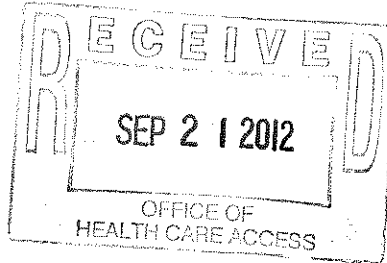


September 21, 2012

Kim Martone  
Director of Operations  
Office of Health Care Access  
410 Capitol Avenue  
MS#13HCA  
Hartford, CT 06134-0308



Dear Ms. Martone,

Enclosed is Saint Francis Hospital and Medical Center's Certificate of Need proposal to acquire a third fixed MRI machine at Saint Francis Hospital and Medical Center to replace 3 days a week mobile MRI services.

Please call me with any questions or concerns at 860-714-5573.

We appreciate your attention in this matter.

Sincerely,

  
**Christopher Hartley**  
Senior Vice President  
Planning & Business Development  
Government Relations

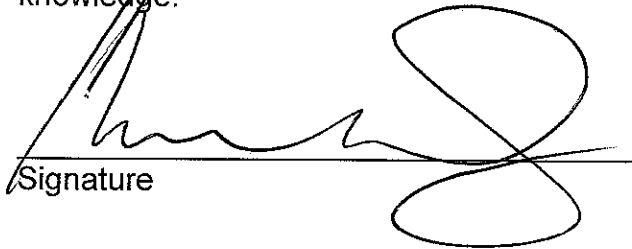
Enclosures

**AFFIDAVIT**

Applicant: **Saint Francis Hospital and Medical Center**

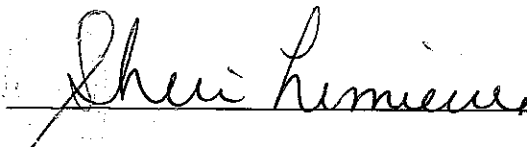
Project Title: **Acquisition of Fixed MRI**

I, **Christopher Dadlez, President and Chief Executive Officer**  
Of **Saint Francis Hospital and Medical Center** being duly sworn, depose and  
state that **Saint Francis Hospital and Medical Center's** information submitted  
in this Certificate of Need Application is accurate and correct to the best of my  
knowledge.

  
\_\_\_\_\_  
Signature

9/18/12  
\_\_\_\_\_  
Date

Subscribed and sworn to before me on September 18, 2012

  
\_\_\_\_\_  
Notary Public/Commissioner of Superior Court

My commission expires: July 31, 2014



**The Hartford Courant.**

A TRIBUNE PUBLISHING COMPANY

# Affidavit of Publication

State of Connecticut

Friday, August 24, 2012

County of Hartford

I, Rena Matus, do solemnly swear that I am Financial Operations Assistant of the Hartford Courant, printed and published daily, in the state of Connecticut and that from my own personal knowledge and reference to the files of said publication the advertisement of Public Notice was inserted in the regular edition.

On dates as follows: 8/22/2012	\$40.30
8/23/2012	\$35.30
8/24/2012	\$35.30

"Under the Connecticut General Statutes 19a-638 of the Department of Public Health, Saint Francis Hospital and Medical Center located at 114 Woodland Street in Hartford, CT 06105 is proposing to acquire a third fixed Magnetic Resonance Imaging (MRI) machine to be located on the campus of Saint Francis Hospital and Medical Center located at 114 Woodland Street in Hartford, CT 06105. The proposed capital expenditure is \$3,818,000. Saint Francis Hospital and Medical Center will file the Certificate of Need for this project with the Department of Public Health through the Office of Health Care Access."

In the amount of \$110.90  
ST FRANCIS HOSP. & MED. CENT  
328283  
ZONE 6

*Rena Matus* Financial Operations Assistant  
Rena Matus

Subscribed and sworn to before me on August 24, 2012

*Renee N. Janes* Notary Public

**RENEE N. JANES**  
**NOTARY PUBLIC**  
MY COMMISSION EXPIRES MAR. 31, 2013

2513972

## Application Checklist

### Instructions:

1. Please check each box below, as appropriate; and
2. The completed checklist *must* be submitted as the first page of the CON application.

- Attached is the CON application filing fee in the form of a certified, cashier or business check made out to the "Treasurer State of Connecticut" in the amount of \$500.

### For OHCA Use Only:

Docket No.: \_\_\_\_\_ Check No.: \_\_\_\_\_  
OHCA Verified by: \_\_\_\_\_ Date: \_\_\_\_\_

- Attached is evidence demonstrating that public notice has been published in a suitable newspaper that relates to the location of the proposal, 3 days in a row, at least 20 days prior to the submission of the CON application to OHCA. (OHCA requests that the Applicant fax a courtesy copy to OHCA (860) 428-7053, at the time of the publication)
- Attached is a paginated hard copy of the CON application including a completed affidavit, signed and notarized by the appropriate individuals.
- Attached are completed Financial Attachments I and II.
- Submission includes one (1) original and four (4) hard copies with each set placed in 3-ring binders.

**Note:** A CON application may be filed with OHCA electronically through email, if the total number of pages submitted is 50 pages or less. In this case, the CON Application must be emailed to [ohca@ct.gov](mailto:ohca@ct.gov).

**Important:** For CON applications (less than 50 pages) filed electronically through email, the signed affidavit and the check in the amount of \$500 must be delivered to OHCA in hardcopy.

- The following have been submitted on a CD
1. A scanned copy of each submission in its entirety, including all attachments in Adobe (.pdf) format.
  2. An electronic copy of the documents in MS Word and MS Excel as appropriate.



**State of Connecticut  
Office of Health Care Access  
Certificate of Need Application**

**Instructions:** Please complete all sections of the Certificate of Need (“CON”) application. If any section or question is not relevant to your project, a response of “Not Applicable” may be deemed an acceptable answer. If there is more than one applicant, identify the name and all contact information for each applicant. OHCA will assign a Docket Number to the CON application once the application is received by OHCA.

**Docket Number:**

**Applicant: Saint Francis Hospital and Medical Center**

**Contact Person: Christopher Hartley**

**Contact Person’s**

**Title: Senior Vice President Planning, Business Development and Government Relations**

**Contact Person’s**

**Address: 114 Woodland Street Hartford, CT 06105**

**Contact Person’s**

**Phone Number: 860-714-5573**

**Contact Person’s**

**Fax Number: 860-714-8093**

**Contact Person’s**

**Email Address: [Chartley@stfranciscare.org](mailto:Chartley@stfranciscare.org)**

**Project Town: Hartford, CT**

**Project Name: Acquisition of Fixed MRI**

**Statute Reference: Section 19a-638, C.G.S.**

**Estimated Total**

**Capital Expenditure: \$3,818,000**

## **1. Project Description: Acquisition of Equipment**

a. Please provide a narrative detailing the proposal.

**Saint Francis Hospital and Medical Center is a tertiary, acute care general hospital that provides a wide variety of health care services to patients in need of inpatient and outpatient care since 1897. Saint Francis Hospital and Medical Center is designated as a Level 2 Trauma Center by the American College of Surgeons. Saint Francis Hospital and Medical Center serves over 32,000 inpatients and over 300,000 outpatients each year. Saint Francis Hospital and Medical Center is committed to providing each patient the “Best Care for a Lifetime”.**

**This high quality commitment has been recognized by several entities over the last several years. The following is a summary and description of all the awards given to Saint Francis since 2009.**

**Joint Commission Accreditation Hospitals- Please see Attachment 1.**

***Most Wired – 2012 – recognized by *Hospitals & Health Networks Magazine* for making progress toward adoption of Information Technology. (Embargo Date: July 10, 2012)***

***Connecticut Quality Improvement Award Gold Prize – was given to Saint Francis Hospital by the Connecticut Quality Improvement Association for our work in improving the Universal Protocol in our operating room, using the Safe Surgery Checklist. (June 2012)***

***The LeapFrog Group “A” Score –Saint Francis Hospital and Medical Center was only one of four hospitals in the state to receive an “A” grade on the organization’s Hospital Safety Score. The Hospital Safety Score<sup>SM</sup> was calculated under the guidance of The Leapfrog Group’s Blue Ribbon Expert Panel using publicly available data on patient injuries, medical and medication errors, and infections. U.S. hospitals were assigned an A, B, C, D, or F for their safety. (June 2012)***

***HealthGrades<sup>®</sup> Patient Safety Excellence Award<sup>™</sup> – for patient safety indicators from the Agency for Healthcare Research and Quality (AHRQ) to identify patient safety incidence rates, placing Saint Francis in the top 5% in the nation for patient safety, and the only Connecticut hospital to achieve this distinction. (May 2012)***

***American Heart Association/American Stroke Association *Get With the Guidelines Gold Plus Award* – to the Hoffman Heart and Vascular Institute for providing excellent care to heart failure patients. Saint Francis is one of the only three hospitals statewide to receive this award. (May 2012)***

***Silver Healthy Hospital Award, Stryker – for outstanding performance in reducing environmental harm and improving overall hospital quality through medical device remanufacturing and reprocessing. For 2011, Saint Francis saved \$235,600 and had a total waste avoidance of 11,900 pounds. (April 2012)***

***Outcome Excellence Award – the outpatient rehabilitation staff at 95 Woodland Street received this award from Focus on Therapeutic Outcomes (FOTO) for exceeding the predicted national target for outcomes and patient satisfaction over a one-year period. The targets were met for two consecutive years, for both 2010 and 2011. (April 2012)***

**2012 Top Performer** – the inpatient rehabilitation team at Mount Sinai Rehabilitation Hospital received an Outstanding Performance Award from the Uniform Data Systems database for its top ten percent ranking out of 800 programs across the United States. (April 2012)

**The Blue Ribbon Award** – for the John T. O’Connell Tower presented at the 17<sup>th</sup> Annual Awards Showcase from the Real Estate Exchange. This is the most significant annual awards event in commercial real estate in Connecticut and a celebration of excellence in the industry. (April 2012)

**The BUILDCT 2012 Award** – for the John T. O’Connell Tower best new large construction project greater than \$10 million from the Association of General Contractors. The award was given to Saint Francis Hospital and Medical Center; TRO/Jung Brannen, the architect and engineer; and Turner Construction Company, the construction manager. (March 2012)

**Connecticut Quality Improvement Award Silver Innovation Prize** – for the creation of the Connecticut Institute for Primary Care Innovation. (August 2011)

**American Heart Association/American Stroke Association Get With The Guidelines Gold Plus Award** – for achievement in using evidence-based guidelines in the treatment of stroke patients. (August 2011)

**Most Wired – 2011** – recognized by *Hospitals & Health Networks Magazine* for making progress toward adoption of Information Technology. (July 2011)

**Community Value Five-Star Hospital** – recognized by Cleverly & Associates, a healthcare industry intelligence and education consultancy for value provided to the community, based on financial viability, facility reinvestments, low-cost structures, and high-quality patient care. (July 2011)

**Practice Greenhealth Partner for Change with Distinction** – for outstanding environmental achievement in healthcare. (April 2011)

**HealthGrades<sup>®</sup> Patient Safety Excellence Award<sup>™</sup>** – for patient safety indicators from the Agency for Healthcare Research and Quality (AHRQ) to identify patient safety incidence rates. (March 2011)

**The American Society for Metabolic and Bariatric Surgery and the Surgical Review Corporation Bariatric Surgery Center of Excellence<sup>®</sup> Designation** – for demonstrating an unparalleled ability to consistently deliver safe, effective, evidence-based care. (March 2011)

**Focus on Therapeutic Outcomes, Inc. Outcomes Excellence Award** – for exceeding the national average for functional change in the patients treated at the Center for Rehabilitation and Sports Medicine. (March 2011)

***The American College of Cardiology Foundation NCDR ACTION Registry Gold Performance Award*** – for implementing a higher standard of care and reaching the aggressive goal of treating coronary artery disease patients with 85 percent compliance with American College of Cardiology/American Heart Association clinical guidelines and recommendations. (December 2010)

***The American Alliance of Healthcare Providers Choice Award*** – for implementing an excellent healthcare program that successfully results in courteous, compassionate, and caring service to patients, families, and the community. (July 2010)

***Most Wired “Most Improved” Award*** – for the Hospital’s level of achievement in business and administrative management, clinical quality and safety, continuum of care, and infrastructure. Based on a survey by *Hospitals & Health Networks Magazine*, McKesson Corporation and the College of Healthcare Information Management Executives. (July 2010)

***Practice Greenhealth Partner for Change Award*** – for continuously improving and expanding upon mercury elimination, waste reduction and pollution prevention. Presented by Practice Greenhealth, a national membership organization for healthcare facilities committed to environmentally responsible operations. (May 2010)

***Anthem Blue Cross and Blue Shield Blue Distinction Center for Knee and Hip Replacement*** – In recognition of clinical excellence in knee and hip replacement surgery. (January 2010)

***American Heart Association/American Stroke Association Get With The Guidelines Gold Plus Performance Achievement Award*** – In recognition of implementing excellent care for stroke patients, according to evidence-based guidelines. (January 2010)

***U.S. Department of Health and Human Services Silver-2 Medal*** – In recognition of efforts promoting organ donation. (October 2009)

***Employer Support of the Guard and Reserves Program – Connecticut Above and Beyond Award*** for support of Hospital employees who are members of National Guard and Reserves. (July 2009)

***Practice Greenhealth Partner for Change Award*** – for continuously improving and expanding upon mercury elimination, waste reduction and pollution prevention. Presented by Practice Greenhealth, a national membership organization for healthcare facilities committed to environmentally responsible operations. (May 2009)

***ENERGY STAR Label*** – for superior energy efficiency and environmental protection. Awarded by the U.S. Environmental Protection Agency. Saint Francis was previously awarded ENERGY STAR labels in 2003 and 2006. (April 2009)

***Connecticut Breastfeeding Coalition Breastfeeding Friendly Employer Award*** – Given for Saint Francis’ efforts in supporting breastfeeding by working mothers. (January 2009)

As you can see from the listing of recent awards above, Saint Francis Hospital and Medical Center has been recognized for its excellence by a wide range of programs who oversee quality service delivery.



To maintain this excellence in care, Saint Francis Hospital and Medical Center must maintain its diagnostic capabilities at the highest levels. The Department of Radiology and Imaging Services provides diagnostic imaging services to approximately 200,000 inpatient, emergency department patients and outpatients annually, as well as serving as a major diagnostic support service for over 600 local community hospital physicians across all specialties.

Saint Francis Hospital and Medical Center is currently in the process realigning its clinical sections into clinical 'Service Lines' that will, in conjunction with St Francis Health Care Partners (SFHCP), the parent Accountable Care Organization (ACO), and Johnson Memorial Medical Center (JMMC), coordinate and provide specialty care services for the entire ACO network across the continuum of care from the community physician to the hospital setting. As a tertiary level facility serving central and north central Connecticut, Saint Francis Hospital and Medical Center must provide access to contemporary, state of the art services through our specialty service lines, including pertinent imaging applications.

In addition, Saint Francis Hospital and Medical Center has also contributed to the community as a key partner with the University of Connecticut School of Medicine and other centers of higher education serving as a clinical site for training Nurses, Physician Assistants, Medical Students and Physicians during their Residency and Fellowship across numerous specialties. The Department of Radiology and Imaging Services serves as a training facility for Radiologists, supporting both the University of Connecticut School of Medicine Radiology Residency Program and the Saint Francis Hospital and Medical Center post-doctorate MRI Fellowship Program. In addition, the Department of Radiology and Imaging Services is a clinical affiliate site for the following college Radiologic and Diagnostic Imaging Technology Student Programs; Capital Community College, Gateway Community College, University of Hartford and Quinnipiac University.

The Department of Radiology and Imaging Services at Saint Francis Hospital and Medical Center functions as a key support platform for the numerous services provided at Saint Francis Hospital and Medical Center and the associated clinical affiliates in the ACO network. Given its role as a tertiary level facility serving central Connecticut, it is essential that Saint Francis Hospital and Medical Center have access to imaging services that are not only timely, but also contemporary and on par with other tertiary level facilities across the nation.

Saint Francis Hospital and Medical Center proposes to purchase a state of the art second generation 3T magnet (Siemens Magnetom Skyra) which will replace a mobile service at Saint Francis Hospital and Medical Center's main campus as well as supplement the capabilities to its two 1.5Tesla MRI units currently on site that are at capacity.

The many unique, critical applications of MRI have led MR to become one of the most critical diagnostic imaging technologies offered by Saint Francis Hospital and Medical Center. Despite the national and regional economic downturn, MRI volume has continued to increase. Saint Francis Hospital and Medical Center is currently served by two fixed 1.5Tesla MRI units approved by the Office of Health Care Access (OHCA). Saint Francis Hospital and Medical Center is also served 3 days a week by a 7 day a week mobile service which is split between the hospital campus and an access site in Avon, this mobile service has also been approved by OHCA.

**The MRI volume at Saint Francis Hospital and Medical Center has steadily increased over time. Most recently, in FY 2010 there were 11,316 total MRI exams and in FY 2011 11,580 MRI exams performed for a 2.3% year over year increase. In reviewing the 2012 MRI volume to date, Saint Francis Hospital and Medical Center projects it will serve over 12,337 patients in FY 2012 which is an increase of 6.5%. The two fixed 1.5T MRI scanners are currently operating 24 hours, 7 days a week to support inpatient and outpatient operations. This has lead to increasing difficulty balancing the needs of the emergency room and hospital for "STAT" examinations on critically ill patients. This has also resulted in scheduling backlogs for routine outpatient work. In addition, as a tertiary level facility Saint Francis Hospital and Medical Center attracts complex cases and has specialized in studies that other facilities in the community do not perform such as Cardiac MRI, MR Spectroscopy and complex body MR and MR angiography applications. Given the complexity of these studies many exams can easily take up to twice as long as routine examinations.**

**The 3 day week mobile service at 95 Woodland Street Health Enhancement Center located across the street from Saint Francis Hospital and Medical Center has provided some flexibility but is limited to regular business hours and can only be used for routine outpatient examinations as it is not suited for inpatient work. Volumes on the mobile service have essentially peaked, in FY 2010 a total of 706 examinations were performed, in FY 2011 a total of 405 examinations were performed and the projected volume for FY 2012 is 684 examinations.**

**Saint Francis Hospital and Medical Center proposes to replace the 3 day a week mobile service with a third internalized hospital based service which will be provided by a state of the art second generation 3T magnet (Siemens Magnetom Skyra). Saint Francis Hospital and Medical Center believes that not only do Saint Francis Hospital and Medical Center's current volumes, case mix, and volume trends support this addition but that having a third state of the art fixed magnet is necessary to maintain our operations and meet the demands of both Saint Francis Hospital and Medical Center and our ACO network of referring clinicians making up SFHCP and affiliated institutions. As a tertiary level training facility Saint Francis Hospital and Medical Center must continue to provide state of the art, contemporary services that may not be available in the community at large. Saint Francis Hospital and Medical Center must be able to provide the complex, and sometimes time intensive studies that other facilities may be unable to perform while still having the operational flexibility and ready access to MRI service to meet the ever increasing requirements for shorter lengths of stay (LOS), improved patient safety, and timely diagnosis and treatment required of a modern 21<sup>st</sup> century hospital.**

**Saint Francis Hospital and Medical Center plans to eliminate the three days of mobile MRI service provided by Alliance Imaging, Inc at the 95 Woodland Street location, terminating the contractual agreement for the service at this location. The remaining four days of mobile MRI service provided by Alliance Imaging at the Avon location will remain in place under an existing contractual agreement and no other change in the Alliance contract will be needed.**

- b. Provide letters that have been received in support of the proposal.

**Please refer to Attachment 2 for letters of support.**

- c. Provide the Manufacturer, Model, Number of slices/tesla strength of the proposed scanner (as appropriate to each piece of equipment).

**The proposed new fixed MRI manufacturer is Siemens and the model is Magnetom Skyra 3T (tesla strength)**

- d. List each of the Applicant's sites and the imaging modalities and other services currently offered by location.

**Saint Francis Hospital and Medical Center Main Campus, 114 Woodland St., Hartford/  
Department of Radiology and Imaging Services:**

- **Diagnostic X-Ray**
- **CT Scan**
- **MRI**
- **PET/CT**
- **Nuclear Medicine ( General and Cardiac)**
- **Ultrasound**
- **Interventional Radiology/Special Procedures**
- **Mammography/Needle Localizations**

**Comprehensive Breast Center, 95 Woodland St., Hartford:**

- **Mammography (Screening and Diagnostic)**
- **Breast Ultrasound**
- **Stereotactic Breast Biopsy**
- **Bone Density**
- **Diagnostic X- Ray**
- **MRI (mobile service)**

**Saint Francis Care Access Centers:**

- **35 Nod Road, Avon: MRI ( mobile service)**
- **7 Elm Street, Enfield: Diagnostic X-Ray**

**Burgdorf Health Center, 131 Coventry St., Hartford:**

- **Diagnostic X-Ray**

**Mount Sinai Campus, 500 Blue Hills Ave., Hartford:**

- **Diagnostic X-Ray**
- **Ultrasound**

**Medical Office Building, 1000 Asylum Street, Hartford:**

- **Diagnostic X-Ray**

## **2. Clear Public Need**

- a. Explain why there is a clear public need for the proposed equipment. Provide evidence that demonstrates this need.

**Magnetic Resonance Imaging (MRI) is now a ubiquitous clinical tool which has revolutionized the diagnosis and management of a wide variety of diseases. Based on the principle of spatially encoding the radio signal emitted by water protons placed within a magnetic field after stimulation with radiofrequency waves, the first MR scanners entered clinical practice in the early 1980s. These early units were used primarily for imaging the brain, but over the ensuing three decades continued advances in MRI have resulted in a wide variety of imaging applications encompassing the entire body.**

**MRI units are frequently denoted by the field strength of their magnet measured in Teslas (T). The current standard for high field magnets is 1.5 T; these units are ubiquitous and make the images most people are used to seeing in the media on a daily basis. The advantage of higher field strength magnets is an improved Signal to Noise Ratio (SNR) of the emitted radiofrequency waves which allow for improved image quality, better spatial resolution, and faster scan times.**

**During the early 2000s, the first 3T magnets entered clinical practice. The main advantage of 3T over 1.5T is an almost doubling in the SNR with the stronger magnet which improves speed and image quality. Perhaps more importantly, 3T magnets have a much greater 'chemical shift' between water and fat protons. This opens the door for several unique applications for 3T MR which can not be done well or at all with the lower field strength magnets. While early 3T magnets suffered from some image quality and speed problems related to the higher field strength and chemical shift, these issues have been for the most part resolved with the second generation of 3T MRI.**

**Saint Francis Hospital and Medical Center plans to purchase a state of the art second generation 3T magnet (Siemens Magnetom Skyra) which will replace a mobile service at Saint Francis Hospital and Medical Center and supplement the capacity to Saint Francis Hospital and Medical Center's two current 1.5T units which are reaching saturation levels.**

**There are also unique clinical applications that can only be performed on a 3T platform which are expected clinical applications available at tertiary level facilities across the country. As there are currently no other 3T units in central or north central Connecticut, patients within Saint Francis Hospital and Medical Center network currently have to travel out of the region to have these studies performed or will forego the procedure, which can result in less than optimal patient care. These applications and the clinical service lines they support will be discussed in the following narrative.**

**There are several applications that the two current 1.5 T units at Saint Francis Hospital and Medical Center cannot perform but are optimally performed on a 3T unit. These applications revolve around the increasing need for robust non contrast cardiovascular imaging to protect certain renal disease patients from the effects of gadolinium contrast agents and the emerging need for functional neuro-imaging to support Saint Francis Hospital and Medical Center's growing neuroscience program.**

Please review the more detailed discussion of the impact of these new 3T applications on MRI volume in section 3g below.

- b. Provide the utilization of existing health care facilities and health care services in the Applicant's service area.

See below table.

The Hospital based MRI facilities are the following:

Hospital	Number of MRI Machines	FY 2010 Total Volume	FY 2011 Total Volume	Increase/Decrease And Percent difference ft'11 over 'FY'10
Bristol	1	3,465	3,232	(233) (7%)
CCMC	1	3,634	4,094	460 13%
Charlotte Hungerford	1	6,434	6,480	46 1%
Hospital of Central CT	1	6,965	7,703	738 11%
Hartford Hospital	2	8,322	7,742	(580) (7%)
John Dempsey	1	7,185	6,876	(309) (4%)
Johnson Memorial	1	1,378	1,511	133 10%
Manchester Memorial	1	3,840	3,731	(109) (3%)
Middlesex Hospital	1	10,803	10,579	(224) (2%)
Midstate Medical Center	1	6,942	7,534	592 9%
Rockville General	1	1,896	1,833	(63) (3%)
Saint Francis Hospital and Medical Center	3	13,849*	14,221*	372 3%
Total	13	74,713	75,536	823 1.1%

Source: OHCA Financial form 450 twelve month filing for FY 2010 and FY 2011

\*Note: The volume numbers in the OHCA form 450 are higher than the volume numbers used in the utilization projections elsewhere in this application because these numbers include volume for the Avon outpatient site and are based on MRI revenue codes that reflect charges not necessarily procedures performed.

- c. Complete **Table 1** for each piece of equipment of the type proposed currently operated by the Applicant at each of the Applicant's sites.

**Table 1: Existing Equipment Operated by the Applicant**

<b>Provider Name Street Address Town, Zip Code</b>	<b>Description of Service *</b>	<b>Hours/Days of Operation **</b>	<b>Utilization ***</b>
Saint Francis Hospital and Medical Center 114 Woodland Street Hartford CT 06105	Siemens Symphony 1.5 Tesla MRI Closed	Mon-Fri 24 hours Sat-Sun 6:00am-10:30pm	6,604 Exams 07/01/2011- 07/01/2012
Saint Francis Hospital and Medical Center 114 Woodland Street Hartford CT 06105	Siemens Avanto 1.5 Tesla MRI Closed	Mon-Fri 24 hours Sat-Sun 6:00am-10:30pm	4,978 Exams 07/01/2011- 07/01/2012
Saint Francis Hospital and Medical Center 95 Woodland Street Hartford CT 06105	Siemens Symphony 1.5 Tesla MRI Closed (Alliance Imaging Mobile Service)	Tuesday, Wednesday, and Friday 8:00am- 5:00pm	620 exams 06/01/2011- 06/01/2012

\* Include equipment strength (e.g. slices, tesla strength), whether the unit is open or closed (for MRI)

\*\* Days of the week unit is operational, and start and end time for each day; and

\*\*\* Number of scans/exams performed on each unit for the most recent 12-month period (identify period).

- d. Provide the following regarding the proposal's location:

- i. The rationale for locating the proposed equipment at the proposed site;

**The proposed fixed unit is proposed to be located on the Saint Francis Hospital and Medical Center at 114 Woodland Street in the MRI department located on the first floor of building one. It will be adjacent to one of the existing fixed MRI unit.**

- ii. The population to be served, including specific evidence such as incidence, prevalence, or other demographic data that demonstrates need;

**Please refer to the response to the question below 2 d. iii.**

- iii. How and where the proposed patient population is currently being served;

**The proposed patient population is currently being served by Saint Francis Hospital and Medical Center at its site located at 95 Woodland Street Health Enhancement Center with its mobile MRI. Hence, the patients being served there would shift to the new fixed unit proposed on the first floor of Saint Francis Hospital and Medical Center's MRI department. In addition to outpatients, Saint Francis Hospital and Medical Center's inpatients will benefit from the utilization of this MRI in a more timely fashion than if the additional machine was not present.**

- iv. All existing providers (name, address) of the proposed service in the towns listed above and in nearby towns;

**As noted above there are no other 3T MRI units in the Saint Francis service area**

- v. The effect of the proposal on existing providers; and

**This project will not affect other area providers as Saint Francis Hospital and Medical Center will use this equipment to serve its existing patient base. In addition, the health care delivery system in Connecticut will benefit from this proposal as patients within the Saint Francis Hospital and Medical Center system will have access to 3T state of the art MRI applications which will improve patient safety and care. These include but are not limited to fast accurate MR Spectroscopy at 3T, complex vascular imaging without the risk of contrast exposure in patients with renal disease, as well as functional brain mapping to help plan and preserve critical areas of the brain in patients undergoing open surgical or Cyberknife treatments for brain tumors, vascular malformations, and other lesions.**

- vi. If the proposal involves a new site of service, identify the service area towns and the basis for their selection.

**This question is not applicable since Saint Francis is proposing to serve the same MRI population that currently uses its hospital MRI scanners and the mobile unit located at 95 Woodland in Hartford, CT.**

- e. Explain why the proposal will not result in an unnecessary duplication of existing or approved health care services.

**This project will not be a duplication of services since there currently is no 3T MRI technology in Saint Francis Hospital and Medical Center's service area. The current MRI units at Saint Francis have reached full capacity. This new equipment will serve its existing patient base. In addition, the health care delivery system in Connecticut will benefit from this proposal as patients will be able to be served on state-of – the art equipment without lengthy delays. Furthermore, no new licenses will be required as a result of this project.**

### 3. Actual and Projected Volume

- a. Complete the following tables for the past three fiscal years (“FY”), current fiscal year (“CFY”), and first three projected FYs of the proposal, for each of the Applicant’s existing and proposed pieces of equipment (of the type proposed, at the proposed location only). In Table 2a, report the units of service by piece of equipment, and in Table 2b, report the units of service by type of exam (e.g. if specializing in orthopedic, neurosurgery, or if there are scans that can be performed on the proposed scanner that the Applicant is unable to perform on its existing scanners).

**Table 2a: Historical, Current, and Projected Volume, by Equipment Unit**

Scanner Type	Actual Volume (Last 3 Completed FYs October - September)			CFY Volume*	Projected Volume (First 3 Full Operational FYs- October - September)**			
	FY 2009	FY 2010	FY 2011	FY 2012 annualized	FY 2013	FY 2014	FY 2015	FY 2016
<b>Avanto 1.5 Tesla MRI</b>								
Emergency	136	132	122	143	148	100	102	104
Inpatient	1,181	1,266	1,156	1,406	1,434	971	990	1,010
Outpatient	3,097	3,161	3,377	3,378	3,443	2,278	2,324	2,369
<b>Total</b>	<b>4,414</b>	<b>4,559</b>	<b>4,655</b>	<b>4,927</b>	<b>5,025</b>	<b>3,349</b>	<b>3,416</b>	<b>3,483</b>
<b>Symphony 1.5 Tesla MRI</b>								
Emergency	339	357	338	323	329	137	140	143
Inpatient	2,537	2,272	2,471	2,684	2,738	1,325	1,351	1,378
Outpatient	3,149	3,221	3,605	3,712	3,786	3,107	3,169	3,232
<b>Total</b>	<b>6,025</b>	<b>5,850</b>	<b>6,414</b>	<b>6,719</b>	<b>6,853</b>	<b>4,569</b>	<b>4,660</b>	<b>4,753</b>
<b>Symphony Mobile 1.5 Tesla MRI</b>								
Emergency	0	0	0	0	0	0	0	0
Inpatient	0	0	0	0	0	0	0	0
Outpatient	1,451	907	511	691	705	0	0	0
<b>Total</b>	<b>1,451</b>	<b>907</b>	<b>511</b>	<b>691</b>	<b>705</b>	<b>0</b>	<b>0</b>	<b>0</b>
<b>Skyra 3.0 Tesla MRI</b>								
Emergency	0	0	0	0	0	148	151	154
Inpatient	0	0	0	0	0	1,426	1,456	1,485
Outpatient	0	0	0	0	0	3,341	3,406	3,474
<b>Total</b>	<b>0</b>	<b>0</b>	<b>0</b>	<b>0</b>	<b>0</b>	<b>4,915</b>	<b>5,013</b>	<b>5,113</b>
<b>G T</b>	<b>11,890</b>	<b>11,316</b>	<b>11,580</b>	<b>12,337</b>	<b>12,583</b>	<b>12,833</b>	<b>13,089</b>	<b>13,349</b>

\* For periods greater than 6 months, report annualized volume, identifying the number of actual months covered and the method of annualizing. For periods less than six months, report actual volume and identify the period covered. **FY’2012 is annualized using October – July 2012 data.**

\*\* If the first year of the proposal is only a partial year, provide the first partial year and then the first three full FYs. Add columns as necessary. **See above**

\*\*\* Identify each scanner separately and add lines as necessary. Also break out inpatient/outpatient/ED volumes if applicable. **See above**

\*\*\*\* Fill in years. In a footnote, identify the period covered by the Applicant’s FY (e.g. July 1-June 30, calendar year, etc.). **See above**



**Table 2b: Historical, Current, and Projected Volume, by Type of Scan/Exam**

	Actual Volume (Last 3 Completed FYs October 1, - September 30)			CFY Volume*	Projected Volume (First 3 Full Operational FYs (October 1- September 30)**			
	FY 2009	FY 2010	FY 2011	FY'12 annualized	FY 2013	FY 2014	FY 2015	FY 2016
<b>Service type***</b>								
<b>Neuro</b>	7,809	7,665	7,746	8,559	8,730	8,905	9,082	9,263
<b>Ortho</b>	2,077	1,807	1,896	1,856	1,893	1,930	1,969	2,008
<b>Cardiac</b>	95	89	112	109	111	113	115	117
<b>Breast</b>	799	707	699	705	719	733	748	763
<b>Body</b>	1,110	1,048	1,127	1,108	1,130	1,152	1,175	1,198
<b>Total</b>	11,890	11,316	11,580	12,337	12,583	12,833	13,089	13,349

\* For periods greater than 6 months, report annualized volume, identifying the number of actual months covered and the method of annualizing. For periods less than six months, report actual volume and identify the period covered. **FY'12 is annualized using October – July volumes.**

\*\* If the first year of the proposal is only a partial year, provide the first partial year and then the first three full FYs. Add columns as necessary. **N/A**

\*\*\* Identify each type of scan/exam (e.g. orthopedic, neurosurgery or if there are scans/exams that can be performed on the proposed piece of equipment that the Applicant is unable to perform on its existing equipment) and add lines as necessary. **See above**

\*\*\*\* Fill in years. In a footnote, identify the period covered by the Applicant's FY (e.g. July 1-June 30, calendar year, etc.). **See above**

- b. Provide a breakdown, by town, of the volumes provided in Table 2a for the most recently completed full FY.

**Please refer to Attachment 3.**

- c. Describe existing referral patterns in the area to be served by the proposal.

**Saint Francis Hospital and Medical Center has seen a significant increase in the number of patients presenting for surgical and radiosurgical (Cyberknife) treatment of brain tumors. For 2010 SFHMC treated 181 patients and for 2011 SFHMC treated 219 patients with primary and metastatic disease to the brain for a year over year increase of 20%. We anticipate continued growth of our Oncology and Neuroscience programs as part of the SFHCP ACO. Our service lines will require the appropriate tools to stay contemporary and we have identified functional neuroimaging as a key need for the institution as this is fast becoming a necessary clinical tool to support a robust Neuro Oncology and Neuroscience program.**

- d. Explain how the existing referral patterns will be affected by the proposal.

**The proposed replacement of the existing mobile MRI unit with the fixed –based MRI unit ((Siemens Magnetom Skyra) will provide current referring physician’s greater opportunity to service their patients. This proposal will improve the delivery of health care in greater Hartford area and beyond. Increasing access to MRI services at Saint Francis Hospital and Medical Center will clearly benefit Saint Francis Hospital and Medical Center’s existing patients as well as Saint Francis Hospital and Medical Center’s referring physicians. Replacement of the mobile MRI service with the fixed MRI unit will provide seven days weekly availability, increased diagnostic capabilities and improved clinical image quality. Referring physicians will have access to 3T technology at Saint Francis Hospital and Medical Center which is currently not available in Hartford or surrounding area.**

- e. Explain any increases and/or decreases in volume seen in the tables above.

**The increases in patient volume have been based on historical trends of the past three fiscal years and a conservative estimation of future growth. Equal redistribution of exams utilizing three fixed MRI units at Saint Francis Hospital and Medical Center explains the decrease in exams per unit over the next three fiscal years projected volumes with a net increase in volume of 2% each of the next three years.**

- f. Provide a detailed explanation of all assumptions used in the derivation/ calculation of the projected volume by scanner and scan type.

**Saint Francis Hospital and Medical Center anticipates a continued growth in the demand for MRI services based on historical trends and the increased demand for advanced MRI examinations such as Cardiac imaging, Breast imaging and interventional procedures and Neurological studies as a few examples. The Department of Radiology and Imaging Services at Saint Francis Hospital and Medical Center functions as a key clinical support platform for the numerous services provided at Saint Francis Hospital and Medical Center and the associated clinical affiliates in the ACO network. Given its role as a tertiary level facility serving central Connecticut, it is reasonable to anticipate continued future growth.**

- g. Provide a copy of any articles, studies, or reports that support the need to acquire the proposed scanner, along with a brief explanation regarding the relevance of the selected articles.

**In 2000, Nephrogenic Systemic Fibrosis (NSF) was described in the literature as an emerging disease resulting in rapid decline due to the generalized deposition of collagen within tissues. NSF affects patients with impaired renal function and has been strongly associated with the recent administration of gadolinium contrast in these patients. Although a firm causative mechanistic relationship has not been established, based on the strong association of this disorder with gadolinium use in patients with impaired renal function the FDA has issued guidelines that Gadolinium contrast should only be used in patients with impaired renal function when absolutely necessary. This is the standard of care to which Saint Francis Hospital and Medical Center now adheres. (See article 1 contained in Attachment 4)**

With the emergence of NSF radiologists at Saint Francis Hospital and Medical Center have had to fall back on non contrast MRA techniques using Time of Flight (TOF) and Phase Contrast (PC) techniques available using the hospital's older generation of magnets. Unfortunately these studies have often proved to be inadequate. Fortunately, with the advent of 3T new robust techniques to perform MRA without the administration of contrast agents have emerged which can replicate the temporal and spatial resolution of contrast enhanced MRA. Techniques now entering clinical practice focus on two approaches. One such technique involves gating blood flow and imaging differences in signal intensity within pulsatile blood flow during 3D Half Fourier Fast Spin Echo acquisition (FSE) or Balanced Steady State Free Precession (bSSFP) acquisitions. Various vendors have approached this differently, but these techniques together fall under the categorization of Fresh Blood Imaging (FBI). The second image enhancing approach involves using spin labeling techniques where a volume of moving blood will be labeled with an RF pulse prior to allowing the pulse to flow into a target tissue or organ which has be 'prepped' with an inversion pulse to suppress background signal resulting in a pure image of inflowing blood. These techniques are collectively called Time-Spatial Labeling Inversion Pulse techniques (Time SLIP). In addition to these two 3T MRI diagnostic new techniques which will now be available, the Saint Francis Hospital and Medical Center Radiology Department uses the other MRI diagnostic techniques of TOF and PC imaging. These two techniques are also significantly improved using the 3T (See articles 2 and 3 contained in Attachment 4).

There is also a very high association of cardiovascular disease among patients with chronic renal failure. In fact cardiovascular disease accounts for up to 40% of all deaths in patients with chronic renal disease. The loss of the ability to non-invasively image some of these patients after the emergence of NSF has complicated their care significantly as there is truly no other way to perform adequate non invasive vascular imaging of these patients. Thus, the installation of the proposed 3T magnet at Saint Francis Hospital and Medical Center will allow the institution to provide high quality non contrast MRA using the new techniques described above to this critical patient population. (See article 4 contained in Attachment 4).

In addition, the higher field strength of 3T results in an increased relaxation time for soft tissues relative contrast enhancement. This increased relaxation time when combined with the higher signal to noise ratio of 3T technology will allow Saint Francis Hospital and Medical Center to dramatically reduce the dose of gadolinium the Saint Francis Hospital and Medical Center Radiology Department currently has to administer to all patients including those on whom Saint Francis Hospital and Medical Center Radiology Department performs contrast enhanced MRA. Given the large population of patients with early renal impairment or transient renal impairment, any reduction in administered gadolinium will help improve the safety and quality of the exam for all patients. (See articles 5 and 6 contained in Attachment 4).

## Clinical Functional Neuroimaging and Treatment Planning

The surgical, non invasive, and medical treatment of brain tumors and other medical and functional diseases of the brain such as Multiple Sclerosis (MS) have evolved hand in hand with the improved ability to localize both diseased and non diseased brain. These improvements have also enhanced the ability of physicians to functionally map brain activity. The brain is an interconnected network of cortical and subcortical neural tissue where each region specializes in processing and storing information ranging from basic motor reflex and autonomic functions, to the various higher level functions of perception, memory, processing, planning, and thought which together encompass consciousness. One of the practical challenges of medical and surgical treatment of brain disorders is determining not only “where” a lesion is but “what” does the normal tissue around the lesion do functionally and how is it connected to everything else.

All areas of the brain function in unison and contribute to normal higher and lower mental function. Certain areas however are termed “eloquent”, meaning that damage to these areas has immediate irreversible functional consequence. Damage to these areas may result in paralysis, loss of the ability to speak, loss of the ability to comprehend speech, blindness, loss of sensation or other functional loss. In addition, the deep structure of the brain is made up of innumerable white matter fibers that interconnect the various processing regions of the brain allowing the whole ensemble to function in unison. Major collections of fibers that interconnect one region of the brain to another are termed white matter “tracts” and damage to these connections, either surgically or due to a demyelinating condition such as MS can result in severe functional impairment.

In the 1990’s it was discovered that areas of active brain tissue increase their local blood flow through physiological auto regulation, this increased flow results in a slight change in the ratio of oxygenated to deoxygenated hemoglobin within a region of the brain. Oxyhemoglobin is diamagnetic and deoxyhemoglobin is paramagnetic with vastly different  $T2^*$  relaxation times. Fast gradient techniques can in real time detect the changes in  $T2^*$  relaxation of neural tissue, these techniques are collectively termed BOLD (Blood Oxygenation Level Dependent) imaging and have become a critical tool for neuroscience ushering in the era of Functional MRI or fMRI. BOLD techniques are greatly limited at lower field strength magnets but they have contributed greatly to neuroscience research, dramatically helping Saint Francis Hospital and Medical Center Radiology Department to better understand how the brain functions. Higher field strength magnets such as 3T units are increasingly sensitive to the small susceptibility changes within tissues seen with the BOLD effect. This combined with the added signal inherent with the higher field strength makes 3T MR units perfectly suited to perform fMRI as a viable clinical tool. (See article 7 contained in Attachment 4).

At the same time that fMRI techniques have evolved to map eloquent cortical structures, applications to simultaneously map white matter tracts have also emerged using diffusion tensor imaging techniques (DTI). Diffusion imaging was part of the early evolution of MRI and allowed imaging of the bulk flow of water within tissues by determining the speed at which water protons move from one area to other by phase encoding the position and velocity of water protons in tissue. Free water protons exhibit Brownian motion and are free to move in all directions unrestricted based on their kinetic energy, such motion is said to be isotropic.

**Water protons within tissue are restricted in their motion by their local environment and exhibit varying degrees of restricted motion, which is termed anisotropy (restricted diffusion).**

**Modern high field 3T magnets can determine the vector of isotropy and anisotropy for a given volume of tissue. In the brain, water protons in white matter tracks demonstrate a high degree of isotropic motion (non-restricted diffusion) along the course of white matter fiber tracts. By generating a vector representation of the maximum diffusion in each volume of white matter in the brain, maps of the fiber tracts connecting the various regions within a living brain can be non invasively generated. DTI generated maps can be used for evaluating the location of critical white matter tracts that need to be surgically preserved, or DTI can be used to evaluate the integrity of white matter tracts in medical conditions such as MS. (See article 8 contained in Attachment 4).**

**DTI and fMRI techniques are now feasible for routine clinical work with the advent of newer more robust 3T platforms such as the Siemens Magnetom Skyra unit which Saint Francis Hospital and Medical Center seeks approval to purchase at this time. 3T MRI and software packages for fMRI and DTI imaging are now FDA approved for clinical use and are used routinely to identify key cortical structures and fiber tracts that need to be preserved during surgical and non surgical treatment. Studies have shown that preoperative mapping with fMRI and DTI imaging improves surgical outcomes by helping the treating physician appropriately identify patients who would be successful surgical candidates and better plan surgery or radiotherapy treatments to minimize damage to key areas for all patients who meet the criteria outlined in this study. (See articles 9 and 10 contained in Attachment 4).**

#### **4. Quality Measures**

- a. Submit a list of all key professional, administrative, clinical, and direct service personnel related to the proposal. Attach a copy of their Curriculum Vitae.

**Please refer to Attachment 5 for a copy of the CV's.**

- b. Explain how the proposal contributes to the quality of health care delivery in the region.

**This Certificate of Need proposal will ensure patients will have the opportunity to receive MR scans on the very latest state of the art MRI scanning technology. The improved speed, image quality and capabilities with this new technology will ensure that Saint Francis Hospital and Medical Center continues to be of the highest quality to serve its patients needing MRI scanning services.**

**In addition, Saint Francis Hospital and Medical Center along with Mount Sinai Rehabilitation, Inc. are both accredited by the Joint Commission on Accreditation of Hospitals. Both were recently reaccredited by JCAHO in 2011 for three years.**

#### **5. Organizational and Financial Information**

- a. Identify the Applicant's ownership type(s) (e.g. Corporation, PC, LLC, etc.).

**Saint Francis Hospital and Medical Center is a non profit Organization.**

- b. Does the Applicant have non-profit status?  
 Yes (Provide documentation)  No
- c. Provide a copy of the State of Connecticut, Department of Public Health license(s) currently held by the Applicant and indicate any additional licensure categories being sought in relation to the proposal.

**Please see Attachment 6 for a copy of Saint Francis Hospital and Medical Center's current license. Saint Francis Hospital and Medical Center is not seeking any other new license.**

d. Financial Statements

- i. If the Applicant is a Connecticut hospital: Pursuant to Section 19a-644, C.G.S., each hospital licensed by the Department of Public Health is required to file with OHCA copies of the hospital's audited financial statements. If the hospital has filed its most recently completed fiscal year audited financial statements, the hospital may reference that filing for this proposal.

**Saint Francis Hospital and Medical Center files its audited financial statements with OHCA as part of its annual filing.**

- ii. If the Applicant is not a Connecticut hospital (other health care facilities): Audited financial statements for the most recently completed fiscal year. If audited financial statements do not exist, in lieu of audited financial statements, provide other financial documentation (e.g. unaudited balance sheet, statement of operations, tax return, or other set of books.)

**This question is not applicable since Saint Francis Hospital and Medical Center files its audited financial statements with OHCA as part of its annual filing.**

- e. Submit a final version of all capital expenditures/costs as follows:

**Table 3: Proposed Capital Expenditures/Costs**

Medical Equipment Purchase	\$223,266
Imaging Equipment Purchase	\$2,659,616
Non-Medical Equipment Purchase	\$22,118
Land/Building Purchase *	\$0
Construction/Renovation **	\$763,000
Other Non-Construction – A/E Fees	\$150,000
<b>Total Capital Expenditure (TCE)</b>	<b>\$3,818,000</b>
Medical Equipment Lease (Fair Market Value) ***	\$0
Imaging Equipment Lease (Fair Market Value) ***	\$0
Non-Medical Equipment Lease (Fair Market Value) ***	\$0
Fair Market Value of Space ***	\$0
<b>Total Capital Cost (TCC)</b>	<b>\$3,818,000</b>
<b>Total Project Cost (TCE + TCC)</b>	<b>\$3,818,000</b>
Capitalized Financing Costs (Informational Purpose Only)	\$0
Total Capital Expenditure with Cap. Fin. Costs	\$3,818,000

\* If the proposal involves a land/building purchase, attach a real estate property appraisal including the amount; the useful life of the building; and a schedule of depreciation.

**This question is not applicable since this proposal does not include a building purchase.**

\*\* If the proposal involves construction/renovations, attach a description of the proposed building work, including the gross square feet; existing and proposed floor plans; commencement date for the construction/ renovation; completion date of the construction/renovation; and commencement of operations date.

**The MRI renovation is to replace the mobile unit located at an outpatient clinic across the street at 95 Woodland Street. The proposed location will be at 114 Woodland Street as an expansion of the existing MRI suite located at the corner of Woodland and Collins Street on Level 1 of Building 2. The project will consist of approximately 1800 square feet of interior renovation. The renovation will include replacing a portion of the existing floor slab to meet structural and vibration requirements for the new MRI unit; a new MRI imaging room with required shielding, infrastructure improvements required for the use of the MRI unit, a holding bay, control room, toilet room, patient changing, and appropriate MRI/ACR (American College of Radiology) safety zoning required for patient and staff safety. The use of the mobile unit across the street will cease upon the opening of the new MRI unit.**

**Please see Attachment 7 for drawings.**

**The anticipated construction start date is February 2013 with the anticipated construction completion September 2013 and anticipated commencement of operations November 2013.**

\*\*\* If the proposal involves a capital or operating equipment lease and/or purchase, attach a vendor quote or invoice; schedule of depreciation; useful life of the equipment; and anticipated residual value at the end of the lease or loan term.

**Please refer to Attachment 8.**

- f. List all funding or financing sources for the proposal and the dollar amount of each. Provide applicable details such as interest rate; term; monthly payment; pledges and funds received to date; letter of interest or approval from a lending institution.

**Saint Francis Hospital and Medical Center will fund the \$3,818,000 for the project through funded depreciation.**

- g. Demonstrate how this proposal will affect the financial strength of the state's health care system.

**There are several positive benefits to the addition of 3T MRI technology to the diagnostic armamentarium of Saint Francis Hospital and Medical Center.**

**These benefits include:**

**The ability to provide better diagnostic images for a selected number of patients(those with kidney failure, MS and certain heart conditions) that will allow better, safer treatment planning. This improvement in diagnosis should also lead to shorter lengths of stay and improved health outcomes with less possibility of readmission;**

**The increased availability of MRI services on site at Saint Francis Hospital and Medical Center on a 24 hour 7 day a week basis will also allow the hospital to improve in and outpatient through put in general .This throughput improvement should also help shorten length of stay for inpatients and shorten the time to treatment for outpatients as well;**

**As Saint Francis Hospital and Medical Center's MRI scanners are already operating at a high level the availability of a third machine should allow more routine maintenance during regular business hours thus lowering costs to the institution;**

**As a major tertiary teaching institution the availability of the latest technology is essential to training tomorrow's health professionals as to the most appropriate applications of MRI technology and most cost effective approach to the use of this equipment.**

**Though the benefits of adding 3T MRI to Saint Francis Hospital and Medical Center are clear Saint Francis Hospital and Medical Center is not aware of a specific formula that would allow it to quantify the statewide financial benefits of the addition of a 3T MRI to one institution in the financial strength of the state as a whole.**



**6. Patient Population Mix: Current and Projected**

- a. Provide the current and projected patient population mix (based on the number of patients, not based on revenue) with the CON proposal for the proposed program.

**Table 4: Patient Population Mix**

	<b>Current** FY ***</b>	<b>Year 1 FY ***</b>	<b>Year 2 FY ***</b>	<b>Year 3 FY ***</b>
Medicare*				
Medicaid*				
CHAMPUS & TriCare				
<b>Total Government</b>				
Commercial Insurers*				
Uninsured				
Workers Compensation				
<b>Total Non-Government</b>				
<b>Total Payer Mix</b>				

\* Includes managed care activity.

\*\* New programs may leave the "current" column blank.

\*\*\* Fill in years. Ensure the period covered by this table corresponds to the period covered in the projections provided.

**Please refer to Attachment 9.**

- b. Provide the basis for/assumptions used to project the patient population mix.

**The basis for the projected patient population mix is equivalent discharges.**

**7. Financial Attachments I & II**

- a. Provide a summary of revenue, expense, and volume statistics, without the CON project, incremental to the CON project, and with the CON project. **Complete Financial Attachment I.** (Note that the actual results for the fiscal year reported in the first column must agree with the Applicant's audited financial statements.) The projections must include the first three full fiscal years of the project.

**Please refer to Attachment 9.**

- b. Provide a three year projection of incremental revenue, expense, and volume statistics attributable to the proposal by payer. **Complete Financial Attachment II.** The projections must include the first three full fiscal years of the project.

**Please refer to Attachment 9.**

- c. Provide the assumptions utilized in developing **both Financial Attachments I and II** (e.g., full-time equivalents, volume statistics, other expenses, revenue and expense % increases, project commencement of operation date, etc.).

**Please refer to Attachment 9.**

- d. Provide documentation or the basis to support the proposed rates for each of the FYs as reported in Financial Attachment II. Provide a copy of the rate schedule for the proposed service(s).

**Please refer to Attachment 9.**

- e. Provide the minimum number of units required to show an incremental gain from operations for each fiscal year.

**The minimum number of MRI exams required to show an incremental gain from operations by fiscal year are as follows:**

**FY 2014 - 49**

**FY 2015 - 419**

**FY 2016 - 415**

- f. Explain any projected incremental losses from operations contained in the financial projections that result from the implementation and operation of the CON proposal.

**There are no incremental losses from operations contained in the financial projections that result from the implementation of the CON proposal.**

- g. Describe how this proposal is cost effective.

**This Certificate of Need proposal will ensure patients will have the opportunity to receive MR scans on the very latest MRI scanning technology. Any current delays and lost productivity will no longer occur. The enhanced speed and image quality with this new technology will ensure that Saint Francis Hospital and Medical Center continues to be of the highest quality to serve its patients needing scanner services.**

# **ATTACHMENT 1**

**Saint Francis  
Hospital and Medical Center  
Hartford, CT**

has been Accredited by



**The Joint Commission**

Which has surveyed this organization and found it to meet the requirements for the

**Hospital Accreditation Program**

October 29, 2011

Accreditation is customarily valid for up to 36 months.

Isabel V. Hoverman, MD, MACP  
Chair, Board of Commissioners

Organization ID #: 5669  
Print/Reprint Date: 02/07/12

Mark R. Chassin, MD, FACP, MPP, MPH  
President

The Joint Commission is an independent, not-for-profit, national body that oversees the safety and quality of health care and other services provided in accredited organizations. Information about accredited organizations may be provided directly to The Joint Commission at 1-800-994-6610. Information regarding accreditation and the accreditation performance of individual organizations can be obtained through The Joint Commission's web site at [www.jointcommission.org](http://www.jointcommission.org).



This reproduction of the original accreditation certificate has been issued for use in regulatory/payer agency verification of accreditation by The Joint Commission. Please consult Quality Check on The Joint Commission's website to confirm the organization's current accreditation status and for a listing of the organization's locations of care.

# **ATTACHMENT 2**

August 23, 2012

To whom it may concern:

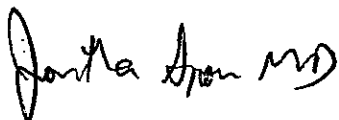
As a medical oncologist, MRI technology has become a routine component of our medical practice, and specifically in the past several years has resulted in increased usage for two particular oncology indications. More women with newly diagnosed breast cancer are undergoing breast MRI to assist with surgical treatment planning because of the ability of MRI to more precisely define the extent of a primary tumor in the breast than other modalities and also to detect second primary lesions that were missed by mammography and ultrasound but which require therapy. These scenarios occur with sufficient frequency that they are more than just anecdotal; we are currently performing a retrospective analysis to determine the fraction of our breast cancer patients who had MRI performed which affected treatment.

Secondly, MRI is critical for imaging of the spinal cord and brain. A large percentage of patients with advanced cancer will at some time require evaluation for possible presence of brain metastases or spinal cord involvement. MRI is indispensable for these indications, and provides much more definitive information than CT. As frequent users of MRI services, as volume has increased, we have noted the delay in time to scheduling outpatient MRI despite the extended hours of operation. For cancer patients where there is a suspicion of a spinal cord or brain problem, speed of diagnosis can be critical in determining clinical outcome. The number of patients seen here in the Cancer Center has continued to grow at least 5% yearly, and so in conjunction with the increasing number of cancer patients in the population, our use of this service will certainly increase.

The increased information available from the 3 Tesla MRI will allow dramatically improved outcomes for our cancer patients having brain tumors resected, so that the surgeon can more precisely plan his surgery with the least possible morbidity and better long-term function for the patient.

In summary, I fully support the acquisition of this new MRI unit, both to accommodate the needs of the growing numbers of cancer patients served by St. Francis, as well as to allow the type of patient-oriented cutting-edge care that has been a hallmark of St. Francis. If I can provide any further information, please contact me at (860) 714-5392.

Sincerely,



Jonathan Sporn, MD  
Chief, Section of Hematology-Oncology, St Francis Hospital and Medical Center  
Professor of Medicine, University of Connecticut School of Medicine



August 24, 2012

RE: MRI CON

To Whom It May Concern:

St. Francis Hospital and Medical Center serves a large population of patients in Central Connecticut with underlying cardiovascular disease. Cardiovascular disease is a systemic process which can result in ischemic heart disease, stroke, or peripheral vascular disease, and which is associated with significant impacts on morbidity, mortality, and quality of life. The realignment of clinical services to coordinate a continuum of care between community based care and care in the acute setting, places a premium on the diagnostic modalities necessary to provide high-quality, safe, cost-effective cardiovascular imaging services for the patient population we serve.

Non-invasive vascular imaging using cross-sectional techniques such as MRI and CT has revolutionized the management of vascular disease, decreasing the time from development of symptoms to definitive diagnosis, and reducing the necessity for more costly and risky invasive diagnostic techniques. Advanced non-invasive vascular imaging also facilitates identification of patients who are best served by less expensive and less risky minimally invasive therapeutic procedures.

Chronic renal insufficiency is commonly associated with and often caused by systemic cardiovascular disease. Up to 40% of patients with underlying cardiovascular disease have or will develop some degree of renal insufficiency, complicating the use of standard diagnostic and therapeutic techniques. The contrast agents often necessary for standard CT and MRI imaging increase risk in many patients with vascular disease and associated renal insufficiency. Iodinated CT contrast agents are nephrotoxic, and gadolinium contrast agents used for MRI have been shown to be associated with nephrogenic systemic fibrosis, a progressive, irreversible renal disease. As a result, it is often difficult to perform non-invasive vascular imaging in the large subset of patients with vascular and renal disease.

Recent advances in MRI technology and the emergence of high-field three-tesla (3T) magnets have now made it possible to non-invasively image the vascular system without administration of contrast agents. The 3T MRI imaging system proposed in this CON is a critical diagnostic tool which will allow diagnosis, treatment selection, and risk stratification in the large population of patients with cardiovascular disease who have associated renal dysfunction.

Sincerely,

Daniel J. Diver, M.D.  
Chief, Section of Cardiology  
Director, Hoffman Heart and Vascular Institute  
St. Francis Hospital and Medical Center

DJD/jbw

# **ATTACHMENT 3**



MRI Exam Count by Town-FY2011		
HARTFORD	CT	2,373
WEST HARTFORD	CT	1,081
EAST HARTFORD	CT	751
BLOOMFIELD	CT	715
WINDSOR	CT	517
MANCHESTER	CT	397
ENFIELD	CT	353
NEWINGTON	CT	279
WETHERSFIELD	CT	253
SOUTH WINDSOR	CT	216
AVON	CT	215
BRISTOL	CT	206
NEW BRITAIN	CT	200
SIMSBURY	CT	186
WINDSOR LOCKS	CT	177
GLASTONBURY	CT	177
ROCKY HILL	CT	176
VERNON	CT	169
SUFFIELD	CT	140
FARMINGTON	CT	131
GRANBY	CT	96
SOUTHINGTON	CT	93
CANTON	CT	92
ELLINGTON	CT	82
TOLLAND	CT	81
EAST GRANBY	CT	75
MIDDLETOWN	CT	73
EAST WINDSOR	CT	72
MERIDEN	CT	68
SOMERS	CT	63
BROAD BROOK	CT	62
BURLINGTON	CT	59
UNIONVILLE	CT	54
CROMWELL	CT	52
BERLIN	CT	51
COVENTRY	CT	49
PLAINVILLE	CT	48
TORRINGTON	CT	47
MARLBOROUGH	CT	47
WEST SIMSBURY	CT	46
COLCHESTER	CT	44
WEST SUFFIELD	CT	41
BOLTON	CT	39
EAST HAMPTON	CT	36
BARKHAMSTED	CT	31
SOUTH GLASTON	CT	28
NORTH GRANBY	CT	28
STAFFORD SPRI	CT	26
EAST HARTLAND	CT	26
WALLINGFORD	CT	25
PORTLAND	CT	25
NEW HARTFORD	CT	24
HEBRON	CT	24
PLANTSVILLE	CT	23

<b>MRI Exam Count by Town-FY2011</b>		
WATERBURY	CT	21
OLD SAYBROOK	CT	21
COLUMBIA	CT	21
WILLINGTON	CT	20
TERRYVILLE	CT	19
LEBANON	CT	19
KENSINGTON	CT	18
WINSTED	CT	17
VERNON ROCKVI	CT	17
STORRS MANSFI	CT	17
SPRINGFIELD	MA	17
SOUTHWICK	MA	17
CHESHIRE	CT	16
WINCHESTER	CT	15
WILLIMANTIC	CT	15
WEATOGUE	CT	15
W HARTFORD	CT	15
NORWICH	CT	15
HARWINTON	CT	14
UNION	CT	13
TARIFFVILLE	CT	13
MOODUS	CT	13
WOLCOTT	CT	12
WEST GRANBY	CT	12
DANIELSON	CT	12
BROOKLYN	NY	12
PLYMOUTH	CT	11
NORFOLK	CT	11
CHESTER	CT	10
ASHFORD	CT	10
N/A		10
MANSFIELD CEN	CT	9
HIGGANUM	CT	9
COLLINSVILLE	CT	8
CANAAN	CT	8
WESTFIELD	MA	7
THOMASTON	CT	7
OLD LYME	CT	7
NIANTIC	CT	7
NEW HAVEN	CT	7
HARTLAND	CT	7
EAST HADDAM	CT	7
ANDOVER	CT	7
WESTPORT	CT	6
STAMFORD	CT	6
ROCKVILLE	CT	6
NORWALK	CT	6
LYME	CT	6
WESTBROOK	CT	5
WATERFORD	CT	5
STOWE	VT	5
STORRS	CT	5
SOUTH GLASTONBU	CT	5
SHARON	CT	5

MRI Exam Count by Town-FY2011			
PUTNAM	CT	5	
PROSPECT	CT	5	
PARK CITY	UT	5	
OAKDALE	CT	5	
NORTH HAVEN	CT	5	
MIDDLEFIELD	CT	5	
MIDDLE HADDAM	CT	5	
LONGMEADOW	MA	5	
LITCHFIELD	CT	5	
DURHAM	CT	5	
CHICOPEE	MA	5	
CHAPLIN	CT	5	
CANTON CENTER	CT	5	
BETHLEHEM	CT	5	
BANGOR	ME	5	
WEST HAVEN	CT	4	
WAKEFIELD	RI	4	
STAFFORD SPIN	CT	4	
SALEM	CT	4	
POQUONOCK	CT	4	
PLAINFIELD	CT	4	
NEWTOWN	CT	4	
MOOSUP	CT	4	
MILFORD	CT	4	
MANSFIELD	CT	4	
HAMDEN	CT	4	
GUILFORD	CT	4	
GROTON	CT	4	
GOSHEN	CT	4	
EAST LYME	CT	4	
EAST BERLIN	CT	4	
COLEBROOK	CT	4	
CANTERBURY	CT	4	
BRONX	NY	4	
BRIDGEPORT	CT	4	
BISHOPS CORNE	CT	4	
AMSTON	CT	4	
WOODBURY	CT	3	
WINDHAM	CT	3	
WILBRAHAM	MA	3	
WATERTOWN	CT	3	
TRUMBULL	CT	3	
THOMPSON	CT	3	
STAFFORD SPRINGS	CT	3	
RIVERTON	CT	3	
RIVER VIEW	FL	3	
RIDGEFIELD	CT	3	
PEQUABUCK	CT	3	
OAKVILLE	CT	3	
NORTH WINDHAM	CT	3	
NEW YORK	NY	3	
MYSTIC	CT	3	
MERRICK	NY	3	
MADISON	CT	3	

MRI Exam Count by Town-FY2011			
LEDYARD		CT	3
LARGO		FL	3
IVORYTON		CT	3
GRT BARRINGTN		MA	3
GRANVILLE		MA	3
GALES FERRY		CT	3
FEEDING HILLS		MA	3
FALLS VILLAGE		CT	3
EASTFORD		CT	3
DAYVILLE		CT	3
CHATHAM		MA	3
CANADA		CT	3
BOZRAH		CT	3
0612FORD		CT	3
WORCESTER		MA	2
WOODSTOCK		CT	2
WINSTEAD		CT	2
WHITE HAVEN		PA	2
WEST WILLINGN		CT	2
WEST HARFTORD		CT	2
WALES		MA	2
VIERA		FL	2
VERNON ROCKVL		CT	2
TEANECK		NJ	2
SURPRISE		AZ	2
SUNNYSIDE		NY	2
STRATFORD		CT	2
STAFFORDVILLE		CT	2
STAFFORD SPRS		CT	2
STAFFORD SPR		CT	2
STAFFOR SPRIN		CT	2
ST CATHERINE		XX	2
SAN MATEO		CA	2
S WINDSOR		CT	2
S GLASTONBURY		CT	2
ROXBURY		CT	2
ROCKFALL		CT	2
PRESTON		CT	2
POMFRET CENTE		CT	2
OAKLAND		ME	2
NOTTINGHAM		NH	2
NORTH GROSVENORDA		CT	2
NORTH ANDOVER		MA	2
NEW LONDON		CT	2
NEW BRITIAN		CT	2
N.WINDHAM		CT	2
N LAUDERDALE		FL	2
N GRANBY		CT	2
MONTVILLE		CT	2
MERRIMACK		NH	2
MEMPHIS		TN	2
MCCLELLENVILL		SC	2
LUDLOW		MA	2
LISBON		CT	2

<b>MRI Exam Count by Town-FY2011</b>		
LEWISTON	ME	2
KILLINGWORTH	CT	2
JUPITER	FL	2
JEWETT CITY	CT	2
HOMESTEAD	FL	2
HARRISONBURG	VA	2
GT BARRINGTON	MA	2
GREEN COVE SPRINGS	FL	2
GOLETA	CA	2
FREEDOM	NH	2
FENWICK ISLAN	DE	2
FAR ROCKAWAY	NY	2
ELLENTON	FL	2
EAST NORTHPOR	NY	2
EAST LONGMEAD	MA	2
EAST HAVEN	CT	2
DERBY	CT	2
CLINTON	CT	2
CHARLTON	MA	2
BROADBROOK	CT	2
BETHELHEM	CT	2
ARLINGTON	VA	2
AGAWAM	MA	2
ZEPHYRHILLS	FL	1
YUMA	AZ	1
YANTIC	CT	1
WOODSTOCK VAL	CT	1
WOODMERE	NY	1
WINSBORO	SC	1
WILINGTON	CT	1
WILDWOOD	FL	1
WHIPPANY	NJ	1
WESTERLY	RI	1
WEST SPRINGFI	MA	1
WEST NEW YORK	NJ	1
WEST HARFORD	CT	1
WEST FIELD	MA	1
WEST CHESTER	PA	1
WEATOQUE	CT	1
WAUREGAN	CT	1
WASHINGTON DE	CT	1
WASHINGTON	DC	1
WARE	MA	1
WALTHAM	MA	1
W SPRINGFIELD	MA	1
W GREENWICH	RI	1
VERNON ROCKVILLE	CT	1
UNCASVILLE	CT	1
TOPSFIELD	MA	1
TITUSVILLE	FL	1
THE VILLAGES	FL	1
TAUNTON	MA	1
TAFTVILLE	CT	1
SWAMPSCOTT	MA	1

MRI Exam Count by Town-FY2011		
STURBRIDGE	MA	1
STORRS MANSFIEL	CT	1
STONINGTON	CT	1
STEVENSVILLE	MT	1
STAFFORD SPRG	CT	1
STAFFORD SP	CT	1
STAFFORD	CT	1
SPRINGFIELD	MA	1
SPRAGUE	CT	1
SOUTHBURY	CT	1
SOUTHBRIDGE	MA	1
SOUTH KENT	CT	1
SOMERVILLE	MA	1
SO WINDSOR	CT	1
SHERMAN	CT	1
SHELTON	CT	1
SCOTTSDALE	AZ	1
SCOTLAND	CT	1
SAYRE	PA	1
SALISBURY	CT	1
RUMFORD	RI	1
ROCKYHILL	CT	1
RIDGEWOOD	NJ	1
RICHMOND	VA	1
RICHLAND	PA	1
RAYNHAM	MA	1
PUNTA GORDA	FL	1
PONTE VEDRA	FL	1
POMFRET CENTER	CT	1
PLEASANT VALL	CT	1
PINE MEADOW	CT	1
PASCOAG	RI	1
PARK RIDGE	NJ	1
OXFORD	CT	1
ONECO	CT	1
NORTHVILLE	MI	1
NORTHFORD	CT	1
NORTHFIELD	CT	1
NORTHAMPTON	MA	1
NORTH PALM BE	FL	1
NORTH FRANKLI	CT	1
NORTH EASTHAM	MA	1
NEWPORT	NY	1
NAUGATUCK	CT	1
NASHUA	NH	1
NAPLES	FL	1
N WINDHAM	CT	1
MUNSON	MA	1
MILLERTON	NY	1
MILLBRAE	CA	1
MIDDLEBURY	CT	1
MASHPEE	MA	1
MARION	CT	1
MAHOPAC	NY	1

<b>MRI Exam Count by Town-FY2011</b>		
MACUNGIE	PA	1
LOWELL	MA	1
LINCOLN	RI	1
LEWISVILLE	TX	1
LAWRENCEVILLE	NJ	1
LAUDERHILL	FL	1
KISSIMMEE	FL	1
KIHEI	HI	1
JAMAICA	NY	1
HURST	TX	1
HOPKINTON	MA	1
HOLYOKE	MA	1
HOLMES	NY	1
HICKSVILLE	NY	1
HERNANDO	FL	1
HANOVER	CT	1
HAMPTON	NH	1
HAMPDEN	ME	1
HADDAM	CT	1
GRISWOLD	CT	1
GRIMESLAND	NC	1
FORRESTVILLE	CT	1
FENTON	MI	1
ESSEX	CT	1
ELMWOOD	CT	1
EASTHARTFORD	CT	1
EAST WINSOR	CT	1
EAST SPRINGFI	MA	1
E. HARTFORD	CT	1
E GRANBY	CT	1
DULUTH	GA	1
DOUGLAS	GA	1
DORCHESTER	MA	1
DELRAY BEACH	FL	1
DANBURY	CT	1
DALLAS	TX	1
COPPELL	TX	1
COBURG	OR	1
CHARLOTTE	NC	1
CHARLESTOWN	RI	1
CASTLETON ON HUDSON	NY	1
BROWNSVILLE	VT	1
BROOKFIELD	CT	1
BRIMFIELD	MA	1
BRANFORD	CT	1
BONDVILLE	VT	1
BEVERLY HILLS	CA	1
BARKHAMSTEAD	CT	1
BAREFOOT BAY	FL	1
AUBURN	NY	1
ATMORE	AL	1
AMENIA	NY	1
6106 HARTFORD	CT	1
<b>Total</b>		11,580

<b>MRI Exam Count by Town-FY2011</b>			
<b>Source: SF Radiology Dept.</b>			
<b>file:h: mr exams by town 8 10 12</b>			



# ATTACHMENT 4

# ARTICLE 1

# Gadolinium-based MR Contrast Agents and Nephrogenic Systemic Fibrosis<sup>1</sup>

Phillip H. Kuo, MD, PhD  
Emanuel Kanal, MD  
Ali K. Abu-Alfa, MD  
Shawn E. Cowper, MD

**N**ephrogenic systemic fibrosis (NSF), described in 2000 (1), is an emerging systemic disorder characterized by widespread tissue fibrosis. Originally known as nephrogenic fibrosing dermopathy because of its dominant cutaneous findings, the nomenclature was revised in recent years to reflect an increased understanding of its systemic effects (1,2). While the precise cause of NSF remains a mystery, it is known to occur only in patients with renal disease—generally in those requiring dialysis. NSF may develop rapidly and can sometimes result in patients becoming confined to a wheelchair within a few weeks. More commonly, the skin thickening is insidious and can be confused clinically with peripheral edema. Pathophysiologically, NSF results in increased tissue deposition of collagen, commonly resulting in thickening and hardening of the skin of the extremities and often culminating in immobility and contractures of the joints. In some patients, there is clinical involvement of other tissues (lung, skeletal muscle, heart, diaphragm, esophagus, etc), although the patient may not be clinically symptomatic (3). While NSF sometimes stabilizes, it rarely spontaneously remits. No consistently effective therapy exists, although rapid correction in renal function (by medical or surgical means) generally results in a cessation of progression and often in a reversal of symptoms (4).

With renal dysfunction at the core of this condition, the possibility that renally excreted endogenous or exogenous substances may be triggering NSF has been of great interest. Since NSF appears not to have existed prior to 1997, suspicion that a recently introduced agent might be the culprit has been rampant, but investigation by several authors and by the Centers for Disease Control and Prevention has so far failed to identify a single causative medication (3). Of great interest, the author of a recent article (5) has suggested that

administration of intravenous contrast material for magnetic resonance (MR) imaging (ie, gadolinium chelates) has been associated with a small cluster of patients with NSF in Austria (five of nine imaged patients). A Web-based medical advisory originating in Denmark claims that, since January 2002, approximately 400 patients with severely impaired renal function were administered gadolinium-based MR contrast material; 20 patients (5%) subsequently were diagnosed with NSF (6). Other unpublished U.S. experience (S.E.C., October 2006) suggests an approximate incidence of 3% for the development of NSF in the setting of severe renal failure and administration of intravenous contrast material for MR imaging.

An international NSF registry at Yale University (New Haven, Conn) maintains records on over 215 patients with NSF worldwide. A survey now underway has revealed that more than 95% of all NSF patients surveyed (currently approximately 100) have been exposed to a gadolinium chelate within 2–3 months prior to disease onset. The majority of the patients were being maintained with dialysis. However, a number of patients with impaired renal function have been reported to the registry, the severity of whose disease has been difficult to determine retrospectively.

To the best of our knowledge, the overwhelming majority of known NSF cases at this point (~90%) represent patients who had previously received gadodiamide (Omniscan; GE Healthcare, Princeton, NJ) (7). Nevertheless, there have been reports of NSF cases associated with other agents. As of October 26, 2006, there have been a total of 57 cases of NSF associated with prior gadolinium-based MR contrast agent administration reported to the U.S. Food and Drug Administration (FDA)

Published online before print  
10.1148/radiol.2423061640

Radiology 2007; 242:647–649

<sup>1</sup>From the Department of Diagnostic Radiology, (P.H.K.), Department of Internal Medicine, Section of Nephrology (A.K.A.), and Department of Dermatology and Pathology (S.E.C.), Yale School of Medicine, 333 Cedar St, PO Box 208042, New Haven, CT 06520-8042; and Department of Radiology, University of Pittsburgh Medical Center, Pittsburgh, Pa (E.K.). Received September 21, 2006; revision requested November 13; revision received December 11; final version accepted December 15. Address correspondence to P.H.K. (e-mail: [phillip.kuo@yale.edu](mailto:phillip.kuo@yale.edu)).

Authors stated no financial relationship to disclose.

© RSNA, 2007

MedWatch Web site (<http://www.fda.gov/medwatch>). Of the 57 cases of NSF reported to the FDA to date, six are definitely associated with gadopentetate dimeglumine (Magnevist; Berlex Imaging, Montville, NJ); two, with gadoversetamide (OptiMARK; Mallinckrodt, St Louis, Mo); and three, with gadodiamide plus gadoversetamide associated; for three other cases, the associated specific gadolinium-based MR contrast agent was not definitively identified. For the remainder, gadodiamide was the associated agent (George Mills, MD [FDA], personal communication, October 26, 2006). The FDA has sufficient confidence in these MedWatch reports to induce an update to their Public Health Advisory in the near future (George Mills, MD, personal communication, October 26, 2006). While the FDA fully recognizes that the reports available at this time focus on gadodiamide, the FDA nevertheless continues to be concerned that this may be a class issue rather than a specific agent issue (George Mills, MD, personal communication, October 26, 2006).

Both standard- and high-dose administrations of these agents have been recorded, and multiple administrations have been reported. In some cases, patients were exposed to additional contrast enhanced MR imaging procedures in an effort to investigate the patient's sudden and inexplicable lower extremity skin hardening (S.E.C., unpublished data, October 2006).

Although a causative relationship between gadolinium chelates and NSF has not been firmly established, the data are certainly suspicious that such a relationship may exist. This suspicion has been compounded by the recent detection of gadolinium in tissue biopsy specimens from some patients with known NSF (8,9), including some in whom the biopsy was performed as long as 11 months after the original intravenous administration of the gadolinium-based MR contrast agent (8).

If such a causative relationship exists, some questions that immediately emerge include the following: (a) How do renal failure and MR contrast agents trigger NSF? Is the effect related to the

extended half-life of these agents far beyond the typical expected 70–90 minutes exhibited by those with normal renal function (10)? (b) Are other factors necessary to place a patient at risk? (c) Does the proinflammatory milieu in renal failure contribute to the fibrotic response (11)? (d) Is metabolic acidosis necessary for the disease to occur (5)? (e) Why did the initial reports appear in 1997, when gadolinium-containing contrast agents had already been used in patients with renal failure for several years? (f) Is the gadolinium, gadolinium chelate complex, or the chelator the culprit?

While at this time there are more questions than answers, the recognition of an epidemiologic association between the administration of gadolinium-based MR contrast agents and the development of NSF prompts caution in the use of these agents in the setting of renal disease. The FDA currently provides recommendations posted on their Web site and quoted below (12):

Gadolinium-containing contrast agents, especially at high doses, should be used only if clearly necessary in patients with advanced kidney failure (those currently requiring dialysis or with a Glomerular Filtration Rate (GFR) = 15 cc/min or less).

It may be prudent to institute prompt dialysis in patients with advanced kidney dysfunction who receive a gadolinium contrast MRA. Although there are no data to determine the utility of dialysis to prevent or treat NSF/NFD [nephrogenic fibrosing dermopathy] in patients with decreased kidney function, average excretory rates of gadolinium are 78%, 96%, and 99% in the first to third hemodialysis sessions, respectively (Okada et al, *Acta Radiologica*, vol 42 p. 339, May 2001).

Although there is evidence associating the development of NSF in patients with renal failure with only some, but not all, of the FDA-approved gadolinium-based MR contrast agents to date, prudence dictates that we apply our concern to all gadolinium-based MR contrast agents in this regard until more definitive infor-

mation is forthcoming. For the use of all gadolinium-based MR contrast agents in patients with stage 4 or 5 chronic kidney disease (ie, patients maintained with either hemodialysis or peritoneal dialysis) or patients with a GFR of less than 30 mL/min/1.73 m<sup>2</sup>, we follow the approach listed below. We share this solely as our approach rather than as an official recommendation of any kind.

1. In consultation with the ordering physician, we consider alternative imaging or nonimaging modalities that may provide the requested clinical diagnostic data at a lower potential risk. The benefits and risks of an MR study with the addition of contrast material should be evaluated on an individual basis for each patient.

2. We administer gadolinium-based MR contrast agents to a patient with stage 4 or 5 chronic kidney disease or with acute kidney injury and markedly impaired GFR or who undergoes dialysis, if prescribed by a state-licensed physician. We inform patients of the benefits, risks, and alternatives, based on currently available information, and prospectively record in writing the disclosure and the informed consent.

3. If administration of a gadolinium-based MR contrast agent is deemed necessary, we consider using the lowest dose needed to reliably provide the diagnostic information being clinically sought. In the absence of a specific reason to the contrary, consider a default dose of no more than half the standard dose for these patients.

4. We perform any additional non-enhanced sequences that may be helpful, and we monitor the study to evaluate for the continuing necessity of contrast agent.

5. For patients maintained with hemodialysis, we ensure hemodialysis treatment as soon as possible, ideally within 3 hours after the administration of the gadolinium-containing contrast agent. A second dialysis session within 24 hours can also be performed if it is clinically safe to do so.

6. For patients undergoing peritoneal dialysis, we ensure that patients have no periods with a dry abdomen (ie, peritoneal cavity contains no dialysate),

and we perform more frequent manual exchanges or additional automated peritoneal dialysis cycles for at least 48 hours after administration. However, there are data to suggest that hemodialysis clears the gadolinium-based MR contrast agent more effectively than does peritoneal dialysis (10). Therefore, we consider hemodialysis for patients undergoing peritoneal dialysis who may still have a functional vascular access for hemodialysis, for patients thought to be at higher risk because of the dose used or prior recent exposure, and for those who have other risk factors, according to the judgment of the nephrologist.

7. Insufficient data exist to estimate the risk of developing NSF in relationship to the GFR in patients with chronic kidney disease who are not maintained with dialysis. The primary concern would be for patients with stage 4 chronic kidney disease (defined as GFR of 15–30 mL/min/1.73 m<sup>2</sup>). On the other hand, initiating hemodialysis in patients without vascular access for the sole purpose of removing gadolinium-based MR contrast material entails some risks and discomfort, including the potential need for permanent hemodialysis sooner than anticipated. As such, initiating hemodialysis for the sole purpose of removing a gadolinium chelate needs to be evaluated on an individual basis, and a risk-benefit assessment must be made regarding the need for gadolinium chelate administration versus the risks of developing NSF and/or initiating dialysis.

8. We refrain from administering gadolinium-based MR contrast agents to patients in whom there may be relatively protected spaces that the gadolinium chelates might enter but from which they may not readily be cleared. An example of such a space is the amni-

otic fluid, where at least some of these contrast agents can accumulate shortly after intravenous administration, as observed by one of the authors (E.K.).

9. If there is a diagnosis or clinical suspicion of NSF in the patient, we discourage exposure to any gadolinium chelates.

10. In light of the observation that the overwhelming majority of cases of NSF are associated with prior gadodiamide administration specifically, we do not administer this agent to patients with any renal disease.

At this time, the relationship between NSF and gadolinium chelates remains unclear. Further studies are now underway at the Centers for Disease Control Prevention, the FDA, and in the medical regulatory agencies of the European Union. If we encounter NSF in a patient, we proceed as follows:

1. We ascertain whether there is a history of administration of a gadolinium-based MR contrast agent in the weeks or months preceding the initial diagnosis. We record the date of administration and the dose and brand of the contrast agent administered, as well as the date of onset or diagnosis of NSF (as precisely as possible).

2. We report the event to the FDA (or appropriate non-U.S. regulatory agency) online through the MedWatch reporting program (<http://www.fda.gov/medwatch/>) or by phone (1-800-FDA-1088).

3. We report the case to the NSF registry at Yale University (<http://www.icnfd.org>).

#### References

- Cowper SE, Robin HS, Steinberg SM, Su LD, Gupta S, LeBoit PE. Scleromyxoedema-like cutaneous diseases in renal-dialysis patients. *Lancet* 2000;356:1000–1001.
- Cowper SE, Su LD, Bhawan J, Robin HS, LeBoit PE. Nephrogenic fibrosing dermatopathy. *Am J Dermatopathol* 2001;23:383–393.
- Cowper SE, Boyer PJ. Nephrogenic systemic fibrosis: an update. *Curr Rheumatol Rep* 2006;8:151–157.
- Cowper SE. Nephrogenic systemic fibrosis: the nosological and conceptual evolution of nephrogenic fibrosing dermatopathy. *Am J Kidney Dis* 2005;46:763–765.
- Grobner T. Gadolinium: a specific trigger for the development of nephrogenic fibrosing dermatopathy and nephrogenic systemic fibrosis? *Nephrol Dial Transplant* 2006;21:1104–1108.
- Stenver DI. Investigation of the safety of MRI contrast medium Omniscan. Danish Medicines Agency. <http://www.dkma.dk/1024/vistUKLSArtikel.asp?artikelID=8931>. Published May 29, 2006. Accessed December 7, 2006.
- Thomsen HS. Nephrogenic systemic fibrosis: a serious late adverse reaction to gadodiamide. *Eur Radiol* 2006;16:2619–2621.
- High WA, Ayers RA, Chandler J, Zito G, Cowper SE. Gadolinium is detectable within the tissues of patients with nephrogenic systemic fibrosis. *J Am Acad Dermatol* [in press].
- Boyd AS, Zic JA, Abraham JL. Gadolinium deposition in nephrogenic fibrosing dermatopathy. *J Am Acad Dermatol* [in press].
- Joffe P, Thomsen HS, Meusel M. Pharmacokinetics of gadodiamide injection in patients with severe renal insufficiency and patients undergoing hemodialysis or continuous ambulatory peritoneal dialysis. *Acad Radiol* 1998;5:491–502.
- Stenvinkel P, Alvestrand A. Inflammation in end-stage renal disease: sources, consequences, and therapy. *Semin Dial* 2002;15:329–337.
- U.S. Food and Drug Administration. Public health advisory: gadolinium-containing contrast agents for magnetic resonance imaging (MRI)—Omniscan, OptiMARK, Magnevist, ProHance, and MultiHance. Department of Health and Human Services. [http://www.fda.gov/cder/drug/advisory/gadolinium\\_agents.htm](http://www.fda.gov/cder/drug/advisory/gadolinium_agents.htm). Published June 8, 2006. Accessed December 7, 2006.

## **ARTICLE 2**

## Review

## Non-Contrast Enhanced MR Angiography: Established Techniques

### CME

Mitsue Miyazaki, PhD<sup>1,2\*</sup> and Masaaki Akahane, MD<sup>3</sup>

This article is accredited as a journal-based CME activity. If you wish to receive credit for this activity, please refer to the website: [www.wileyhealthlearning.com](http://www.wileyhealthlearning.com)

#### ACCREDITATION AND DESIGNATION STATEMENT

Blackwell Futura Media Services designates this journal-based CME activity for a maximum of 1 *AMA PRA Category 1 Credit*<sup>™</sup>. Physicians should only claim credit commensurate with the extent of their participation in the activity.

Blackwell Futura Media Services is accredited by the Accreditation Council for Continuing Medical Education to provide continuing medical education for physicians.

#### EDUCATIONAL OBJECTIVES

Upon completion of this educational activity, participants will be better able to discuss recent advancements in established NC-MRA techniques and clinical applications.

#### ACTIVITY DISCLOSURES

No commercial support has been accepted related to the development or publication of this activity.

##### Faculty Disclosures:

The following contributors have no conflicts of interest to disclose:

Editor-in-Chief: C. Leon Partain, MD, PhD

CME Editor: Scott B. Reeder, MD, PhD

CME Committee: Scott Nagle, MD, PhD, Pratik Mukherjee, MD, PhD, Shreyas Vasawala, MD, PhD, Bonnie Joe, MD, PhD, Tim Leiner, MD, PhD, Sabine Weckbach, MD, Frank Korosec, PhD

Authors: Mitsue Miyazaki, PhD, Masaaki Akahane, MD

This manuscript underwent peer review in line with the standards of editorial integrity and publication ethics maintained by *Journal of Magnetic Resonance Imaging*. The

peer reviewers have no relevant financial relationships. The peer review process for *Journal of Magnetic Resonance Imaging* is double-blinded. As such, the identities of the reviewers are not disclosed in line with the standard accepted practices of medical journal peer review.

Conflicts of interest have been identified and resolved in accordance with Blackwell Futura Media Services's Policy on Activity Disclosure and Conflict of Interest. No relevant financial relationships exist for any individual in control of the content and therefore there were no conflicts to resolve.

#### INSTRUCTIONS ON RECEIVING CREDIT

For information on applicability and acceptance of CME credit for this activity, please consult your professional licensing board.

This activity is designed to be completed within an hour; physicians should claim only those credits that reflect the time actually spent in the activity. To successfully earn credit, participants must complete the activity during the valid credit period.

Follow these steps to earn credit:

- Log on to [www.wileyhealthlearning.com](http://www.wileyhealthlearning.com)
- Read the target audience, educational objectives, and activity disclosures.
- Read the article in print or online format.
- Reflect on the article.
- Access the CME Exam, and choose the best answer to each question.
- Complete the required evaluation component of the activity.

This activity will be available for CME credit for twelve months following its publication date. At that time, it will be reviewed and potentially updated and extended for an additional period.

<sup>1</sup>Toshiba Medical Research Institute USA, Vernon Hills, Illinois, USA.

<sup>2</sup>Toshiba Medical Systems Corp., Tochigi, Japan.

<sup>3</sup>Department of Radiology, University of Tokyo Hospital, Tokyo, Japan.

\*Address reprint requests to: M.M., Toshiba Medical Research Institute, USA, 706 N. Deerpath Drive, Vernon Hills, IL 60061. E-mail: [mmiyazaki@tmriusa.com](mailto:mmiyazaki@tmriusa.com)

Received April 23, 2011; Accepted July 29, 2011.

DOI 10.1002/jmri.22789

View this article online at [wileyonlinelibrary.com](http://wileyonlinelibrary.com).

Until recently, time-of-flight (TOF) and phase contrast (PC) were the only non-contrast MR angiography (NC-MRA) techniques practically used in clinical. In the decade, NC-MRA have been gained a revival of an interest among the MR researchers and scientists, in part because of safety concerns related to the possible link between gadolinium-based contrast agents and nephrogenic systemic fibrosis (NSF). This article introduces other established NC-MRA techniques, such as ECG-gated partial Fourier fast spin echo (FSE) and balanced steady-state free precession (bSSFP), both with and without arterial spin labeling. Then, the article focuses on two main applications: peripheral run-off and renal MRA. Recently, both applications have achieved remarkable advancements and have become a viable clinical option as an alternative to contrast-enhanced (CE) MRA. In addition, developments on the horizon including whole body MRA applications and further advancement at 3 Tesla are discussed.

**Key Words:** non-contrast MRA; non-contrast MR venography; spin labeling; time-spatial labeling inversion pulse (time-SLIP); fresh blood imaging (FBI)

**J. Magn. Reson. Imaging 2012;35:1-19.**

© 2011 Wiley Periodicals, Inc.

CONTRAST-ENHANCED MR angiography (CE-MRA) with gadolinium-based contrast materials was widely accepted for abdominal MRA after its introduction in 1994 by Prince (1). Since its inception, the CE-MRA technique has been meticulously refined to adjust to each part of the body. On the other hand, since the early days of clinical magnetic resonance imaging and long before the development of CE-MRA techniques, traditional non-contrast MR angiography (NC-MRA) techniques, such as time of flight (TOF) and phase contrast (PC), have been developed and widely applied in various applications. Three-dimensional (3D) TOF is currently used in intracranial MRA, two-dimensional (2D) MRA is used in carotid and distal peripheral MRA (2,3), and PC MRA is used mostly for quantitative flow measurements in various applications (4,5). Long acquisition time and almost unavoidable motion artifacts hinder the use of these techniques in the abdomen and peripheral run-off MRA.

The renaissance of interest in NC-MRA for other parts of body has been contributed to factors including improved MR hardware, sequence improvements, and parallel imaging (6,7). A concern about a possible link between gadolinium-based contrast agents and nephrogenic systemic fibrosis (NSF) (8), especially in patients with renal insufficiency, has stimulated further development of alternative techniques that do not require exogenous contrast material. The original NC-MRA research was motivated in Japan, due to the relatively high cost and dose limitations of gadolinium based contrast material (9) in addition to intrinsic desires of performing totally noninvasive and contrast free examinations from healthcare professionals and patients.

In late 1990 to early 2000, the 3D fast spin echo (FSE) based sequences using electrocardiographic (ECG) gating were developed to provide 3D NC-MRA images of bright blood vessels by triggering every slice encoding at the same cardiac phase (10,11). This technique was

later extended by using different cardiac trigger delay times to separate arteries from veins. This further development enabled the FSE-based NC-MRA technique to be applied for peripheral run-off MRA (12,13).

Balanced steady-state free-precession (bSSFP) sequences, initially described as early as 1958 (14), have become commercially available in early 2000 and used in a wide range of applications (15). The high signal-to-noise ratio (SNR) and intrinsic T2/T1 contrast provide high blood signal efficiency, making the bSSFP sequence an appropriate choice for angiography applications.

To depict particular vessels, the methodology of arterial spin labeling (ASL) was originally developed using spin echo and gradient echo type sequences for carotid angiography (16,17). Later, the ASL-based approach was adapted to MR angiography in various parts of the body using faster acquisition sequences like half-Fourier FSE and bSSFP (18-20). However, application of these techniques requires other considerations, such as arterial and venous flow patterns, T1 and T2 of blood compared with the background tissues, and relative susceptibility of the different parts of body (i.e. air/tissue interface in lungs). The details of these considerations are described elsewhere (21).

The purpose of this article is to provide the latest information of the established NC-MRA techniques. The focus is on the basics of NC-MRA sequences, various spin labeling techniques, clinical applications in specific arteries and veins, and new developments, including whole-body MRA and NC-MRA at 3 Tesla (T).

## FRESH BLOOD IMAGING (FBI): ECG-GATED 3D HALF-FOURIER FSE

Early examples of NC-MRA were reported in the 1980s with a spin echo technique using ECG-gating to demonstrate pulsatile flow and to produce a 2D projection image in lower extremities (22,23). Improvements in both hardware and software have made it possible to extend this technique to 3D, enabling acquisition to observe the vessels in detail within a reasonable scan time. Furthermore, shortening of the echo-train-spacing (ETS) in 3D half-Fourier FSE and parallel imaging have made this technique clinically feasible to provide bright blood on commercially available MRI scanners without administration of contrast material.

### Principles of the Technique

The NC-MRA technique, fresh blood imaging (FBI) using an ECG-gated 3D half-Fourier FSE sequence relies on a signal difference between systolic and diastolic triggered acquisitions (10,12). The technique relies on the black arterial signal, or flow void, due to the spin-dephasing effects of fast arterial flow during systole. During diastole, arteries have slow flow and are thus depicted with high signal. In contrast, venous blood is bright throughout the cardiac cycle, due to its moderately constant slow flow. Because this



technique relies on the blood-flow velocity, ECG gating or peripheral-pulse gating (PPG) is required for selectively acquiring data during the desired cardiac phases. To obtain each slice at the same cardiac phase, slice encoding is triggered with the same cardiac delay time in the 3D half-Fourier FSE sequence. The contrast of the image in half-Fourier FSE is determined by the effective echo time ( $TE_{eff}$ ); moderate to heavily T2-weighted images are obtained by selecting short to long  $TE_{eff}$ s.

The following are essential concepts to achieve bright blood NC-MRA images with this technique. In FSE-based acquisitions, blurring in the phase encode (PE) direction caused by T2 decay of the MR signal is unavoidable. This T2-blurring effect of FSE-based sequences is due to the sampling multiple echoes per shot across extended echo times, unlike spin-echo sequences which acquire only one echo per shot (24). The T2 blurring effects of artery, vein, and muscle have been analyzed using a point spread function (PSF) approach (11). The shorter the T2 value, the greater the spread of one pixel's signal across neighboring pixels, as indicated by increasing a full-width at half-maximum (FWHM) of the PSF. The FWHM can be improved by shortening echo train spacing (ETS), increasing the number of shots (reducing the echo train length), and the application of parallel imaging. Parallel imaging techniques permit shorter total data sampling periods resulting in reduced T2 blurring. However, in FSE-based sequences, parallel imaging does not affect the scan time because the repetition time (TR) is fixed as it is related to cardiac cycles. Another consideration is that flowing spins, such as blood, lose signal due to flow dephasing effects. Short echo train spacing produces less spin dephasing thereby better capturing the flowing blood signals. Another solution to reduce flow dephasing is to apply rectilinear or centric  $k$ -space ordering, which intrinsically results in less flow dephasing near the center of  $k$ -space along the PE direction (25). To summarize, to effectively obtain bright blood by means of the ECG-gated half-Fourier FSE technique, a combination of the following techniques is used: short echo train spacing, reduction of acquisition window using parallel imaging, and rectilinear  $k$ -space ordering. Lastly, depending on the application, additional prepulses, like a short tau inversion recovery (STIR), can be used in conjunction with 3D half-Fourier FSE to achieve fat suppression. Furthermore, FSE-based sequences allow the selecting of the  $TE_{eff}$  to control the contrast in T2-weighted images.

#### Applications

**Pulmonary MRA.** Using 3D half-Fourier FSE acquisitions, appropriate ECG delay(s) for diastolic and/or systolic-triggering need to be selected for the various applications. Figure 1a shows the relationship between the flow velocities of the ascending aorta, the descending aorta, and the superior vena cava (SVC) at the various ECG-triggering phases or delays measured using the 2D PC technique. Figure 1b shows the corresponding signal intensities during

each ECG delay obtained using half-Fourier FSE. A preparatory, "ECG-prep" sequence that produces 2D single-shot images at incremental triggering times of arbitrary steps can be used to find the specific trigger delay (TD) for systole, when arterial blood is black (flow voids), and for diastole when arteries are bright, as shown in Figure 1c (10). Each single-shot 2D acquisition is acquired in 2 or 3 R-R intervals at incremental delays to produce separate images for each phase. Depending on the preference, the 2D PC technique is often used to determine the systolic and diastolic delays as an alternative to the ECG-prep scan.

Before moving to the 3D acquisition methods, it is noteworthy to mention the image result of the ECG-triggered images; subtraction of the systolic- from diastolic-triggered images provides a NC-MRA projection image. Lung perfusion projection images obtained using ECG-prep are presented on a healthy volunteer in Figure 2a,b and a patient with a pulmonary thromboembolism in Figure 2c,d. The signal difference of pulmonary vessels between diastole and systole provides NC pulmonary perfusion MRA (Fig. 2a-c). The hypo-intensity defect is due to the pulmonary thromboembolism in Fig. 2c), which matches with digital subtraction angiography (DSA) image (Fig. 2d). This signal difference of systole and diastole was intensively investigated in both human and canine imaging (26,27).

#### Thoracic and Abdominal MRA

In thoracic and abdominal MRA, the vessels are large enough, and it is often not required to separate arteries from veins, as the diastolic triggering depicts bright blood in both artery and vein. In addition, an advantage in imaging the pulmonary and aortic arch is that background and lung signals in the images are negligible (9,10). In those regions with relatively fast flow, typically the PE direction should be selected to be parallel to the direction of flow (cranio-caudal) to reduce the effect of signal blurring due to PSF. This orientation requires the application of presaturation bands superior and inferior to avoid wrap-around artifacts. Figure 3 compares images obtained in the thoracic arch acquired by CE-MRA and NC FBI. The FBI source images clearly demonstrate the intimal flap and tear as well as pleural and pericardial effusions with the synchronized ECG triggering. The corresponding CE-MRA source images acquired after the FBI scans reveal the patent lumen and the intimal flap and tear by the difference in the contrast arrival timing. Clinical evaluation of the thoracic and abdominal regions with NC FBI images was performed in a prospective study of 75 patients with arterial diseases referred for NC FBI (34 dissection, 27 aneurysm, 4 arterial occlusion, 10 surgical bypass). Image quality of the NC FBI images graded excellent in 45, satisfactory in 25, and poor in 5 patients. With all 34 dissection cases, the intimal flap was consistently visualized (9).

#### Peripheral MRA

Due to small vessel size and complicated intermingling between arteries and veins in distal legs and

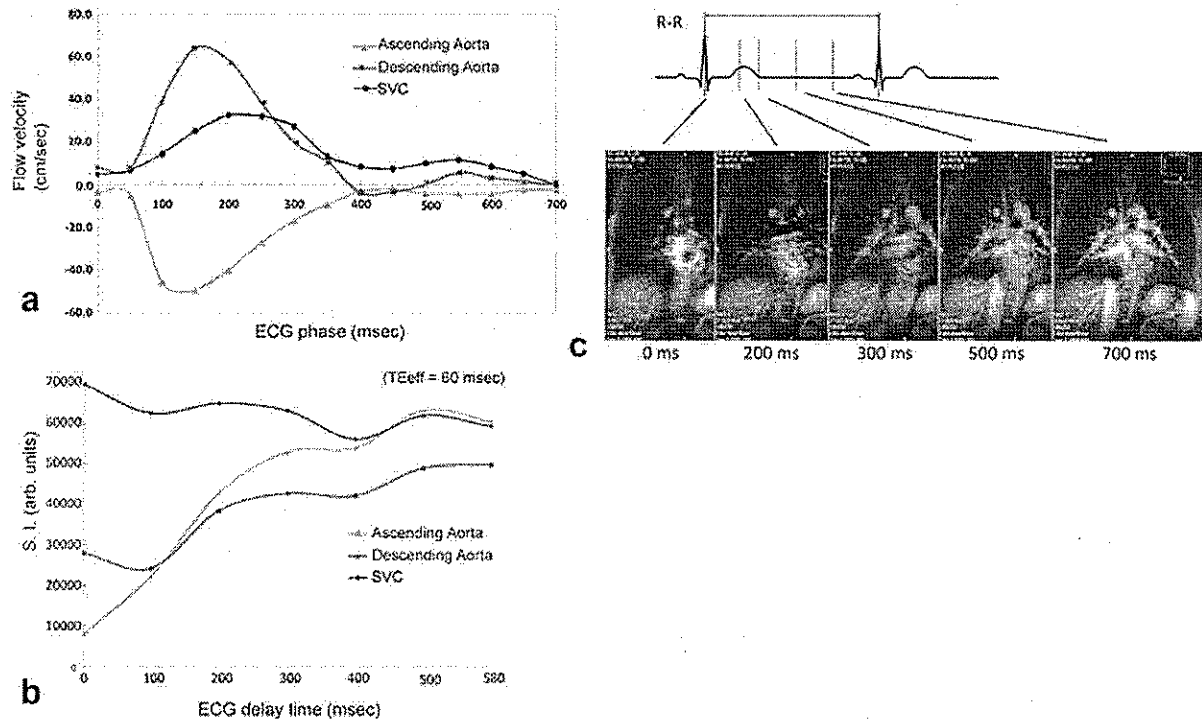


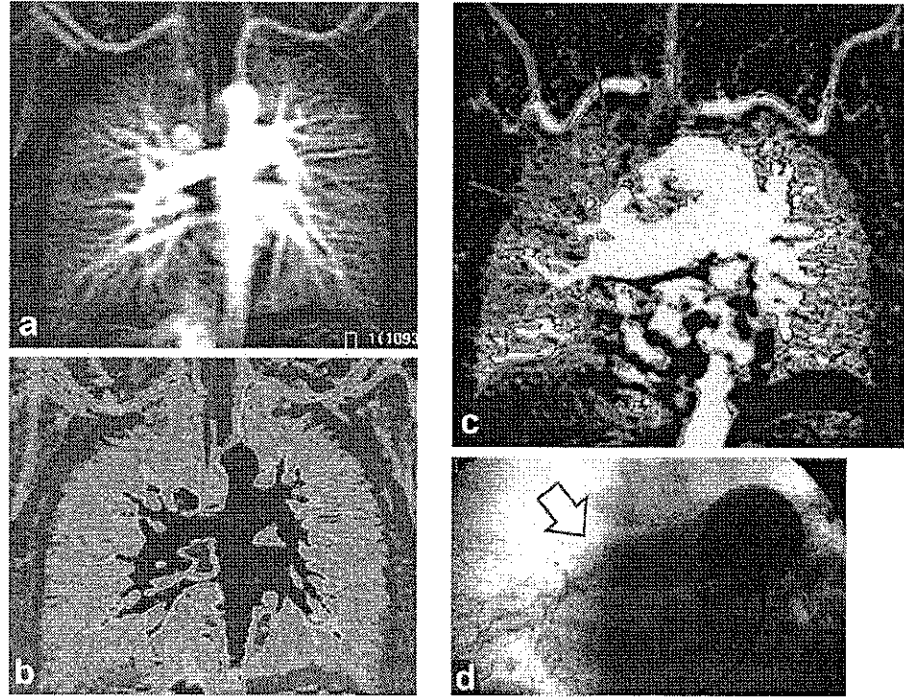
**Figure 1.** a: A graph shows the flow velocity versus ECG phases. The ascending and descending aorta show faster flow at systole with opposite directions. Superior vena cava shows moderate flow throughout the cardiac cycle. b: Signal intensity in arbitrary units vs. ECG delay times. Ascending and descending aorta show low signals during systole, while both show high signal during diastole. The superior vena cava (SVC) shows moderate signal intensity throughout cardiac cycle. c: The result of the ECG-prep scan presents various single shot projection images at different cardiac phases. The systolic trigger delay at 200 ms shows flow void or dark blood; whereas, the diastolic trigger delay at 700 ms shows bright blood. (Reproduced, with permission, from *J Magn Reson Imaging* 2000;12:776-783.)

hands, a diastolic and systolic subtraction method is required to depict arterial or venous trees separately. Unlike thoracic and abdominal MRA where one uses the PE direction in parallel with flow, selecting the PE direction perpendicular to the main flow vector gains an intrinsic dephasing effect. This dephasing effect is attributed to the constant RO gradient versus the lesser PE gradient near the center of  $k$ -space using rectilinear ordering. Additionally, applying flow-spoiling pulses in the RO direction can add an extra dephasing effect during systole, which is aptly named flow-spoiled fresh-blood imaging (FS-FBI) (12). The FS-FBI technique allows separation of arteries from veins in the peripheral run-off region. The percentage of the flow-spoiling gradient is defined as a percentage relative to one-half the entire RO gradient area (12). The flow-spoiling gradient pulses accentuate the differences in signal between systolic and diastolic phases, without affecting slower flowing venous blood and the stationary background signals.

In general, to avoid misregistration artifacts, a continuous acquisition of systolic and diastolic triggering is performed to collect systolic and diastolic images without interruption. Figure 4a illustrates the schematics of continuous systolic scans with each slice encoding with the same delay from the R wave, followed by the diastolic scans. At each slice encoding, a single shot half-Fourier FSE is acquired with a STIR

pulse for fat suppression. Operators can preset the system to subtract systolic from diastolic triggered source images, which conveniently generates the arteriogram after the maximum intensity projection (MIP) processing. In practice, the generally ideal RO flow compensation or spoiler gradient value is preset at each segment (i.e., iliac, thigh, and calf) on patients and healthy volunteers. Often, older patients with slower flow require a stronger RO spoiler pulse. Vessels in the hand and feet with slower flowing blood are also imaged with this approach using stronger flow spoiling pulses to differentiate systolic signal from diastolic signal. Determining systolic and diastolic triggering timing becomes crucial to generate optimal signal difference. It is recommended that the ECG-prep scan use similar scan parameters as the 3D acquisition, such as R-R interval, effective TE, orientation of the PE direction, application of a prepulse such as STIR for fat-suppression, and single-shot acquisition window duration. The multi phase ECG-prep acquisition is typically incremented by 50 ms or 100 ms with TR of 2 or 3 R-R intervals to observe single shot 2D images across the entire cardiac cycle. For processing, first, the delay time corresponding to the lowest signal in the artery of interest is selected as the optimal systolic triggering delay. Second, the subtraction of the optimal systolic image from all the ECG-prep images is generated to be input to the

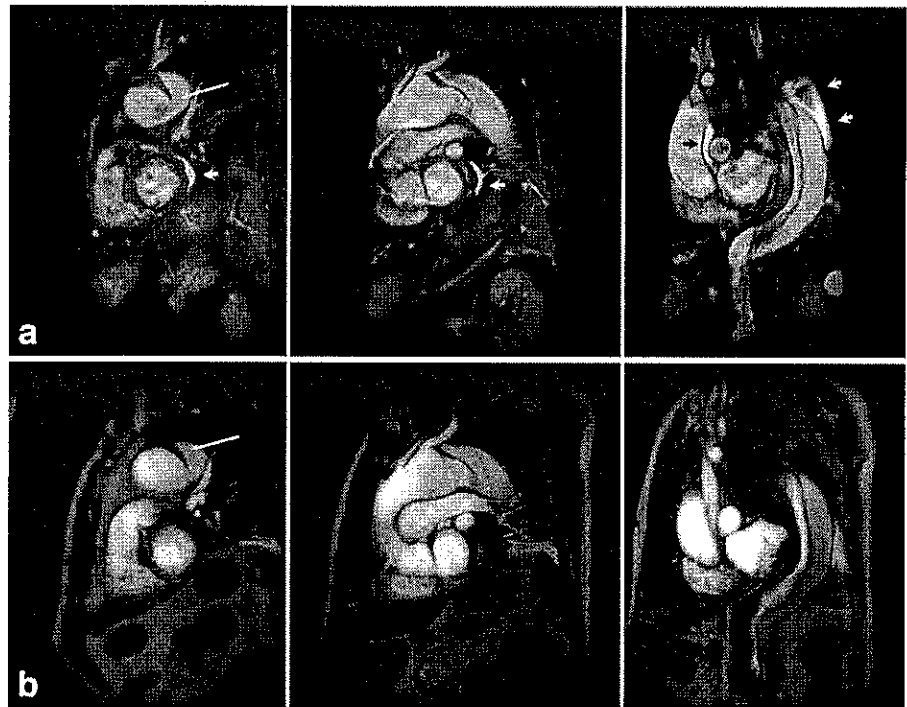
**Figure 2.** a: A projection image of pulmonary NC-MRA by subtraction of systolic from diastolic image on a healthy volunteer at 1.0T. b: A color illustration showing the high signal regions in red. c: A projection image of a patient with pulmonary thromboembolism at 0.5T. Lack of signal at the right upper lobe indicates thromboembolism with less blood supply (arrows). d: The digital subtraction angiography image indicates the similar finding as noncontrast 2D projection image in c. Image courtesy to Dr. Katsumi Nakamura of Kyoritsu Tobata Hospital, Japan.



identification of the optimal diastolic delay time. In this subtracted set, the delay time corresponding to the highest signal intensity in the artery of interest is chosen as the optimal diastolic triggering delay. As shown in Figure 4b, this manual calculation procedure is sometimes cumbersome; it is often difficult for the user to determine the optimal systolic and diastolic triggering delays. This time-consuming procedure

is even more difficult when the signal intensities of diastole are similar in all images. To overcome this problem, graphic display software, FBI-Navi, has been developed to provide a simple graph of signal intensity verses ECG phases (28). The FBI-Navi algorithm manipulates all the images of the ECG-prep scan, and automatically summarizes the arterial signals in the different cardiac phases. Figure 4c shows a variation

**Figure 3.** a: FBI NC-MRA contiguous source images showing a dissecting aorta with clear depiction of tear (arrow). Effusion regions are seen on the T2-weighted images (arrowheads). b: Corresponding CE-MRA of aortic arch on the same patient. CE-MRA reveals the depiction of true lumen and false lumen by bolus chase and a dissection tear (arrow). (Reproduced, with permission, from J Magn Reson Imaging 2001;14:113-119.)



of the arterial signal intensity presented in a 2D graph to select the delay timing: the low signal intensity corresponding to systolic and the high signal corresponding to diastolic triggering delays. The determination of diastole should be based on the beginning to the middle of a plateau area, because the single shot acquisition duration is approximately 100–250 ms for a  $256 \times 256$  matrix, depending on the parallel imaging factor. Figure 4d shows typical images of diastolic and systolic MIP images. Subtraction of the systolic from the diastolic images generates the arteriogram after the MIP processing.

Evaluation of the FS-FBI technique using ECG-gated half-Fourier FSE was performed on patients with peripheral diseases (29–31). In the preliminary study in 2002, Urata et al. compared the ECG-gated FS-FBI method with CE-MRA in 26 patients and reported that NC-MRA method was comparable to CE-MRA in 24/44 regions, while 15 were inferior and 5 were superior, when tested in a total of 56 regions (18 iliac, 20 femoral, and 18 calf area) in 26 patients that were diagnosed or had suspected arterial occlusive disease (29). To avoid the overestimation of stenoses, the investigators in this study suggested that diastolic images, depicting both arteries and veins, always be evaluated in addition to the subtracted MIP images. In a separate study, Lim et al compared the NC MRA method in the calf station including pedal arteries with the conventional bolus chase imaging and 3D time-resolved contrast-enhanced imaging in 36 patients (30). In their study, serious artifacts lead to poor diagnostic confidence in 17 patients (47.2%). Among the patients with satisfactory diagnostic confidence, accuracy, sensitivity, and negative predictive values were 92.2%, 92.4%, and 97.5, respectively. One limitation of the study was that only the subtracted MIP images were evaluated. Recently, Nakamura et al. have reported a comparison of NC FS-FBI with 16 row computed tomographic angiography (CTA) on 13 patients in arterial vasculature including the aortoiliac, femoral, and popliteocrural arteries (31). In the hemodynamically significant stenosis evaluation compared with CT, FS-FBI had an overall sensitivity of 97%, specificity of 96%, accuracy of 96%, and positive and negative predictive values of 88% and 99%, respectively. Due to its high negative predictive value, it may be possible to use FS-FBI for screening purposes. Figure 5a,b shows images of a patient comparing NC FS-FBI and 16-row CT. Both images shows similar arterial anatomical depiction, where the CTA image shows calcified areas and the NC FS-FBI image shows no calcification.

Most recently, two separate clinical evaluations of a similar technique reported using different vendors present a controversial result. Heneder et al reported the comparison of NC MRA in 36 patients with peripheral arterial occlusive disease was inferior in image quality to CE MRA and time-resolved MRA in the calf region at 3T (32). In the results of this study, the negative predictive value and sensitivity of NC MRA ranges from 97.8 to 100% and the specificity and positive predictive value ranged from 72.8 to 85.5% and 66.7 to 78.2%, respectively. They reported that the

major limitation was patient-induced motion. On the contrary, Gutzeit et al reported that excellent overall image quality was observed for NC MRA in the thigh and calf regions, yet insufficient diagnostic quality was observed in pedal arteries. Their NC MRA study yielded a mean sensitivity of 95.6%, specificity of 97.4%, positive and negative predictive values of 87.2 and 99.2%, accuracy of 97.1% for the thigh segments and a mean sensitivity of 95.2%, specificity of 87.5%, positive and negative predictive values of 83.2 and 96.6%, accuracy of 90.5% for the calf segments (33). The reasons for the considerably better depiction and higher scores could be the additional effort of using self-developed pillows and pads to provide support under the patient's calf for easy and comfortable positioning to reduce motion-related artifacts. To improve the depiction of the pedal arteries, a stronger RO spoiler may be required to differentiate slow flow in the pedal arteries as compared to arteries in the thigh and calf (12,31).

The FS-FBI NC MRA technique relies on systolic and diastolic signal differences. In the case of a severe stenosis, the signals in both systolic and diastolic images become similar due to turbulent flow, and their subtraction causes loss of signal in the final subtraction angiogram. Therefore, it is recommended to review diastolic source images when there is a positive finding (31). In addition, it is noteworthy to consider the flow sensitivity dependency on the flip angle of the refocusing pulses, as reported by Storey et al (34). With decreased refocusing flip angle, the faster flow components of blood experience unbalanced refocusing effects, resulting in signal loss in the main arteries. However, with decreased refocusing flip angle, the distal branch arteries are better visualized in the final subtraction angiogram.

#### *Non-contrast MR Venography*

The FS-FBI images contain both arterial and venous information, as in Figure 5c,d. The arterial images are obtained as a result of the subtraction of systolic from diastolic source images. One additional subtraction of those subtracted arterial images from the systolic source images, followed by the MIP processing, provides a venous image. Ono et al. have reported that the aortoiliac station requires an additional scan with the PE direction in the craniocaudal orientation with presaturation pulses to ensure the depiction of the superior vena cava (13). Outside the iliac region, just systolic triggering is acquired for venous images, which were considered to have relatively slower flow in the femoral and popliteal region. A recent clinical evaluation of FBI venography on 32 patients based on finding deep vein thrombosis compared with DSA provides 100% identification by two reviewers on all three stations. The corresponding sensitivities were 100% and 99.6% for the two reviewers (35).

#### **BALANCED SSFP**

Balanced steady-state free precession (bSSFP) provides a high signal efficiency and intrinsic T2/T1

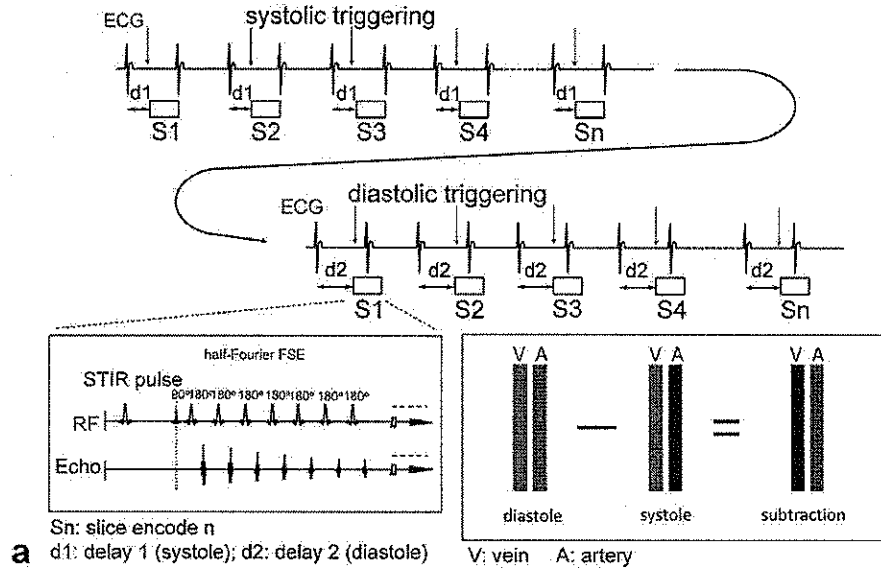
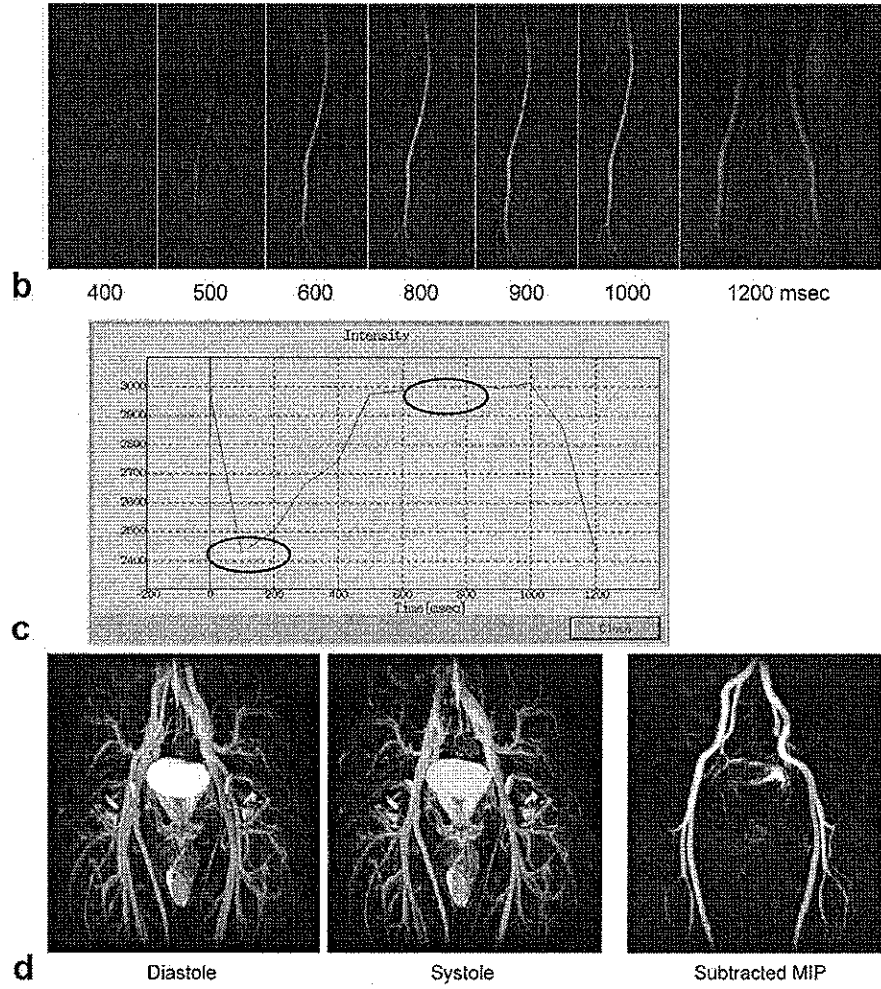


**Figure 4. a:** A 3D half-Fourier FSE with a continuous systolic and diastolic acquisition. Each slice (S1, S2, ... Sn) is imaged in one single-shot acquisition using half-Fourier FSE. One trigger delay (d1) is timed for systole for one 3D acquisition, while a second (d2) is timed for diastole. Acquisitions are performed every other or every third heart beat. To generate a bright blood angiogram, the systolic images (where artery appears dark) are subtracted from diastolic images. **b:** Manual subtraction images from the ECG-prep scan by subtraction the systolic image from all the other source images. (Reproduced, with permission from Magn Reson Med 2011;65:595-602.) **c:** Typical result of an FBI-Navi algorithm, indicating the best triggering time at systolic and diastolic delays. **d:** Typical 3D MIP images of both systolic and diastolic images, indicating diastolic triggering with both arteries and veins in bright blood, whereas systolic triggering shows black blood arteries and bright blood veins. The subtraction of diastolic and systolic sources images followed by an MIP procession provides the arterial image after MIP (right).



contrast, which is relevant for NC-MRA with minimal flow dependency (15). The sequence consists of an  $\alpha/2$  preparation pulse, dummy pulses for spin-conditioning, and an alternating radiofrequency (RF) excita-

tion pulse train, which offers fully balanced spins in all three directions, for high SNR and high contrast for blood signal. The merit of this application is obvious; however, the sensitivity of bSSFP to  $B_0$  field

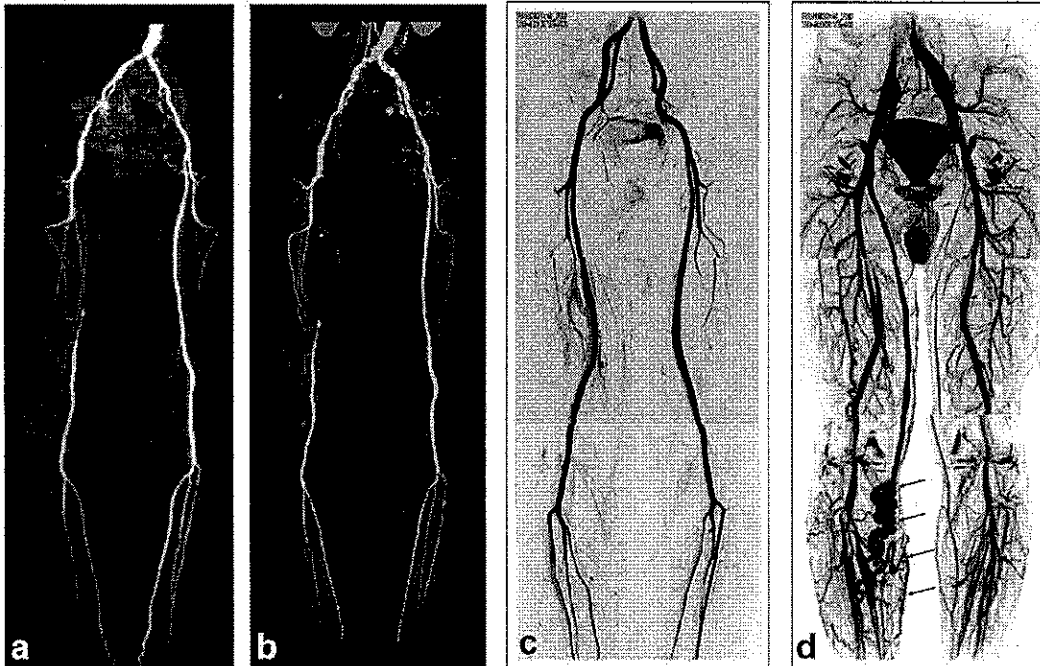


**Figure 5.** **a:** Three-station FBI run-off image on a 66-year-old patient with occlusions of the right superficial femoral artery and the right anterior tibial artery. Flow-spoiler pulses with 0, +10, and +20% were applied at the aortoiliac, femoral, and popliteocrural stations, respectively. **b:** A 16-row CTA image. Good agreement between the two modalities for depicting normal to occlusion regions with collateral branches. (Reproduced, with permission from *Magn Reson Med* 2011;65:595-602.) **c:** Arterial MIP images of three-station peripheral run-offs on a patient acquired using FS-FBI with spoiler pulses of 0, +10%, and 20% in the iliac, femoral, and popliteal regions, respectively. **d:** The additional subtraction of arterial images from systolic images provides venous images. Note that varicose veins (arrows) are unambiguously depicted in the popliteal station. Because of double subtraction, fluid is depicted in d. Image courtesy to Dr. Katsumi Nakamura of Kyoritsu Tobata Hospital, Japan.

inhomogeneity makes the technique susceptible to off-resonance banding artifact, unlike FSE-based sequences. Recent advances in software and hardware to shorten the TR of the excitation pulse train have helped to improve the robustness of bSSFP in the presence of inhomogeneous  $B_0$  fields.

Two alternative approaches using bSSFP for peripheral MRA applications include flow-sensitive dephasing (FSD) bSSFP and quiescent-interval single-shot (QISS) (36,37). Like FBI, the FSD bSSFP technique also uses subtraction of black blood systolic images from bright blood diastolic images by applying a motion-sensitizing bipolar-gradient FSD module only in systole. The advantage of the technique is that the FSD module can be incorporated in multiple directions as applying motion sensitization in the RO and PE directions independently as demonstrated in hands (38). The QISS technique, which leverages the inflow effect combined with ECG gating, comprises a slice-selective saturation pulse to suppress the stationary background signal, a traveling saturation pulse to suppress upstream venous signals, a quiescent interval of 228 ms, and followed by 2D multislice bSSFP read-out with chemical shift-selective fat saturation pulse. The merits of QISS are its short acquisition time and ease of use. However, the technique requires shimming in each segment and is limited in resolution in the slice direction, which is typically craniocaudal (37).

## SPIN LABELING TECHNIQUE

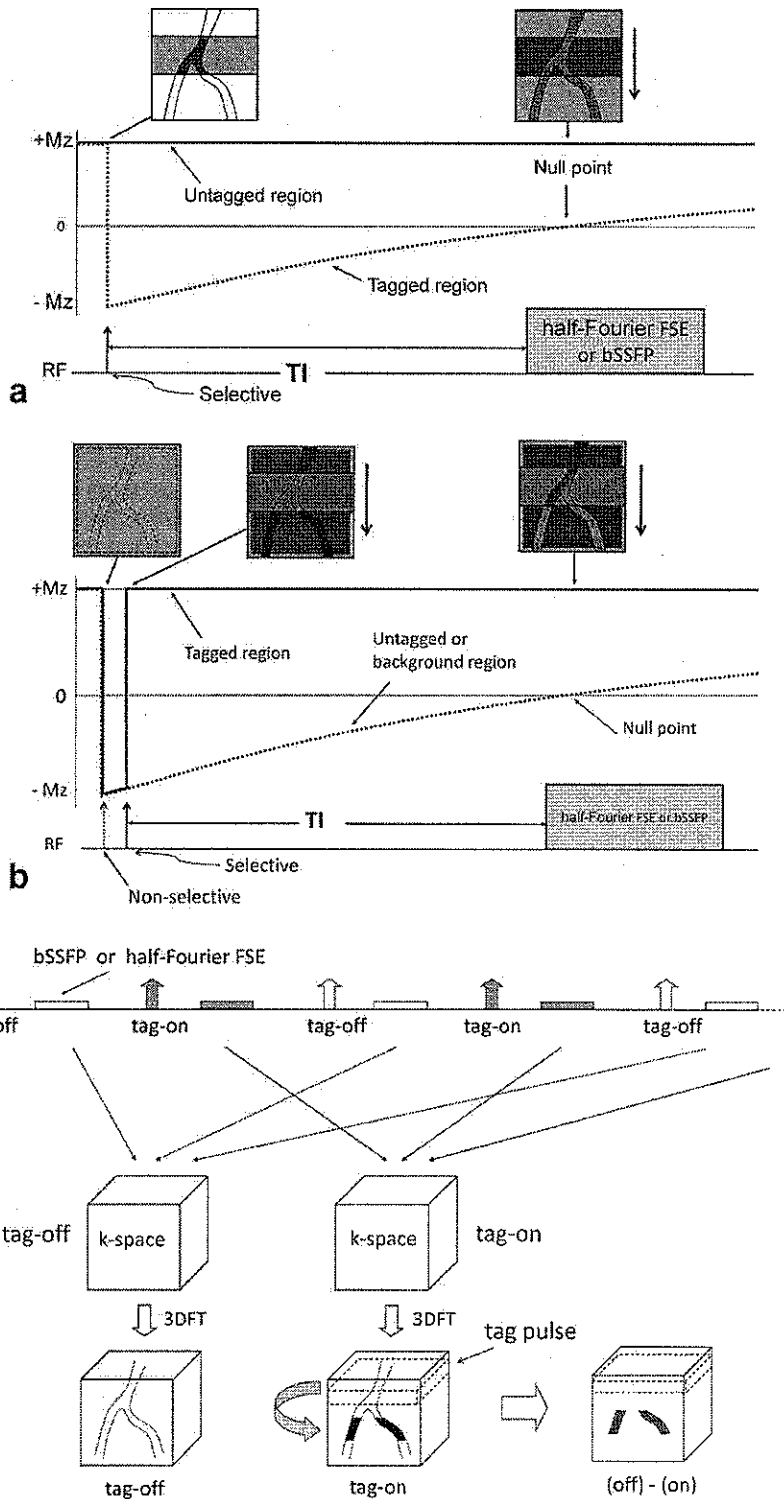
### Background

In late 1980s, Nishimura et al reported a method using one image acquired with a selective inversion recovery pulse (IR) to tag the vessel of interest combined with another image acquired with a nonselective IR pulse, to generate image contrast after subtraction (16). Later this method was expanded to an arterial spin labeling technique (ASL) technique called Signal Targeting with Alternating Radiofrequency (STAR) (17,39).

Both the half-Fourier FSE and bSSFP sequences allow single-shot imaging by acquiring multiple echoes (18,19). This feature enables short scan times and the possibility of adding various prepulses, such as a fat-suppression pulse, an inversion pulse, and/or a spin labeling pulse. Both half-Fourier FSE and bSSFP sequences offer bright-blood imaging. However, unless they are combined with a spin labeling technique, the background signal still hinders the depiction of blood vessels.

With regard to MRA and MR venography with spin labeling, there are several characteristic differences between half-Fourier FSE and bSSFP. As mentioned above, bSSFP requires good  $B_0$  field homogeneity (15), which is not a problem for half-Fourier FSE. However, limitations of half-Fourier FSE are flow dependency and the direction dependency of the PE direction to the orientation of the vessels. Therefore, application of

**Figure 6.** Sequence diagrams of the flow-in and flow-out techniques with the magnetization states, indicated by illustrative blood vessel images. **a:** The flow-in technique: The tagging pulse inverts the spins in the tagged region, which then recover exponentially by means of spin lattice (T1) relaxation, while untagged blood flows into the tagged region. Selection of TI to make the spins of the tagged region (background) near the null point yields the best contrast between the untagged fresh blood and the background signal. The illustrative images show the tagged region and time course of blood flowing into the tagged region. **b:** The flow-out technique: The first nonselective IR pulse inverts all magnetization in the region; which is immediately followed by a spatially selective tagging pulse in any orientation to selectively restore the magnetization in the tagged region to its original value. Therefore, the tagged blood flowing out of the tagged regions appears as bright-blood signal. The spins outside of the tagged region, which experienced only the nonselective IR pulse, have undergone T1 relaxation. Thus, the contrast between blood and background is highest when TI is the near null point for the background. Note that the illustrative images show the tagged region and the time course of out-flow of the marked blood. **c:** An alternate tag-on/off subtraction technique. The tag-on and tag-off data series were acquired alternately and both sets of data were each Fourier transformed separately, followed by the subtraction.



half-Fourier FSE is suitable for imaging relatively slower flow vessels like pulmonary vessels, portal veins, hepatic veins, and arteries in hands and feet. In contrast, bSSFP allows acquisition in arbitrary cardiac phases. In addition, the flow independent characteristic of bSSFP allows imaging of fast flow vessels, such as in cardiac, aortic arch, aorta, and renal MRA.

**Three Spin Labeling Techniques**

Three types of spin labeling technique for time-spatial labeling inversion pulse (time-SLIP) are described below: flow-in, flow-out, and alternate tag-on/off subtraction (18). All time-SLIP techniques can be combined with half-Fourier FSE or bSSFP sequences, with

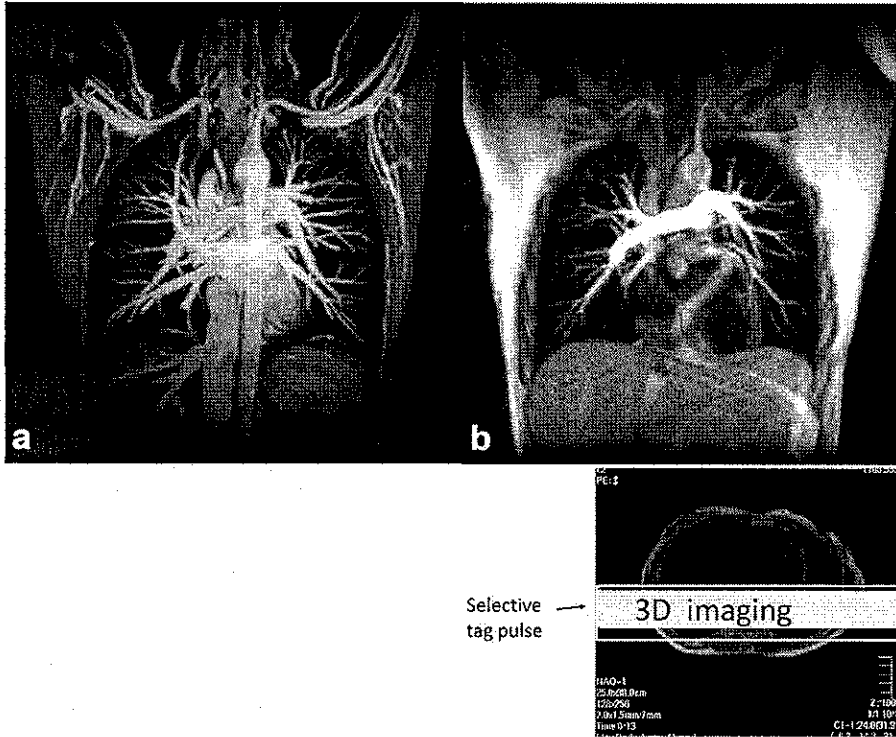


**Figure 7. a:** Pulmonary NC-MRA acquired using FBI (3D half-Fourier FSE using diastolic ECG triggering) on a healthy female volunteer (28 years old) at 1.0T. Both arteries and veins are depicted. **b:** Spatial-selective tag pulse was applied on the pulmonary trees. Waiting approximately TI of 800 ms, followed by the 3D half-Fourier FSE using diastolic ECG triggering data acquisition, permits depiction of only the pulmonary arteries.

2D or 3D acquisition, and with ECG (or PPG) gating, respiratory gating, or both.

Figure 6a-c shows flow-in, flow-out, and alternate tag-on/off subtraction techniques, respectively. Figure 6a,b shows a sequence and the corresponding magnetization states of signals for both untagged and tagged regions. The flow-in technique (Fig. 6a) applies a spatially (or slab) selective inversion recovery (IR) (tagging) pulse to saturate a region of interest. Untagged spins flow into the tagged region during the inversion recovery time (TI). The flow-out technique (Fig. 6b) applies both a nonselective IR pulse and a spatially selective IR pulse. Unlike the flow-in technique, double inversions using the nonselective and selective pulses restore the tagged spins to the +Mz axis which later flow out from the tagged region. The untagged spins undergo T1 relaxation ideally crossing through the null point at TI. The alternate tag-on/off subtraction technique (Fig. 6c) consists of a series of interleaved tag-on and tag-off acquisitions to generate two separate images. These images are individually reconstructed and then subtracted to yield the final angiogram. This technique allows depiction of only signals of the tagged region by the cancellation of the background signal by means of subtraction. In all three techniques, the orientation of the tag pulse can be adjusted freely to achieve any oblique orientation relative to the scan plane.

The characteristic difference of the techniques is that the flow-in and flow-out techniques require careful selection of TI to null the background signal, whereas the alternate tag-on/off technique generates images without the background signals (removed by means of subtraction) regardless of the selection of TI.

This independency of TI selection permits the study of perfusion in a time-resolved manner by repeated acquisitions with many different TIs. However, the main drawback of the alternate tag-on/off technique is that the scan time is doubled.

### Applications of the Flow-In Technique

#### Thoracic MRA

An example of the time-SLIP flow-in technique is shown on the pulmonary arteries in Figure 7. In Figure 7a, the FBI or 3D half-Fourier FSE image triggered during diastole presents both pulmonary arteries and veins. Applying the time-SLIP pulse to saturate the background signals, waiting for a TI of 800 ms, followed by readout using 3D half-Fourier FSE triggering during diastole, provides imaging of pulmonary arteries. The freshly pumped blood from the heart flowing into the pulmonary region is depicted with the right to left PE direction. The bSSFP sequence can be used in this area as well with the time-SLIP flow-in technique. The proximal pulmonary arteries may be better depicted in bSSFP due to the flow independency of the technique, whereas the distal vessels may be better depicted in the half-Fourier FSE, because it is less susceptible to air in the lung using a spin echo based sequence.

#### Renal MRA

**Clinical Background.** Renal artery stenosis (RAS) is a primary focus for renal NC-MR angiography. The choice of the best imaging technique for the evaluation of patients suspected of having RAS remains





**Figure 8.** A 59-year-old male with a history of renal artery bypass grafting for a renal artery aneurysm, suspected of having renovascular hypertension. The patient underwent NC-MRA using the flow-in technique with 3D bSSFP (TI = 1900 ms) and STIR. **a:** Oblique coronal reconstruction image with maximum intensity projection (MIP) shows stenosis of the lower branch of the graft (arrow). Note that the signal intensity of the graft just peripheral to the stenosis decreased (arrowheads) probably because of turbulent flow. **b:** Significant stenosis was confirmed by intra-arterial digital subtraction angiography using carbon dioxide (arrow), and percutaneous transluminal angioplasty (PTA) followed by stent placement was performed.

controversial. Duplex ultrasonography is completely noninvasive and relatively inexpensive. The criteria for RAS include increased peak systolic velocity of the renal artery and high ratio of the peak systolic velocities between the renal artery and the aorta. Resistance index value is reported to be useful for prediction of the outcome of revascularization (40). However, the test is operator dependent and limited by obesity and gas. Anatomical variations of renal arteries and distal reconstitution by collateral vessels may cause

false negative results. Therefore, combined use of Doppler study with another imaging method that provides anatomical details of renal arteries may be highly desired.

Contrast-enhanced (CE)-CTA and CE-MRA are both well-established techniques for the depiction of detailed anatomical information of renal arteries. Diagnostic performance of these studies is satisfactory (41,42). However, CE-CTA requires iodinated contrast media, which carries a risk of contrast

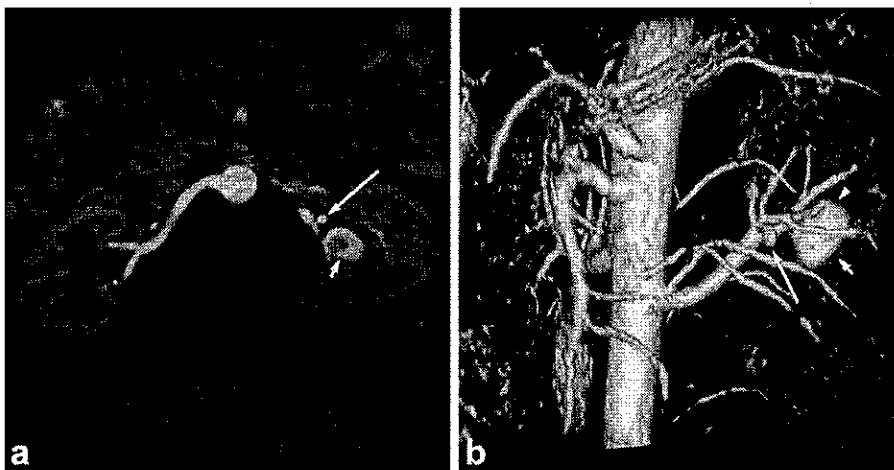


**Figure 9.** A 31-year-old male with suspected of having an aneurysm of the left renal artery by screening ultrasonography underwent NC-MRA using the flow-in technique with bSSFP read-out. **a:** The source image of NC-MRA acquired with an inversion time (TI) of 1400 ms and frequency selective fat suppression, which shows bright signal in the arterial structures with good suppression of the veins and the background signal. Both large (arrowhead) and small (arrow) saccular aneurysms in the branches of left renal artery are clearly depicted. **b:** The volume rendering image revealed the geometric relationship between the aneurysms and the parent vessels.

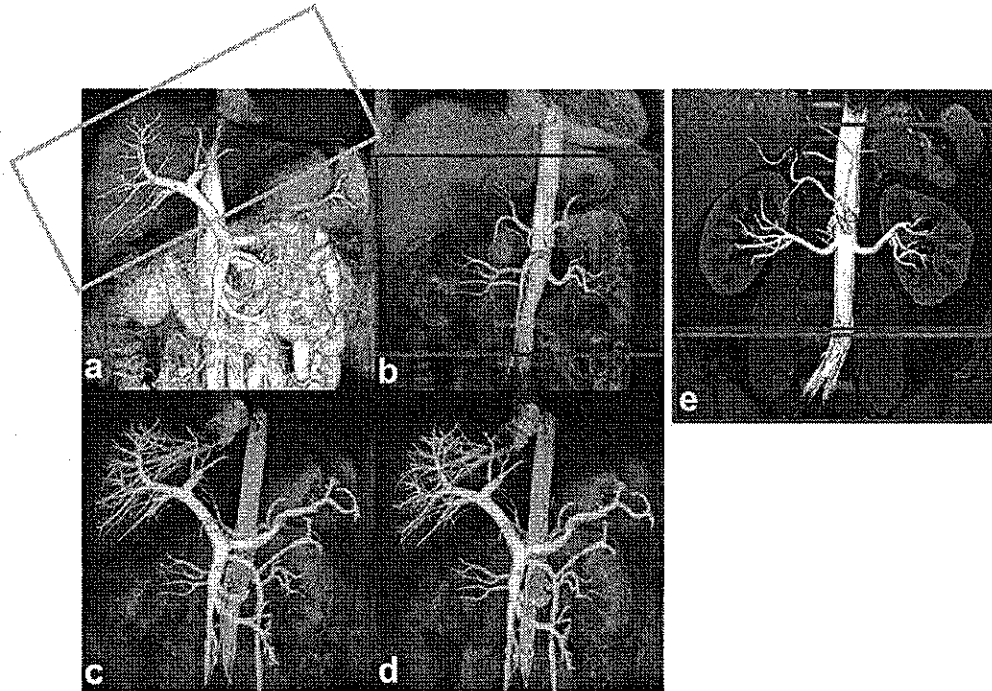


**Figure 10.** Examples of time-SLIP flow-in techniques. **a:** Portal veins are depicted by applying the tag pulse (yellow line) oblique to the liver so that splenic vein and superior vena cava (SVC) flow into the portal veins in the liver using bSSFP read-out. **b:** The time-SLIP flow-in image presents hepatic artery and renal arteries. The tag pulse (red line) is placed relatively higher to depict hepatic artery. **c,d:** Stereoscopic image pair of three fusion images showing portal veins, hepatic artery with renal arteries, and hepatic veins. Image courtesy to Dr. Hiroyuki Isoda of Kyoto University, Kyoto, Japan. **e:** Renal artery and hepatic artery are well depicted with a slightly higher tag position. Image courtesy to Ms. Ayako Ninomiya of Toshiba Medical Systems Corp., Japan.

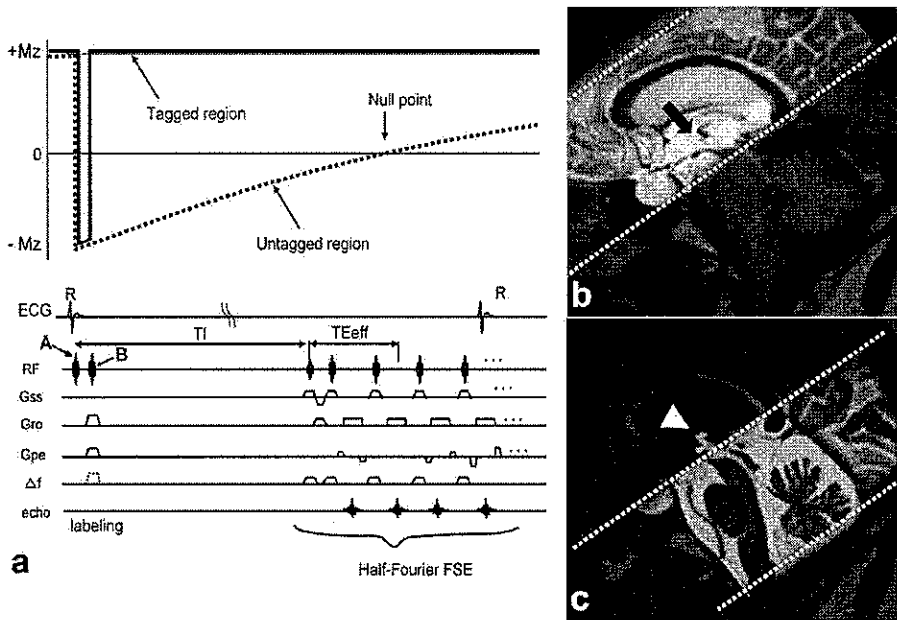


**Figure 11. a:** Sequence chart and magnetization states of untagged (nonselective) and tagged (selective) spins. An initial non-selective pulse inverts all magnetizations to  $-M_z$ , then restored by a selective pulse to  $+M_z$  state. Whereas untagged spins experience the  $T_1$  recovery process evolving from  $-M_z$  to  $+M_z$ . Around the null points of the background signals, tagged and untagged signals have good contrast. **b:** The sagittal time-SLIP pulse at  $T_I$  of 3600 ms on CSF in the lateral and third ventricles. Note that the signal void (arrow) is depicted as turbulent flow of CSF in the third ventricle. **c:** The sagittal time-SLIP pulse at  $T_I$  of 3600 ms on CSF in the aqueduct and fourth ventricle. The CSF flows out from the aqueduct into the third ventricle is remarkably depicted by high signal intensity. (Reproduced, with permission, from Radiology 2008;249:644-652.)

nephropathy among patients with chronic kidney disease. Potential risks of radiation exposure associated with CT scans are also a main concern, especially in younger patients. Nephrogenic systemic fibrosis is another considerable risk for patients under hemodialysis in terms of Gadolinium-enhanced MR angiography.

**Technical Background.** NC-MRA is free of radiation exposure and exogenous contrast media, as it uses blood as an endogenous contrast material. This safety aspect of NC-MRA methods is especially advantageous in the evaluation of renal arteries among patients with severe chronic kidney disease, who are not under hemodialysis, and patients with high risk of allergic adverse reactions. Patients unable to comply with long breathholding may well tolerate the use of respiratory gating as a preferable method in the renal NC-MRA application. Originally, real time motion correction was applied with the technique to compensate for the motion, as applied in coronary MRA (43,44). However, now, the use of respiratory gating is preferable in the renal NC-MRA examination. Early NC-MRA techniques, such as TOF and PC MRA, were not comparable to CE-MRA or CE-CTA. However, the flow-in spin labeling NC-MRA technique with bSSFP provides renal angiogram with excellent image quality. Recent studies showed that state-of-the-art renal NC-MRA is comparable to DSA (45,46).

There are several critical points to consider for successful flow-in renal NC-MRA technique. The flowing blood and renal parenchyma (medulla and cortex) contrast is maximized at around TI of 1100 ms in healthy volunteers (47). Nevertheless one needs to consider the blood travel time and the background signal recovery. In a clinical setting, the optimal TI (blood travel time) tends to be longer in the elderly than the younger patients. Because the arterial blood velocity is slower in elder patients, the extent of opacified arterial structures will be lesser in the elderly if the same TI is applied. If TI is inadequately short, accessory renal arteries arising from the caudal portion of the aorta or iliac arteries will be missed, causing the false negative rate to increase. As the TI increases, the extent of arterial opacification becomes greater; however, contrast between arteries and background decreases, and motion artifact caused by the initiation of the next inspiration increases. Therefore, the TI should be the factor which maximizes the contrast between blood and background. In our clinical experience, the TI of 1400 ms is long enough for young and healthy patients, but it is not enough for older or atherosclerotic patients. The TI of around 1900 ms is recommended for the assessment of atherosclerotic renal artery stenosis. Short-tau inversion-recovery (STIR) fat suppression is preferable to a chemical shift-selective fat-saturation (CHESS) pulse to maintain good contrast between arterial blood and background, as reported by Shonai et al (48).

Control of breathing is crucial for good image quality, especially in cases where long inversion times such as 1900 ms are used. If the respiratory cycle is not long enough, inspiration of the next cycle will

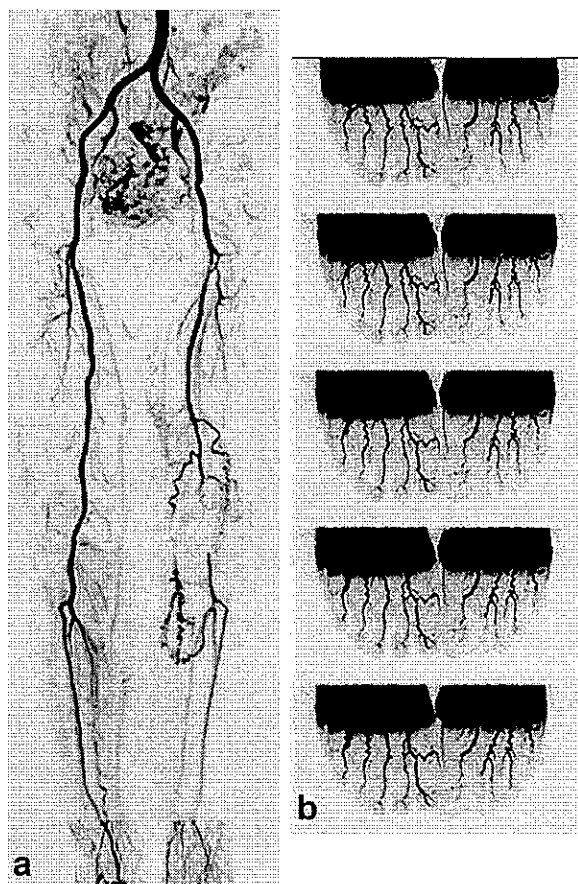


**Figure 12.** a: FS-FBI images of the patient with a femoral occlusion showing collateral vessels. b: The corresponding digital arteries of the same patient showing in time-resolved time-SLIP NC-MRA images with different TI times. Increasing the TI times (top to bottom), the left blood supply in the left foot is somewhat slower than the right foot. Image courtesy to Dr. Jun Isogai of Hasuda Hospital, Saitama, Japan.

begin during the data acquisition, which causes motion artifacts. Moreover, an unsteady respiratory cycle results in nonuniform background signals shot-to-shot due to the different TI recovery period of each shot. Unsteady respiration may be related to variable diaphragmatic position in the expiratory phase which causes motion blurring. Proper instruction to the patients on how to breathe slowly before the examination is important. As reported by Parienty et al, active control of breathing by an integrated auto-voice system or recorded voice instruction is helpful to achieve steady respiratory cycles (45).

Positioning of the inversion pulse (tag) for younger, healthy patients versus elderly and atherosclerotic patients also varies. The upper edge of the tag slab is the starting point of the inflow of the hyper-intense blood, i.e., endogenous contrast media. The more caudal the starting point of the tag, the more distal the bright blood reaches in the kidneys (45). In most cases, the upper edge of the tag slab is aligned with the superior pole of the kidney at the higher position (usually left). However, the slab can be placed more caudally in

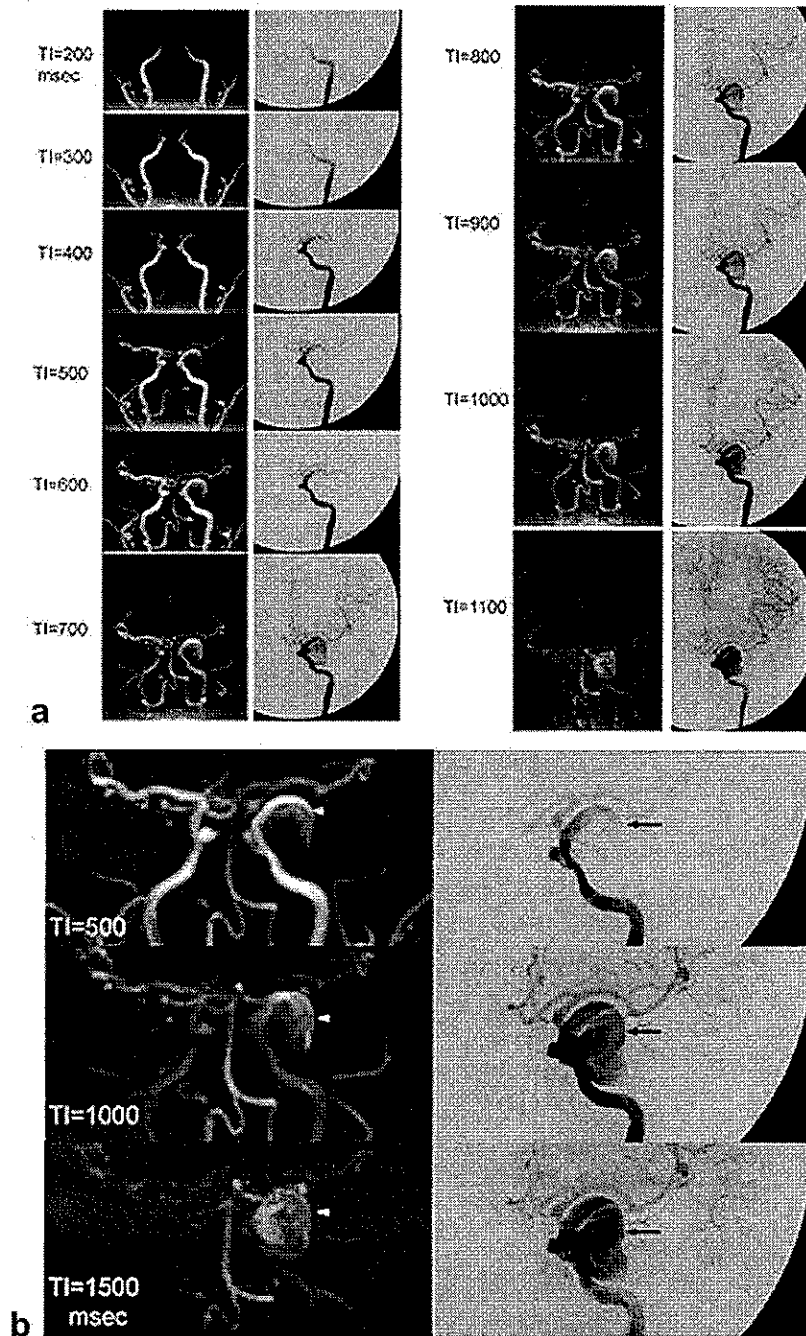


**Figure 13.** A 62-year-old female with a giant aneurysm of the left internal carotid artery. **a:** Time-resolved NC-MR angiography with multiple inversion times in increments of 100 ms. The corresponding DSA images are on the right. **b:** The same patient data in increments of 500 ms revealed turbulent flow gradually pouring into the aneurysm (arrowheads), which was well correlated with corresponding catheter angiogram (arrows).

cases where the blood flow is so slow that the bright blood does not reach distal branches sufficiently.

The coronal imaging plane is advantageous for depiction of accessory branches arising from the caudal portion of the aorta or iliac arteries. The wide coverage of coronal scanning also prevents failure of the visualization of main renal arteries originating from different positions of the aorta. The minor disadvantage of the coronal scanning compared with axial scanning includes relatively weak inflow effect and slight decrease of spatial resolution, particularly in the anterior-posterior direction. Ostial stenosis of accessory

renal arteries branching off from the anterior aspect of the aorta is better examined in the axial source images rather than the coronal images, because of the better in-plane resolution. When extra examination time is permitted, combination of both coronal acquisition with a wide coverage and the targeted axial acquisition of main renal arteries maximize the diagnostic performance, as reported by Parienty et al (45).

**Pitfalls and Considerations.** Interpretation of NC-MRA for RAS is similar to that of CE-MRA, but some specific knowledge is helpful to maintain diagnostic

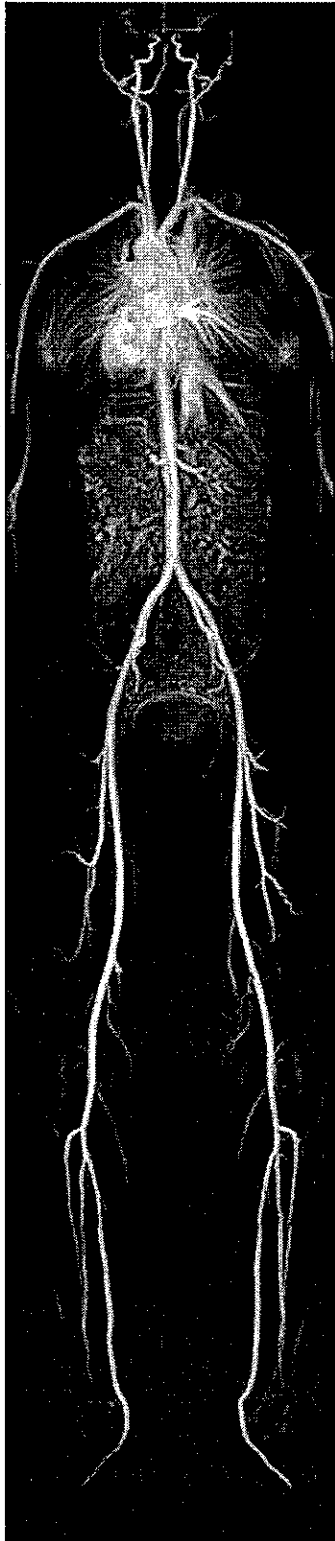


**Figure 14.** Whole-body NC-MRA on a healthy volunteer. Various techniques were applied in various parts of the body; time-SLIP bSSFP in carotid, FBI in thoracic region, time-SLIP renal, and FS-FBI in peripheral run-offs. Image courtesy to Yuichi Yamashita and Takao Yamamoto, Toshiba Medical Systems Corp., Japan.

performance. There is a tendency toward overestimation of stenoses in NC-MRA caused by signal loss due to turbulent rapid flow. Signal intensity of the blood just distal to a significant stenosis also decreases, so severe stenosis can be misinterpreted as occlusion, especially in the MIP images of the full slab without masking. This misinterpretation can easily be avoided by the examination of source images and/or partial MIP images, as indicated in Figure 8. Another point to note is that attention needs to be paid to the accessory branches. Failure in depiction of accessory renal arteries accounts for a considerable portion of false-negative results in NC-MRA studies. The key finding to be aware of with regard to hidden accessory renal arteries is the partially lack of intraparenchymal branches at the lower pole of the kidney. An additional scan can visualize these branches with placing the tag pulse far caudally (45).

In approximately 10% to 23% of patients who undergo renal transplantation, stenosis of the artery occurs in the transplanted kidney, which may cause posttransplant hypertension and graft dysfunction. NC-MRA is considered to be a reliable test for the assessment of transplanted renal artery in combination with Duplex ultrasonography (49).

Other potential applications of renal NC-MRA include renal artery aneurysm, arteriovenous fistula, and evaluation of vasculitis such as polyarteritis nodosa. Figure 9 shows an example of renal artery aneurysms in a patient. NC-MRA is potentially superior to CE-MRA or CE-CTA for depiction of intraparenchymal branches, because it is free from disturbance by parenchymal enhancement. Good contrast between arteries and the renal parenchyma is essential for the evaluation of intra parenchymal branches. Improvement in spatial resolution permits possible evaluation of smaller branch vessels. Applications in 3T or higher magnetic field scanners provide better contrast and higher spatial resolution, which is discussed later.

#### *Abdominal MRA*

Other applications of flow-in time-SLIP are portal veins (50), hepatic arteries (51), and hepatic veins (52). Shimada et al compared the portal depiction difference between half-Fourier FSE and bSSFP combined with time-SLIP (53). In depiction of the hepatic veins, double tag pulses were applied with one tag on the upper liver to suppress the aorta, and the other tag placed below the liver to suppress the signals from the portal veins (52). Figure 10 shows various applications of the time-SLIP flow-in technique. There are reports studying the distribution of portal vein using a similar technique, which uses the tag pulse on the splenic vein and the superior mesenteric vein (SMV) (54). This was observed as black blood to flow out from the tagged splenic blood and SMV. Further functional study of the portal vein was performed with the intake of a meal (55). Other applications of NC-MRA in abdomen are discussed in details elsewhere (56).

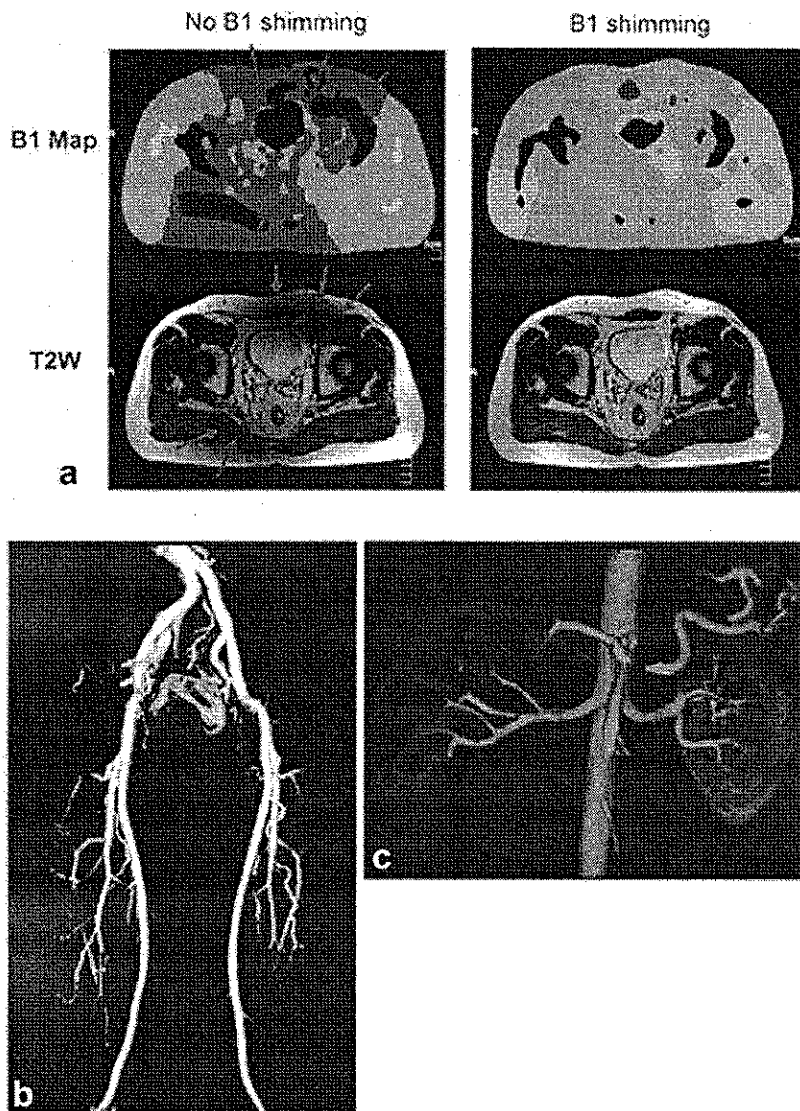


**Figure 15. a:** With no  $B_1$  shimming, the  $B_1$  map and T2-weighted image show unevenness in signal distribution or shading within the image, (arrows) whereas, with  $B_1$  shimming, signal distribution is uniform in both map and T2-weighted images. **b:** 3T image of iliac to femoral NC-MRA. Note that there is no shading in the vessel image. **c:** The 3T renal NC-MRA in a volume rendered image with high SNR and good blood to background contrast. (Image courtesy to Drs. Yoshinori Hamamura, Toshiba Medical Research Institute, USA and Kazuya Okamoto, Toshiba Medical Systems Corp., Japan.)

#### Application of the Flow-Out Technique

The flow-out technique consists of a nonselective pulse followed by a selective pulse. The spins that experience both pulses remain at  $+M_z$  and flow out from the tagged region, whereas the spins that experience only the nonselective pulse slowly recover to  $+M_z$  by means of  $T_1$  relaxation. A good example of time-SLIP flow-out is studying the cerebrospinal fluid (CSF). Yamada et al. have applied 2D time-SLIP using half-Fourier FSE with various TI values to observe the CSF flow out from the tagged region (57). Figure 11 shows the sequence diagram and magnetization states followed by nonselective and selective RF pulses. CSF is unambiguously depicted to flow out from the tagged regions. Note that CSF has a longer  $T_1$  value so that the null point of CSF is relatively long, as compared to blood.

The differences between the flow-in and flow-out techniques are discussed below. As in applications of

renal MRA and portal veins, the flow-in technique suppresses the region of interest (ROI) by applying only the selective pulse and waiting for a TI time to allow blood from all vessels and all directions to flow into the ROI. Therefore, we do not know which vessels contribute most in the angiogram. Of course, in the renal arteries, blood signals from the aorta contribute to the renal arteries. However, as presented in Figure 10a, the blood supply to the portal vein comes from contributions from both the splenic and the superior mesenteric veins. Therefore, the flow-in technique is most suitable to be used for angiography purposes. On the contrary, the flow-out technique allows depiction of CSF or blood supply by only the selectively tagged region. Depending on the application, the contribution of the tagged signal may be isolated to distinct vessels. Consequently, the flow-out technique is most suitable to studying the supply functionality aspects of moving objects like CSF and blood flow.

Table 1  
Summary of Various Non-contrast Techniques and Their Possible Applications With Characteristics and Limitations

Techniques		Typical Applications	Characteristics and Limitations
ECG-gated half-Fourier FSE		Peripheral MRA and MRV, Abdominal vessels	Vessel Morphology, Less susceptible to field heterogeneity
bSSFP		Coronary MRA, Pulmonary and Abdominal vessels	Vessel Morphology, Susceptible to field heterogeneity
Spin Labeling (Time-SLIP)	Flow-in	Renal MRA, Aorta, Portal veins	MR angiography, Limited TI for nulling of background signal
	Flow-out	MRA and MRV, CSF Flow	Flow function, Limited TI for nulling of background signal
	Alternate Tag On/Off subtraction	Perfusion, Time-resolved MRA	Allows selecting any TI times, double the scan time

**Application of the Alternate Tag-on/off Subtraction Technique**

As mentioned, the alternate tag-on/off subtraction technique is a combination of both tag-on and tag-off acquisitions followed by subtraction. Therefore, it requires twice the scan time of the flow-in and flow-out techniques individually. However, the advantage is that a wide range of TI values can be used, unlike the flow-in and flow-out techniques that require selecting the TI at or near the null point. A reported application of the alternate tag-on/off subtraction technique is the study the portal vein distribution of blood flow using a single breathhold 3D half-Fourier FSE technique (58). The technique permits selective tagging of the splenic vein and the mesenteric vein to separately study the intraportal distribution under physiological conditions.

Moreover, because the alternate tag-on/off subtraction technique allows repeated acquisitions with various TI values, the detailed blood flow can be depicted in a time-resolved manner, like in a perfusion process. The perfusion information can be obtained without contrast media and with good cancellation of background signal between the tagged and untagged images (59,60).

Another example of the alternate tag-on/off technique is NC-MRA of feet as shown in Figure 12. With an increasing TI, the slower blood flow to the digital arteries on the left leg can be seen due to the femoral occlusion with collateral vessels. Another example of time-resolved NC-MRA is carotid MRA in Figure 13. Because the TI increment has no limitation (60), unlike time-resolved CE-MRA, one can achieve arbitrary time resolution by applying finite increments of TI. Of course, the number of time increments proportionally increases the total scan time. As an example, the carotid arteries are depicted with 100-ms incre-

ments, which were compared with DSA in Figure 13a. As TI is increased, the carotid blood flow progresses further away from the tagged region. The blood flow is correlated well with the timing of DSA, as shown in Figure 13b where the depiction of tagged blood entering in the aneurysm is comparable to the DSA results. Furthermore, time-resolved NC-MRA presents hemodynamics of the arteriovenous malformation or fistula and distinction of feeding arteries in the pelvis and lower extremity (61).

**FUTURE DIRECTIONS**

Previously, the established techniques for NC-MRA are discussed with regard to its application in various body parts. Two of the new perspectives for NC-MRA are whole-body MRA and 3T MRA. The whole-body NC-MRA requires multiple coil arrangements with high parallel imaging factors, presenting blood vessels from the head to toe, which was achieved with a combination of techniques: 3D TOF in the head to cervical regions, FBI in the thoracic region, time-SLIP with bSSFP in the abdomen, and FS-FBI in the aortoiliac to popliteal regions (62). Figure 14 presents a whole-body NC-MRA image using various techniques, such as time-SLIP carotid, FBI thoracic, time-SLIP abdomen, and FS-FBI for iliac to popliteal MRA.

Another prospect is 3T MRA. The dominant challenge for NC-MRA at 3T is the short B<sub>1</sub> wavelength problem resulting in nonuniform B<sub>1</sub> transmit field at higher field strengths (34,63,64). In addition, SAR is problematic for NC-MRA at 3T due to its use of RF-intensive sequences such as half-Fourier FSE and bSSFP at 3T. The problem is exacerbated by the requirement of high flip angles needed to produce high-intensity blood signal and good blood-to-background contrast (34). One approach to mitigate B<sub>1</sub> nonuniformity is B<sub>1</sub> shimming. Figure 15a shows T2-weighted images with and without application of B<sub>1</sub> shimming, along with their associated B<sub>1</sub> maps. Multiple-phase transmission with B<sub>1</sub> shimming allows evenness of RF penetration, resulting in uniform NC-MRA images.

The benefits of 3T for NC-MRA include not only increased SNR, but also the advantages of longer T<sub>1</sub> relaxation time. High signal intensity at 3T makes better depictions of arteries (65). With a longer T<sub>1</sub> value at 3T, the time-SLIP flow in technique allows longer TI

Table 2  
Acronyms of Various NC-MRA Techniques

	ECG-gated half-Fourier FSE	Spin-labeling
Toshiba	FBI	Time-SLIP
Siemens	Native SPACE	Native trueFISP
Philips	TRANCE	b-TRANCE
GE	3D delta Flow	Inflow-IR

FBI = fresh blood imaging; Time-SLIP = time-spatial labeling inversion pulse.

than at 1.5T, which results in good contrast between blood and background signals. Lanzman et al. have compared renal NC-MRA in healthy volunteers at 1.5T and 3T (66). No difference was seen in the evaluation of the first and second branch segments; however, 3T NC-MRA showed significant improvement over 1.5T in imaging of the third and the fourth branch segments. Figure 15b,c shows FS-FBI aortoiliac NC-MRA image and time-SLIP flow-in renal NC-MRA at 3T, respectively.

## SUMMARY

Both peripheral and renal NC-MRA techniques are discussed with regard to technical points and clinical remarks. Three different NC-MRA time-SLIP techniques are described as flow-in, flow-out, and alternate tag-on/off subtraction. Depending on the application and specific target vessel, time-SLIP can be selectively combined with half-Fourier FSE or bSSFP in 2D and 3D acquisitions. The flow-in technique works well for observing inflow of blood into the vessels of interest, which is suitable for visualization of their angiographic morphology. The flow-out technique allows selective observation of outflow from the tagged vessels. The alternate tag-on/off subtraction technique allows observation of only the tagged vessels without background signal, at the cost of doubling the scan time. To select the appropriate technique, it is important to understand the target vessel system in each clinical application. Table 1 summarizes the NC MRA techniques and possible applications with characteristics and limitations. Those established techniques are commercially available and a summary of commercial names are summarized in Table 2.

## ACKNOWLEDGMENTS

Authors thank Dr. Leping Zha, Dr. Andrew Wheaton, and Mr. Robert Anderson of Toshiba Medical Research Institute, USA for technical assistance.

## REFERENCES

- Prince MR. Gadolinium-enhanced MR aortography. *Radiology* 1994;191:155-164.
- Masaryk TJ, Laub GA, Modic MT, Ross JS, Haacke EM. Carotid-CNS MR flow imaging. *Magn Reson Med* 1990;14:308-314.
- Laub GA. Time-of-flight method of MRA. *Magn Reson Imaging Clin N Am* 1995;3:391-398.
- Dumoulin CL, Souza SP, Walker MF, Wagle W. Three-dimensional phase contrast angiography. *Magn Reson Med* 1989;9:139-149.
- Dumoulin CL, Yucel EK, Vock P, et al. Two- and three-dimensional phase contrast MRA of the abdomen. *J Comput Assist Tomogr* 1990;14:779-784.
- Sodickson DK, Manning WJ. Simultaneous acquisition of spatial harmonics (SMASH): fast imaging with radiofrequency coil arrays. *Magn Reson Med* 1997;38:591-603.
- Pruessmann KP, Weiger M, Scheidegger MB, Boesiger P. SENSE: sensitivity encoding for fast MRI. *Magn Reson Med* 1999;42:952-962.
- Bubaescu I, Izzedine H. Gadolinium-induced nephrotoxicity. *Int J Clin Pract* 2003;62:1113-1118.
- Urata J, Miyazaki M, Wada H, Nakaura T, Yamashita Y, Takahashi M. Clinical evaluation of aortic diseases using nonenhanced MRA with ECG-triggered 3D half-Fourier FSE. *J Magn Reson Imaging* 2001;14:113-119.
- Miyazaki M, Sugiura S, Tateishi F, Wada H, Kassai Y, Abe H. Non-contrast-enhanced MRA using 3D ECG-synchronized half-Fourier fast spin echo. *J Magn Reson Imaging* 2000;12:776-783.
- Miyazaki M, Ichinose N, Sugiura S, Kassai Y, Kanazawa H, Machida Y. A novel MR angiography technique: swap phase encode extended data (SPEED) acquisition using half-Fourier RARE. *J Magn Reson Imaging* 1998;8:505-507.
- Miyazaki M, Takai H, Sugiura S, Wada H, Kuwahara R, Urata J. Peripheral MRA: separation of arteries from veins with flow-spoiled gradient pulses in electrocardiography-triggered three-dimensional half-Fourier fast spin-echo imaging. *Radiology* 2003;227:890-896.
- Ono A, Murase K, Taniguchi T, et al. Deep vein thrombosis using non-contrast-enhanced MR venography with electro-cardiographically-gated three-dimensional half-Fourier FSE: preliminary experience. *Magn Reson Med* 2009;61:907-917.
- Carr HY. Steady-state free precession in nuclear magnetic resonance. *Phys Rev* 1958;112:1693-1701.
- Scheffler K, Lehnardt S. Principles and applications of balanced SSFP techniques. *Eur Radiol* 2003;13:2409-2418.
- Nishimura DG, Macovski A, Pauly JM, Conolly SM. MRA by selective inversion recovery. *Magn Reson Med* 1987;4:193-202.
- Edelman RR, Siewert B, Adamis M, Gaa J, Laub G, Wiclopolski P. Signal targeting with alternating radiofrequency (STAR) sequences: application to MRA. *Magn Reson Med* 1994;31:233-238.
- Kanazawa H, Miyazaki M. Time-spatial labeling inversion tag (t-SLIT) using a selective IR-tag on/off pulse in 2D and 3D half-Fourier FSE as arterial spin labeling. In: Proceedings of the 10th Annual Meeting of ISMRM, Honolulu, 2002. (abstract 140).
- Stuber M, Bornert P, Spuentrup E, Botnar RM, Manning WJ. Selective three-dimensional visualization of the coronary arterial lumen using arterial spin tagging. *Magn Reson Med* 2002;47:322-329.
- Yui M, Miyazaki M, Kanazawa H, Okamoto K. Aortic arch to intracranial 3D MRA with t-SLIT 3D-SSFP using a neurovascular-attached QD head SPEEDER coil. In: Proceedings of the 12th Annual Meeting of ISMRM, Kyoto, 2004. (abstract 2121).
- Miyazaki M, Lee VS. Non-contrast-enhanced magnetic resonance angiography: state-of-the-art. *Radiology* 2008;248:20-43.
- Wedeen VJ, Meuli RA, Edelman RR, et al. Projective imaging of pulsatile flow with magnetic resonance. *Science* 1985;230:946-948.
- Meuli RA, Wedeen VJ, Geller SC, et al. MR gated subtraction angiography: evaluation of lower extremities. *Radiology* 1986;159:411-418.
- Constable RT, Gore JC. The loss of small objects in variable TE imaging: implications for FSE, RARE, and EPI. *Magn Reson Med* 1992;28:9-24.
- Hinks RS, Constable RT. Gradient moment nulling in fast spin echo. *Magn Reson Med* 1994;32:698-706.
- Kawanami S, Nakamura K, Miyazaki M, Sugiura S, Yamamoto S, Nakata H. Flow-weighted MRI of the Lungs with the ECG-gated half-Fourier FSE technique: evaluation of the effect of the cardiac cycle. *Magn Reson Med Sci* 2002;1:137-147.
- Suga K, Ogasawara N, Okada M, Tsukuda T, Matsunaga N, Miyazaki M. Lung perfusion impairments in pulmonary embolic and airway obstruction with noncontrast MR imaging. *J Appl Physiol* 2002;92:2439-2451.
- Furudate N, Miyazaki M. FBI-Navi for easy determination of diastolic and systolic triggering phases in non-contrast fresh blood imaging (FBI). In: Proceedings of the 17th Annual Meeting of ISMRM, Toronto, 2008. (abstract 2902).
- Urata J, Wada H, Kuwahara R, Miyazaki M, Nishiharu T, Yamashita Y. Evaluation of lower extremity arterial diseases using flow-dephasing spoiler gradient pulses in ECG-triggered 3D half-Fourier FSE: initial experience. In: Proceedings of the 10th Annual Meeting of ISMRM, Honolulu, 2002. (abstract 1750).
- Lim RP, Hecht EM, Xu J, et al. 3D Non-gadolinium enhanced ECG-gated MRA of the distal lower extremities: preliminary clinical experience. *J Magn Reson Imaging* 2008;28:181-189.
- Nakamura K, Miyazaki M, Kuroki K, Yamamoto A, Hiramine A, Admiraal-Behloul F. Non-contrast-enhanced peripheral MRA: technical optimization of flow-spoiled fresh blood imaging for screening peripheral arterial diseases. *Magn Reson Med* 2011;65:595-602.



32. Haneder S, Attenberger UI, Riffel P, Henzler T, Schoenberg SO, Michaely HJ. Magnetic resonance angiography (MRA) of the calf station at 3.0 T: intraindividual comparison of non-enhanced ECG-gated flow-dependent MRA, continuous table movement MRA and time-resolved MRA. *Eur Radiol* 2011;21:1452-1461.
33. Gutzelt A, Stutter R, Froehlich JM, et al. ECG-triggered non-contrast-enhanced MR angiography (TRANCE) versus digital subtraction (DSA) in patients with peripheral arterial occlusive disease of the lower extremities. *Eur Radiol* 2011;21:1979-1987.
34. Storey P, Atanasova I, Lim RP, Xu J, Chen Q, Lee VS. Tailoring the flow sensitivity of fast spin-echo sequences for non-contrast-enhanced peripheral MRA. *Magn Reson Med* 2010;64:1098-1108.
35. Ono A, Murase K, Taniguchi T, et al. Deep vein thrombosis: diagnostic value of non-contrast-enhanced MR venography using electrocardiography-triggered three dimensional half-Fourier PSE. *Magn Reson Med* 2010;64:88-97.
36. Fan Z, Sheehan J, Bi X, Liu X, Carr J, Li D. 3D noncontrast MR angiography of the distal lower extremities using flow-sensitive dephasing (FSD)-prepared balanced SSFP. *Magn Reson Med* 2009;62:1523-1532.
37. Edelman RR, Sheehan JJ, Dunkle E, Schindler N, Carr J, Koktzoğlu I. Quiescent-interval single-shot unenhanced magnetic resonance angiography of peripheral vascular disease: technical considerations and clinical feasibility. *Magn Reson Med* 2010;63:951-958.
38. Sheehan JJ, Fan Z, Davarpanah AH, et al. Nonenhanced MR angiography of the hand with flow-sensitive dephasing-prepared balanced SSFP sequence: initial experience with systemic sclerosis. *Radiology* 2011;256:248-256.
39. Wielopolski PA, Adamis M, Prasad P, Gaa J, Edelman R. Breath-hold 3D STAR MR angiography of the renal arteries using segmented echo planar imaging. *Magn Reson Med* 1995;33:432-438.
40. Radermacher J, Chavan A, Bleck J, et al. Use of Doppler ultrasonography to predict the outcome of therapy for renal-artery stenosis. *N Engl J Med* 2001;344:410-417.
41. Olbricht CJ, Paul K, Prokop M, et al. Minimally invasive diagnosis of renal artery stenosis by spiral computed tomography angiography. *Kidney Int* 1995;48:1332-1337.
42. Garovic VD, Achauer MA, Kittner T, et al. Comparison of gadolinium-enhanced MR angiography to intraarterial digital subtraction angiography for evaluation of renal artery stenosis: results of a phase III multicenter trial. *J Magn Reson Imaging* 2010;31:390-397.
43. Spuentrup E, Manning WJ, Bornert P, Kissinger KV, Botnar RM, Stuber M. Renal arteries: navigator-gated balanced fast field-echo projection MRA with aortic spin labeling: initial experience. *Radiology* 2002;225:589-596.
44. Katoh M, Buecker A, Stuber M, Gunther RW, Spuentrup E. Free-breathing renal MRA with steady-state free-precession (SSFP) and slab-selective spin inversion: initial results. *Kidney Int* 2004;66:1272-1278.
45. Parienty I, Rostoker G, Jouniaux F, Plotin M, Admiraal-Behloul F, Miyazaki M. Renal artery stenosis evaluation in chronic kidney disease patients: nonenhanced time-spatial labeling inversion-pulse three-dimensional MR angiography with regulated breathing versus DSA. *Radiology* 2011;259:592-601.
46. Wyttenbach R, Braghetti A, Wyss M, et al. Renal artery assessment with nonenhanced steady-state free precession versus contrast-enhanced MR angiography. *Radiology* 2007;245:186-195.
47. Takahashi J, Tsuji Y, Hamada Y, et al. Non-contrast-enhanced renal MRA using time-spatial labeling pulse (t-SLIP) with 3D balanced SSFP. Proceedings of the 15th Annual Meeting of ISMRM, Berlin, 2007. (abstract 179).
48. Shonai T, Takahashi T, Ikeguchi H, Miyazaki M, Amano K, Yui M. Improved arterial visibility using STIR fat suppression in non-contrast-enhanced Time-Spatial Labeling Pulse (Time-SLIP) renal MRA. *J Magn Reson Imaging* 2009;29:1471-1477.
49. Lanzman RS, Voiculescu A, Walther C, et al. ECG-gated nonenhanced 3D steady-state free precession MR angiography in assessment of transplant renal arteries: comparison with DSA. *Radiology* 2009;252:914-921.
50. Shimada K, Isoda H, Okada T, Kamae et al. Unenhanced MR portography with a half-Fourier fast spin-echo sequence and time-space labeling inversion pulses: preliminary results. *AJR Am J Roentgenol* 2009;193:106-112.
51. Shimada K, Isoda H, Okada T, et al. Non-contrast-enhanced hepatic MRA with true steady-state free-precession and time spatial labeling inversion pulse: optimization of the technique and preliminary results. *Eur J Radiol* 2009;70:111-117.
52. Shimada K, Isoda H, Okada T, et al. Non-contrast-enhanced MRA for selective visualization of the hepatic vein and inferior vena cava with true steady-state free-precession sequence and time-spatial labeling inversion pulses: preliminary results. *J Magn Reson Imaging* 2009;29:474-479.
53. Shimada K, Isoda H, Okada T, et al. Non-contrast-enhanced MR portography with time-spatial labeling inversion pulses: comparison of imaging with three-dimensional half-Fourier fast spin-echo and true steady-state free-precession sequences. *J Magn Reson Imaging* 2009;29:1140-1146.
54. Ito K, Koike S, Shimizu S, et al. Intraportal Venous Flow Distribution: evaluation with single breath-hold ECG-triggered three-dimensional half-Fourier fast spin-echo MR imaging and a selective inversion-recovery tagging pulse. *AJR Am J Roentgenol* 2002;178:343-348.
55. Tsukuda T, Ito K, Koike S, Sasaki et al. Pre- and postprandial alterations of portal venous flow: evaluation with single breath-hold three-dimensional half-Fourier fast spin-echo MR imaging and a selective inversion recovery tagging pulse. *J Magn Reson Imaging* 2005;22:527-533.
56. Miyazaki M, Isoda H. Non-contrast-enhanced MR angiography of the abdomen. *Eur J Radiol* 2011 [Epub ahead of print].
57. Yamada S, Miyazaki M, Kanazawa H, et al. MRI visualization of cerebrospinal fluid movement with spin labeling: preliminary results in normal and pathophysiological conditions. *Radiology* 2008;249:644-652.
58. Ito K, Shimizu A, Tsukada T, et al. Evaluation of intraportal venous flow distribution by unenhanced MR angiography using three-dimensional fast spin-echo with a selective tagging pulse: efficacy of subtraction of tag-on and tag-off images acquired during a single breath-hold. *J Magn Reson Imaging* 2009;29:1224-1229.
59. Isogai J, Miyazaki M, Shimada T, et al. Non-contrast MRA of the toes using time-spatial labeling inversion pulse (time-SLIP) and optimization of flow-spoiled gradient pulses for the assessment of foot arteries in flow-spoiled fresh blood imaging (FBI). In: Proceedings of the 16th Annual Meeting of ISMRM, Toronto, 2008. (abstract 2901).
60. Hori M, Shraga N, Watanabe Y, et al., Time-resolved three-dimensional magnetic resonance digital subtraction angiography without contrast material in the brain: initial investigation. *J Magn Reson Imaging* 2009;30:214-218.
61. Akahane M, Sato J, Komatsu S, Watanabe Y, Satake Y, Ohtomo K. Nonenhanced time-resolved MR angiography for the arteriovenous malformation/fistula of the pelvis and the lower extremity. In: Proceedings of the 18th Annual Meeting of ISMRM, Stockholm, 2010. (abstract 3762).
62. Nakamura K, Yamamoto A, Nagashima R, Haraoka K, Miyazaki M. Non-contrast-enhanced whole-body MR angiography. In: Proceedings of the 18th Annual Meeting of ISMRM, Stockholm, 2010. (abstract 4441).
63. Vernickel P, Roschmarin P, Findeklec C, Ludeke KM, Overweg J, et al. Eight-channel transmit/receive body MRI coil at 3T. *Magn Reson Med* 2007;58:381-389.
64. Sung K, Nayak K. Measurement and characterization of RF non-uniformity over the heart at 3T using body coil transmission. *J Magn Reson Imaging* 2008;27:643-648.
65. Miyazaki M, Yamashita Y, Wheaton A, et al. Noncontrast MRA at 3T. In: Proceedings of the 19th Annual Meeting of ISMRM, Montreal, 2011. (abstract 3349).
66. Lanzman RS, Kropil P, Schmitt P, et al. Nonenhanced free-breathing ECG-gated steady-state free precession 3D MRA of the renal arteries: comparison between 1.5T and 3T. *AJR Am J Roentgenol* 2010;194:794-798.

## **ARTICLE 3**

## Magnetic Resonance Angiography at 3.0 Tesla: Initial Clinical Experience

Norbert G. Campeau, M.D., John Huston III, M.D., Matt A. Bernstein, Ph.D., Chen Lin, Ph.D., and  
Gordon F. Gibbs, M.D.

---

**Summary:** Magnetic resonance (MR) angiography has undergone significant development over the past decade. It has gone from being a novelty application of MR with limited clinical use to replacing catheter angiography in some clinical applications. One of the principal limitations inherent to all MR angiographic techniques is that they remain signal limited when pushed to the limits of higher resolution and short acquisition time. Developments in magnetic gradient hardware, coil design, and pulse sequences now are well optimized for MR angiography obtained at 1.5-T main magnetic field (B-field) strength, with acquisition times and imaging matrix size near their optimal limits, respectively. Recently, the United States Food and Drug Administration (FDA) approved use of clinical magnetic resonance imaging with main magnetic field strengths of up to 4 T. Before FDA approval, use of MR with magnetic field strengths much greater than 1.5 T was essentially reserved for investigational or research applications. The main advantage of high B-field imaging is a significant improvement in the signal-to-noise ratio (SNR), which increases in an approximately linear fashion with field strength in the range of 1.5 to 3.0 T. This increased SNR is directly available when performing MR angiographic acquisitions at higher magnetic field strengths, allowing for better resolution and conspicuity of vessels with similar acquisition times. Little has been reported on the benefits of performing MR angiography at magnetic field strengths >1.5 T. The purpose of this article is to summarize our current experience with intracranial and cervical MR angiographic techniques at 3.0 T. **Key Words:** Magnetic resonance angiography—3.0 Tesla.

---

Magnetic resonance (MR) angiography consists of several techniques using magnetic resonance pulse sequences specifically devised to provide angiographic contrast, allowing depiction and characterization of blood vessels (1). MR angiography is currently beginning its second decade of clinical development. The basis of MR angiographic contrast derived from time-of-flight (TOF) techniques and phase-contrast (PC) techniques reflects blood flow patterns and velocities, and remains distinct from contrast mechanisms that form the basis of conventional X-ray angiography. Newer contrast-enhanced (CE) MR angiographic techniques exploit the lumen-filling characteris-

tics of injected contrast, and the basis for angiographic contrast is physiologically similar to conventional angiography.

MR angiography has made substantial technical advances in the past decade and is now widely used in many clinical applications (2). Advances in scanner hardware including higher performance gradients with faster rise times, and greater maximum amplitudes have been very beneficial for MR angiography. Improvements in pulse sequence design and improved coil design also have greatly improved the quality of MR angiography possible today, even when compared to only a few years ago. Recently, high-resolution CE MR angiographic techniques have been developed that are of sufficient quality and resolution to allow MR angiography to replace conventional catheter angiography for preoperative evaluation of patients before endarterectomy at many institutions. One

---

From the Department of Radiology, Mayo Clinic and Foundation, Rochester, Minnesota, U.S.A.

Address correspondence and reprint requests to Dr. Norbert G. Campeau, Department of Radiology, Mayo Clinic, 200 First Street SW, Rochester MN, 55905, U.S.A.

of the main limitations of all MR angiographic techniques, however, is that they remain inherently signal limited when pushed to the limits of higher resolution with short acquisition time. The principal advantage of high B-field imaging is improvement in the signal-to-noise ratio (SNR), which increases in an approximately linear fashion with field strength in the range from 1.5 to 3.0 T.

The United States Food and Drug Administration (FDA) recently approved use of clinical magnetic resonance imaging (MRI) at magnetic field strengths of up to 4 T. Before this approval, imaging at higher B-fields typically was used only for investigation or research applications. With the change in FDA regulations, MRI and MR angiography now routinely can be acquired from patients in a clinical setting at such higher magnetic field strengths, yielding a significant improvement in available SNR. There have been some reports regarding MR angiography at low magnetic field strength (3), but little has been reported on the benefits of performing MR angiography at magnetic field strengths  $>1.5$  T (4). The purpose of this article is to summarize our current experience with intracranial and cervical MR angiographic techniques at 3.0 T.

### SIGNA VH/i 3.0-T MR SCANNER

All studies were performed on a commercially available Signa VH/i 3.0-T MR Scanner (General Electric Medical Systems, Waukesha, Wisconsin, U.S.A.), equipped with 40 mT/m, 150 T/m/s gradients, and a 28-cm-diameter transmit-receive birdcage head coil (5,6). A prototype transmit-receive cervical coil was supplied by Advanced Imaging Research Inc. (Cleveland, OH, U.S.A.). The scanner (Fig. 1) also is equipped with a higher order resistive shim set ( $z^2$ ,  $z^3$ ,  $xy$ ,  $xz$ ,  $yz$ , and  $x^2-y^2$ ) and autoshim software (7). Automated higher-order shimming is performed once at the start of each patient study and produces an extremely uniform magnetic field (shim), which is beneficial for imaging, MR angiography, and spectroscopy. The automated shimming process requires 10 seconds of scan time, with the remainder of the shimming process including volume of interest definition and analysis typically requiring approximately 2 minutes. The system has received 510(k) clearance from the FDA. Calorimetric experiments (8) performed with Institutional Review Board approval established a 14-W radiofrequency (RF) power limit for our specific head coil and power monitoring system. The 14-W limit accounts for both the FDA's 3 W/kg limit for the head, as well as power losses in the head coil. Thus, each coil has its own measured RF power limit. Preliminary development work adapting and optimizing pulse sequences for clinical imaging and MR angiography at 3.0 T began in August 1999. Routine clinical imaging of

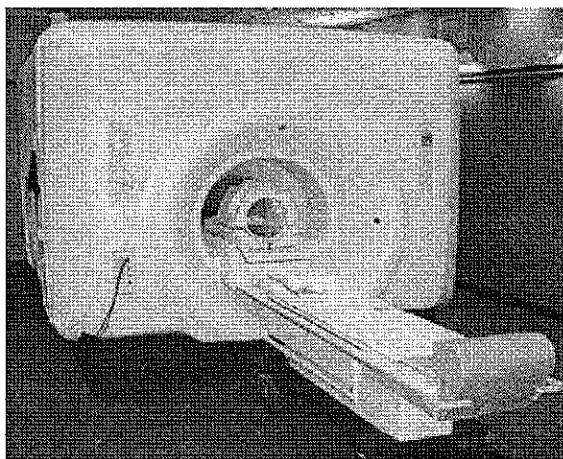


**FIG. 1.** Signa VH/i 3.0 T MR Scanner (General Electric Medical Systems). The scanner is equipped with a Magnex 3T-94 actively shielded magnet, 40 mT/m, 150 T/m/s gradients, and a 28-cm-diameter transmit-receive birdcage head coil. The bore aperture is 55 cm wide and 2.6 m in length. The scanner uses an operator console interface that is nearly identical to that used on 1.5-T Signa LX MR scanners.

patients began in October 1999, with a single shift schedule consisting of nine 1-hour examinations per day. The goal of this conservative scheduling was to provide generous imaging time for the 3.0-T examinations to perform extra sequences to optimize imaging at 3.0 T. At the time of manuscript preparation (January 2001),  $>2,300$  patients have been imaged on the 3.0-T scanner, with MR angiography performed on  $>350$  patients (approximately 15% of patients). The fraction of patients having MR angiography at 3.0 T will be increased in the future, as patients requiring MR angiography now are preferentially scheduled on the 3.0-T scanner rather than on a conventional 1.5-T scanner. Overall examination times at 3.0 T are similar to those at 1.5 T. If desired, patient throughput on the 3.0-T scanner can be similar to 1.5 T.

### INCREASED SNR AT 3.0 T

The principal advantage of high B-field imaging is improvement in SNR, which increases linearly with field strength in the range from 1.5 to 3.0 T. SNR measurements performed using phantoms demonstrated a slightly greater than twofold increase ( $2.03 \pm 0.06$ ) in SNR at 3.0 T compared to a conventional 1.5-T scanner (Signa LX; General Electric Medical Systems). These results (Fig. 2) are consistent with the expected linear increase in SNR with magnetic field strength. The advantages of this increased SNR are readily apparent, especially for MR angiographic applications, which are inherently, signal limited by necessity of high spatial resolution and short

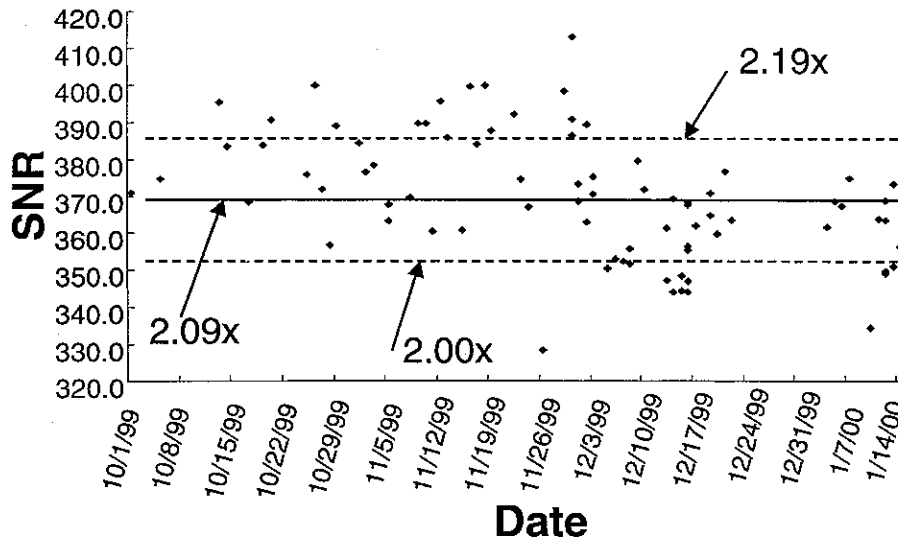


**FIG. 2.** Increased signal-to-noise ratio (SNR) at 3.0 T. The principal advantage of high B-field imaging is improvement in SNR, which increases linearly with field strength in the range from 1.5 to 3.0 T. Multiple SNR measurements performed using quality control phantoms demonstrated a slightly greater than two-fold increase ( $2.09 \pm 0.05$ ) in SNR at 3.0 T compared to a conventional 1.5-T scanner (Signa LX; GE Medical Systems). This increased SNR may be used to improve image resolution and decrease acquisition time.

acquisition time. SNR is essentially a “currency” that may be spent in various ways. SNR can be used to reduce acquisition time, improve spatial resolution, or a combination of both. For a given pulse sequence with identical imaging parameters, a single excitation (Nex) 3.0-T scan is equivalent to a 4-Nex 1.5-T scan. If the receiver bandwidth is doubled at 3.0 T to keep the chemical shift (measured in pixels) the same, then the 1-Nex 3.0-T scan is equivalent to a 2-Nex 1.5-T scan.

**LIMITATIONS OF IMAGING AT 3.0 T**

The main limitation of imaging at higher magnetic field strengths is RF heating, because specific absorption rate (SAR) or deposited RF energy scales approximately quadratically with the strength of the main magnetic field in the range from 1.5 to 3.0 T. The limitation of increased SAR is greatest for pulse sequences, which are RF intensive, such as fast spin echo (FSE) and fluid-attenuated inversion recovery (FLAIR), and results in acquisition of a decreased number of sections per unit time compared to 1.5 T. SAR limitations do not generally limit MR angiographic techniques at 3.0 T, and TOF, PC, and CE techniques can all be performed with similar imaging volumes and similar number of sections (Tables 1 and 2). SAR effects currently restrict use of magnetization transfer (MT) at 3.0 T, but these limitations can be overcome using special techniques for applying the MT pulse (9).

Additional limitations of imaging at 3.0 T compared to 1.5 T include an increase in the magnitude of the susceptibility changes (Fig. 3), and a doubling of chemical shift artifact. The magnitude of the chemical shift and suscep-

tibility effects may be restored to values similar to 1.5-T imaging by doubling the receiver bandwidth. A 3.0-T scan with double the receiver bandwidth still has approximately 40% higher SNR than a similar scan performed at 1.5 T.

Currently, there is a paucity of MRI safety data at 3.0 T for biomedical implant devices, implanted metallic su-

**TABLE I.** 1.5-T versus 3.0-T two-dimensional, time-of-flight, magnetic resonance angiographic pulse sequence parameters

Parameter	1.5 T	3.0 T
Pulse sequence	SPGR	Fast SPGR
TR (ms)	38	27
TE (ms)	8.7 fractional echo	8.8 fractional echo
Flip angle	60°	40°
Scan plane	Axial	Axial
Matrix (frequency × phase)	256 × 128	256 × 128
Number of excitations (Nex)	1	1
Field of view (cm)	16	40
Phase field of view	1.0	0.5
Section thickness (mm)	1.5	1.5
Number of locations	80	80
Saturation band (mm thick)	40	40
Frequency direction	Antero-posterior	Antero-posterior
Bandwidth (kHz)	16	16
Options	Flow compensation Sequential saturation band	Flow compensation Sequential saturation band Variable bandwidth
Scan time (min)	7:06	4:45

For the 3.0-T acquisition, the TR and flip angle are reduced to account for the increased saturation occurring from the magnetic field-dependent increase in the T1 relaxation times. The reduced TR results in a shorter acquisition time for the 3.0-T scan compared to a comparable 1.5-T scan.

**TABLE 2.** 1.5-T versus 3.0-T three-dimensional, time-of-flight, multiple overlapping thin slabs acquisition, magnetic resonance angiographic pulse sequence parameters

Parameter	1.5 T	3.0 T
Pulse sequence	SPGR	SPGR
Mode	3D	3D
TR (ms)	43	38
TE (ms)	6.9	3.4
Flip angle	25°	25°
Scan plane	Axial	Axial
Matrix (frequency × phase)	256 × 224	288 × 224
Number of excitation (Nex)	1	1
Field of view (cm)	18	18
Phase field of view	0.9	0.9
Section thickness (mm)	1.4	1.4
Locations per slab/overlap	23/6	23/6
Frequency direction	Antero-posterior	Antero-posterior
Bandwidth (kHz)	16	16
Options	Flow compensation Magnetization transfer Zip 512 (frequency and phase directions)	Flow compensation Variable bandwidth Zip 512 (frequency and phase directions)
	Zip 2 (Z direction)	Zip 2 (Z direction)
	Extended dynamic range	Extended dynamic range
Scan time	4:08 min per slab (2 slabs for COW) (3 slabs for COW + VB)	4:02 min per slab (2 slabs for COW) (3 slabs for COW + VB)

The 3.0-T acquisition uses a slightly shorter TR, with similar flip angle. The TE is chosen such that fat and water are out of phase. Because water and fat will move into and out of phase twice as often at 3.0-T, the TE for the 3.0-T acquisition was chosen to be approximately half that of the 1.5-T acquisition. The spatial resolution is increased for the 3.0-T acquisition, resulting in decreased intravoxel dephasing artifact due to the decreased heterogeneity of spins within the smaller voxels.

COW, circle of Willis; VB, vertebrobasilar system; Zip, zero fill interpolation.

tures, aneurysm clips, and metallic prostheses (Fig. 4). This poses an additional minor limitation to performing MRI at 3.0 T, resulting in the occasional need to reschedule MR examinations on a 1.5-T scanner due to lack of safety data. As results from testing of such devices become available, this limitation will become less prevalent in the future. There is also a slight increase in the incidence of claustrophobia on the 3.0-T scanner, resulting from the smaller 55-cm-diameter magnet bore of the 3.0-T scanner compared to the 60-cm bore aperture for a conventional 1.5-T scanner (Signa LX; GE Medical Systems). There is also a slightly increased incidence of patients not fitting into the 3.0-T scanner, also resulting from the smaller 55-cm magnet bore diameter of the 3.0-T scanner. The MRI/MR angiographic examinations for these pa-

tients usually are completed satisfactorily on the wider-bore 1.5-T scanner.

### MAGNETIC FIELD-DEPENDENT CHANGES IN T1 RELAXATION TIMES

T1 relaxation times are largely field strength dependent (10). The value of the T2 relaxation times generally remains unchanged or decreases slightly with magnetic field strength. In our experience, the T1 relaxation time of brain parenchyma increases by 25–40% from 1.5 to 3.0 T. The T1 of some materials, such as cerebrospinal (CSF) fluid, blood, and solutions of gadolinium chelates, also remains essentially unchanged with magnetic field strength. The observed changes in the relaxation times are beneficial for MR angiography at 3.0 T, resulting in better background suppression with preserved signal from the vessels. These magnetic field dependent effects on the T1 relaxation times are beneficial for MR angiography performed at higher field strengths. The differential changes in T1 values between blood and brain parenchyma can lead to an increase in vascular conspicuity that is complementary to the effects resulting from the increased SNR available at 3.0 T on the basis of magnetic field strength alone.

Similarly, the conspicuity of contrast enhancing areas is more prominent at 3.0 T compared to 1.5 T, because of the differential magnetic field strength-dependent changes in the T1 relaxation times for nonenhancing background tissues and enhancing parenchyma and vessels. In our experience, parenchymal contrast enhancement at 3.0 T is similar to that resulting from administration of triple dose of gadolinium at 1.5 T (5). This latter effect is beneficial for both conventional MRI and contrast-enhanced MR angiography (CE MR angiography) at 3.0 T. Specifically, in the case of CE MR angiography, this leads to improved conspicuity of CE vessels at 3.0 T compared to similar acquisitions obtained at 1.5 T.

### MR ANGIOGRAPHIC IMAGING TECHNIQUES AT 3.0 T

All of the principal MR angiographic imaging techniques currently available at 1.5 T for MR angiography of the circle of Willis, vertebrobasilar system, and cervical carotid arteries, as well as MR venography (MRV) of the intracranial veins and dural venous sinuses, have been implemented on our 3.0-T scanner. This includes techniques based on TOF, PC, and bolus gadolinium CE MR angiography. The main benefit of higher field MR angi-

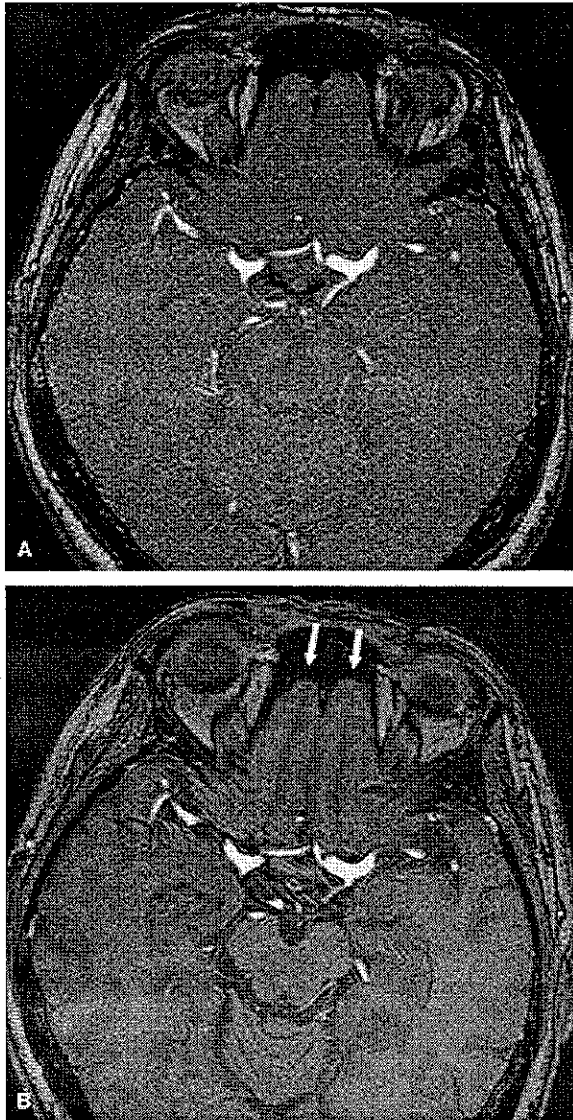


**FIG. 3.** Increased susceptibility changes at 3.0 T. Axial 3D time-of-flight (TOF) source images obtained at similar levels from the same patient at 1.5 T (A) and 3.0 T (B) demonstrate mildly increased susceptibility artifact on the 3.0-T image (arrows). The susceptibility artifact is most prominent at air-bone interfaces. It once was believed that susceptibility artifact at 3.0 T would be so severe that it would preclude clinical imaging at such field strengths. This is not the case, and susceptibility artifact typically does not result in significant degradation of MR angiographic acquisitions at 3.0 T. The magnitude of the susceptibility effects may be restored to values identical to 1.5-T imaging by doubling the receiver bandwidth on the 3.0-T acquisition. A 3.0-T scan with double the receiver bandwidth still has 40% higher SNR than a similar scan performed at 1.5 T. The increased SNR of the 3.0-T image (B) is readily apparent and yields a substantial improvement in anatomic depiction, vascular conspicuity, improved gray-white matter differentiation, and better discrimination between brain parenchyma and cerebrospinal fluid compared to the 1.5-T image (A). The 3.0-T TOF images are more prone to flow-related artifacts than images from 1.5-T acquisitions (see Fig. 13).

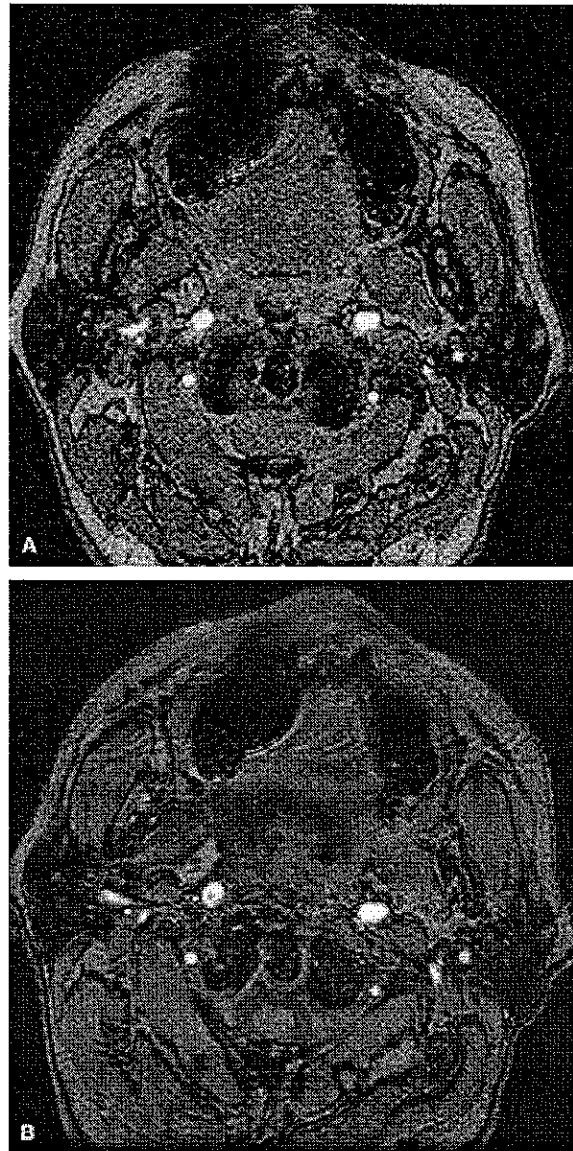


**FIG. 4.** Metallic dental artifact from 3D time-of-flight source images obtained at a similar location in the same patient at 1.5 T (Fig. 4A) and 3.0 T (Fig. 4B) is comparable at the two field strengths. Although metallic artifact is generally more marked at 3.0 T than at 1.5 T, it usually does not result in significant degradation of MR angiographic acquisitions. Note the improved signal-to-noise ratio and better anatomic depiction of structures on the 3.0-T image (Fig. 4B). To date, we have not imaged any patients with intracranial aneurysm clips because of safety concerns. There currently is a paucity of data available at 3.0 T regarding the safety of performing MR examinations on patients with surgically implanted metallic clips, sutures, and biomedical devices, which precludes examination of such patients at 3.0 T.

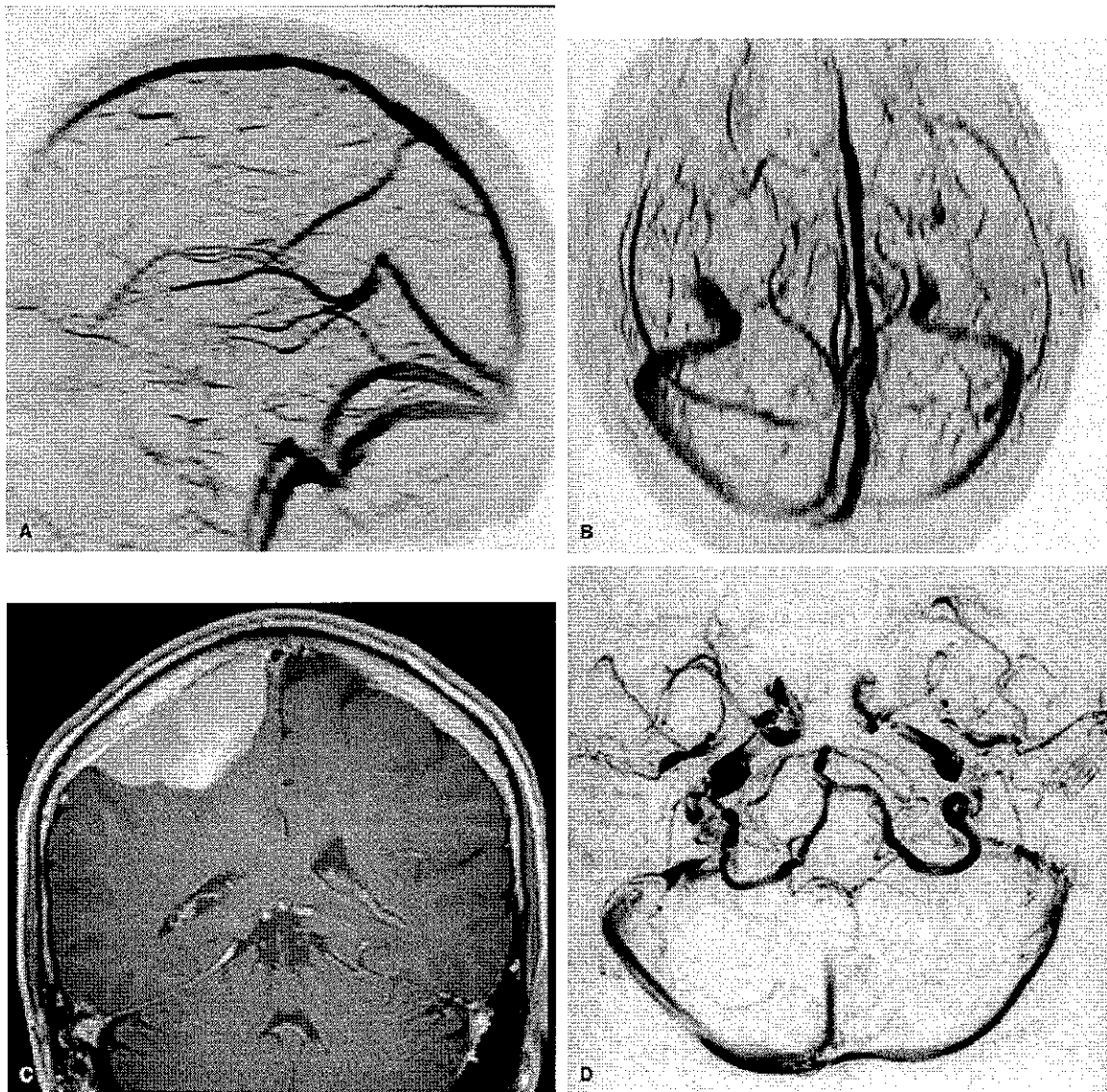


**FIG. 5.** Two-dimensional time-of-flight (TOF) magnetic resonance venography (MRV) at 3.0 T. The principal use of 2D TOF for intracranial applications is for MRV of the intracranial veins and major dural venous sinuses. Oblique sagittal maximum intensity projection (MIP) (A) and superior MIP (B) from a 3.0-T 2D TOF MRV in a patient with a right parasagittal meningioma (C). There is no evidence of sinus occlusion; however, the meningioma displaces a portion of the superior sagittal sinus and results in some mass effect upon the right vein of Trolard (A,B: arrows). The left transverse sinus is congenitally small and is best seen on an axial slab 2D phase-contrast MRV (D), obtained in the same patient at 3.0 T. Our MRV protocol for evaluation of sinus thrombosis at 3.0 T typically includes at least one phase-contrast acquisition in addition to the TOF acquisition.

ography is that the available increased SNR allows acquisition of a higher-resolution acquisition matrix with similar imaging time.

### TOF TECHNIQUES

TOF MR angiographic techniques are based on contrast provided by flow-related enhancement, which is derived

from entry of unsaturated (fully magnetized) blood into an imaging section of interest in which the magnetization of stationary tissue is saturated. All TOF sequences, including two-dimensional (2D), three-dimensional (3D), and multiple overlapping thin slab acquisition (MOTSA), rely on flow-related enhancement as the basis for their contrast.



## TWO-DIMENSIONAL TOF

Two-dimensional TOF techniques were introduced in 1989 (11) and basically consist of acquiring a stack of contiguous or slightly overlapped 2D sections. The technique is best suited for applications where the orientation of each 2D section is perpendicular to the long axis of the vessel of imaging interest. Two-dimensional TOF typically has been used for MR angiography of the cervical carotid arteries, which can take advantage of this preferred geometry. Two-dimensional TOF has relatively poor spatial resolution, but better temporal resolution, than 3D TOF techniques, which is beneficial for imaging rapid pulsatile flow typically present within the cervical carotid arteries.

Two-dimensional TOF differs from conventional multislice spin echo in that slices are acquired sequentially one after each other, and not simultaneously. The sequence parameters are chosen to maximize the flow-related enhancement of in-flowing unsaturated blood, yielding a dark background with bright vessels. Vessels that course within the axial 2D section may become magnetically saturated and lose signal intensity. Once a stack of slices has been acquired, a 3D angiogram is generated using a maximum intensity projection (MIP) algorithm. Use of saturation bands in combination with 2D TOF techniques may be used to suppress signal from either venous or arterial structures. This is typically done by placing the saturation band immediately below or above the imaging volume of interest, respectively. The effectiveness of the saturation bands is best when they are applied orthogonal to the principal direction of blood flow. The parameters used for 2D TOF MR angiographic acquisitions at 1.5 and 3.0 T are listed in Table 1.

The principal use of 2D TOF for intracranial applications is for MR venography (MRV) of the veins and major dural venous sinuses (Fig. 5).

Our 3.0-T scanner does not currently have a body coil (planned development in 2001); therefore it requires use of coils that have transmit-receive capability. Recently, a transmit-receive volume neck coil for use at 3.0 T was developed (Advanced Imaging Research Inc., Cleveland, OH, U.S.A.). This coil is suitable for performing cervical MR angiography at 3.0 T and has been used to acquire 2D TOF images of the cervical carotid and vertebral arteries (Fig. 6). The 2D TOF also is used as part of the cervical MR angiographic protocol, mainly as a scout for the bolus gadolinium MR angiography of the cervical carotid and vertebral arteries (Fig. 7).

## THREE-DIMENSIONAL TOF

Three-dimensional TOF is ideal for imaging the intracranial circulation, including the circle of Willis and ver-

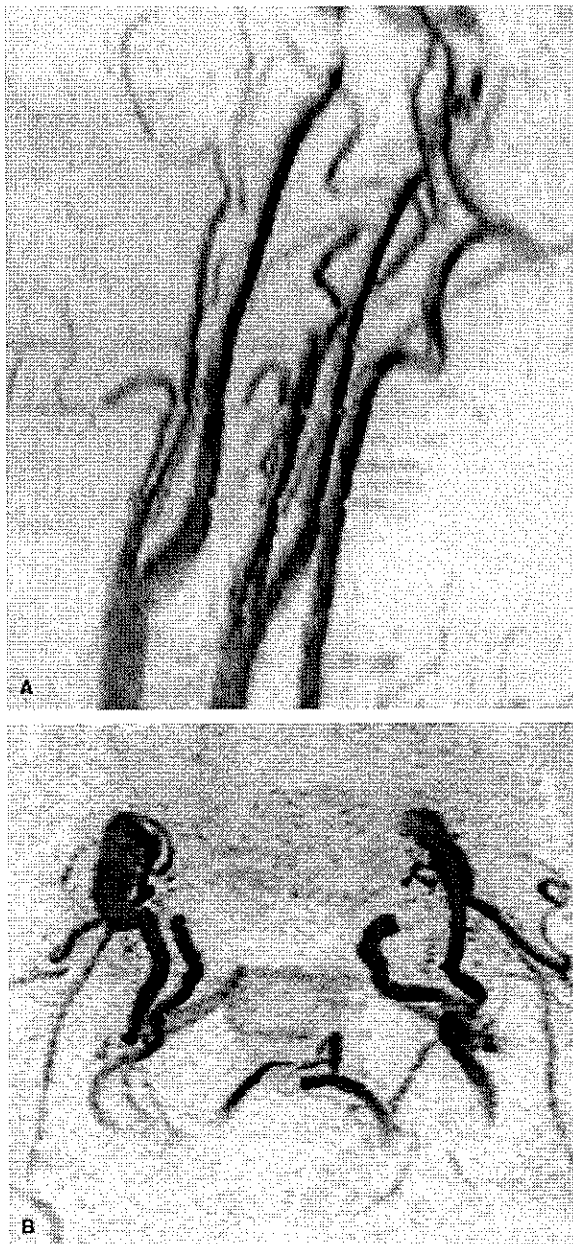
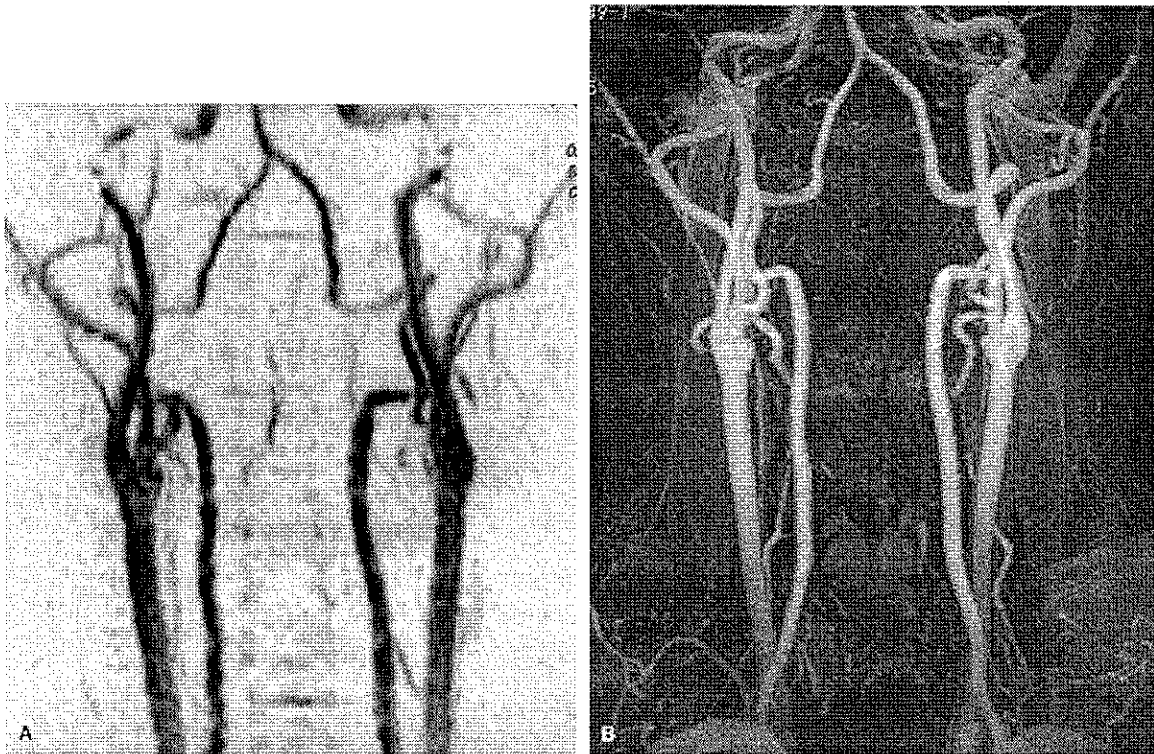


FIG. 6. Two-dimensional time-of-flight (TOF) cervical MR angiography at 3.0 T. Oblique sagittal maximum intensity projection (A) and axial collapse (B) from a 3.0-T 2D TOF MR angiographic acquisition obtained in a patient with minimal atheromatous involvement of the carotid bifurcations. This study was obtained using a transmit-receive volume neck coil. Development of a body coil (planned for 2001) will allow use of receive-only coils, which may yield additional improvement in image quality. The appearance and interpretation of these images is similar to that at 1.5 T.



**FIG. 7.** Comparison of 3.0-T 2D time-of-flight (TOF) cervical MR angiography with 3.0-T bolus gadolinium contrast-enhanced cervical MR angiography acquired from the same patient. **A:** Coronal 2D TOF maximum intensity projection. **B:** Corresponding coronal projection from a bolus gadolinium cervical MR angiography. No vascular abnormality is identified. In this case, the 2D TOF cervical MR angiography was acquired as part of the bolus gadolinium contrast-enhanced cervical MR angiographic protocol. The role of the 2D TOF cervical MR angiography is twofold. First, the axial collapse (not shown) serves as a scout image used to prescribe the bolus gadolinium cervical MR angiography, ensuring that the vertebral and carotid arteries are completely included in the acquired volume. Second, a stenosis that is associated with the presence of a flow void on the 2D TOF images usually is indicative of a surgically significant stenosis. The bolus gadolinium cervical MR angiography (**B**) yields excellent anatomic depiction that is clearly better than that obtained with the 2D TOF technique (**A**). An elliptic centric phase-encoding algorithm allows MR angiographic acquisitions with excellent venous suppression.

tebrobasilar system. Three-dimensional TOF MR angiography has already demonstrated significant clinical utility, such as examining patients with suspected aneurysms, following-up aneurysms, and evaluating vascular malformations. Compared with 2D TOF techniques, single-slab 3D TOF is more prone to signal loss due to flow saturation. One way to overcome this limitation is to use MOTSA, which provides decreased sensitivity to the effects of flow saturation but preserves the increased SNR available from a 3D technique, resulting in better images (12). MOTSA provides a good compromise between the increased SNR available with a 3D technique with less effects of saturation and is used for routine intracranial TOF imaging at our institution (Fig. 8). The parameters used for 3D TOF MR angiography for 1.5- and 3.0-T acquisitions are listed in Table 2.

#### DIFFERENCES BETWEEN TOF MR ANGIOGRAPHY AT 1.5 AND 3.0 T

##### Increased background suppression at 3.0 T

Pulse sequences used for TOF acquisitions consist of gradient-recalled echo sequences with flow compensation. Parameters that affect the degree of background saturation (suppression) include the repetition time (TR) and flip angle. When TR becomes shorter than the longitudinal relaxation times (T<sub>1</sub>) of the tissues imaged, magnetization becomes saturated. For a given TR, tissues with longer T<sub>1</sub> relaxation times will demonstrate greater saturation. Typical TR for TOF pulse sequences range from 20 to 50 ms, which is shorter than any T<sub>1</sub> within physiological tissues, except perhaps areas of gadolinium enhancement or methemoglobin associated with subacute hemorrhage. As

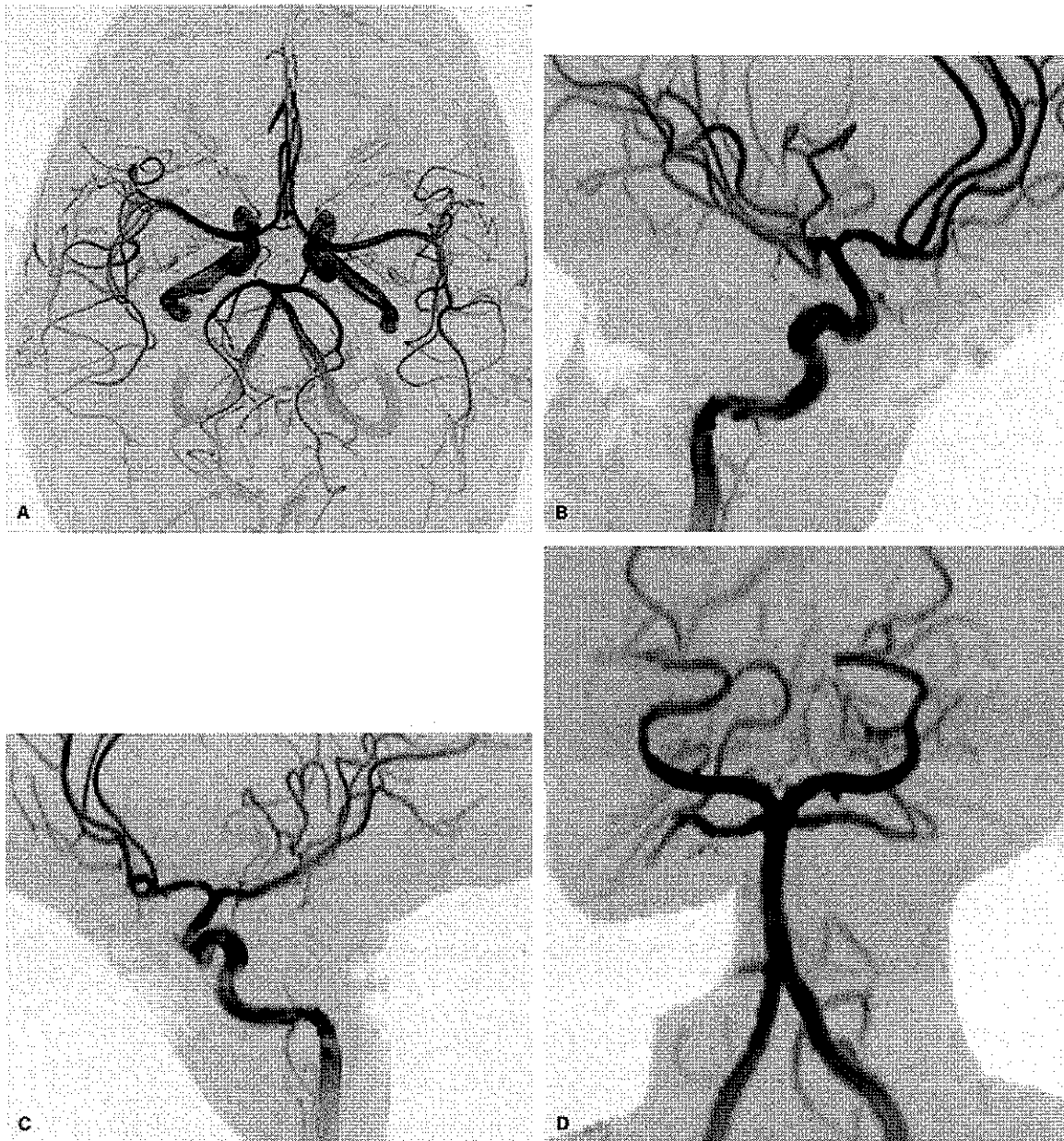


**FIG. 8.** Three-dimensional time-of-flight (TOF) MR angiography of the intracranial circulation including the circle of Willis and vertebrobasilar system acquired at 3.0 T in a 17-year-old boy being evaluated for headaches. The axial maximum intensity projection (MIP) collapse (A), MIP subvolumes from the right (B) and left (C) anterior intracranial vascular territories, and vertebrobasilar system (D) demonstrate the high quality of 3D TOF MR angiography possible at 3.0 T. The study is normal, with no evidence of aneurysm or hemodynamically significant stenosis. Note the excellent background suppression and excellent conspicuity of the vascular structures. This implementation of 3D TOF MR angiography uses the multiple overlapping thin slab acquisition technique, which provides a compromise between the increased SNR available with a 3D technique having less saturation effects.

mentioned earlier, the T1 relaxation times for most tissues are dependent on the magnetic field strength and are longer for higher magnetic field strengths. Because the T1 relaxation time of brain parenchyma increases approximately

25–40% from 1.5 to 3.0 T, with little change in the T1 of blood, there is a differential decrease in the relative difference. Therefore, for a given TR there will be greater background suppression at 3.0 T compared to 1.5 T (Fig. 9).

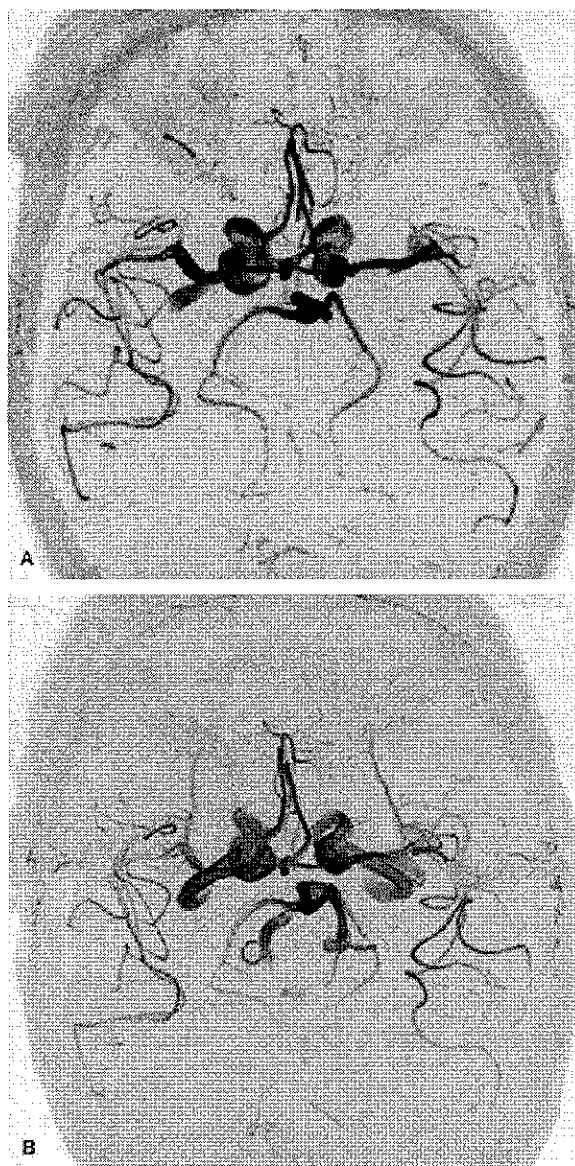


**FIG. 9.** Improved background suppression for 3D time-of-flight (TOF) MR angiography at 3.0 T. Comparison of 3D TOF MR angiography axial collapsed images from the same patient acquired at 1.5 T (A) and 3.0 T (B) demonstrates better suppression of background signal at 3.0 T. Part of the improved background suppression arises from observed magnetic field strength-dependent increases in the relaxation times of blood, cerebrospinal fluid, and brain parenchyma, which make these tissues more prone to saturation at 3.0 T when the pulse sequence repetition time TR is similar to that used at 1.5 T. The pulse sequence parameters used for these 1.5-T and 3.0-T acquisitions are listed in Table 2.

#### Effect on in-plane blood saturation

As the TR becomes shorter, blood traversing a given imaging volume will be subjected to more RF pulses. The contrast between fully saturated blood entering the slab

and the background will progressively decrease as the blood moves within the imaging volume. This will result in variation of contrast across the slab and potential complete saturation of blood remaining in the imaging plane for an extended duration. TR needs to be adjusted in order to compromise between the degree of background saturation and saturation of in-plane blood. At 3.0 T, there is little change in the T1 relaxation time of blood, making in-plane saturation effects similar at 1.5 and 3.0 T for similar slab thickness. Also, because there is more signal available at 3.0 T, fully saturated blood may be pulsed more often at 3.0 T before becoming completely saturated (Figs. 10 and 11).

#### Effect of flip angle on contrast

Similarly, for a given flip angle, the degree of background saturation will be greater at 3.0 T compared to 1.5 T. Both the degree of background suppression and blood saturation will depend on the magnitude of the flip angle. There is a trade-off between desired background suppression and the amount of blood saturation. A large flip angle approaching  $90^\circ$  will yield excellent background suppression, but flowing blood will not travel far before also becoming suppressed. A low flip angle prevents blood saturation, but does not provide good background suppression. The optimal flip angle depends on the application, with 3D TOF techniques using flip angles ranging from  $15^\circ$  to  $35^\circ$ , and 2D TOF techniques using flip angles ranging from  $40^\circ$  to  $90^\circ$ . Because the T1 relaxation time of tissues is dependent on the strength of the main magnetic field and increases with increasing field strength, it is generally beneficial to use lower flip angles for TOF MR angiographic techniques at higher field strength. By lowering the flip angle, saturation effects will be less prominent for MR angiography obtained at higher fields, while maintaining adequate background subtraction.

#### Thickness of imaging volume

The thickness of the imaging section will affect blood saturation, as the traversing blood will remain within a thicker volume for a longer duration of time, experiencing more TR pulses. The possibility for complete saturation of blood remaining in the imaging plane for an extended duration will increase with increasing volume thickness. Again, because there is little change in the T1 relaxation time of blood at 1.5 and 3.0 T, the in-plane saturation effects will be similar at 3.0 T compared to 1.5 T for blood vessels. Because of the differential increase in the T1 relaxation times of background tissue, the "venetian blind" effect between the MOTSA slabs is more obvious at 3.0 T compared to 1.5 T using our current acquisition parameters (Fig. 10). This venetian blind effect mildly reduces

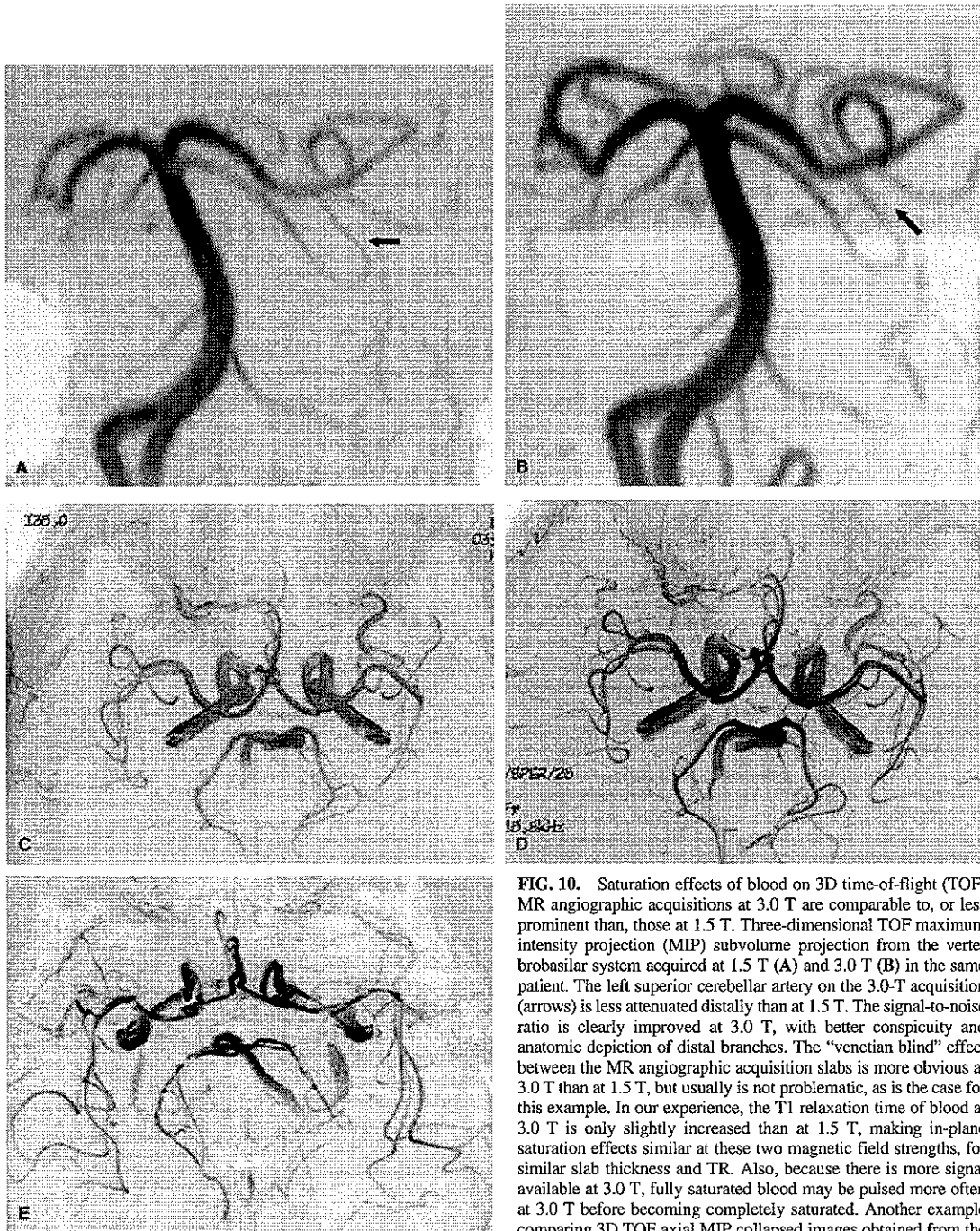


**FIG. 10.** Saturation effects of blood on 3D time-of-flight (TOF) MR angiographic acquisitions at 3.0 T are comparable to, or less prominent than, those at 1.5 T. Three-dimensional TOF maximum intensity projection (MIP) subvolume projection from the vertebrobasilar system acquired at 1.5 T (A) and 3.0 T (B) in the same patient. The left superior cerebellar artery on the 3.0-T acquisition (arrows) is less attenuated distally than at 1.5 T. The signal-to-noise ratio is clearly improved at 3.0 T, with better conspicuity and anatomic depiction of distal branches. The "venetian blind" effect between the MR angiographic acquisition slabs is more obvious at 3.0 T than at 1.5 T, but usually is not problematic, as is the case for this example. In our experience, the T1 relaxation time of blood at 3.0 T is only slightly increased than at 1.5 T, making in-plane saturation effects similar at these two magnetic field strengths, for similar slab thickness and TR. Also, because there is more signal available at 3.0 T, fully saturated blood may be pulsed more often at 3.0 T before becoming completely saturated. Another example comparing 3D TOF axial MIP collapsed images obtained from the same patient at 1.5 T (C) and 3.0 T (D) again demonstrates improved

visualization of flow in distal branches on the 3.0-T image. E: The 3D TOF axial MIP collapsed image obtained at 3.0 T in another patient demonstrates multiple areas of segmental narrowing presumed to represent intracranial atherosclerosis. There is good visualization of flow seen distal to several relatively high-grade stenoses.

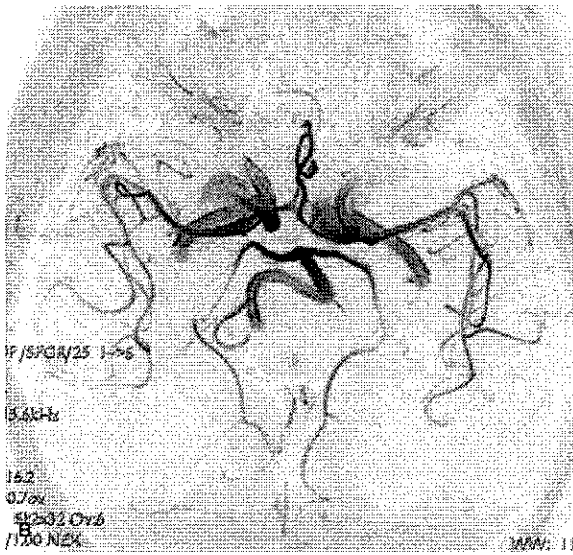
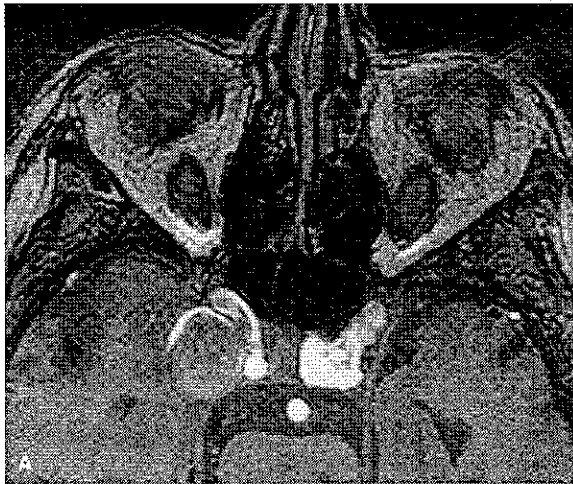


**FIG. 11.** Saturation effects can make evaluation of large or partially thrombosed aneurysms problematic with 3D time-of-flight (TOF) MR angiography. **A:** Axial source image from 3D time-of-flight (TOF) MR angiography acquired at 3.0 T demonstrates bilateral giant aneurysms of the cavernous portions of the internal carotid arteries. **B:** Maximum intensity projection axial collapsed image from the same acquisition fails to adequately depict the morphology of the aneurysms. Similar results would be expected for a 1.5-T 3D TOF MR angiographic acquisition.

the conspicuity of vessels in the distal portions of the acquisition slab on the 3.0-T MR angiographic acquisitions. Variation of TR across k-space may be helpful to improve the vessel/background contrast and reduce the venetian blind artifact, with the added benefit of reduced acquisition time (13,14).

#### Image matrix resolution

The size of the imaging matrix is limited in the frequency-encoding direction by low SNR and within the

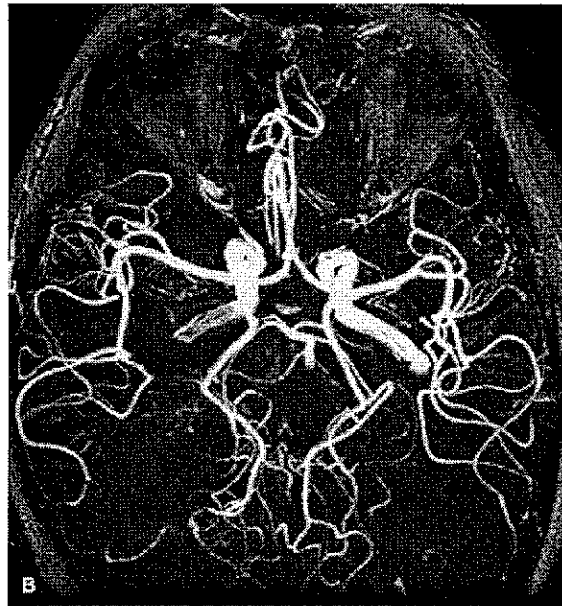
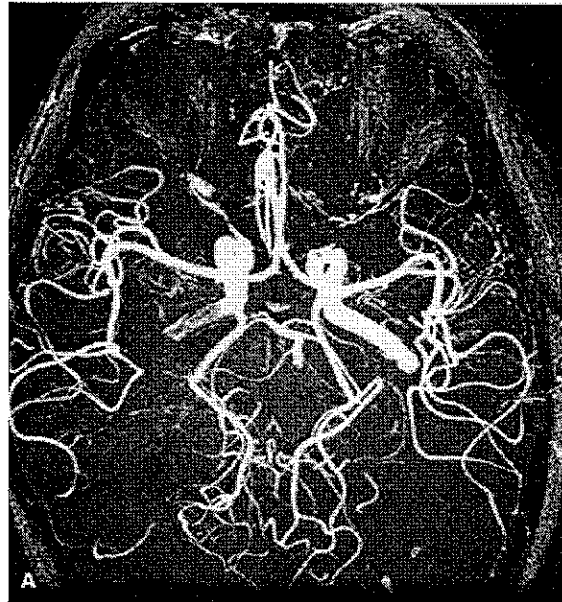


**FIG. 12.** Magnetization transfer (MT). Projection images from 3D time-of-flight (TOF) MR angiographic acquisitions obtained without (A) and with use of magnetization transfer (B); other parameters are identical. MT can be used to improve MR angiographic acquisitions by further suppressing background signal, resulting in improved conspicuity of vessels. MT is used on all 1.5-T 3D TOF MR angiographic acquisitions at our institution. Implementation of MT at 3.0 T has required modification of pulse sequences because of power deposition/specific absorption rate limitations and currently is not implemented into the clinical 3D TOF MR angiographic pulse sequence, but will be in the near future.

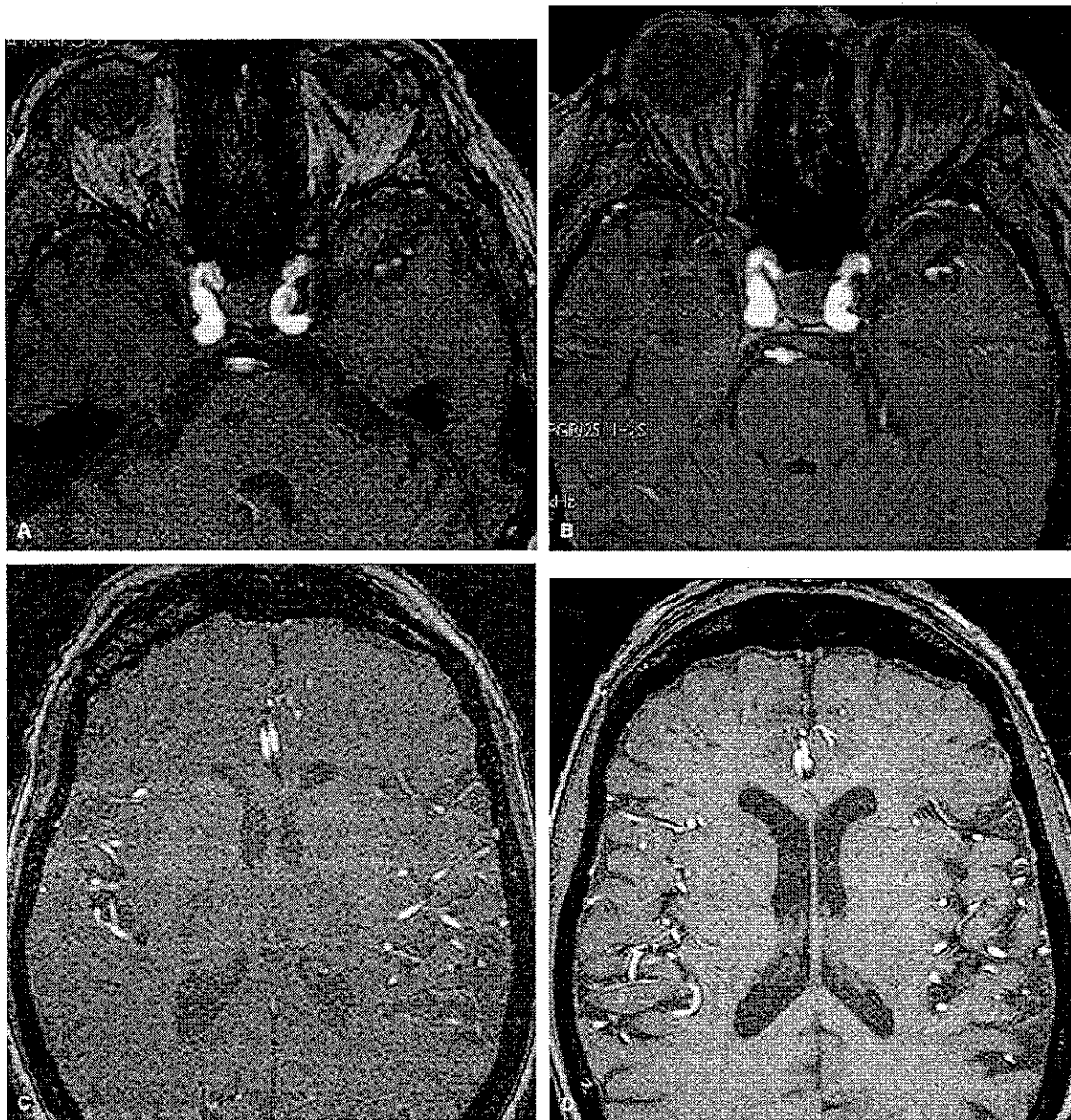


**FIG. 13.** Flow-related artifacts. Our current technique for 3D time-of-flight (TOF) MR angiography at 3.0 T uses a TE of 3.4 ms, which is approximately half that used in 1.5-T acquisitions (TE = 6.9 ms). This shorter TE reduces time available for flow compensation pulses. As a result, the 3.0-T MR angiographic images are more prone to flow-related artifacts. Source images from 3D TOF MR angiography obtained at 1.5 T (A) and 3.0 T (B) demonstrate increased vascular ghosting in the phase-encoding direction on the 3.0-T image. This typically is most marked at the level of the cavernous internal carotid arteries and circle of Willis (see Fig. 3). Additional examples of source images from comparable levels in another patient acquired at 1.5 T (C) and 3.0 T (D) demonstrate mildly increased flow artifact on the 3.0-T acquisition. The increased signal-to-noise ratio is clearly evident on the 3.0-T image.

phase-encoding direction by both SNR and acquisition time. Because SNR is increased at 3.0 T, the imaging matrix can be increased compared to 1.5 T. An additional benefit of increasing the size of the matrix is a reduction in the amount of partial voluming artifact. The smaller

voxels are less subject to the intravoxel dephasing artifact present with voxels that include greater heterogeneity of spins. Because of the increased SNR available at 3.0 T, use of higher spatial resolution can readily be obtained with reasonable acquisition times, taking advantage of the

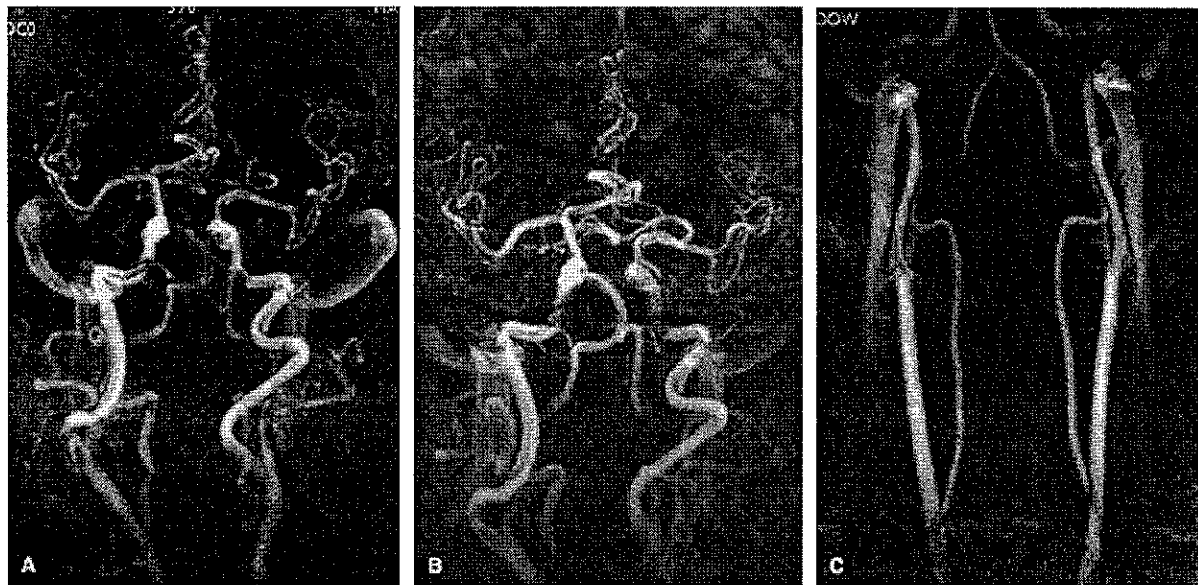


**FIG. 14.** Two-dimensional phase-contrast (PC) slab MR angiography. Use of 2D PC slab MR angiography at 3.0 T is similar to that at 1.5 T and is useful for providing initial scout images used in prescribing additional intracranial and cervical MR angiographic acquisitions. Comparison of coronal 1.5 T (A) and 3.0 T (B) 2D PC slab MR angiographic images from the same patient demonstrates increased noise on the 3.0-T image most prominent in the region of the cerebral hemispheres. A component of this is due to imaging of cerebrospinal fluid pulsatility on the 3.0-T acquisition due to increased sensitivity to slower flow for a given velocity-encoding gradient amplitude (VENC). C: The 3.0-T coronal 2D PC slab cervical MR angiography obtained using the transmit-receive volume neck coil. With suitable VENC, 2D PC slab MR angiography is useful as an adjunct to time-of-flight MRV acquisitions (see Fig. 5D).

synergistic benefits of less dephasing artifact within the smaller voxels.

#### Magnetization transfer

Magnetization transfer is a technique used to further reduce signal from background tissue, yielding improved conspicuity of vessels (9). The technique is beneficial for MR angiography at 3.0 T, providing additional suppression of background signal (Fig. 12). Implementation of magnetization transfer into the routine clinical MR angiographic pulse sequences currently is under way, but has required modification of pulse sequences because of power deposition/SAR limitations at 3.0 T. As such, magnetization transfer was not initially used into our routine 3D TOF MR angiographic acquisitions at 3.0 T, but will be in the near future.

#### Water-lipid chemical shift effects

There is a fixed chemical shift difference for protons within water and lipid of approximately 3.4 ppm, arising principally from the electronegativity of the unshielded electron pair in water. The water and lipid components precess at slightly different frequencies when placed in an identical external magnetic field. Protons from water and fat will first be in phase at each 4.7 ms at 1.5 T. The

Larmor frequency at 3.0 T is 127 MHz, or double that at 1.5 T (63.5 MHz). Therefore, at 3.0 T, fat and water will move into and out of phase twice as often at 3.0 T, or at every 2.35-ms interval. Three-dimensional TOF MR angiography is best performed with water and fat out of phase. Our current technique for 3D TOF MR angiography at 3.0 T uses a TE of 3.4 ms, which is approximately half that used in 1.5-T acquisitions (TE = 6.9 ms). Use of a shorter TE for 3.0-T acquisitions reduces the time available for applying flow compensation gradients, which may contribute to increased flow artifacts observed at 3.0 T. The 3.0-T MR angiographic images can be more prone to flow-related artifacts (Fig. 13) for a variety of reasons. One simple reason is the flow artifacts are less likely to be buried in the noise: a higher SNR also means a higher artifact-to-noise ratio.

#### PC MR ANGIOGRAPHIC TECHNIQUES

PC techniques differ from TOF techniques in that the basis of contrast is generated from addition of specially designed bipolar velocity- or flow-encoding gradients that yield predictable acquired phase differences for nonstationary tissues. For each RF excitation, the bipolar gradients are applied twice, with altered polarity, so that sta-



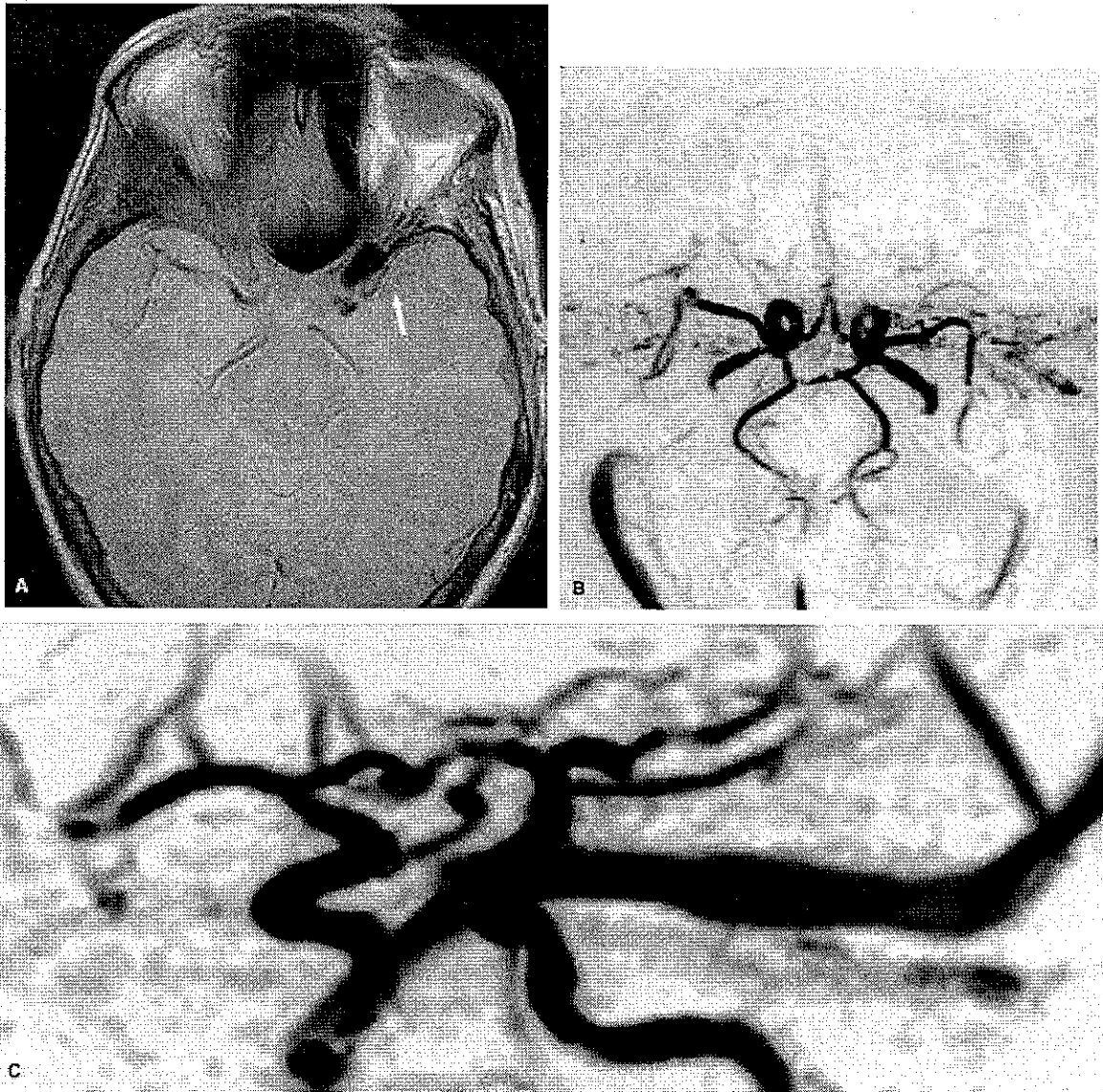


**FIG. 15.** Intracranial 3D phase-contrast (PC) MR angiography at 3.0 T. Three-dimensional PC MR angiography is used much less frequently than 3D time-of-flight (TOF) MR angiography for evaluation of the circle of Willis and vertebrobasilar system, largely due to the relatively long acquisition time compared to similar TOF-based MR angiography. Three-dimensional PC MR angiography often is performed when MR angiography is desired following administration of gadolinium, in which case the T1 relaxation effects of intravascular gadolinium significantly degrade TOF-based MR angiography, especially in the region of the cavernous sinuses where venous flow obscures detail of the cavernous internal carotid arteries. Such was the case in this example in which an axial 3.0-T proton density image (A) demonstrates an oblong signal void in the left juxtacavernous region (arrow), suspicious in appearance for an aneurysm. Three-dimensional PC MR angiographic axial collapse (B) and oblique maximum intensity projection (C) images of the circle of Willis were obtained at the same setting at 3.0 T. Gadolinium was administered before MR angiography. The 3D PC MR angiography demonstrates no evidence for aneurysm. Computed tomography (not shown) later showed findings were due to a pneumatized left clinoid process.

tionary spins do not acquire any phase (15,16). The velocity-encoding gradients result in a phase shift for moving spins that is dependent on the magnitude of the applied gradient and on both the direction and velocity of flow. These velocity-encoding gradients may be applied on any or all of three orthogonal axes. Generally, for quan-

titative analysis of flow, images sensitized to motion only in a single direction perpendicular to the imaging plane are acquired. For qualitative analysis, however, often images sensitive to flow in all three directions are acquired, and the square root of the sum of the squares is calculated to form an image sensitive to flow speed, regardless of the

TABLE 3. 1.5-T and 3.0-T two-dimensional, phase-contrast magnetic resonance angiographic parameters

Parameter	1.5 T	3.0 T
Pulse sequence	Phase contrast	Phase contrast
Mode	2D	2D
TR (ms)	40	40
TE	Minimum	Minimum
Flip angle	20°	20°
Scan plane	Axial or coronal	Axial or coronal
Matrix (frequency × phase)	512 × 256	512 × 256
Field of view (cm)	22	22
Phase field of view	0.7	0.75
Slab thickness (mm)	80–90	80–90
Frequency direction	Superior-inferior	Superior-inferior
Bandwidth (kHz)	32	32
Options	Flow reconstruction = complex VENC = 60 cm/s MR angiography VENC = 20 cm/s MR venography Collapse = on	Flow reconstruction = complex VENC = 60 cm/s MR angiography VENC = 20 cm/s MR venography Collapse = on
Scan time	2:45 min/4 Nex 3:05 min/6 Nex	2:45 min/4 Nex 3:05 min/6 Nex

These parameters are similar for 1.5-T and 3.0-T acquisitions. These acquisitions provide useful scout images for prescribing intracranial or cervical MR angiographic studies and are useful for MR venographic studies when a suitable VENC is chosen. VENC, velocity-encoding gradient magnitude.

direction of flow. The echo time (TE) for PC MR angiographic sequences usually is chosen as the minimum possible and will be similar for 1.5- and 3.0-T acquisitions because the time required to play out the velocity-encoding gradients depends largely on the rise time and maximal amplitude of the magnetic gradients and not the main magnetic field strength. For identical parameters, a 3.0-T PC MR angiographic acquisition will have twice the SNR of a 1.5-T acquisition. The value of the velocity-encoding gradient (VENC) may be reduced to increase sensitivity to slow flow. This feature is useful in the evaluation of venous thrombosis or thrombosed aneurysms, where TOF MR angiography often suffers from saturation effects. Although PC MR angiography can be sensitive to slow flow, use of a VENC that is too small can lead to aliasing in regions of higher flow rates. Use of a VENC that is too large decreases the sensitivity to slow flow. This usually necessitates separate studies for MR angiographic and MRV examinations. For a given VENC, however, slower flow will be better imaged at 3.0 T due to the increased signal available over a comparable 1.5-T acquisition, making a priori selection of a higher VENC less problematic at 3.0 T.

## TWO-DIMENSIONAL PC MR ANGIOGRAPHY

Two-dimensional PC imaging is used mainly for obtaining a scout image used in prescribing intracranial TOF MR angiographic pulse sequences (Fig. 14). It is useful in MRV as an adjunct to TOF MRV (Fig. 5D). Because the mechanism of contrast for PC MR angiographic tech-

niques depends solely on flow, it is less prone to false-negative results that may occur with TOF MR angiography in the setting of acute thrombus. In such cases, the high T1 signal of thrombus cannot be distinguished from fully magnetized in-flowing blood using TOF MR angiography. Benefits of PC MRV at higher field strength include increased SNR and better depiction of smaller vessels and slow flow.

The 2D PC techniques also may be used to provide quantitative CSF flow measurement. Quantitative CSF flow measurements obtained at the level of the cerebral aqueduct have been shown useful in the evaluation of normal pressure hydrocephalus.

## THREE-DIMENSIONAL PC MR ANGIOGRAPHY

Three-dimensional PC imaging may be used to evaluate intracranial arterial flow, although it is generally inferior to 3D TOF techniques because of decreased resolution and increased sensitivity to degradation by pulsed or disturbed flow (17). In our clinical practice, use of 3D PC MR angiography for evaluation of the circle of Willis and vertebrobasilar system typically is reserved for MR angiographic acquisitions obtained following administration of gadolinium. In such cases, TOF MR angiographic acquisitions usually are substantially degraded from the presence of venous structures, which cannot be suppressed adequately due to the marked T1 shortening of blood resulting from intravascular gadolinium. With careful selection of the velocity-encoding gradients, the 3D PC technique in the postgadolinium setting is less "contaminated"

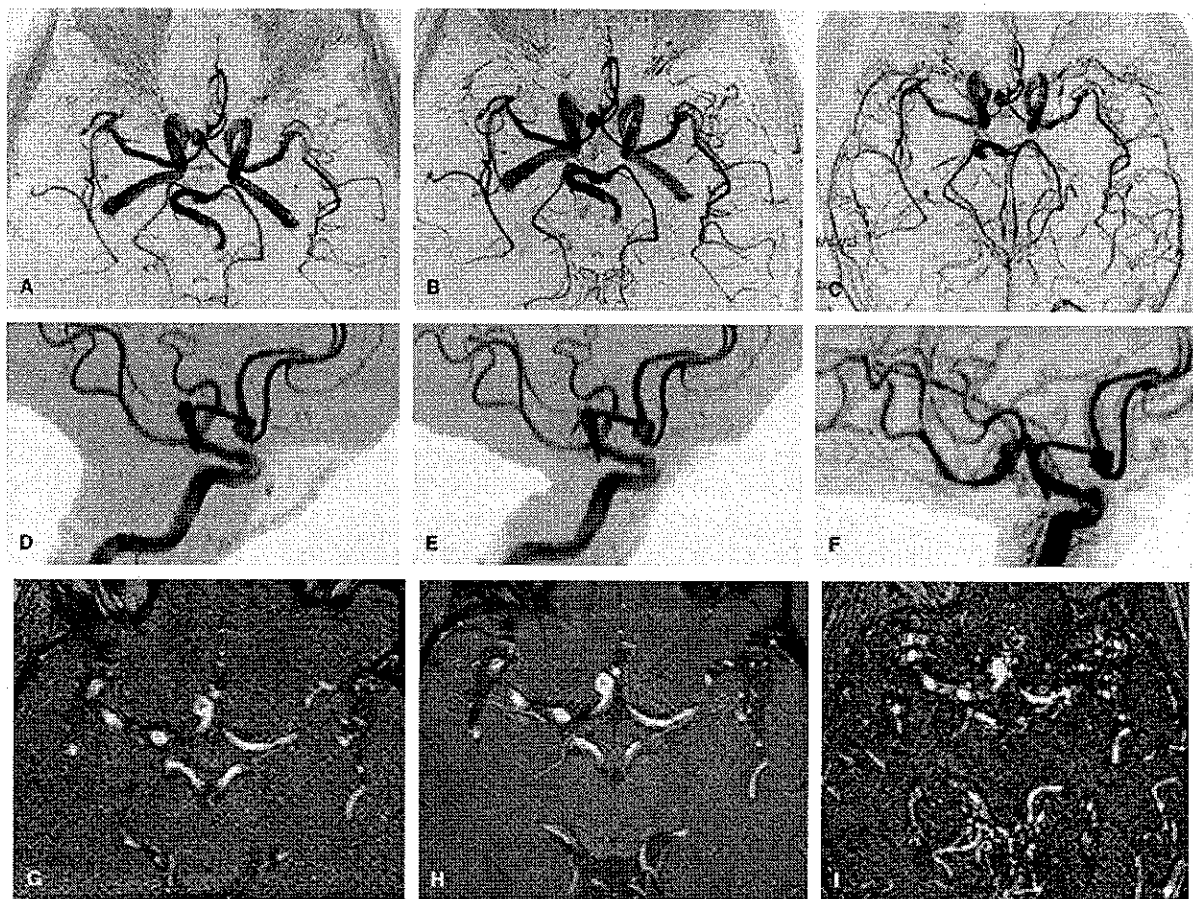


**FIG. 16.** The 3.0-T contrast-enhanced (CE) intracranial MR angiography. Comparison of 1.5-T time-of-flight (TOF) MR angiography, 3.0-T TOF MR angiography, and 3.0-T CE MR angiography in a patient with a known right anterior communicating artery aneurysm. Axial maximum intensity projection collapse from 1.5-T TOF (A), 3.0-T TOF (B), and 3.0-T CE MR angiography (C). Right internal carotid (IVI) subvolume projection from 1.5-T TOF (D), 3.0-T TOF (E), and 3.0-T CE MR angiography (F). Source images from 1.5-T TOF (G), 3.0-T TOF (H), and 3.0-T CE MR angiography (I). The aneurysm is well seen using all three techniques. The CE MR angiographic acquisition demonstrates more peripheral vascular branches than either TOF technique. Examination of the source images (G–I) demonstrates that the 3.0-T TOF acquisition has the most signal-to-noise ratio of the three. The 3.0-T TOF images demonstrate vascular artifact that is slightly more prominent than on the other techniques. Contrast and vascular conspicuity of peripheral branches is best using CE MR angiography. CE MR angiography suffers the least from saturation effects due to the relaxivity effects of the intravascular gadolinium.

by adjacent venous structures, especially in the region of the cavernous sinuses and adjacent to the deep venous structures (Fig. 15).

### CE MR ANGIOGRAPHY

CE MR angiography at 3.0 T currently is being adopted at our institution for both intracranial and cervical MR angiographic applications. CE MR angiographic techniques exploit the lumen-filling characteristics of injected contrast material, providing a basis for contrast, which is more analogous to that of conventional catheter-based X-ray angiography (18).

### INTRACRANIAL CE MR ANGIOGRAPHY

A current study comparing intracranial 3.0-T CE MR angiography with conventional 3.0-T TOF MR angiography currently is under way at our institution. The CE MR angiographic imaging protocol is derived from a similar technique (19,20) developed at our institution for bolus gadolinium cervical MR angiography (Table 3). The pulse sequence uses a 3D gradient-echo elliptic centric view order acquisition. Examples of intracranial CE-MR angiographic examinations are shown in Figs. 16 and 17. The examinations were acquired in a scan time of 51 seconds, producing 48 axial source images, each 1.2 mm thick, with a field of view (FOV) of 220 × 154 mm and imaging

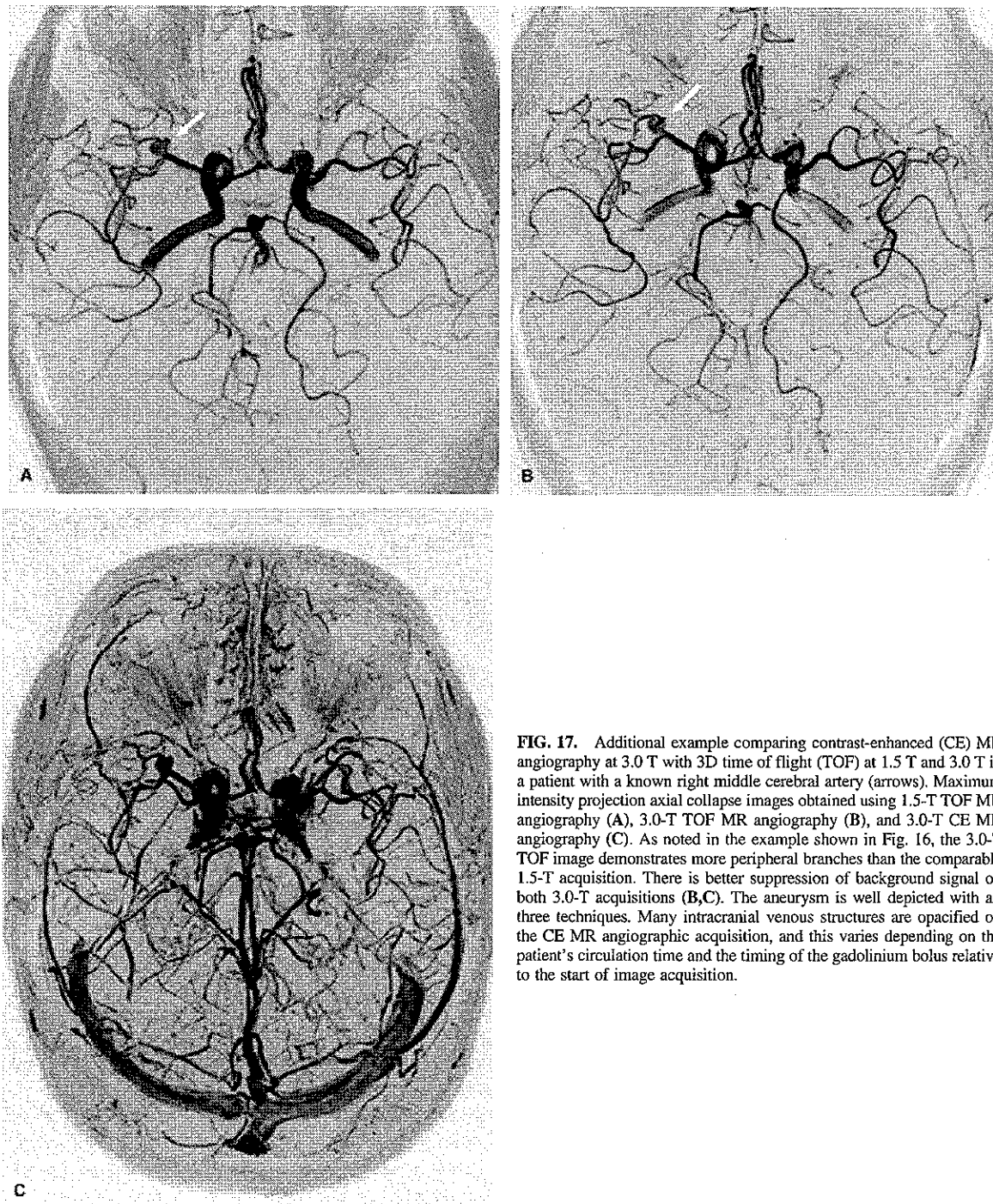


**FIG. 17.** Additional example comparing contrast-enhanced (CE) MR angiography at 3.0 T with 3D time of flight (TOF) at 1.5 T and 3.0 T in a patient with a known right middle cerebral artery (arrows). Maximum intensity projection axial collapse images obtained using 1.5-T TOF MR angiography (A), 3.0-T TOF MR angiography (B), and 3.0-T CE MR angiography (C). As noted in the example shown in Fig. 16, the 3.0-T TOF image demonstrates more peripheral branches than the comparable 1.5-T acquisition. There is better suppression of background signal on both 3.0-T acquisitions (B,C). The aneurysm is well depicted with all three techniques. Many intracranial venous structures are opacified on the CE MR angiographic acquisition, and this varies depending on the patient's circulation time and the timing of the gadolinium bolus relative to the start of image acquisition.

**TABLE 4.** 3.0-T versus 1.5-T bolus gadolinium cervical magnetic resonance angiographic pulse sequence parameters

Parameter	1.5 T	3.0 T
Pulse sequence	Elliptical Centric SPGR	Elliptical Centric SPGR
Mode	3D	3D
TR (ms)	6.7	6.7
TE (ms)	1.5 fractional echo (minimum)	1.5 fractional echo (minimum)
Flip angle	45°	33°
Scan plane	Coronal	Coronal
Matrix (frequency × phase)	256 × 224	416 × 224
Number of excitations 1 (Nex)	1	1
Field of view (cm)	22	22
Phase field of view	0.7	0.7
Section thickness (mm)	1.4	1.4
Number of locations	48	48
Frequency direction	Superior-inferior	Superior-inferior
Bandwidth (kHz)	32	31.2
Options	Variable bandwidth Zip 512 (frequency and phase directions)	Variable bandwidth Zip 512 (frequency and phase directions)
Scan time (min)	0:51	0:51

The parameters are essentially identical, except for reduced radiofrequency flip angle and increased matrix resolution at 3.0 T. Zip, zero fill interpolation.

matrix of 416 × 224 voxels. The TR/TE was 6.7/1.5 ms, the flip angle was 30 to 40°, receiver bandwidth of 150 Hz/pixel. Depending on the section thickness, the voxel size was 0.529 × 0.982 × 1.2 mm = 0.62 mm<sup>3</sup> (before three-direction zero filling). A power injector (Spectris; MedRad, Pittsburgh, PA, U.S.A.) injected 25 ml of gadoteridol (Braaco, Milan Italy) into the right antecubital vein at a rate of 3 ml/s, followed by a 25-ml saline flush injected at 2 ml/s. Bolus timing was performed using standard fluoroscopic software, using a 2-ml gadoteridol test dose followed by a 20-ml saline flush (19). Intracranial CE MR angiography is promising to be superior to TOF MR angiography for evaluating large aneurysms that are susceptible to signal loss resulting from flow saturation, evaluating partially thrombosed aneurysms, and characterizing the neck of the aneurysms.

#### BOLUS GADOLINIUM CERVICAL MR ANGIOGRAPHY

One of the biggest success stories of MR angiography of the carotid arteries has come with introduction of elliptic centric CE sequences, which produce high-resolution arterial images with excellent venous suppression (19,20). CE MR angiographic techniques exploit the lumen-filling

characteristics of injected contrast material and eventually may challenge conventional angiography as the “gold standard” for evaluation of atheromatous carotid artery stenosis. The technique at 3.0 T is similar to the 1.5-T technique and uses a coronal elliptic centric pulse sequence (Table 4). Our 3.0-T scanner currently does not have a body coil (planned development in 2001); therefore, initial results were obtained with the prototype transmit-receive cervical coil. This coil is suitable for performing bolus gadolinium cervical MR angiography on the 3.0-T scanner (Fig. 18).

Analysis of the bolus gadolinium MR angiographic pulse sequence in use at our institution (21) yielded an analytical expression for the point spread function for the elliptic centric view order, using data provided from experimentally measured gadolinium contrast bolus profiles in nine patients. The analysis demonstrated that isotropic spatial resolution of 1 mm before zero filling is possible for an FOV large enough to include both carotid and vertebral arteries within the imaging volume. Compared to the spatial resolution of conventional X-ray angiography (512 line pairs in a 4.5-inch FOV for digital subtraction angiography [DSA]), the spatial resolution of 3D CE MR angiography remains limited.

Insights gained within that study (21) were that significant residual contrast remains within the vascular compartment after the first pass of 0.1–0.15 mmol/kg bolus of gadolinium. The analytical point spread function expresses the square root dependence of full width at half-maximum on TR and Y and Z fields of view. Consequently, resolution is maximized when these quantities are reduced maximally. Reducing the FOV in either phase-encoding direction yields improved resolution in both of the phase-encoding directions. The benefits of performing CE MR angiography at 3.0 T over 1.5 T are readily apparent, considering the limited SNR available from a combination of short TR imaging and small FOV.

#### FUTURE DEVELOPMENTS OF MR ANGIOGRAPHY AT 3.0 T

MR angiography at higher magnetic field strength is in its infancy and likely will undergo significant improvement in the near future with the proliferation of higher magnetic field MR scanners. The pulse sequence parameters we implemented are a good first start, but certainly will continue to be optimized.

New coil development will improve uniformity, coverage, and SNR. These improvements will continue to benefit MR angiography at higher field strength. With devel-

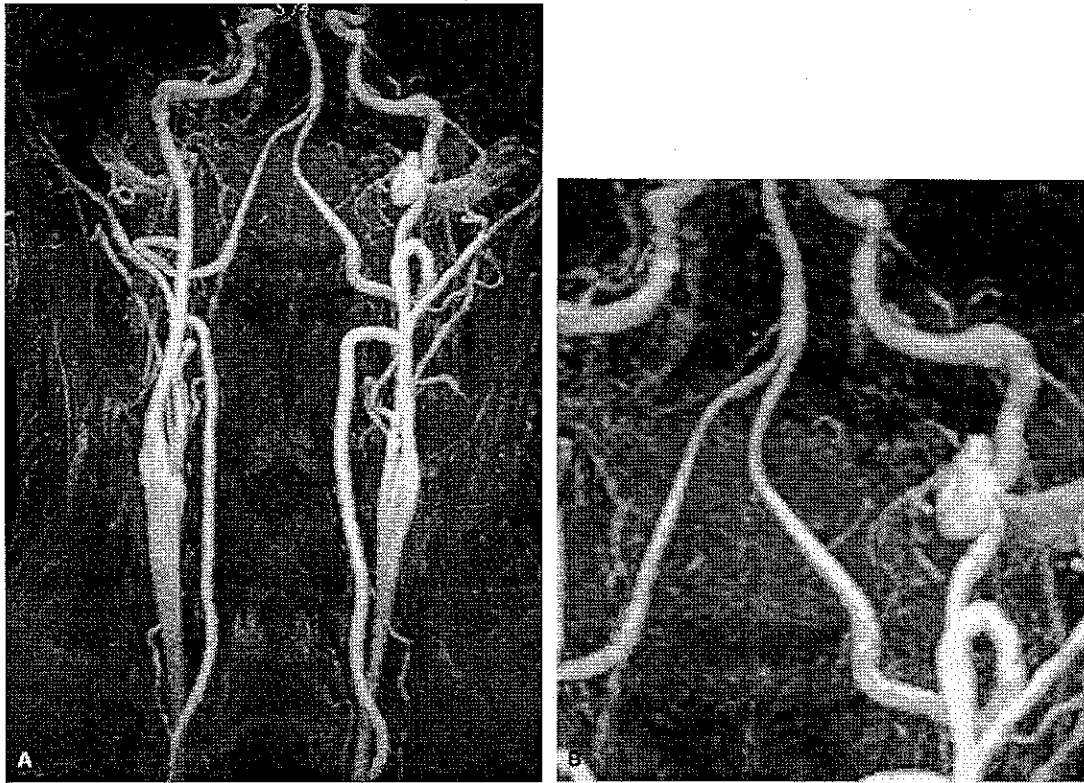


FIG. 18. The 3.0-T bolus gadolinium cervical MR angiography. Coronal maximum intensity projection (MIP) collapse image from 3.0-T bolus gadolinium cervical MR angiography (A) demonstrates findings consistent with a pseudoaneurysm complicating a dissection of the upper left cervical internal carotid artery in a 37-year-old man (B). The study was acquired with a transmit-receive volume neck coil. The pulse sequence uses an elliptic centric k-space view order that allows for good venous suppression within the images.

opment of a body coil, MR angiography at 3.0 T will be extended to nonneurological applications. Applications to cardiac MR angiography, renal angiography, peripheral angiography of upper and lower extremities, and pulmonary angiography are likely to demonstrate significant benefit when acquired at higher magnetic field strength.

Increased spatial resolution MR angiography will become routine when acquired using higher B-fields. Voxel dimensions for 3.0-T TOF MR angiographic acquisitions now typically are one third that of conventional X-ray DSA. This discrepancy in imaging resolution between MR angiography and DSA-based techniques will continue to be narrowed in the future. Postprocessing higher spatial resolution MR angiographic datasets will necessitate improvement in computer processing speed. It currently is time consuming to process a  $1,024 \times 1,024$  MR angiographic dataset on the operator's console using standard MR angiographic image processing software due to the large dataset size.

## SUMMARY

MR angiography has made substantial clinical improvement since its inception slightly more than a decade ago. One of the principal limitations of MR angiography continues to be low SNR. Performing MR angiography at higher magnetic field strengths provides this SNR boost, because available SNR scales linearly with main magnetic field strength. The physics of imaging at higher magnetic field strength are synergistic, providing improved MR angiography. MR angiography will continue to evolve with new techniques and new clinical applications. Our initial experience shows that MR angiography benefits significantly when performed at higher magnetic field strength. In summary, the benefits at 3.0 T are clear. They include increased SNR, better background suppression leading to better vessel conspicuity, and identification of smaller vessels and more distal branches. Early work using elliptic centric CE MR angiography at 3.0 T consistently produces

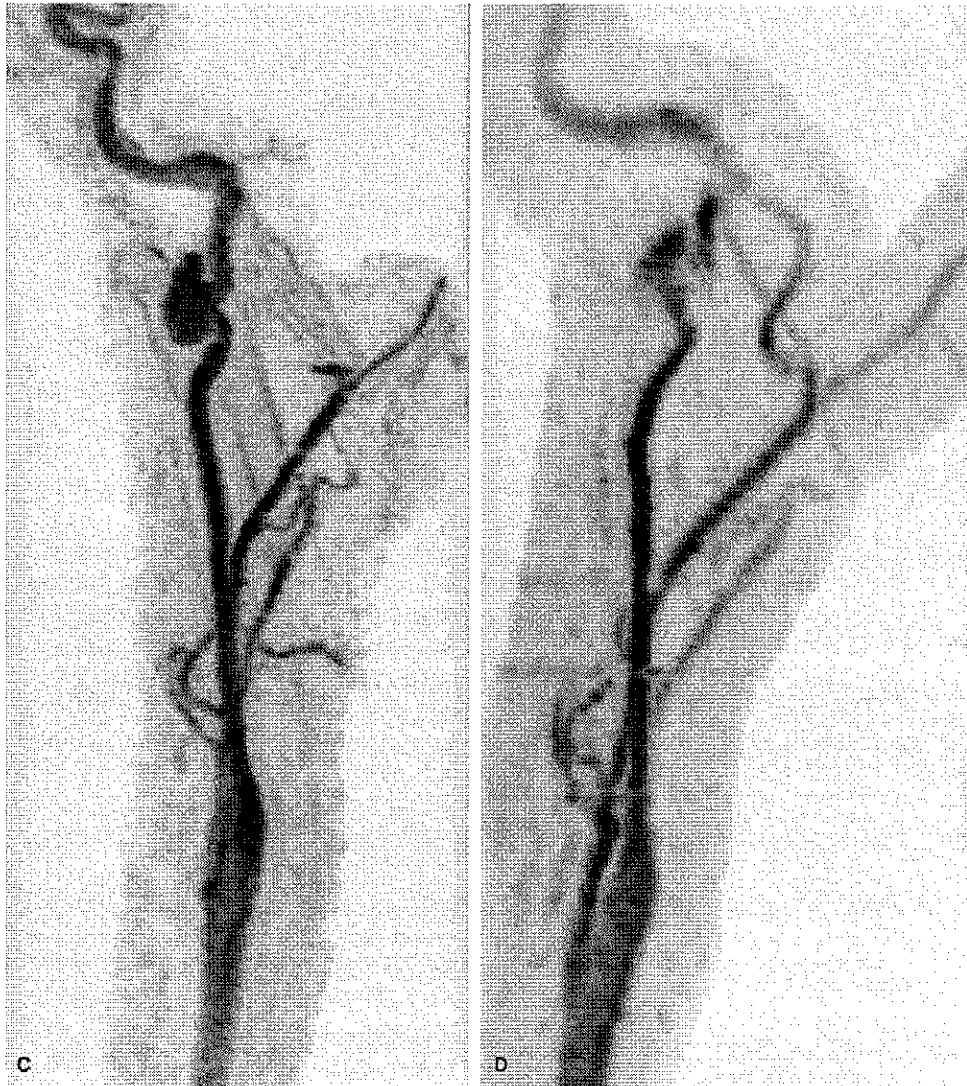


FIG. 18. (cont.) Corresponding left carotid IVI subvolume projection from the bolus gadolinium MR angiography acquisition (C), and 3.0-T 2D time-of-flight (TOF) acquisition (D) obtained during the same imaging session. Note the excellent signal-to-noise ratio and anatomic depiction present on the contrast-enhanced images. The 2D TOF image (D) is more prone to patient motion and swallowing artifacts, due in part to the increased acquisition time associated with the 2D TOF technique and from stacked axial image acquisition. The pulse sequence parameters used for the 3.0-T bolus gadolinium MR angiography are listed in Table 4.

high-resolution, venous-suppressed images of the carotid arteries.

MR angiography at high field strength is in its infancy in comparison to the current stage of MR angiographic development on conventional 1.5-T scanners. Initial results are promising. Continued improvements in hardware and software undoubtedly will continue over the next few years, likely at an accelerated pace given the increase of high field scanners in clinical practice.

**Acknowledgment:** The authors thank Ravi Srinivasan, Presi-

dent, Advanced Imaging Research, Inc., for providing the 3.0-T volume neck coil used for cervical MR angiographic studies.

#### REFERENCES

1. Keller PJ, Drayer BP, Fram EK, eds. Magnetic resonance angiography. *Neuroimaging Clin North Am* 1992;2:623-692.
2. Masaryk TJ, Perl J II, Dagirmanjian A, et al. Magnetic resonance angiography: Neuroradiological applications. In: Stark DD, Bradley WG, eds. *Magnetic resonance imaging*, 3rd ed. St. Louis: Mosby, 1999:1277-316.
3. Foster JD, Kovelski J. Magnetic resonance angiography of the head and neck in an open scanner. In: Rothschild PA, Reinking Roths-

- child D, eds. *Open MRI*. Philadelphia: Lippincott Williams & Wilkins, 2000:337-346.
4. Bernstein MA, Huston J III, Felmlee JP, et al. Neuro MRA at 3.0T and 40 mT/m: Initial experience. *Acta Radiol* 2000;18(Suppl.):422.
  5. Campeau NG, Huston J III, Wood CP, et al. Clinical MR imaging of the brain at 3.0 Tesla: Initial clinical experience. Proceedings of the 86th Scientific Assembly of RSNA. *Radiology* 2000;217(suppl):675.
  6. Bernstein MA, Huston J III, Jack CR, et al. Routine clinical brain MR imaging at 3.0T: Initial experience. *Proc Intl Soc Mag Reson Med* 2000;8:1994.
  7. Kim DH, Adalsteinsson E, Glover G, et al. SVD regularization algorithm for improved high-order shimming. *Proc Intl Soc Mag Reson Med* 2000;8:1685.
  8. Felmlee JP, Bernstein MA, Huston J III. Analysis of RF heating at 3.0T. *Proc Intl Soc Magn Reson Med* 2000;8:A2002.
  9. Parker DL, Buswell HR, Goodrich KC, et al. The application of magnetization transfer to MR angiography with reduced total power. *Magn Reson Med* 1995;34:283-6.
  10. Bottomley PA, Foster TH, Argersinger RE, et al. A review of normal tissue hydrogen NMR relaxation times from 1-100 MHz: Dependence on tissue type, NMR frequency, temperature, species, excision, and age. *Med Phys* 1984;11:425-48.
  11. Keller PJ, Drayer BP, Fram EK, et al. MR angiography with two-dimensional acquisition and three-dimensional display. *Radiology* 1989;173:527-32.
  12. Davis WL, Blatter DD, Harnsberger HR, et al. Intracranial MR angiography: Comparison of single-volume three-dimensional time-of-flight and multiple overlapping thin slab acquisition techniques. *AJR Am J Roentgenol* 1994;163:915-20.
  13. Butts RK, Faraneh F, Riederer SJ, et al. T2 weighted spin-echo pulse sequence with variable repetition and echo times for reduction of MR image acquisition time. *Radiology* 1991;180:551-6.
  14. Tkach J, Lin W, Duda JJ Jr, et al. Optimizing three-dimensional time-of-flight MR angiography with variable TR. *Radiology* 1994;191:805-11.
  15. Laub G, Kaiser W. MR angiography with gradient moment refocusing. *J Comput Assist Tomogr* 1988;12:377-82.
  16. Axel L, Morton D. MR flow imaging by phase compensated/uncompensated difference images. *J Comput Assist Tomogr* 1987;11:31-4.
  17. Oelerich M, Lentschig MG, Zunker P, et al. Intracranial vascular stenosis and occlusion: Comparison of 3D time-of-flight and 3D phase-contrast MR angiography. *Neuroradiology* 1998;40:567-73.
  18. Laub G. Principles of contrast-enhanced MR angiography. Basic and clinical applications. *Magn Reson Imaging Clin North Am* 1999;7:783-95.
  19. Huston J III, Fain SB, Riederer SJ, et al. Carotid arteries: Maximizing arterial to venous contrast in fluoroscopically triggered contrast-enhanced MR angiography with elliptic centric view ordering. *Radiology* 1999;211:265-73.
  20. Wilman AH, Riederer SJ, Huston J III, et al. Arterial phase carotid and vertebral artery imaging in 3D contrast-enhanced MR angiography by combining fluoroscopic triggering with an elliptical centric acquisition order. *Magn Reson Med* 1998;40:24-5.
  21. Fain SB, Riederer SJ, Bernstein MA, et al. Theoretical limits of spatial resolution in elliptical-centric contrast-enhanced 3D-MRA. *Magn Reson Med* 1999;42:1106-16.



# ARTICLE 4

## Chronic renal disease

Malvinder S Parmar

Early identification and active management of patients with renal impairment in primary care can improve outcomes

The number of patients with end stage renal disease is growing worldwide. About 20-30 patients have some degree of renal dysfunction for each patient who needs renal replacement treatment.<sup>1</sup> Diabetes and hypertension are the two most common causes of end stage renal disease and are associated with a high risk of death from cardiovascular disease.

Mortality in patients with end stage renal disease remains 10-20 times higher than that in the general population. The focus in recent years has thus shifted to optimising the care of these patients during the phase of chronic kidney disease, before the onset of end stage renal disease. This review summarises current knowledge about the various stages of chronic renal disease, the risk factors that lead to progression of disease, and their association with common cardiovascular risk factors. It also provides strategies for intervention at an early stage of the disease process, which can readily be implemented in primary care, to improve the overall morbidity and mortality associated with chronic renal disease.

### Sources and search criteria

I searched Medline to identify recent articles (1992-2001) related to the management of chronic renal disease and its complications. Key words used included chronic kidney disease, chronic renal failure, kidney disease, end stage renal disease, anaemia, erythropoietin, ischaemic heart disease, cardiac disease, lipid disorders, hyperparathyroidism, calcium, phosphate, nutrition, diabetes, and hypertension in relation to kidney disease. I also referred to the recent clinical practice guidelines published by the National Kidney Foundation.<sup>2</sup>

### Diagnosis

Chronic renal failure is defined as either kidney damage or glomerular filtration rate less than 60 ml/min for three months or more.<sup>2</sup> This is invariably a progressive process that results in end stage renal disease.

Serum creatinine is commonly used to estimate creatinine clearance but is a poor predictor of glomerular filtration rate, as it may be influenced in unpredictable ways by assay techniques, endogenous and exogenous substances, renal tubular handling of

### Summary points

Significant renal dysfunction might be present even when serum creatinine is normal or only slightly abnormal

Renal function declines progressively once creatinine clearance falls by about 25% of normal, but symptoms are often not apparent until renal failure is advanced

The baseline rate of urinary protein excretion is the best single predictor of disease progression

The prevalence of common cardiovascular risk factors is high in chronic renal disease; early identification and effective control of these risk factors is important to improve outcomes

Cardiovascular disease accounts for 40% of all deaths in chronic renal disease

Potentially reversible causes should be sought when renal function suddenly declines

Irreversible but modifiable complications (anaemia, cardiovascular disease, metabolic bone disease, malnutrition) begin early in the course of renal failure

creatinine, and other factors (age, sex, body weight, muscle mass, diet, drugs).<sup>3</sup> Glomerular filtration rate is the "gold standard" for determining kidney function, but its measurement remains cumbersome. For practical purposes, calculated creatinine clearance is used as a correlate of glomerular filtration rate and is commonly estimated by using the Cockcroft-Gault formula or the recently described modification of diet in renal disease equation (box 1).<sup>1,2</sup>

### Stages of chronic renal disease

Chronic renal disease is divided into five stages on the basis of renal function (table, fig 1). Pathogenesis of progression is complex and is beyond the scope of this review. However, renal disease often progresses by

Timmins and District Hospital, Timmins, ON, Canada

Malvinder S Parmar  
director of dialysis

Correspondence to:  
707 Ross Avenue  
East, Suite 108,  
Timmins, ON,  
Canada P4N 8R1  
atbeat@ntl.  
sympatico.ca

BMJ 2002;325:85-90



Additional  
references appear  
on bmj.com

**Box 1: Methods for estimating creatinine clearance (glomerular filtration rate) in ml/min/1.73 m<sup>2</sup>**

**Cockcroft-Gault formula:<sup>1</sup>**

$$\text{Creatinine clearance} = \frac{(140 - \text{age})(\text{weight in kilograms})}{\text{Serum creatinine } (\mu\text{mol/l}) \times 0.81} \times (0.85 \text{ if female})$$

**Modification of diet in renal disease equation:<sup>2</sup>**

$$\text{Glomerular filtration rate} = 186.3 \times (\text{serum creatinine})^{-1.154} \times \text{age}^{0.203} \times (0.742 \text{ if female}) \times (1.21 \text{ if black})$$

**Box 2: Risk factors for chronic renal disease**

**Risk factors**

(Factors that increase the risk of kidney damage)

- Age
- Diabetes\*
- Hypertension\*
- Family history of renal disease
- Renal transplant

**Initiation factors**

(Factors that initiate kidney damage)

- Diabetes\*
- Hypertension\*
- Autoimmune diseases
- Primary glomerulopathies
- Systemic infections
- Nephrotoxic agents

**Progression factors**

(Factors that cause progressive decline in renal function after onset of kidney damage)

- Persistent activity of underlying disease
- Persistent proteinuria
- Elevated blood pressure\*
- Elevated blood glucose\*
- High protein/phosphate diet
- Hyperlipidaemia\*
- Hyperphosphataemia
- Anaemia
- Cardiovascular disease
- Smoking\*
- Other factors: elevated angiotensin II, hyperaldosteronism, increased endothelin, decreased nitric oxide

\*Common modifiable cardiovascular risk factors

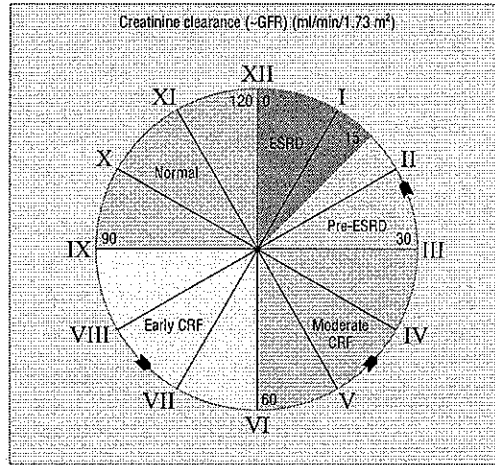


**Fig 1** Continuum of renal disease (anticlockwise model) (CRF=chronic renal failure; ESRD=end stage renal disease; GFR=glomerular filtration rate)

“common pathway” mechanisms, irrespective of the initiating insult.’ In animal models, a reduction in nephron mass exposes the remaining nephrons to adaptive haemodynamic changes that sustain renal function initially but are detrimental in the long term.<sup>5</sup>

**Early detection**

Renal disease is often progressive once glomerular filtration rate falls by 25% of normal. Early detection is important to prevent further injury and progressive loss of renal function.

Patients at high risk (box 2) should undergo evaluation for markers of kidney damage (albuminuria (box 3), abnormal urine sediment, elevated serum creatinine) and for renal function (estimation of glomerular filtration rate from serum creatinine) initially and at periodic intervals depending on the underlying disease process and stage of renal disease. Potentially reversible causes (box 4) should be identified and effectively treated if a sudden decline in renal function is observed.

Stages of renal dysfunction (adapted from National Kidney Foundation—K/DOQI)<sup>6</sup>

Stage	Description	Creatinine clearance (~ GFR) (ml/min/1.73 m <sup>2</sup> )	Metabolic consequences
1	Normal or increased GFR—people at increased risk (box 2) or with early renal damage	>90	
2	Early renal insufficiency	60-89*	Concentration of parathyroid hormone starts to rise (GFR ~60-80)
3	Moderate renal failure (chronic renal failure)	30-59	Decrease in calcium absorption (GFR<50) Lipoprotein activity falls Malnutrition Onset of left ventricular hypertrophy Onset of anaemia (erythropoietin deficiency)
4	Severe renal failure (pre-end stage renal disease)	15-29	Triglyceride concentrations start to rise Hyperphosphataemia Metabolic acidosis Tendency to hyperkalaemia
5	End stage renal disease (uraemia)	<15	Azolaemia develops

GFR=glomerular filtration rate.

\*May be normal for age.

**Box 3: Definition of urinary albumin or protein excretion**

- Normal albumin excretion: < 30 mg/24 hours
- Microalbuminuria: 20-200 µg/min or 30-300 mg/24 hour or
  - in men—urine albumin/creatinine 2.5-25 mg/mmol
  - in women—urine albumin/creatinine 3.5-35 mg/mmol
- Macroalbuminuria (overt proteinuria): > 300 mg/24 hour
- Nephrotic range proteinuria: > 3 g/24 hour

**Box 4: Potentially reversible causes of worsening renal function**

- Effective circulatory volume depletion: dehydration, heart failure, sepsis
- Obstruction: urinary tract obstruction
- Uncontrolled hypertension
- Toxic causes: nephrotoxic or radiocontrast agents

**Diabetes**

Diabetes is a common cause of chronic renal failure and accounts for a large part of the growth in end stage renal disease in North America.<sup>3</sup> Effective control of blood glucose and blood pressure reduces the renal complications of diabetes.

Meticulous control of blood glucose has been conclusively shown to reduce the development of microalbuminuria by 35% in type 1 diabetes (diabetes control and complications trial)<sup>6</sup> and in type 2 diabetes (United Kingdom prospective diabetes study).<sup>7</sup> Other studies have indicated that glycaemic control can reduce the progression of diabetic renal disease.<sup>8</sup> Adequate control of blood pressure with a variety of antihypertensive agents, including angiotensin converting enzyme inhibitors, has been shown to delay the progression of albuminuria in both type 1 and type 2 diabetes.<sup>9,10</sup> Recently, angiotensin receptor blockers have been shown to have renoprotective effects in both early and late nephropathy due to type 2 diabetes.<sup>11-13</sup> Box 5 shows strategies for managing diabetic nephropathy.

**Hypertension**

Hypertension is a well established cause, a common complication, and an important risk factor for progression of renal disease. Controlling hypertension is the most important intervention to slow the progression of renal disease.<sup>14</sup>

Any antihypertensive agents may be appropriate, but angiotensin converting enzyme inhibitors are particularly effective in slowing progression of renal insufficiency in patients with and without diabetes by reducing the effects of angiotensin II on renal haemodynamics, local growth factors, and perhaps glomerular permeability.<sup>9,15</sup> Non-dihydropyridine calcium channel blockers have also been shown to retard progression of renal insufficiency in patients with type 2 diabetes. Recently, angiotensin receptor blockers (irbesartan and losartan) have been shown to have a renoprotective effect in diabetic nephropathy, independent

**Box 5: Management strategies for diabetic nephropathy**

(Ensure effective control of common cardiovascular risk factors—for example, lipids, smoking—at all times)

- Initial stage (normal albumin excretion, < 30 mg/24 hours):
  - Optimal glycaemic control (haemoglobin A<sub>1c</sub> < 7%)
  - Target blood pressure < 130/80 mm Hg
  - Monitor urinary albumin excretion
- Incipient nephropathy (microalbuminuria, 30-300 mg/24 hour or 20-200 µg/min):
  - Optimal glycaemic control (haemoglobin A<sub>1c</sub> < 7%)
  - Target blood pressure < 125/75 mm Hg
  - Control urinary albumin excretion, irrespective of blood pressure
  - Angiotensin inhibition
- Overt nephropathy (albumin excretion > 300):
  - Optimal glycaemic control (haemoglobin A<sub>1c</sub> < 7%)
  - Target blood pressure < 125/75 mm Hg
  - Control urinary protein excretion
  - Angiotensin inhibition, irrespective of blood pressure
  - Avoid malnutrition
  - Modest protein restriction, in selected groups
- Nephropathy with renal dysfunction:
  - Optimal glycaemic control; avoid frequent hypoglycaemia
  - Target blood pressure < 125/75 mm Hg
  - Angiotensin inhibition
  - Watch for hyperkalaemia
  - Avoid malnutrition; consider protein and phosphate restriction
- End stage renal disease:
  - Renal replacement—transplantation or dialysis
  - Monitor for hyperkalaemia
  - Hold angiotensin inhibition (when glomerular filtration < 15 ml/min) in selected patients

of reduction in blood pressure.<sup>11-13</sup> Early detection and effective treatment of hypertension to target levels is essential (box 6). The benefit of aggressive control of blood pressure is most pronounced in patients with urinary protein excretion of > 3 g/24 hours.<sup>14</sup>

**Proteinuria**

Proteinuria, previously considered a marker of renal disease, is itself pathogenic and is the single best predictor of disease progression.<sup>16</sup> Reducing urinary protein excretion slows the progressive decline in renal function in both diabetic and non-diabetic kidney disease.

Angiotensin blockade with angiotensin converting enzyme inhibitors or angiotensin receptor blockers is more effective at comparable levels of blood pressure control than conventional antihypertensive agents in reducing proteinuria, decline in glomerular filtration rate, and progression to end stage renal disease.<sup>11-14,16,17,18,19</sup>

**Intake of dietary protein**

The role of dietary protein restriction in chronic renal disease remains controversial.<sup>15,16,17</sup> The largest con-

**Box 6: Target blood pressure in renal disease<sup>16</sup>**

- Blood pressure of < 130/85 mm Hg in all patients with renal disease
- Blood pressure of < 125/75 mm Hg in patients with proteinuric renal disease (urinary protein excretion ≥ 1 g/24 hours)

trolled study initially failed to find an effect of protein restriction,<sup>17</sup> but secondary analysis based on achieved protein intake suggested that a low protein diet slowed the progression. However, early dietary review is necessary to ensure adequate energy intake, maintain optimal nutrition, and avoid malnutrition.

#### Dyslipidaemia

Lipid abnormalities may be evident with only mild renal impairment and contribute to progression of chronic renal disease and increased cardiovascular morbidity and mortality. A meta-analysis of 13 controlled trials showed that hydroxymethyl glutaryl coenzyme A reductase inhibitors (statins) decreased proteinuria and preserved glomerular filtration rate in patients with renal disease, an effect not entirely explained by reduction in blood cholesterol.<sup>18</sup>

#### Phosphate and parathyroid hormone

Hyperparathyroidism is one of the earliest manifestations of impaired renal function,<sup>19</sup> and minor changes in bones have been found in patients with a glomerular filtration rate of 60 ml/min.<sup>20</sup> Precipitation of calcium phosphate in renal tissue begins early, may influence the rate of progression of renal disease, and is closely related to hyperphosphataemia and calcium phosphate (Ca×P) product. Precipitation of calcium phosphate should be reduced by adequate fluid intake, modest dietary phosphate restriction, and administration of phosphate binders to correct serum phosphate. Dietary phosphate should be restricted before the glomerular filtration rate falls below 40 ml/min and before the development of hyperparathyroidism. The use of vitamin D supplements during chronic renal disease is controversial.

#### Smoking

Smoking, besides increasing the risk of cardiovascular events, is an independent risk factor for development of end stage renal disease in men with kidney disease.<sup>21</sup> Smoking cessation alone may reduce the risk of disease progression by 30% in patients with type 2 diabetes.<sup>22</sup>

#### Anaemia

Anaemia of chronic renal disease begins when the glomerular filtration rate falls below 30-35% of normal and is normochromic and normocytic. This is primarily caused by decreased production of erythropoietin by the failing kidney,<sup>23</sup> but other potential causes should be considered. Whether anaemia accelerates the progression of renal disease is controversial. However, it is independently associated with the development of left ventricular hypertrophy and other cardiovascular complications in a vicious cycle (fig 2).<sup>24</sup>

Treatment of anaemia with recombinant human erythropoietin may slow progression of chronic renal disease but requires further study. Treatment of anaemia results in partial regression of left ventricular hypertrophy in both patients with pre-end stage renal disease and patients receiving dialysis and has reduced the frequency of heart failure and hospitalisation among patients receiving dialysis.<sup>25 26</sup>

Both National Kidney Foundation and European best practice guidelines recommend evaluation of anaemia when haemoglobin is <11 g/dl and consideration of recombinant human erythropoietin if

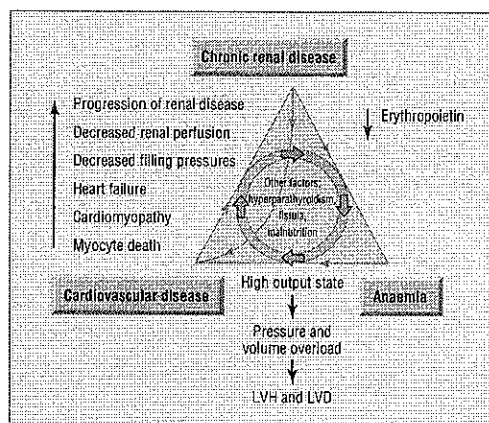


Fig 2 Perpetuating triad of chronic kidney disease, anaemia, and cardiovascular disease (LVH=left ventricular hypertrophy; LVD=left ventricular dilatation)

haemoglobin is consistently <11 g/dl to maintain a target haemoglobin of >11 g/dl.<sup>27 28</sup>

### Prevention or attenuation of complications and comorbidities

#### Malnutrition

The prevalence of hypoalbuminaemia is high among patients beginning dialysis, is of multifactorial origin, and is associated with poor outcome. Hypoalbuminaemia may be a reflection of chronic inflammation rather than of nutrition in itself. Spontaneous intake of protein begins to decrease when the glomerular filtration rate falls below 50 ml/min. Progressive decline in renal function causes decreased appetite, thereby increasing the risk of malnutrition. Hence early dietary review is important to avoid malnutrition. Adequate dialysis is also important in maintaining optimal nutrition.

#### Cardiovascular disease

The prevalence, incidence, and prognosis of clinical cardiovascular disease in renal failure is not known with precision, but it begins early and is independently associated with increased cardiovascular and all cause mortality.<sup>31</sup> Both traditional and uraemia specific risk factors (anaemia, hyperphosphataemia, hyperparathyroidism) contribute to the increased prevalence of cardiovascular disease.<sup>29</sup> Cardiac disease, including left ventricular structural and functional disorders, is an important and potentially treatable comorbidity of early kidney disease.

No specific recommendations exist for either primary or secondary prevention of cardiovascular disease in patients with chronic renal disease. Current practice is mostly derived from studies in patients with diabetic or non-renal disease. At present, in the absence of evidence, clinical judgment indicates effective control of modifiable and uraemia specific risk factors at an early stage of renal disease; definitive guidelines for intervention await well designed, adequately powered prospective studies.

### Preparing patient for renal replacement treatment

Integrated care by the primary care physician, nephrologist, and renal team from an early stage is

vital to reduce the overall morbidity and mortality associated with chronic renal disease. Practical points helpful at this stage of renal disease include

- Patients should be referred to a nephrologist before serum creatinine is 150-180 µmol/l
- Patients receiving comprehensive care by the renal team have shown slower rates of decline in renal function, greater probability of starting dialysis with higher haemoglobin, better calcium control, a permanent access, and a greater likelihood of choosing peritoneal dialysis<sup>w12</sup>
- Patients with progressive renal failure should be educated to save vessels of the non-dominant arm for future haemodialysis access; they should have a permanent vascular access (preferably arteriovenous fistula) created when the glomerular filtration rate falls below 25 ml/min or renal replacement treatment is anticipated within a year
- Patients starting dialysis at relatively higher levels of residual renal function (early starts) have better solute clearance, less malnutrition, better volume control, and less morbidity and mortality than patients starting at traditional low levels of renal function (late starts).<sup>w13</sup>

**Conclusion**

Chronic renal failure represents a critical period in the evolution of chronic renal disease and is associated with complications and comorbidities that begin early in the course of the disease. These conditions are initially subclinical but progress relentlessly and may eventually become symptomatic and irreversible. Early in the course of chronic renal failure, these conditions are amenable to interventions with relatively simple treatments that have the potential to prevent adverse outcomes. Fig 3 summarises strategies for effective management of chronic renal disease. By acknowledging these facts, we have an excellent opportunity to change the paradigm of management of chronic renal failure and improve patient outcomes.

Competing interests: None declared.

- 1 Jones C, McQuillan G, Kusek J, Eberhardt M, Herman W, Coresh J, et al. Serum creatinine levels in the US population: third national health and nutrition examination survey [correction appears in *Am J Kidney Dis* 2000;35:178]. *Am J Kidney Dis* 1998;32:992-9.
- 2 National Kidney Foundation—K/DOQI. Clinical practice guidelines for chronic kidney disease: evaluation, classification and stratification. *Am J Kidney Dis* 2002;39(suppl 1):S1-266.
- 3 Walsler M. Assessing renal function from creatinine measurements in adults with chronic renal failure. *Am J Kidney Dis* 1998;32:1-22.
- 4 Remuzzi G, Bertani T. Pathophysiology of progressive nephropathies. *N Engl J Med* 1998;339:1448-56.
- 5 Brenner BM, Meyer TW, Hostetter TH. Dietary protein intake and the progressive nature of kidney disease: the role of hemodynamically mediated glomerular injury in the pathogenesis of progressive glomerular sclerosis in aging, renal ablation, and intrinsic renal disease. *N Engl J Med* 1982;307:652-9.
- 6 The Diabetes Control and Complications Trial (DCCT) Research Group. Effect of intensive therapy on the development and progression of nephropathy in the DCCT. *Kidney Int* 1995;47:1703-20.
- 7 UK Prospective Diabetes Study Group. Tight blood pressure control and risk of macrovascular and microvascular complications in type 2 diabetes: UKPDS 38. *BMJ* 1998;317:703-13.
- 8 Wang P, Lau J, Chalmers T. Meta-analysis of the effects of intensive blood-glucose control on late complications of type 1 diabetes. *Lancet* 1993;341:1306-9.
- 9 Lewis E, Hunsicker L, Bain R, Rhode R. The effect of angiotensin converting enzyme inhibition on diabetic nephropathy. *N Engl J Med* 1993;329:1456-62.
- 10 Parving H-H, Osterby R, Anderson P, Husech W. Diabetic nephropathy. In: Brenner B, ed. *The kidney*. Philadelphia, PA: Saunders, 1996:1864-92.
- 11 Parving H-H, Lehnert H, Brochner-Mortensen J, Gomis R, Anderson S, Arner P for the Irbesartan in Patients with Type 2 Diabetes and Microalbuminuria Study Group. The effect of irbesartan on the develop-

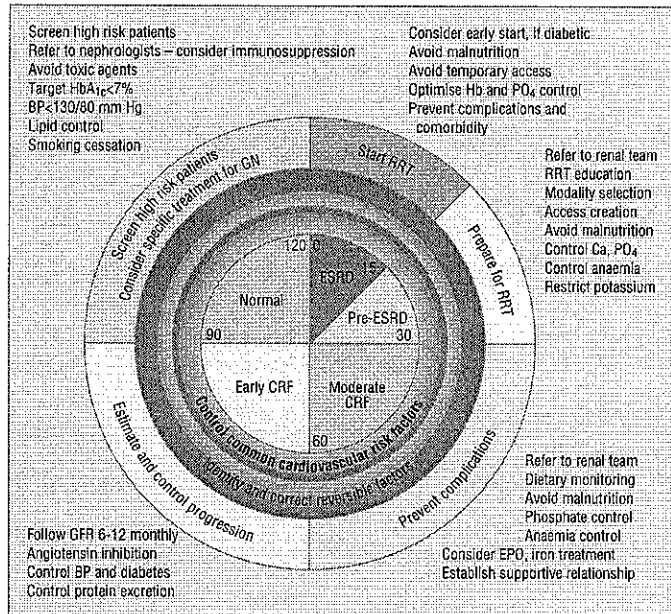


**Fig 3** Strategies for active management of chronic renal disease (BP=blood pressure; Ca=calcium; CRF=chronic renal failure; EPO=erythropoietin; ESRD=end stage renal disease; GN=glomerulonephritis; GFR=glomerular filtration rate; Hb=haemoglobin; PO<sub>4</sub>=phosphate; RRT=renal replacement treatment)

ment of diabetic nephropathy in patients with type 2 Diabetes. *N Engl J Med* 2001;345:870-8.

- 12 Lewis EJ, Hunsicker LG, Clarke WR, Berl T, Pohl MA, Lewis JB, et al for the Collaborative Study Group. Renoprotective effect of the angiotensin-receptor antagonist irbesartan in patients with nephropathy due to type 2 diabetes. *N Engl J Med* 2001;345:861-69.
- 13 Brenner BM, Cooper ME, Zeeuw D, Keane WF, Mitch WE, Parving H-H, et al for the RENAAL Study Investigators. Effects of losartan on renal and cardiovascular outcomes in patients with type 2 diabetes and nephropathy. *N Engl J Med* 2001;345:861-9.
- 14 Mogensen CE, Neldam I, Tikkanen I, Oren S, Viskoper R, Watts RW, et al. Randomised controlled trial of dual blockade renin-angiotensin system in patients with hypertension, microalbuminuria, and non-insulin

**Additional educational resources**

- Tomson GRV. Recent advances: nephrology. *BMJ* 2000;320:98-101
- Mason PD, Pusey CD. Glomerulonephritis: diagnosis and treatment. *BMJ* 1994;309:1557-63
- Walker R. Recent advances: general management of end stage renal disease. *BMJ* 1997;315:1429-32
- Ifudu O. Care of patients undergoing hemodialysis. *N Engl J Med* 1998;339:1054-62
- Remuzzi G, Schieppati A, Ruggenti P. Clinical practice: nephropathy in patients with type 2 diabetes. *N Engl J Med* 2002;346:1145-51
- National Kidney Foundation—K/DOQI. Clinical practice guidelines for chronic kidney disease: evaluation, classification and stratification. *Am J Kidney Dis* 2002;39(suppl 1):S1-266

**Patient information**

- **Kidney School** ([www.kidneyschool.org](http://www.kidneyschool.org))—an interactive, web-based program designed to help people learn what they need to know to understand renal disease and its treatment, adjust to renal disease, make good medical choices, and live as fully as possible
- **Doc-To-Me** ([www.doctome.com](http://www.doctome.com))—presents concise, informative, and authoritative pre-end stage renal disease lectures: "Staying healthy with bad kidneys"
- **Kidney Incorporated** ([www.hdialysis.com](http://www.hdialysis.com))—provides general information about kidneys, pre-end stage renal disease care, and dialysis treatment

- dependent diabetes: the candesartan and lisinopril microalbuminuria (CALM) study. *BMJ* 2000;321:1440-4.
- 15 Klahr S. Is there still a role for a diet very low in protein, with or without supplements, in the management of patients with end-stage renal disease? *Curr Opin Nephrol Hypertens* 1998;5:384-7.
  - 16 Levey AS, Adler S, Caggiula AW, England BK, Greene T, Hunsicker LG, et al. Effects of dietary protein restriction on the progression of advanced renal disease in the modification of diet in renal disease study. *Am J Kidney Dis* 1996;27:652-63.
  - 17 Modification of Diet in Renal Disease Study Group. Effects of diet and antihypertensive therapy on creatinine clearance and serum creatinine in the modification of diet in renal disease study. *J Am Soc Nephrol* 1996;7:556-66.
  - 18 Fried LF, Orchard TJ, Kasiske BL. Effect of lipid reduction on the progression of renal disease: a meta-analysis. *Kidney Int* 2001;59:260-9.
  - 19 Martinez I, Saracho R, Montenegro J, Llach F. The importance of dietary calcium and phosphorus in the secondary hyperparathyroidism of patients with early renal failure. *Am J Kidney Dis* 1997;29:496-502.
  - 20 Coen G, Mazzaferro S, Ballant P, Sardella D, Chicca S, Manni M, et al. Renal bone disease in 76 patients with varying degrees of predialysis chronic renal failure: a cross-sectional study. *Nephrol Dial Transplant* 1998;11:813-9.
  - 21 Orth S, Stockmann A, Conradt C, Ritz E, Ferro M, Kreuzer W, et al. Smoking as a risk factor for end-stage renal failure in men with primary renal disease. *Kidney Int* 1998;54:926-31.
  - 22 Ritz E, Ogata H, Orth SR. Smoking a factor promoting onset and progression of diabetic nephropathy. *Diabetes Metab* 2000;26(suppl 4):54-63.
  - 23 Eschbach JW. The anemia of chronic renal failure. *Kidney Int* 1989;35:134-48.
  - 24 Foley RN, Parfrey PS, Harnett JD, Kent GM, Murray DC, Barre PE. The impact of anemia on cardiomyopathy, morbidity and mortality in end-stage renal disease. *Am J Kidney Dis* 1996;28:53-61.
  - 25 Portoles J, Torralbo A, Martin P, Rodrigo J, Herrero J, Barrientos A. Cardiovascular effects of recombinant human erythropoietin in predialysis patients. *Am J Kidney Dis* 1997;29:541-8.
  - 26 Eschbach JW, Aquilino T, Haley NR, Fan MH, Blagg CR. The long-term effects of recombinant human erythropoietin on the cardiovascular system. *Clin Nephrol* 1992;38:S96-103.
  - 27 National Kidney Foundation—Dialysis Outcomes Quality Initiative. Guidelines for the treatment of anemia of chronic renal failure. *Am J Kidney Dis* 1997;30(suppl 3):S150-91.
  - 28 European best practice guidelines for the management of anaemia in patients with chronic renal failure. *Nephrol Dial Transplant* 1999;14(suppl 5):1-50.
  - 29 Foley RN, Parfrey PS. Cardiac disease in chronic uremia: clinical outcomes and risk factors. *Adv Ren Rep Place Ther* 1997;4:234-8.

(Accepted 31 May 2002)

## Lesson of the week

# Antenatal screening for rubella—infection or immunity?

Nilesh M Mehta, Roslyn M Thomas

**Interpret antenatal screening tests for rubella cautiously in recent immigrants and in women with a rash in early pregnancy**

Neonatal Intensive Care Unit, Northwick Park Hospital, Harrow HA1 3UJ

Nilesh M Mehta specialist registrar  
Roslyn M Thomas consultant paediatrician

Correspondence to: R M Thomas ros.thomas@nwlh.nhs.uk

*BMJ* 2002;325:90-1

Rubella vaccination among schoolgirls and susceptible women in the United Kingdom since 1970 has dramatically reduced the number of cases of congenital rubella syndrome and terminations of pregnancies related to rubella infection.<sup>1</sup> In 1988 the combined measles, mumps, and rubella vaccine was introduced for children aged 12-15 months. Reported cases of congenital rubella syndrome declined significantly, with only a few notified cases of infection among immigrants and in infants whose mothers acquired the infection while travelling overseas in early pregnancy. Immune status of pregnant women is determined by routine antenatal screening for rubella IgG antibody, so that susceptible women can receive postpartum vaccination.

We report two infants with congenital rubella syndrome whose mothers had recently arrived from abroad. Both mothers had a rash in early pregnancy in their country of origin, which was not elicited when they booked for antenatal care in the United Kingdom.

## Case reports

### Case 1

A 22 year old primiparous Sri Lankan woman had routine antenatal screening tests at 20 weeks' gestation, soon after her arrival in the United Kingdom. The laboratory reported presence of rubella IgG antibody, "consistent with immunity." The infant was born with severe symmetrical intrauterine growth restriction, purpura, thrombocytopenia, and a patent ductus arteriosus. Cranial ultrasonography showed bilateral periventricular calcification (fig 1). Skeletal radiographs showed linear radiolucencies in the metaphyses of the long bones and lucent areas in the iliac bones, consistent with osteitis (fig 2). Ophthalmological examination showed a unilateral cataract on the first day after birth and progressive bilateral cataracts by 3

weeks of age. Congenital rubella syndrome was suspected, and the mother confirmed that she had had a transient rash at 6-8 weeks' gestation in Sri Lanka. Rubella specific IgM was detected in the infant's blood taken at 11 days of age, and excretion of rubella virus was subsequently confirmed in the infant's saliva and urine. Audiological testing showed major bilateral sensorineural hearing loss by 12 weeks. Retesting of the mother's antenatal serum with IgM and IgG avidity tests gave results compatible with acquired rubella infection during early gestation.

### Case 2

Soon after her arrival in the United Kingdom a 29 year old primiparous Nigerian woman gave birth at 38 weeks' gestation to an infant with severe symmetrical intrauterine growth restriction. The woman's antenatal tests in Nigeria did not include rubella screening. The infant had interstitial pneumonitis, thrombocytopenia, and a patent ductus arteriosus. Ophthalmological examination showed bilateral cataracts by 3 weeks of

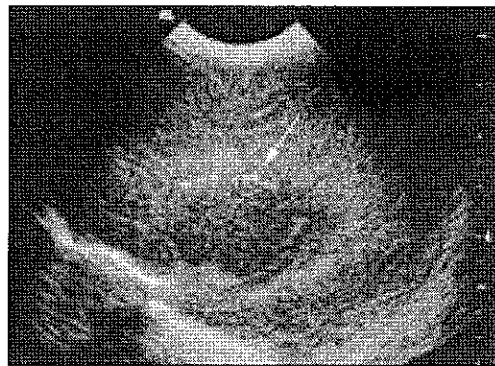


Fig 1 Cranial ultrasound scan showing linear calcification in the brain parenchyma in the parasagittal plane

## **ARTICLE 5**



## MR Contrast Agent at High-Field MRI (3 Tesla)

Siegfried Trattig, MD, Ahmed Ba-Ssalamah, MD, Iris-Melanie Noebauer-Huhmann, MD, Markus Barth, PhD, Stefan Wolfsberger, MD, Katja Pinker, MD, and Engelbert Knosp, MD

**Abstract:** Tumor-to-brain contrast after gadolinium administration using MP-RAGE and T1-SE scans in patients with primary and secondary brain tumors was significantly higher at 3 T than at 1.5 T. The subjective assessment of cumulative triple-dose 3 Tesla images obtained the best results in the detection of brain metastases compared with other sequences followed by 1.5 T cumulative triple-dose enhanced images. In macroadenomas of the hypophysis, contrast-enhanced 3 T MRI was superior to standard MRI in the diagnosis of cavernous sinus infiltration and in visualization of cranial nerves within the cavernous sinus. Due to higher spatial resolution, contrast-enhanced MR venography at 3 T showed more details in and around tumors than at 1.5 T, additionally enhanced by stronger susceptibility weighting and higher signal-to-noise ratio at 3 T. In summary, administration of gadolinium-based contrast agent produces higher contrast between tumor and normal brain at 3 T than at 1.5 T, helps to detect more cerebral metastases at 3 T versus 1.5 T in single and cumulative triple dose, improves the evaluation of macroadenomas of the hypophysis, and makes MR venography at 3 T clinically attractive with increase in spatial resolution within the same measurement time, thus providing more detailed information.

**Key Words:** 3 Tesla MRI, high-field strength, gadolinium, MRI contrast agent, brain tumors, metastases, MR venography

(*Top Magn Reson Imaging* 2003;14:365–375)

### INTRODUCTION

The recent introduction of clinical magnetic resonance (MR) scanners operating at magnetic field strengths >1.5 Tesla (T) marks a revolution in MR imaging (MRI). Since about 1998, the major MR scanner vendors began to offer high-field scanners, typically operating at 3 T. This new generation of compact 3 T magnets feature identical geometric dimensions as well as the same user environment as the state-of-the-art 1.5 T systems. They offer access to most MR techniques and at

the same time capitalize on the advantages of high-field MRI and MR spectroscopy.<sup>1–6</sup> Such a combination shows promise to open the door to routine clinical use of 3 T MR systems.

The increasing availability of such high-field scanners in the near future raises the question of how contrast agents behave at 3 T and, in particular, whether high-field scanners will improve the radiologic evaluation of intracranial tumors after administration of contrast agents.

Additionally, it can be hypothesized that techniques that benefit from the higher field such as BOLD (Blood Oxygenation Level Dependent) imaging may be further improved by contrast agent administration.

### TECHNICAL CONSIDERATIONS AND BASIC CONTRAST AGENT STUDY

Contrast-enhanced MRI has become the method of choice for visualization of most abnormalities of the brain. The intravenous administration of gadolinium-DTPA for contrast-enhanced images has proved to be valuable in the evaluation of primary brain tumors and metastases. Most of these tumors enhance with the use of contrast agents, with improved tumor delineation and evaluation of internal tumor structure. An intravenous dose of 0.1 mmol/kg has been established as the optimum dose on routine scanners.

It is well known that the magnetic field strength influences the effect of contrast agent.

The effect on behavior of contrast agents at different field strengths depends on two basic mechanisms: the nuclear magnetic relaxation dispersion and the field-dependent relaxation of tissue.<sup>7</sup>

The *nuclear magnetic relaxation dispersion* or *relaxivity* of a paramagnetic ion to water protons, described by the Solomon-Bloembergen-Morgan equation, decreases at higher magnetic fields.<sup>8</sup> The relaxivity of gadodiamide has been tested in lower and higher field strengths up to 2 T. A decrease that becomes slower and is nearly proportional to the field strength above 0.4 T has been demonstrated in vitro.<sup>9</sup>

The *water proton relaxation rates* (1/T1) of brain tissues decrease when the field strength increases from 1.5 to 3 T.<sup>10</sup> Thus, the intrinsic T1 of tissue increases with field strength.<sup>7</sup> The rates at which excited protons relax are known to be functions of the applied magnetic field. In general, for semisolid tissues the longitudinal or spin-lattice relaxation rate

From the Centre of Excellence "High-Field MR," Department of Radiology (Drs Trattig, Ba-Ssalamah, Barth, Noebauer-Huhmann, and Pinker) and the Department of Neurosurgery (Drs Wolfsberger and Knosp), University Hospital of Vienna Medical School, Vienna, Austria.

Reprints: Siegfried Trattig, MD, Centre of Excellence "High-Field MR," Department of Radiology, University Hospital of Vienna Medical School, Währinger Gürtel 18-20, A-1090 Vienna, Austria (e-mail: siegfried.trattig@univie.ac.at).

Copyright © 2003 by Lippincott Williams & Wilkins

( $R1 = 1/T1$ ) decreases with field strength, while the transverse or spin-spin relaxation rate ( $R2 = 1/T2$ ) is only slightly affected. The  $R1$  rate has been observed to decrease about 20% to 30% between 1.5 T and 3 T. This corresponds to an increase in  $T1$  relaxation time of between 35% and 40%. Thus, the signal enhancement in  $T1$ -weighted MR images produced by the administration of a standard dose of gadolinium contrast agent should depend on actual relaxation times of nonenhanced (gray and white matter) and enhanced (tumor) tissues at a particular magnetic field. As  $T1$  is shorter at lower magnetic fields, a further decrease caused by administration of contrast agent seems to produce less contrast than at higher field strengths. The magnetic field dependence of contrast enhancement in tumors was addressed in several studies.<sup>11-14</sup> The contrast effect of gadodiamide in brain tumors compared with normal brain has been found to be greater at 1.5 T than at 0.3 T.<sup>12</sup> In a different study, an increase in contrast enhancement in brain tumors was found at 2.0 T compared with 0.5 T.<sup>13</sup> A recent study proved that a higher dose is required for low-field MR scanners operating at 0.2 T.<sup>14</sup>

In a recent study performed by Noebauer-Huhmann et al.,<sup>15</sup> it could be demonstrated that in  $T1$ -weighted 3D-gradient echo sequence with magnetization preparation (MP-RAGE), and even in  $T1$ -SE not optimized for 3 T (identical parameters on 1.5 and 3 T were used, despite the longer  $T1$ -relaxation times on the 3 T MR unit) after gadolinium-based contrast agent administration the contrast between brain tumor or metastasis and the surrounding normal brain was markedly higher at 3 T compared with 1.5 T (Figs. 1, 2). These results confirm previous expectations that although both the relaxation rate of the unenhanced tissue and the relaxivity of the contrast agent decrease with increasing field strength, it is not a proportional process.

The better tumor-to-brain contrast after gadolinium administration on the higher field can be clinically used to reduce the amount of contrast media in routine contrast studies of the brain. Thus, a recent presentation showed that using the half standard dose of gadolinium-DTPA at 3 T provided a similar tumor brain contrast compared with 1.5 T.<sup>16</sup>

## CLINICAL APPLICATIONS

### Detection of Brain Metastases

In patients with cancer, intracranial metastases are diagnosed before or with the primary tumor in about 20%.<sup>17</sup> The diagnosis of intracranial metastases in patients with cancer is important for prognosis and therapy, since staging of the primary tumor is changed and more aggressive therapeutic regimens are necessary. Patients with multiple brain metastases are usually treated with whole brain radiation and/or chemotherapy without surgery. It has been reported that patients with solitary metastasis who undergo resection have an increased survival time and an improved quality of life compared with patients with solitary metastasis and chemotherapy alone.<sup>18</sup>

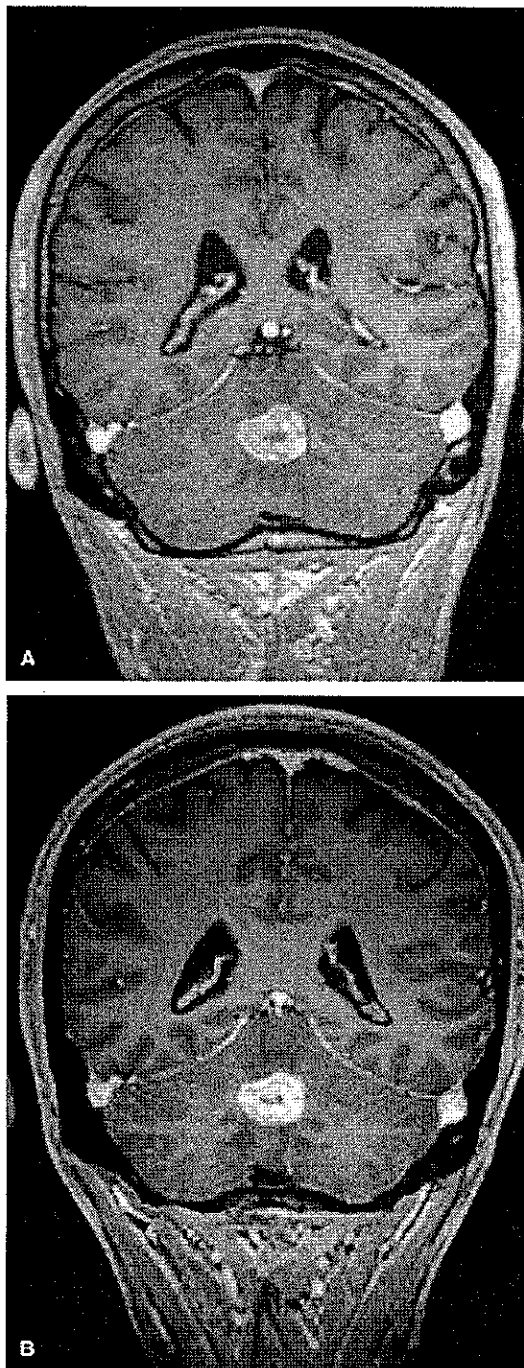


**FIGURE 1.** Metastasis in the cerebellar vermis on MP-RAGE image after intravenous contrast agent administration in the coronal plane on 1.5 T (a) and on a corresponding 3.0 T image (b). The tumor-to-brain contrast is higher on 3.0 T than on 1.5 T.

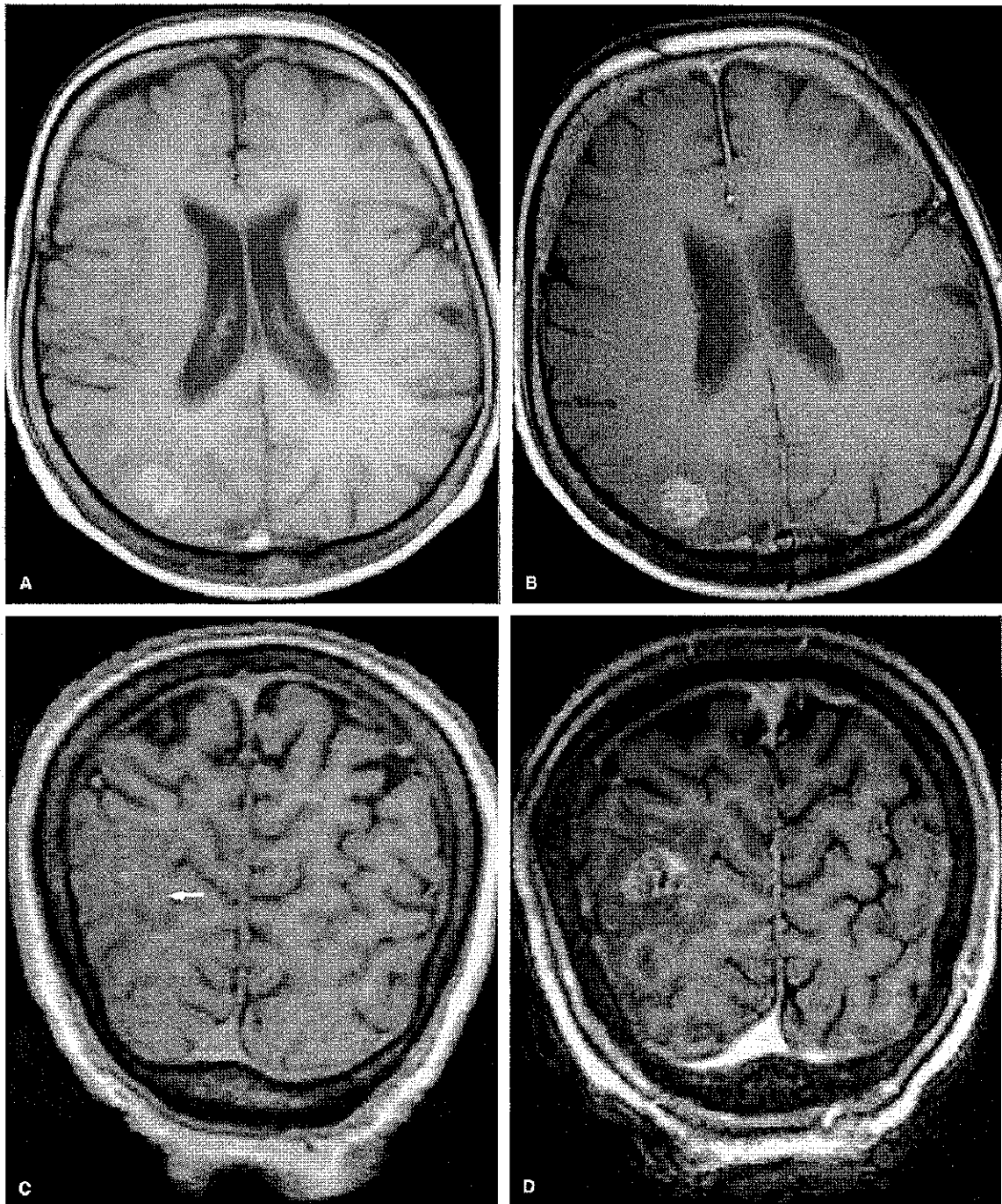


**FIGURE 2.** Glioma in the right parieto-occipital region demonstrated on postcontrast axial T1-SE image on 1.5 T (a) and 3.0 T (b) and on postcontrast coronal MP-RAGE image on 1.5 T (c) (arrow) and 3.0 T (d). The lesion is much better seen on postcontrast 3.0 T SE and MP-RAGE images.

The decision regarding a conservative versus a surgical approach depends on the number of brain metastases detected by radiology. A single lesion was found by CT and MRI in up to 50% of all patients with intracerebral metastases.<sup>19</sup> In many

departments of neurosurgery, up to 2 metastases would be removed surgically or with gamma knife therapy, whereas in patients with more than 2 metastases whole brain radiation and chemotherapy are performed.

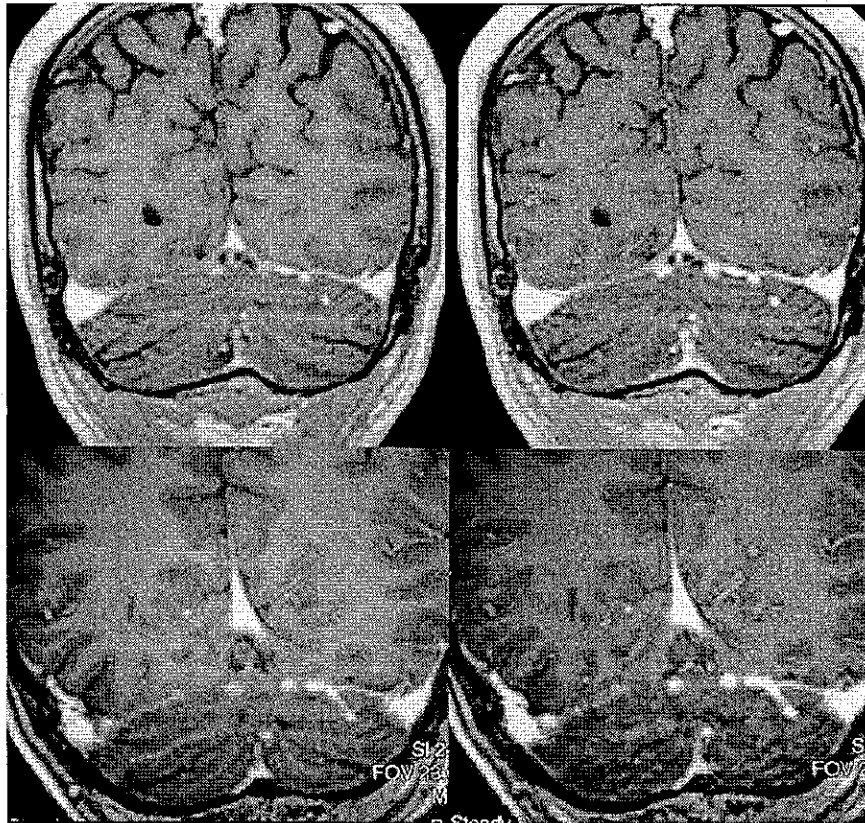


**FIGURE 3.** Four metastases in the posterior fossa are shown on coronal MP-RAGE image after intravenous contrast agent administration on 1.5 T image single dose (left upper), on corresponding 3.0 T image single dose (left lower), on 1.5 T image triple dose (right upper), and corresponding 3.0 T image triple dose (right lower). Note that on single dose examinations lesions are better delineated on 3.0 T than at 1.5 T, whereas triple dose examinations on both field strengths depict lesions with excellent contrast.

Thus, from a radiologic viewpoint, it is important to increase the detection rate of brain metastases for optimal patient treatment. Even with MRI, though clearly superior to CT, the detection of small metastases is a challenge, since small metastases frequently located at the corticomedulullary junction may not be associated with vasogenic edema or mass effect.<sup>20</sup> Therefore, a reasonably high lesion contrast and high spatial resolution are required.

An improved lesion contrast can be achieved by using either a higher dose of contrast agent or a higher field strength.

An intravenous administration of 0.1 mmol/L gadolinium-chelate has been widely accepted as a standard dose for routine examinations of cerebral diseases on routine MR scanners.<sup>21</sup> However, an improvement of lesion contrast has also been demonstrated with higher doses of gadolinium-chelate,<sup>22</sup> in particular in brain diseases with subtle enhancement or small lesions.

Another way to increase the conspicuity of small lesions is the use of MR scanners operating at a higher field, such as 3

T. The higher field strength not only improves the signal-to-noise ratio, providing the basis for high-resolution imaging, but also the T1 relaxation times of gray and white matter become longer.<sup>7,8</sup> The later effect reduces the T1 contrast of brain on T1-weighted spin-echo sequences without contrast agent administration, but it has the advantage that the uptake of contrast agent produces a more significant shortening of the T1 relaxation time at higher field strengths. This can be attributed to the field strength dependence of the T1 relaxation time that is well known and has been investigated previously on a 3 T whole body scanner.<sup>15</sup>

In a recent study by Ba-Ssalamah et al.<sup>23</sup> in which a single (standard) dose and a cumulative triple dose (a double dose 10 minutes after a standard dose) was compared at 3 T with 1.5 T in patients with known or clinically suspected brain metastases, the cumulative triple-dose images at 3 T and 1.5 T were markedly better for detection of brain metastases with an average of 4.1 lesions per patient, whereas an average of 3.4 lesions per patient were seen on the single-dose 3 T and 1.5 T.

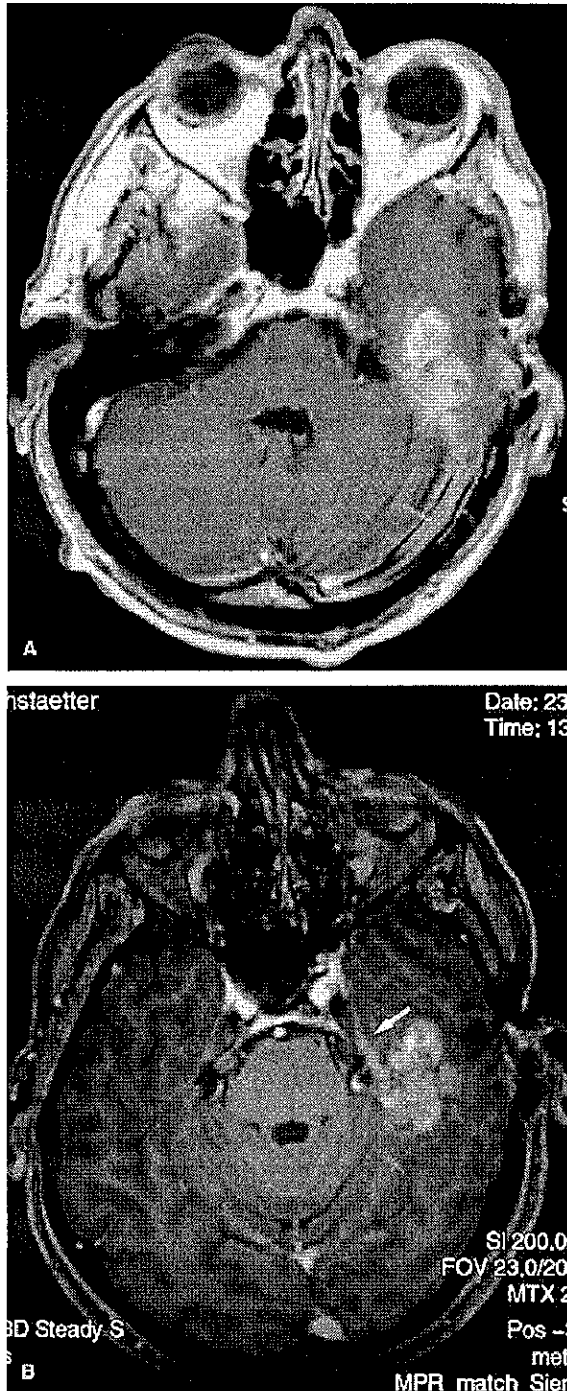


**FIGURE 4.** A multilobulated metastasis in the left temporal lobe with infiltration of the left tentorial dura is shown on axial postcontrast MP-RAGE image on 1.5 T (a) and 3.0 T (b) (arrow). Dural infiltration is more conspicuous on 3.0 T than on 1.5 T.

The subjective assessment of cumulative triple-dose 3 T images obtained the best results compared with other sequences, detecting 84 metastases, followed by 1.5 T cumulative triple-dose enhanced images with 81 brain metastases (Fig. 3). The objective assessment confirmed these results showing significantly higher signal-to-noise and contrast-to-noise ratios with 3 T compared with 1.5 T.

There was a significant difference between the cumulative triple dose and single dose for both field strengths in the detection of lesions <5 mm; however, no significant difference was found in the detection of lesions >5 mm.

In two cases, in which leptomeningeal infiltration was observed, the enhancing pattern identified in the high field strength single-dose MR scan was better visualized than on the standard field strength single-dose MR scan (Fig. 4).

Although it could be demonstrated in this study<sup>23</sup> that high field strength MRI is clinically beneficial in assessing brain metastases, it is an expensive approach so far. The same study also revealed that a cumulative triple-dose contrast administration as an independent influencing factor improves lesion contrast even more than a high field strength. The advantage of higher contrast dosage for the detection of brain metastases has been described previously<sup>6</sup> and was confirmed by the results of the recent study.<sup>23</sup>

However, it could be demonstrated that high field strength and cumulative triple contrast dosage have synergistic effects and can therefore be used together advantageously. An optimized imaging technique is of importance in patients in whom the detection of additional brain lesions may alter therapy dramatically. Discussing optimized imaging possibilities for low-contrast enhancing lesions, one has to keep in mind that there are a number of additional techniques that might improve the conspicuity of this type of lesions, including delayed acquisition of postcontrast images<sup>24</sup> or magnetization transfer sequences.<sup>25</sup>

### Evaluation of Macroadenomas of the Hypophysis

At present, magnetic resonance imaging is considered the standard diagnostic tool for endosellar and parasellar structures. However, the currently established 1.0 to 1.5 T MR scanners have certain drawbacks in the imaging of sellar lesions for diagnosis and surgery:

Invasion of the parasellar spaces has been reported in 6% to 10% of pituitary adenomas.<sup>26</sup> Preoperative knowledge about the integrity of the medial cavernous sinus border is crucial as 1) parasellar invasion may increase surgical morbidity due to intense bleeding from the venous compartments and injury to the intracavernous carotid artery segment and cranial nerves<sup>27</sup>; 2) decreases the likelihood of surgical cure as tumor remnants may remain inside the cavernous sinus compartments<sup>28</sup>; and 3) indicates a biologically more aggressive tumor as demonstrated by an increased proliferation rate.<sup>29</sup> Incom-

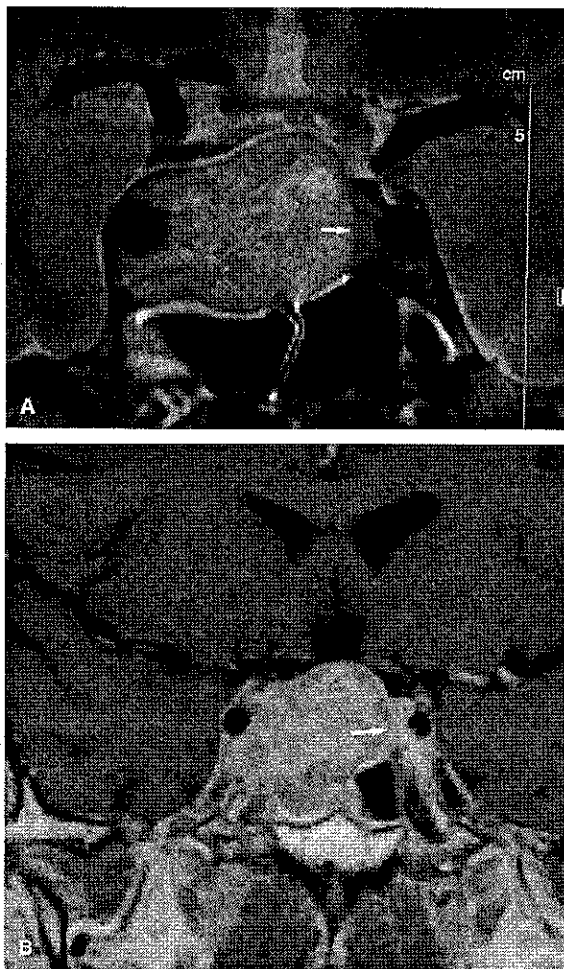


**FIGURE 5.** Cavernous sinus infiltration by macroadenoma on the right demonstrated on RARE-TSE (a) and postcontrast MP-RAGE (b) in the coronal plane. Notice that the left intact medial border of the cavernous sinus is well delineated on both sequences (arrow).

plete resection and tumor regrowth at an increased pace compared with noninvasive adenomas with the need for additional therapy such as focal irradiation, stereotactic radiosurgery, or reoperation are therefore characteristics of these lesions.

While the classic teaching is that a dural layer borders the pituitary gland laterally and constitutes the medial wall of the cavernous sinus,<sup>30</sup> recent anatomic-histologic studies have shown that it is actually a layer of mesenchymal loose circumferential fibers that is embedding the gland.<sup>31,32</sup> As this wall is fragile and thin, the lateral expansion of sellar lesions is common and its demonstration on contrast-enhanced MRI is often beyond spatial resolution. Dietemann et al. reported on 50 normal pituitaries scanned at 1.5 T MRI using a fast inversion recovery sequence and found a medial wall of the cavernous sinus only in a minority of cases.<sup>31</sup> A clear delineation of the

thin medial border of the cavernous sinus was also rarely seen in other studies<sup>33–35</sup> and, thus, cannot be taken into consideration for the diagnosis of invasion of the venous space. To increase the predictive value of MRI, classifications based on indirect signs of parasellar tumor extension through the medial cavernous sinus wall such as the Knosp classification,<sup>36</sup> angle of tumor surrounding the internal carotid artery (ICA), and tumor extension into the cavernous sinus compartments are routinely used.<sup>33</sup>

In a recent study performed by Wolfsberger et al.<sup>37</sup> on a 3 T MR unit, a high resolution imaging protocol was developed and performed on patients with macroadenomas of the hypophysis in comparison with a 1.5 T unit.

The results of 16 patients demonstrated that contrast-enhanced high-field, high-resolution MRI was superior in predicting tumor invasion into the cavernous sinus border by direct delineation of the medial border as a distinct line between the sellar lesion and the venous spaces (Fig. 5). The integrity or infiltration of the medial cavernous sinus border in 32 cases was correctly predicted in 84% of 3 T versus 59% of 1.5 T MR images with a statistically significant difference in specificity. However, comparison of sensitivities did not reach significance because of the small number of only six infiltrated cavernous sinuses.

This study also focused on the visualization of cranial nerves running through the lateral wall of the cavernous sinus by means of contrast-enhanced high-resolution, high-field MRI in comparison with standard (1.5 T) MRI.

The intracavernous segments of the cranial nerves III, IV, V<sub>1</sub>, V<sub>2</sub>, and VI are embedded in a sheath made of the superficial and deep dural layers of the lateral cavernous sinus wall.<sup>38–40</sup> 3 T MRI proved to be superior over standard MRI as it delineated significantly more hypointense spots on postcontrast series inside the lateral wall of the cavernous sinus at the anatomic positions of the cranial nerves.<sup>37</sup> The abducent nerve was the least common nerve to visualize as a spot between intracavernous ICA and IV/V<sub>1</sub>. This coincides with the results of Korogi et al.<sup>41</sup> who found the V<sub>1</sub>/VI nerve complex in only 28% of conventional postcontrast images. However, if they used the filling defects of contrast media on dynamic MRI studies as an indirect sign for cranial nerve location, detection improved to 75% but still they were only distinguishing paired cranial nerve complexes. With a median diameter of <1 mm, the trochlear nerve is the smallest of the intracavernous cranial nerves traveling below the oculomotor nerve and superolateral to the origin of the inferolateral trunk, its tentorial branch, and the intracavernous ICA. In the study by Wolfsberger et al.,<sup>37</sup> a hypointense spot separated from the oculomotor nerve was found in 67% of cases, which they attributed to intracavernous course of the trochlear nerve. In the 1.5 T MRI study of Daniels et al.,<sup>42</sup> the trochlear nerve could never be visualized independently of the oculomotor nerve. Depiction of the intracavernous segments of the cranial nerves is important because

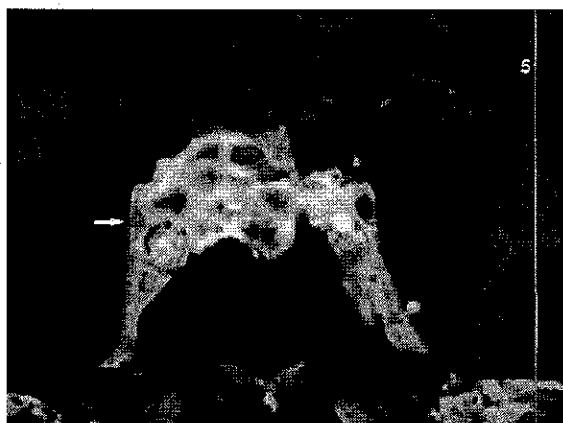


FIGURE 6. Patient with ophthalmoplegia on the right. On postcontrast 3.0 T coronal MP-RAGE image a hemorrhagic macroadenoma of the hypophysis infiltrates the right cavernous sinus with signs of compression of the third cranial nerve (arrow).

it may clinically contribute to the diagnosis of ophthalmoplegia in case of a tumor causing compression or ischemia of the nerve (Fig. 6).

Localization of the pituitary gland may be crucial for maintaining its integrity during surgery, particularly in case of an endosellar location of the pituitary gland and endoscopic approach with a small opening of the sellar floor. However, in case of large sellar lesions, the gland and the optic chiasm may be flattened to an extent where it cannot reliably be identified any more. It could be demonstrated that the contrast enhancement of the pituitary gland on T1-weighted images was stronger on 3 T compared with standard MRI and the signal of the optic chiasm was of higher signal intensity on noncontrast T1-weighted MP-RAGE images on 3 T versus T1-SE weighted MRI.<sup>37</sup> Stronger enhancement in high-field MR scanners after application of contrast agent has been reported,<sup>15</sup> the hyperintensity of the white fiber tracts such as the optochiasmatic system is attributed to the inversion recovery and heavily T1-weighted MP-RAGE sequence compared with standard spin-echo sequences usually applied in standard MR examinations. Both effects were found particularly helpful in delineating the compressed and flattened pituitary and optochiasmatic structures from the sellar lesion, which may allow prediction of the

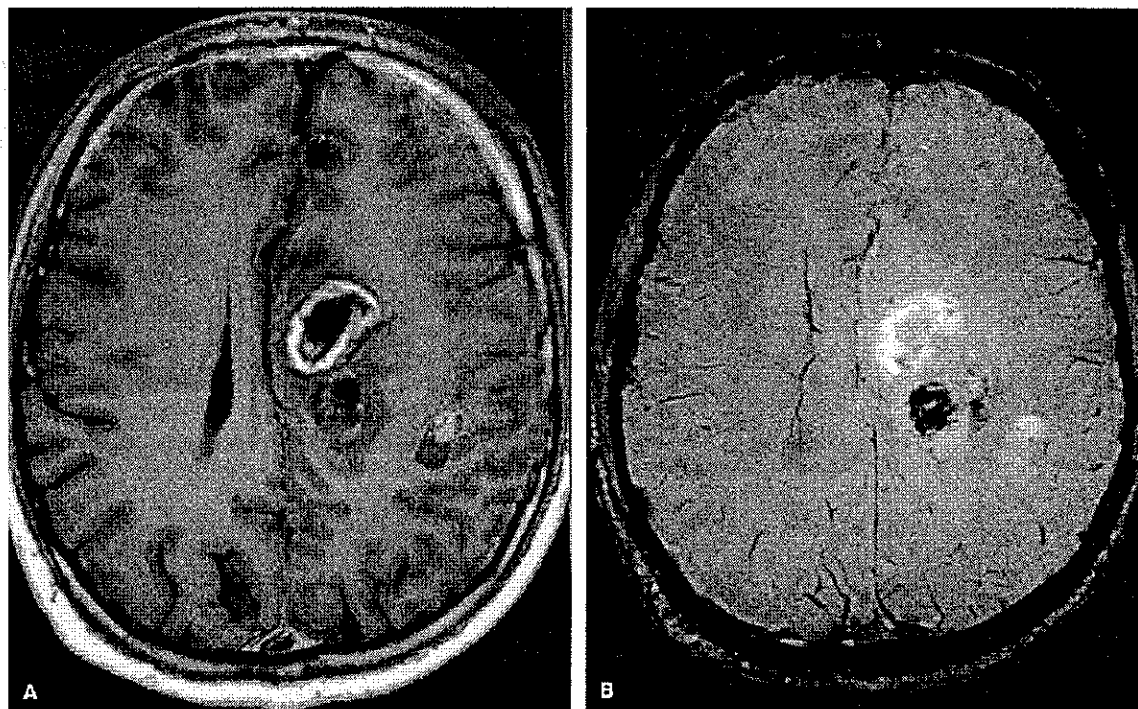
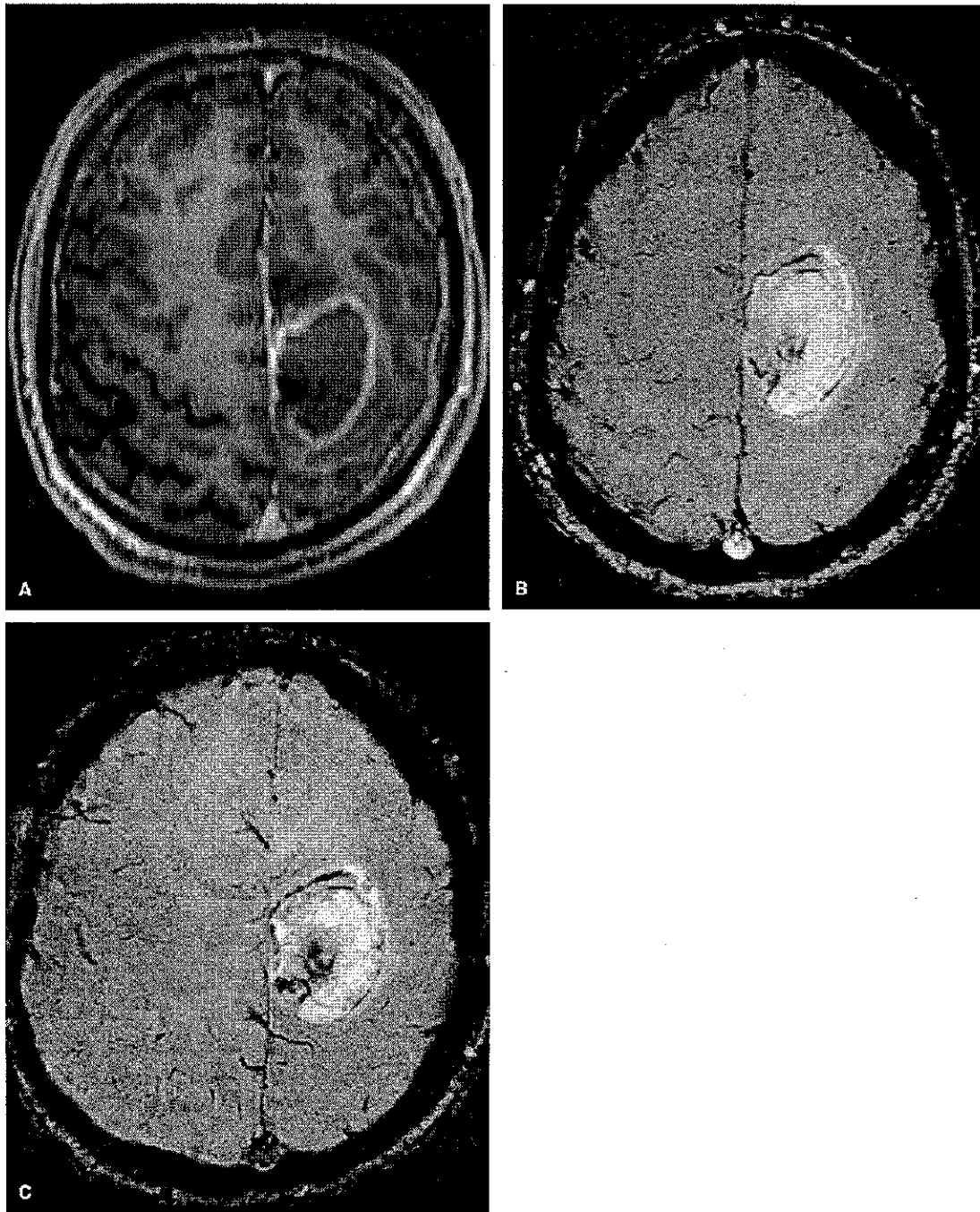


FIGURE 7. A histologically proven multifocal glioblastoma grade 4 is demonstrated on axial postcontrast IR-RARE (a) and on CE-MRV image (b). The multifocal lesion consists of smaller components with nodular contrast uptake and one larger component with rim enhancement. On CE-MRV image more structures with different features can be seen: a prominent inhomogeneous hypointense region in one part of the tumor. Some of the smaller hyperintense lesions show susceptibility effects and some show no effect. Notice that the large rim-enhancing part of the tumor shows no susceptibility effect at all.



**FIGURE 8.** A histologically proven high-grade glioma (grade 3) is shown on axial postcontrast MP-RAGE image (a) and on corresponding CE-MRV images on 1.5 T (b) and 3.0 T (c). The rim-enhancing tumor shows peripheral and central hypointensities on CE-MRV, corresponding to susceptibility effects with tubular appearance in the periphery. Note that on 3.0 T more details are visualized than on 1.5 T.



visual deficit in case of a tumor with large suprasellar extension according to the amount of distortion and dislocation of the optic chiasm and nerves.

### CONTRAST-ENHANCED MR VENOGRAPHY

Three-dimensional (3D) high-resolution magnetic resonance venography (MRV) has been introduced recently to study the normal venous architecture in the human brain utilizing Blood Oxygenation Level Dependent (BOLD)-induced phase effects between venous blood and surrounding brain parenchyma.<sup>43-45</sup> The visualization of small veins in the human brain noninvasively at submillimeter resolution by MRV has been used to provide detailed images of the venous architecture in diseases such as arteriovenous malformations,<sup>46-48</sup> occult vascular lesions,<sup>49</sup> and multiple sclerosis.<sup>50</sup> With these pathologies MRV offered important additional diagnostic information not easily obtained with other imaging modalities. One limitation for the full clinical application of MRV at 1.5 T is the long measurement time due to the long echo time and the high spatial resolution needed.

In a recent study by Barth et al.,<sup>51</sup> MRV protocols were developed to obtain both sufficient volume coverage and high spatial resolution within reasonable measurement times. Two approaches were taken to reduce measurement time:

1. A higher field strength (3 T) to increase the signal-to-noise ratio, which is doubled on 3 T in comparison to 1.5 T. In addition, the phase difference between blood and surrounding tissue also increase linearly with field strength<sup>52</sup> and  $T_2^*$  decreases with field strength.<sup>10</sup> First studies performed at 3 T<sup>47</sup> and on recently developed 8 T whole body scanners<sup>53,54</sup> showed superior delineation of small veins with significantly reduced scan time.
2. A standard dose of contrast agent was administered intravenously. It could be demonstrated that application of a T1-reducing contrast agent increased the blood signal fraction available for signal cancellation with surrounding tissue by inducing an extra phase shift.<sup>55</sup>

In the study by Barth et al.,<sup>51</sup> both approaches combined, ie, contrast-enhanced MRV (CE-MRV) at 3 T, led to optimum signal cancellation at a shorter echo time and, consequently, repetition time (TR).

Due to the higher field strength, the magnetization available for MRI was significantly increased so that the reduction in measurement time did not lead to reduced signal-to-noise ratio. A further decrease in measurement time might be possible using a double dose of contrast agent (0.2 mmol/kg), further enhancing visualization of venous structures as shown by a basic study of Lin et al.<sup>55</sup> performed at 1.5 T.

CE-MRV of highly vascularized tumors showed complex and variable venous patterns in various types of tumors and in different parts of the lesions (edema, contrast-enhancing area, central and/or necrotic part of the lesion) similar to findings in case studies at 1.5 T<sup>48,52</sup> (Fig. 7). This might be due to

the increased blood supply and particular vascular patterns around fast-growing (malignant) tumors. MRV can be used in principle to obtain vascular density and the associated blood volume, information that may help to assess the increased microvasculature that is associated with (re)growing tumors<sup>56</sup> as well as to detect nonviable tissue<sup>57</sup> or to identify increases or decreases of microvasculature during therapy.

Results of several other studies suggest that venous structures are very important to estimate the oxygen supply of tumors,<sup>58-66</sup> so in principle MRV has the potential to probe angiogenesis; however, further investigations (eg, by direct comparison of CE-MRV images with histologic sections or PET images) might show whether MRV can be used to estimate microvasculature or oxygen supply of tumors.

At 3 T, volume coverage and spatial resolution of the CE-MRV protocol were sufficient for routine examinations of patients with tumors and could be performed within a reasonable measurement time.<sup>51</sup> With the same measurement time, less details were visible on CE-MRV images at 1.5 T (Fig. 8). If the same resolution had been chosen at 1.5 T, CE-MRV measurement time would have increased by 25% compared with 3 T, still without having stronger susceptibility weighting and intrinsic higher signal-to-noise ratio available at 3 T.

### CONCLUSION

Administration of gadolinium-based contrast agent produces higher contrast between tumor and normal brain at 3 T than at 1.5 T, helps to detect more cerebral metastases at 3 T versus 1.5 T in single and cumulative triple dose, improves the preoperative evaluation of macroadenomas of the hypophysis and makes MRV at 3 T clinically attractive with increase in spatial resolution within the same measurement time, thus providing more detailed information.

### REFERENCES

1. Vaughan JT, Garwood M, Collins CM, et al. 7T vs. 4T: RF power, homogeneity and signal-to-noise comparison in head images. *Magn Reson Med.* 2001;46:24-30.
2. Bernstein MA, Huston J, Jack CR, et al. Routine clinical brain MR imaging at 3.0 T: initial experience. *Proc Int Soc Mag Reson Med.* 2000;8:1994.
3. Bernstein MA, Huston J, Lin C, et al. High-resolution intracranial and cervical MRA at 3.0 T: technical considerations and initial experience. *Magn Reson Med.* 2001;46:955-962.
4. Thulborn KR. Clinical rationale for very-high-field (3.0 Tesla) functional magnetic resonance imaging. *Top Magn Reson Imag.* 1999;10:37-50.
5. Gonen O, Gruber S, Li BS, et al. Multivoxel 3D proton spectroscopy in the brain at 1.5 T versus 3.0 T: signal-to-noise ratio and resolution comparison. *AJNR Am J Neuroradiol.* 2001;22:1727-1731.
6. Hunsche S, Moseley ME, Stoeter P, et al. Diffusion-tensor MR imaging at 1.5 and 3.0 T: initial observations. *Radiology.* 2001;221:550-556.
7. Rinck PA, Fischer HW, Van der Bist D, et al. Field-cycling relaxometry: medical applications. *Radiology.* 1988;168:843-849.
8. Wood ML, Hardy PA. Proton relaxation enhancement. *J Magn Res Imaging.* 1993;3:149-156.
9. Rinck PA, Muller RN. Field strength and dose dependence of contrast

- enhancement by Gadolinium-based MR contrast agents. *Eur Radiol.* 1999;9:998-1004.
10. Wansapura JP, Holland SK, Dunn RS, et al. NMR relaxation times in the human brain at 3.0 Tesla. *J Magn Res Imaging.* 1999;9:531-538.
  11. Elster AD. Field-strength dependence of Gadolinium enhancement: theory and implications. *AJNR Am J Neuroradiol.* 1994;15:1420-1423.
  12. Akeson P, Vikhoff B, Stahlberg F, et al. Brain lesion contrast in MR Imaging: dependence of field strength and concentration of gadodiamide injection in patients and phantoms. *Acta Radiol.* 1997;38:14-18.
  13. Chang KH, Ra DG, Han MH, et al. Contrast enhancement of brain tumors at different MR field strengths: comparison of 0.5 T and 2.0 T. *AJNR Am J Neuroradiol.* 1994;15:1413-1419.
  14. Hausteijn J, Laniado M, Niendorf H-P, et al. Administration of Gadopentate dimeglumine in MR imaging of intracranial tumors: dosage and field strength. *AJNR Am J Neuroradiol.* 1992;13:1199-1206.
  15. Nöbauer-Huhmann JM, Ba-Ssalamah A, Mlynarik V, et al. Magnetic resonance imaging contrast enhancement of brain tumors at 3 Tesla versus 1.5 Tesla. *Invest Radiol.* 2002;37:114-119.
  16. Krautmacher C, Tschampa H, Born MC, et al. MRI of contrast enhancing brain tumors at 3 Tesla versus 1.5 Tesla: first clinical results evaluating T1-weighted SE, FFE and MDEFT sequences. *Eur Congr Radiol.* 2003;437.
  17. Posner JB, Chernik NL. Intracranial metastases from systemic cancer. *Adv Neurol.* 1978;19:579-592.
  18. Martini N. Operable lung cancer. *CA Cancer J Clin.* 1993;43:201-214.
  19. Delattre JY, Krol G, Thaler HT, et al. Distribution of brain metastases. *Arch Neurol.* 1988;45:741-744.
  20. Healy ME, Hessclink J, Press GA, et al. Increased detection of intracranial metastases with intravenous Gd-DTPA. *Radiology.* 1987;165:619-624.
  21. Yuh WT, Fisher DJ, Engelken JD, et al. MR evaluation of CNS tumors: dose comparison study with gadopentetate dimeglumine and gadoteridol. *Radiology.* 1991;180:485-491.
  22. Runge VM, Kirsch JE, Burke VI, et al. High-dose gadoteridol in MR imaging of intracranial neoplasms. *J Magn Reson Imaging.* 1992;2:9-18.
  23. Ba-Ssalamah A, Nöbauer-Huhmann JM, Pinker K, et al. The effect of contrast dose and field strength in the MR detection of brain metastases. *Invest Radiol.* 2003;38:414-421.
  24. Yuh WT, Tali ET, Nguyen HD, et al. The effect of contrast dose, imaging time and lesion size in the MR detection of intracerebral metastases. *AJNR Am J Neuroradiol.* 1995;16:373-380.
  25. Finelli DA, Hurst GC, Karaman BA, et al. Use of magnetization transfer for improved contrast on gradient-echo MR images of the cervical spine. *Radiology.* 1994;193:165-171.
  26. Fahlbusch R, Buchfelder M. Transsphenoidal surgery of parasellar pituitary adenomas. *Acta Neurochir (Wien).* 1988;92:93-99.
  27. Thapar K, Laws ER Jr. Pituitary surgery. In: Thapar K, Kovacs K, Scheithauer BW, et al., eds. *Diagnosis and Management of Pituitary Tumors.* Totowa, NJ: Humana, 2001;225-246.
  28. Knosp E, Kitz K, Steiner E, et al. Pituitary adenomas with parasellar invasion. *Acta Neurochir Suppl (Wien).* 1991;53:65-71.
  29. Knosp E, Kitz K, Perneczky A. Proliferation activity in pituitary adenomas: measurement by monoclonal antibody Ki-67. *Neurosurgery.* 1989;25:927-930.
  30. Taptas JN. The so-called cavernous sinus: a review of the controversy and its implications for neurosurgeons. *Neurosurgery.* 1982;11:712-717.
  31. Dietemann JL, Kehrli P, Maillot C, et al. Is there a dural wall between the cavernous sinus and the pituitary fossa? Anatomical and MRI findings. *Neuroradiology.* 1998;40:627-630.
  32. Kehrli P, Ali M, Reis M Jr, et al. Anatomy and embryology of the lateral sellar compartment (cavernous sinus) medial wall. *Neurol Res.* 1998;20:585-592.
  33. Cottier JP, Destrieux C, Brunereau L, et al. Cavernous sinus invasion by pituitary adenoma: MR imaging. *Radiology.* 2000;215:463-469.
  34. Scotti G, Yu CY, Dillon WP, et al. MR imaging of cavernous sinus involvement by pituitary adenomas. *AJR Am J Roentgenol.* 1988;151:799-806.
  35. Steiner E, Imhof H, Knosp E. Gd-DTPA enhanced high resolution MR imaging of pituitary adenomas. *Radiographics.* 1989;9:587-598.
  36. Knosp E, Steiner E, Kitz K, et al. Pituitary adenomas with invasion of the cavernous sinus space: a magnetic resonance imaging classification compared with surgical findings. *Neurosurgery.* 1993;33:610-617.
  37. Wolfsberger S, Ba-Ssalamah A, Pinker K, et al. Application of 3 Tesla magnetic resonance imaging for diagnosis and surgery of sellar lesions. *Neurosurgery.* (in press)
  38. Rhoton AL Jr. The cavernous sinus, the cavernous venous plexus and the carotid collar. *Neurosurgery.* 2002;51:375-410.
  39. Lang J. *Skull Base and Related Structures.* Stuttgart, Germany: Schattauer, 1995;186-191.
  40. Umansky F, Nathan H. The lateral wall of the cavernous sinus: with special reference to the nerves related to it. *J Neurosurg.* 1982;56:228-234.
  41. Korogi Y, Takahashi M, Sakamoto Y, et al. Cavernous sinus: correlation between anatomic and dynamic gadolinium-enhanced MR imaging findings. *Radiology.* 1991;180:235-237.
  42. Daniels DL, Pech P, Mark L, et al. Magnetic resonance imaging of the cavernous sinus. *AJR Am J Roentgenol.* 1985;144:1009-1014.
  43. Reichenbach JR, Venkatesan R, Schillinger DJ, et al. Small vessels in the human brain: MR venography with deoxyhemoglobin as an intrinsic contrast agent. *Radiology.* 1997;204:272-277.
  44. Reichenbach JR, Jonetz-Mentzel L, Fitzek C, et al. High-resolution blood oxygen-level dependent MR venography (HRBV): a new technique. *Neuroradiology.* 2001;43:364-369.
  45. Reichenbach JR, Essig M, Haacke EM, et al. High-resolution venography of the brain using magnetic resonance imaging. *MAGMA.* 1998;6:62-69.
  46. Essig M, Reichenbach JR, Schad LR, et al. High-resolution MR venography of cerebral arteriovenous malformations. *Magn Reson Imaging.* 1999;17:1417-1425.
  47. Reichenbach JR, Barth M, Haacke EM, et al. High resolution MR venography at 3.0 Tesla. *J Comput Assist Tomogr.* 2000;24:949-957.
  48. Schad LR. Improved target volume characterization in stereotactic treatment planning of brain lesions by using high-resolution BOLD MR-venography. *NMR Biomed.* 2001;14:478-483.
  49. Lee BC, Vo KD, Kido DK, et al. MR high-resolution blood oxygenation level-dependent venography of occult (low-flow) vascular lesions. *AJNR Am J Neuroradiol.* 1999;20:1239-1342.
  50. Tan IL, van Schijndel RA, Pouwels PJ, et al. MR venography of multiple sclerosis. *AJNR Am J Neuroradiol.* 2000;21:1039-1042.
  51. Barth M, Nöbauer-Huhmann JM, Reichenbach JR, et al. High resolution three-dimensional contrast-enhanced blood oxygenation level-dependent magnetic resonance venography of brain tumors at 3 Tesla: first clinical experience and comparison with 1.5 Tesla. *Invest Radiol.* 2003;38:408-413.
  52. Reichenbach JR, Haacke EM. High-resolution BOLD venographic imaging: a window into brain function. *NMR Biomed.* 2001;14:453-467.
  53. Novak V, Abduljalil A, Kangarlu A, et al. Intracranial ossifications and microangiopathy at 8 Tesla MRI. *Magn Reson Imaging.* 2001;19:1133-1137.
  54. Abduljalil AM, Schmalbrock P, Novak V, et al. Phase venous vessels enhancement in high field brain MR imaging. *Proc ISMRM.* 2002;1045.
  55. Lin W, Mukherjee P, An H, et al. Improving high-resolution MR bold venographic imaging using at T1 reducing contrast agent. *J Magn Reson Imaging.* 1999;10:118-123.
  56. Tynniinen O, Aronen HJ, Ruhala M, et al. MRI enhancement and microvascular density in gliomas: correlation with tumor cell proliferation. *Invest Radiol.* 1999;34:427-434.
  57. Henry RG, Vigneron DB, Fischbein NJ, et al. Comparison of relative cerebral blood volume and proton spectroscopy in patients with treated gliomas. *AJNR Am J Neuroradiol.* 2000;21:357-366.
  58. Kuperman V, Rivicr JN, Lewis MZ, et al. Changes in T2\*-weighted images during hyperoxia differentiate tumors from normal tissue. *Magn Reson Med.* 1995;33:318-325.
  59. Karczmar GS, Kuperman VY, Rivicr NJ, et al. Magnetic resonance measurement of response to hyperoxia differentiates tumors from normal tissue and may be sensitive to oxygen consumption. *Invest Radiol.* 1994;29 (suppl 2):161-163.
  60. Rodrigues LM, Maxwell RJ, McSheehy PM, et al. In vivo detection of ifosfamide by 31P-MRS in rat tumors: increased uptake and cytotoxicity induced by carbogen breathing in GH3 prolactinomas. *Br J Cancer.* 1997;75:62-68.

61. Robinson SP, Howe FA, Griffiths JR. Noninvasive monitoring of carbogen-induced changes in tumor blood flow and oxygenation by functional magnetic resonance imaging. *Int J Radiat Oncol Biol Phys.* 1995;33:855-859.
62. Robinson SP, Collingridge DR, Howe FA, et al. Tumour response to hypercapnia and hyperoxia monitored by FLOOD magnetic resonance imaging. *NMR Biomed.* 1999;12:98-106.
63. Howe FA, Robinson SP, Rodrigues LM, et al. Flow and oxygenation dependent (FLOOD) contrast MR imaging to monitor the response of rat tumors to carbogen breathing. *Magn Reson Imaging.* 1999;17:1307-1318.
64. Howe FA, Robinson SP, McIntyre DJ, et al. Issues in flow and oxygenation dependent contrast (FLOOD) imaging of tumors. *NMR Biomed.* 2001;14:497-506.
65. McSheehy PM, Robinson SP, Ojugo AS, et al. Carbogen breathing increases 5-fluorouracil uptake and cytotoxicity in hypoxic murine RIF-1 tumors: a magnetic resonance study in vivo. *Cancer Res.* 1998;58:1185-1194.
66. Robinson SP, Howe FA, Rodrigues LM, et al. Magnetic resonance imaging techniques for monitoring changes in tumor oxygenation and blood flow. *Semin Radiat Oncol.* 1998;8:197-207.

## **ARTICLE 6**

# Magnetic Resonance Angiography of Chest and Abdomen at 3 T

Ulrich Kramer, MD,\* Kambiz Nael, MD,† Michael Fenchel, MD,\* and Stephan Miller, MD\*

**Abstract:** During the past decade, contrast-enhanced magnetic resonance angiography (CE-MRA) has been proven to be a powerful tool to visualize the thoracoabdominal vasculature and, consequently, has become a widely accepted noninvasive imaging modality. With the more recent introduction of high-field whole-body magnetic resonance scanners, a further improvement of diagnostic accuracy can be expected. General considerations for performing high-resolution CE-MRA at higher field strength include the benefits of higher signal-to-noise ratio and an improved contrast between vascular and background tissues. Although there are many positive attributes for performing CE-MRA at 3 T, there are also some tradeoffs, such as static magnetic field inhomogeneity and increase in specific absorption rate. This review describes the main technical innovations of advanced CE-MRA techniques at 3 T, illustrated by characteristic cases.

**Key Words:** 3 T, abdominal aorta, magnetic resonance angiography, parallel imaging, technical developments

(*Top Magn Reson Imaging* 2007;18:105–115)

During the past decade, 3-dimensional (3-D) contrast-enhanced magnetic resonance angiography (CE-MRA) has become a widely accepted, reliable, and noninvasive tool for evaluation of thoracoabdominal vasculature.<sup>1–3</sup> Furthermore, CE-MRA has high sensitivity and specificity estimates when compared with the generally accepted standard of reference, the intra-arterial digital subtraction x-ray angiography (DSA), of almost all vascular territories.<sup>4–6</sup> In addition, when focusing on abdominal imaging, in several studies, CE-magnetic resonance angiography (MRA) has been proven to be a powerful tool to visualize abdominal vasculature and, nowadays, is even comparable with computed tomographic angiography (CTA) and is superior to ultrasound.<sup>7–9</sup> Although CE-MRA is more expensive and less readily available compared with ultrasound or CTA, the added information provided by MRA has resulted in its widespread use as the modality of choice for a variety of vascular disorders.<sup>10,11</sup>

From the \*Department of Diagnostic Radiology, University of Tuebingen, Germany and †Department of Radiological Sciences, David Geffen School of Medicine, University of California Los Angeles, Los Angeles, CA.

Reprints: Ulrich Kramer, MD, Department of Diagnostic Radiology, University of Tuebingen, Hoppe-Seyler-Str. 3, 72076 Tuebingen, Germany (e-mail: ulrich.kramer@med.uni-tuebingen.de).  
Copyright © 2007 by Lippincott Williams & Wilkins

## DIFFERENT TECHNIQUES OF MRA

Most commonly used techniques for imaging the thoracoabdominal aorta are time-of-flight (TOF) MRA and 3-D CE-MRA.

Two-dimensional TOF MRA is a relatively simple technique based on the inflow of unsaturated blood into a saturated slice (imaging volume). Saturation of the tissue in the slice is achieved by submitting it to radio frequency (RF) pulses with a repetition time much shorter than the tissue T1 values, thereby decreasing its longitudinal magnetization vector. Because inflowing unsaturated blood still has a large longitudinal magnetization vector, it will be seen in the image slice as an area of high signal intensity. Apart from scan times of several minutes, 2 major types of artifacts can be distinguished in TOF MRA: flow voids and ghosting artifacts. Flow voids can be caused by in-plane saturation or post-stenotic turbulence effects. Ghosting artifacts can be found as a consequence of vessel pulsatility or large variations in flow velocity during the cardiac cycle. Therefore, TOF MRA is only successfully applied in nonmoving structures with good inflow properties, such as extracranial and intracranial vasculatures.

Consequently, the need to overcome these limitations of noncontrast MRA techniques has driven the development and clinical use of CE-MRA in the thoracic and the abdominal aortas. The drawbacks of TOF imaging include long imaging times, inability to see in-plane and small vessels, and loss of signal in aneurismal vascular structures secondary to turbulent flow. On the other hand, CE-MRA is fast, avoids saturation effects, is flow-independent, and offers substantially higher spatial and temporal resolution compared with noncontrast techniques.

The aims of this article are to describe the technical approaches to CE-MRA of the thoracoabdominal aorta at 3 T and to provide an overview of the relevant clinical applications in this vascular territory.

## MRA IN COMPARISON WITH CONVENTIONAL INTRA-ARTERIAL ANGIOGRAPHY

Magnetic resonance angiography has several advantages over conventional angiography. Digital subtraction x-ray angiography is invasive and exposes patients to radiation and nephrotoxic iodinated contrast agent. Furthermore, it may be associated with additional complications, such as atheroembolism, retroperitoneal hemorrhage, or pseudoaneurysm formation. In contrast to this, the reliability of MRA is not affected by impaired renal function or the

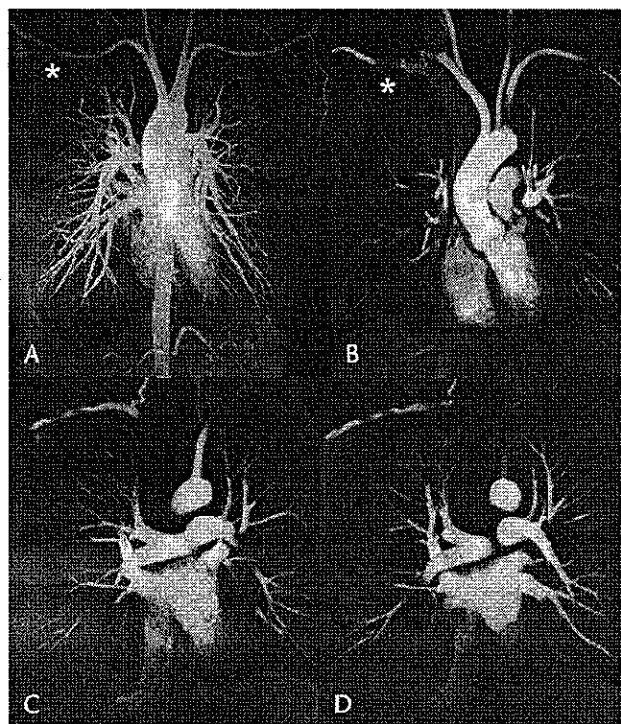


**FIGURE 1.** High-spatial-resolution CE-MRA in a 33-year-old male volunteer. Full-thickness MIP (A) and 3 consecutive coronal thin-MIP images (B–D) of the same volunteer are shown. Images reveal up to the fifth-order pulmonary branches with good definition. Note the typical T2\* artefact causing local signal loss (\*) in the right subclavian artery.

presence of bilateral renovascular disease.<sup>5,12,13</sup> Moreover, it is unnecessary to hydrate the patients or to stop the use of diuretics before the examination. Another suggested advantage of MRA is the possibility of evaluating not only arterial but also venous vasculature. The general lack of nephrotoxicity of these magnetic resonance (MR) contrast agents is an especially important advantage for patients with poor renal function, particularly in the workup of suspected renal artery stenosis. In this way, conventional angiography for diagnosis can be avoided in a large number of patients and be reserved for those patients with clinically significant stenosis who may benefit from intervention.<sup>14,15</sup>

Nevertheless, conventional angiography, especially of the renal arteries, remains the criterion standard for evaluation of vascular anatomy; the major advantage is a convincingly high spatial resolution (in-plane resolution, up to  $0.3 \text{ mm}^2$ ) allowing for precise assessment of number, length, and morphology of arterial and venous vessels or for determining the presence of vascular stenosis.

### HIGH-FIELD CE-MRA AT 3 T

With the more recent introduction of high-field whole-body MR scanners to the clinical environment, the resultant approximate doubling in signal-to-noise ratio (SNR) at 3 T can

be used to increase spatial and/or temporal resolution. There is the potential to acquire high-spatial resolution data sets with an isotropic resolution of  $1 \text{ mm}^3$  or even less. To detect vessel details, such as narrowing, even in segmental arteries (eg, renal arteries), isotropic data sets are desirable. Multiplanar reformatting comparable with that of high-resolution CT volume data sets requires isotropic data to avoid geometric distortions and to ensure accurate delineation of the vasculature (Fig. 1).<sup>16–19</sup> Furthermore, another potential benefit of high-field MRA includes the prolongation of the longitudinal tissue relaxation time T1 in background tissue, leading to an increased contrast to noise ratio (CNR) between contrast-enhanced vascular structures (Gd-chelates) and the surrounding background tissue. Importantly, SNR and CNR gain may be used at 3 T to increase spatial resolution to avoid partial volume effects and, hence, decrease diagnostic accuracy because it is an often-reported limitation at 1.5 T when grading vascular stenoses, owing to moderate spatial resolution (in-plane resolution,  $>1.5 \text{ mm}$ ). Consequently, nowadays, high-field CE-MRA can compete with multi-detector CTA in resolution parameters, and further improvements of diagnostic accuracy can be expected (Fig. 2).<sup>20</sup> By using parallel imaging techniques, such as sensitivity encoding or simultaneous acquisition of spatial harmonics, and high

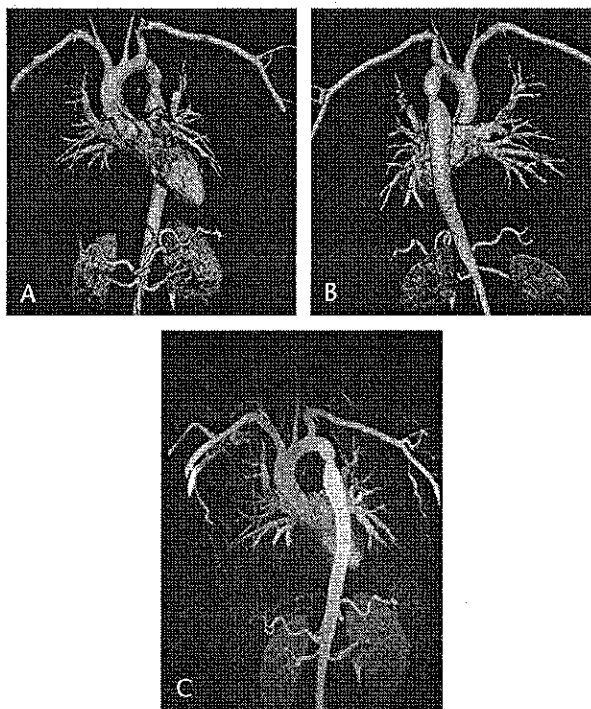


**FIGURE 2.** Images obtained from a 28-year-old male patient with coarctation of the aorta. Volume-rendered (A, B) images in an anterior and posterior view and maximum-intensity projection (MIP). High-grade aortic isthmus stenosis is also shown (C). Note the additional findings, such as an accessory renal artery on the left side owing to extended field of view and high spatial resolution.

acceleration factors, this can be realized without any prolongation of the acquisition time.

**PARALLEL IMAGING TECHNIQUES**

Increasing the spatial resolution requires larger imaging matrices, which means longer repetition time (TR) values in the 3-D angiographic sequences. Moreover, by reducing slice thickness, more slices have to be acquired for the assessment of a given imaging volume of interest. As a consequence, imaging time and breath holding may become too long and, therefore, unacceptable for patient examinations. Fast image acquisition is also required to minimize motion artifacts, which originate not only from respiration but also from diaphragm and bowel motion.

Parallel MR imaging techniques use spatial information contained in the sensitivity profiles of the elements of a coil array.<sup>21,22</sup> This allows for a reduction of the number of spatial encoding steps. As a consequence, the MR acquisition time can be shortened, whereas spatial resolution of the image is preserved.<sup>23,24</sup> Unfortunately, this improvement in scan time is associated inseparably with a loss of SNR because signal loss scales with the square root of the parallel-imaging acceleration factor. In theory, the maximum attainable acceleration factor for parallel imaging is

equal to the number of coil elements along the phase-encoding direction. Therefore, at field strength of 1.5 T, where SNR may already be marginal, the use of parallel imaging is strongly restricted. Signal-to-noise ratio penalties usually limit the maximum acceleration factor to about 2 for most applications at 1.5 T. Thus, the SNR improvements observed at 3 T may help compensate for parallel imaging-related SNR loss (Fig. 3).<sup>23,25</sup>

However, parallel imaging can be used to convert a higher SNR to increased resolution or speed without increasing specific absorption rates (SARs). In addition, the CNR for CE-MRA at higher field strength is dramatically increased because of increased tissue T1 value. The decreased scan time is advantageous in 2 ways. First, shorter acquisition times also allow high-quality studies in patients who are not able to hold their breath as required. Second, reduced scan times can help to ameliorate the depiction of the distal parts of the renal arteries.<sup>11,17,26</sup>

Although there are many positive aspects for performing CE-MRA at 3 T, there are also some tradeoffs that limit effectiveness in certain applications. For instance, the general limitations of 3-T imaging include static magnetic field and RF magnetic field inhomogeneities, increase in SAR that might lead to patient heating, increased magnetic

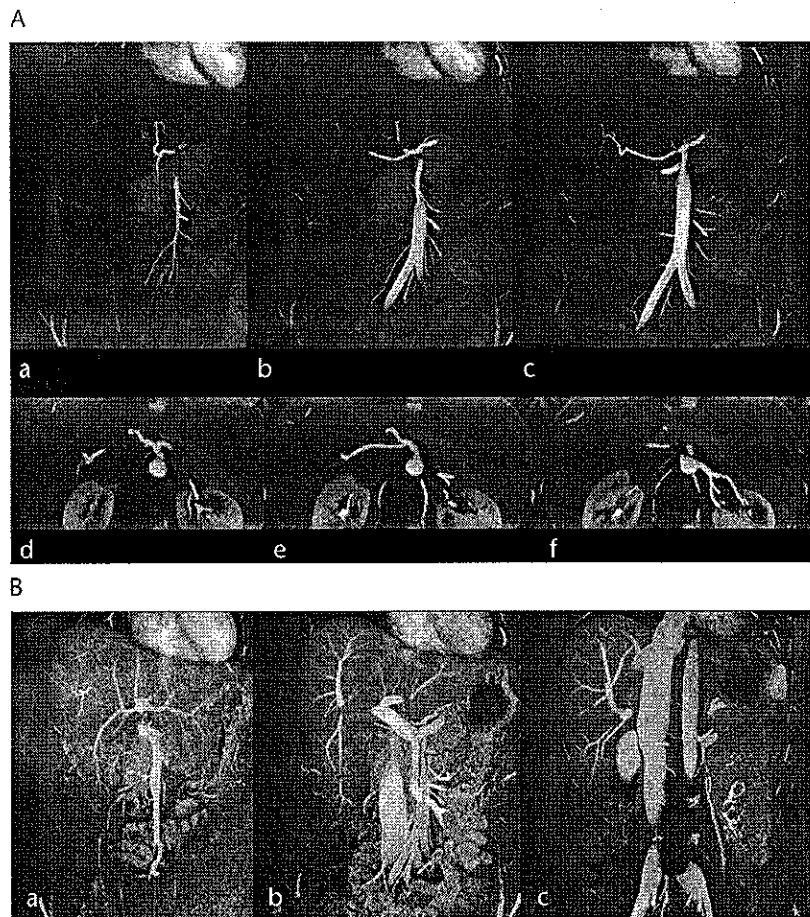


**FIGURE 3.** A, Coronal (a–c) and transverse (d–f) reformatted MR images from unsubtracted CE-MRA 3-D data set of a 35-year-old volunteer show detailed information of the abdominal aorta and its major branches. Celiac trunk, hepatic artery, and superior mesenteric artery can be clearly marked off. B, Coronal (a–c) reformatted MR images obtained from the same volunteer. In a second scan, portal vein and hepatic veins are visualized.

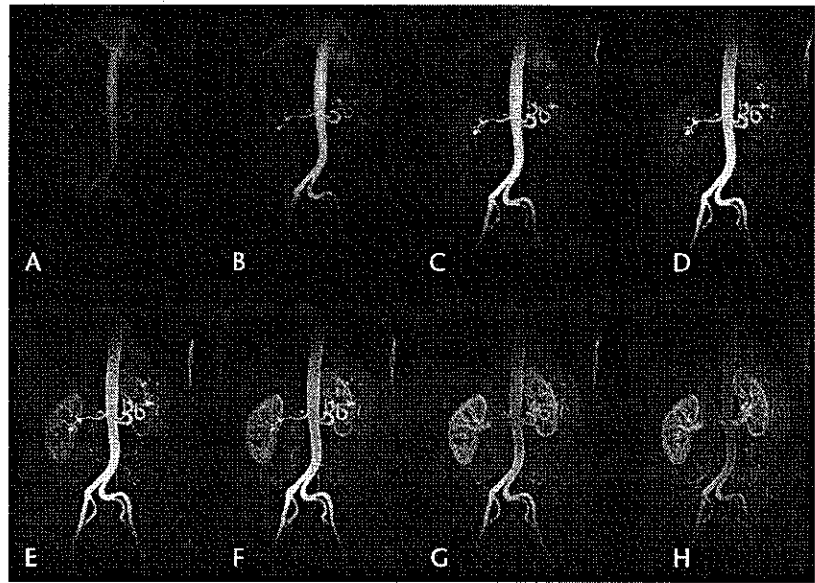


**FIGURE 4.** Coronal MIP images from 3-D time-resolved CE-MRA in a 34-year-old male volunteer (sample interval, 1.4 seconds) show sequential filling of abdominal aorta, renal arteries, renal parenchyma, and renal veins. Vascular details (eg, early branching of the right renal artery) and homogeneity of parenchymal enhancement can be observed.

susceptibility associated with metal artifacts, and issues associated with RF penetration in large patients.<sup>19,27</sup>

### ADVANTAGES AT 3 T

As mentioned previously, the improved SNR associated with 3 T can be traded for improved temporal resolution in

dynamic MR acquisition sequences. The improved temporal resolution can be achieved through standard techniques, including partial Fourier imaging, parallel imaging, and undersampled projection reconstruction methods. The improved temporal resolution can therefore be traded for shorter breath-hold periods or be used to provide greater diagnostic information about the temporal passage of contrast during CE-MRA studies (Figs. 4, 5).

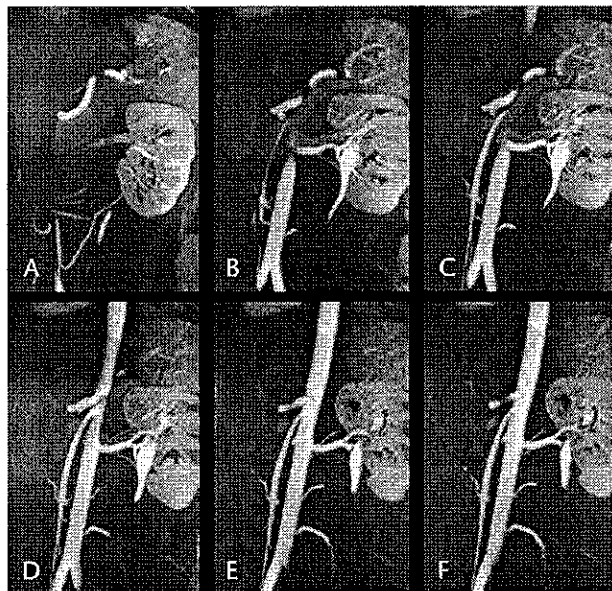


**FIGURE 5.** Six consecutive thin-MIP images of the left renal artery derived from the contrast-enhanced 3-D data set of a 35-year-old female patient with suspected renal artery stenosis are shown. Hilar branching and intraparenchymal segmental arteries can be evaluated.

### DISADVANTAGES AT 3 T

Despite these significant advantages, several limitations have to be taken into account when discussing CE-MRA at 3 T. First, the increase in magnetic field strength results in an increase in the SAR that is roughly proportional to the square of the B1 field value. It means that doubling the field strength from 1.5 T to 3 T causes a 4-fold increase in the SAR. This rise in SAR translates into a greater risk for tissue heating and, hence, greater potential for discomfort or even burns; more than ever, MRA pulse sequences usually use rapid acquisition, high flip angles, and short repetition times. To avoid SAR limitations, flip angle can be adapted without significant degradation of image quality. Second, an additional issue at 3 T is related to the static magnetic field inhomogeneities introduced by air/tissue interfaces in certain anatomical regions. Because most MRA techniques use gradient echo imaging, these susceptibility artifacts are relatively amplified. Third, for CE-MRA, the higher field strength might result in a slight increase in signal loss related to T2\* that is associated with very high concentrations of gadolinium agents (eg, in the subclavian vein), which may result in obscuration of the arterial signal (Fig. 1). Finally, in very large patients, the issues associated with RF signal penetration during excitation of protons and the nonuniformities in the B1 field can result in variations in signal intensity, especially for the center of the body. Although these



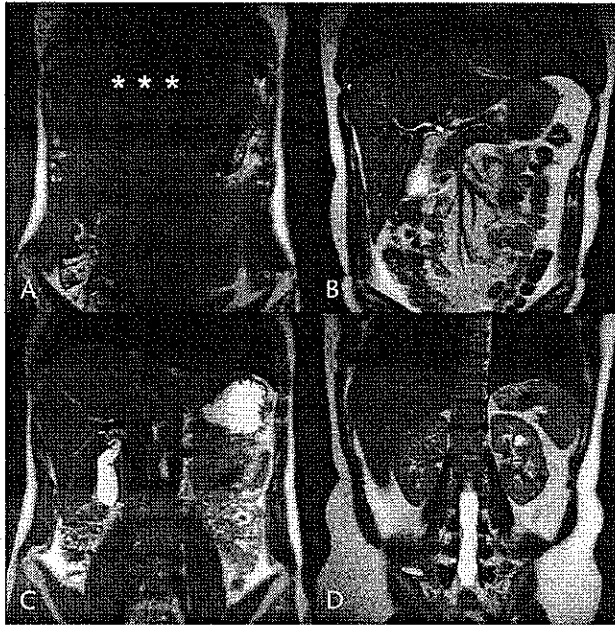


**FIGURE 6.** Coronal T2-weighted half-Fourier single-shot turbo spin-echo images of the abdomen obtained from a 42-year-old male volunteer. Dielectric resonance artefacts (\*) causing local signal loss in the ventral parts of the liver are shown. There is no image degradation in the course of the abdominal aorta caused by its dorsal position.

effects of B1 field are less prominent in the head, in large patients, the effects of reduced RF penetration in the abdomen can be significant. In many patients, areas of signal loss can be observed, owing to the so-called *dielectric resonance effect*. This effect, which is caused by the shorter wavelength of RF signal at 3 T, is greatest when intensive RF sequences are applied (Figs. 6, 7). Nevertheless, in our experience, these effects typically do not affect the performance of abdominal MRA because signal behavior is relatively independent from B1-field inhomogeneities in the setting of administered contrast agent.

### CLINICAL APPLICATIONS

Magnetic resonance imaging was performed on a 3-T whole-body system (Magnetom Trio; Siemens Medical Solutions, Erlangen, Germany) with total imaging matrix parallel-imaging capabilities in combination with phased-array surface coils. The gradient system operates with a maximum gradient strength of 45 mT/m and a maximum slew rate of 200 mT/m per millisecond. Breath-hold acquisitions were performed at end expiration.

### THORACIC AND ABDOMINAL AORTA

Although CT is more practicable and available for patients in an acute setting such as aortic trauma or aortic dissection, 3-D CE-MRA of the aorta has been established as the imaging modality of choice for a variety of pathological

findings and for congenital malformations.<sup>5,8,13,20,28–32</sup> Imaging can be performed either to establish the diagnosis or to follow up patients with congenital heart disease. The major advantage of CE-MRA is the possibility to combine noninvasive luminal imaging and imaging of extra-aortic structures without recourse to ionizing radiation or potentially nephrotoxic iodinated contrast agents.

If evaluation of the thoracic aorta is necessary, cross-sectional imaging should be performed, in addition to MRA, to gain as much information as possible. In certain cases, it may be also important to look at the anatomy of the left ventricle or left ventricular outflow tract to determine whether aortic insufficiency or stenosis has resulted in dilatation of the left ventricle.

The most common indications for CE-MRA of the thoracoabdominal aorta include aneurysms, aortic dissection, and atherosclerosis with occlusive diseases (Figs. 8, 9). When there is an aortic dissection, CE-MRA studies must evaluate the extent of the dissection, the sizes of the true and the false lumina, the patency of the false lumen, and the potential abdominal branch vessel involvement. In some cases, a second CE-MRA study of the abdomen may be required to assess the distal dissections extending into the abdominal aorta and into the renal or mesenteric arteries. Significantly visually lower parenchymal enhancement, in comparison with the contralateral paired viscera (eg, the kidney), can be read as a sign of poor prognosis. Additional dark-blood

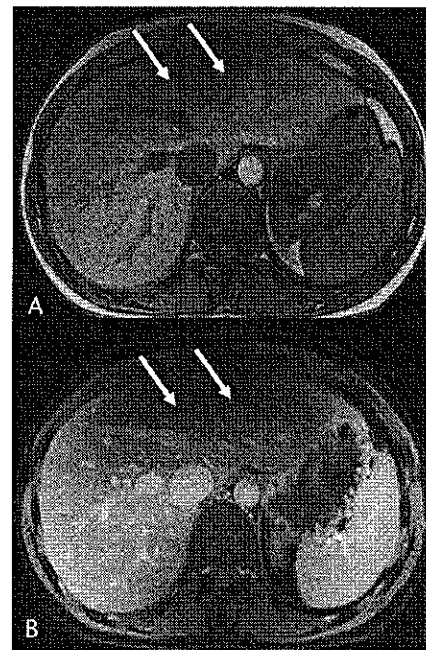


**FIGURE 7.** Transverse T1-weighted turbo spin echo slice of the upper abdomen (A) before and (B) after administration of contrast agent. Typical B1 inhomogeneities causing local signal loss (arrows) can be found. These artefacts do not interfere and are not relevant for CE-MRA because of anatomical position in the field of view.

techniques may help to differentiate intramural hematoma from a thrombosed false lumen in aortic dissection.

Second, contrast-enhanced MR imaging is considered to provide detailed information about the anatomy of the abdominal aorta and its visceral branches (Fig. 10). This is mandatory for the accurate surgical planning of liver resection or transplantation or for the planning of catheter-related interventional procedures, such as chemoembolization. Additional venous and portal-venous angiograms can be obtained to evaluate portal hypertension or detect venous anomalies.<sup>11,26</sup> For example, a severe stenosis of the celiac trunk precludes the placement of an intra-arterial catheter into the hepatic artery for selective, preoperative intra-arterial chemotherapy. Furthermore, in potential live kidney donors, detailed information about renal arterial and venous vasculature enables a decision to be made as to whether a kidney is suitable for transplantation. The presence of accessory arteries, early branching arteries, anomalous venous anatomy, and ureteral abnormalities may influence the choice of kidney, which is required before nephrectomy.<sup>16</sup> In addition, in post-transplant setting, CE-MRA became established as modality of choice for the assessment of hepatic artery, portal vein stenosis, and renal anastomotic stenosis (Fig. 11). Finally, CE-MRA represents an ideal imaging technique for evaluation of patients with suspected abdominal aortic occlusion. Moreover, CE-MRA has been shown to be an excellent tool to image the vessels distal to the aortic occlusion. This is clinically important to evaluate the status of the distal runoff vessels. A further benefit of CE-MRA relates to the fact that different imaging approaches can be used to supplement angiographic images. For instance, in malignant diseases, MRA is often performed for assessment of arterial feeding vessels or venous infiltration of an abdominal mass. In these cases, a comprehensive examination protocol combining morphological and angiographic images is recommended.

### SCAN PROTOCOLS

Patients are imaged in a supine position and, if possible, the arms should be placed above the head to avoid wrap-around artifacts. Breath-hold imaging for thoracoabdominal MRA is mandatory and significantly improves image quality; during breath hold, the patient should be instructed to do this in slight expiration to avoid too great pressure in the thorax and to avoid the possibility of insufficient compactness of the bolus.

Inasmuch as the anatomy of the thoracic aorta can be variable and complex because of the underlying disease, localizer imaging should be performed before positioning the slab for the final CE-MRA scan. Additional dark-blood cross-sectional imaging is required when intramural hematoma of the aorta is possible. This condition might be missed on contrast-enhanced images because the hematoma may have a high signal similar to that of the contrast-enhanced vessel lumen. Furthermore, cross-sectional imaging might be helpful to evaluate not only the vessel wall but also the surrounding soft tissue. For example, when an aortic aneurysm is present, associated features, such as thrombus or ulceration, can be visualized. Moreover, the true size of an

aneurysm may be underestimated by using CE-MRA because CE-MRA is primarily a luminogram similar to conventional DSA. Because the background is suppressed on CE-MRA to depict the vessels accurately, it may become difficult to visualize the outer wall of the aneurysm even on native slices.

For CE-MRA of the thoracic and the abdominal aorta, we usually prescribe the imaging volume as a coronal or coronal-oblique acquisition. Three-dimensional gradient-recalled heavily T1-weighted sequences are used, where the imaging of an arterial bed is synchronized with the arrival of a bolus of contrast media. The volume of contrast agent and the method of injection are coordinated with the imaging protocol. Furthermore, imaging parameters should be adjusted to provide the optimum balance between spatial resolution and anatomical coverage within a comfortable breath hold. One of the goals in optimizing the sequence parameters is to keep the scan time of the 3-D data set to a minimum so that acquisition can be achieved in a single breath hold. This can be realized by using short TR and TE values. The short TR value permits an overall reduction of the imaging time, whereas a short TE value helps in minimizing T2\* effects.

Typical sequence parameters in clinical protocols for thoracoabdominal CE-MRA at 3 T are summarized in Table 1.

Time-resolved MRA can be used as a complimentary study or, in many instances, can provide all the relevant diagnostic information required.<sup>33-36</sup> At our institution, for time-resolved MRA, we use an ultra-fast spoiled 3-D gradient-recalled echo sequence with asymmetrical k-space sampling and echo sharing in all 3 axes to further shorten the acquisition time. The higher the temporal resolution, the more accurate the hemodynamics can be assessed. Because only

**TABLE 1.** Sequence Parameters for Thoracoabdominal CE-MRA at 3 T

	Conventional CE-MRA	Time-Resolved CE-MRA
Orientation	Coronal	Coronal
Repetition time (ms)	3.0	2.55
Echo time (ms)	1.14	1.05
Flip angle (degrees)	19–23*	12–18*
Slice thickness (mm)	1.0	3.0
FOV read (mm)	380–450*	450–500*
FOV phase (%)	75	68.8
Base resolution	512	512
Phase resolution (%)	80	75
No. slices	72–96*	32*
Matrix size	512 × 336	512 × 264
Voxel size (mm)	1.1 × 0.9 × 1.0	1.3 × 1.0 × 3.0
PAT mode	GRAPPA	GRAPPA
Acceleration factor	3	3
Reference lines	24	24
Bandwidth (Hz/px)	650	750
Contrast (mL)	15–20 at 2 mL/s	5 at 4 mL/s
Scan time (s)	16–19*	1.6 per slab

\*Data depends on patient adjustment.  
FOV indicates field of view; GRAPPA, generalized autocalibrating partially parallel acquisitions; PAT, parallel acquisition technique.

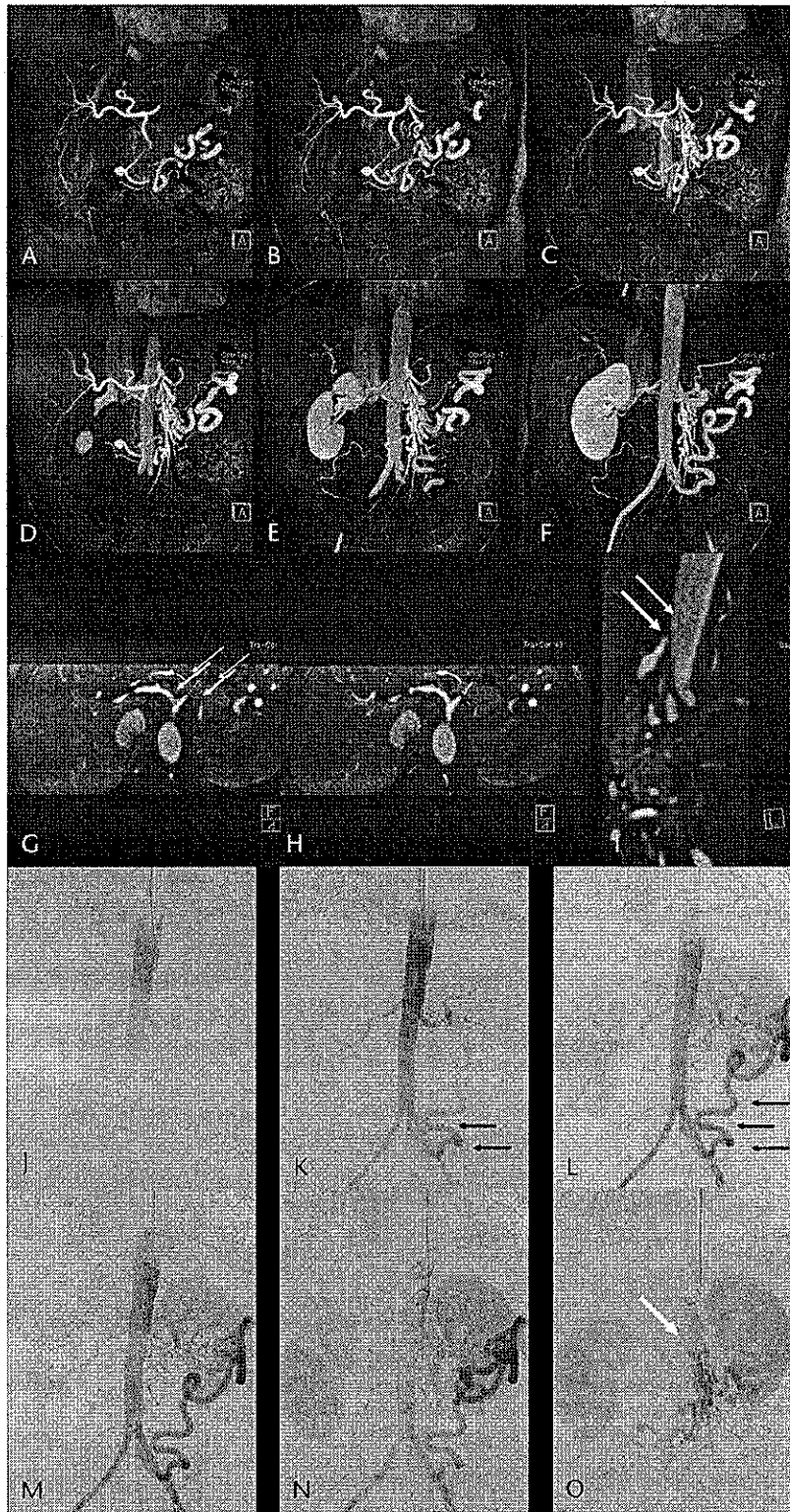


**FIGURE 8.** Images obtained from a 56-year-old woman with history of abdominal angina. Coronal (A–F), transverse (G–H), and sagittal (I) multiplanar reformats from CE-MRA show severe stenosis of the celiac trunk (white arrow). Note the delayed enhancement of the celiac arteries caused by a retrograde filling via the inferior mesenteric artery, which is dilated (black arrows). Preoperative DSA (J–O) confirmed the findings described in MRA. Because of high-grade stenosis of the celiac trunk, interventional stent placement failed.

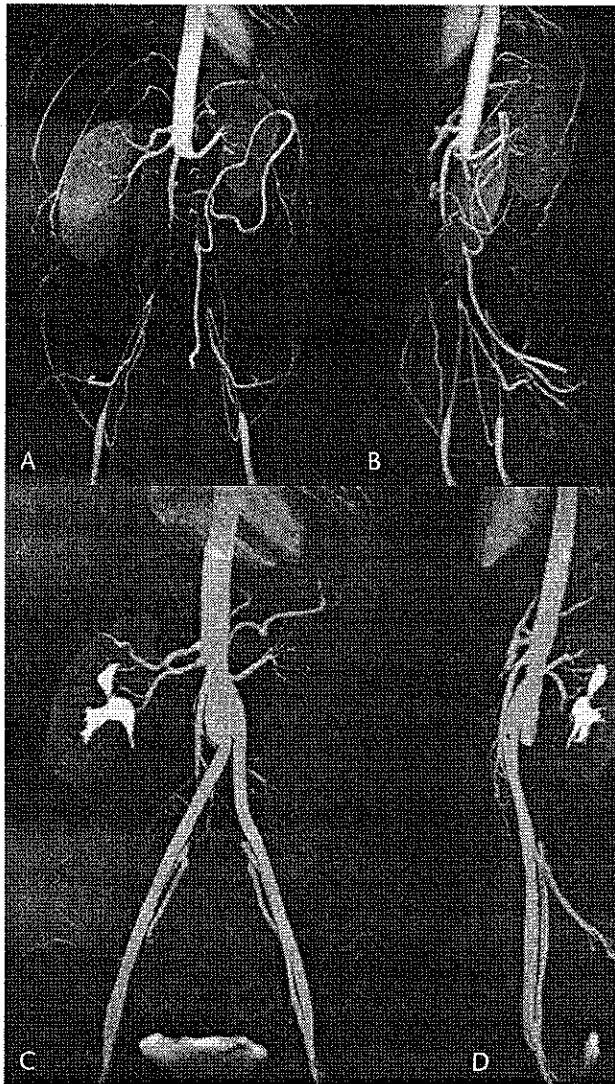


**FIGURE 9.** Coronal and sagittal MIP images obtained from a 38-year-old female patient with Leriche syndrome are shown (A, B). Postoperative imaging demonstrates regular perfusion of the prosthesis and the runoff vessels (C, D). Images (C) and (D) were derived from a whole-body angiography performed on a 1.5-T system.

small amounts of contrast agent (3–5 mL) for time-resolved scans are needed, static and dynamic MRA scans can be combined in a single examination for comprehensive imaging.

In our opinion, time-resolved CE-MRA is especially useful in aortic dissection or congenital heart diseases. For instance, sequential filling in the true and the false lumens, the entry and the exit points of the dissection, pseudo aneurysms, and intramural hematomas may have characteristic appearances. In patients with coarctation, time-resolved CE-MRA may show sequential filling of chest wall collaterals. For pulmonary vasculature, time-resolved tech-

niques can be used to combine dynamic and morphological information and provide insight into cardiopulmonary hemodynamics.<sup>37,38</sup> Analysis of perfusion data provides several parameters of physiological relevance, including the time to peak, mean transit time, and maximum signal intensity. Computer-assisted color mapping can permit visual assessment of regional perfusion. Nowadays, dynamic pulmonary MRA at 3 T provides functional and perfusion information and has been shown to be feasible in the detection of perfusion defects. Possible clinical indications include pulmonary embolism, pulmonary arterial hypertension, and pulmonary arteriovenous malformations.

Nevertheless, MR imaging of the pulmonary vasculature is still challenging for a variety of reasons, most importantly because of respiratory motion and susceptibility artifacts at air-tissue interfaces. Because faster imaging protocols and dedicated surface coils are available, high-resolution pulmonary CE-MRA can now resolve up to fifth-order pulmonary branches in a comfortable breath hold. Infiltration of vessels in cases of mediastinal or lung tumors can be assessed reliably. If a mediastinal mass is suspected, additional scans of venous phases should be performed because a major complication of these tumors is the obstruction of the veins, caused by compressive effects or direct tumor invasion. Therefore, combined vascular and soft tissue imaging before and after contrast is useful in visualizing tumor extension and involvement of vasculature, which is an important issue for presurgical planning.

### PITFALLS

A typical pitfall in imaging the thoracic or the abdominal aorta, especially in patients with advanced atherosclerotic disease or increased tortuosity of the thoracic aorta, is incomplete coverage of the anatomy. Therefore, a preliminary unenhanced scan should be reviewed to look for aliasing or incomplete coverage before contrast agent is applied. Another important issue in imaging the thoracoabdominal aorta is ringing or stripe artifacts. These artifacts in the lumen of the aorta are caused by incorrect timing of the contrast agent bolus. If the contrast agent arrives too late,



**FIGURE 10.** Volume-rendered images in different projections of a 48-year-old male patient after renal transplantation are shown. A patch plastic due to intraoperative vascular injury of the external iliac artery can be found. There is no evidence of anastomotic stenosis.



**FIGURE 11.** Images obtained from a 72-year-old female patient with suspected infrarenal aortic aneurysm. Coronal (A) and sagittal (B) full-thickness MIP and transverse reformatted MR images (C–H) reveal ectatic aortic bifurcation and atherosclerotic tortuosity of the abdominal aorta. The origin of the inferior mesenteric artery can be reliably identified (arrow). Additional bilateral renal artery stenoses were found.

central parts of the k-space will be acquired when the maximum concentration of gadolinium has not been reached. If a significantly higher concentration of gadolinium in the area of interest is found during the acquisition of the peripheral parts of the k-space, artifactual longitudinal dark stripes within the aortic lumen may occur, which can simulate an aortic dissection. To avoid or compensate for this kind of artifact, a second 3-D data set should be performed immediately after the first scan. If these lines also appear on the second data set, a diagnosis of an aortic dissection is likely. Finally, when imaging the abdominal aorta and its branches, blurring artifacts of branching vessels (eg, renal arteries) may appear because of respiratory motion. In patients who are not able to follow the breath-hold instructions, these kinds of artifacts often cannot be avoided.

#### REVIEW OF LITERATURE

A large number of studies have shown MR imaging at field strength of 1.5 T to be able to achieve sensitivities and

specificities of 90% to 100% for the diagnosis of aortic dissection, aneurysms, or occlusion.<sup>4,14,28–31,39–42</sup> Accordingly, this technique represents the modality of choice for both elective examination of suspicious aortic disease and for follow-up studies.

Nevertheless, to our knowledge, the experience with CE-MRA at 3 T for imaging the thoracoabdominal aorta or its major intra-abdominal branches is still limited. Other than volunteer studies or feasibility studies with restricted number of subjects, there are no data available focusing on severe aortic diseases. Nael et al<sup>19</sup> recently published their initial experiences in 32 patients for abdominal CE-MRA. Furthermore, there are some experiences in renal artery imaging at 3 T, indicating that high-spatial resolution 3-D CE-MRA is feasible, and results are promising for a comprehensive evaluation in the settings of renovascular disease.<sup>17,20,43</sup> Among others, Fenchel et al<sup>17</sup> reported the potential of dedicated phased-array coils with 32 elements for abdominal CE-MRA by using high acceleration factors (up to 6) in a

volunteer study. For pulmonary vasculature, Nael et al<sup>37,38</sup> reported CE-MRA at 3 T to be able to depict morphological and functional abnormalities in patients with pulmonary arterial hypertension in encouraging detail when compared with the findings in volunteer studies.

## CONCLUSIONS

Contrast-enhanced magnetic resonance angiography at 3 T is advantageous in terms of improved SNR; thus, measurement time can be reduced and/or spatial resolution can be increased without corruption of the signal yield. These improvements are substantial and result in significantly improved clinical MRA. Limitations at 3 T include an increased sensitivity to RF field inhomogeneity, tissue heating, and static magnetic field inhomogeneity.

## REFERENCES

- Prince MR, Yucel EK, Kaufman JA, et al. Dynamic gadolinium-enhanced three-dimensional abdominal MR arteriography. *J Magn Reson Imaging*. 1993;3:877-881.
- Prince MR, Narasimham DL, Stanley JC, et al. Breath-hold gadolinium-enhanced MR angiography of the abdominal aorta and its major branches. *Radiology*. 1995;197:785-792.
- Lee VS, Martin DJ, Krinsky GA, et al. Gadolinium-enhanced MR angiography: artifacts and pitfalls. *AJR Am J Roentgenol*. 2000;175:197-205.
- De Cobelli F, Vanzulli A, Sironi S, et al. Renal artery stenosis: evaluation with breath-hold, three-dimensional, dynamic, gadolinium-enhanced versus three-dimensional, phase-contrast MR angiography. *Radiology*. 1997;205:689-695.
- Schoenberg SO, Rieger J, Weber CH, et al. High-spatial-resolution MR angiography of renal arteries with integrated parallel acquisitions: comparison with digital subtraction angiography and US. *Radiology*. 2005;235:687-698.
- Nael K, Saleh R, Lee M, et al. High-spatial-resolution contrast-enhanced MR angiography of abdominal arteries with parallel acquisition at 3.0 T: initial experience in 32 patients. *AJR Am J Roentgenol*. 2006;187:W77-W85.
- Kawamoto S, Fishman EK. MDCT angiography of living laparoscopic renal donors. *Abdom Imaging*. 2006;31:361-373.
- Baden JG, Racy DJ, Grist TM. Contrast-enhanced three-dimensional magnetic resonance angiography of the mesenteric vasculature. *J Magn Reson Imaging*. 1999;10:369-375.
- Baskaran V, Perelcs FS, Nemcek AA Jr, et al. Gadolinium-enhanced 3D MR angiography of renal artery stenosis: a pilot comparison of maximum intensity projection, multiplanar reformatting, and 3D volume-rendering postprocessing algorithms. *Acad Radiol*. 2002;9:50-59.
- Fenchel M, Scheule AM, Stauder NI, et al. Atherosclerotic disease: whole-body cardiovascular imaging with MR system with 32 receiver channels and total-body surface coil technology—initial clinical results. *Radiology*. 2006;238:280-291.
- Nael K, Laub G, Finn JP. Three-dimensional contrast-enhanced MR angiography of the thoraco-abdominal vessels. *Magn Reson Imaging Clin N Am*. 2005;13:359-380.
- Giessing M, Kroencke TJ, Taupitz M, et al. Gadolinium-enhanced three-dimensional magnetic resonance angiography versus conventional digital subtraction angiography: which modality is superior in evaluating living kidney donors? *Transplantation*. 2003;76:1000-1002.
- Fain SB, King BF, Breen JF, et al. High-spatial-resolution contrast-enhanced MR angiography of the renal arteries: a prospective comparison with digital subtraction angiography. *Radiology*. 2001;218:481-490.
- Vasbinder GB, Nelemans PJ, Kessels AG, et al. Accuracy of computed tomographic angiography and magnetic resonance angiography for diagnosing renal artery stenosis. *Ann Intern Med*. 2004;141:674-682.
- Vasbinder GB, Nelemans PJ, Kessels AG, et al. Diagnostic tests for renal artery stenosis in patients suspected of having renovascular hypertension: a meta-analysis. *Ann Intern Med*. 2001;135:401-411.
- Kramer U, Nael K, Laub G, et al. High-resolution magnetic resonance angiography of the renal arteries using parallel imaging acquisition techniques at 3.0 T: initial experience. *Invest Radiol*. 2006;41:125-132.
- Fenchel M, Nael K, Deshpande VS, et al. Renal magnetic resonance angiography at 3.0 tesla using a 32-element phased-array coil system and parallel imaging in 2 directions. *Invest Radiol*. 2006;41:697-703.
- Nael K, Ruehm SG, Michaely HJ, et al. High spatial-resolution CE-MRA of the carotid circulation with parallel imaging: comparison of image quality between 2 different acceleration factors at 3.0 tesla. *Invest Radiol*. 2006;41:391-399.
- Nael K, Saleh R, Lee M, et al. High-spatial-resolution contrast-enhanced MR angiography of abdominal arteries with parallel acquisition at 3.0 T: initial experience in 32 patients. *AJR Am J Roentgenol*. 2006;187:W77-W85.
- Kramer U, Nael K, Laub G, et al. High-resolution magnetic resonance angiography of the renal arteries using parallel imaging acquisition techniques at 3.0 T: initial experience. *Invest Radiol*. 2006;41:125-132.
- Griswold MA, Jakob PM, Heidemann RM, et al. Generalized autocalibrating partially parallel acquisitions (GRAPPA). *Magn Reson Med*. 2002;47:1202-1210.
- Heidemann RM, Ozsarlak O, Parizel PM, et al. A brief review of parallel magnetic resonance imaging. *Eur Radiol*. 2003;13:2323-2337.
- Pruessmann KP. Parallel imaging at high field strength: synergies and joint potential. *Top Magn Reson Imaging*. 2004;15:237-244.
- Griswold MA, Kammengieser S, Heidemann RM, et al. Field-of-view limitations in parallel imaging. *Magn Reson Med*. 2004;52:1118-1126.
- Fenchel M, Nael K, Ruehm S, et al. Isotropic high spatial resolution magnetic resonance angiography of the supra-aortic arteries using two-dimensional parallel imaging (iPAT2) at 3 tesla: a feasibility study. *Invest Radiol*. 2006;41:545-552.
- Michaely HJ, Dietrich O, Nael K, et al. MRA of abdominal vessels: technical advances. *Eur Radiol*. 2006;16:1637-1650.
- Campeau NG, Huston J III, Bernstein MA, et al. Magnetic resonance angiography at 3.0 tesla: initial clinical experience. *Top Magn Reson Imaging*. 2001;12:183-204.
- Matsunaga N, Hayashi K, Okada M, et al. Magnetic resonance imaging features of aortic diseases. *Top Magn Reson Imaging*. 2003;14:253-266.
- Khan IA, Nair CK. Clinical, diagnostic, and management perspectives of aortic dissection. *Chest*. 2002;122:311-328.
- Tatli S, Yucel EK, Lipton MJ. CT and MR imaging of the thoracic aorta: current techniques and clinical applications. *Radiol Clin North Am*. 2004;42:565-585.
- Chan HH, Tai KS, Yip LK. Patient with Leriche's syndrome and concomitant superior mesenteric aneurysm: evaluation with contrast-enhanced three-dimensional magnetic resonance angiography, computed tomography angiography and digital subtraction angiography. *Australas Radiol*. 2005;49:233-237.
- Fink C, Hallscheidt PJ, Hosch WP, et al. Preoperative evaluation of living renal donors: value of contrast-enhanced 3D magnetic resonance angiography and comparison of three rendering algorithms. *Eur Radiol*. 2003;13:794-801.
- Frydrychowicz A, Bley TA, Winterer JT, et al. Accelerated time-resolved 3D contrast-enhanced MR angiography at 3 T: clinical experience in 31 patients. *MAGMA*. 2006;19:187-195.
- Finn JP, Baskaran V, Carr JC, et al. Thorax: low-dose contrast-enhanced three-dimensional MR angiography with subsecond temporal resolution—initial results. *Radiology*. 2002;224:896-904.
- Fink C, Ley S, Kroeker R, et al. Time-resolved contrast-enhanced three-dimensional magnetic resonance angiography of the chest: combination of parallel imaging with view sharing (TREAT). *Invest Radiol*. 2005;40:40-48.
- Nael K, Michaely HJ, Villablanca P, et al. Time-resolved contrast enhanced magnetic resonance angiography of the head and neck at 3.0 tesla: initial results. *Invest Radiol*. 2006;41:116-124.

37. Nael K, Michaely HJ, Kramer U, et al. Pulmonary circulation: contrast-enhanced 3.0-T MR angiography—initial results. *Radiology*. 2006;240:858–868.
38. Nael K, Michaely HJ, Lee M, et al. Dynamic pulmonary perfusion and flow quantification with MR imaging, 3.0 T vs. 1.5 T: initial results. *J Magn Reson Imaging*. 2006;24:333–339.
39. Russo V, Renzulli M, Buttazzi K, et al. Acquired diseases of the thoracic aorta: role of MRI and MRA. *Eur Radiol*. 2006;16:852–865.
40. Loewe C, Schillinger M, Haumer M, et al. MRA versus DSA in the assessment of occlusive disease in the aortic arch vessels: accuracy in detecting the severity, number, and length of stenoses. *J Endovasc Ther*. 2004;11:152–160.
41. Carr JC, Finn JP. MR imaging of the thoracic aorta. *Magn Reson Imaging Clin N Am*. 2003;11:135–148.
42. Willmann JK, Wildermuth S, Pfammatter T, et al. Aortoiliac and renal arteries: prospective intraindividual comparison of contrast-enhanced three-dimensional MR angiography and multi-detector row CT angiography. *Radiology*. 2003;226:798–811.
43. Michaely HJ, Nael K, Schoenberg SO, et al. The feasibility of spatial high-resolution magnetic resonance angiography (MRA) of the renal arteries at 3.0 T. *Rofo*. 2005;177:800–804.

## **ARTICLE 7**



J.J. Pillai

# The Evolution of Clinical Functional Imaging during the Past 2 Decades and Its Current Impact on Neurosurgical Planning

**SUMMARY:** BOLD fMRI has, during the past decade, made a major transition from a purely research imaging technique to a viable clinical technique used primarily for presurgical planning in patients with brain tumors and other resectable brain lesions. This review article briefly examines the history and evolution of clinical functional imaging, with particular emphasis on how the use of BOLD fMRI for neurosurgical planning has changed during the past 2 decades. Even more important, this article describes the many published studies during that same period that have examined the overall clinical impact that BOLD and DTI have made on surgical planning.

**ABBREVIATIONS:** AF = arcuate fasciculus; ASFNR = American Society of Functional Neuroradiology; BOLD = blood oxygen level-dependent; CPT = current procedural terminology; CPU = central processing unit; CSM = intraoperative cortical stimulation mapping; DTI = diffusion tensor imaging; DTT = diffusion tensor tractography; EPI = echo-planar imaging; FA = fractional anisotropy; FDA = US Food and Drug Administration; fMRI = functional MR imaging; GLM = general linear model; MEG = magnetoencephalography; PACS = picture archiving and communication system; QC = quality control; RAM = random access memory; SPM = Statistical Parametric Mapping; TL = temporal lobe; TLE = temporal lobe epilepsy; Wada = intracarotid sodium amobarbital test

fMRI is a physiologic imaging technique that has rapidly evolved since the early 1990s when Ogawa et al<sup>1-3</sup> first described the BOLD principle, which was based on animal imaging studies and was considered novel. Human imaging applications arose only in 1991, when Belliveau et al<sup>4</sup> described mapping of the human visual cortex by using fMRI. Since those early days, fMRI has burgeoned into one of the most useful research techniques in modern cognitive neuroscience, with use by a wide variety of researchers in fields as diverse as psychology, neurology, psychiatry, and linguistics. However, clinical use of fMRI is a relatively recent phenomenon, with only slightly more than a decade of collective experience. This review article examines the history and evolution of clinical functional imaging, with special emphasis on BOLD and, to a lesser extent, DTI applications in clinical brain tumor imaging, which have served as early models for the clinical translation and maturation of these imaging modalities. In addition, this article describes the clinical impact that BOLD and DTI have made on surgical planning.

The ASFNR was established in 2004 to address the unique concerns relating to clinical use of functional imaging, comprising not only BOLD imaging but also DTI, perfusion imaging, MEG/magnetic source imaging, and molecular and metabolic imaging, including MR spectroscopy. As all of these physiologic imaging modalities enter mainstream clinical neuroradiology, a growing need to establish national standards for their clinical use and standardized quality control metrics has emerged. The ASFNR, by planned launch of a multicenter study that will assess the effectiveness of BOLD

and DTI in surgical planning, is well-poised for this role. The steadily increasing membership of the ASFNR and successful annual meetings, such as the one conducted in late February 2009 in San Antonio, Texas, are a testament not only to the increasing popularity of these techniques but also to the growing need for incorporation of these modalities into mainstream clinical neuroradiology practice. While a description of all the research and clinical applications of these diverse physiologic and metabolic imaging modalities that are embraced by the ASFNR is clearly beyond the scope of this article, we can examine the technique that has historically served as the springboard for the birth of the ASFNR—BOLD imaging—and, to a lesser extent, the complementary role of DTI in presurgical mapping, which are the main currently accepted clinical applications of these techniques. There are broadly 3 main categories of patients who commonly undergo preoperative fMRI: 1) patients with structural brain lesions in close proximity to eloquent cortex who need preoperative functional risk assessment, 2) patients who need determination of preoperative language hemispheric lateralization (and possibly, in the future, memory lateralization), and 3) patients with epilepsy needing preoperative seizure-focus localization with electroencephalographic-correlated fMRI.<sup>5</sup> We will focus on the first 2 categories in this article.

## The Early Era of Clinical BOLD Imaging

In the early days of BOLD imaging (the 1990s), all such imaging was conducted at most centers under institutional review board-approved research protocols because no accepted clinical application existed, and much investigation into the basic principles of BOLD contrast was necessary. Because EPI was relatively new and most MR imaging scanners were operating at field strengths of 1.5T or below, with limited gradient strengths and low slew rates, BOLD imaging was relatively difficult to perform. While FDA-approved EPI sequences were

From the Division of Neuroradiology, Russell H. Morgan Department of Radiology and Radiological Science, Johns Hopkins University School of Medicine, Baltimore, Maryland.

Please address correspondence Jay J. Pillai, MD, Division of Neuroradiology, The Johns Hopkins Hospital, Phipps Bldg, 8-100, 600 N Wolfe St, Baltimore, MD 21287; e-mail: jpillai@jhmi.edu

DOI 10.3174/ajnr.A1845

developed by scanner manufacturers, the software for BOLD image analysis was not FDA-approved but was rather designed strictly for research applications.

Because paradigms for motor, language, and visual mapping were just beginning to emerge and limited literature was available regarding optimal paradigm design and stimulus-presentation techniques, much of the work being conducted in the realm of paradigm design and implementation was home grown at a number of academic institutions. Many different software packages were available for BOLD processing, but no consensus existed as to which was most appropriate for clinical use and multiple approaches to data processing existed.<sup>6</sup> Some of these packages relied on the GLM for statistical analysis (eg, SPM, University College London, London, UK),<sup>7</sup> while others relied on cross-correlation approaches, *t* test analyses, independent component analysis, or multiple different options for data analysis (eg, Analysis of Functional NeuroImages; Medical College of Wisconsin, Milwaukee, Wisconsin).<sup>8</sup> Even within each of these general approaches, much debate existed as to the optimal statistical thresholding for research and clinical applications. Different iterations of the software were developed during the years (eg, SPM evolved from the early SPM96 to the current SPM8), and new, more conservative statistical approaches evolved (eg, various corrections for multiple comparisons, the false discovery rate).<sup>9</sup>

During the early era of clinical BOLD imaging, the same basic interdisciplinary approach that served as the hallmark of BOLD research applied equally to clinical examinations. Often an MR imaging physicist or 2, research assistants, image-processing personnel, a statistician, and, at some centers, a psychologist or neurologist were participants in a multidisciplinary fMRI research team along with a neuro-radiologist either with or without a dedicated MR imaging technologist. The fMRI systems used had to be essentially assembled by the research team, with stimulus-presentation software and hardware, patient-monitoring equipment, and paradigm design and implementation all independently developed or purchased from different vendors. No integrated commercially available fMRI system existed, and the home grown systems were not designed to be MR imaging technologist-driven.

Although unprecedented high-resolution structural brain imaging had been realized with the advent of structural MR imaging in the early 1980s, study of in vivo higher level cognitive function was not possible before the advent of BOLD fMRI. BOLD imaging allowed assessment not only of sensorimotor and visual function but also of complex language, memory, emotion, and even higher level reasoning functions, such as abstract mathematic reasoning.<sup>10</sup> BOLD imaging complemented established but relatively spatial-resolution-limited electrophysiologic methods such as electroencephalography and transcranial magnetic stimulation for the study of brain function, and it preceded the emergence of MEG as a readily available alternative technique. This has led to an explosion of BOLD-related literature in the cognitive neurosciences during the past 2 decades. Even unlikely applications such as in the medicolegal arena with evaluation of truth-telling have recently been noted.<sup>11,12</sup>

## **BOLD fMRI Validation Studies during the Early Era**

### ***BOLD Motor Mapping***

During the early era of functional imaging, many individual institution-based clinical validation studies emerged that strove to compare BOLD results with those of the intracarotid sodium amobarbital (Wada) test for language lateralization and intraoperative cortical stimulation mapping for language and motor cortex localization. For example, many studies have compared CSM with preoperative motor fMRI; these studies have found high correlations between the 2 modalities.<sup>13-20</sup>

### ***BOLD Language Mapping Compared with Wada Testing***

Language mapping has been less standardized than motor mapping across medical centers and has thus been more difficult to validate than simple sensorimotor mapping. Nevertheless, many studies have compared preoperative BOLD imaging with the Wada test for language lateralization. For example, Binder et al<sup>21</sup> studied 22 patients with epilepsy with both Wada testing and fMRI by using a semantic decision task and found high correlation between the lateralization on fMRI and Wada testing ( $r = 0.96$ ). Bahn et al<sup>22</sup> also found similar results (100% concordance) in a comparison of language fMRI to Wada lateralization in their study of 7 patients with epilepsy. Similarly, Hertz-Pannier et al<sup>23</sup> reported perfect language lateralization concordance between Wada and preoperative fMRI results by using a word-generation task in a group of 6 children with partial epilepsy. Sabbah et al<sup>24</sup> reported language lateralization concordance in 19 of 20 patients with epilepsy between preoperative Wada testing and fMRI by using a silent word-generation task. Meneses et al<sup>25</sup> also studied 5 patients with epilepsy with a verbal-fluency fMRI language task and have similarly reported 100% lateralization concordance with Wada testing. On the basis of these and other studies, many epileptologists now think that fMRI is adequate for language lateralization, though the failure thus far to establish widely accepted memory activation paradigms still makes fMRI fall short of a definite substitute for the Wada test for overall hemispheric lateralization. Nevertheless, many believe that fMRI is well on its way to serving as a reliable noninvasive substitute for the Wada test.<sup>26</sup>

### ***BOLD Language Mapping Compared with Intraoperative Mapping***

Other studies were performed comparing preoperative language fMRI results with those of awake intraoperative CSM results. For example, Yetkin et al<sup>13</sup> in their study of 28 patients who performed finger, lip, and tongue motor tasks in addition to silent word-generation and counting tasks, found 100% concordance between the fMRI activation sites and intraoperative stimulation sites within 20 mm and 87% concordance within 10 mm. Furthermore, Benson et al<sup>27</sup> reported correct language lateralization by using a verb-generation task in 22 of 23 patients who also underwent either Wada testing ( $n = 12$ ) or CSM ( $n = 11$ ) as a reference standard. Hirsch et al,<sup>16</sup> in their study of 125 patients and 63 controls using multiple fMRI tasks, found sensitivities for detection of the Broca area of 93% and 77% and for the Wernicke area of 100% and 91%, respec-

tively, for the control and patient groups; they also noted overall concordance with CSM and Wada results.

### **Memory Mapping with BOLD fMRI**

While memory mapping has been the subject of extensive research during the past decade, it has not yet gained widespread clinical acceptance despite the publication of 3 validation studies, which have compared preoperative memory fMRI lateralization with preoperative Wada test results and/or postoperative memory outcome.<sup>28-30</sup> For example, Janszky et al<sup>28</sup> in their study of 16 patients with right mesial TLE who performed the Roland hometown walking test found a high correlation ( $r = 0.71$ ) between the preoperative fMRI memory lateralization and individual postoperative memory outcome following right anterior TL resection. Similarly, Richardson et al<sup>30</sup> noted high correlations between preoperative fMRI hippocampal encoding asymmetry and postoperative memory outcome in their study of 10 patients with left TLE who underwent a verbal-encoding task.

In the study of Rabin et al<sup>29</sup> of 35 patients with TLE and 30 healthy controls who performed a complex visual-scene-encoding memory task, the authors evaluated medial TL regions of interest that encompassed the hippocampus, parahippocampal gyrus, and fusiform gyrus. The control subjects showed almost symmetric activation within these regions of interest, whereas the patients with TLE showed greater asymmetry. Preoperative fMRI activation asymmetry ratios from the regions of interest correlated significantly with both memory lateralization by preoperative Wada testing and postoperative memory outcome, as determined by a change in scene recognition between presurgical and postsurgical evaluations.<sup>29</sup>

### **Limitations in the Early Era of Functional Imaging**

Many of these studies were fairly unsophisticated because in that era, export of postprocessed functional activation maps into neuronavigation systems was not possible and most radiology departments did not even have PACS, but were rather relying on hard copy films. Neurosurgeons using such data at most centers had access to only relatively primitive neuronavigation systems that only permitted use of 3D structural brain images; for this reason, hard copy images of BOLD results were often posted in the surgical suites for planning purposes. As PACS servers became more common around the turn of the century with the digitization of radiology departments, more impetus for electronic transfer of functional activation maps to PACS servers developed. Along with the development of PACS, we have seen a tremendous increase in computational capacity since the 1990s. In those days, much of the processing of BOLD data was extremely time-consuming due to relatively slow CPU processing capability and relatively low memory (RAM) capacity of high-end computer workstations in that era, and the data-storage needs were colossal, considering that a single clinical study could exceed 1 gigabyte of data. It was not uncommon for a single clinical fMRI study to require up to 8–12 hours of processing by using GLM approaches. A minimum of 1 terabyte of storage capacity was considered optimal in those days, which seems minute compared with the requirements of the current era.

Multimodality image fusion, now the standard, was not

widely available due to the inherent limitations of BOLD processing and coregistration with other functional imaging datasets. For example, coregistration with DTI maps, such as FA-weighted color directional maps or DTT, was generally not feasible because different research software packages were used for generation of the DTI maps, which were not necessarily compatible with the software used for the BOLD image analysis. Scanner vendors did not provide commercially available software for DTI processing, and only standard 3-direction diffusion encoding was available for generation of typical diffusion-weighted images and postprocessed apparent diffusion coefficient maps. Similarly, dynamic susceptibility contrast perfusion MR imaging was in its infancy as well, and commercially available software generally allowed only acquisition of time-to-peak maps and basic cerebral blood volume maps, not corrected for contrast-leakage effects or capable of providing permeability information. Even the phenomenon of neurovascular uncoupling had not yet been described, and many of the potential pitfalls of the clinical application of BOLD imaging were just being acknowledged for the first time.

### **Advances in the Current Era of Functional Imaging**

In the current era of functional imaging, arising at the start of the current millennium, what was originally a novelty from a cognitive neuroscience investigation standpoint has evolved into an essential element in such exploration of human brain function, and this has led to development of new models of language function (eg, the ventral and dorsal stream model) and working memory based on empiric evidence provided by functional neuroimaging.<sup>31</sup>

Furthermore, BOLD imaging has made a major transition from a research to a clinically viable imaging technique. The development of the new CPT codes for fMRI in January 2007 signifies this transition to an essential clinical tool that has elevated the surgical standard of care. From the very beginning, our neurosurgical colleagues have been primarily responsible for advocating the clinical use of this technique, and currently neurosurgeons at a growing number of academic medical centers consider the combination of BOLD and DTI to be an indispensable component of their practices. Such imaging has influenced preoperative risk assessment, intraoperative mapping strategy, and surgical trajectory.

Many major improvements in the current decade of clinical functional imaging have made performance of these examinations much more streamlined and practical. Newer commercially available fully integrated FDA-approved fMRI systems are now available that offer turnkey solutions from a data-acquisition and paradigm-delivery standpoint as well as rapid and often technologist-driven streamlined processing. No institutional review board protocol is needed for use of these FDA-approved clinical systems. A variety of well-documented paradigms are available for motor, language, and visual mapping. Three-dimensional fusion of DTI and BOLD datasets and delivery of postprocessed images to PACS servers and neuronavigation systems are now possible due to software improvements. Image-processing time has been drastically reduced to  $\leq 1$  hour for BOLD processing, largely due to vastly more powerful computer workstations with faster CPUs and greater RAM. While the need for increased data-storage ca-

CPT Codes for fMRI <sup>35</sup>	
Code No.	Description
70554 fMRI brain by technologist	Includes test selection and administration of repetitive body part movement and/or visual stimulation, not requiring physician or psychologist administration.
70555 fMRI brain by physician/psychologist	Requires physician or psychologist administration of entire neurofunctional testing.
96020 functional brain mapping (must be used with 70555)	Neurofunctional testing selection and administration during noninvasive imaging functional brain mapping, with test administered entirely by a physician or psychologist, with review of test results and report.

capacity has grown, the cost associated with incremental expansion of data-storage capability has decreased substantially. Perfusion imaging or cerebrovascular reactivity mapping is also performed at many centers along with BOLD fMRI to evaluate the potential for lesion-related neurovascular uncoupling.

#### **Establishment of CPT Codes Reflecting Advances of the Current Era**

The establishment of the CPT codes has been based both on the numerous single-center clinical validation studies described above and on several landmark studies that have shown the great value of preoperative functional imaging in surgical planning.<sup>32-34</sup> See the Table for a description of these codes.<sup>35</sup> Specifically, in the study of Petrella et al<sup>32</sup> of 39 patients with brain tumors who underwent preoperative fMRI, the BOLD fMRI altered treatment planning in 19 patients ( $P < .05$ ) and resulted in reduced surgical time (15–60 minutes) in 22 patients. Medina et al<sup>33</sup> evaluated 60 patients with preoperative language ( $n = 53$ ), motor ( $n = 33$ ), or visual ( $n = 7$ ) fMRI. In 38 (63%) patients, fMRI helped to avoid further studies, including the Wada test. In their series, intraoperative mapping was altered in 31 (52%) patients, and overall surgical planning was altered in 25 (42%) patients by the preoperative fMRI results.<sup>33</sup> Roessler et al<sup>34</sup> studied 22 patients with gliomas near the motor cortex who underwent both preoperative fMRI on a 3T MR imaging system and CSM. fMRI detected the primary motor cortex in all patients, but CSM was possible in only 17 of 22 patients (77.3%). The authors reported 100% agreement between CSM localization and fMRI localization of the primary motor cortex within 10 mm.<sup>34</sup>

#### **Complementary Role of DTI in Eloquent White Matter Mapping**

DTI for depiction of eloquent white matter has been as useful in clinical practice as BOLD imaging for delineation of eloquent cortex because surgical severing of these white matter tracts can produce similar postoperative neurologic deficits. Many scanner vendors now offer streamlined DTI and DTT packages, and the overall value of DTI for preoperative risk assessment is excellent.<sup>36</sup> See Fig 1 for an example of how the combination of BOLD and DTI is used in the evaluation of a patient with a brain tumor.

#### **Emerging Role of BOLD and DTI in Neuronavigation**

One relatively recent advance has been the ability to import digital BOLD and DTI data directly into neuronavigation systems. Some of the neuronavigation companies even offer their own BOLD and DTI processing software, including software for basic tractography. Several recent studies have shown great

promise for DTI incorporation into neuronavigation systems for surgical planning,<sup>37-40</sup> and similar studies have shown the added value of BOLD results when incorporated into neuronavigation systems.<sup>41</sup> Each of these studies will be described briefly.

In the study of Bello et al<sup>37</sup> of 52 patients with low-grade gliomas and 12 patients with high-grade gliomas, the authors found a high correlation between DTI fiber tracking results and those of intraoperative subcortical mapping; the overall sensitivity was 95% for detection of the corticospinal tract and 97% for detection of language tracts, by using intraoperative mapping as the criterion standard. The combination of both methods decreased surgery duration, patient fatigue, and the incidence of intraoperative seizures.<sup>37</sup>

Wu et al<sup>38</sup> studied 238 patients with brain tumors involving the pyramidal tract to determine the impact of the use of preoperative DTI in neuronavigation on postsurgical outcome and long-term survival; 118 underwent DTI, while 120 underwent only standard 3D structural imaging for neuronavigation. Postoperative motor deterioration occurred in 32.8% of the control cases, compared with only 15.3% in the DTI group ( $P < .001$ ). In addition, significantly higher 6-month Karnofsky Performance Scale scores were noted in the DTI group.<sup>38</sup> In 81 patients with high-grade gliomas, the median survival of patients undergoing preoperative DTI was 21.2 months compared with only 14.0 months for the control patients ( $P = .048$ ).<sup>38</sup>

Coenen et al<sup>39</sup> compared the location of the preoperative DTI-based pyramidal tract outlined in neuronavigation with the tract outlined in surgery through subcortical intraoperative mapping in 13 patients with tumors adjacent to the pyramidal tracts or in perirolandic regions. They found that in 11 of the 13 patients (92%), the motor pathways were correctly predicted by preoperative DTT, by using subcortical intraoperative mapping as the criterion standard.<sup>39</sup>

Berman et al<sup>40</sup> performed DTT of the corticospinal tract with DTT overlay on T1- and T2-weighted anatomic images for import into a neuronavigation system for surgical planning in a total of 9 patients with gliomas; in 7 patients, additional magnetic source imaging was performed to identify the functional somatosensory cortex. Intraoperative subcortical stimulation mapping of the corticospinal tract was performed by using a bipolar electrode with a total of 16 subcortical motor stimulations identified in the 9 patients.<sup>40</sup> The mean distance between stimulation sites and DTT-determined tracts was  $8.7 \pm 3.1$  mm, which included the inherent error associated with both the actual DTT technique and the stereotactic navigation/image coregistration.<sup>40</sup>

Krishnan et al<sup>41</sup> investigated the correlation between the lesion-to-fMRI voxel activation distance and the occurrence of new postoperative motor deficits in 54 patients with peri-

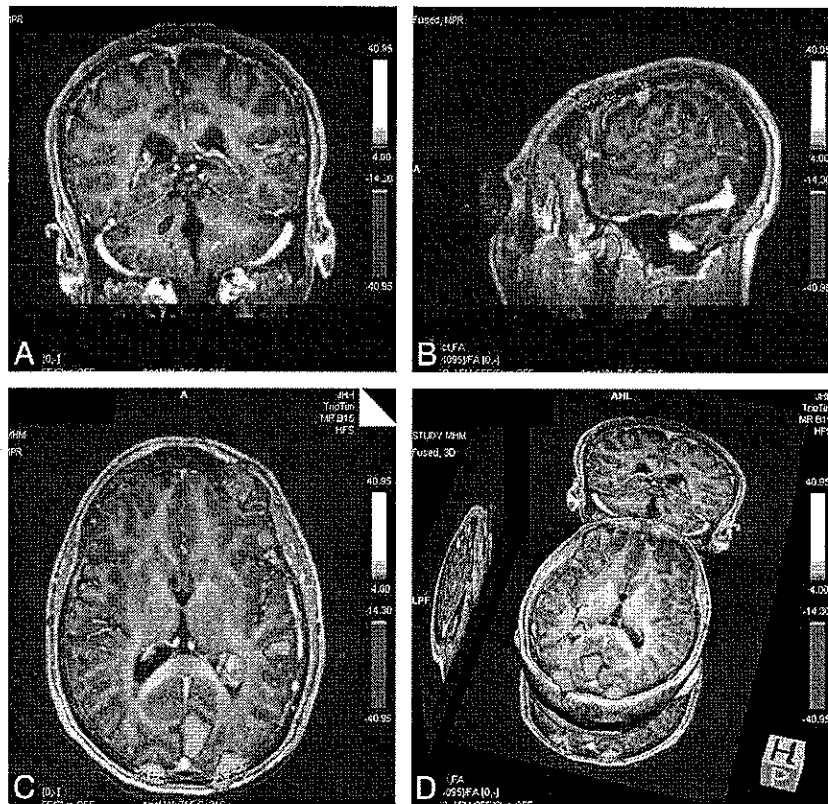


**Fig 1.** Multiplanar views of language BOLD activation overlaid on FA-weighted color directional diffusion maps superimposed on postgadolinium 3D magnetization-prepared rapid acquisition of gradient echo high-resolution anatomic images in a patient with a left trigonal intraventricular mass. The BOLD paradigm used is a silent word-generation task. Red-green-blue coding convention is used for DTI display, in which red refers to mediolateral; blue, to superoinferior; and green, to anteroposterior preferential diffusion. Note the activation of both Broca and Wernicke areas in the left hemisphere in this left-language-dominant patient.

rolandic lesions who performed hand, foot, and tongue motor fMRI tasks. In 45 patients, gross total resection was accomplished, while 80%–95% of resection was performed in the remaining 9 patients; postoperative neurologic status was noted to be improved relative to baseline in 29.6% of patients, unchanged in 53.7%, and worsened in 16.7%.<sup>41</sup> The authors concluded that a lesion-to-activation distance of <5 mm may be associated with a higher risk of postsurgical neurologic deterioration, whereas within a 10-mm range, CSM should be performed for safe resection, while for distances of >10 mm, a complete resection can be safely accomplished.<sup>41</sup>

See Fig 2A, -B for examples of language and motor BOLD-activation maps imported into a neuronavigation system.

### New Insights and Challenges Provided by Clinical Functional Imaging

During the past 2 decades, fMRI has not only served a vital role in presurgical mapping in patients with resectable brain lesions but has also contributed greatly to the evolution of our knowledge regarding language processing and overall cortical and subcortical language representation in the human brain.<sup>31</sup> The classic model of language processing, invoking the Broca area (left inferior frontal gyrus) and Wernicke area (posterior left superior temporal gyrus) as well as the AF, which connects the expressive language areas to the receptive language cortex, has recently been replaced with a more complex model describing a more expansive language network. In particular, the

new concept of “dual-stream model,” which has been described in the current decade, has been recently evaluated with fMRI/DTT by Saur et al.<sup>31</sup> These authors observed that sublexical speech repetition is subserved by a dorsal pathway, connecting the superior TL and the premotor cortices in the frontal lobe via the AF and superior longitudinal fasciculus.<sup>31</sup> In addition, higher level language comprehension is mediated by a ventral pathway connecting the middle TL and ventrolateral prefrontal cortex via the extreme capsule.<sup>31</sup> The dorsal pathway involves sensorimotor mapping of sound to articulation, whereas linguistic processing of sound to meaning involves the ventral pathway.<sup>31</sup>

Some technical pitfalls of clinical BOLD imaging have been highlighted as a result of the growing use of this technique. Foremost among these is the phenomenon of neurovascular uncoupling, which refers to the uncoupling of the regional microvascular blood flow changes from adjacent neuronal activity often seen in high-grade brain tumors with tumor angiogenesis or in arteriovenous malformations that alter local cerebral hemodynamics; many biochemical mediators of the neurovascular coupling have been implicated, such as nitrous oxide, certain neurotransmitters, etc.<sup>42-44</sup> Cerebral vascular reactivity mapping by using carbon dioxide challenges or breath-holding, MR perfusion imaging to assess the presence of regional hyperperfusion, and complementary intraoperative mapping evaluation are methods that different centers are

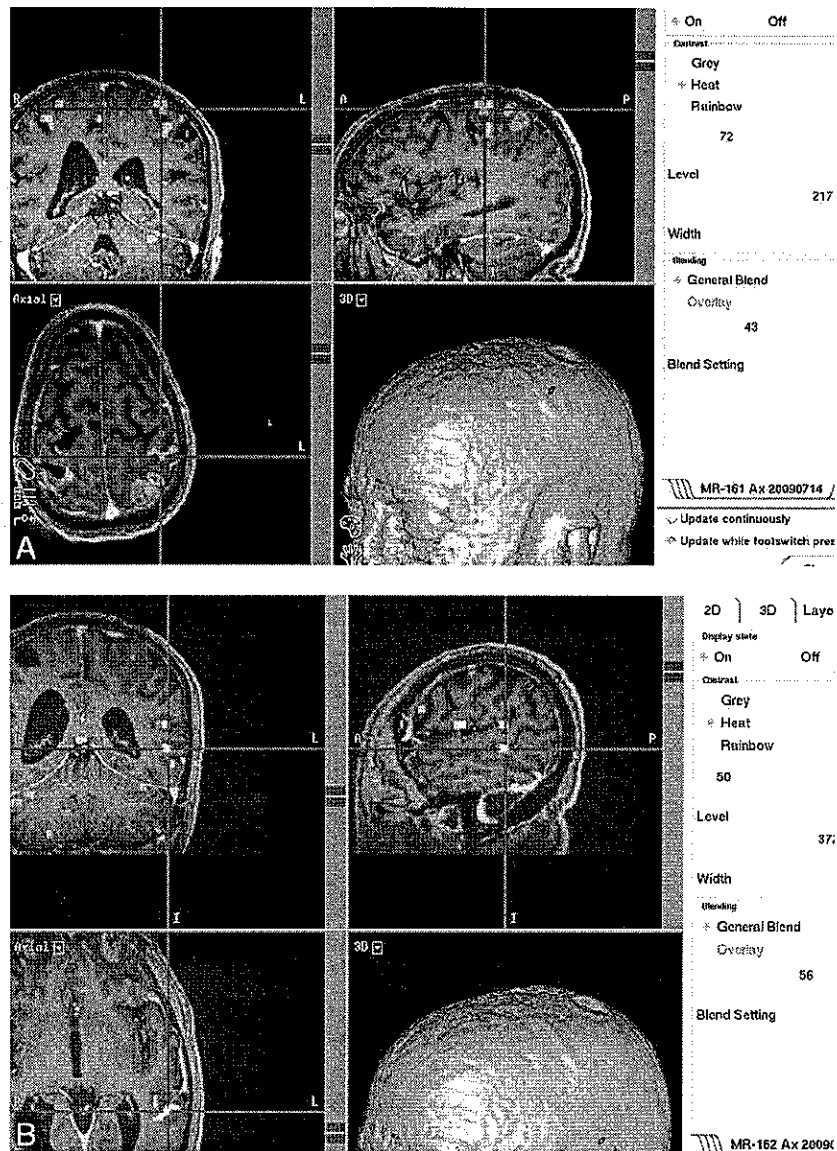


**Fig 2.** BOLD activation maps imported into a neuronavigation system. *A*, Hand motor activation from an alternating finger-tapping paradigm, with the 3D cursor placed on activation seen anterior to a left parietal lobe tumor. *B*, Language activation (combination of silent word-generation and rhyming tasks), with the 3D cursor on temporal lobe receptive cortical activation, in close proximity to the classic Wernicke area.

using in the current era to assess the validity of BOLD activation in light of this important limitation.

Another emerging problem is lack of standardization, which affects DTT as well as BOLD; many different software packages exist for tractography, including traditional DTI-based methods (such as the fiber assignment by continuous tracking algorithm),<sup>45-47</sup> as well as more sophisticated methods that take into account each eigenvector within an individual voxel, such as high angular resolution diffusion imaging<sup>48-50</sup> or diffusion spectrum imaging.<sup>51</sup>

### The Future of Functional Neuroimaging

The future of clinical functional imaging holds the opportunity for neuroradiologists to work more closely with neurosurgical colleagues as preoperative functional imaging becomes progressively incorporated into the evolving surgical

standard of care. Challenges in a revenue-driven radiology practice model will have to be met with demonstration of the added value of functional imaging in overall patient care, and neurosurgical end-users will continue to provide this necessary impetus for development in this field. Although currently limited to major tertiary care academic centers, clinical functional imaging will likely soon make its way to private practices and smaller academic centers as vendors provide increasingly sophisticated streamlined and integrated packages. In the future, with increasing use of higher field intraoperative MR imaging systems, integration of presurgical and possibly even intraoperative functional imaging data into neuronavigation systems with effective real-time brain-shift correction may become a reality, and this will affect the future role of the functional neuroradiologist. In addition, the need to train neuro-radiology fellows in functional imaging is being increasingly

recognized; therefore, fellowship programs will need to provide trainees with more exposure to physiologic/functional imaging in the near future.

## References

- Ogawa S, Lee TM, Nayak AS, et al. Oxygenation-sensitive contrast in magnetic resonance image of rodent brain at high magnetic fields. *Magn Reson Med* 1990;14:68–78
- Ogawa S, Lee TM. Magnetic resonance imaging of blood vessels at high fields: in vivo and in vitro measurements and image simulation. *Magn Reson Med* 1990;16:9–18
- Ogawa S, Lee TM, Kay AR, et al. Brain magnetic resonance imaging with contrast dependent on blood oxygenation. *Proc Natl Acad Sci U S A* 1990;87:9868–72
- Belliveau JW, Kennedy DN Jr, McKinstry RC, et al. Functional mapping of the human visual cortex by magnetic resonance imaging. *Science* 1991;254:716–19
- Chakraborty A, McEvoy AW. Presurgical functional mapping with functional MRI. *Curr Opin Neurol* 2008;21:446–51
- Gold S, Christian B, Arndt S, et al. Functional MRI statistical software packages: a comparative analysis. *Hum Brain Mapp* 1998;6:73–84
- Friston KJ, Jezzard P, Turner R. Analysis of functional MRI time-series. *Hum Brain Mapp* 1994;1:153–71
- Cox RW. AFNI: software for analysis and visualization of functional magnetic resonance neuroimages. *Comput Biomed Res* 1996;29:162–73
- Genovese CR, Lazar NA, Nichols T. Thresholding of statistical maps in functional neuroimaging using the false discovery rate. *Neuroimage* 2002;15:870–78
- Kroger JK, Nystrom LE, Cohen JD, et al. Distinct neural substrates for deductive and mathematical processing. *Brain Res* 2008;1243:86–103
- Kozel FA, Johnson KA, Mu Q, et al. Detecting deception using functional magnetic resonance imaging. *Biol Psychiatry* 2005;58:605–13. Epub 2005 Sep 26
- Mohamed FB, Faro SH, Gordon NJ, et al. Brain mapping of deception and truth telling about an ecologically valid situation: functional MR imaging and polygraph investigation—initial experience. *Radiology* 2006;238:67–88
- Yetkin FZ, Mueller WM, Morris GL, et al. Functional MR activation correlated with intraoperative cortical mapping. *AJNR Am J Neuroradiol* 1997;18:1311–15
- Roux FE, Boulanouar K, Ranjeva JP, et al. Usefulness of motor functional MRI correlated to cortical mapping in Rolandic low-grade astrocytomas. *Acta Neurochir (Wien)* 1999;141:71–79
- Roux FE, Boulanouar K, Ranjeva JP, et al. Cortical intraoperative stimulation in brain tumors as a tool to evaluate spatial data from motor functional MRI. *Invest Radiol* 1999;34:225–29
- Hirsch J, Ruge MI, Kim KH, et al. An integrated functional magnetic resonance imaging procedure for preoperative mapping of cortical areas associated with tactile, motor, language, and visual functions. *Neurosurgery* 2000;47:711–21, discussion 721–22
- Roux FE, Ibarrola D, Tremoulet M, et al. Methodological and technical issues for integrating functional magnetic resonance imaging data in a neuronavigational system. *Neurosurgery* 2001;9:1145–56, discussion 1156–57
- Krings T, Schreckenberger M, Rohde V, et al. Functional MRI and 18F FDG-positron emission tomography for presurgical planning: comparison with electrical cortical stimulation. *Acta Neurochir (Wien)* 2002;144:889–99
- Wu JS, Zhou LF, Chen W, et al. Prospective comparison of functional magnetic resonance imaging and intraoperative motor evoked potential monitoring for cortical mapping of primary motor areas [in Chinese]. *Zhonghua Wai Ke Za Zhi* 2005;43:1141–45
- Xie J, Chen XZ, Jiang T, et al. Preoperative blood oxygen level-dependent functional magnetic resonance imaging in patients with gliomas involving the motor cortical areas. *Chin Med J (Engl)* 2008;121:631–35
- Binder JR, Swanson SJ, Hammeke TA, et al. Determination of language dominance using functional MRI: a comparison with the Wada test. *Neurology* 1996;46:978–84
- Bahn MM, Lin W, Silbergeld DL, et al. Localization of language cortices by functional MR imaging compared with intracarotid amobarbital hemispheric sedation. *AJR Am J Roentgenol* 1997;169:575–79
- Hertz-Pannier L, Gaillard WD, Mott SH, et al. Noninvasive assessment of language dominance in children and adolescents with functional MRI: a preliminary study. *Neurology* 1997;48:1003–12
- Sabbah P, Chassoux F, Leveque C, et al. Functional MR imaging in assessment of language dominance in epileptic patients. *Neuroimage* 2003;18:460–67
- Meneses MS, Rocha SF, Blood MR, et al. Functional magnetic resonance imaging in the determination of dominant language cerebral area [in Portuguese]. *Arq Neuropsiquiatr* 2004;62:61–67. Epub 2004 Apr 28
- Abou-Khalil B. An update on determination of language dominance in screening for epilepsy surgery: the Wada test and newer noninvasive alternatives. *Epilepsia* 2007;48:442–55. Epub 2007 Feb 21
- Benson RR, FitzGerald DB, LeSueur LL, et al. Language dominance determined by whole brain functional MRI in patients with brain lesions. *Neurology* 1999;10:52:798–809
- Janszky J, Jokeit H, Kontopoulou K, et al. Functional MRI predicts memory performance after right mesiotemporal epilepsy surgery. *Epilepsia* 2005;46:244–50
- Rabin ML, Narayan VM, Kimberg DY, et al. Functional MRI predicts post-surgical memory following temporal lobectomy. *Brain* 2004;127(pt 10):2286–98
- Richardson MP, Strange BA, Thompson PJ, et al. Pre-operative verbal memory fMRI predicts post-operative memory decline after left temporal lobe resection. *Brain* 2004;127(pt 11):2419–26
- Saur D, Kreher BW, Schnell S, et al. Ventral and dorsal pathways for language. *Proc Natl Acad Sci U S A* 2008;105:18035–40
- Petrella JR, Shah LM, Harris KM, et al. Preoperative functional MR imaging localization of language and motor areas: effect on therapeutic decision making in patients with potentially resectable brain tumors. *Radiology* 2006;240:793–802
- Medina LS, Bernal B, Dunoyer C, et al. Seizure disorders: functional MR imaging for diagnostic evaluation and surgical treatment—prospective study. *Radiology* 2005;236:247–53
- Roessler K, Donat M, Lanzenberger R, et al. Evaluation of preoperative high magnetic field motor functional MRI (3 Tesla) in glioma patients by navigated electrocortical stimulation and postoperative outcome. *J Neurol Neurosurg Psychiatry* 2005;76:1152–57
- Bobholz JA, Rao SM, Saykin AJ, et al. Clinical use of functional magnetic resonance imaging: reflections on the new CPT codes. *Neuropsychol Rev* 2007;17:189–91
- Ulmer JL, Salvan CV, Mueller WM, et al. The role of diffusion tensor imaging in establishing the proximity of tumor borders to functional brain systems: implications for preoperative risk assessments and postoperative outcomes. *Technol Cancer Res Treat* 2004;3:567–76
- Bello L, Gambini A, Castellano A, et al. Motor and language DTI fiber tracking combined with intraoperative subcortical mapping for surgical removal of gliomas. *Neuroimage* 2008;39:369–82
- Wu JS, Zhou LF, Tang WJ, et al. Clinical evaluation and follow-up outcome of diffusion tensor imaging-based functional neuronavigation: a prospective, controlled study in patients with gliomas involving pyramidal tracts. *Neurosurgery* 2007;61:935–48, discussion 948–49
- Coenen VA, Krings T, Axer H, et al. Intraoperative three-dimensional visualization of the pyramidal tract in a neuronavigation system (PTV) reliably predicts true position of principal motor pathways. *Surg Neurol* 2003;60:381–90
- Berman JL, Berger MS, Chung SW, et al. Accuracy of diffusion tensor magnetic resonance imaging tractography assessed using intraoperative subcortical stimulation mapping and magnetic source imaging. *J Neurosurg* 2007;107:488–94
- Krishnan R, Raabe A, Hattingen E, et al. Functional magnetic resonance imaging-integrated neuronavigation: correlation between lesion-to-motor cortex distance and outcome. *Neurosurgery* 2004;55:904–14
- Ulmer JL, Krouwer HG, Mueller WM, et al. Pseudo-reorganization of language cortical function at fMRI imaging: a consequence of tumor-induced neurovascular uncoupling. *AJNR Am J Neuroradiol* 2003;24:213–17
- Holodny AI, Schulder M, Liu WC et al. The effect of brain tumors on BOLD functional MR imaging activation in the adjacent motor cortex: implications for image-guided neurosurgery. *AJNR Am J Neuroradiol* 2000;21:1415–22
- Schreiber A, Hubbe U, Ziyeh S, et al. The influence of gliomas and nonglial space-occupying lesions on blood-oxygen-level-dependent contrast enhancement. *AJNR Am J Neuroradiol* 2000;21:1055–63
- Mori S, Crain BJ, Chacko VP, et al. Three dimensional tracking of axonal projections in the brain by magnetic resonance imaging. *Ann Neurol* 1999;45:265–69
- Basser PJ, Pajevic S, Pierpaoli C, et al. In vivo fiber tractography using DT-MRI data. *Magn Reson Med* 2000;44:625–32
- Conturo TE, Lori NF, Cull TS, et al. Tracking neuronal fiber pathways in the living human brain. *Proc Natl Acad Sci U S A* 1999;96:10422–27
- Berman JL, Chung S, Mukherjee P, et al. Probabilistic streamlines q-ball tractography using the residual bootstrap. *Neuroimage* 2008;39:215–22
- Hess CP, Mukherjee P, Han ET, et al. Q-ball reconstruction of multimodal fiber orientations using the spherical harmonic basis. *Magn Reson Med* 2006;56:104–17
- Mukherjee P, Chung SW, Berman JL, et al. Diffusion tensor MR imaging and fiber tractography: technical considerations. *AJNR Am J Neuroradiol* 2008;29:843–52
- Kuo LW, Chen JH, Wedeen VJ, et al. Optimization of diffusion spectrum imaging and q-ball imaging on clinical MRI system. *Neuroimage* 2008;41:7–18. Epub 2008 Feb 26

## **ARTICLE 8**



# Diffusion Tensor Magnetic Resonance Imaging in Multiple Sclerosis

Daniel Goldberg-Zimring, PhD

Andrea U. J. Mewes, MD

Mahnaz Maddah, MSc

Simon K. Warfield, PhD

## ABSTRACT

Multiple sclerosis (MS), a demyelinating disease, occurs principally in the white matter (WM) of the central nervous system. Conventional magnetic resonance imaging (MRI) is sensitive to some, but not all, brain changes associated with MS. Diffusion-weighted imaging (DWI) provides information about water diffusion in tissue and diffusion tensor MRI (DT-MRI) about fiber direction, allowing for the identification of WM abnormalities that are not apparent on conventional MRI images. These techniques can quantitatively characterize the local microstructure of tissues. MS-associated disease processes lead to regions characterized by an increased amount of water diffusion and a decrease in the anisotropy of diffusion direction. These changes have been found to produce different patterns in MS patients presenting different courses of the disease. Changes in water diffusion may allow examination of the type, appearance, enhancement, and location of lesions not readily visible by other means. Ongoing studies of MS are integrating conventional MRI and DT-MRI measures with connectivity-based regional assessment, aiming to provide a better understanding of the nature and the location of WM lesions. This integration and the development of novel image-processing and visualization techniques may improve the understanding of WM architecture and its disruption in MS. This article presents a brief history of DWI, its basic principles and applications in the study of MS, a review of the properties and applications of DT-MRI, and their use in the study of MS. In addition, this article illustrates the methodology for the analysis of DT-MRI in ongoing studies of MS.

Key words: Diffusion-weighted imaging, diffusion tensor, DT-MRI, multiple sclerosis, magnetic resonance imaging, diffusivity, lesion, tractography.

Goldberg-Zimring D, Mewes AUJ,  
Maddah M, Warfield SK.

Diffusion tensor magnetic resonance  
imaging in multiple sclerosis.  
*J Neuroimaging* 2005;15:68S-81S.  
DOI: 10.1177/1051228405283363.

Multiple sclerosis (MS) is a demyelinating disease occurring in the white matter (WM) and gray matter (GM) of

the central nervous system. In conventional magnetic resonance imaging (MRI), MS lesions located in the WM produce a hyperintense signal in both proton density and T2-weighted images, while the hypointense T1-weighted lesions are considered to be chronic.<sup>1</sup>

In MS patients, WM may be disrupted in areas not apparent on conventional T2-weighted MRI. Abnormalities of normal-appearing WM (NAWM) on T2-weighted MRI have been detected using magnetization transfer imaging (MTI),<sup>2,4</sup> diffusion-weighted imaging (DWI),<sup>5,9</sup> diffusion tensor MRI (DT-MRI),<sup>6,10-13</sup> and magnetic resonance spectroscopy (MRS).<sup>14-16</sup> (For separate, detailed discussions of MTI and MRS, please see the accompanying articles in this supplement.<sup>4,16</sup>)

In general, MS patients present an increased amount of water diffusion and a decreased anisotropy of diffusion direction in the region of the lesions, in the surrounding lesion tissue, and in the remote NAWM. These changes are believed to be the result of either damage and removal of highly aligned cellular structures or replacement of axonal fibers with amorphous cells<sup>7,9,17,18</sup> and are apparently dependent on the clinical course of the patient.

The correlation between WM lesion burden in MRI and clinical outcome measures is significant but not strong.<sup>19</sup> WM lesion burden is typically measured over the entire brain, which may underestimate the significance of the underlying connectivity of WM and the

Received August 18, 2005, and in revised form September 27, 2005. Accepted for publication October 6, 2005.

From the Computational Radiology Laboratory, Department of Radiology, Brigham and Women's Hospital, Harvard Medical School, Boston, Massachusetts (DG-Z, AUJM, SKW); the Computer Science and Artificial Intelligence Laboratory, Massachusetts Institute of Technology, Cambridge (MM); and the Computational Radiology Laboratory, Department of Radiology, Children's Hospital, Harvard Medical School, Boston, Massachusetts (SKW).

Address correspondence to Daniel Goldberg-Zimring, PhD, Department of Radiology, Brigham and Women's Hospital, Harvard Medical School, 75 Francis Street, Boston, MA 02115. E-mail: daniel@bwh.harvard.edu.

cumulative effects on WM damage in functionally eloquent WM tracts.<sup>18,20</sup>

Recent advances in DT-MRI and image-processing techniques are providing the image acquisition and visualization technology to enable *in vivo* assessment of the WM architecture of the human brain. These technologies will enable future studies of the relationship between WM disruption, WM connectivity, and clinical measures and will ultimately lead to improved monitoring of patients, better prediction of the course of the disease, and more rapid assessment of new treatments or therapies. (For separate, detailed discussions of image-processing techniques, please see the accompanying article in this supplement.<sup>21</sup>)

This article presents a brief history of DWI and its basic principles and applications in the study of MS, followed by a review of the properties and applications of DT-MRI and its use in the study of MS. In addition, it presents a proposed methodology for the analysis of DT-MRI in ongoing studies of MS.

## Diffusion-Weighted Imaging

### *Brief History*

DWI allows quantitative measurement of the molecular motion of water. DWI is based on the continuous agitation of minute suspended particles, which is a phenomenon known as Brownian movement, named after Robert Brown, who observed the constant movement of pollen grains in 1827.<sup>22</sup> Brown suspended some of the pollen grains in water and examined them closely, only to see them "filled with particles" that were "very evidently in motion." He was soon satisfied that the movement "arose neither from currents in the fluid, nor from its gradual evaporation, but belonged to the particle itself."<sup>22</sup> The kinetic force in Brownian movement is directly related to particle size, and the vector of the force that gives rise to the movement is not consistent, nor does it result in motion in a specific direction. Through his investigation of Brownian movement (frequently referred to as Brownian motion), Albert Einstein showed that according to the molecular-kinetic theory of heat, bodies of microscopically visible size suspended in a liquid perform movements of such magnitude that they can be easily observed using a microscope, on account of the molecular motions of heat.<sup>23</sup> This theoretical formulation was also independently derived by Sutherland,<sup>24</sup> and it has been referred to as the Sutherland-Einstein equation.<sup>25</sup> This analysis of Brownian motion led to the formulation of the Boltzmann constant.

Early nuclear magnetic resonance (NMR) efforts to observe diffusion were performed by Stejskal and Tanner.<sup>26</sup> They derived the effect of a time-dependent magnetic gradient on the spin-echo experiment, particularly in the presence of spin diffusion. In 1986, Le Bihan et al<sup>27</sup> developed an MRI technique to observe intravoxel incoherent motions resulting from the distribution of phases in a single voxel when appropriate magnetic field gradient pulses are applied. They studied the diffusion coefficients measured on images of water and acetone phantoms. They also analyzed neurological images from healthy controls and patients by estimating the amount of water diffusion in tissue by means of the apparent diffusion coefficient (ADC) and found differences between various normal and pathologic tissues. ADC is a scalar measure that reflects the amount of apparent diffusivity in a particular direction.<sup>28</sup> One of the first and most widely used clinical applications of DWI is the evaluation of brain stroke (ischemia). DWI is the most sensitive method for detecting acute ischemia *in vivo*,<sup>29,30</sup> allowing for the distinction between old and new strokes<sup>30,31</sup> and helping to differentiate early stroke from other focal brain processes, which is not possible with conventional MRI.

### *Basic Principles*

The measurement and characterization of water diffusion in tissues is based on the quantification of the random motion of water molecules in tissues. This random motion provides microscopic *in vivo* information about tissue architecture that is not provided by conventional MRI. In pure water, individual molecules present a constant random motion in all directions, but in the environment of brain tissue, this random motion is restricted in different ways. The main factors affecting water diffusion are the structural components and temperature of the tissues. Isotropic diffusion occurs largely in tissues with incoherent structures such as those in the brain ventricles and in adult cortical GM, where the apparent diffusion restriction is equal in all directions. Anisotropic diffusion is present in tissues such as those in regions of WM fiber tracts, where water diffusion has a preferred orientation.<sup>5,6</sup>

In DWI, a single field gradient pulse is applied during image acquisition, providing a quantitative measurement of water diffusion.<sup>27</sup> This quantitative measurement of the diffusion in the gradient direction is determined by the amount of attenuation in the signal resulting from the randomization of the NMR spin phase caused by the diffusion of water molecules. Thus, only diffusion in the direction of the applied gradient can be detected. As the diffusion of water is 3-dimensional (3D), 3 orthogonal measures of direction are required to calculate the mean

diffusivity ( $\bar{D}$ ) for each voxel. The bulk  $\bar{D}$  is the 3D analog of the ADC and is an intrinsic property of the tissues and has no directional dependence. It has also been called trace ADC or mean trace.<sup>28</sup>

### DWI in MS

In the brain's WM, the mobility of the water is restricted by structures such as myelinated and unmyelinated axons that are oriented along the fiber tracts, and the direction of highest diffusivity coincides with the tissue's fiber tract axis.<sup>32,33</sup> The pathological elements of MS have the potential to alter the permeability or geometry of structural barriers to molecular diffusion of water in the brain.<sup>7</sup>

The first study to use DWI in MS was performed by Larsson et al.<sup>34</sup> They studied acute and chronic MS lesions and found diffusion to be higher in acute plaques compared with chronic plaques, suggesting a probable relation between the degree of demyelination and the increase of extracellular water space. Another study performed by Droogan et al.<sup>35</sup> found a higher  $\bar{D}$  and reduced anisotropy in MS lesions as compared with NAWM, with the highest  $\bar{D}$  values measured in T1-weighted hypointense and enhanced lesions. A slightly higher  $\bar{D}$  and reduced anisotropy were also found in the WM of the MS patients as compared with healthy controls. However, no differences in  $\bar{D}$  between patients with different disease phenotypes were observed, and no correlations with disability were seen. In a study of lesions presenting different patterns of enhancement (eg, nonenhancement, homogeneously enhanced, and ring enhanced), Roychowdhury et al.<sup>36</sup> aimed to determine whether the  $\bar{D}$  pattern corresponded to the MRI findings and whether it accounted for histopathologic characteristics of different lesion types. This correspondence was observed, as all 3 types of lesions had a higher  $\bar{D}$  than the NAWM. There was also a significant difference in the mean  $\bar{D}$  between homogeneously enhanced and ring-enhanced as well as between homogeneously enhanced and nonenhanced lesions.

Longitudinal studies have analyzed the changes in diffusion properties in NAWM regions and subsequently presented new enhancing lesions, finding an increasing  $\bar{D}$  in the prelesion NAWM<sup>37,38</sup> and at the time of lesion enhancement.<sup>37</sup> These observations suggested that alterations in the tissue integrity, such as edema and demyelination, occur before the formation of new MS lesions. Werring et al.<sup>37</sup> also observed an increase in  $\bar{D}$  in matched contralateral NAWM regions at the time of the first noted lesion enhancement, suggesting that structural damage is also caused in connected areas of NAWM. In an additional longitudinal study performed by Caramia et al.,<sup>39</sup>  $\bar{D}$  was monitored to identify changes occurring in

the NAWM, the linkage to T2-weighted lesion load, and the correlation with clinical parameters in early MS patients with clinically isolated symptoms. At baseline, they did not find any difference in the  $\bar{D}$  between patients and healthy controls; after 12 months, the  $\bar{D}$  in patients was significantly higher and correlated with T2-weighted lesion load. For those patients presenting an increase in  $\bar{D}$  above a confidence interval, disability status also deteriorated. Similarly, Schmierer et al.<sup>40</sup> observed the changes in  $\bar{D}$  in NAWM in patients with primary-progressive MS (PPMS) over a 1-year period. Serial DWI showed progressive changes in the NAWM in patients with PPMS, with an increment of the  $\bar{D}$  associated with an increase of the T1-weighted and T2-weighted lesion load. They also found the  $\bar{D}$  in frontal NAWM to be associated with disability.

In MS, the changes in diffusion are not exclusively located in the WM; they can also be observed in the normal-appearing GM (NAGM). Cercignani et al.<sup>41</sup> measured  $\bar{D}$  in both the NAWM and NAGM in MS patients and found that  $\bar{D}$  in healthy controls was higher in both NAWM and NAGM than in MS patients. Fabiano et al.<sup>42</sup> analyzed the changes in  $\bar{D}$  in the thalamus of MS patients and observed increased water diffusion, which was partly associated with clinical course, lesion load, and brain atrophy. These results suggest that in MS, subtle changes also occur in the NAGM.

### Diffusion Tensor MRI

#### Estimation of DT From DT-MRI

DT-MRI, initially proposed by Basser et al.,<sup>32</sup> differs from DWI in that in DT-MRI, a tensor describing local water diffusion is calculated for each voxel from measurements of diffusion of at least 6 noncollinear, noncoplanar gradients. The tensors  $D$  are then estimated by solving a system of equations with the form<sup>43</sup>

$$\ln(S_k) = \ln(S_0) - b\hat{g}_k^T D \hat{g}_k, \quad (1)$$

where  $k = 1 \dots n$ , in which  $n$  is the number of gradients.  $S_k$  represents the signal intensities in the presence of diffusion-sensitizing gradients, and  $g_k - S_0$  is the baseline signal intensity obtained from the absence of a diffusion-sensitizing field gradient.

Diffusion tensors are often visualized as ellipsoids with the size and shape reflecting the degree of diffusion along each principal axis and may be represented by symmetric  $3 \times 3$  matrices. The principal axes correspond to the eigenvectors of the tensor ( $e_1$ ,  $e_2$ , and  $e_3$ ), and the relative size of each axis is determined by the eigenvalues of the tensor ( $\lambda_1$ ,  $\lambda_2$ , and  $\lambda_3$ ).<sup>32</sup> An elliptical representation of a tensor is depicted in Figure 1.

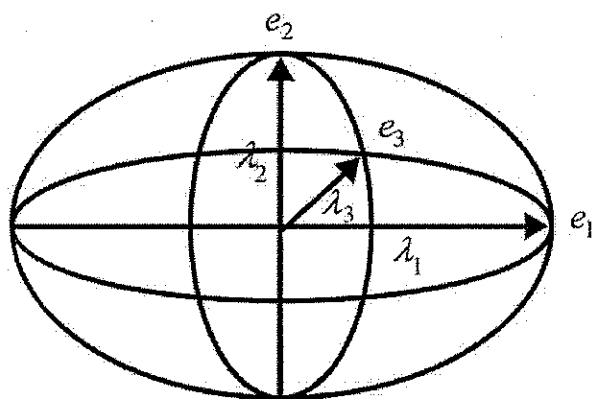


**Fig 1.** Elliptical representation of a tensor, reflecting the degree of diffusion along each principal axis and may be represented by symmetrical  $3 \times 3$  matrices. The principal axes correspond to the eigenvectors of the tensor ( $e_1$ ,  $e_2$ , and  $e_3$ ), and the relative size of each axis is determined by the eigenvalues of the tensor ( $\lambda_1$ ,  $\lambda_2$ , and  $\lambda_3$ ).

### Tensor Representation

In DT-MRI, a tensor describes the local water diffusion per voxel. In isotropic diffusion, characteristic of the adult human brain GM and cerebrospinal fluid, the magnitude of the diffusion is equal in all directions, and the corresponding tensor shape is spherical. Anisotropic diffusion, found in the adult human brain WM, is represented by ellipsoids with variable magnitude of their axes. The shape characteristics of this ellipsoid may be summarized with basic geometric measures<sup>43</sup>: (1) linear, when the diffusion is mainly in the direction of the largest eigenvalue ( $\lambda_1 \gg \lambda_2 \approx \lambda_3$ ); (2) planar, when the diffusion is restricted to a plane spanned by the 2 eigenvectors of the 2 largest eigenvalues ( $\lambda_1 \approx \lambda_2 \gg \lambda_3$ ); and (3) spherical, when the diffusion is equal in all directions ( $\lambda_1 \approx \lambda_2 \approx \lambda_3$ ). By using the largest eigenvalues of the tensor, the linear, planar, and spherical measures can be obtained by, respectively,

$$c_l = \frac{\lambda_1 - \lambda_2}{\lambda_1} \quad (2)$$

$$c_p = \frac{\lambda_2 - \lambda_3}{\lambda_1} \quad (3)$$

$$c_s = \frac{\lambda_3}{\lambda_1} \quad (4)$$

where  $c_l$ ,  $c_p$ , and  $c_s$  lie in the range  $[0, 1]$  and their sum is equal to 1.

### Scalar Measurements

The 2 primary measurements derived from DT-MRI and its tensor representation, based on the normalized vari-

ance of the eigenvalues, include (1) the bulk mean diffusivity, a measure of the amount of water diffusion in tissue, which is equal to one third of the trace of the diffusion tensor:

$$\bar{D} = \frac{\text{Trace}(D)}{3} = \frac{\lambda_1 + \lambda_2 + \lambda_3}{3} \quad (5)$$

and (2) the fractional anisotropy (FA), a measure of the anisotropy of diffusion direction,<sup>6,11,17,18,44,45</sup> which is represented by

$$FA = \frac{1}{\sqrt{2}} \frac{\sqrt{(\lambda_1 - \lambda_2)^2 + (\lambda_2 - \lambda_3)^2 + (\lambda_1 - \lambda_3)^2}}{\sqrt{\lambda_1^2 + \lambda_2^2 + \lambda_3^2}} \quad (6)$$

### Tractography

Tensor visualization allows for representation of the information contained in DT-MRI data. This is the first step for the construction of fiber tracts.<sup>5,46,47</sup> The eigenvector corresponding to the largest eigenvalue indicates the primary orientation of the local brain structure; therefore, it is possible to assess a bulk average of the in vivo axonal connectivity using DT-MRI.<sup>43</sup> The in-plane component of the measured fiber direction is usually represented by headless arrows,<sup>46-48</sup> with the length of the arrows being proportional to the relative anisotropy and orientation indicated by color coding. DT-MRI may be used to delineate WM fiber tracts and thus construct 3D tracts, traces of the pathways representing WM fiber tracts by means of connected diffusion tensors.<sup>43,49-51</sup> Mori et al<sup>52</sup> constructed such representations by starting from a seed pixel and stepping along a line in both the retrograde and orthograde directions according to the largest eigenvector at each pixel. Different criteria were defined to determine when and where to terminate the tracking procedure and hence to identify particular WM pathways of interest. The tracking was performed for every pixel inside the brain, and only those fibers that penetrated previously defined regions of interest were retained. Wakana et al<sup>53</sup> applied the same technique to reconstruct the 3D trajectories of 17 prominent WM tracts. These tracts were superimposed on coregistered anatomic MR images, and parcellation maps of the WM were created, which were later coregistered to DT-imaging color maps to assign visible structures.

Recent work has been carried out in the construction of intersubject atlases from DT-MRI data. Jones et al<sup>54</sup> described spatial averaging of scans from 10 healthy adults and demonstrated success in bringing fiber tracts into correspondence. Mori et al<sup>52</sup> successfully extracted certain corresponding fiber tracts and then detected a different pattern of anisotropy along a certain tract in an adrenoleukodystrophy patient as compared to the

healthy individuals. The feasibility of selection and extraction of specific tracts from scans has also been recently demonstrated,<sup>55</sup> as shown also in a study of pyramidal tracts in MS patients.<sup>18</sup> Average DT-MRI atlases have been constructed by aligning the DT-MRI data using a nonlinear registration approach, which uses all the components of the tensor.<sup>56</sup> This enables the topology and morphology representative of a group of patients to be modeled by the combination of the intensity average and the shape average derived from the mean of deformation fields.<sup>57</sup>

#### *DT-MRI in MS*

The geometry of diffusion tensors can quantitatively characterize the local structure in tissues. The density of the fibers, the degree of myelination, the average fiber tract diameter, and the directional similarity of the fibers in the voxel all affect the shape of the diffusion ellipsoid.<sup>43</sup> Investigation of these properties through several ongoing research studies may provide a better understanding of the pathologic processes involved in MS.

DT-MRI-derived metrics have been found to show tissue damage not only in the area of the T1- and T2-weighted lesion but also in the lesion's surrounding area and in remote NAWM and NAGM as a result of Wallerian degeneration. Kealy et al<sup>58,59</sup> compared the T2-weighted size of MS lesions with lesion size as defined on FA maps. They found a significantly reduced anisotropy both inside the T2-weighted lesions and in the immediately adjacent NAWM regions, indicating that the real size of the lesions is often substantially greater in DT-MRI than what is seen in conventional MRI. Similarly, Guo et al<sup>60</sup> found that the anisotropy and the  $\bar{D}$  values were more abnormal in the lesions and their periphery than in more distant regions. A generally increased  $\bar{D}$  and a reduced FA, especially in brain regions normally presenting a high anisotropy, such as the corpus callosum (CC) and the internal capsule,<sup>61,62</sup> are common changes in the DT-MRI parameters in the NAWM of MS patients. In a more detailed and recent study of the NAWM of the CC of MS patients,<sup>63</sup> a significantly reduced FA in the anterior and posterior midbody subdivisions of the CC was observed. Compared to healthy controls, almost no changes in the FA of the genu of the CC were found, while the splenium showed an insignificant trend to reduced FA values.

Some studies have investigated the pathologic severity of tissue damage in MS based on the DT-MRI metrics observed in different types of lesions. Werring et al<sup>44</sup> observed the highest diffusion in destructive T1-weighted hypointense lesions, whereas the greatest change in anisotropy was found in inflammatory contrast-enhanced lesions. Two different studies<sup>6,45</sup> found that in nonacute

enhanced T1-weighted hypointense lesions, the FA was lower than that of T1-weighted isointense lesions. However, significantly higher  $\bar{D}$ <sup>45</sup> and similar  $\bar{D}$  values<sup>6</sup> were also observed when comparing enhancing and nonenhancing MS lesions.

DT-MRI also has been used with the aim of studying and characterizing the damage caused by MS in its different stages and phenotypes. A study comparing early-onset MS (mean disease duration <1.5 years) in young patients (mean age 14.1 years) with healthy controls with DT-MRI<sup>64</sup> found only a slight increase in  $\bar{D}$  of the NAWM. Griffin et al<sup>65</sup> analyzed the changes in macroscopically normal-appearing brain tissue (NABT) in early relapsing-remitting MS (RRMS) patients (mean disease duration 1.7 years), finding significant differences in FA,  $\bar{D}$ , and volume ratio between lesions and NAWM. However, they did not find a significant difference in the NAWM and NAGM between patients and healthy controls, nor did they find any correlation with clinical outcome measures. To determine whether DT-MRI observable disease effects could be detected in early MS (mean disease duration 1.6 years), Rashid et al<sup>66</sup> analyzed the changes in FA,  $\bar{D}$ , and volume ratio in both the NABT and the whole brain tissue, finding only an increased FA. Studying the normal-appearing CC in RRMS patients having a relatively short disease duration of 2.7 years<sup>67</sup> revealed that FA and  $\bar{D}$  are more severe in normal-appearing CC regions than in other NAWM regions. These studies suggest that in early-stage disease, the pathological changes are minor or localized in specific brain structures such as the CC.

Studies comparing DT-MRI-derived measures concur that the damage caused by MS is higher in more progressive forms of the disease. Cercignani et al<sup>68</sup> quantified tissue damage on T2-weighted lesions and NAWM by means of  $\bar{D}$ , FA, and intervoxel coherence (C, which represents the degree of similarity of orientation of adjacent voxels) from PPMS, RRMS, and secondary-progressive MS (SPMS) patients. They found that the CC of SPMS patients had a higher  $\bar{D}$  and a lower FA and C than did patients with either RRMS or PPMS. SPMS patients also had a higher average lesion  $\bar{D}$  than both RRMS and PPMS did. Similar results were obtained by Rovaris et al<sup>69</sup> for both NAWM and NAGM, with a significantly different  $\bar{D}$  and not significantly different FA when comparing SPMS to PPMS patients. In another study quantifying the extent of GM damage as seen on DT-MRI maps of RRMS, PPMS, and SPMS patients,<sup>70</sup> significant differences were found between controls and patients with only the progressive forms of the disease. The authors also found some differences between RRMS and SPMS patients as well as some differences between PPMS and

SPMS patients, confirming GM damage in MS, which is also related to disease progression.

Longitudinal studies have also been carried out using DT-MRI-derived parameters. Cassol et al<sup>71</sup> monitored the evolution of trace and of FA in the NAWM of MS patients and found that both trace and FA indicated a recovery after the acute phase in RRMS patients and a progressive shift toward abnormal values in SPMS patients. In another study, over a 1-year period,<sup>72</sup> tissue changes beyond the resolution of conventional MRI were detected in the NAGM of patients with progressive MS. These observations indicated that the damage in the GM does not depend only on the T2-weighted lesion load and the reduction of brain volume and may be an additional result of accumulated disability in progressive MS.

The microscopic and more localized analysis of tissue damage that is possible with DT-MRI, as well as its capability to detect remote damage in normal-appearing tissue, is allowing some improvement in the correlation of MRI studies with clinical disability. Ciccarelli et al<sup>11</sup> observed that the FA and  $\bar{D}$  in the cerebral peduncles were inversely correlated with the Expanded Disability Status Scale (EDSS) and pyramidal functional scores. RRMS patients had a strong correlation between the FA and the EDSS in both supra- and infratentorial NAWM, while in PPMS and SPMS patients, disease duration correlated strongly with  $\bar{D}$  in infratentorial NAWM and with FA in the cerebral peduncles. In a study of the correlation between cognitive impairment in RRMS patients and DT-MRI,<sup>17</sup> no correlation between any of the neuropsychological test scores and brain volume, average lesion FA, and whole brain tissue FA was found. However, moderate correlations were found between neuropsychological scores exploring language, attention, and memory and DT-MRI quantitative metrics such as FA and  $\bar{D}$  histograms of whole brain tissue, NABT, NAWM, and NAGM. This seems to reflect the severity of language, attention, and memory deficits in RRMS patients. Using an algorithm to identify specific tracts and measure disease burden within them, Wilson et al<sup>18</sup> assessed pyramidal tract damage caused by MS with a measure derived from the relative anisotropy along the tracts. This measurement in the pyramidal tract correlated significantly with both the EDSS and, to a greater extent, with the pyramidal functional system score (FSS). In a similar way, Lin et al<sup>20</sup> measured the average  $\bar{D}$  ( $\bar{D}_{av}$ ) along the pyramidal tract and CC. They found a correlation between the pyramidal tract  $\bar{D}_{av}$  and pyramidal FSS and between CC  $\bar{D}_{av}$  and the Paced Auditory Serial Addition Test, a neuropsychological test commonly used on MS patients. They also found that the global, but not the localized, T2-weighted lesion correlated with  $\bar{D}_{av}$  of

both the pyramidal tract and CC. The results obtained by Wilson et al<sup>18</sup> and Lin et al<sup>20</sup> show that an increased specificity in monitoring the progression of motor and cognitive impairment in MS may be obtained by matching specific WM tracts with specific clinical scoring systems.

## Proposed Methodology for the Analysis of DT-MRI in Ongoing Studies of MS

### Image Acquisition

High-resolution MRI was acquired from MS patients and healthy controls using a 3T Signa System (GE Medical Systems, Milwaukee, WI). The acquired sets of images included the following: (1) line scan diffusion images (TR/TE = 93/55 milliseconds, field of view [FOV] = 270 cm, matrix size = 256 × 256) using a b = 1000 s/mm<sup>2</sup>, 1 baseline and 6 noncollinear and noncoplanar directions, 60 contiguous 2-mm-thick axial sections for each direction; (2) MPRAGE3D T1-weighted (TR/TE = 8/3.2 milliseconds, inversion preparation time = 725 milliseconds, postdelay time = 1400 milliseconds, FOV = 240 cm, matrix size = 256 × 256), 124 contiguous 1.3-mm-thick sagittal sections; (3) 3DFSE T2-weighted (TR/TE = 4300/8 milliseconds, FOV = 240 cm, matrix size = 256 × 256), 160 contiguous 1-mm-thick sagittal sections; and (4) fluid-attenuated inversion recovery (FLAIR; TR/TE = 8000/8 milliseconds, inversion time = 2450 milliseconds, FOV = 240 cm, matrix size = 256 × 256), 80 contiguous 1.5-mm-thick sagittal sections.

### Alignment of Conventional and DT-MRI

Although the T1-weighted, T2-weighted, and FLAIR images were acquired during the same session, slight head movements were expected to occur. Therefore, T2-weighted and FLAIR images were aligned with the T1-weighted images using an ITK implementation (www.itk.org) of a rigid registration algorithm based on the maximization of mutual information.<sup>73</sup>

Following the rigid registration of conventional MRI, an outline of the intracranial cavity (ICC) masks containing brain parenchyma and cerebrospinal fluid were manually obtained from both the DT-MRI baseline and the T1-weighted MRI. These ICC masks were later applied to the original baseline and T1-weighted sets of images, respectively, to get the segmentation of the ICC. The T1-weighted ICC mask was also used to segment the ICC from the T2-weighted and FLAIR images.

The T1-weighted, T2-weighted, and FLAIR ICCs were then registered onto the baseline ICC using an affine registration algorithm.<sup>74</sup> This algorithm computes an optimal alignment using a robust least-squares method to esti-

mate the rigid body or affine transform that best fits a set of local block match calculations.

#### *Interactive Identification of Particular Fiber Tracts*

Raw data were converted to derive DT information using custom software and were then loaded into 3D slicer ([www.slicer.org](http://www.slicer.org)). The regions of interest (ROIs) were outlined by an expert based on information from the FA map and an additional map, which encodes the direction of the largest eigenvector. This map is known as a color by orientation (CBO) map.<sup>62</sup> The FA map was thresholded to identify regions of anisotropic WM. Based on the CBO map, which allows ready visualization of changes in fiber orientation, the binary label map was segmented into different anatomically defined ROIs. Ambiguities in the CBO map were resolved by seeding single tracts and observing the trajectory.

#### *Assessment of Disease Burden From DT- and Conventional MRI*

The correlation between conventional MRI-derived measures of MS lesion burden and clinical measures of disease status has not been strong and may be at least in part because most MRI-derived measures ignore the different functional significance of different regions of the WM. (For an in-depth discussion of the clinical-MRI paradox, please see the accompanying article in this supplement.<sup>76</sup>) This could be addressed by defining a specific set of regions of WM fiber tracts as observed with DT-MRI and measuring lesion burden from DT- and conventional MRI that reflect alterations in the WM in those regions.

Several measures are possible, including the minimum (min), maximum (max), and mean  $\pm$  standard deviation of the FA and ADC, as well as for the linear, planar, and circular measurements from (1) inside the lesion, (2) a peripheral ROI surrounding the lesion, and (3) a "healthy" symmetric area corresponding to the mirror-image reflection across the midline. MS lesions can be identified and segmented by analyzing the previously aligned sets of images (eg, conventional MRIs registered to the DT-MRI baseline) using established methods.<sup>76</sup>

Beyond single summary measures, distributions of parameters such as the FA along the fiber tracts contained in anatomically defined ROIs may be determined and may reflect the resulting disruption caused by MS. This analysis includes the estimation of tracts<sup>77</sup> aligned with conventional MRI from which the MS lesions are segmented.

#### *Quantitative Assessment*

Compared to the information obtained from the FA map, the information about changes in fiber direction contained in the CBO map is more useful for the interactive

identification of fiber tracts. In Figure 2A, for example, the internal capsule appears as a bright structure in the FA map, and separating the anterior and posterior crus of the internal capsule is not possible. In contrast, in the CBO scalar map (Fig 2B), it is possible to separately identify the anterior crus (blue contour on the right and yellow contour on the left) and posterior crus (orange contour on the right and green contour on the left). Differentiation between different ROIs lying close to each other and appearing bright in the FA map (Fig 2A) is also possible due to the different orientation visible in the CBO map (Fig 2B). In this way, the limbic system (sky blue contour on the right and pink contour on the left) was differentiated from the CC (Fig 2B in green). The identification of the major fiber tracts allows the construction of DT-MRI-based digital atlases such as the one depicted in Figure 2C along with representations of fiber tracts generated anatomically.

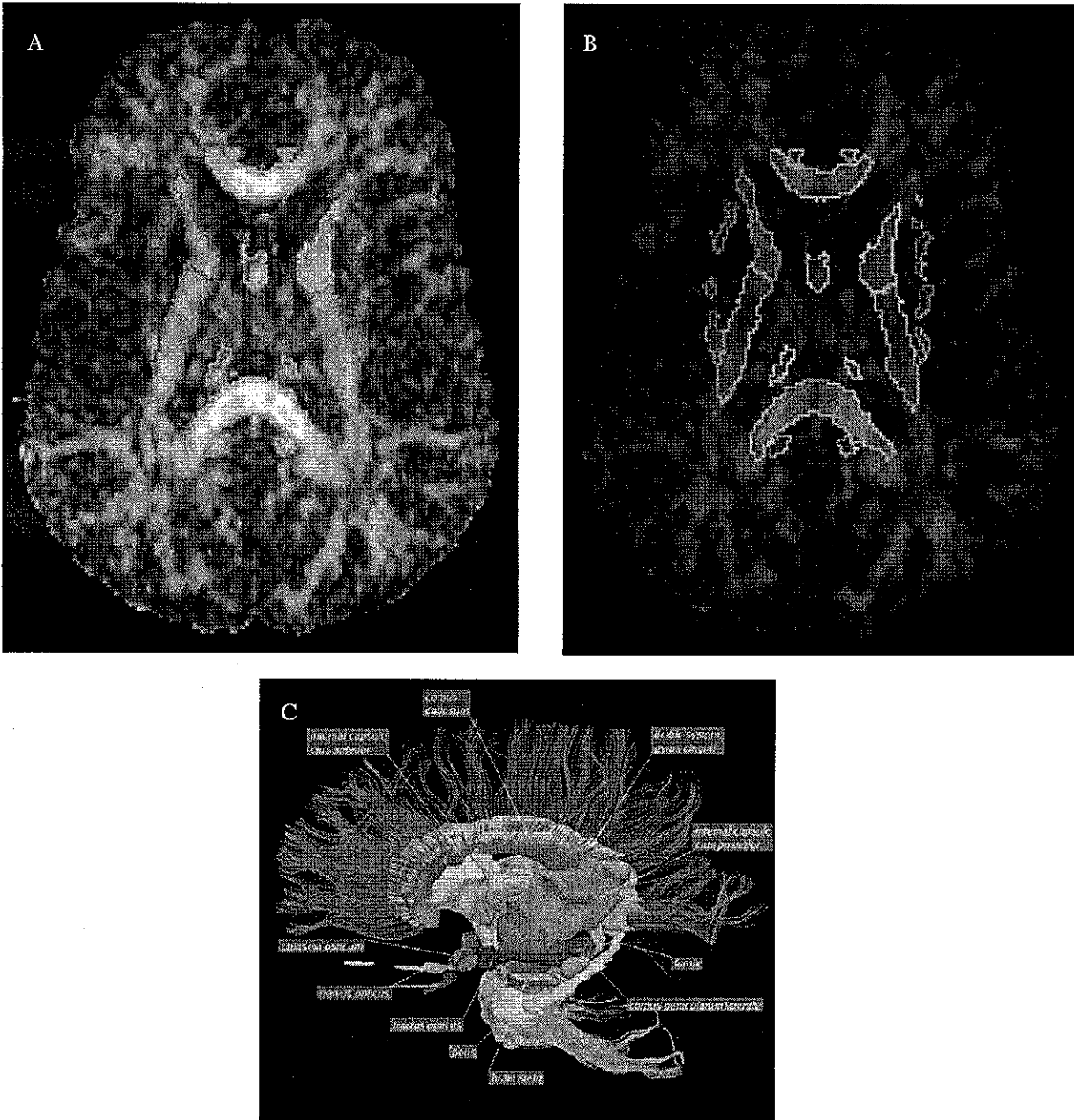
The min, max, and mean  $\pm$  standard deviation of the FA, ADC, linear, planar, and spherical measurements were obtained for an MS lesion visible on conventional MRI. Table 1 summarizes the measurements from inside the lesion, from the lesion's periphery, and from the lesion's mirror-image area. As can be observed, there is a decrease in the mean FA and an increase in the mean ADC as the measurement is done closer to the area where the lesion is located. Similar results were obtained for the planar and spherical measurements.

Figure 3A shows the analyzed lesion (arrow) as seen in the baseline image slice of an MS patient's DT-MRI scan, while Figure 3B presents the same slice depicting diffusion tensors represented as glyphs and color coded by the spherical measure  $c_1$  of the local diffusion tensor.

To illustrate the analysis of changes in FA along the fiber tracts, an MS lesion on the posterior part of the CC was identified. Identification of the lesion was performed using the sets of conventional MRI (Fig 4A). In addition, an apparent area of NAWM located relatively close to the MS lesion was identified from the FA (Fig 4B) and CBO (Fig 4C) maps. From the obtained changes in FA measured along the fibers of the constructed fiber tracts (Figs 5A, B), a significant drop in the FA value corresponding to the lesion (yellow in Figs 5A, B) may be observed, while the slight drop corresponds to the apparent area of NAWM (blue in Figs 5A, B).

#### **Summary**

DWI and DT-MRI have been widely used in studies conducted with the purpose of better understanding the pathogenesis of MS, its natural course, and the nature and location of WM abnormalities, as well as the correlation



**Fig 2.** Axial slice from the diffusion tensor magnetic resonance imaging of a healthy volunteer, shown as a fractional anisotropy map (A) and as a color by orientation (CBO) map (B). In both images, a manually drawn labeled atlas of the major fiber tracts is superimposed. The fiber tracts were identified based on the information provided by the CBO map. In this way, the tracts were drawn on every single slice in which they appeared. (C) This figure illustrates white matter fiber tracts in 2 ways. Some white matter fiber tracts generated by streamline tractography are visualized as thin lines (blue for fibers associated with the corpus callosum and peach for fibers generated in the pons and continuing into the medial pedunculi of the cerebellum). In joint analysis of DT-MRI and conventional MRI, it is of interest to associate particular voxels of the conventional MRI with streamline tractography from particular regions and, in doing so, to define volumetric regions of interest. In this figure, several such white matter regions are visualized as color-coded solid 3-dimensional models.

between MS lesions and the clinical outcome measures. It is now known that the FA decreases while the ADC increases in the areas affected by MS abnormalities, the NAWM and the NAGM. These changes have been found

to be particularly high in patients presenting a more severe course of the disease, such as SPMS, than in less severe courses, such as early-onset MS and RRMS patients. Changing patterns of DT-MRI measurements depending



Table 1. Minimum, Maximum, and  $\bar{x} \pm SD$  for the FA, ADC, Linear, Planar, and Spherical Measurements for an Identified MS Lesion

	Inside the Lesion	Lesion's Periphery	Lesion's Mirror Image
FA			
Min	0.102	0.133	0.120
Max	0.585	0.600	0.590
$\bar{x} \pm SD$	0.344 $\pm$ 0.092	0.395 $\pm$ 0.084	0.385 $\pm$ 0.092
ADC ( $\times 10^{-3}$ mm <sup>2</sup> /s)			
Min	0.840	0.745	0.798
Max	1.511	1.280	1.196
$\bar{x} \pm SD$	1.230 $\pm$ 0.150	1.023 $\pm$ 0.101	1.000 $\pm$ 0.070
Linear			
Min	0.015	0.024	0.001
Max	0.278	0.374	0.293
$\bar{x} \pm SD$	0.137 $\pm$ 0.057	0.156 $\pm$ 0.069	0.132 $\pm$ 0.064
Planar			
Min	0.008	0.011	0.021
Max	0.515	0.661	0.664
$\bar{x} \pm SD$	0.190 $\pm$ 0.115	0.243 $\pm$ 0.145	0.285 $\pm$ 0.132
Spherical			
Min	0.300	0.223	0.229
Max	0.874	0.853	0.847
$\bar{x} \pm SD$	0.644 $\pm$ 0.116	0.566 $\pm$ 0.120	0.550 $\pm$ 0.125

FA = fractional anisotropy, ADC = apparent diffusion coefficient, MS = multiple sclerosis. Measurements were obtained from inside the lesion, the lesion's periphery, and the lesion's mirror-image area.

on the type, appearance, and enhancement of MS lesions and/or their location in different brain structures have also been found.

The integration of both DT- and conventional MRI measures together with connectivity-based regional assessment and the development of novel image analysis and visualization techniques could provide better means to understand the nature and the location of WM abnormalities. The relationship between WM disruption, WM connectivity, and clinical measures will potentially allow clinicians to better correlate fiber tract disruption and MS symptoms such as cognitive impairment. Furthermore, it would ultimately lead to improved monitoring of patients, better prediction of the course of the disease, and more rapid assessment of new treatments or therapies.

This work was partially supported by grants NIH-R21MH067054, NIH-P41RR13218, NIH-R01LM007861; National Multiple Sclerosis Society Award No. RG 3478A2/2; Whitaker Foundation Research Grant, NSF ITR 0426558; and a research grant from CIMIT. This supplement was supported by an educational grant from Teva Neuroscience. BioScience Communications contributed to the editorial refinement of this article and to the production of this supplement. Authors may have accepted honoraria for their supplement contributions.

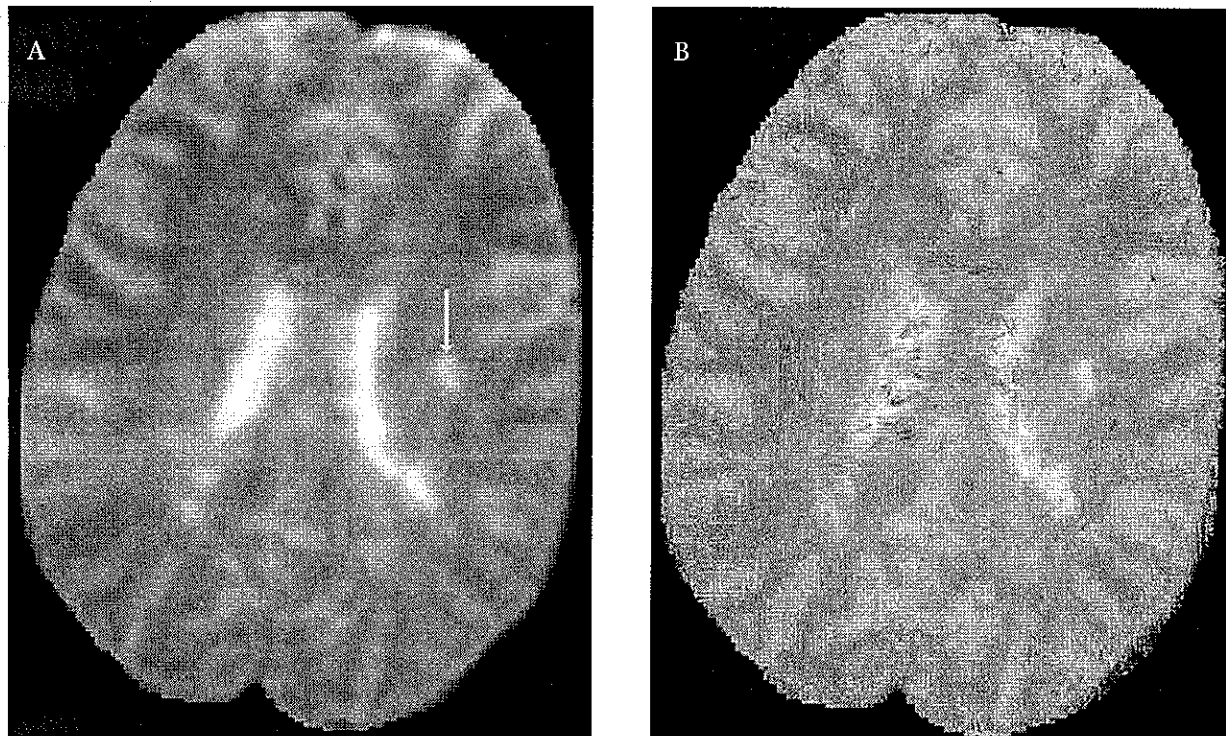
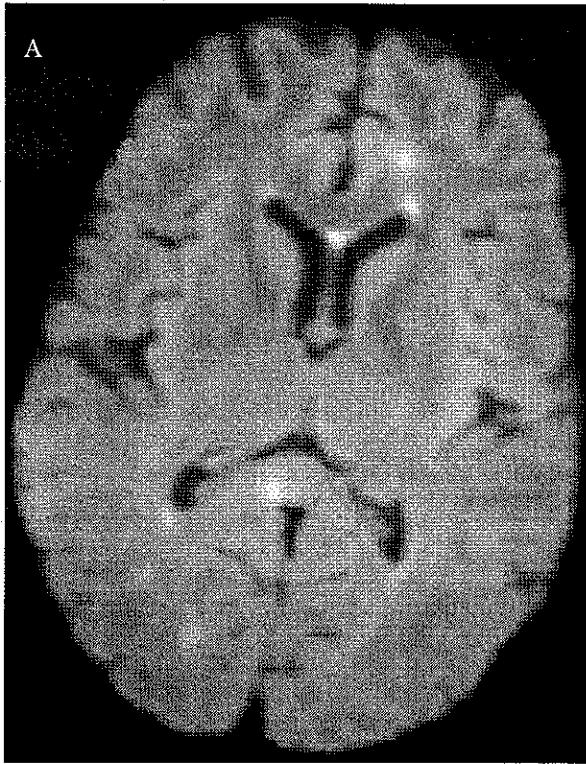
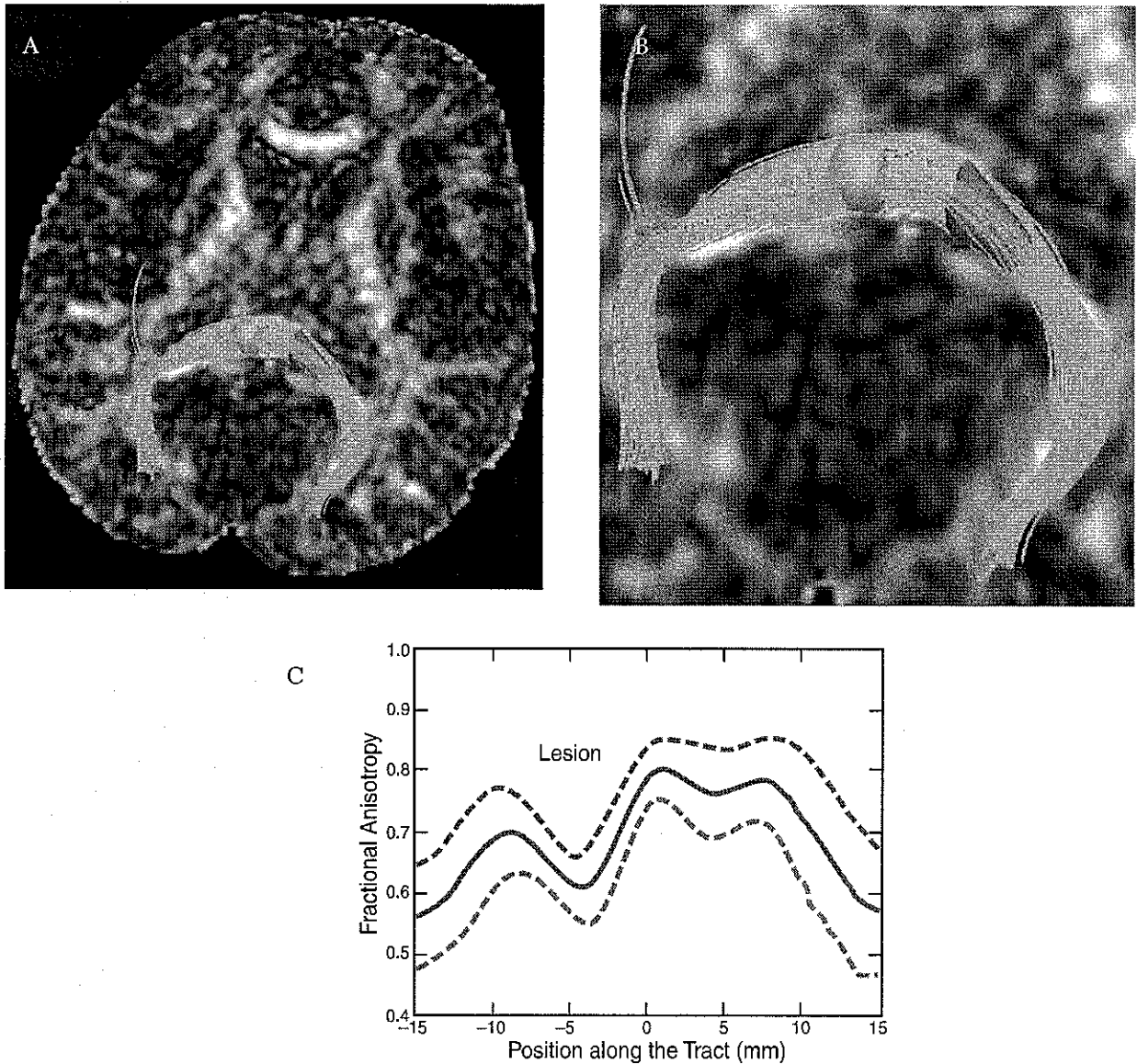


Fig 3. (A) The baseline source of the diffusion tensor magnetic resonance imaging scan of a patient with multiple sclerosis presenting with white matter (WM) lesions. (B) Diffusion tensors represented as glyphs and color coded by the degree of isotropy of the local diffusion tensor: red where the diffusion is most isotropic and blue where the diffusion is most anisotropic. Note that the WM lesions present an increased isotropic diffusion. Results in Table 1 correspond to the WM lesion on the left hemisphere (arrow).



**Fig 4.** A multiple sclerosis (MS) lesion (yellow) and an apparent area of normal-appearing white matter (NAWM; blue) detected in the posterior part of the corpus callosum. Different from the MS lesion, which can be observed in conventional magnetic resonance images (MRIs) (A) and diffusion tensor (DT)-MRI-derived maps such as fractional anisotropy (B), the NAWM can be observed only from DT-MRI-derived color by orientation maps (C).



**Fig 5.** (A) Tractography of the posterior part of the corpus callosum, which is disrupted by a multiple sclerosis lesion (yellow) and an apparent area of normal-appearing white matter (NAWM; blue, see also Fig 3). (B) A magnified view of the fibers clearly passing through the lesion and the NAWM. (C) Changes in fractional anisotropy (FA) measured along the fibers tracts depicted in (A). These changes are represented as the mean (solid line)  $\pm$  standard deviation (dashed lines). Position from the brain midline is indicated on the abscissa. The significant drop in the FA value corresponds to the lesion (yellow in [A] and [B]), while the slight drop corresponds to the apparent area of NAWM (blue in [A] and [B]).

## References

1. Truyen L, van Waesberghe JH, van Walderveen MA, et al. Accumulation of hypointense lesions ("black holes") on T1 spin-echo MRI correlated with disease progression in multiple sclerosis. *Neurology* 1996;47:1469-1476.
2. Filippi M, Rocca MA, Martino G, Horsfield MA, Comi G. Magnetization transfer changes in the normal appearing white matter precede the appearance of enhancing lesions in patients with multiple sclerosis. *Ann Neurol* 1998;43:809-814.
3. Horsfield MA, Barker GJ, Barkhof F, Miller DH, Thompson AJ, Filippi M. Guidelines for using quantitative magnetization transfer magnetic resonance imaging for monitoring treatment of multiple sclerosis. *J Magn Reson Imaging* 2003;17:389-397.
4. Horsfield MA. Magnetization transfer imaging in multiple sclerosis. *J Neuroimaging* 2005;15(suppl 1):58S-67S.

5. Pierpaoli C, Jezzard P, Basser PJ, Barnett A, Di Chiro G. Diffusion tensor MR imaging of the human brain. *Radiology* 1996;201:637-648.
6. Filippi M, Cercignani M, Inglese M, Horsfield MA, Comi G. Diffusion tensor magnetic resonance imaging in multiple sclerosis. *Neurology* 2001;56:304-311.
7. Filippi M, Inglese M. Overview of diffusion-weighted magnetic resonance studies in multiple sclerosis. *J Neurol Sci* 2001;186:S37-S43.
8. Horsfield MA. Using diffusion-weighted MRI in multicenter clinical trials for multiple sclerosis. *J Neurol Sci* 2001;186:S51-S54.
9. Horsfield MA, Jones DK. Applications of diffusion-weighted and diffusion tensor MRI to white matter diseases: a review. *NMR Biomed* 2002;15:570-577.
10. Filippi M, Iannucci G, Cercignani M, Assunta Rocca M, Pratesi A, Comi G. A quantitative study of water diffusion in multiple sclerosis lesions and normal-appearing white matter using echo-planar imaging. *Arch Neurol* 2000;57:1017-1021.
11. Ciccarelli O, Werring DJ, Wheeler-Kingshott CA, et al. Investigation of MS normal-appearing brain using diffusion tensor MRI with clinical correlations. *Neurology* 2001;56:926-933.
12. Tamura H, Takahashi S, Kurihara N, Yamada S, Hatazawa J, Okudera T. Practical visualization of internal structure of white matter for image interpretation: staining a spin-echo T2-weighted image with three echo-planar diffusion-weighted images. *AJNR Am J Neuroradiol* 2003;24:401-409.
13. Rocca MA, Iannucci G, Rovaris M, Comi G, Filippi M. Occult tissue damage in patients with primary progressive multiple sclerosis is independent of T2-visible lesions—a diffusion tensor MR study. *J Neurol* 2003;250:456-460.
14. Fu L, Matthews PM, De Stefano N, et al. Imaging axonal damage of normal-appearing white matter in multiple sclerosis. *Brain* 1998;121:103-113.
15. Pelletier D, Nelson SJ, Oh J, et al. MRI lesion volume heterogeneity in primary progressive MS in relation with axonal damage and brain atrophy. *J Neurol Neurosurg Psychiatry* 2003;74:950-952.
16. Narayana PA. Magnetic resonance spectroscopy in the monitoring of multiple sclerosis. *J Neuroimaging* 2005;15(suppl 1):46S-57S.
17. Rovaris M, Iannucci G, Falautano M, et al. Cognitive dysfunction in patients with mildly disabling relapsing-remitting multiple sclerosis: an exploratory study with diffusion tensor MR imaging. *J Neurol Sci* 2002;195:103-109.
18. Wilson M, Tench CR, Morgan PS, Blumhardt LD. Pyramidal tract mapping by diffusion tensor magnetic resonance imaging in multiple sclerosis: improving correlations with disability. *J Neurol Neurosurg Psychiatry* 2003;74:203-207.
19. Khouri SJ, Guttmann CRG, Orav EJ, et al. Longitudinal MRI imaging in multiple sclerosis: correlation between disability and lesion burden. *Neurology* 1994;44:2120-2124.
20. Lin X, Tench CR, Morgan PS, Niepel G, Constantinescu CS. "Importance sampling" in MS: use of diffusion tensor tractography to quantify pathology related to specific impairment. *J Neurol Sci* 2005;237:13-19.
21. Liu L, Meier D, Polgar-Turcsanyi M, Karkocha P, Bakshi R, Guttmann CRG. Multiple sclerosis medical image analysis and information management. *J Neuroimaging* 2005;15(suppl 1):103S-117S.
22. Ford BJ. Brownian movement in Clarkia pollen: a reprise of the first observations. *The Microscope* 1992;40:235-241. Available at: <http://www.brianjford.com/wbbrowna.htm>. Accessed September 27, 2005.
23. Einstein A. Investigations on the theory of the Brownian movement. Fürth R, ed; Cowper AD, trans-ed. Mineola, NY: Dover; 1956:1-18. Available at: [http://lorentz.phl.jhu.edu/AnnusMirabilis/AeReserveArticles/eins\\_brownian.pdf](http://lorentz.phl.jhu.edu/AnnusMirabilis/AeReserveArticles/eins_brownian.pdf). Accessed September 27, 2005.
24. Sutherland W. A dynamical theory of diffusion for nonelectrolytes and the molecular mass of albumin. *Philosophical Magazine* 1905;S6:781-785.
25. Pais A. *Subtle Is the Lord: The Science and the Life of Albert Einstein*. New York, NY: Oxford University Press; 1982.
26. Stejskal EO, Tanner JE. Spin diffusion measurements: spin echoes in the presence of a time-dependent field gradient. *J Chem Phys* 1965;42:288-292.
27. Le Bihan D, Breton E, Lallemand D, Grenier P, Cabanis E, Laval-Jeantet M. MR imaging of intravoxel incoherent motions: application of diffusion and perfusion in neurologic disorders. *Radiology* 1986;161:401-407.
28. Basser PJ, Jones DK. Diffusion-tensor MRI: theory, experimental design and data analysis—a technical review. *NMR Biomed* 2002;15:456-467.
29. Moseley ME, Cohen Y, Mintorovitch J, et al. Early detection of regional cerebral ischemia in cats: comparison of diffusion- and T<sub>2</sub>-weighted MRI and spectroscopy. *Magn Reson Med* 1990;14:330-346.
30. Warach S, Chien D, Li W, Ronthal M, Edelman RR. Fast magnetic resonance diffusion-weighted imaging of acute human stroke. *Neurology* 1992;42:1717-1723.
31. Warach S, Gaa J, Siewert B, Wielopolski P, Edelman RR. Acute human stroke studied by whole brain echo planar diffusion-weighted magnetic resonance imaging. *Ann Neurol* 1995;37:231-241.
32. Basser PJ, Mattiello J, LeBihan D. MR diffusion tensor spectroscopy and imaging. *Biophys J* 1994;66:259-267.
33. Beaulieu C, Allen PS. Determinants of anisotropic water diffusion in nerves. *Magn Reson Med* 1994;31:394-400.
34. Larsson HBW, Thomsen C, Frederiksen J, Stubgaard M, Henriksen O. In vivo magnetic resonance diffusion measurements in the brain of patients with multiple sclerosis. *Magn Reson Imaging* 1992;10:7-12.
35. Droogan AG, Clark CA, Werring DJ, Barker GJ, McDonald WI, Miller DH. Comparison of multiple sclerosis clinical subgroups using navigated spin echo diffusion-weighted imaging. *Magn Reson Imaging* 1999;17:653-661.
36. Roychowdhury S, Maldjian JA, Grossman RI. Multiple sclerosis: comparison of trace apparent diffusion coefficient with MR enhancement pattern of lesions. *AJNR Am J Neuroradiol* 2000;21:869-874.
37. Werring DJ, Brassat D, Droogan AG, et al. The pathogenesis of lesion and normal-appearing white matter changes in multiple sclerosis: a serial diffusion MRI study. *Brain* 2000;123:1667-1676.
38. Rocca MA, Cercignani M, Iannucci G, Comi G, Filippi M. Weekly diffusion-weighted imaging of normal-appearing white matter in MS. *Neurology* 2000;55:882-884.
39. Caramia F, Fantano P, Di Legge S, et al. A longitudinal study of MR diffusion changes in normal appearing white matter of patients with early multiple sclerosis. *Magn Reson Imaging* 2002;20:383-388.

40. Schmierer K, Altmann DR, Kassim N, et al. Progressive change in primary progressive multiple sclerosis normal-appearing white matter: a serial diffusion magnetic resonance imaging study. *Mult Scler* 2004;10:182-187.
41. Cercignani M, Bozzali M, Iannucci G, Comi G, Filippi M. Magnetization transfer ratio and mean diffusivity of normal appearing white and grey matter from patients with multiple sclerosis. *J Neurol Neurosurg Psychiatry* 2001;70:311-317.
42. Fabiano AJ, Sharma J, Weinstock-Guttman B, et al. Thalamic involvement in multiple sclerosis: a diffusion-weighted magnetic resonance imaging study. *J Neuroimaging* 2003;13:307-314.
43. Westin CF, Maier SE, Mamata H, Nabavi A, Jolesz FA, Kikinis R. Processing and visualization for diffusion tensor MRI. *Med Image Anal* 2002;6:93-108.
44. Werring DJ, Clark CA, Barker GJ, Thompson AJ, Miller DH. Diffusion tensor imaging of lesions and normal-appearing white matter in multiple sclerosis. *Neurology* 1999;52:1626-1632.
45. Bammer R, Augustin M, Strasser-Fuchs S, et al. Magnetic resonance diffusion tensor imaging for characterizing diffuse and focal white matter abnormalities in multiple sclerosis. *Magn Reson Med* 2000;44:583-591.
46. Peled S, Gudbjartsson H, Westin CF, Kikinis R, Jolesz FA. Magnetic resonance imaging shows orientation and asymmetry of white matter fiber tracts. *Brain Res* 1998;780:27-33.
47. Westin CF, Maier S, Khidhir B, Everett P, Jolesz F, Kikinis R. Image processing for diffusion tensor magnetic resonance imaging. Paper presented at: Second International Conference on Medical Image Computing and Computer-Assisted Intervention; September 19-22, 1999; Cambridge, UK.
48. Mamata H, Mamata Y, Westin CF, et al. High-resolution line scan diffusion tensor MR imaging of white matter fiber tract anatomy. *AJNR Am J Neuroradiol* 2002;23:67-75.
49. Basser PJ, Pajevic S, Pierpaoli C, Duda J, Aldroubi A. In vivo fiber tractography using DT-MRI data. *Magn Reson Med* 2000;44:625-632.
50. Conturo TE, Lori NF, Cull TS, et al. Tracking neuronal fiber pathways in the living human brain. *Proc Natl Acad Sci U S A* 1999;96:10422-10427.
51. Jones DK, Simmons A, Williams SCR, Horsfield MA. Non-invasive assessment of axonal fiber connectivity in the human brain via diffusion tensor MRI. *Magn Reson Med* 1999;42:37-41.
52. Mori S, Kaufmann WE, Davatzikos C, et al. Imaging cortical association tracts in the human brain using diffusion-tensor-based axonal tracking. *Magn Reson Med* 2002;47:215-223.
53. Wakana S, Jiang H, Nagae-Poetscher LM, van Zijl PCM, Mori S. Fiber tract-based atlas of human white matter anatomy. *Radiology* 2004;230:77-87.
54. Jones DK, Griffin LD, Alexander DC, et al. Spatial normalization and averaging of diffusion tensor MRI data sets. *Neuroimage* 2002;17:592-617.
55. Catani M, Howard RJ, Pajevic S, Jones DK. Virtual in vivo interactive dissection of white matter fasciculi in the human brain. *Neuroimage* 2002;17:77-94.
56. Guimond A, Meunier J, Thirion J-P. Average brain models: a convergence study. *Comput Vis Image Underst* 1999;77:192-210.
57. Park HJ, Kubicki M, Shenton ME, et al. Spatial normalization of diffusion tensor MRI using multiple channels. *Neuroimage* 2003;20:1995-2009.
58. Kealy SM, Kim Y, Whiting WL, Madden DJ, Provenzale JM. Determination of multiple sclerosis plaque size with diffusion-tensor MR imaging: comparison study with healthy volunteers. *Radiology* 2005;236:615-620.
59. Kealy SM, Kim Y, Provenzale JM. Redefinition of multiple sclerosis plaque size using diffusion tensor MRI. *AJR Am J Roentgenol* 2004;183:497-503.
60. Guo AC, MacFall JR, Provenzale JM. Multiple sclerosis: diffusion tensor MR imaging for evaluation of normal-appearing white matter. *Radiology* 2002;222:729-736.
61. Henry RG, Oh J, Nelson SJ, Pelletier D. Directional diffusion in relapsing-remitting multiple sclerosis: a possible in vivo signature of Wallerian degeneration. *J Magn Reson Imaging* 2003;18:420-426.
62. Coombs BD, Best A, Brown MS, et al. Multiple sclerosis pathology in the normal and abnormal appearing white matter of the corpus callosum by diffusion tensor imaging. *Mult Scler* 2004;10:392-397.
63. Hasan KM, Gupta RK, Santos RM, Wolinsky JS, Narayana PA. Diffusion tensor fractional anisotropy of the normal-appearing seven segments of the corpus callosum in healthy adults and relapsing-remitting multiple sclerosis patients. *J Magn Reson Imaging* 2005;21:735-743.
64. Mezzapesa DM, Rocca MA, Falini A, et al. A preliminary diffusion tensor and magnetization transfer magnetic resonance imaging study of early-onset multiple sclerosis. *Arch Neurol* 2004;61:366-368.
65. Griffin CM, Chard DT, Ciccarelli O, et al. Diffusion tensor imaging in early relapsing-remitting multiple sclerosis. *Mult Scler* 2001;7:290-297.
66. Rashid W, Hadjiprocopis A, Griffin CM, et al. Diffusion tensor imaging of early relapsing-remitting multiple sclerosis with histogram analysis using automated segmentation and brain volume correction. *Mult Scler* 2004;10:9-15.
67. Ge Y, Law M, Johnson G, et al. Preferential occult injury of corpus callosum in multiple sclerosis measured by diffusion tensor imaging. *J Magn Reson Imaging* 2004;20:1-7.
68. Cercignani M, Bozzali M, Iannucci G, Comi G, Filippi M. Intra-voxel and inter-voxel coherence in patients with multiple sclerosis assessed using diffusion tensor MRI. *J Neurol* 2002;249:875-883.
69. Rovaris M, Bozzali M, Iannucci G, et al. Assessment of normal-appearing white and gray matter in patients with primary progressive multiple sclerosis: a diffusion-tensor magnetic resonance imaging study. *Arch Neurol* 2002;59:1406-1412.
70. Bozzali M, Cercignani M, Sormani MP, Comi G, Filippi M. Quantification of brain gray matter damage in different MS phenotypes by use of diffusion tensor MR imaging. *AJNR Am J Neuroradiol* 2002;23:985-988.
71. Cassol E, Ranjeva JP, Ibarrola D, et al. Diffusion tensor imaging in multiple sclerosis: a tool for monitoring changes in normal-appearing white matter. *Mult Scler* 2004;10:188-196.
72. Rovaris M, Iannucci G, Falautano M, et al. Cognitive dysfunction in patients with mildly disabling relapsing-remitting multiple sclerosis: an exploratory study with diffusion tensor MR imaging. *J Neurol Sci* 2002;103:109.
73. Viola P, Wells WM. Alignment by maximization of mutual information. *International Journal of Computer Vision* 1997;24:137-154.

74. Ourselin S, Roche A, Subsol G, Pennec X, Ayache N. Reconstructing a 3D structure from serial histological sections. *Image and Vision Computing* 2000;19:25-31.
75. Zivadinov R, Leist TP. Clinical-magnetic resonance imaging correlations in multiple sclerosis. *J Neuroimaging* 2005;15(suppl 1):10S-21S.
76. Warfield S, Dengler J, Zaers J, et al. Automatic identification of grey matter structures from MRI to improve the segmentation of white matter lesions. *J Image Guid Surg* 1995;1:326-338.
77. Maddah M, Mewes AUJ, Haker S, Grimson WEL, Warfield SK. Automated atlas-based clustering of white matter fiber tracts from DTMRI. Paper presented at: Eighth International Conference on Medical Image Computing and Computer-Assisted Intervention; October 26-29, 2005; Palm Springs, CA.

## **ARTICLE 9**

## FUNCTIONAL BRAIN MAPPING AND ITS APPLICATIONS TO NEUROSURGERY

Suzanne Tharin, M.D., Ph.D.

Department of Neurosurgery,  
Brigham and Women's Hospital,  
Harvard Medical School,  
Boston, Massachusetts

Alexandra Golby, M.D.

Department of Neurosurgery,  
Brigham and Women's Hospital,  
Harvard Medical School,  
Boston, Massachusetts

Reprint requests:

Alexandra Golby, M.D.,  
Department of Neurosurgery,  
Brigham and Women's Hospital,  
Harvard Medical School,  
75 Francis Street,  
Boston, MA 02115.  
Email: agolby@bwh.harvard.edu

Received, January 19, 2006.

Accepted, August 30, 2006.

FUNCTIONAL BRAIN MAPPING may be useful for both preoperative planning and intraoperative neurosurgical decision making. "Gold standard" functional studies such as direct electrical stimulation and recording are complemented by newer, less invasive techniques such as functional magnetic resonance imaging. Less invasive techniques allow more areas of the brain to be mapped in more subjects (including healthy subjects) more often (including pre- and postoperatively). Expansion of the armamentarium of tools allows convergent evidence from multiple brain mapping techniques to bear on pre- and intraoperative decision making. Functional imaging techniques are used to map motor, sensory, language, and memory areas in neurosurgical patients with conditions as diverse as brain tumors, vascular lesions, and epilepsy. In the future, coregistration of high resolution anatomic and physiological data from multiple complementary sources will be used to plan more neurosurgical procedures, including minimally invasive procedures. Along the way, new insights on fundamental processes such as the biology of tumors and brain plasticity are likely to be revealed.

**KEY WORDS:** Brain mapping, Diffusion tensor imaging, Functional magnetic resonance imaging, Preoperative planning, Transcranial magnetic stimulation

*Neurosurgery* 60(ONS Suppl 2):ONS-185-ONS-202, 2007

DOI: 10.1227/01.NEU.0000255386.95464.52

The goal of neurosurgical resection of brain lesions is maximal excision with minimal permanent injury to the surrounding normal brain tissue and, more importantly, no resultant neurological deficit. A new deficit may be caused by damage to cortical areas immediately surrounding a lesion, as well as to the white matter at the depths of the lesion and to brain tissue involved in the surgical approach. Central to minimally morbid surgery is an understanding of the anatomic and physiological relationship of a lesion to surrounding eloquent brain tissue. Functional brain imaging provides information on the anatomic localization of a variety of brain functions, such as movement, sensation, speech and memory, as well as of white matter tracts connecting critical areas. Together with conventional imaging methods used to localize the lesion, functional imaging can be helpful in defining the relationship of the lesion to critical brain structures for operative planning. Although neurosurgeons have long used invasive brain mapping techniques, recent technological advances have led to several additional less invasive methods for mapping brain function. These methods differ not only in their

methodology and physiological basis but also in their level of spatial and temporal resolution, their invasiveness, and their cost.

Conceptually, one may ascribe function to a given area of brain by observing it, blocking it, or stimulating it. Observational methods reveal increased electrical or metabolic activity in specific brain regions while a certain behavior, such as movement or speech, is performed. Such methods demonstrate involvement of various brain areas in a specific function, without demonstrating either necessity or sufficiency. Blocking (or inhibition) methods localize function by reversibly inhibiting neuronal functioning in specific brain areas and looking for a consequent reversible functional deficit. Inhibition methods demonstrate the necessity of a given area to a specific function and are useful in that they mimic the effect of surgical resection. However, inhibition methods cannot demonstrate sufficiency. For example, primary auditory pathways are necessary for the perception of speech, but they do not serve to decode speech. Stimulation or activation methods involve stimulation of a target brain area with the goal of eliciting a specific neurological response, such as movement of a specific body



part. Stimulation demonstrates sufficiency and can mimic an activating lesion such as a seizure focus. Some techniques, such as electric cortical stimulation (ECS), may be used for both activation and inhibition. Given incomplete information inherent in any single technique, convergent information from multiple methods may be the most useful in operative planning. In this review, we will describe the various functional mapping techniques, their utility in assessing particular functions, and their application to neurosurgical disease processes.

## TECHNIQUES

### Observational

#### *Positron Emission Tomography*

In positron emission tomographic (PET) imaging, a radioactive tracer compound labeled with a positron-emitting isotope such as  $^{15}\text{O}$  is administered. The patient is then imaged in a scanner containing rings of scintillation detectors that determine the position of the isotopes within the body. PET may be used to measure cerebral blood flow, cerebral glucose metabolism, and dopamine receptor occupancy, among other functions.  $\text{H}_2^{15}\text{O}$  PET is used to measure cerebral blood flow. Hemodynamic changes thus measured may be used as a surrogate for neuronal cell activation. When  $\text{H}_2^{15}\text{O}$  PET is used for functional brain mapping, the patient performs a task and cerebral blood flow, as quantified by the tracer, is measured. Blood flow under control conditions is then subtracted from blood flow during task performance to obtain regions of increased flow thought to subservise the task in question. When fluoro deoxyglucose (FDG)-PET is used for functional brain mapping, the patient performs a task and cerebral metabolism, as measured by FDG uptake, is measured and compared to uptake under control conditions (170).

One advantage of PET is its ability to study a wide range of functions: any brain function that can be called upon with a behavioral task can be studied by PET. Specificity of the PET image will be dependent on specificity of the behavioral and control task paradigm and implementation. Disadvantages of PET include a poor signal-to-noise ratio when compared with functional MRI (fMRI), only moderate spatial resolution (the best PET scanners have spatial resolution of 4 mm), and poor temporal resolution owing to imaging time and the temporal delay in measuring metabolic changes as a proxy for neuronal changes. Moreover, PET is relatively invasive as it involves administration of radioactive tracer, limiting the number of studies in any individual patient and excluding certain patient populations such as children. PET studies also require expensive, dedicated equipment and personnel and, ideally, access to a cyclotron for the production of tracers. Because it is hemodynamically based, PET is vulnerable to processes that uncouple neural and hemodynamic events. Like any observational technique, it has the disadvantage of not differentiating essential from participating areas.

PET has been used in preoperative planning, including motor and somatosensory mapping (158, 180). PET studies have also examined brain changes that are associated with neurological

diseases such as Alzheimer's disease (108), as well as those that accompany functional recovery from neurological injury such as stroke (19). Perhaps the most common use of PET in neurosurgical planning is its utility in the localization of seizure foci (2, 34, 35, 171, 172). Technological developments in PET continue. In the future, PET imaging may be used to delineate areas of abnormal brain function or altered neurochemistry, thereby guiding resections or pinpointing functional targets.

#### *fMRI*

Like PET, fMRI measures change in cerebral blood flow as a surrogate for neuronal activity. The most commonly used fMRI method measures blood oxygen level-dependent (BOLD) changes in the magnetic resonance signal. Neuronal activity results in increased blood flow through local capillaries. The increased perfusion outstrips the increased demand, resulting in an increase in the ratio of oxyhemoglobin (oxy-Hb) to deoxyhemoglobin (deoxy-Hb) (39). The iron in deoxy-Hb is paramagnetic and reduces the T2 signal. The relative increase in oxy-Hb concentration with neuronal activity results in an increase in the T2 signal with neuronal activity, forming the basis of BOLD imaging (124). For each voxel, the BOLD signal during performance of a task is compared with that during the resting or control state. Unlike PET, BOLD signal change represents a ratio rather than an absolute physiological measure. The change in signal is small, on the order of 0.5 to 5% (6). To obtain an acceptable signal-to-noise ratio, the BOLD signal is averaged over multiple repeated trials and then subjected to statistical analysis. fMRI investigations are normally carried out according to one of two types of experimental paradigms: block design or event-related paradigms (28, 51). In block design, multiple trials of a task or stimulus presentations (a task block) are alternated with multiple trials or presentations of a control task (a control block). The fMRI signals from these two (or more) types of blocks, task versus control, are compared. This is a high sensitivity method but does not allow for analysis of data according to the subject's performance (e.g., speed or accuracy). The second type of fMRI protocol is the event-related protocol in which single trials of a task or tasks are compared. This allows analysis of fMRI data based on the subject's performance on the task but is a lower sensitivity technique (28, 51). Finally, the BOLD map is superimposed on the detailed neuroanatomy derived from the conventional structural magnetic resonance imaging (MRI). Perfusion imaging using arterial spin labeling (ASL), a second fMRI method in which magnetically labeled arterial blood water, delivered as a bolus, is used as a tracer, is a less commonly used technique.

There is evidence in humans and primates that the fMRI signal is proportional to the neuronal firing rate (61, 142) and to local field potentials (97). The same has been demonstrated in rodents (125, 191). fMRI has been validated against PET, transcranial magnetic stimulation (TMS), and ECS for localization of the motor cortex in patients with lesions displacing the central sulcus, demonstrating overlapping (<1 cm) maps in the majority of cases (88). The typical spatial resolution of fMRI is 2 to 5 mm, which is generally higher than PET (192). Advanced

MRI techniques, including higher field strengths (81, 133, 190) and parallel imaging (94, 164), can provide increased signal-to-noise ratios, increased spatial resolution, or shortened acquisition times. The latency of the observed signal change in BOLD imaging is several seconds, making the temporal resolution of fMRI poor when compared with techniques such as ECS or electroencephalography (EEG).

Functional MRI is noninvasive and, therefore, repeatable, both for many runs in a single session (unlike Wada testing) and on multiple occasions to follow patients over time. Because of its noninvasiveness and safety, fMRI is suitable for use in children. Unlike Wada testing, fMRI can provide localization and not merely lateralization of critical functions such as language and memory. Finally, fMRI is able to demonstrate functional activations in the depths of cortical sulci, not just at the cortical surface, an advantage over the "gold standard" electrocortical stimulation (ECS). Disadvantages of fMRI include sensitivity to motion-related artifacts, including those arising from the heartbeat, breathing, and head motion. This has proven particularly problematic for language mapping, generally precluding the use of tasks involving overt spoken language. Furthermore, the technique is sensitive to signal from large draining veins, although this is less prevalent at higher field strengths (45). fMRI also does not have the proven clinical track record of Wada testing or intraoperative mapping.

Neurosurgical applications of fMRI include preoperative localization of primary motor and sensory cortices. As with any emerging technique, validation against standard techniques is a requirement for adoption into mainstream use. Many groups have now examined the validity of fMRI in localizing motor (101, 149, 151), somatosensory (101), and visual (63) areas versus ECS. fMRI has also been used to determine hemispheric language lateralization, and correlates well with Wada findings (27). Although fMRI may soon be substituted for Wada testing for the preoperative determination of language lateralization, and may indeed offer many advantages (discussed below), the technique is has not yet been well correlated with ECS in finer language localization studies (150); thus, its use remains an adjunct as experimental efforts to improve its agreement with standard techniques continue. Several groups have also used fMRI to determine memory lateralization in patients with medically refractory medial temporal lobe (MTL) epilepsy and have also demonstrated good agreement with Wada testing (14, 30, 48). Asymmetric MTL activation has also been shown to be increased contralateral to the side of the seizure focus (9, 48, 72), as well as to be predictive of postoperative memory deficits after mesial temporal resection (71). Spike-triggered fMRI has also been used to localize seizure foci for surgical resection in intractable epilepsy (29, 65, 156, 157).

#### Anisotropic Diffusion Tensor Imaging

Although not strictly a functional study, diffusion tensor imaging (DTI) is able to demonstrate white matter tracts by using MRI to measure the direction of diffusion of water molecules as a marker for the axis of these tracts. The technique is based on the restriction of diffusion of water by axonal mem-

branes and myelin. Water diffusion in axon tracts is direction-dependent, or anisotropic. For physiological reasons that are incompletely understood, water will diffuse least in a direction perpendicular to fiber tracts and most in a direction parallel to them (114). In DTI, magnetic field gradients are applied in multiple orientations. The diffusion tensor is a matrix (mathematical model) that is used to estimate the direction of maximum diffusivity of water molecules based upon MRI data for every voxel. This direction of maximum diffusivity corresponds to the axis of white matter tracts in that voxel (73). Typical spatial resolution in DTI is a voxel size of  $2 \times 2 \times 5 \text{ mm}^3$ , although this is improving quickly (69). An advantage of DTI is that it specifically examines white matter, which is poorly imaged by other functional techniques. One limitation is that it offers little specific information on the functional status or substrates of these tracts. The technique also suffers from poor signal-to-noise ratio (69) and is vulnerable to artifact from air spaces. Other difficulties include imaging crossing tracts, although acquisition and computational advances are continuously being made, providing solutions to these and other issues. *Figure 1* presents a preoperative DTI tractography image incorporating fiber clustering algorithms (123) and demonstrating the relationship of the tumor to adjacent tracts.

DTI may be used to visualize major white matter tracts, including the cingulum, superior and inferior occipitofrontal fasciculi, uncinate fasciculus, arcuate fasciculus, occipitotemporal fasciculus, the corticospinal, corticobulbar and corticopontine tracts, the optic radiations, corpus callosum, and anterior commissure (73). The same authors report occasional but inconsistent visualization of the optic tract, fornix, and tapetum (73). DTI has been used to image the effect of neoplasms on the integrity and trajectory of white matter tracts (187). Four patterns of anisotropy have been observed: normal signal with altered position or direction, corresponding to tract displace-



**FIGURE 1.** Functional MRI study of a 17-year-old patient with a low grade tumor (DNET) in the primary motor cortex region. Left panel shows an axial view of activation associated with tongue movement. Right panel shows a coronal view of activation associated with finger tapping. These results demonstrate the usefulness of fMRI to study multiple functions in a single sitting as well as to display results in various planes.

ment; decreased but present signal with normal direction and location, thought to correspond to vasogenic edema; decreased signal with disrupted direction maps, thought to correspond to infiltration; and loss of anisotropic signal corresponding to fiber tract obliteration or destruction (73). Histopathological studies for validation are still lacking, however, owing to the difficulty in performing such studies. Information on white matter tracts may be useful in operative planning to assist in the avoidance of displaced tracts and those affected by edema or tumor and to allow the surgeon greater confidence when working in areas of brain where critical white matter tracts might be expected but where DTI reveals preexisting tract destruction. There is also some evidence that low-grade tumors may contain white matter tracts within the boundaries of the tumor (163).

Tummala et al. (173) have used DTI of the optic radiations to facilitate complete resection of tumors with no postoperative visual field deficit in two pediatric patients. Berman et al. (13) have combined motor ECS with DTI of motor fiber tracts to visualize motor areas as well as their descending axons in patients with gliomas. This approach could be generalized to sensory and language mapping in awake craniotomies. A few groups have described the use of DTI with fMRI to evaluate the motor cortex and its descending tracts in patients with tumors near the motor cortex (76, 89, 113, 130, 187). Reliable integration of DTI datasets into standard neuronavigation systems by coregistration with fiber tract data with standard anatomic data will greatly facilitate the routine use of this technology. Nimsky et al. have described such integration of DTI data into a standard intraoperative neuronavigation system (119, 122). The authors have recently used this technique to visualize the pyramidal tracts and optic radiations during surgery in 16 patients with space-occupying lesions residing in the vicinity of the above-mentioned tracts (119). Combining DTI with fMRI allows imaging of a particular functional area as well as its connections to other areas, noninvasively, before surgery.

#### *Electrocorticography and Electroencephalography*

Electrocorticography is the direct recording of electrical potentials associated with brain activity from the cerebral cortex. A widely used application of electrocorticography is the localization of the central sulcus by means of phase reversal of somatosensory evoked potentials (SSEP-PR) (189). The EEG is a recording of the summed post-synaptic potentials of populations of cortical neurons. The EEG waveform assumes certain characteristic shapes in different states of arousal, with seizure activity, during the inter-ictal period, and in various disease states. The EEG may be recorded by means of extracranial (scalp) electrodes or intracranial electrodes (depth electrodes or subdural grids and strips). To pursue intracranial electrode placement, there must be sufficient evidence to limit the possible sites of epileptogenesis because clinical considerations necessarily limit coverage with these invasively placed electrodes. On the basis of the scalp EEG and other data, sites are selected for implantation with either depth or subdural electrodes. Depth electrodes are implanted using stereotactic guidance and are most commonly used to monitor the medial temporal lobe

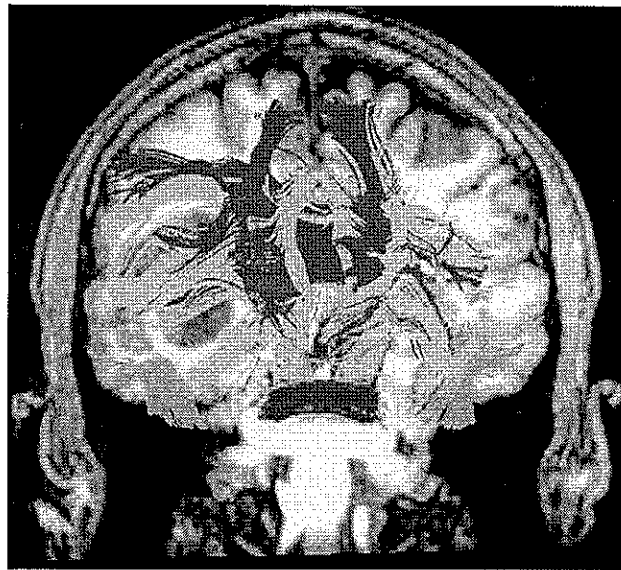


**FIGURE 2.** A coronal brain slice with super-imposed diffusion tensor tractography. The tractography demonstrates alteration in the arrangement of the tracts around the tumor in the temporal lobe. Tracts have been grouped and color-coded into clusters of similarly shaped tracts, which facilitate interpretation of the findings.

structures. Subdural electrodes, arranged in grids and strips, may be used to record from larger areas of cortex including intrahemispheric or subtemporal locations. Each technique has its strengths and limitations in terms of risk, brain coverage, and ease of placement; therefore, individualized determination of the appropriate method is important (57). In both cases, the electrodes can be used to stimulate and record, thereby allowing extraoperative functional mapping (115). Because of the necessity of an additional operative session and risks of hemorrhage, infection, or cerebral edema in 1 to 4% of patients (175), this technique has limited indications. In addition, the need for intracranial recording has declined as other, less invasive, preoperative studies that allow more patients to proceed directly to resective surgery without this step have been developed and validated. Like scalp EEG, intracranial EEG is characterized by excellent temporal resolution; because it does not suffer from distortion from the scalp and cranium, intracranial EEG has much better spatial resolution than scalp EEG. Because intracranial EEG is much more invasive than scalp EEG, it has found use only in limited situations, primarily in epilepsy surgery. Invasive recordings from the human brain can provide unique opportunities to study fundamental processes at fine temporal and spatial resolution (33).

#### *Magnetoencephalography*

Magnetoencephalography (MEG) is a non-invasive method of measuring brain activity by measuring the magnetic fields that accompany neuronal activity. MEG is similar to EEG but is based on magnetic field changes rather than voltage changes.

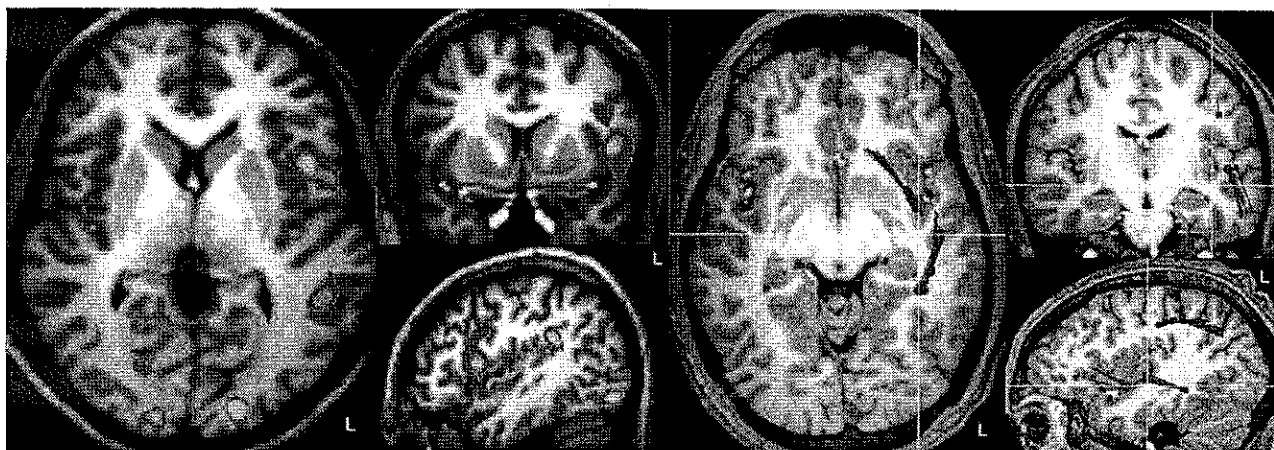


**FIGURE 3.** Language mapping using both MEG and fMRI in the same subject using identical behavioral paradigms. Note that MEG generates equivalent current dipole models that tend to be located deep to the actual cortical surface, whereas fMRI generates statistically color-coded maps located more

superficially. Language lateralization is clearly to the left using both methodologies. Whereas MEG results favor temporal lobe activations, fMRI results favor frontal lobe activations.

Neural activity can be described as the generation and propagation of ion currents. The longitudinal current flow generated by several thousands of neurons firing synchronously can be detected at the scalp surface using a biomagnetometer. MEG data are gathered using a biomagnetometer made up of wire induction coils arranged in an array covering the entire head. The magnetic fields produced by neural activity induce electric currents in these coils and can be used to reconstruct an image of the distribution of evoked neural electrical activity of brain function in real-time. Because the electrical current generated by the magnetic field is very small, superconductors must be used to overcome the impedance of the recording wire. Superconducting quantum interference devices are used to record the conductance change caused by the small magnetic fields associated with neuronal activity. MEG source localization is generally modeled as the equivalent current dipole. When MEG is used for mapping the functional cortex, a stimulus task is presented multiple times. The resulting evoked neuromagnetic signals are then averaged over 80 or more trials to separate the signal produced by a focal population of active neurons from background activity.

MEG has several advantages and disadvantages. Like EEG, MEG has excellent temporal resolution on the order of 1 millisecond. Unlike surface EEG, however, the MEG signal is not attenuated by the cranium and scalp and has better spatial resolution of approximately 2 mm and better signal-to-noise ratio (136). MEG is also a reimbursable procedure, both for epileptic focus localization and for functional mapping. Because MEG source localization is modeled as the equivalent current dipole, several simultaneous sources may be inaccurately represented in MEG datasets by a spatially intermediate single location. MEG also tends to localize function deep to the cortical surface. MEG scanners require dedicated personnel as well as magnetic- and radio frequency-shielded rooms similar to MRI. The

technique is extremely vulnerable to environmental magnetic noise, including the earth's magnetic field and the magnetically noisy environment in hospitals. Currently, MEG scanners are very expensive (> \$2 million capital equipment costs) and have limited availability. At this time, their use is mainly restricted to centers pursuing research programs.

In neurosurgical practice, MEG is used primarily in the presurgical evaluation of epilepsy patients to localize epileptogenic foci (83). The use of MEG has more recently expanded to stereotactic and image-guided surgery to aid in the safe resection of lesions adjacent to eloquent cortex (128, 145). Magnetic source imaging is the coregistration of MEG data to a structural image to facilitate the anatomofunctional correlations and to incorporate this information into stereotactic neuronavigation systems (37). Several studies report good correlation between preoperative MEG functional data and intraoperative maps of sensory and motor evoked potentials and electrocortical mapping (42, 43, 77, 144, 168). Several groups have merged functional MEG data with anatomic data to locate key functional cortex near and within cortical lesions, including arteriovenous malformations, gliomas, and brain metastases. Rezai et al. have reported a technique of integrating MEG functional mapping data for both motor and sensory tasks into a stereotactic database for use intraoperatively, as well as for preoperative planning (145). Their system combined MEG data with CT scans, MRI scans, and digital angiography in an interactive stereotactic system and was used in 10 patients undergoing surgical resection of lesions involving the sensorimotor cortex. Similarly, McDonald et al. (106) report the successful combination of both fMRI and MEG data into a frameless stereotactic system that also incorporates digital registration of cortical stimulation sites. These techniques allow the simultaneous viewing of both structural and functional brain anatomy and their spatial relationship to brain lesions,

which may allow the surgeon to resect more aggressively without violating functional cortical areas.

### Optical Imaging

Brain tissue exhibits optical properties such as scattering and absorption, which can be measured directly at the brain surface. It has been shown that these intrinsic optical signals (IOSs) vary as a function of neuronal activity. At least three types of IOSs are generated by neuronal activity: light scattering signals, some of which may be intrinsic to the neurons themselves; changes in absorption spectra of molecules like Hb, cytochrome and reduced nicotinamide adenine dinucleotide; and IOSs related to changes in blood volume as measured by overall changes in Hb absorption (40). So, like PET and BOLD-fMRI, imaging of intrinsic optical signals (IIOS) depends primarily on changes in local cerebral blood volume and oxygenation. Unlike BOLD-fMRI, changes in blood volume and Hb oxygenation may be measured separately by selecting the appropriate wavelengths (54). IIOS can be used to map functional areas and has been validated against ECS (52). IIOS may be used as a basis for imaging both normal and seizure activity in patients undergoing craniotomy (54). Advantages of optical imaging include low cost and high spatial and temporal resolution. Its limitations are similar to those described above for ECS, including that it is not available preoperatively, that it requires a craniotomy, and that it yields information about only the cortical surface. Optical imaging has not yet been widely adopted for neurosurgical purposes. Finally, a few groups have reported the use of infrared or near-infrared imaging of neuronal activity through the intact cranium (66, 161), although such work remains very preliminary.

### Inhibition and Activation

#### Intracarotid Amytal or Wada Test

The intracarotid amytal (IAT), or Wada, test is an inhibition method in which the territory perfused by the internal carotid artery (ICA) on one side of the brain is temporarily anesthetized by injection of sodium amytal into the ICA. After the observed onset of contralateral hemiparesis and EEG changes, a battery of behavioral tests is applied. Wada testing was initially developed to lateralize language dominance in patients undergoing electroconvulsive therapy but has long been used for language lateralization in preoperative patients with medically intractable epilepsy (181, 182). It was subsequently modified to test lateralization of memory and to assess the risk of postoperative amnesia in patients undergoing temporal lobectomy for medial temporal lobe epilepsy (111). The spatial resolution of the Wada test is usually hemispheric. However, Wada testing has been used in a more highly localized manner with selective catheterization, e.g., to investigate function of the mesial temporal structures in epilepsy patients (17). Temporal resolution is not applicable to this technique. Because it is an inhibition method, the Wada test mimics the effect of surgical resection.

Wada testing is limited in that the examiner has only a few minutes to test each hemisphere. The test is invasive, carrying

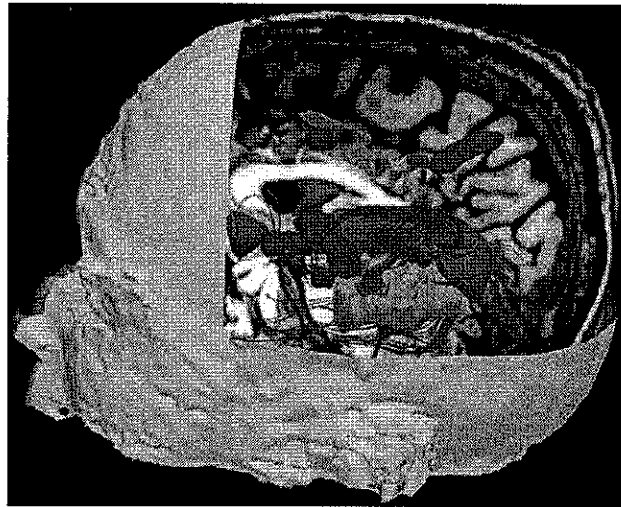


**FIGURE 4.** A cut-away 3-dimensional model incorporates multi-modality brain mapping data. The segmented tumour is shown in green, fMRI activations in purple, MEG activations in blue, and cortical stimulation sites in red. White matter tracts around the lesion are demonstrated in yellow. This type of image demonstrates the complexity of displaying multiple data types as well as the potential utility. In this case, the non-invasive data accurately predicted that the patient experienced language difficulties during resection at the posterior margin of the tumour, even though there were no positive stimulation sites there.

a 0.6 to 1% risk of stroke (58). The transient hemiparesis and cognitive deficits elicited during the test may be upsetting to patients. Agitation and even obtundation can preclude language testing in some individuals. Because of its invasive nature, Wada testing is not readily repeatable. Technically, the test is potentially confounded by cross flow between hemispheres when it exists, resulting in anesthesia of both hemispheres from a unilateral injection. In terms of lateralization of MTL function, in most people, the majority of the MTL is not perfused by the ICA, so inhibition during Wada testing is thought to be indirect and may not be complete.

#### Electrocortical Stimulation

Since the 1930s, direct electrocortical stimulation (ECS) testing has been the gold standard method for mapping brain function in preparation for surgical resection (126, 132). The motor cortex is mapped intraoperatively by stimulating the pre- and postcentral gyri, as well as the premotor area (PMA) and supplementary motor area (SMA). ECS for motor mapping (12, 126) may be performed under general anesthesia without muscle relaxants. Low frequency stimulation delivered to the motor cortex causes contralateral muscular contractions. Kombos et al. (85) have reported the use of monopolar ECS in which muscle action potentials are recorded as a surrogate for movement, which seems to be accompanied by a decreased risk of intraoperative seizure (85). In motor mapping, ECS is used as an activation technique.

To test language functions, it is necessary that the patient remain awake and able to perform certain tasks such as counting or naming (110). Awake craniotomy for language mapping is typically performed using a combination of local anesthetic field block and short acting general agents to induce a rapidly reversible hypnotic state. Once the scalp, cranium, and dura are opened, the sedation is allowed to wear off so that the patient may cooperate with behavioral testing. During the cortical stimulation testing, the patient is awake and asked to perform language tests such as counting or naming while the surgeon stimulates the cortical surface. Areas in which cortical stimulation induces speech arrest or paraphasic errors are considered essential for language function. In this case, ECS is used as an inhibition technique causing disruption in normal neuronal firing. Because the bipolar stimulating electrodes have a 5-mm tip separation, a 1-cm margin is generally respected during the subsequent resection. In their study of 40 patients undergoing removal of gliomas in the dominant temporal lobe, Haglund et al. (53) reported that among patients without preoperative language deficits, 87% had no deficits postoperatively using the above methods.

ECS can also be performed extraoperatively. This option is used primarily for epilepsy surgery for the mapping of the seizure focus through the chronic (~1 wk) implantation of intracranial electrodes. In addition to electrocorticography, cortical stimulation for the determination of eloquent cortex may also be performed during this time period. When indicated, this technique has the advantage of allowing significant time and a sufficiently relaxed and cooperative patient to allow detailed cognitive testing. However, like intraoperative ECS, this technique can only sample from limited regions and is, therefore, not suitable for certain investigations.

In spite of the excellent spatial resolution and predictive value of this technique for cortical mapping, the most obvious drawback is that it requires a craniotomy. In fact, it requires a wide craniotomy that exposes not only the lesion but also adjacent eloquent cortical regions suspected of being jeopardized by the resection. This technique, therefore, does not allow for preoperative planning. ECS language mapping requires that the patient be able to cooperate in performing these tasks during an awake craniotomy. Most children and some adults are unable to tolerate being awake for such a procedure. Even cooperative patients may have trouble maintaining task performance over the course of the investigation. Awake craniotomy generally requires dedicated neuroanesthesia support and a sufficient caseload to provide training and expertise and, hence, may not be available in many centers.

Cortical stimulation testing is also limited by the difficulty of examining the sulcal depths that comprise as much as two-thirds of the cortical surface (25), the deep structures of the mesial temporal lobe, or the underlying white matter. For example, it is not uncommon for patients who have undergone cortical mapping and resection respecting the boundaries of the eloquent cortex to nevertheless be left with neurological deficits secondary to damage to associated white matter tracts. To minimize such occurrences, a few groups have reported suc-

cess using white matter stimulation intraoperatively to define critical tracts (80). Berman et al. (13) have reported the combined use of cortical ECS with DTI to image motor cortex and its descending tracts in patients with gliomas.

### TMS

TMS involves the stimulation or inhibition of neuronal electrical activity via a magnetic field delivered at the scalp. The technique emerged from the discovery of the related technique of transcranial electrical stimulation (TES), in which electric currents applied to the scalp were used to activate cortical neurons (109). Unfortunately in TES a minority of the applied current flowed in the desired direction through the skin and scalp to the cortex, with the remaining majority of the applied current traveling between the stimulating electrodes, activating pain receptors and causing unwanted contraction of scalp muscles. Thus, TES through an intact cranium has not proved a useful technique. Barker et al. (7) subsequently discovered that a magnetic field could be used to set up an electrical stimulus across the scalp and cranium. In TMS, a current is discharged into an electromagnetic coil held over the cranium; this discharge creates a magnetic field that induces a perpendicular electric field. The field is conducted through the living tissues of the skin and cranium and produces an electric current in the cortex, without causing pain in the patient (155). TMS may be used as an activation technique, as is the case when single pulse TMS is used to map the motor cortex (86, 102). It may also be used as an inhibition technique, as in the use of repetitive TMS to disrupt language processing (82, 131) and may be used for the determination of language lateralization (74). Single pulse TMS has temporal resolution on the order of milliseconds; the effects of repetitive TMS can last on the order of seconds. A great advantage of TMS is that it is the only noninvasive inhibition technique. Disadvantages include poor spatial resolution and the risk of repetitive TMS causing seizures (155). Although there has been relatively little reported use of TMS in surgical planning, Krings et al. (86) have described the correlation of TMS with ECS in motor mapping in two patients with tumors near the central sulcus. Neggers et al. (116) have recently developed a frameless stereotactic navigation system for delivering TMS and validated their results showing correlation with fMRI and ECS to within 5mm in motor cortex. Recent reports also describe the coregistration of TMS and fMRI data to investigate visual processing and lateralization of different aspects of memory processing (155). Despite one study reporting that TMS does not replicate Wada testing (36), the above-mentioned reports suggest tremendous promise for the technique in operative planning in the future.

## APPLICATIONS TO SPECIFIC FUNCTIONS

### 1. Motor Mapping

A variety of functional imaging techniques are routinely used in motor mapping in patients with tumors in the vicinity of the motor strip (84, 85) or with suspected seizure foci near primary motor cortex (70). Voluntary movement is associated

with activation of primary motor cortex (M1), premotor area (PMA), supplementary motor area (SMA) and superior parietal lobule (SPL).

Pre-operatively, fMRI is used in many centers to delineate brain regions activated with motor tasks. Many groups have validated fMRI against ECS in localizing motor areas (101, 149, 151, 193). In a recent study of 33 patients with tumors near the central sulcus, Majos et al. found 84% agreement between pre-operative fMRI and intraoperative ECS in identification of motor areas and 83% agreement in the identification of sensory centers between the two techniques. When sensory and motor data are combined, the agreement between fMRI and ECS increased to 98% (101). Roessler et al. recently used 3-Tesla fMRI and ECS to guide resection of gliomas in motor cortex (148). In those patients for whom the two modalities could be correlated (17 of 22), there was 100% agreement between fMRI and ECS data within 1cm.

Intraoperatively, motor cortex may be mapped using bipolar ECS as described above (12, 126). Motor areas may also be mapped either intra- or extra-operatively by recording Bereitschaftspotentials (BPs) (70). These are slow electrical potentials recorded in the awake patient from motor cortex prior to the initiation of voluntary movements and represent excitatory post-synaptic potentials (EPSPs) of cortical pyramidal neurons. Often recorded via chronic subdural electrodes, BPs have the advantages of recording activity associated with planning and execution of voluntary movement, no induction of seizure activity, and yielding information for any type of movement of any part of the body (70). The disadvantage of recording BPs is that they require a very cooperative patient as movements need to be repeated at least 50 times to obtain averaged waveforms (70).

A few groups have recently reported cases in which fMRI was combined with DTI to image motor cortex and its descending (pyramidal) tracts in a patients with lesions residing within or next to primary motor cortex (76, 113, 130). Berman et al. have combined motor ECS with DTI of motor fiber tracts to visualize motor areas as well as their descending axons in patients with gliomas (13).

Several studies have shown altered motor maps in patients with lesions near motor areas. Yousry et al. have found alterations in the cortical representation of the motor hand area in intact patients with space-occupying lesions near the central sulcus (193). Using fMRI to study patients with tumors located in the vicinity of the motor strip, Krings et al. found decreasing activation in primary motor cortex in proportion to the degree of pre-operative hemiparesis (89). They also noted increasing activation in secondary motor areas with increasing pre-operative weakness. Decreased activation in M1 was thought to reflect either loss of cortical neurons or changes in cerebral blood flow secondary to the lesion; increased activation in secondary areas may represent redundant circuitry and form the basis for functional recovery following resection (89). Motor cortex may also be frequently (and unpredictably) shifted by mass lesions. These accounts of the alterations of motor maps illustrate the potential plasticity of the adult brain.

## 2. Language Lateralization

fMRI and Wada are used for language lateralization in patients with MTL epilepsy and in those with tumors of the frontal and temporal lobes. Wada testing with comprehensive language assessment (98) reliably lateralizes language function. Benbadis et al. have demonstrated poor correlation between language lateralization based solely on speech arrest when compared to lateralization by Wada testing based on comprehensive language assessment and lateralization by fMRI in 12 patients with intractable epilepsy, suggesting that speech arrest alone is an unreliable method of preoperative language lateralization (10). Woerman et al. compared language lateralization by fMRI and Wada in 100 patients with temporal lobe epilepsy (TLE) or extra-temporal epilepsy and found 91% concordance in the results of the two tests (188). In their study, fMRI falsely categorized language lateralization in only 3% of left-sided TLE patients but in 25% of left-sided extratemporal epilepsy patients. This large study using a simple word-generation task and a rapid (15 min) acquisition time suggests that fMRI may reduce the need for Wada testing in TLE but is less useful in the determination of language lateralization in extra-temporal epilepsy. Other studies have reported 100% concordance in language lateralization between fMRI and Wada testing in patients with temporal lobe epilepsy (21, 41). Furthermore, Aldenkamp et al. have obtained the expected language dominance distribution in right-handed healthy volunteers using fMRI and a silent word generation task (4). Lehericy et al. have demonstrated that frontal, not temporal, asymmetry of language dominance correlated with Wada testing (93). Further validation of fMRI for preoperative language lateralization comes from studies demonstrating atypical (bilateral or right-dominant) language dominance in 22 to 24% of non-right-handed subjects (140, 169), in agreement with earlier findings using Wada testing of left-handed epileptic patients (141). Furthermore, Fernandez et al. have recently demonstrated high within-test and test-retest intrasubject reproducibility for language lateralization fMRI in patients with epilepsy (38). In addition to carrying fewer risks, fMRI has the advantage of taking less time and costing less than Wada testing. Medina et al. performed cost analysis demonstrating that Wada testing costs 3.7 times more than fMRI (107).

One frequently identified shortcoming of fMRI in language mapping is that, for reasons of motion artifact, silent word generation tests are generally used, as opposed to spoken tests standard during Wada testing. Aldenkamp et al. addressed this issue with the development of a protocol involving alternating scan acquisition with overt naming of pictures (4). Interestingly, the authors found that overt naming lateralizes poorly in fMRI, with all subjects showing bilateral activation. Silent word generation on the other hand, lateralizes well, validating this method (4). Bilateral activation with overt language tasks probably results from non-language-specific activations in face motor, auditory and other areas. Region of interest analysis in putative language areas during overt language tasks may still effectively show lateralization (167). The finding of Aldenkamp

et al. also illustrates the inherent difference between observational and inhibition techniques: although both hemispheres are activated by overt naming, only one may be necessary for language function (that side which, when inhibited during Wada testing, results in aphasia). Furthermore, an important difference between the two techniques is illustrated: in fMRI both hemispheres are tested simultaneously, whereas in Wada testing each hemisphere is tested alone. Despite the fact that Wada testing, as an inhibition technique, mimics the effects of resection, fMRI may come closer to replicating the context (both hemispheres active) of behavior in the postoperative patient. Binder et al. noted a linear relationship between the intensity of right hemispheric activation on fMRI and the severity of language deficits observed on Wada testing of right-dominant individuals (15), suggesting a role for fMRI in predicting the severity of language deficits in right hemisphere surgery in this population and underscoring the possible advantage of the fMRI with its graded output over the Wada test with binary output (166).

### 3. Language Localization

While the emphasis in patients undergoing anterior temporal lobectomy has been on lateralization of temporal lobe speech areas for operative planning, fMRI and PET studies have demonstrated significant involvement of other cortical regions in language. These are particularly pertinent to patients with seizure foci or mass lesions away from the MTL but within these other speech areas. Some of these areas can be preferentially activated with different protocols, such as frontal regions with word generation paradigms (93, 140). Patients with epilepsy show greater variability of language dominance (166) and increased activation of contralateral language areas (21) than healthy control subjects on fMRI. These data point to additional areas that may produce deficits with resective surgery but also to areas of cortex that may be recruited during recovery from surgery or longstanding injury to primary language areas. They also underscore that an observational technique like fMRI cannot distinguish essential from participating, but non-essential, areas.

In epilepsy patients undergoing EEG monitoring via implanted electrodes and awake intraoperative patients undergoing lesion resection, ECS may be used to map specific areas involved in various aspects of language. In these as well as other patients, fMRI may be used in a complementary fashion. While fMRI protocols in current use have demonstrated excellent concordance with Wada testing for language lateralization, correlation between pre- and postoperative fMRI and intraoperative cortical mapping remains inconsistent in studies. In a study of 14 right-handed patients with left hemisphere tumors, Roux et al. (150) compared language areas activated by naming and verb generation tasks with intraoperative speech mapping using ECS. The authors identified 22 language sites with cortical stimulation, 5 of which were concordant with sites identified by fMRI, but 17 of which were not associated with fMRI signal. Based on these findings they conclude that while fMRI is a helpful adjunct its failure to identify speech areas identified by ECS in the operating room makes it insufficient to form the basis of

critical pre-operative decision making prior to resection. Postoperative fMRI of a subset of their patients identified language foci that correlated with those identified intraoperatively with ECS in only 6 of 8 patients examined, with complete agreement in only 3 of 8 patients (150). The authors note that sensitivity and specificity of fMRI can be improved by combining data from both tasks, suggesting that modification of the behavioral paradigms used could improve correlation with ECS data. In patients with MTL epilepsy, on the other hand, Carpentier et al. have demonstrated concordance in intrahemispheric language maps generated by fMRI and via cortical stimulation (21). The authors did find additional areas identified by fMRI, partly owing to limited coverage of cortex by electrodes and partly owing to the fundamental differences between fMRI, an observational technique, and ECS, an inhibition technique.

## APPLICATIONS TO SPECIFIC DISEASE PROCESSES

### Tumor

In patients with brain tumors, the goal of maximizing resection competes with that of not causing any additional neurological symptoms. Many patients with primary tumors of the central nervous system have infiltrative lesions; thus, resections are performed for reduction of mass effect and disease burden but generally not for cure. Thus, minimizing resultant neurological deficits and associated reduction in quality of life is paramount. Similarly, patients with brain metastases usually have limited life expectancies, and palliative surgery must not worsen existing symptoms or introduce new deficits. There is data to suggest that the degree of resection of low-grade gliomas correlates with long-term survival (11, 24, 96, 134, 186), although the evidence remains controversial (79, 105). Because low-grade gliomas can have a slow clinical course, the need to balance aggressive resection with postoperative morbidity, particularly in the neurologically intact patient, is heightened when they are located within or near eloquent brain. Preoperative fMRI has been widely used either alone (3, 56, 87, 89, 185) or in combination with ECS (64, 88, 151) to map eloquent cortex in the vicinity of low-grade gliomas before resection; in some cases, it has been used in conjunction with intraoperative MRI scanning (56).

Owing to their infiltrative nature, low-grade gliomas may have functional tissue within the tumor (127, 163). Indeed, Russel et al. (154) have found that resection of low-grade gliomas involving the supplementary motor area (SMA) results in a higher incidence of transient weakness (SMA syndrome) than the resection of high-grade gliomas in the same region, presumably owing to the presence of more functional SMA cortex within the lower-grade lesions. Detailed and accurate functional imaging is, therefore, particularly important for planning their resection.

Tumors of higher grade present a somewhat different set of challenges. There is inconsistent evidence that the degree of resection of a glioblastoma multiforme (GBM) correlates with time to progression and median survival (78). However, with the best median survival times being 1 to 2 years (78, 91), the



time for postoperative recovery and the duration of even transient deficits are particularly relevant for GBM patients. The transient hemiparesis of the SMA syndrome, for instance (154), which usually resolves within weeks to months, could represent an unacceptable morbidity when the expected survival of the patient may not significantly exceed that time.

The BOLD effect is sensitive to altered regional blood flow as is found in high-grade tumors of the central nervous system (16). Higher-grade tumors are associated with hemodynamic-neural uncoupling, and fMRI data must be interpreted accordingly with this in mind. Perhaps owing in part to this effect, Liu et al. (95) have reported that BOLD fMRI activation volume in the SMA is affected by both tumor type (intra- versus extra-axial) and distance from the motor cortex. Edema surrounding the tumor can also affect the MRI signal. Although a potential source of error in the interpretation of fMRI, this effect has been capitalized on in DTI to distinguish between primary and metastatic brain tumors. In the area of edema surrounding a metastasis, there is an increase in the diffusion of water along white matter tracts, whereas a decrease in diffusion is generally noted in primary brain tumors, presumably owing to their infiltrative nature (99, 100, 139).

DTI may also be used to image the effect of tumor on fiber tracts, as well as to measure early response to therapy in densely cellular tumors (62). FDG-PET and SPECT are commonly used to distinguish radiation necrosis from tumor recurrence in cases in which MRI data was ambiguous (18).

Functional imaging has revealed new information concerning plasticity and suppressed activity in patients with tumors and neurological deficits. Roux et al. (149) have shown recovery of function and of fMRI signal in patients with tumors in the primary motor cortex with preoperative weakness and with no pre- or intraoperative fMRI or ECS activation in the affected cortex.

There will likely be an increased role for functional imaging in the guidance of minimally invasive techniques such as focused ultrasound, laser thermal ablation, stereotactic radiosurgery, and other, emerging techniques in patients with brain tumors.

### Vascular

Location within eloquent cortex is an unfavorable prognostic factor for the surgical resection of arteriovenous malformations (AVMs) (165). However, because AVMs are congenital lesions and in view of the plasticity of the developing and even adult brain, eloquent cortex may not reside in the expected position owing to reorganization of functional areas during embryonic development or as a consequence of hemorrhage or steal in the adult (178, 179). Functional imaging is, therefore, particularly helpful and has been described by several groups in planning therapies in these patients (8, 20, 102). Shimamura et al. (162) have recently reported the use of preoperative MEG to localize the central sulcus in patients with AVMs residing near the motor cortex. They describe two cases of displacement of the functional central sulcus from the expected anatomic location in patients with peri-Rolandic AVMs, presumably demonstrating plasticity related to these congenital

lesions. This is important in the selection of surgical versus expectant management or radiosurgical treatment options. Cannestra et al. (20) have used fMRI and Wada testing to identify those patients with dominant hemisphere pre-Sylvian AVMs who are suitable for surgery with intraoperative ECS and optical imaging.

Many types of abnormal blood flow may be associated with AVMs, including altered vasoreactivity, steal, and shunting (102). For this reason, BOLD fMRI data, which depend on alterations in cerebral blood flow associated with neuronal activity, must be interpreted with caution in these patients. Indeed, Lehericy et al. (92) have demonstrated cases of incorrect language lateralization on fMRI in patients with dominant hemispheric AVMs residing near language areas. Functional imaging studies have also been reported in the preoperative planning of resections of cavernous malformations (31, 113).

### Epilepsy

In patients with severe or medically intractable epilepsy, surgical resection of the epileptogenic focus may represent the best treatment option (184). Distinct from resections of tumors or vascular lesions, in epilepsy surgery, functional imaging is sometimes used for the localization of the lesion itself, in addition to lateralization and localization of critical functions.

Seizure foci may be localized during seizure activity (ictal imaging), between seizures (inter-ictal imaging), or both. These areas tend to be hyperactive and hyperperfused during a seizure and hypoactive and hypoperfused when compared with normal brain between seizures. Traditionally, subdural grids and strips in combination with depth electrodes have been used to localize seizure foci based on ictal and interictal recordings (70). Intraoperative optical imaging may be used to localize and confirm seizure foci, both ictally and interictally (54). Ictal SPECT (177) and MEG (83) may be used to localize epileptogenic foci non-invasively. Spike triggered fMRI (29, 65, 156, 157), FDG-PET (2, 34, 35, 172) and  $H_{215}^{O}PET$  (171) may be used interictally to localize neocortical seizure foci as well as to lateralize MTL seizure foci.

MEG scans are more commonly used for interictal observations. Although the correlation is not universally accepted, several studies have reported good correspondence between MEG recorded interictal spikes and seizure foci. In a series of 11 children with neocortical epilepsy, Minassian et al. (112) reported a strong regional correspondence between the location of MEG identified interictal spikes and ictal activity confirmed by subdural grid electrode recordings. Wheless et al. (183) compared the accuracy of MEG for locating seizure activity with MRI scans, scalp video EEG, and interictal and ictal subdural grid electrode recording, as determined by each method's ability to predict the clinical success of surgical resection. They found that MEG was second only to ictal intracranial recordings in predicting a positive surgical outcome but made no direct comparison between the anatomic location of seizure foci determined by each method. Mamelak et al. (103) compared MEG interictal data with intracranial electrode monitoring in 23 epilepsy patients. They found that MEG accurately localized

seizure foci to the correct lobe and was, thereby, useful in guiding the placement of subdural electrodes, particularly in neocortical epilepsy.

The critical function of greatest concern in patients with medial temporal lobe (MTL) epilepsy is the encoding and retrieval of memory. For these patients, preoperative functional imaging may be particularly helpful for assessing risk of memory deficit, as the structures of the medial temporal lobe, including the hippocampus, amygdala and parahippocampal cortices, are substrates for memory formation (138). This is illustrated by the dense anterograde amnesia observed in a now famous patient after bilateral medial temporal lobectomy for intractable epilepsy (160). Lateralization and localization of MTL activation varies depending on the modality (verbal versus nonverbal) and the stage (encoding versus retrieval) of memory task tested (47, 138). Wada testing is the current gold standard used to screen candidates for anterior temporal lobectomy at risk of postoperative amnesia. The limitations of Wada testing of memory include cost, invasiveness, and perfusion of part of the MTL by the posterior circulation, and are discussed above. fMRI is increasingly used to lateralize memory function in candidates for anterior temporal lobectomy. A number of studies have compared Wada testing to fMRI in these patients (138). In general, patients with MTL epilepsy show greater activation of the contralateral MTL during memory testing (48, 75, 146), and excellent agreement exists in memory lateralization between Wada and fMRI testing in the same patient (30, 48). Unfortunately, fMRI is subject to geometric distortion as well as loss of signal in this region, particularly in the anterior MTL (138). It must also be remembered that loss of fMRI signal in a sclerotic MTL may merely reflect loss of tissue, rather than complete relocalization of function (138).

### Other

As functional brain mapping techniques become less invasive, they may be used to investigate increasing numbers of disease processes, as well as to suggest targets for functional neurosurgical interventions to treat these conditions. Roux et al. (152) have described a case of the use of fMRI to guide placement of a chronic motor cortex stimulator for the treatment of phantom limb pain. Casey et al. (22) have used  $H_2^{15}O$  PET to image brain activity in an experimental model of heat allodynia, a kind of neuropathic pain. The authors show altered forebrain activity in this setting compared to perception of normal heat pain. These reports suggest that functional imaging might be used both to better understand the mechanisms, as well as identify potential targets for functional neurosurgical interventions in pathological pain conditions. Other groups have described the use of functional imaging techniques to identify alterations in activity in various brain regions in depression (5, 32, 49, 50) and obsessive compulsive disorder (174, 176). Again, research of this type may eventually identify targets for functional neurosurgical interventions for a wide variety of disorders.

### Future Directions

As illustrated in *Table 1*, current functional brain mapping techniques suffer from limitations in either temporal or spatial resolution, or are highly invasive. It follows that resolution and quality of data can be improved by integrating, or coregistering, data from multiple complimentary sources (26).

Improved integration of functional data with conventional imaging data and neuronavigation systems is also needed (129, 153). Although pre- and intraoperative coregistration of data from multiple functional mapping techniques has yet to find its way into mainstream use, an increasing number of studies suggesting its utility may be found in the literature. For instance, Roessler et al. (148) recently used 3-Tesla fMRI and ECS to maximize resection of gliomas in motor cortex with no permanent morbidity. Cannestra et al. (20) have combined preoperative fMRI and Wada testing with intraoperative ECS and optical imaging in the selection of treatment and preoperative planning in patients with dominant pre-Sylvian AVMs. Krishnan et al. (90) describe the use of neuronavigation-integrated fMRI, combined with intraoperative ECS, to predict and minimize risk of new postoperative neurological deficit in resection of tumors near motor cortex. Two recent studies describe the use of neuronavigation-integrated fMRI together with intraoperative cortical mapping to improve the accuracy of placement of epidural chronic motor cortex stimulation for intractable neuropathic pain (46, 135).

A problem common to the intraoperative use of preoperative mapping techniques is the failure to take into account brain shift after the opening of the craniotomy flap and dura. Shifts of up to 24 mm at the cortical surface have been described (60). Causes of brain shift include patient positioning and gravity, edema, administration of osmotic diuretics, drainage of CSF, retraction, and resection (23, 59, 60, 117, 137). Furthermore, investigations of brain shift have revealed that displacement of the cortical surface and of deeper structures are uncorrelated (60, 143). Because of this, and because of the heterogeneity among lesions encountered in the operating room, intraoperative MRI is necessary to address this problem by providing images of the brain during surgery (55). Recently, multiple groups have put forward algorithms to update neuronavigation systems with intraoperative MRI images after brain shift (23, 60). Imaging or modeling intraoperative brain shift and applying these transformations to preoperative functional datasets will allow more accurate intraoperative information to be available to the surgeon.

In addition to adjusting preoperatively acquired images to compensate for brain shift, future prospects will include the intraoperative acquisition of functional data, such as intraoperative DTI and fMRI. Nimsy et al. (120) have demonstrated the feasibility of intraoperative DTI to assess shift of white matter tracts. By comparing DTI data acquired pre- and intraoperatively, the authors describe variable and sometimes marked shifting (8 mm inward–15 mm outward) of white matter tracts during the resection of adjacent mass lesions (120, 121). Schulder et al. (159) have described the use of low-field intra-

**TABLE 1. Functional brain mapping techniques\***

Technique	Basis	Spatial resolution	Temporal resolution	Invasiveness	Applications
PET	Perfusion, metabolism	≥4 mm	Several seconds	++	Identification of seizure foci
fMRI	Perfusion	2–5 mm	Several seconds	+	Localization of language and memory; localization of motor, sensory areas; identification of seizure foci
DTI	Restricted water diffusion	<1 mm <sup>3</sup>	N/A	+	Localization of WM tracts; assessment of integrity of WM tracts
Scalp EEG	Electrical potentials	Poor	Milliseconds	+	Lateralization of seizure foci
Intracranial EEG	Electrical potentials	Poor	Milliseconds	++++	Localization of seizure foci for resection
MEG	Magnetic potentials	Poor	Milliseconds	+	Localization of seizure foci, localization of motor, language cortex, emerging applications
IIOS	Intrinsic optical signals	Excellent	Milliseconds	++++	Intraoperative motor and sensory mapping
IAT	Reversible anesthesia	Usually hemispheric	N/A	+++	Lateralization of language and memory
ECS	Direct electrical stimulation	Excellent	Instantaneous	++++	Intraoperative motor, sensory and language mapping
TMS	Applied magnetic stimulation	Medium	Milliseconds to seconds	+ to ++	Localization of motor areas, emerging applications

\* PET, positron emission tomography; fMRI, functional magnetic resonance imaging; DTI, diffusion tensor imaging; N/A, not applicable; WM, white matter; EEG, electroencephalography; MEG, magnetoencephalography; IIOS, imaging of intrinsic optical signals; IAT, intracarotid amyltal test; ECS, electrocortical stimulation testing; TMS, transcranial magnetic stimulation.

operative fMRI of the motor cortex. Intraoperative fMRI would be facilitated by the use of high field strength systems (>1.5 T) (118). Gasser et al. (44) have demonstrated the feasibility of high field intraoperative fMRI. The authors used peripheral sensory stimulation and measured fMRI activation of sensory cortex, which was verified with phase reversal of SSEPs.

New minimally invasive functional imaging techniques such as functional transcranial Doppler ultrasound imaging (fTCDs) are finding increasing use in preoperative planning. Rihs et al. (147) have recently validated fTCDs for determination of language lateralization against Wada testing and have demonstrated the utility of fTCDs when patients may be unable to undergo Wada testing. fTCDs have also been used to map areas involved in visual (1) and auditory (104) perception. Studies comparing the reliability of less invasive methods with that of the more invasive gold standard techniques will pave the way for increasingly noninvasive testing. As fMRI has revealed, non-invasive studies carry the advantage of applicability to more patient populations, including children, repeatability during a session, repeatability over the patient’s clinical course, and whole-brain coverage. In addition, the ability to prepare preoperative, non-invasive functional brain maps will be particularly important as more minimally invasive treatments are developed.

Functional imaging may also find use in monitoring the response of tumors to treatment. Henson et al. (62) have suggested that the use of BOLD fMRI to measure oxygen levels

within tumors (68) could be used in monitoring the efficacy of agents that increase deoxyribonucleic acid damage from chemotherapy or radiation, and are currently investigating this in animal models (67).

### CONCLUSIONS

Functional imaging is playing an increasing role in neurosurgical planning. The use of newer, less invasive techniques has enabled the assessment of more brain areas in individual patients, as well as the imaging of many functions in healthy subjects. One theme emerging from these more recent studies is that of plasticity, both of the developing brain, best illustrated by the relocation of functions in patients with AVMs, and the adult brain, best seen in patients with slowly progressive lesions or during recovery. The combination of functional imaging with conventional imaging, image-guidance, and intraoperative imaging systems will lead to our ability to perform more complete and precise resections of lesions while preserving neurological functions. Functional brain mapping stands to eventually change the way intracranial processes are treated by creating a road map of brain function that not only defines eloquent “no-go” areas but also illuminates potential functional targets. Such a non-invasively obtained road map will be critical to the development of minimally invasive therapies.

## REFERENCES

1. Aaslid R: Visually evoked dynamic blood flow response of the human cerebral circulation. *Stroke* 18:771-775, 1987.
2. Abou-Khalil BW, Siegel GJ, Sackellares JC, Gilman S, Hichwa R, Marshall R: Positron emission tomography studies of cerebral glucose metabolism in chronic partial epilepsy. *Ann Neurol* 22:480-486, 1987.
3. Achten E, Jackson GD, Cameron JA, Abbott DF, Stella DL, Fabinyi GC: Presurgical evaluation of the motor hand area with functional MR imaging in patients with tumors and dysplastic lesions. *Radiology* 210:529-538, 1999.
4. Aldenkamp AP, Boon PA, Deblaere K, Achten E, Backes WH, Boon P, Hofman P, Troost J, Vandemaële P, Vermeulen J, Vonck K, Wilmink J: Usefulness of language and memory testing during intracarotid amobarbital testing: observations from an fMRI study. *Acta Neurol Scand* 108:147-152, 2003.
5. Anand A, Li Y, Wang Y, Wu J, Gao S, Bukhari L, Mathews VP, Kalnin A, Lowe MJ: Activity and connectivity of brain mood regulating circuit in depression: A functional magnetic resonance study. *Biol Psychiatry* 57:1079-1088, 2005.
6. Bandettini PA, Wong EC, Hinks RS, Tikhonov RS, Hyde JS: Time course EPI of human brain function during task activation. *Magn Reson Med* 25:390-397, 1992.
7. Barker AT, Jalinous R, Freeston IL: Non-invasive magnetic stimulation of human motor cortex. *Lancet* 1:1106-1107, 1985.
8. Baumann SB, Noll DC, Kondziolka DS, Schneider W, Nichols TE, Mintun MA, Lewine JD, Yonas H, Orrison WW Jr, Scabassi RJ: Comparison of functional magnetic resonance imaging with positron emission tomography and magnetoencephalography to identify the motor cortex in a patient with an arteriovenous malformation. *J Image Guid Surg* 1:191-197, 1995.
9. Bellgowan PS, Binder JR, Swanson SJ, Hammeke TA, Springer JA, Frost JA, Mueller WM, Morris GL: Side of seizure focus predicts left medial temporal lobe activation during verbal encoding. *Neurology* 51:479-484, 1998.
10. Benbadis SR, Binder JR, Swanson SJ, Fischer M, Hammeke TA, Morris GL, Frost JA, Springer JA: Is speech arrest during wada testing a valid method for determining hemispheric representation of language? *Brain Lang* 65:441-446, 1998.
11. Berger MS, Deliganis AV, Dobbins J, Keles GE: The effect of extent of resection on recurrence in patients with low grade cerebral hemisphere gliomas. *Cancer* 74:1784-1791, 1994 (comment).
12. Berger MS, Kincaid J, Ojemann GA, Lettich E: Brain mapping techniques to maximize resection, safety, and seizure control in children with brain tumors. *Neurosurgery* 25:786-792, 1989.
13. Berman JJ, Berger MS, Mukherjee P, Henry RG: Diffusion-tensor imaging-guided tracking of fibers of the pyramidal tract combined with intraoperative cortical stimulation mapping in patients with gliomas. *J Neurosurg* 101:66-72, 2004.
14. Binder J, Bellgowan P, Frost J, Hammeke T, Springer J, Rao S, Prieto T, O'Reilly W, Cox R: Functional MRI demonstrates left medial temporal lobe activation during verbal episodic memory encoding. *Neuroimage* 3:S530, 1996.
15. Binder JR, Swanson SJ, Hammeke TA, Morris GL, Mueller WM, Fischer M, Benbadis S, Frost JA, Rao SM, Haughton VM: Determination of language dominance using functional MRI: A comparison with the Wada test. *Neurology* 46:978-984, 1996.
16. Bogomolny DL, Petrovich NM, Hou BL, Peck KK, Kim MJ, Holodny AI: Functional MRI in the brain tumor patient. *Top Magn Reson Imaging* 15:325-335, 2004.
17. Brassel F, Weissenborn K, Ruckert N, Hussein S, Becker H: Superselective intra-arterial amytal (Wada test) in temporal lobe epilepsy: basics for neuro-radiological investigations. *Neuroradiology* 38:417-421, 1996.
18. Buchpiguel CA, Alavi JB, Alavi A, Kenyon LC: PET versus SPECT in distinguishing radiation necrosis from tumor recurrence in the brain. *J Nucl Med* 36:159-164, 1995.
19. Calautti C, Leroy F, Guincestre JY, Marie RM, Baron JC: Sequential activation brain mapping after subcortical stroke: Changes in hemispheric balance and recovery. *Neuroreport* 12:3883-3886, 2001.
20. Carnestra AF, Pouratian N, Forage J, Bookheimer SY, Martin NA, Toga AW: Functional magnetic resonance imaging and optical imaging for dominant-hemisphere perisylvian arteriovenous malformations. *Neurosurgery* 55: 804-814, 2004.
21. Carpentier A, Pugh KR, Westerveld M, Studholme C, Skrinjar O, Thompson JL, Spencer DD, Constable RT: Functional MRI of language processing: Dependence on input modality and temporal lobe epilepsy. *Epilepsia* 42:1241-1254, 2001.
22. Casey KL, Lorenz J, Minoshima S: Insights into the pathophysiology of neuropathic pain through functional brain imaging. *Exp Neurol* 184 [Suppl 1]:S80-S88, 2003.
23. Clatz O, Delingette H, Talos IF, Golby AJ, Kikinis R, Jolesz FA, Ayache N, Warfield SK: Robust nonrigid registration to capture brain shift from intra-operative MRI. *IEEE Trans Med Imaging* 24:1417-1427, 2005.
24. Claus EB, Horlacher A, Hsu L, Schwartz RB, Dello-Iacono D, Talos F, Jolesz FA, Black PM: Survival rates in patients with low-grade glioma after intra-operative magnetic resonance image guidance. *Cancer* 103:1227-1233, 2005.
25. Cosgrove GR, Buchbinder BR, Jiang H: Functional magnetic resonance imaging for intracranial navigation. *Neurosurg Clin N Am* 7:313-322, 1996.
26. Dale AM, Halgren E: Spatiotemporal mapping of brain activity by integration of multiple imaging modalities. *Curr Opin Neurobiol* 11:202-208, 2001.
27. Desmond JE, Sum JM, Wagner AD, Demb JB, Shear PK, Glover GH, Gabrieli JD, Morrell MJ: Functional MRI measurement of language lateralization in Wada-tested patients. *Brain* 118:1411-1419, 1995.
28. Detre JA: fMRI: Applications in epilepsy. *Epilepsia* 45 [Suppl 4]:26-31, 2004.
29. Detre JA, Alsop DC, Aguirre GK, Sperling MR: Coupling of cortical and thalamic ictal activity in human partial epilepsy: Demonstration by functional magnetic resonance imaging. *Epilepsia* 37:657-661, 1996.
30. Detre JA, Maccotta L, King D, Alsop DC, Glosser G, D'Esposito M, Zarahn E, Aguirre GK, French JA: Functional MRI lateralization of memory in temporal lobe epilepsy. *Neurology* 50:926-932, 1998.
31. Duffau H, Fontaine D: Successful resection of a left insular cavernous angioma using neuronavigation and intraoperative language mapping. *Acta Neurochir (Wien)* 147:205-208, 2005.
32. Ebert D, Ebmeier KP: The role of the cingulate gyrus in depression: From functional anatomy to neurochemistry. *Biol Psychiatry* 39:1044-1050, 1996.
33. Engel AK, Moll CK, Fried I, Ojemann GA: Invasive recordings from the human brain: clinical insights and beyond. *Nat Rev Neurosci* 6:35-47, 2005.
34. Engel J Jr, Brown WJ, Kuhl DE, Phelps ME, Mazziotta JC, Crandall PH: Pathological findings underlying focal temporal lobe hypometabolism in partial epilepsy. *Ann Neurol* 12:518-528, 1982.
35. Engel J Jr, Kuhl DE, Phelps ME, Crandall PH: Comparative localization of epileptic foci in partial epilepsy by PCT and EEG. *Ann Neurol* 12:529-537, 1982.
36. Epstein CM, Woodard JL, Stringer AY, Bakay RA, Henry TR, Pennell PB, Litt B: Repetitive transcranial magnetic stimulation does not replicate the Wada test. *Neurology* 55:1025-1027, 2000.
37. Fagaly R: Neuromagnetic instrumentation, in Sato S (ed): *Advances in Neurology: Magnetoencephalography*. New York, Raven Press, 1990, pp 11-32.
38. Fernandez G, Specht K, Weis S, Tendolkar I, Reuber M, Fell J, Klaver P, Ruhlman J, Reul J, Elger CE: Intrasubject reproducibility of presurgical language lateralization and mapping using fMRI. *Neurology* 60:969-975, 2003.
39. Fox PT, Raichle ME: Focal physiological uncoupling of cerebral blood flow and oxidative metabolism during somatosensory stimulation in human subjects. *Proc Natl Acad Sci U S A* 83:1140-1144, 1986.
40. Frostig RD, Lieke EE, Ts'o DY, Grinvald A: Cortical functional architecture and local coupling between neuronal activity and the microcirculation revealed by in vivo high-resolution optical imaging of intrinsic signals. *Proc Natl Acad Sci U S A* 87:6082-6086, 1990.
41. Gaillard WD, Balsamo L, Xu B, Grandin CB, Branietki SH, Papero PH, Weinstein S, Conry J, Pearl PL, Sachs B, Sato S, Jabbari B, Vezina LG, Frattali C, Theodore WH: Language dominance in partial epilepsy patients identified with an fMRI reading task. *Neurology* 59:256-265, 2002 (comment).
42. Gallen CC, Bucholz R, Sobel DF: Intracranial neurosurgery guided by functional imaging. *Surg Neurol* 42:523-530, 1994.
43. Gallen CC, Schwartz BJ, Bucholz RD, Malik G, Barkley GL, Smith J, Tung H, Copeland B, Bruno L, Assam S, Hirschkoef E, Bloom F: Presurgical localization of functional cortex using magnetic source imaging. *J Neurosurg* 82:988-994, 1995.
44. Gasser T, Ganslandt O, Sandalcioglu E, Stolke D, Fahlbusch R, Nimsky C: Intraoperative functional MRI: Implementation and preliminary experience. *Neuroimage* 26:685-693, 2005.

45. Gati JS, Menon RS, Ugurbil K, Rutt BK: Experimental determination of the BOLD field strength dependence in vessels and tissue. *Magn Reson Med* 38:296-302, 1997.
46. Gharabaghi A, Hellwig D, Rosahl SK, Shahidi R, Schrader C, Freund HJ, Samii M: Volumetric image guidance for motor cortex stimulation: Integration of three-dimensional cortical anatomy and functional imaging. *Neurosurgery* 57 [Suppl 1]:114-120, 2005.
47. Golby AJ, Poldrack RA, Brewer JB, Spencer D, Desmond JE, Aron AP, Gabrieli JD: Material-specific lateralization in the medial temporal lobe and prefrontal cortex during memory encoding. *Brain* 124:1841-1854, 2001.
48. Golby AJ, Poldrack RA, Illes J, Chen D, Desmond JE, Gabrieli JD: Memory lateralization in medial temporal lobe epilepsy assessed by functional MRI. *Epilepsia* 43:855-863, 2002.
49. Goldapple K, Segal Z, Garson C, Lau M, Bieling P, Kennedy S, Mayberg H: Modulation of cortical-limbic pathways in major depression: Treatment-specific effects of cognitive behavior therapy. *Arch Gen Psychiatry* 61:34-41, 2004.
50. Goodwin GM: Functional imaging, affective disorder and dementia. *Br Med Bull* 52:495-512, 1996.
51. Gore JC: Principles and practice of functional MRI of the human brain. *J Clin Invest* 112:4-9, 2003.
52. Grinvald A, Lieke E, Frostig RD, Gilbert CD, Wiesel TN: Functional architecture of cortex revealed by optical imaging of intrinsic signals. *Nature* 324:361-364, 1986.
53. Haglund MM, Berger MS, Shamseldin M, Lettich E, Ojemann GA: Cortical localization of temporal lobe language sites in patients with gliomas. *Neurosurgery* 34:567-576, 1994.
54. Haglund MM, Hochman DW: Optical imaging of epileptiform activity in human neocortex. *Epilepsia* 45 [Suppl 4]:43-47, 2004.
55. Hall WA, Liu H, Martin AJ, Pozza CH, Maxwell RE, Truwit CL: Safety, efficacy, and functionality of high-field strength interventional magnetic resonance imaging for neurosurgery. *Neurosurgery* 46:632-642, 2000.
56. Hall WA, Liu H, Truwit CL: Functional magnetic resonance imaging-guided resection of low-grade gliomas. *Surg Neurol* 64:20-27, 2005.
57. Hamer H, Morris H: Indications for invasive video-electroencephalographic monitoring, in Lucers HO, Comair YG (eds): *Epilepsy Surgery*. Philadelphia, Lippincott Williams & Wilkins, 2001, pp 559-566.
58. Hankey GJ, Warlow CP, Sellar RJ: Cerebral angiographic risk in mild cerebrovascular disease. *Stroke* 21:209-222, 1990.
59. Hartkens T, Hill DL, Castellano-Smith AD, Hawkes DJ, Maurer CR Jr, Martin AJ, Hall WA, Liu H, Truwit CL: Measurement and analysis of brain deformation during neurosurgery. *IEEE Trans Med Imaging* 22:82-92, 2003.
60. Hastreiter P, Rezk-Salama C, Soza G, Bauer M, Greiner G, Fahlbusch R, Ganslandt O, Nimsky C: Strategies for brain shift evaluation. *Med Image Anal* 8:447-464, 2004.
61. Heeger DJ, Huk AC, Geisler WS, Albrecht DG: Spikes versus BOLD: What does neuroimaging tell us about neuronal activity? *Nat Neurosci* 3:631-633, 2000 (comment).
62. Henson JW, Gaviani P, Gonzalez RG: MRI in treatment of adult gliomas. *Lancet Oncol* 6:167-175, 2005.
63. Hirsch J, Ruge MI, Kim KH, Correa DD, Victor JD, Relkin NR, Labar DR, Krol G, Bilsky MH, Souweidane MM, DeAngelis LM, Gutin PH: An integrated functional magnetic resonance imaging procedure for preoperative mapping of cortical areas associated with tactile, motor, language, and visual functions. *Neurosurgery* 47:711-722, 2000.
64. Deleted in proof.
65. Hoffmann A, Jager L, Werhahn KJ, Jaschke M, Noachter S, Reiser M: Electroencephalography during functional echo-planar imaging: Detection of epileptic spikes using post-processing methods. *Magn Reson Med* 44:791-798, 2000.
66. Hoshino T, Sakatani K, Katayama Y, Fujiwara N, Murata Y, Kobayashi K, Fukaya C, Yamamoto T: Application of multichannel near-infrared spectroscopic topography to physiological monitoring of the cortex during cortical mapping: Technical case report. *Surg Neurol* 64:272-275, 2005.
67. Hou H, Khan N, O'Hara JA, Grinberg OY, Dunn JE, Abajian MA, Wilmot CM, Makki M, Demidenko E, Lu S, Steffen RP, Swartz HM: Effect of RSR13, an allosteric hemoglobin modifier, on oxygenation in murine tumors: An *in vivo* electron paramagnetic resonance oximetry and bold MRI study. *Int J Radiat Oncol Biol Phys* 59:834-843, 2004.
68. Hsu YY, Chang CN, Jung SM, Lim KE, Huang JC, Fang SY, Liu HL: Blood oxygenation level-dependent MRI of cerebral gliomas during breath holding. *J Magn Reson Imaging* 19:160-167, 2004.
69. Hunsche S, Moseley ME, Stoeter P, Hedehus M: Diffusion-tensor MR imaging at 1.5 and 3.0 T: Initial observations. *Radiology* 221:550-556, 2001.
70. Ikeda A, Miyamoto S, Shibusaki H: Cortical motor mapping in epilepsy patients: Information from subdural electrodes in presurgical evaluation. *Epilepsia* 43 [Suppl 9]:56-60, 2002.
71. Janszky J, Jokeit H, Kontopoulou K, Mertens M, Ebner A, Pohlmann-Eden B, Woermann FG: Functional MRI predicts memory performance after right mesiotemporal epilepsy surgery. *Epilepsia* 46:244-250, 2005.
72. Janszky J, Ollech I, Jokeit H, Kontopoulou K, Mertens M, Pohlmann-Eden B, Ebner A, Woermann FG: Epileptic activity influences the lateralization of mesiotemporal fMRI activity. *Neurology* 63:1813-1817, 2004.
73. Jellison BJ, Field AS, Medow J, Lazar M, Salamat MS, Alexander AL: Diffusion tensor imaging of cerebral white matter: A pictorial review of physics, fiber tract anatomy, and tumor imaging patterns. *AJNR Am J Neuroradiol* 25:356-369, 2004.
74. Jennum P, Friberg L, Fuglsang-Frederiksen A, Dam M: Speech localization using repetitive transcranial magnetic stimulation. *Neurology* 44:269-273, 1994.
75. Jokeit H, Okujava M, Woermann FG: Memory fMRI lateralizes temporal lobe epilepsy. *Neurology* 57:1786-1793, 2001.
76. Kamada K, Houkin K, Takeuchi F, Ishii N, Ikeda J, Sawamura Y, Kuriki S, Kawaguchi H, Iwasaki Y: Visualization of the eloquent motor system by integration of MEG, functional, and anisotropic diffusion-weighted MRI in functional neuronavigation. *Surg Neurol* 59:352-362, 2003.
77. Kamada K, Takeuchi F, Kuriki S, Oshiro O, Houkin K, Abe H: Functional neurosurgical simulation with brain surface magnetic resonance images and magnetoencephalography. *Neurosurgery* 33:269-273, 1993.
78. Keles GE, Anderson B, Berger MS: The effect of extent of resection on time to tumor progression and survival in patients with glioblastoma multiforme of the cerebral hemisphere. *Surg Neurol* 52:371-379, 1999.
79. Keles GE, Lamborn KR, Berger MS: Low-grade hemispheric gliomas in adults: A critical review of extent of resection as a factor influencing outcome. *J Neurosurg* 95:735-745, 2001 (comment).
80. Keles GE, Lundin DA, Lamborn KR, Chang EF, Ojemann G, Berger MS: Intraoperative subcortical stimulation mapping for hemispherical perirolandic gliomas located within or adjacent to the descending motor pathways: Evaluation of morbidity and assessment of functional outcome in 294 patients. *J Neurosurg* 100:369-375, 2004 (comment).
81. Kim DS, Garwood M: High-field magnetic resonance techniques for brain research. *Curr Opin Neurobiol* 13:612-619, 2003.
82. Knecht S, Fieol A, Drager B, Breitenstein C, Sommer J, Henningsen H, Ringelstein EB, Pascual-Leone A: Degree of language lateralization determines susceptibility to unilateral brain lesions. *Nat Neurosci* 5:695-699, 2002 (comment).
83. Knowlton RC, Shih J: Magnetoencephalography in epilepsy. *Epilepsia* 45 [Suppl 4]:61-71, 2004.
84. Kombos T, Suess O, Funk T, Kern BC, Brock M: Intra-operative mapping of the motor cortex during surgery in and around the motor cortex. *Acta Neurochir (Wien)* 142:263-268, 2000.
85. Kombos T, Suess O, Kern BC, Funk T, Hoell T, Kopetsch O, Brock M: Comparison between monopolar and bipolar electrical stimulation of the motor cortex. *Acta Neurochir (Wien)* 141:1295-1301, 1999.
86. Krings T, Buchbinder BR, Butler WE, Chiappa KH, Jiang HJ, Rosen BR, Cosgrove GR: Stereotactic transcranial magnetic stimulation: Correlation with direct electrical cortical stimulation. *Neurosurgery* 41:1319-1326, 1997.
87. Krings T, Reinges MH, Erberich S, Kemeny S, Rohde V, Spetzger U, Korinth M, Willmes K, Gilsbach JM, Thron A: Functional MRI for presurgical planning: Problems, artefacts, and solution strategies. *J Neurol Neurosurg Psychiatry* 70:749-760, 2001.
88. Krings T, Schreckenberger M, Rohde V, Foltys H, Spetzger U, Sabri O, Reinges MH, Kemeny S, Meyer PT, Moller-Hartmann W, Korinth M, Gilsbach JM, Buell U, Thron A: Metabolic and electrophysiological validation of functional MRI. *J Neurol Neurosurg Psychiatry* 71:762-771, 2001.

89. Krings T, Topper R, Willmes K, Reinges MH, Gilsbach JM, Thron A: Activation in primary and secondary motor areas in patients with CNS neoplasms and weakness. *Neurology* 58:381-390, 2002.
90. Krishnan R, Raabe A, Hattingen E, Szelenyi A, Yahya H, Hermann E, Zimmermann M, Seifert V: Functional magnetic resonance imaging-integrated neuronavigation: Correlation between lesion-to-motor cortex distance and outcome. *Neurosurgery* 55:904-915, 2004.
91. Lacroix M, Abi-Said D, Fourney DR, Gokaslan ZL, Shi W, DeMonte F, Lang FF, McCutcheon IE, Hassenbusch SJ, Holland E, Hess K, Michael C, Miller D, Sawaya R: A multivariate analysis of 416 patients with glioblastoma multiforme: Prognosis, extent of resection, and survival. *J Neurosurg* 95:190-198, 2001 (comment).
92. Lehericy S, Biondi A, Sourour N, Vlaicu M, du Montcel ST, Cohen L, Vivas E, Capelle L, Faillot T, Casasco A, Le Bihan D, Marsault C: Arteriovenous brain malformations: Is functional MR imaging reliable for studying language reorganization in patients? Initial observations. *Radiology* 223:672-682, 2002.
93. Lehericy S, Cohen L, Bazin B, Samson S, Giacomini E, Rougetet R, Hertz-Pannier L, Le Bihan D, Marsault C, Baulac M: Functional MR evaluation of temporal and frontal language dominance compared with the Wada test. *Neurology* 54:1625-1633, 2000.
94. Lin FH, Huang TY, Chen NK, Wang FN, Stufflebeam SM, Belliveau JW, Wald LL, Kwong KK: Functional MRI using regularized parallel imaging acquisition. *Magn Reson Med* 54:343-353, 2005.
95. Liu WC, Feldman SC, Schulder M, Kalnin AJ, Holodny AI, Zimmerman A, Sinensky R, Rao S: The effect of tumour type and distance on activation in the motor cortex. *Neuroradiology* 47:813-819, 2005.
96. Lo SS, Cho KH, Hall WA, Hernandez WL, Kossow RJ, Lee CK, Clark HB: Does the extent of surgery have an impact on the survival of patients who receive postoperative radiation therapy for supratentorial low-grade gliomas? *Int J Cancer* 96 [Suppl]:71-78, 2001.
97. Logothetis NK, Pauls J, Augath M, Trinath T, Oeltermann A: Neurophysiological investigation of the basis of the fMRI signal. *Nature* 412:150-157, 2001 (comment).
98. Loring DW, Murro AM, Meador KJ, Lee GP, Gratton CA, Nichols ME, Gallagher BB, King DW, Smith JR: Wada memory testing and hippocampal volume measurements in the evaluation for temporal lobectomy. *Neurology* 43:1789-1793, 1993 (comment).
99. Lu S, Ahn D, Johnson G, Cha S: Peritumoral diffusion tensor imaging of high-grade gliomas and metastatic brain tumors. *AJNR Am J Neuroradiol* 24:937-941, 2003.
100. Lu S, Ahn D, Johnson G, Law M, Zagzag D, Grossman RI: Diffusion-tensor MR imaging of intracranial neoplasia and associated peritumoral edema: Introduction of the tumor infiltration index. *Radiology* 232:221-228, 2004.
101. Majos A, Tybor K, Stefanczyk L, Goraj B: Cortical mapping by functional magnetic resonance imaging in patients with brain tumors. *Eur Radiol* 15:1148-1158, 2005.
102. Maldjian J, Atlas SW, Howard RS 2nd, Greenstein E, Alsop D, Detre JA, Listerud J, D'Esposito M, Flamm ES: Functional magnetic resonance imaging of regional brain activity in patients with intracerebral arteriovenous malformations before surgical or endovascular therapy. *J Neurosurg* 84:477-483, 1996 (comment).
103. Mamelak AN, Lopez N, Akhtari M, Sutherling WW: Magnetoencephalography-directed surgery in patients with neocortical epilepsy. *J Neurosurg* 97:865-873, 2002.
104. Matteis M, Silvestrini M, Troisi E, Cupini LM, Caltagirone C: Transcranial doppler assessment of cerebral flow velocity during perception and recognition of melodies. *J Neurol Sci* 149:57-61, 1997.
105. McCormack BM, Miller DC, Budzilovich GN, Voorhees GJ, Ransohoff J: Treatment and survival of low-grade astrocytoma in adults—1977-1988. *Neurosurgery* 31:636-642, 1992.
106. McDonald JD, Chong BW, Lewine JD, Jones G, Burr RB, McDonald PR, Koehler SB, Tsuruda J, Orrison WW, Heilbrun MP: Integration of preoperative and intraoperative functional brain mapping in a frameless stereotactic environment for lesions near eloquent cortex. Technical note. *J Neurosurg* 90:591-598, 1999.
107. Medina LS, Aguirre E, Bernal B, Altman NR: Functional MR imaging versus Wada test for evaluation of language lateralization: Cost analysis. *Radiology* 230:49-54, 2004.
108. Meltzer CC, Zubieta JK, Brandt J, Tune LE, Mayberg HS, Frost JJ: Regional hypometabolism in Alzheimer's disease as measured by positron emission tomography after correction for effects of partial volume averaging. *Neurology* 47:454-461, 1996.
109. Merton PA, Morton HB: Stimulation of the cerebral cortex in the intact human subject. *Nature* 285:227, 1980.
110. Meyer FB, Bates LM, Goerss SJ, Friedman JA, Windschitl WL, Duffy JR, Perkins WJ, O'Neill BP: Awake craniotomy for aggressive resection of primary gliomas located in eloquent brain. *Mayo Clin Proc* 76:677-687, 2001.
111. Milner B, Branch C, Rasmussen T: Study of short-term memory after intracarotid injection of sodium amytal. *Trans Am Neurol Assoc* 87:224-226, 1962.
112. Minassian BA, Otsubo H, Weiss S, Elliott I, Rutka JT, Snead OC 3rd: Magnetoencephalographic localization in pediatric epilepsy surgery: Comparison with invasive intracranial electroencephalography. *Ann Neurol* 46:627-633, 1999.
113. Moller-Hartmann W, Krings T, Coenen VA, Mayfrank L, Weidemann J, Kranzlein H, Thron A: Preoperative assessment of motor cortex and pyramidal tracts in central cavernoma employing functional and diffusion-weighted magnetic resonance imaging. *Surg Neurol* 58:302-308, 2002.
114. Moseley ME, Cohen Y, Kucharczyk J, Mintorovitch J, Asgari HS, Wendland MF, Tsuruda J, Norman D: Diffusion-weighted MR imaging of anisotropic water diffusion in cat central nervous system. *Radiology* 176:439-445, 1990.
115. Mueller WM, Morris GL 3rd: Intraoperative and extraoperative identification of eloquent brain using stimulation mapping. *Neurosurg Clin N Am* 4:217-222, 1993.
116. Neggess SF, Langerak TR, Schutter DJ, Mandl RC, Ramsey NF, Lemmens PJ, Postma A: A stereotactic method for image-guided transcranial magnetic stimulation validated with fMRI and motor-evoked potentials. *Neuroimage* 21:1805-1817, 2004.
117. Nimsky C, Ganslandt O, Cerny S, Hastreiter P, Greiner G, Fahlbusch R: Quantification of, visualization of, and compensation for brain shift using intraoperative magnetic resonance imaging. *Neurosurgery* 47:1070-1080, 2000.
118. Nimsky C, Ganslandt O, Fahlbusch R: Comparing 0.2 tesla with 1.5 tesla intraoperative magnetic resonance imaging analysis of setup, workflow, and efficiency. *Acad Radiol* 12:1065-1079, 2005.
119. Nimsky C, Ganslandt O, Fahlbusch R: Implementation of fiber tract navigation. *Neurosurgery* 58 [Suppl 2]:ONS-292-ONS304, 2006.
120. Nimsky C, Ganslandt O, Hastreiter P, Wang R, Benner T, Sorensen AG, Fahlbusch R: Intraoperative diffusion-tensor MR imaging: Shifting of white matter tracts during neurosurgical procedures—Initial experience. *Radiology* 234:218-225, 2005.
121. Nimsky C, Ganslandt O, Hastreiter P, Wang R, Benner T, Sorensen AG, Fahlbusch R: Preoperative and intraoperative diffusion tensor imaging-based fiber tracking in glioma surgery. *Neurosurgery* 56:130-138, 2005.
122. Nimsky C, Grummich P, Sorensen AG, Fahlbusch R, Ganslandt O: Visualization of the pyramidal tract in glioma surgery by integrating diffusion tensor imaging in functional neuronavigation. *Zentralbl Neurochir* 66:133-141, 2005.
123. O'Donnell L, Westin CF: White matter tract clustering and correspondence in populations. *Med Image Comput Assist Interv Int Conf Med Image Comput Assist Interv* 8:140-147, 2005.
124. Ogawa S, Lee TM, Kay AR, Tank DW: Brain magnetic resonance imaging with contrast dependent on blood oxygenation. *Proc Natl Acad Sci U S A* 87:9868-9872, 1990.
125. Ogawa S, Lee TM, Stepnoski R, Chen W, Zhu XH, Ugurbil K: An approach to probe some neural systems interaction by functional MRI at neural time scale down to milliseconds. *Proc Natl Acad Sci U S A* 97:11026-11031, 2000.
126. Ojemann G, Ojemann J, Lettich E, Berger M: Cortical language localization in left, dominant hemisphere. An electrical stimulation mapping investigation in 117 patients. *J Neurosurg* 71:316-326, 1989.
127. Ojemann JG, Miller JW, Silbergeld DL: Preserved function in brain invaded by tumor. *Neurosurgery* 39:253-259, 1996.
128. Orrison WW Jr: Magnetic source imaging in stereotactic and functional neurosurgery. *Stereotact Funct Neurosurg* 72:89-94, 1999.

129. O'Shea JP, Branco DM, Petrovich N, Knierim K, Golby AJ: Integrated image and function-guided surgery in eloquent cortex: A technique report. *Int J Med Robot Comput Assist Surg* 2:75-83, 2006.
130. Parmar H, Sitoh YY, Yeo TT: Combined magnetic resonance tractography and functional magnetic resonance imaging in evaluation of brain tumors involving the motor system. *J Comput Assist Tomogr* 28:551-556, 2004.
131. Pascual-Leone A, Gates JR, Dhuna A: Induction of speech arrest and counting errors with rapid-rate transcranial magnetic stimulation. *Neurology* 41:697-702, 1991 (comment).
132. Penfield W: The cerebral cortex and consciousness, in *The Harvey Lectures*, Baltimore, Williams & Wilkins Co., 1937, pp 35-69.
133. Pfeuffer J, Adriany G, Shmuel A, Yacoub E, Van De Moortele PF, Hu X, Ugurbil K: Perfusion-based high-resolution functional imaging in the human brain at 7 Tesla. *Magn Reson Med* 47:903-911, 2002.
134. Philippon JH, Clemenceau SH, Fauchon FH, Foncin JF: Supratentorial low-grade astrocytomas in adults. *Neurosurgery* 32:554-559, 1993.
135. Piroette B, Voordecker P, Neugroschl C, Baleriaux D, Wikler D, Metens T, Denolin V, Joffroy A, Massager N, Brotchi J, Levivier M: Combination of functional magnetic resonance imaging-guided neuronavigation and intraoperative cortical brain mapping improves targeting of motor cortex stimulation in neuropathic pain. *Neurosurgery* 56:344-359, 2005.
136. Pizzella V, Romani G: Principles of magnetoencephalography, in Sato S (ed): *Magnetoencephalography*. New York, Raven Press, 1990, pp 1-9.
137. Platenik LA, Miga MI, Roberts DW, Lunn KE, Kennedy FE, Hartov A, Paulsen KD: In vivo quantification of retraction deformation modeling for updated image-guidance during neurosurgery. *IEEE Trans Biomed Eng* 49:823-835, 2002.
138. Powell HW, Koepp MJ, Richardson MP, Symms MR, Thompson PJ, Duncan JS: The application of functional MRI of memory in temporal lobe epilepsy: A clinical review. *Epilepsia* 45:855-863, 2004.
139. Provenzale JM, McGraw P, Mhatre P, Guo AC, Delong D: Peritumoral brain regions in gliomas and meningiomas: Investigation with isotropic diffusion-weighted MR imaging and diffusion-tensor MR imaging. *Radiology* 232:451-460, 2004.
140. Pujol J, Deus J, Losilla JM, Capdevila A: Cerebral lateralization of language in normal left-handed people studied by functional MRI. *Neurology* 52:1038-1043, 1999.
141. Rasmussen T, Milner B: The role of early left-brain injury in determining lateralization of cerebral speech functions. *Ann NY Acad Sci* 299:355-369, 1977.
142. Rees G, Friston K, Koch C: A direct quantitative relationship between the functional properties of human and macaque V5. *Nat Neurosci* 3:716-723, 2000 (comment).
143. Reinges MH, Nguyen HH, Krings T, Hutter BO, Rohde V, Gilsbach JM: Course of brain shift during microsurgical resection of supratentorial cerebral lesions: Limits of conventional neuronavigation. *Acta Neurochir (Wien)* 146:369-377, 2004.
144. Rezai AR, Hund M, Kronberg E, Deletis V, Zonenshayn M, Cappell J, Ribary U, Llinas R, Kelly PJ: Introduction of magnetoencephalography to stereotactic techniques. *Stereotact Funct Neurosurg* 65:37-41, 1995.
145. Rezai AR, Hund M, Kronberg E, Zonenshayn M, Cappell J, Ribary U, Kall B, Llinas R, Kelly PJ: The interactive use of magnetoencephalography in stereotactic image-guided neurosurgery. *Neurosurgery* 39:92-102, 1996.
146. Richardson MP, Strange BA, Duncan JS, Dolan RJ: Preserved verbal memory function in left medial temporal pathology involves reorganisation of function to right medial temporal lobe. *Neuroimage* 20 [Suppl 1]:S112-S119, 2003.
147. Rihs F, Sturzenegger M, Gutbrod K, Schroth G, Mattle HP: Determination of language dominance: Wada test confirms functional transcranial Doppler sonography. *Neurology* 52:1591-1596, 1999.
148. Roessler K, Donat M, Lanzemberger R, Novak K, Geissler A, Gartus A, Tahamtan AR, Milakara D, Czech T, Barth M, Knosp E, Beisteiner R: Evaluation of preoperative high magnetic field motor functional MRI (3 Tesla) in glioma patients by navigated electrocortical stimulation and postoperative outcome. *J Neurol Neurosurg Psychiatry* 76:1152-1157, 2005.
149. Roux FE, Boulanouar K, Ibarrola D, Tremoulet M, Chollet F, Berry I: Functional MRI and intraoperative brain mapping to evaluate brain plasticity in patients with brain tumours and hemiparesis. *J Neurol Neurosurg Psychiatry* 69:453-463, 2000.
150. Roux FE, Boulanouar K, Lotterie JA, Mejdoubi M, LeSage JP, Berry I: Language functional magnetic resonance imaging in preoperative assessment of language areas: Correlation with direct cortical stimulation. *Neurosurgery* 52:1335-1347, 2003.
151. Roux FE, Boulanouar K, Ranjeva JP, Tremoulet M, Henry P, Manelfe C, Sabatier J, Berry I: Usefulness of motor functional MRI correlated to cortical mapping in Rolandic low-grade astrocytomas. *Acta Neurochir (Wien)* 141:71-79, 1999.
152. Roux FE, Ibarrola D, Lazorthes Y, Berry I: Chronic motor cortex stimulation for phantom limb pain: A functional magnetic resonance imaging study: Technical case report. *Neurosurgery* 48:681-688, 2001.
153. Roux FE, Ibarrola D, Tremoulet M, Lazorthes Y, Henry P, Sol JC, Berry I: Methodological and technical issues for integrating functional magnetic resonance imaging data in a neuronavigational system. *Neurosurgery* 49:1145-1157, 2001.
154. Russell SM, Kelly PJ: Incidence and clinical evolution of postoperative deficits after volumetric stereotactic resection of glial neoplasms involving the supplementary motor area. *Neurosurgery* 52:506-516, 2003.
155. Sack AT, Linden DE: Combining transcranial magnetic stimulation and functional imaging in cognitive brain research: Possibilities and limitations. *Brain Res Brain Res Rev* 43:41-56, 2003.
156. Salek-Haddadi A, Friston KJ, Lemieux L, Fish DR: Studying spontaneous EEG activity with fMRI. *Brain Res Brain Res Rev* 43:110-133, 2003.
157. Salek-Haddadi A, Lemieux L, Merschhemke M, Friston KJ, Duncan JS, Fish DR: Functional magnetic resonance imaging of human absence seizures. *Ann Neurol* 53:663-667, 2003.
158. Schreckenberger M, Spetzger U, Sabri O, Meyer PT, Zeggel T, Zimny M, Gilsbach J, Buell U: Localisation of motor areas in brain tumour patients: A comparison of preoperative [18F]FDG-PET and intraoperative cortical electrostimulation. *Eur J Nucl Med* 28:1394-1403, 2001.
159. Schulder M, Azmi H, Biswal B: Functional magnetic resonance imaging in a low-field intraoperative scanner. *Stereotact Funct Neurosurg* 80:125-131, 2003.
160. Scoville WB, Milner B: Loss of recent memory after bilateral hippocampal lesions. *J Neurol Neurosurg Psychiatry* 20:11-21, 1957.
161. Shevelev IA: Functional imaging of the brain by infrared radiation (thermoencephalography). *Prog Neurobiol* 56:269-305, 1998.
162. Shimamura N, Ohkuma H, Ogane K, Manabe H, Yagihashi A, Kikkawa T, Suzuki S: Displacement of central sulcus in cerebral arteriovenous malformation situated in the peri-motor cortex as assessed by magnetoencephalographic study. *Acta Neurochir (Wien)* 146:363-368, 2004.
163. Skirboll SS, Ojemann GA, Berger MS, Lettich E, Winn HR: Functional cortex and subcortical white matter located within gliomas. *Neurosurgery* 38:678-685, 1996.
164. Sodickson DK, Hardy CJ, Zhu Y, Giaquinto RO, Gross P, Kenwood G, Niendorf T, Lejay H, McKenzie CA, Ohliger MA, Grant AK, Rofsky NM: Rapid volumetric MRI using parallel imaging with order-of-magnitude accelerations and a 32-element RF coil array: Feasibility and implications. *Acad Radiol* 12:626-635, 2005.
165. Spetzler RF, Martin NA: A proposed grading system for arteriovenous malformations. *J Neurosurg* 65:476-483, 1986.
166. Springer JA, Binder JR, Hammeke TA, Swanson SJ, Frost JA, Bellgowan PS, Brewer CC, Perry HM, Morris GL, Mueller WM: Language dominance in neurologically normal and epilepsy subjects: A functional MRI study. *Brain* 122:2033-2046, 1999.
167. Suarez RO, O'Shea JP, Whalen S, Golby AJ: Determination of cerebral dominance from vocalized language using region of interest analysis: An MEG and fMRI comparative study. Presented at the 35th Annual Society for Neuroscience Meeting, Washington, DC, November, 2005. (abstr).
168. Sutherling WW, Crandall PH, Darcey TM, Becker DP, Levesque MF, Barth DS: The magnetic and electric fields agree with intracranial localizations of somatosensory cortex. *Neurology* 38:1705-1714, 1988.
169. Szafarski JP, Binder JR, Possing ET, Mckiernan KA, Ward BD, Hammeke TA: Language lateralization in left-handed and ambidextrous people: fMRI data. *Neurology* 59:238-244, 2002.
170. Tai YF, Piccini P: Applications of positron emission tomography (PET) in neurology. *J Neurol Neurosurg Psychiatry* 75:669-676, 2004.

171. Tatlidil R, Xiong J, Luther S: Presurgical lateralization of seizure focus and language dominant hemisphere with O-15 water PET imaging. *Acta Neurol Scand* 102:73-80, 2000.
172. Theodore WH, Sato S, Kufta C, Balish MB, Bromfield EB, Leiderman DB: Temporal lobectomy for uncontrolled seizures: The role of positron emission tomography. *Ann Neurol* 32:789-794, 1992.
173. Tummala RP, Chu RM, Liu H, T T, Hall WA: Application of diffusion tensor imaging to magnetic-resonance-guided brain tumor resection. *Pediatr Neurosurg* 39:39-43, 2003.
174. Ursu S, Stenger VA, Shear MK, Jones MR, Carter CS: Overactive action monitoring in obsessive-compulsive disorder: Evidence from functional magnetic resonance imaging. *Psychol Sci* 14:347-353, 2003.
175. Van Buren J: Complications of surgical procedures in the diagnosis and treatment of epilepsy, in Engel J (ed): *Surgical treatment of the epilepsies*. New York, Raven Press, 1987, pp 465-475.
176. van der Wee NJ, Ramsey NF, Jansma JM, Denys DA, van Megen HJ, Westenberg HM, Kahn RS: Spatial working memory deficits in obsessive compulsive disorder are associated with excessive engagement of the medial frontal cortex. *Neuroimage* 20:2271-2280, 2003.
177. Van Paesschen W: Ictal SPECT. *Epilepsia* 45 [Suppl 4]:35-40, 2004.
178. Vates GE, Lawton MT, Wilson CB, McDermott MW, Halbach VV, Roberts TP, Rowley HA: Magnetic source imaging demonstrates altered cortical distribution of function in patients with arteriovenous malformations. *Neurosurgery* 51:614-627, 2002.
179. Vikingsstad EM, Cao Y, Thomas AJ, Johnson AF, Malik GM, Welch KM: Language hemispheric dominance in patients with congenital lesions of eloquent brain. *Neurosurgery* 47:562-570, 2000.
180. Viñas FC, Zamorano L, Mueller RA, Jiang Z, Chugani H, Fuerst D, Muzik O, Mangner TJ, Diaz FG: [15O]-water PET and intraoperative brain mapping: A comparison in the localization of eloquent cortex. *Neurolog Res* 19:601-608, 1997.
181. Wada J: A new method for determination of the side of cerebral speech dominance: A preliminary report on the intracarotid injection of sodium amyltal in man. *Igaku Seibutsugaku* 14:221-222, 1949.
182. Wada J, Rasmussen T: Intracarotid injection of sodium amyltal for the lateralization of cerebral speech dominance: Experimental and clinical observations. *J Neurosurg* 17:226-282, 1960.
183. Wheless JW, Willmore LJ, Breier JL, Katakai M, Smith JR, King DW, Meador KJ, Park YD, Loring DW, Clifton GL, Baumgartner J, Thomas AB, Constantinou JE, Papanicolaou AC: A comparison of magnetoencephalography, MRI, and V-EEG in patients evaluated for epilepsy surgery. *Epilepsia* 40:931-941, 1999.
184. Wiebe S, Blume WT, Girvin JP, Eliasziw M: Effectiveness and Efficiency of Surgery for Temporal Lobe Epilepsy Study Group: A randomized, controlled trial of surgery for temporal-lobe epilepsy. *N Engl J Med* 345:311-318, 2001 (comment).
185. Wilkinson ID, Romanowski CA, Jellinek DA, Morris J, Griffiths PD: Motor functional MRI for pre-operative and intraoperative neurosurgical guidance. *Br J Radiol* 76:98-103, 2003.
186. Wisoff JH, Boyett JM, Berger MS, Brant C, Li H, Yates AJ, McGuire-Cullen P, Turski PA, Sutton LN, Allen JC, Packer RJ, Finlay JL: Current neurosurgical management and the impact of the extent of resection in the treatment of malignant gliomas of childhood: A report of the Children's Cancer Group trial no. CCG-945. *J Neurosurg* 89:52-59, 1998 (comment).
187. Witwer BP, Mofakhar R, Hasan KM, Deshmukh P, Houghton V, Field A, Arfanakis K, Noyes J, Moritz CH, Meyerand ME, Rowley HA, Alexander AL, Badie B: Diffusion-tensor imaging of white matter tracts in patients with cerebral neoplasm. *J Neurosurg* 97:568-575, 2002.
188. Woermann FG, Jokeit H, Luerding R, Freitag H, Schulz R, Guertler S, Okujava M, Wolf P, Tuxhorn I, Ebner A: Language lateralization by Wada test and fMRI in 100 patients with epilepsy. *Neurology* 61:699-701, 2003.
189. Wood CC, Spencer DD, Allison T, McCarthy G, Williamson PD, Goff WR: Localization of human sensorimotor cortex during surgery by cortical surface recording of somatosensory evoked potentials. *J Neurosurg* 68:99-111, 1988.
190. Yacoub E, Shmuel A, Pfeuffer J, Van De Moortele PF, Adriany G, Andersen P, Vaughan JT, Merkle H, Ugurbil K, Hu X: Imaging brain function in humans at 7 Tesla. *Magn Reson Med* 45:588-594, 2001.
191. Yang X, Hyder F, Shulman RG: Functional MRI BOLD signal coincides with electrical activity in the rat whisker barrels. *Magn Reson Med* 38:874-877, 1997.
192. Yoo SS, Talos IF, Golby AJ, Black PM, Panych LP: Evaluating requirements for spatial resolution of fMRI for neurosurgical planning. *Hum Brain Mapp* 21:34-43, 2004.
193. Yousry TA, Schmid UD, Jassoy AG, Schmidt D, Eisner WE, Reulen HJ, Reiser MF, Lissner J: Topography of the cortical motor hand area: Prospective study with functional MR imaging and direct motor mapping at surgery. *Radiology* 195:23-29, 1995.

**Acknowledgments**

This research was supported by grants to AJG from the National Institutes of Health (K08 NS048063 and U41 RR019703) and the Brain Science Foundation.

**COMMENTS**

Today, the complexity of imaging and neurophysiological techniques are increasingly similar in their application. This review provides a comprehensive and systematic overview of current and available functional brain mapping techniques and their application to neurosurgery. The diverse presentation of not only functional imaging techniques such as functional magnetic resonance imaging, positron emission tomography, and single-photon emission computed tomography, but also of neurophysiological mapping techniques such as electroencephalography, magnetoencephalography, and transcranial magnetic stimulation is very useful because it stresses the strengths and limitations of each of the techniques. The elaborate discussion of these pre-operative mapping techniques and their comparison with intraoperative electrical stimulation applied directly to the cortex is beneficial for judging the value of each technique value and is essential for understanding their complementary application. In specific neurosurgical context, this article is a helpful guide for the application of functional brain mapping techniques.

**Volker Seifert  
Andrea Szelenyi  
Essen, Germany**

Functional brain mapping is an important tool in modern neurosurgery. The sophisticated use of these techniques allows for extended resections without causing additional morbidity. Tharin and Golby provide an excellent overview on the currently available mapping techniques. They distinguish observational techniques, such as positron-emission tomography, functional magnetic resonance imaging, diffusion tensor imaging, electrocorticography, electroencephalography, magnetoencephalography, and optical imaging, as well as inhibition and activation techniques such as intracarotid amobarbital/Wada testing, electrocortical stimulation, and transcranial magnetic stimulation. The application of these techniques, grouped by various functional systems (i.e., motor, language lateralization, language localization), are presented by their use in tumor, vascular, and epilepsy surgery. Registration of the various functional modalities to high resolution, anatomical magnetic resonance datasets opens the possibility to integrate all of these data in a navigational setup, leading to so-called functional neuronavigation.

This functional navigation allows the direct visualization of the mapping results in the surgical field, allowing pre- and intraoperative modalities to be compared easily. This concept of registering data to the standard anatomical image setup is open for further data beyond the standard anatomical and functional imaging. Adding data from magnetic resonance spectroscopy and other molecular imaging modalities



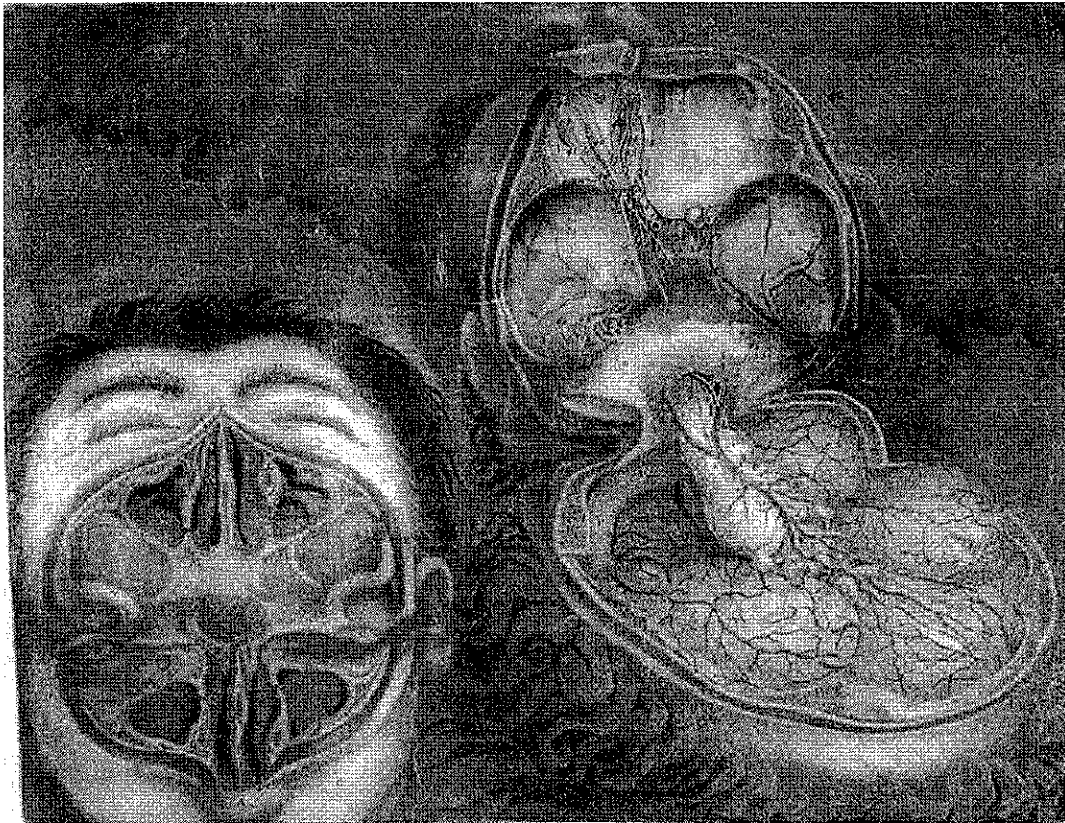
enables the correlation of histology to the results of advanced imaging modalities, which proves or disproves their clinical value. This results in the so-called multimodal navigation setup. Besides the challenge of registering these data with a low error, a big challenge is finding the most suitable presentation of all of these data in the surgical field. The goal must be to avoid disturbing the surgeon during his work by an information overflow and present only the data necessary to achieve the maximum benefit for the patient. Furthermore, the overall application accuracy of modern navigation systems has always been of concern to surgeons, especially intraoperative events such as brain shift outdating the preoperative data, which must be compensated for. The combination of intraoperative imaging with a multimodal navigational setup offers the best possibility to solve these challenges.

Christopher Nimsky  
Erlangen, Germany

Until neurorestoration is realized in practical terms, neurosurgeons will continue to be faced with the need to meticulously preserve neurological function while surgically treating pathologies of the nervous system with eloquence of tissue defining not only surgical risk but

also operable versus inoperable lesions. Over the past several decades, the ability to preoperatively define the anatomic substrate in neurosurgery has increased dramatically, and sophisticated imaging is available in all but the most modest of venues. In addition, the fusion of imaging and surgery has been brought into the operating room with the routine use of image-guided, frame-based stereotaxy and frameless neuronavigation technology. The availability of intraoperative magnetic resonance imaging is also increasing. Although the ability to define the preoperative anatomy has dramatically evolved and gained widespread utility, the routine use of methods of localization of cerebral function within the anatomic structures, both cortical and subcortical, has perhaps lagged behind. In this topic review, the authors provide a timely overview of the principal modalities for functional brain mapping. These topics cover tools that, although familiar to most neurosurgeons, are used less widely than anatomic imaging. Ultimately, the developments described in this review will lead to the fusion of anatomy datasets and functional imaging to guide surgery and increase safety in manipulating the least forgiving of surgical substrates.

Charles Y. Liu  
Los Angeles, California



Jacques Fabian Gautier d'Agoty, 1717–1785, *Myologie complete en couleur et grandeur naturelle*. Paris: Gautier & Quillau, 1746. (courtesy of Killam Library, Special Collections, Dalhousie University, Halifax, Nova Scotia and the U.S. National Library of Medicine, National Institutes of Health, Bethesda, Maryland).

# **ARTICLE 10**

# Functional Magnetic Resonance Imaging–Guided Brain Tumor Resection

Walter A. Hall, MD, MBA, Peter Kim, MD, PhD, and Charles L. Truwit, MD

**Objectives:** We evaluated the safety and efficacy of using functional magnetic resonance imaging (fMRI) brain activation data obtained at both 1.5 and 3 T to guide brain tumor resections using 1.5-T intraoperative MRI (ioMRI) guidance.

**Materials and Methods:** From January 1997 to March 2006, fMRI was performed on 29 patients before attempted brain tumor resection. Functional MRI was used to identify and coregister areas of brain activation for motor (n = 18), speech (n = 6), motor and speech (n = 4), and short-term memory and speech (n = 1) with respect to the tumor using a 1.5-T and two 3-T MRI scanners. Surgical resection was accomplished using 2 different 1.5-T ioMRI systems. The appropriate MRI scan sequences were obtained during surgery to determine and maximize the extent of the surgical resection depending on the tumor type.

**Results:** Of 29 patients, 20 (69%) had radiographically complete fMRI-guided tumor resections and 2 (7%) had successful MRI-guided brain biopsy because of the proximity of their astrocytomas to the eloquent cortex. The tumors were oligodendrogliomas (n = 16), astrocytomas (n = 4), meningiomas (n = 3), glioblastomas multiforme (n = 2), a pleomorphic astrocytoma (n = 1), and a dysembryoplastic neuroepithelial tumor (n = 1). The preoperative fMRI data were accurate in all cases. After tumor resection, 7 patients (26%) had transient neurologic deficits that resolved completely within 1 month of the surgical procedure in all cases. No adverse events associated with ferromagnetic instrumentation occurred.

**Conclusions:** Functional MRI was accurate for localizing areas of eloquent neurologic function before ioMRI-guided brain tumor resection.

**Key Words:** brain activation, brain neoplasms, brain tumor, functional magnetic resonance imaging, magnetic resonance imaging

(*Top Magn Reson Imaging* 2008;19:205–212)

Neurosurgeons have been using intraoperative magnetic resonance imaging (ioMRI) guidance to help direct the resection of brain tumors for more than a decade. Before the advent of ioMRI, neurosurgeons relied on stereotactic techniques including neuronavigation to assist in the performance

of image-guided surgery. Unfortunately, these surgical modalities are based on imaging obtained before the surgery and therefore do not account for the brain shift that will result from the egress of cerebrospinal fluid once the cranium is opened. These limitations provided the most compelling reason for the development of ioMRI whereby the neurosurgeon can detect the occurrence of brain shift and institute corrective measures in near real time, which ensures that the procedure will be performed in a safe and successful manner. Intraoperative MRI also offers the surgeon the additional advantages of exquisite soft tissue discrimination, the ability to view the surgical site in 3 dimensions, and confirmation of the absence of a hematoma resulting from surgery before leaving the operating suite.<sup>1–3</sup>

The ideal field strength for ioMRI has yet to be determined, and those used have ranged from 0.12 to 3.0 T.<sup>4</sup> The first operational ioMRI system that was installed was a 0.5-T double-coil design (Sigma SP; General Electric Medical Systems, Milwaukee, Wis) in which the neurosurgeon operated between the coils and image acquisition could be continuous.<sup>1</sup> All ioMRI systems that are used for surgical guidance allow for basic T<sub>1</sub>- and T<sub>2</sub>-weighted imaging capabilities; however, only high-field strength systems that are 1.5 T or higher enable the performance of MR spectroscopy, MR venography, MR angiography, brain activation studies, chemical shift imaging, diffusion-weighted imaging, and perfusion studies.<sup>1,5,6</sup> Each high-field imaging technique provides a significant surgical safety advantage for the neurosurgeon and the patient. Intracranial vascular structures can be visualized and avoided during surgery to prevent inadvertent injury using MR angiography and MR venography. The diagnostic yield of brain biopsy can be enhanced by using MR spectroscopy and chemical shift imaging to target areas of elevated phosphocholine, which are felt to represent the site of rapid membrane turnover suggestive of recurrent or progressive tumor growth. Mapping out the location of functional cortex using brain activation studies can influence the surgical approach to a tumor that will provide the surgeon with a safe trajectory that will result in a good patient outcome and a decrease in medical costs through complication avoidance.<sup>5</sup>

The role of surgery in the management of primary brain tumors remains controversial. Clearly, obtaining a tissue sample is necessary to make an accurate diagnosis that will direct the future management of that patient. However, whether the extent of the tumor resection provides the patient with a survival benefit has been a point of contention for both high- and low-grade gliomas (LGGs).<sup>7,8</sup> For high-grade

From the Department of Neurosurgery, State University of New York Upstate Medical University, Syracuse, NY; and Department of Radiology, Hennepin County Medical Center, Minneapolis, MN.

Reprints: Walter A. Hall, MD, MBA, Department of Neurosurgery, SUNY Upstate Medical University, 750 E Adams St, Syracuse, NY 13210 (e-mail: hallw@upstate.edu).

Copyright © 2009 by Lippincott Williams & Wilkins

gliomas, there are studies that contend and refute the notion that the extent of tumor resection is associated with prolonged survival<sup>8,9</sup> and prognosis,<sup>10</sup> respectively. Similarly, disagreement exists for LGGs regarding whether the extent of the surgical resection correlates with the length of patient survival and the risk of tumor recurrence.<sup>11,12</sup> To address this concern in patients with LGG, we analyzed 65 patients who received postoperative radiation therapy after resection of their tumors to identify those variables that correlated with overall survival and disease-specific survival.<sup>7</sup> In a multivariate analysis, the only predictors of overall and disease-specific survival were the presence of contrast enhancement and the extent of the surgery.<sup>7</sup> Based on our findings as well as on others, it has been our goal in all patients with LGG to attempt complete surgical resection. We have subsequently used ioMRI to ensure the highest likelihood of achieving gross total resection in these tumors. By identifying areas of eloquent cortex using brain activation studies for motor, speech, and memory function using 1.5- and 3-T functional MRI (fMRI), we have been able to resect LGG in locations where surgery was felt to carry a prohibitive risk for causing neurologic morbidity.<sup>3,5</sup> We describe our current paradigm for preoperative fMRI at 3 T for patients with brain tumors before attempted resection of their tumors at 1.5 T and describe our early clinical results.

Although we have performed neurosurgery using ioMRI guidance at 3 T, we have not yet resected a tumor at this field strength.

## MATERIALS AND METHODS

### Magnetic Resonance Imaging Systems

The first MRI system on which we performed brain activation studies was a short-bore 1.5-T scanner (Gyrosan ACS-NT; Philips Medical Systems, Best, the Netherlands) that had strong imaging gradients (23 mT/m, 105 mT/m per millisecond), which allowed for the echo planar imaging (EPI) pulse sequences that are necessary for brain activation studies. Patients had brain activation imaging or blood oxygen level-dependent (BOLD) fMRI either several days before the planned surgical procedure or immediately before the administration of general anesthesia. Patients were asked to perform a series of self-paced tasks several times with periods of rest of equal length between the intervals of activation. Tasks that were performed to demonstrate activation for motor function included finger and toe tapping; short-term memory was assessed through the ability to retain items on a list; and language location was determined by testing silent speech. The imaging protocol that was used for fMRI was a single-shot

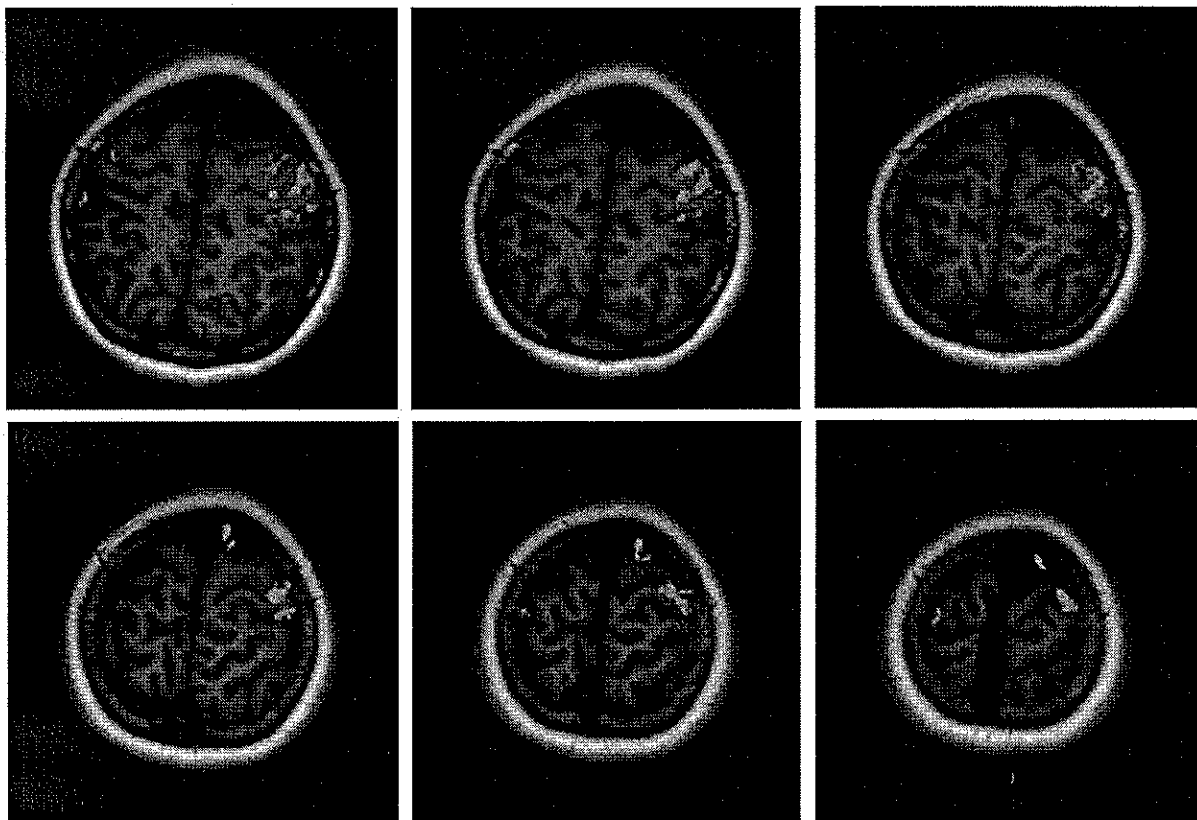


**FIGURE 1.** A 3-T brain activation scan showing the location of the motor cortex after right finger tapping was performed. Axial T<sub>1</sub>-weighted scan showing multiple sequential brain slices displayed from an inferior to a superior direction, each demonstrating brain activation. The brain tumor is clearly anterior to the area of brain activation and was found to be an oligodendroglioma at surgery.

EPI scan (repetition time [TR]/echo time [TE], 3000 milliseconds/40 milliseconds; image matrix,  $64 \times 64$ ; field of view, 210 mm; slice thickness, 7 mm; intersection gap, 1 mm; repetitions, 72; and imaging interval, 4 minutes).<sup>5</sup> Test accuracy was measured by the generation of a wave pattern that was overlaid on a linear graph that indicated when a specific task was and was not being performed. Those areas of BOLD activation were immediately demonstrated on the scanner console on high-quality anatomic images that could be displayed on the liquid crystal display monitors located in the ioMRI suite for review by the neurosurgeon before the start of the surgical case and at any time during the operative procedure. During the surgery, the areas of functional activation were identified with respect to the tumor location on sequential imaging to be avoided despite the demonstration of brain shift. Rigid cranial fixation allowed for the reproduction of the exact scan plane during surgery to enable the neurosurgeon to interpret the scan accurately and identify whether there was residual tumor and how much clearance there was from functional brain tissue.

This prototype MR system had a total length of 180 cm with an inner bore diameter of 60 cm with flared openings on both sides of the magnet. The actively shielded magnet produced a 5-G footprint that had dimensions measuring  $5.0 \times 7.8 \text{ m}^2$ . Two circular loops arranged in a phased array represented the head coil, which allowed excellent access to the patient, and surgery could be performed through 1 coil placed over the operative field. These surface loops provided high-quality imaging comparable to that that could be obtained with a conventional head coil and allowed the neurosurgeon to make intraoperative decisions that may alter the surgical approach.

Two 3-T MRI systems have been used to acquire preoperative brain activation data for motor and speech functions.<sup>3</sup> One short-bore 3-T MR system (Intera; Philips Medical Systems) will generate EPI pulse sequences necessary for brain activation studies using strong imaging gradients (33 mT/m, 180 mT/m per millisecond). The actively shielded magnet produces a 5-G footprint that measures  $7.8 \times 5.0 \text{ m}^2$ . The inner bore diameter is 60 cm, and the overall length is 157 cm.

The imaging software (Philips Medical Systems) for brain activation studies was BOLD and was used for determining the areas of motor and speech functions. Patients performed a series of tasks that resulted in activating the area of interest in which critical neurologic function was thought to be present. The task was self-paced and was repeated several times with the periods of activation separated by intervals of rest of similar lengths. The cortical areas for motor activation were determined by having the patient perform finger or toe tapping (Fig. 1). To evaluate language function, silent speech was performed where patients would think of the names of animals beginning with the start of the alphabet (Fig. 2). Silent speech is tested because true verbalization would result in displacement of the position of the head and inaccurate localization of language function. The protocol for performing fMRI at 3 T using the Philips Medical Systems was a single-shot EPI scan (TR/TE, 3000 milliseconds/35 milliseconds; field of view, 230 mm) with 4-mm-thick slices, a 1-mm

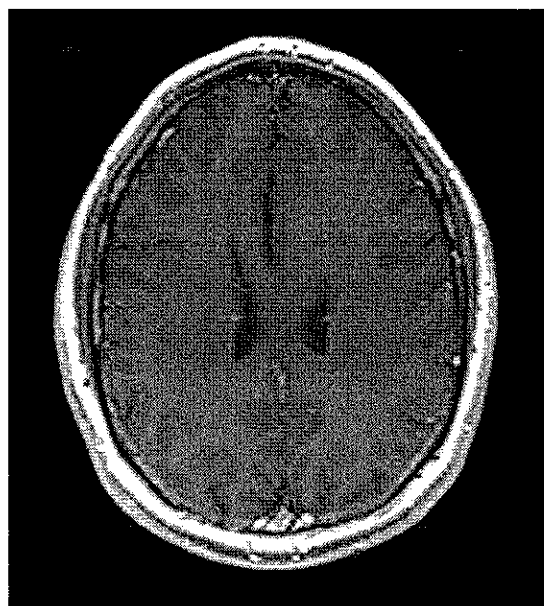


**FIGURE 2.** Axial T<sub>1</sub>-weighted contrast-enhanced brain activation scan performed at 3 T demonstrating the area for cortical localization of silent speech. The tumor is not visible on this scan slice because it is anterior and superior to the area of brain activation.

intersection gap, and an  $80 \times 128$ -image matrix.<sup>3</sup> The imaging interval was 7 minutes over which time the acquisition was repeated sequentially 100 times. Once acquired, the areas of BOLD activation were calculated immediately using the MR scanner computer console and then superimposed on high-quality anatomic images that were displayed on the MRI monitor for either immediate or delayed viewing by the neurosurgeon. In general, the fMRI was performed several days before surgery, and the neurosurgeon would review the results on the day before the planned procedure to determine a safe surgical trajectory to the lesion planned for resection.

The second MRI system for performing brain activation studies is a 3-T scanner (Siemens AD Medical Solutions, Erlangen, Germany) that uses a single-shot EPI sequence (TR/TE, 2660 milliseconds/30 milliseconds; field of view, 192 mm) to generate brain activation images.<sup>3</sup> The image matrix was  $64 \times 64$  with 3-mm-thick scan slices that had a 0.8-mm intersection gap. During the 3-minute imaging interval, the image acquisition was repeated sequentially 60 times. Because the head is rigidly fixed during the operative procedure, those areas of brain activation that were identified preoperatively could be easily and accurately superimposed on the high-quality anatomic images that were obtained during the operative procedure. In this manner, the surgeon was able to avoid those areas of functional brain where damage would result in a postoperative neurologic deficit.

### Intraoperative MRI Systems

The surgical resections were performed using 2 different 1.5-T ioMRI systems, namely, Gyroscan ACS/NT and Intera

I/T (Philips Medical Systems).<sup>1,3,5</sup> The Gyroscan ACS/NT ioMRI system was operational between January 1997 and March 2004. The Inera I/T ioMRI system has been in use since April 2004. The manner in which both ioMRI systems were used to perform surgery was similar, and the operative procedure was initiated after the preoperative brain activation studies obtained at 1.5 or 3 T were reviewed by the neurosurgeon. Within the ioMRI surgical suite, there is a floor-mounted pedestal on which the surgery was performed, which swivels and docks with the on-axis MRI gantry. The MR tabletop moved freely between the scanner and the surgical pedestal and could be locked in place on the pedestal at the center of the magnet during imaging and at a position 40 cm beyond the distal end of the flared opening of the scanner. If the surgery was performed at the near end of the room on the surgical pedestal outside the 5-G line, then non-MRI-compatible surgical instruments could be used. However, if surgery was performed on the opposite side of the magnet, all surgical instrumentation must be MRI-compatible.

The ioMRI suite met all of the requirements for a conventional operating room but could also be used for routine diagnostic MRI when it was not being used for surgery. The ioMRI suite was terminally cleaned the night before a planned surgical procedure and was considered a sterile environment afterwards with all personnel entering the room garbed in surgical attire. The scrub clothes worn by the surgical team were color-coded and pocket-less to prevent the inadvertent entrance of a potentially dangerous ferromagnetic instrument such as a pair of scissors into the ioMRI suite. Using these safety measures, there have not been any untoward events in



**FIGURE 3.** Preoperative 1.5-T axial turbo FLAIR MRI image of a left frontal LGG before surgical manipulation of the brain or the occurrence of brain shift. The brain activation scan result for this patient is shown in Figure 1 and demonstrates that the cortical location for finger tapping function was posterior to the tumor.



**FIGURE 4.** Intraoperative 1.5-T axial turbo FLAIR MR scan of the patient displayed in Figure 3 that demonstrates that the entire preoperative tumor imprint has been resected and the goal of surgery has been achieved.

the ioMRI suite during the performance of more than 1000 surgical procedures since 1997.

At the beginning of the procedure, the head was fixed in a Malcolm-Rand carbon fiber head holder (Elekta, Decatur, Ga) that was attached to the floating table top, which allowed for exact reproduction of scan planes during prolonged operative procedures where repeat imaging was likely because of the type of the tumor being resected or because the lesion location was near eloquent cortex. For low-grade tumors where a complete surgical resection may result in cure or could significantly delay the initiation of adjuvant therapy, multiple imaging updates were usually necessary during surgery. It was essential during surgery to verify with repeat imaging that the surgical approach remained safe and accurate to avoid inadvertent neurologic injury for those tumors that were immediately adjacent to eloquent cortex. The ability to accurately reposition the patient enabled the neurosurgeon to evaluate the operative site for residual disease that was difficult to visualize during surgery due to the brain shift that occurred after part of the tumor was resected.

### Surgical Technique

Patients received general anesthesia in the main operating room before they were transported to the ioMRI suite. Upon arrival in the ioMRI suite, the patient's head was secured in place in the carbon fiber frame that has 4-point titanium pin fixation. One of 2 surface circular loops was placed under the head to create a phased array, and the head was secured in the optimal position to perform the tumor resection. Because we do not combine neuronavigation with ioMRI guidance for the resection of tumors, the cranial opening was localized with respect to the tumor by placing MR-visible markers on the scalp to minimize the size of the craniotomy and the extent of the hair that was shaved. The second circular loop

was placed on the head over the operative field before preparing the patient to obtain preoperative imaging that demonstrated the appearance of the tumor before surgical manipulation (Fig. 3). The intraoperative scans were compared with these baseline images to determine whether the entire tumor had been successfully resected and the goal of surgery had been accomplished (Fig. 4).

After the baseline imaging had been completed, patients were moved to the surgical pedestal where the head was shaved and the operative field was prepared. One of the circular loops was sandwiched between sterile plastic drapes and then stapled directly on to the sterile operative towels. In this way, the surgery was performed through the loop, which did not need to be repositioned during intraoperative imaging. The craniotomy was performed in the near end of the room outside the 5-G line using ferromagnetic surgical instrumentation. Tumors were resected using standard neurosurgical technique, and the intraoperative scanning was obtained to evaluate the extent of the surgical resection. The number of intraoperative scans that were obtained depended on the type of tumor that was being resected. Low-grade gliomas, where a complete surgical resection could prove curative, may ultimately be imaged 3 times during the operative procedure to ensure that all radiographically visible tumor had been removed. Another reason for discontinuation of the surgery was the proximity of residual tumor adjacent to the eloquent cortex that had critical neurologic function as identified by brain activation (Fig. 5).



**FIGURE 5.** Intraoperative 1.5-T axial turbo FLAIR MR image of a patient with a left frontal astrocytoma that is adjacent to the cortical area for right-hand motor activation. An area of increased signal around the resection cavity is suggestive of the presence of residual tumor. The central sulcus is seen posterior to the resection cavity, and the area of increased signal was felt by the surgeon to possibly infiltrate into the motor cortex, which resulted in the discontinuation of the procedure.

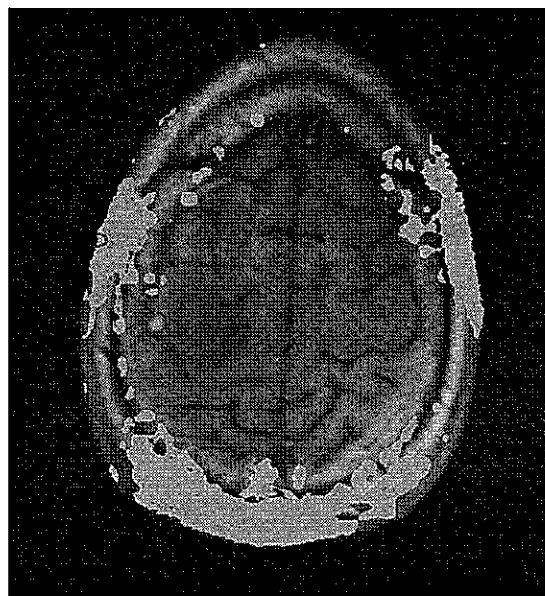


**FIGURE 6.** Axial turbo FLAIR brain activation scan for left finger tapping at 3 T demonstrating the activation immediately lateral to a presumed LGG. Based on the results of the brain activation study, the patient underwent an MRI-guided brain biopsy, which disclosed an astrocytoma. Because of the infiltrative nature of this tumor type, the patient was subsequently treated with adjuvant radiation therapy.

All surgical instruments were withdrawn from the operative field before aligning the surgical pedestal with the MR table and transporting the patient into the scanner. We have not used intraoperative cortical stimulation in combination with fMRI because there has generally been sufficient distance between the tumors being resected and the areas of cortical activation as demonstrated by fMRI, which were easily visualized on anatomic overlays despite the occurrence of brain shift. The completeness of the tumor resection was assessed by the neurosurgeon in consultation with the neuroradiologist.

After the craniotomy was closed before leaving the ioMRI suite, the operative site was imaged one final time to exclude the presence of hematoma. Because of the difficulty encountered in detecting hyperacute blood (intracellular hemoglobin), it was necessary to combine the interpretation of 3 imaging sequences (turbo fluid-attenuated inversion recovery [FLAIR],  $T_2$ -weighted orthogonal half-Fourier acquisition single-shot turbo spin-echo, and  $T_2^*$ -weighted fast low-angle shot gradient echo imaging) to make this determination, usually in the axial plane. When there was concern that an expanding hematoma was in the resection cavity, a repeat scan was performed 15 to 20 minutes later to allow for both enlargement of the clot and the conversion of oxyhemoglobin to deoxyhemoglobin.

### Patient Demographics

From January 1997 to March 2006, 29 patients were considered for 1.5- or 3-T fMRI-guided tumor resection in the 1.5-T ioMRI suite. There were 17 males and 12 females with the ages ranging from 10 to 70 years, mean age of 36 years,

and median age of 41 years. Tumor locations were right frontal ( $n = 10$ ), left frontal ( $n = 12$ ), right parietal ( $n = 1$ ), left temporal ( $n = 5$ ), and left parietal ( $n = 1$ ). Twenty-two patients (76%) presented with seizures, 3 had headaches (10%), and 2 were asymptomatic (7%). The result of the neurologic examination was normal in 27 patients (93%), whereas 2 had expressive aphasia (7%). Twenty-two patients (76%) were having their first neurosurgical procedure. Five patients (17%) had previous incomplete surgical resections of their tumors of which 4 were oligodendrogliomas and 1 was a dysembryoplastic neuroepithelial tumor before being referred for ioMRI-guided surgical resection. Two patients (7%) had ioMRI-guided biopsies only because both of their tumors, which were found to be astrocytomas after pathological examination, were intimately involved with those areas of the brain that activated for hand (Fig. 6) and face motor functions.

## RESULTS

### Tumor Histology

Twenty-seven patients (93%) had radiographically partial or complete fMRI-guided resections of their brain tumors. Two patients (7%) had successful MR-guided brain biopsies of their astrocytomas that were found to be located directly within the motor cortex. The histologic diagnosis from the resected tumors demonstrated 16 oligodendrogliomas (59%), 4 astrocytomas (15%), 3 meningiomas (11%), 2 glioblastomas multiforme (7%), 1 pleomorphic xanthoastrocytoma (4%), and 1 dysembryoplastic neuroepithelial tumor (4%).

### Intraoperative Imaging

Baseline images were obtained before the initiation of surgery to localize the bone flap with respect to the tumor and to minimize size of the cranial opening. The orientation of the head was never changed during the operative procedure, although the tabletop on which the patient was positioned was moved into and out of the scanner during imaging. In most cases, 3 sets of scans were acquired during the surgical procedure. The first scan was performed before surgery with the head in the operative position. The second scan was obtained after it was felt that a complete radiographic resection had been exacted, and the last scan was generated to exclude the presence of hemorrhage in the resection cavity after the craniotomy had been closed before the patient left the ioMRI suite. Functional MRI of all 29 patients localized motor function in 18 patients (62%), speech in 6 (21%), motor and speech in 4 (14%), and speech and memory in 1 (3%). Additional fMRI was not performed once general anesthesia was administered.

The location and type of the tumor influenced the frequency and duration of ioMRI updates. Those tumors located adjacent to areas of brain activation required more frequent updates to avoid those functional areas while maximizing the extent of the surgical resection. Generally, each scan was no longer than 10 to 15 minutes, and scans were rarely repeated within 1 hour of the prior study. Scanning protocols were streamlined to maximize efficiency by only obtaining scans in the most useful orientations for the neurosurgeon to interpret and in the specific scan sequences

that best demonstrated the type of tumor being removed. For patients with LGGs such as oligodendrogliomas and astrocytomas, rapid T<sub>2</sub>-weighted half-Fourier acquisition single-shot turbo spin-echo (scan time, 14 seconds; 16 slices) and high-quality cerebrospinal fluid signal-suppressed T<sub>2</sub>-weighted turbo FLAIR (scan time, 2 minutes; 42 slices) imaging sequences were used to demonstrate the full extent of the tumor.<sup>5</sup> All acquisitions were performed with a field of view of 200 to 230 mm and a 256-image matrix. For those tumors that were enhanced after the administration of contrast, such as malignant gliomas and meningiomas, T<sub>1</sub>-weighted (scan time, 2 minutes 4 seconds; 15 slices) imaging was used during surgery but the administration of contrast was withheld until it was felt that a complete radiographic resection had been achieved to prevent the diffusion of contrast media into the brain parenchyma around the resection cavity where the blood-brain barrier was disrupted owing to tumor cell infiltration and cerebral edema.

In all patients, the radiographic completeness of the surgical resection was determined. The neurosurgeon and the neuroradiologist reviewed the intraoperative images to confirm whether a complete radiographic resection had been achieved as evidenced by the absence of the entire preoperative tumor imprint for LGGs. For enhancing tumors, the surgical resection was considered complete if the entire enhancing portion of the tumor was no longer visible. A radiographically complete surgical resection was achieved in 20 (69%) of 29 patients. Of these 20 patients with complete resections, the tumor types were 11 oligodendrogliomas, 3 astrocytomas, 3 meningiomas, 1 dysembryoplastic neuroepithelial tumor, 1 glioblastoma multiforme, and 1 pleomorphic xanthoastrocytoma. Five patients with oligodendrogliomas had partial resections because of the proximity of their tumors to the motor cortex in 4 and motor and speech cortex in 1. None of these patients with oligodendrogliomas received postoperative adjuvant treatment, and none of their tumors have demonstrated radiographic progression. One patient with an astrocytoma located in the posterior left frontal lobe that was abutting the motor cortex had a partial resection and subsequent adjuvant radiation therapy. Another patient with a recurrent left temporal glioblastoma multiforme infiltrating into the language cortex had a partial resection and then received postoperative chemotherapy. Both astrocytomas that were biopsied because of the intimate involvement of the motor cortex received adjuvant radiation therapy. No clinically significant or radiographically apparent hemorrhage was detected in any patient on postoperative ioMRI.

### Postoperative Morbidity

The incidence on permanent postoperative neurologic morbidity after fMRI-guided brain tumor resection has been low with all transient deficits resolving within 1 month after surgery. Of the 27 patients where an fMRI-guided tumor resection was possible, 7 patients (26%) had transient neurologic impairment. One patient with a superior left temporal astrocytoma experienced a right hemiparesis due to the development of cerebral edema that tracked into the basal ganglia. This patient had no change in their short-term memory function, which was localized preoperatively by fMRI. Motor



apraxias were noted in 3 patients (11%), 2 after resection of meningiomas abutting the motor cortex and 1 after resection of an astrocytoma located in the supplementary motor area. Two patients with posterior left frontal oligodendrogliomas sustained transient speech apraxias, with 1 of them, where there tumor was in the supplementary motor area, also having a temporary motor apraxia. Word finding difficulty, attributed to postoperative cerebral edema, was experienced in 1 patient with a left occipital glioblastoma multiforme that had a radiographic complete surgical resection. In summary, the transient postoperative deficits seen after fMRI-guided brain tumor resection were left hemiparesis (left temporal astrocytoma), speech apraxia (left frontal oligodendroglioma), speech and motor apraxia (left frontal apraxia), word finding difficulty (left occipital glioblastoma multiforme), and 3 motor apraxias (2 right frontal meningiomas and 1 left frontal astrocytoma). No adverse events related to the use of ferromagnetic surgical instrumentation occurred.

## DISCUSSION

The extent of the surgical resection for patients with brain tumors has been reported to correlate with their length of survival.<sup>3</sup> In a series of 65 LGGs treated with surgery and adjuvant radiation therapy that we evaluated at our institution, the only prognostic variables that correlated with overall and disease-specific survival on multivariate analysis were the extent of the surgical resection and whether contrast enhancement was present.<sup>7</sup> Although the optimal treatment of LGGs remains controversial, there is growing evidence that maximizing the extent of the resection prolongs survival, and for some tumors, such as gangliogliomas and dysembryoplastic neuroepithelial tumors, a complete radiographic resection may prove curative.<sup>5</sup> Subtotal resections of LGGs often result from the inability to distinguish visually between tumor tissue and normal brain parenchyma or tumor location near the eloquent cortex bearing neurologic function. During the conventional surgical resection of a LGG located adjacent to functional areas of brain, the surgeon's awareness of the possibility of brain shift will often lead to a conservative approach with the end result being a tumor that is incompletely removed to prevent the inadvertent injury to areas of the brain bearing neural function.

Neuronavigational systems that are either frame-based or frameless provide an increased level of accuracy over conventional neurosurgery by using imaging that is obtained either several days or immediately before surgery. Inaccuracies associated with frame-based and frameless surgical techniques include frame distortion, imaging artifacts associated with the head frame or dental implants, errors associated with setting the coordinates on the frame or its phantom, and fiducial registration.<sup>3</sup> However, the greatest source of inaccuracy encountered during surgery comes from the resulting brain shift that results once the cranium is opened and there is an egress of cerebrospinal fluid. Correction for this occurrence would entail the repeat imaging of the patient and the re-registration of the fiducials, which is time-consuming and significantly lengthens what is already considered a long neurosurgical procedure. Intraoperative MRI enables the

neurosurgeon to detect the degree and extent of the brain shift and allows for the dynamic correction of the brain displacement and the continued resection of any residual brain tumor tissue seen on ioMRI.<sup>3,5</sup> Because of the recognized clinical benefit that results from maximizing the extent of the surgical resection for patients with LGGs, it is necessary to balance the aggressiveness of the surgical resection with the potential risks of causing a permanent postoperative neurologic deficit. In a series of 25 patients with LGGs that were resected using 0.5-T ioMRI guidance, transient neurologic deficits that resolved within 1 month of surgery were experienced in 16% of patients with tumors near the supplementary motor area.<sup>13</sup> Resection of LGGs located within the supplementary motor area will result in a transient neurologic deficit in the form of a hemiparesis that usually resolve within 6 months.<sup>14</sup> In some of our earlier work looking at using 1.5-T fMRI to guide the resection of LGGs, we saw a transient postoperative neurologic deficit rate of 13%, and in a later series of patients where 3-T fMRI was used, the transient neurologic deficit rate was higher at 42%.<sup>3,5</sup> In the series we now report, we saw transient neurologic deficits in 7 (26%) of 27 patients. Another recent report, which evaluated preoperative 3-T fMRI by navigated electrocortical stimulation, demonstrated a transient mild to moderate neurologic deficit rate of 32% where recovery was seen within 3 months of surgery.<sup>15</sup> These seemingly high rates of postoperative neurologic worsening were anticipated, which justifies the necessity of obtaining preoperative brain activation data. It is important to note, as witnessed and described by others, that when using ioMRI guidance to maximize the extent of tumor resection, the resulting deficits will be transient and will usually resolve within 1 month. The rapid resolution of these transient deficits confirms the accuracy of the fMRI data and supports the clinicians' ability to rely on the validity of the information to support their surgical decision making.

In analyzing the first 346 procedures performed at our institution, there were 103 patients whose brain tumors had been resected.<sup>3,5,16</sup> Of these 103 patients with brain tumors, there were 14 cases (14%) where it was felt necessary to obtain preoperative brain activation data by the surgeon to determine a safe surgical approach to the tumor.<sup>3,5,16</sup> Another high-field imaging technique that has been used to avoid inadvertent neurologic injury during brain tumor resection is diffusion tensor imaging.<sup>17</sup> This technique uses the diffusion energy of water to map white matter fiber tracts so that they can be visualized and then avoided at surgery.<sup>17</sup> Although all of the above cited surgical resections for brain tumors have been performed using 1.5-T ioMRI guidance, there are now 3-T ioMRI systems that been installed and used for surgical guidance.<sup>4,18</sup> Although the initial advantages of improved efficiency and decreased patient transient time have been noted, the safety and efficacy of operating in 1.5- and 3-T MR environments seem to be comparable.<sup>3,18</sup>

## REFERENCES

1. Hall WA, Truwit CL. Intraoperative MR-guided neurosurgery. *J Magn Reson Imaging*. 2008;27:368-375.
2. Hall WA, Truwit CL. Intraoperative MR imaging. *Magn Reson Imaging Clin N Am*. 2005;13:533-543.

3. Hall WA, Truwit CL. 3-Tesla functional magnetic resonance imaging-guided tumor resection. *Int J Comput Assist Radiol Surg.* 2007;1:223-230.
4. Truwit CL, Hall WA. Intraoperative magnetic resonance imaging-guided neurosurgery at 3-T. *Neurosurgery.* 2006;58:ONS 338-ONS 346.
5. Hall WA, Liu H, Truwit CL. Functional magnetic resonance imaging-guided resection of low-grade gliomas. *Surg Neurol.* 2005;64:20-27.
6. Hall WA, Liu H, Martin AJ, et al. Intraoperative magnetic resonance imaging. *Top Magn Reson Imaging.* 2000;11:203-212.
7. Lo SS, Cho KH, Hall WA, et al. Does the extent of surgery have an impact on the survival of patients who receive postoperative radiation therapy for supratentorial low-grade gliomas? *Int J Cancer.* 2001;96:71-78.
8. Buckner JC. Factors influencing survival in high-grade gliomas. *Semin Oncol.* 2003;30:10-14.
9. Lacroix M, Abi-Said D, Fourney DR, et al. A multivariate analysis of 416 patients with glioblastoma multiforme: prognosis, extent of resection, and survival. *J Neurosurg.* 2001;95:190-198.
10. Kowalczyk A, Macdonald RL, Amidei C, et al. Quantitative imaging study of extent of surgical resection and prognosis of malignant astrocytomas. *Neurosurgery.* 1997;41:1028-1036.
11. Medbery CA 3rd, Straus KL, Steinberg SM, et al. Low-grade astrocytomas: treatment results and prognostic variables. *Int J Radiat Oncol Biol Phys.* 1988;15:837-841.
12. Claus EB, Horlacher A, Hsu L, et al. Survival rates in patients with low-grade glioma after intraoperative magnetic resonance image guidance. *Cancer.* 2005;103:1227-1233.
13. Martin C, Alexander E III, Wong T, et al. Surgical treatment of low grade gliomas in the intraoperative magnetic resonance imager. *Neurosurgical Focus.* 1998;4:e8.
14. Russell SM, Kelley PJ. Incidence and evolution of post-operative deficits after volumetric stereotactic resection of glial neoplasms involving the supplementary motor area. *Neurosurgery.* 2003;52:506-516.
15. Roessler K, Donat M, Lanzenberger R, et al. Evaluation of preoperative high magnetic field motor functional MRI (3 tesla) in glioma patients by navigated electrocortical stimulation and postoperative outcome. *J Neurol Neurosurg Psychiatry.* 2005;76:1152-1157.
16. Hall WA, Liu H, Maxwell RE, et al. Influence of 1.5-tesla intraoperative MR imaging on surgical decision making. *Acta Neurochir.* 2002;85:29-37.
17. Tummala RP, Chu RM, Liu H, et al. Application of diffusion tensor imaging to magnetic-resonance guided brain tumor resection. *Pediatr Neurosurg.* 2003;39:39-43.
18. Hall WA, Galicich W, Bergman T, et al. 3-Tesla intraoperative MR imaging for neurosurgery. *J Neurooncol.* 2006;77:297-303.

# **ATTACHMENT 5**

# Anthony F Posteraro III, MD

---

Radiology Associates of Hartford  
St Francis Hospital and Medical Center  
1000 Asylum Avenue  
Suite 3201 E  
Hartford, CT 06105  
(860) 525-3322

## Professional Background

Director Nuclear Medicine and Molecular Imaging  
Saint Francis Hospital and Medical Center  
July 2008 – Present

Director Cross Sectional Cardiovascular Imaging  
Saint Francis Hospital and Medical Center  
July 2005 – Present

Radiology Associates of Hartford  
July 2005 – Present

## Appointments

Saint Francis Health Care Partners  
ACO Finance Subcommittee  
January 2011- Present

Saint Francis Health Care Partners  
ACO Data Subcommittee  
March 2012- Present

Director Outpatient Imaging Radiology Associates of Hartford  
July 2011 - Present

Treasurer Radiology Associates of Hartford  
July 2009-June 2011

Secretary Radiology Associates of Hartford  
July 2007-June 2009

## Postgraduate Training

University of Pennsylvania School of Medicine  
Nuclear Medicine Fellowship  
Philadelphia, PA  
July 2004 – June 2005

Brown University Medical School  
Diagnostic Radiology Residency  
Providence, RI  
July 2000 – June 2004

Norwalk Hospital/Yale University School of Medicine  
Medical Residency Program  
Norwalk, CT  
July 1999 – June 2000

## Education

University of Connecticut School of Medicine  
Farmington, CT  
Doctor of Medicine  
May, 1999

University of Connecticut  
Storrs, CT  
Bachelor of Science in Chemistry, *Summa Cum Laude*  
May, 1995

## Awards

- University of Connecticut Health Center Department of Radiology 2008 Teaching Award
- Haffenreffer House Staff Excellence Award, Rhode Island Hospital/Brown Medical School, 2004
- Excellence in Design for Educational Exhibit, 88<sup>th</sup> Annual RSNA Meeting 2002
- Introduction to Research Program, Nominee/Participant, 87<sup>th</sup> Annual RSNA Meeting 2001
- Undergraduate Representative for Commencement, University of Connecticut, 1995
- University Scholar, University of Connecticut, 1995
- Honors Scholar in Chemistry, University of Connecticut, 1995
- Phi Beta Kappa, 1994

## Medical Licensure

State of Connecticut- Active  
State of Rhode Island- Inactive  
State of Pennsylvania- Inactive

## Board Certification

Certificate in Diagnostic Radiology, American Board of Radiology  
American Board of Radiology Certificate of Competence Nuclear Radiology  
American Board of Nuclear Medicine  
Certification Board of Nuclear Cardiology  
Certification Board of Cardiovascular Computed Tomography

## Professional Memberships

American College of Radiology  
Radiological Society of North America  
American Roentgen Ray Society  
Society of Nuclear Medicine

## Publications

- 1) Feld RS, Zink S, Posteraro AF. Empiric Embolization of a Diverticular Bleed with CT Angiographic Mapping: Enlarging the Therapeutic Window of Transcatheter Arterial Intervention. *Journal of Vascular and Interventional Radiology*. 2010; 21: 593 - 595.
- 2) Noce T, Gupta N, Posteraro AF, Kim C. Dual Source Cardiac CT- Technique, Normal Findings, and Variants. *Current Problems in Diagnostic Radiology*. 2010; 39: 37-50.
- 3) Posteraro AF, Dupuy DE, Mayo-Smith WW. Radiofrequency ablation of bony metastatic disease. *Clinical Radiology*. 2004; 59: 803-811.
- 4) Posteraro AF, Atalay, MK. Double inlet left ventricle with transposition of the great vessels. *Medicine and Health Rhode Island*. 2004; 87:182.
- 5) Posteraro AF, Noto RB. Neurologic PET. *Medicine and Health Rhode Island*. 2003; 86:136-138.
- 6) Posteraro AF, Mayo-Smith WW. Bilateral Cystic Ovarian Teratomas. *Medicine and Health Rhode Island*. 2001; 84:19-20.
- 7) Posteraro AF, Mauriello M, Winter SM. Riboflavin treatment of antiretroviral induced lactic acidosis and hepatic steatosis. *Connecticut Medicine*. 2001; 65:387-390.
- 8) Frank HA, Chynwat V, Posteraro AF, Hartwich G, Simonin I, Scheer H. Triplet state energy transfer between the primary donor and the carotenoid in *Rhodobacter Sphaeroides R-26* reaction centers exchanged with modified bacteriochlorophyll pigments and reconstituted with spheroidene. *Photochemistry and Photobiology*. 1996; 64:823-831.

## Presentations

- 1) Noce T, Gupta N, Posteraro AF, Kim C. *Cardiac Anatomy - A Cross Sectional Tour of Normal Cardiac Anatomy and Pitfalls With A Dual Source CT Scanner*. Poster Presentation at the 94<sup>th</sup> Annual Radiological Society of North America, Chicago, IL 2008
- 2) Posteraro AF. *Cardiac Nuclear Imaging Section, Approach to Diagnosis: A Case – Based Imaging Review Course*. Presented at the 107<sup>th</sup> Annual American Roentgen Ray Society, Orlando, FL 2007.
- 3) Posteraro AF. *Today's Tool for Clinical Molecular Imaging*. Presented at New England Roentgen Ray Society Annual Holmes Lecture Innovations in Imaging, Boston, MA. 2007
- 4) Posteraro AF. *PET Imaging Section, Approach to Diagnosis: A Case – Based Imaging Review Course*. Presented at the 106<sup>th</sup> Annual American Roentgen Ray Society, Vancouver, BC. 2006
- 5) Posteraro AF, Dupuy DE, Mayo-Smith WW. *Radiofrequency Ablation of Bony Metastatic Disease*. Poster Presentation at the 88<sup>th</sup> Annual Radiological Society of North America, Chicago, IL. 2002.

- 6) Posteraro AF, Rogg JM, Egglin TK, Cronan, JJ. *Open MRI Imaging: A Panacea?* Presented at the 40<sup>th</sup> Annual American Society of Neuroradiology, Vancouver, BC. 2002.
- 7) Cassese JA, Wallach MT, Posteraro AF. *Ultrasound Measurement of the Colon and Rectum as Screening for Hirschsprung's Disease in Constipated Patients: A Comparison to Barium Enema.* Presented at the 87<sup>th</sup> Annual Radiological Society of North America, Chicago, IL. 2001.

**Allison R. Calvello, MHSA RT (R) (CV) (CT) (MR)**

158 East Chippins Hill Road

Burlington, CT 06013

[arichardson57@comcast.net](mailto:arichardson57@comcast.net)

(H) 860-675-3864

(C) 860-817-4410

**CAREER GOAL:** To become an active participant and leader in a Radiology Department in a progressive hospital

**EMPLOYMENT:**

July 2012 to  
present

**ST. FRANCIS HOSPITAL AND MEDICAL CENTER**  
Hartford, Connecticut

Position: *MRI Supervisor*

- MRI Exams
- Supervise and Train Subordinates
- Purchase and Evaluate Products
- Instruct Student Technologists

December 2009 to  
present

**JEFFERSON RADIOLOGY**  
Hartford, Connecticut

Position: *IT Clinical Support Specialist*  
*3D Technologist*  
*PACS Clinical Specialist*  
*RIS Clinical Specialist*  
*CPR Instructor*

- Process 3D image data sets for Radiologists
- PACS Implementation/Training Team
- RIS Implementation/Training Team
- Liaison for Clinical and IT support
- Workflow Implementation/Training

August 2000  
to present

**HARTFORD HOSPITAL**  
Hartford, Connecticut

Position: *MRI Unit Leader*  
*3D Technologist*  
*Education Coordinator*

- MRI Exams
- Post Process 3D data sets
- Supervise and Train Subordinates
- Schedule patients for procedures
- Purchase and Evaluate Products
- Instruct Student Technologists
- Organize In-Services
- Develop and implement budgets
- Instruct Radiology Residents in MRI Physics



**Allison R. Calvello, MHSA RT (R) (CV) (CT) (MR)**

September 2001  
to May 2011

**UNIVERSITY of HARTFORD**  
West Hartford, Connecticut

Position: *MRI Physics Instructor*

- Instruct MRI students in MRI Physics, Positioning and Instrumentation

June 2011  
To Present

**QUINNIPIAC UNIVERSITY**  
North Haven, Connecticut

Position: *Radiation Physics and Safety Instructor*

- Instruct RA students in Radiation Physics and Safety

June 1989 to  
August 2000

**UCONN HEALTH CENTER/JOHN DEMPSEY HOSPITAL**  
Farmington, Connecticut

Position: *MRI and CT Technologist*  
*Interventional Technologist*

- Interventional/MRI/CT Exams
- Perform/Assist physicians in Interventional and Cardiac Procedures
- Schedule patients for procedures
- Supervise and Train Subordinates
- Purchase and Evaluate Products
- Quality Improvement Team Member/ Work Redesign Committee Member
- Instruct Student Technologists

October 1981  
to June 1989

**CHARLOTTE HUNGERFORD HOSPITAL**  
Torrington, Connecticut

Positions: *Chief of Interventional Radiology*  
*Quality Assurance Technologist*  
*Infection Control Technologist*  
*Accounting Analyst*

**CERTIFICATIONS:**

- **ARRT: 175475**
- **R** (Radiology)
- **CIT** (Cardio-vascular Interventional Technology)
- **CT** (Computed Axial Tomography)
- **MR** (Magnetic Resonance)

**LICENSE:**

State of Connecticut Radiographer: 000982

Allison R. Calvello, MHSA RT (R) (CV) (CT) (MR)

**EDUCATION: SAINT JOSEPH COLLEGE**  
Standish, Maine

- Degree: Masters of Health Services Administration
- G.P.A: 3.9 out of 4.0
- Graduation: December 2005

**UNIVERSITY OF CONNECTICUT**  
Storrs, Connecticut

- Bachelors Degree in General Studies
- Concentration in Business Management/History
- G.P.A.: 3.77 out of 4.00
- Graduated: May 1997
- *Alpha Sigma Lambda* Honor Society
- *Golden Key* National Honor Society

**NAUGATUCK VALLEY COMMUNITY TECHNICAL COLLEGE**  
Waterbury, Connecticut

- Associates Degree in Business Administration: Management
- Graduated: 1994 *Summa Cum Laude*
- G.P.A.: 3.95 out of 4.00
- *Alpha Beta Gamma* Business Honor Society
- *Phi Theta Kappa* National Honor Society

**HARTFORD HOSPITAL SCHOOL of ALLIED HEALTH**  
Hartford, Connecticut

- Radiologic Technology Program
- Class Rank: 1<sup>st</sup>
- Graduated: 1981
- Student of the Year: 1981

**PERSONAL:** Motivated, excellent interpersonal and communication skills, experienced with computers, tutor students, Black Belt in Karate, former V.P. for Board of Directors for credit union, CPR Instructor

## CURRICULUM VITAE

**Leonard J. Quartararo**  
544 Cortland Circle  
Cheshire, CT 06410  
(203) 272-9399

---

### PROFESSIONAL EXPERIENCE

*June 1996 to present*

*Administrative Director, Department of Radiology and Imaging Services, Saint Francis Hospital and Medical Center, Hartford, CT*

Responsible for operations of multiple hospital campus Radiology Services including Saint Francis Hospital and Medical Center Campus, Mount Sinai Campus and Comprehensive Breast Center. In addition, development and management of off-site Out-patient Access Centers including Mobile MRI.

Direct management of 11 clinical and non-clinical section supervisors, responsible for 125 employees, performing approximately 225,000 examinations annually. Imaging Modalities: Radiography, IR, Nuclear Medicine, MRI, CT, Ultrasound, PET/CT and Mammography.

Financial management: annual operating and capital budget.

*1984 to June 1996*

*Assistant Director, Department of Diagnostic Imaging, Yale-New Haven Hospital, New Haven, CT.*

Management of a forty-two room imaging department including: radiography, special procedures, mammography, nuclear medicine, ultrasound, CT, MRI, and out-patient centers.

Direct and coordinate the activities of a management team of fifteen staff, responsible for 250 employees performing over 225,000 examinations annually.

Financial management: annual operating and capital budget.

**PROFESSIONAL EXPERIENCE** *(continued)*

- 1979 - 1984* *Chief Technologist, Nuclear Medicine Department, Yale-New Haven Hospital, New Haven, CT*
- 1978 - 1979* *Cardiac Imaging Technologist, Nuclear Medicine Department, Yale-New Haven Hospital, New Haven, CT*
- 1976 - 1978* *Nuclear Medicine Technologist, Nuclear Medicine Department, Yale-New Haven Hospital, New Haven, CT*
- 1975-1976* *Chief Technologist, Nuclear Medicine Department, Waynesboro Community Hospital, Waynesboro, VA.*

**EDUCATION**

- 1994 - 1996* Rensselaer Polytechnic Institute (Hartford Graduate Center), Hartford, CT  
Masters of Science for Health Care Executives.
- 1984 - 1993* Quinnipiac College, Hamden, CT, School of Allied Health, B.S. in Radiology Sciences with a minor in Health Care Administration.  
- Graduated Cum Laude.  
- National Honor Society - Alpha Sigma Lambda
- 1976* Medical College of Virginia and Virginia Commonwealth University - Administrative Training Institute.
- 1975* University of Virginia and FDA - Quality Assurance Program.
- 1974 - 1975* University of Virginia Medical Center, Charlottesville, VA, School of Nuclear Medicine Technology. Diploma.  
- Ranked second in class.
- 1972 - 1974* Overlook Hospital, Summit, NJ, School of Radiologic Technology.  
Diploma

**EDUCATION** *(continued)*

*1967 - 1971*

Scotch Plains Fanwood High School,  
Scotch Plains, NJ  
Diploma

**ACADEMIC APPOINTMENTS**

*1980 to 1997*

Associate Faculty, School of Allied Health and  
Sciences, Diagnostic Imaging Program, Quinnipiac  
College, Hamden, CT.

*1979 to 1996*

Clinical Instructor, Nuclear Medicine and  
Radiography, Yale-New Haven Hospital in affiliation  
with Gateway Community College, New Haven, CT.

**COMMITTEE MEMBERSHIPS**

*1996 to present*

Hospital Radiation Safety Committee, Saint Francis  
Hospital and Medical Center, Hartford, CT.

*1985 to present*

Committee Member, Directors of Radiology,  
Connecticut Hospital Association (CHA),  
Wallingford, CT.

*1980 - 1985*

Radiation Safety Committee, Yale-New Haven  
Hospital, New Haven, CT.

*1980 - 1985*

Radioisotope Research Committee, Yale-New Haven  
Hospital, New Haven, CT.

*1982*

State Licensure Committee (AD HOC), Connecticut  
Society of Radiologic Technologists.

*1978 - 1979*

National Society of Nuclear Medicine New England  
Chapter, Society of Nuclear Medicine Treasurer.

**NATIONAL BOARD CERTIFICATION**

*1975*

Registered in Nuclear Medicine American Registry  
of Radiologic Technology. Certificate #X-106781.

*1974*

Registered in Radiologic Technology, American  
Registry of Radiologic Technology.  
Certificate #106781.

**PROFESSIONAL MEMBERSHIPS**

American Health Care Radiology Administrators,  
National and North Atlantic Region.  
Membership #4414.

National Society of Nuclear Medicine.  
New England Chapter, Society of Nuclear Medicine,  
Technical Affiliate.

**PUBLICATIONS**

Johnstone, DE, Wackers, FJ, Berger, JH, et al.: Effect  
of Patient Positioning on Left Lateral Thallium-201  
Myocardial Images. JNM 20:183-188, 1979.

Wackers, FJ, Berger, HJ, Johnstone, DE, et al.:  
Multiple Gated Cardiac Blood Pool Imaging for Left  
Ventricular Ejection Fraction: Validation of the  
Technique and Assessment of Variability. American  
Journal of Cardiology, June 1979.

**PAPERS PRESENTED**

Selective Spleen Scanning with Technetium-99m  
Labeled Red Blood Cells. Society of Nuclear  
Medicine, New England Chapter, Hyannis, MA,  
April 1982.

## CURRICULUM VITAE

Michael T. Twohig, M.D.  
22 Brian Woods Drive  
Avon, CT 06001

**Birth Date:** August 27, 1958

**Birthplace:** Springfield, Massachusetts

**Present Position:** Chairman, Department of Radiology  
Saint Francis Hospital and Medical Center  
Hartford, Connecticut  
January 2004 to Present

President and Chief Radiologist  
Radiology Associates of Hartford, P.C.  
Hartford, Connecticut  
December 2003 to Present

Director of Neuroradiologic Services  
Saint Francis Hospital and Medical Center Stroke Center  
2003 to Present

Medical Director, MRI  
Saint Francis Hospital and Medical Center  
Hartford, Connecticut  
1992 to 2011

Director of Neuroradiology  
Saint Francis Hospital and Medical Center  
Hartford, Connecticut  
1992 to Present

Staff Radiologist  
Saint Francis Hospital and Medical Center,  
Hartford, Connecticut  
July 1, 1990 to Present

**Professional Experience:** Vice Chairman  
Department of Radiology  
Saint Francis Hospital and Medical Center  
Hartford, Connecticut  
1995 to 2003

**Professional**

**Experience:**

*(continued)*

Executive Vice President  
Radiology Associates of Hartford, P.C.  
1995 to 2003

New Milford Hospital, New Milford, CT  
General Radiology, June 30, 1988 to June 30, 1990

Meriden-Wallingford Hospital, Meriden, CT  
General Radiology, June 30, 1988 to June 30, 1990

Norwalk Hospital, Norwalk, CT  
MRI .5T GE MRI and CT  
December 1988 to June 30, 1990

Housatonic Valley Radiology Associates, Danbury, CT  
General Radiology, December 1988 to June 1990

**Awards:**

Connecticut Top Docs 2012  
**Connecticut Magazine**  
April 2012

Hartford Area Top Doctors for Radiology  
**Hartford Magazine**  
June 2012

Connecticut Top Docs 2011  
**Connecticut Magazine**  
April 2011

Connecticut Top Docs 2010  
**Connecticut Magazine**  
April 2010

Hartford Area Top Doctors for Radiology  
1 of 5 selected  
**Hartford Magazine**  
June 2011

Hartford Area Top Doctors for Radiology  
1 of 5 selected  
**Hartford Magazine**  
June 2010



Michael T. Twohig, M.D.  
Page 3

Awards:

*(continued)*

Hartford Area Top Doctors for Radiology  
1 of 5 selected  
**Hartford Magazine**  
June 2009

Hartford Area Top Doctors for Radiology  
1 of 5 selected  
**Hartford Magazine**  
June 2008

Hartford Area Top Doctors for Radiology  
1 of 5 selected  
**Hartford Magazine**  
June 2007

Hartford Area Top Doctors for Radiology  
1 of 5 selected  
**Hartford Magazine**  
June 2006

Hartford Area Top Doctors for Radiology  
1 of 4 selected  
**Hartford Magazine**  
June 2005

Hartford Area Top Doctors for Radiology  
1 of 5 selected  
**Hartford Magazine**  
June 2004

Teacher of the Year 1998  
presented by Radiology Residents  
Saint Francis Hospital and Medical Center.  
(Academic year July 1, 1998)

Teacher of the Year 1994  
presented by Radiology Residents  
Saint Francis Hospital and Medical Center.  
(Academic year July 1, 1994)

Michael T. Twohig, M.D.  
Page 4

**Fellowship Training:**

Teacher of the Year 1990  
Yale-New Haven Hospital

Neuroradiology Fellowship  
Yale-New Haven Hospital  
New Haven, Connecticut  
July 1, 1988 to June 30, 1990

**Residency:**

Norwalk Hospital, Norwalk, Connecticut  
Diagnostic Radiology, July 1984 to June 1988  
Co-chief Radiology Resident, July 1986 to June 30, 1987  
Chief Radiology Resident, July 1, 1987 to June 30, 1988

**Additional Residency  
Training:**

Neuroradiology Rotation  
Yale-New Haven Hospital  
March 1, 1986 to May 1, 1986

Pediatric Radiology Rotation  
Yale-New Haven Hospital  
August 1, 1986 to October 1, 1986

Magnetic Resonance Imaging Rotation  
Yale-New Haven Hospital  
November 14, 1986 to December 14, 1986

Armed Forces Institute of Pathology  
Radiology-Pathology Course  
August 10, 1987 to September 18, 1987

Head and Neck Imaging Rotation, Peter Som  
Mount Sinai Medical Center, New York, NY  
February 1, 1988 to February 29, 1988

**Medical:**

New York Medical College, Valhalla, New York  
Medical Degree  
September 1980 to June 1984

**Premedical:**

Boston College, Boston, Massachusetts  
Bachelor of Science, Biology  
September 1976 to June 1980

Michael T. Twohig, M.D.  
Page 5

**Honors:** Summa cum laude  
Phi Beta Kappa

**Board Certifications:** Diplomat National Board of Medical Examiners, 1985  
Radiology, May 1988

**Licensure:** Connecticut

**Appointments:** Senior Attending/Active Staff, Radiology  
Saint Francis Hospital and Medical Center  
December 2000 to Present

Associate Attending Staff, Radiology  
Saint Francis Hospital and Medical Center  
1998 to 2000

Assistant Attending Staff, Radiology  
Saint Francis Hospital and Medical Center  
1990 to 1998

Clinical Instructor, Yale University  
July 1, 1995 to 2008

Assistant Clinical Professor,  
University of Connecticut School of Medicine  
1994 to Present

**Professional Organizations:** Hartford County Medical Society  
Radiological Society of Connecticut  
Radiological Society of North America  
American Medical Association (AMA)  
Phi Beta Kappa Society  
Connecticut Medical Society  
American Society of Neuroradiology (Senior Member)  
American College of Radiology  
Radiological Society of North America  
American College of Physician Executives  
Society of Cardiovascular Computed Tomography  
Society of Body CT and MR

**Committees:**

Quality Committee of the Board  
Saint Francis Hospital and Medical Center  
January 2011 – Present

Physician Recruitment Committee  
Saint Francis Hospital and Medical Center  
May 2010 – July 2011

Strategic Planning Committee Saint Francis Care and  
Saint Francis Hospital and Medical Center Board  
Directors  
April 2010 - Present

Medical Executive Committee (MEC)  
Saint Francis Hospital and Medical Center  
January 2009 - Present

Connecticut Brain Tumor Alliance Medical  
Advisory Board  
Board Member  
October 2008 - Present

Radiology Society of Connecticut Executive Committee  
February 2008 – Present

Stroke Center ED Subgroup  
Saint Francis Hospital and Medical Center  
January 2007 - 2008

Internal Chief's Meeting  
Saint Francis Hospital and Medical Center  
December 2006 – Present

Continuing Medical Education Committee  
Saint Francis Hospital and Medical Center  
January 2006 – Present

Clinical Resource Management Committee – Consultant  
Saint Francis Hospital and Medical Center  
January 2006 - Present

Quality & Patient Safety Committee  
Saint Francis Hospital and Medical Center  
2005 – 2010

**Committees:**

*(continued)*

Medical Affairs Committee (Board of Directors Committee)  
Saint Francis Hospital and Medical Center  
January 2005 – January 2006

Appointed to Medical Staff Council  
Saint Francis Hospital and Medical Center  
2004 - Present

MIRACLES Cabinet  
Medical/Dental Fund Raising Committee  
2004, 2005, 2010, 2011, 2012

Administrative (Stand-up) Committee  
February 2004 to December 2004

Chief's Forum  
Saint Francis Hospital and Medical Center  
February 2004 to Present

Council on Quality  
Saint Francis Hospital and Medical Center  
January 2004 to 2010

MIRACLES – Medical Staff Committee  
November 2002 to Present

Radiology Residency Education Committee  
University of Connecticut and Saint Francis Hospital and  
Medical Center  
2000 - 2011

Alternate to Medical Staff Council  
Saint Francis Hospital and Medical Center  
1998 - 2004

Trauma Advisory Group  
July 1998 -1999

Member, Hospital Committee on Graduate Medical  
Education for Radiology  
July 1994 to 2010

**Quality Projects:**

Kaizen - Initiative on PICC Lines  
March 2004 to Present

Kaizen - ER Quality Initiative  
November 2004 to Present

**Lectures:**

**Contemporary Stroke Imaging**

The Connecticut Society of Radiologic Technologists  
Quinnipiac University – North Haven Campus  
October 1, 2011

**Common and Uncommon Imaging Dilemmas  
Confronting Chiropractors**

CT Chiropractic Association  
May 26, 2010

**Stroke Imaging Diagnostic and Therapeutic  
Implications**

Connecticut Academy of Physician Assistants  
23<sup>rd</sup> Annual Charter Oak Conference  
Mystic Marriott Hotel & Spa, Groton, CT  
April 11, 2010

***Advances in Diagnostic Imaging***

Saint Francis Hospital and Medical Center Annual  
Incorporators Meeting  
Avon Old Farms Inn  
December 7, 2004

***Advances in Diagnostic Imaging***

North End Advisory Group  
Mount Sinai Campus  
November 8, 2004

***Neuroradiology Role in SFH Stroke Center***

Stroke Center Development Committee  
Saint Francis Hospital and Medical Center  
November 7, 2003

**Publications:**

Feeney, J., Jayaraman, V., Luk, S., Shapiro, D., Virk, M., Twohig, M. and Jacobs. L. Retrospective Review of the Costs of Routine Pelvic X-rays in a Trauma Setting. The American Surgeon, March 2011, Vol. 77:337-341

Arias-Camison, J. M., DeSilva, H. N., Panthagani, I., Twohig, M.T. and Bourque, M.D. Scrotal Abscess Mimicking Testicular Torsion in a Premature Infant. Connecticut Medicine, April 2009, 73(4):215-216

Wettstein, Diez, Twohig, Abourizk. The Role of Birth Injury and the Consequences of Inadequately Treated HypoGonadism in Long Standing Pan Hypo Pituitarism. Connecticut Medicine, 1996

Sandoz, Martinez, Kallet, Twohig. Pancreatic Tuberculosis. Connecticut Medicine, 1993; 63(9):531-534.

Twohig, M., Sze, G. AMR of Pediatric Spinal Tumors. In Edwards, M. (ed), Pediatric Magnetic Resonance Imaging, 1990

Sze, G., Twohig, M. A Neoplastic Disease of the Spinal Cord. Scott Atlas (ed), MRI of Brain and Spine. Raven Press, 1990.

**Presentations:**

Poster Presentation at Roentgen Society,  
New Orleans, LA  
May 1999

Poster Presentation at European Radiology Society Meeting. Erbay, Twohig. Agensis of the Internal Carotid Artery, The Role of CT Scan in Diagnosis, 1996.

**Michael Reynolds**

292 Scoville Hill Rd.  
Harwinton, CT 06791  
(860) 485-0307

**Professional Experience:**

***SAINT FRANCIS HOSPITAL AND MEDICAL CENTER, HARTFORD, CT***

**Assistant Director, Radiology / Imaging Services - May 2011 - Present**

Provide administrative and technical management assistance for the efficient supervision of Diagnostic Radiology Imaging Services, including: Diagnostic Radiography, Breast Center, CT Scan, MRI, Nuclear Medicine, Ultrasound, Interventional Angiography, Clerical/Business Service operations. Responsible for independent judgment/action in administrative matters and budget development and control. Assists in the development, interpretation and application of section policies and procedures in accordance with State, Local, Federal and other regulatory agencies (DEP, JCAHO, MQSA, OSHA, and ACR). Provide assistance in developing long range strategic plans supporting the Hospital and Department mission. Provide after hours coverage for emergent issues relating to assigned sections. Has responsibility for special projects as assigned by the Administrative Director. Assumes Department Head responsibilities in the absence of the Administrative Director.

**Supervisor, MRI - April 2009 - July 2012**

Perform MRI procedures. Responsible for the day-to-day operations of the MRI section. Worked closely with Administrative Director of Radiology and Radiologist to supervise and perform MRI examinations, contributing to the efficient operation of the department and promoting the philosophy, to ensure the quality and continuity of patient care. Provides direct patient care to all ages, particularly focusing on the adult patient.

**DIAGNOSTIC IMAGING OF SOUTHBURY**

**Staff MRI/CAT Scan Technologist - August 1999 - April 2009**

Perform MRI and CAT scan procedures. Responsible for all aspects of patient care within the scope of the technologist role. Other responsibilities include establishing new protocols, evaluating equipment for upgrades and new systems. Clinical student development, JCAHO accreditation and review of scheduled patients to ensure appropriate continuum of care.

**WATERBURY HOSPITAL**

**Per Diem Staff CAT Scan Technologist – October 2005 – April 2011**

Perform CAT Scan procedures. Responsible for all aspects of patient care. Obtaining pertinent clinical history, starting I.V. for contrast injections, selection of protocols, reviewing images for quality.



**BRISTOL HOSPITAL**

**Supervisor of Linen Services – July 1994 – April 1999**

Responsible for daily operations of a staff of 14. Development and implementation of policies and procedures. Maintaining and ordering inventory. Interviewing and evaluating staff members.

**Qualifications & Achievements:**

- Associates Degree in Radiologic Technology
- Connecticut State License – Radiographer
- ARRT Certified
- CPR Certified

**Education:**

Quinnipiac University, Hamden, CT  
Health and Science Administration BS  
Current

Naugatuck Valley Community College, Waterbury, CT  
Graduated Associate of Science 3.7 GPA - Radiologic Technology

Morse School of Business  
Certification in Business Management 3.8 CPA

Bristol Central High School, Bristol, CT  
Graduate 1987

Updated: 8/23/12

# **ATTACHMENT 6**

**STATE OF CONNECTICUT**

**Department of Public Health**

**License No. 0054**

**General Hospital**

In accordance with the provisions of the General Statutes of Connecticut Section 19a-493:

Saint Francis Hospital and Medical Center of Hartford, CT d/b/a Saint Francis Hospital and Medical Center is hereby licensed to maintain and operate a General Hospital.

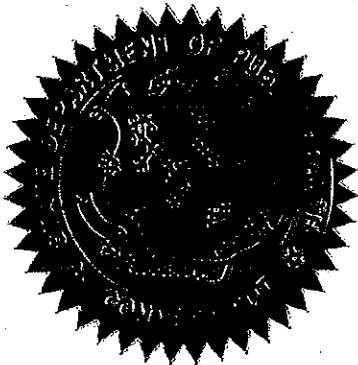
**Saint Francis Hospital and Medical Center** is located at 114 Woodland Street and 500 Blue Hills Avenue, Hartford, CT 06105.

The maximum number of beds shall not exceed at any time:

65 Bassinets

617 General Hospital Beds

This license expires **December 31, 2013** and may be revoked for cause at any time.  
Dated at Hartford, Connecticut, January 1, 2012. RENEWAL.



*Jewel Mullen*

Jewel Mullen, MD, MPH, MPA  
Commissioner

# **ATTACHMENT 7**



2012035 MRI RENOVATION PROJECT- PROPOSED PLAN



# **ATTACHMENT 8**



One Medrad Drive  
 Indianola, PA 15051-0780  
 Phone: (412) 767-2400  
 Fax: (412) 767-4120  
 www.medrad.com

**Quotation**

Quote No : 20141790

Page: 1 of 6  
 Date: 05/10/2012

Customer No: 1001178D

**Quote To:**  
 ST. FRANCIS HOSPITAL AND  
 MEDICAL CENTER  
 114 WOODLAND ST  
 HARTFORD CT 06105-1208

**Validity Period:** 05/10/2012 until 10/30/2013

**We deliver according to the following terms and conditions:**

**Currency:** USD

**Terms of payment:** Net 30 from date of invoice

**Terms of delivery:** Prepaid & Added FOB SHIPPING POINT

ATT: Michael Reynolds  
 MReynold@stfranciscare.org

Todd Rossman  
 Professional Sales Consultant  
 413-519-6094  
 todd.rossman@bayer.com

Item	Description	Qty	Unit Price	Extended Price
1	3012011 SPECTRIS SOLARIS EP MR INJECTOR	1EA	46,950.00	46,950.00
	% Discount			18,310.50-
	Net Value for Item			28,639.50
	<b>***GPO AFFILIATED PRICING</b>			
2	SSI 300 INSTALLATION, SPECTRIS SOLARIS MR INJECTOR	1EA	1,669.00	1,669.00

When applicable, State and Local taxes will be calculated on the order. If you are exempt from taxes, contact customer support at 1(800)633-7231  
 If pricing and terms of this order are based upon your current Group Purchasing Organization (GPO) affiliation, any change to your current affiliation may require a new quote or updated terms and pricing.

Please reference the quote number on your PO and fax to 412-767-4120 for domestic orders or 412-767-1312 for international orders





One Medrad Drive  
 Indianola, PA 15051-0780  
 Phone: (412) 767-2400  
 Fax: (412) 767-4120  
 www.medrad.com

Quote No: 20141790

Page: 2 of 6  
 Date: 05/10/2012

**Quote To:**

ST. FRANCIS HOSPITAL AND  
 MEDICAL CENTER  
 114 WOODLAND ST  
 HARTFORD CT 06105-1208

<b>Sub Total</b>	30,308.50
<b>Total</b>	30,308.50

**NOTE: If using signed quote as a purchase order please complete the following information:**

Print Name: \_\_\_\_\_

Signature: \_\_\_\_\_

Title: \_\_\_\_\_

PO #: \_\_\_\_\_

Phone #: \_\_\_\_\_

EXTENDED WARRANTY OPTIONS FOR SOLARIS:

DirectCARE Basic Solaris 1Yr WX

Extends the One Year Manufacturer's Warranty an additional one (1) year including one (1) annual on-site Predictive Maintenance (PM) in year two from 8 am to 5 pm Monday through Friday. All on-site Service is covered including travel and labor from 8 am to 5 pm Monday through Friday. 24x7 Technical Support available.

Part Number: DCB-SMRS-1W List Price \$5,624.00

**"Act Now" Price: \$4,218.00**

DirectCARE Basic Solaris 2Yr WX

Extends the One Year Manufacturer's Warranty an additional two (2) years including two (2) annual on-site Predictive Maintenance (PMs) in years two and three from 8 am to 5 pm Monday through Friday. All on-site Service is covered including travel and labor from 8 am to 5 pm Monday through Friday. 24x7 Technical Support available.

Part Number: DCB-SMRS-2W List Price \$11,585.00

**"Act Now" Price: \$8,436.00**

**When applicable, State and Local taxes will be calculated on the order. If you are exempt from taxes, contact customer support at 1(800)633-7231**

**If pricing and terms of this order are based upon your current Group Purchasing Organization (GPO) affiliation, any change to your current affiliation may require a new quote or updated terms and pricing.**

Please reference the quote number on your PO and fax to 412-767-4120 for domestic orders or 412-767-1312 for international orders

**200**



One Medrad Drive  
Indianola, PA 15051-0780  
Phone: (412) 767-2400  
Fax: (412) 767-4120  
www.medrad.com

Quote No: 20141790

Page: 3 of 6  
Date: 05/10/2012

**Quote To:**

ST. FRANCIS HOSPITAL AND  
MEDICAL CENTER  
114 WOODLAND ST  
HARTFORD CT 06105-1208

DirectCARE Basic Solaris 3Yr WX

Extends the One Year Manufacturer's Warranty an additional three (3) years including three (3) annual on-site Predictive Maintenance (PMs) in years two, three and four from 8 am to 5 pm Monday through Friday. All on-site Service is covered including travel and labor from 8 am to 5 pm Monday through Friday. 24x7 Technical Support available.

Part Number: DCB-SMRS-3W List Price \$17,904.00

**"Act Now" Price: \$12,654.00**

DirectCARE Basic Solaris 4Yr WX

Extends the One Year Manufacturer's Warranty an additional four (4) years including four (4) annual on-site Predictive Maintenance (PMs) in years two, three, four and five from 8 am to 5 pm Monday through Friday. All on-site Service is covered including travel and labor from 8 am to 5 pm Monday through Friday. 24x7 Technical Support available.

Part Number: DCB-SMRS-4W List Price \$24,602.00

**"Act Now" Price: \$16,872.00**

When applicable, State and Local taxes will be calculated on the order. If you are exempt from taxes, contact customer support at 1(800)633-7231

If pricing and terms of this order are based upon your current Group Purchasing Organization (GPO) affiliation, any change to your current affiliation may require a new quote or updated terms and pricing.

Please reference the quote number on your PO and fax to 412-767-4120 for domestic orders or 412-767-1312 for international orders



One Medrad Drive  
Indianola, PA 15051-0780  
Phone: (412) 767-2400  
Fax: (412) 767-4120  
www.medrad.com

Quote No: 20141790

Page: 4 of 6  
Date: 05/10/2012

#### MEDRAD PRODUCT TERMS AND CONDITIONS

If Customer is a member of a group purchasing organization ("GPO") who has a contract with MEDRAD, the terms of that GPO Agreement will supercede the terms herein.

1. **Modifications.** The prices and terms on this Quote are not subject to verbal changes or other agreements unless approved in writing by MEDRAD's Home Office.
2. **Acceptance.** MEDRAD's products and services are sold only under the terms and conditions stated on this quotation. Acceptance of any Purchase Order is expressly and exclusively made conditional on your assent to these terms and conditions. Any different or additional terms and conditions that may appear in your Purchase Order or any other document sent by you, shall have no effect. MEDRAD expressly objects to and rejects all inconsistent or additional terms, conditions and limitations contained on any of your forms or other writings. If you do not communicate your objection to these terms and conditions in writing and within a reasonable time, or if you accept the goods covered by this Quote, you will be deemed to have accepted these terms and conditions and they will control in all instances. If the Products include embedded software or if you are purchasing software, BY HAVING THE SOFTWARE INSTALLED AND USING THE SOFTWARE PURCHASED HEREUNDER, YOU AGREE TO BE BOUND BY THE TERMS OF THIS AGREEMENT. IF YOU DO NOT AGREE TO THE TERMS OF THIS QUOTE, DO NOT INSTALL OR USE THE SOFTWARE AND NOTIFY MEDRAD IMMEDIATELY.
3. **Pricing.** Prices are based on costs and conditions existing on the date of this Quote and may be changed by MEDRAD before final acceptance. The pricing for products provided pursuant to this Quote may reflect or be subject to discounts, rebates, or other price reduction programs. Please be advised that you are obligated to: a) fully and accurately disclose the amount of any such discounts, rebates, or other price reductions in your cost reports or claims for reimbursement to Medicare, Medicaid, or health care programs requiring such disclosure and b) provide such documentation to representatives of the Secretary of the Department of Health and Human Services and state agencies upon request. Unless noted otherwise, the value of any product listed as \$0.00 on this Quote may constitute a discount that you should evaluate when filing such reports. You may request additional information from MEDRAD in order to meet your reporting or disclosure obligations, by writing to the address set forth in this Quote. All payments are due net thirty (30) days on the total invoiced amount. For all new customers MEDRAD requires a thirty percent (30%) pre-payment for all capital equipment orders, unless otherwise agreed to by MEDRAD's Home Office. MEDRAD's Home Office must approve any payment terms other than net thirty (30) days.
4. **Shipping.** All shipping dates are tentative. MEDRAD will make every reasonable effort to meet shipping dates referenced in this Quote. However, MEDRAD will not be liable for its failure to meet any such date.
5. **Installation.** The cost of installation is not included in the product price and is your responsibility unless otherwise stated. For details on equipment installation, you should consult with your MEDRAD Sales Representative or refer to your Products Manual, which is included with your equipment.

If this Quote includes installation of an overhead counterpoise system (OCS) it is your responsibility to ensure a suitable mounting location for the system. The counterpoise ceiling plate is required to be installed prior to MEDRAD installation of the counterpoise system and installed in accordance with the specifications listed in the installation manual. The OCS ceiling plate should always be installed by a qualified Structural Engineer and/or Architect. In addition, if applicable building codes require the use of a conduit, you are responsible for ensuring that a conduit is available prior to MEDRAD's installation.

If this Quote includes a Certo wireless network it is your responsibility to ensure the approval of the Information Technology Department to allow the operation of the wireless network at your site.

If this Quote includes a Solaris with an Integrated Continuous Battery Charging System (ICBC), installation will require a standard power outlet in the scan room, or authorization to install a filter through the penetration panel.

6. **License.** If the Products include embedded software, or if you are purchasing software, MEDRAD grants to you a non-exclusive license to use

**Please reference the quote number on your PO and fax to 412-767-4120 for domestic orders or 412-767-1312 for international orders**



One Medrad Drive  
Indianola, PA 15051-0780  
Phone: (412) 767-2400  
Fax: (412) 767-4120  
www.medrad.com

Quote No: 20141790

Page: 5 of 6  
Date: 05/10/2012

such software provided by MEDRAD, solely in connection with, or to operate, the Products. Use of the software for any other purpose is strictly prohibited. This license is effective on the date you begin using the Products and software and will continue in effect unless you return the Products or software or if the license is terminated because you breach any provision of these Terms. Upon termination you shall immediately cease use of all software and shall return the Products and software to MEDRAD. The software copyright is owned by MEDRAD and is protected by United States copyright laws and international treaty provisions. MEDRAD does not transfer title to the software to you, but retains the rights to make and license the use of all copies. You shall not copy, translate, disassemble, or decompile nor create or attempt to create, by reverse engineering or otherwise, the source code from the object code of the software. You are not permitted to modify or make derivative works of the software and ownership of any unauthorized modification or derivative work shall vest in MEDRAD.

7. Warranty. MEDRAD warrants that all new MEDRAD products are free from defects in workmanship or material under proper, normal use and service for a period of one year (12 months) from shipment, unless a longer period is provided on the warranty with the products, or as otherwise provided herein.

MEDRAD warrants that all refurbished MEDRAD products shall perform in accordance with the documentation provided, under proper, normal use and service for a period of the shorter of a) 90 days from installation or b) six months from shipment, unless a longer period is provided on the warranty with the products, or as otherwise provided herein.

If this Quote includes an XDS unit which is sold as an upgrade to your existing Stellant unit, the warranty on the XDS will extend for the longer of: a) the warranty (including any extended warranty) on your existing Stellant unit or b) ninety (90) days from the date of installation, but not to exceed six months from the date of shipment.

If this Quote includes a Monitor, peripheral accessories on the Monitor such as pulse oximeter sensors, extension cables, power cables, fiber optic cables, ECG leads, capnography accessories (excluding patient connections), blood pressure cuffs, batteries, and extension tubing are warranted for a period of 90 days from the date of installation, but not to exceed six months from the date of shipment.

If this Quote includes disposable products or angiographic catheters, MEDRAD's warranty shall be limited to repair or replacement of any defective disposable product or angiographic catheter upon receipt of the defective product and a MEDRAD Return Goods Authorization. You acknowledge that the disposables and the equipment are a system and your actions regarding your equipment may invalidate your warranty on the disposables.

During the warranty period, there shall be no charge for any action deemed necessary by MEDRAD, including parts, travel, or labor to fulfill the terms of the warranty, during local business hours of 8:30 a.m. to 5:00 p.m., Monday through Friday, except holidays.

Your actions may invalidate this warranty. If MEDRAD determines that an equipment or disposable problem is due to any of the following, you agree to pay MEDRAD for all labor, travel, material handling and shipping at MEDRAD's, or MEDRAD's agents, standard rates:

- a) Malfunction or damage due to spillage of any type of fluid in or on the unit.
- b) Malfunction due to operator error, including failing to follow specified provisions of the Operations Manual.
- c) Malfunction or damage due to unauthorized modification or repair. Unauthorized actions may jeopardize functionality, reliability, or operator and patient safety. Therefore any unauthorized modification or repair shall render this warranty void and relieve MEDRAD from any further obligation. MEDRAD must review and authorize all modifications and repairs. This service may be obtained by contacting the MEDRAD Service Department.
- d) Malfunction or damage due to the use of non-MEDRAD or non-approved accessories. The use of accessories in connection with the equipment may jeopardize functionality, reliability or operator and patient safety. Therefore any use of non-MEDRAD or non-approved accessories (such as non-MEDRAD disposables or in the case of any PET/CT product, the use of vials or vial shields that are not approved by MEDRAD) shall render this warranty void and relieve MEDRAD from any further obligation.

Please reference the quote number on your PO and fax to 412-767-4120 for domestic orders or 412-767-1312 for international orders



One Medrad Drive  
Indianola, PA 15051-0780  
Phone: (412) 767-2400  
Fax: (412) 767-4120  
www.medrad.com

Quote No: 20141790

Page: 6 of 6  
Date: 05/10/2012

- e) Damage by fire, floods, or other disaster commonly known as "Acts of God".
- f) If the Products include any Counterpoise system, any system malfunction, damage or failures due to improper installation or not meeting MEDRAD's specific requirements for level and plumb and/or loading as specified in the MEDRAD manuals.
- g) If the Products include any Counterpoise system, any ceiling or wall support structure used to mount or support an Injector Head Counterpoise System is excluded from MEDRAD's warranty. MEDRAD does not in any way warrant such structure.

8. Warranty Exclusions. EXCEPT AS PROVIDED IN THE ABOVE WARRANTY SECTION, MEDRAD EXPRESSLY DISCLAIMS ALL WARRANTIES OR CONDITIONS OF ANY KIND, EXPRESS OR IMPLIED, INCLUDING WITHOUT LIMITATION, IMPLIED WARRANTIES OF MERCHANTABILITY, NONINFRINGEMENT AND FITNESS FOR A PARTICULAR PURPOSE (WHETHER OR NOT MEDRAD IS AWARE OF YOUR INTENDED USE OF THE PRODUCT), AND ALL SUCH WARRANTIES ARE EXPRESSLY EXCLUDED. IN NO EVENT SHALL MEDRAD BE LIABLE FOR ANY LOST PROFITS OR INCIDENTAL OR CONSEQUENTIAL DAMAGES ARISING OUT OF OR IN CONNECTION WITH THE USE OR OPERATION OF MEDRAD's PRODUCT OR SERVICE. Some states do not allow the exclusions on limitation of incidental or consequential damages, so the above limitations may not apply. This Limited Warranty gives you specific legal rights and you may also have other rights.

9. Software Warranty. If the Products include embedded software or if you are purchasing software, MEDRAD warrants that the software will substantially conform to the functional specifications contained in the Operations Manual for one year following delivery. This warranty shall not apply if you use the software in a manner that is not authorized or not in accordance with the user instructions or if you modify the Products or the software or if a party other than MEDRAD provides service to the Products or software. MEDRAD does not warrant that the software will operate uninterrupted or that it will be free from minor defects or errors that do not materially affect its performance. Your sole and exclusive remedy for any damages or loss in any way connected with the software whether due to MEDRAD's negligence or breach of any other duty shall be, at MEDRAD's option: i) to bring the performance of the software into substantial compliance with the functional specifications or ii) return of an appropriate portion of any payment by you with respect to the portion of the software that is not functioning.

10. Indemnification. MEDRAD agrees to indemnify, defend and hold you harmless from any liability, loss, expense, cost, claim or judgment (including attorneys fees), arising out of any claim for property damage, or personal injury or death where the product is alleged to have caused or contributed to the damage, injury or death, provided that this indemnification does not extend to injuries, damages or death to the extent caused by the negligence, reckless disregard or intentional acts of you or any third party.

11. Force Majeure. MEDRAD will not be responsible for delays or non-performance directly or indirectly caused by any acts of God, fire, explosion, flood, war, accident, action by governmental authority, inability to procure supplies and raw materials, delays in transportation, work stoppage, court order, and other causes beyond MEDRAD's reasonable control.

12. Compliance With Laws/Export. In addition to any rights and remedies specifically identified here in this Quote, MEDRAD shall have all rights and remedies conferred by law. MEDRAD shall not be required to perform its obligations under this Quote if you have defaulted (e.g. failed to pay) under this Quote or any other contract involving MEDRAD. This Agreement shall be construed in accordance with the laws of the Commonwealth of Pennsylvania, United States of America. You warrant that you are and will remain in compliance with all export and reexport requirements, laws and regulations of the United States of America and any other applicable export and reexport laws and regulations.

13. HIPAA. MEDRAD represents that it is not a Business Associate as defined in the Health Insurance Portability and Accountability Act ("HIPAA"). The functions MEDRAD is required to perform hereunder do not require the use or disclosure of Protected Health Information ("PHI"). To the extent any disclosure of PHI does occur, it is incidental and covered under the incidental disclosure rule found in 45 CFR 164.502(a)(1). In addition, to the extent any such incidental disclosure does occur, MEDRAD agrees to keep all such information confidential.

**Please reference the quote number on your PO and fax to 412-767-4120 for domestic orders or 412-767-1312 for international orders**

## Quotation

**HOLOGIC**<sup>™</sup>

The Women's Health Company

PLEASE REFER TO THIS NUMBER ON  
ALL CORRESPONDENCES AND ORDERS

Quote #: 179577

Buying Group: NONE

Status: Done

TO: Saint Francis Hospital & Medical Center  
114 Woodland St  
Hartford, CT 06105

We are pleased to offer you the products listed on the condition that this Quotation and the attached terms comprise the complete and exclusive statement of the contract between us. This Quotation is based on the information known by Hologic regarding your needs as of the date the Quotation is generated. This Quotation and the attached terms supersede all other quotations, agreements, understandings, warranties and representations, whether written or oral, between us, and may be accepted only in accord with their terms. This offer will remain open for 45 days after the quotation date unless otherwise specified, and is subject to change or withdrawal by Hologic prior to acceptance. To accept, please sign below within the time period for acceptance.

## TAX INFO:

Hologic is required by law to collect all state and local taxes on all sales. If an exemption certificate is not provided by customer at time of order, final invoices will include these amounts. Many states require both specific operator qualifications and/or licensing and registration of x-ray devices. Hologic is not responsible for fulfilling customer's regulatory obligations.

Signed quote and/or purchase order should be forwarded by mail, via e-mail or by fax to:

Skeletal Health (DXA & Mini-C):	Breast Health:	Interventional Breast Solutions (Suros):
HOLOGIC, INC.	HOLOGIC, INC.	HOLOGIC, INC.
35 Crosby Drive	36 Apple Ridge Road	6100 Technology Center Drive
Bedford, MA 01730	Danbury, CT 06810	Indianapolis, IN 46278
ATTN: Sales Administration	ATTN: Sales Administration	ATTN: Sales Administration
Fax: (781) 280-0668	Fax: (203) 731-8463	Fax: (317) 344-7690
Bed-SalesAdmin@hologic.com	Danburyorders@hologic.com	allfieldservicecoordinators@hologic.com

ATTN: Mike Reynolds

Phone: 8607144518

Fax:

Email: mreynold@stfranciscare.org

Quote Date	Hologic Representative	Payment Terms	FOB	Est. Del. Date
May 23, 2012	Elizabeth Dermody Elizabeth.Dermody@hologic.com	Net 30	FACTORY, PREPAID & ADDED	90-120 Days ARO
Qty	Product Model Number and Description	List Price (US\$/Unit)	Unit Price (US\$/Unit)	Extended Price (US\$)
1	PRD-01364 - Sentinelle Breast MRI Tabletop for Siemens Avanto (1.5T, 16Ch) * Coils for both Diagnostic and Interventional Imaging * 16 Channel System * Head Rest with mirror * Surgical grade visco-elastic foam padding * 10 Sterile Biopsy Grids * 2 Days of Applications Training * 1 Year Warranty (as per Hologic Terms and Conditions)	\$118,000.00	\$96,000.00	\$96,000.00
1	4000474-51 - Sentinelle Breast MRI Tabletop Companion Cart Sentinelle Breast MRI Tabletop Companion Cart * Storage * Biopsy Tray * Coil Transfer	\$5,000.00	\$5,000.00	\$5,000.00
1	Trade in of Invivo Breast Coil (7 Ch) - Trade in of Invivo Breast Coil (7 Ch) Trade in of Invivo Breast Coil (7 Ch)	(\$10,000.00)	(\$10,000.00)	(\$10,000.00)
<b>Equipment Total:</b>				<b>\$91,000.00</b>
<b>List Price Total:</b>				<b>\$113,000.00</b>
<b>Discount:</b>				<b>(\$22,000.00)</b>
<b>Final Quote Price:</b>				<b>\$91,000.00</b>

## Notes:

Freight charges are prepaid and added to the invoice.

The buyer is responsible for any additional cost that may accrue as a result of special delivery requirements and handling costs incurred at time of delivery.

## Estimated Optional Lease Pricing Available:

Qty	Product	Monthly Payment (60 months)
1	PRD-01364 - Sentinelle Breast MRI Tabletop for Siemens Avanto (1.5T, 16Ch)	Equipment & Options: \$1,933.48

Assuming you are eligible to lease 100% of the proposed equipment on a five-year basis, these figures are your estimated monthly payments, subject to current rate and credit approval. Contact your local sales agent or call Patrick Dawkins, Lease/Financing Manager for Hologic, at (508)263-8414 or e-mail: hologicleasing@hologic.com

*Hologic may request new customers and established customers to complete our credit application to create or update current credit files. This requirement will be contingent on order amount and prior history with Hologic.*

This Quote is not entered into, pursuant to, or in connection with any group purchasing arrangement of which Customer or Hologic is a party, and is not intended to result in the reporting of sales or the payment of administrative fees to any group purchasing organization. In no event will Hologic be obligated to pay administrative fees to a group purchasing organization, integrated delivery network, or other entity with respect to any single purchase order by Customer under this Quote.

The customer agrees to treat all quoted and sales information as confidential and not to disclose it to any third party other than required by law.

**Buyer Acceptance:**

Saint Francis Hospital & Medical Center

By: \_\_\_\_\_ (signature)

Name and Title: \_\_\_\_\_ (print/type)

Date: \_\_\_\_\_

**Additional Buyer Acceptance (if applicable):**

By: \_\_\_\_\_ (signature)

Name and Title: \_\_\_\_\_ (print/type)

Date: \_\_\_\_\_

**Please provide the Shipping and Billing address here if different from the quote address above  
(If this section is left blank, the product will ship and bill to the address printed at the top)**

Shipping Address: \_\_\_\_\_ Billing Address: \_\_\_\_\_

\_\_\_\_\_

\_\_\_\_\_

\_\_\_\_\_

\_\_\_\_\_

Hologic Approval: John P. Kennedy

Date: May 24, 2012



Invivo Corporation  
 3650 NE 53rd Avenue  
 Gainesville, FL 32609  
 Tel :1-877-INVIVO1  
 Fax :1-352-264-3432

REPRINT

Quote Date : 08/23/2012	Page 1 / 7	Quote Number : 2300282873
----------------------------	---------------	------------------------------

Expiration Date 10/23/2012	
-------------------------------	--

Payment Terms:  
Net 30 Days

## Formal Quote

Shipto: 94020512  
 St Francis Hospital & Medical Ctr  
 114 Woodland St  
 HARTFORD CT 06105-1208  
 UNITED STATES

Quote Contact : Stephanie Giuca  
 Lead Sales Agent :Greg Kingsley  
 Telephone Number :1-877-INVIVO1  
 Fax Number:1-352-264-3432

Sold to : 94020512  
 St Francis Hospital & Medical Ctr  
 114 Woodland St  
 HARTFORD CT 06105-1208  
 UNITED STATES

Customer:  
 St Francis Hospital & Medical Ctr  
 114 Woodland St  
 HARTFORD CT 06105-1208  
 UNITED STATES

Special Comments:

Customer Number: 94020512

Federal EIN: 13-3429115

Incoterms: FOB FACTORY

Item	Article - type number/ description	Quantity	Unit	Unit price	Total amount (USD)
0010	865214 Expression MRI Patient Monitor 000000000000865214	1.000	PCE	15,000.00	15,000.00
	A01 Accessories Kit	1.000		0.00	0.00
	C02 Network Channel B	1.000		0.00	0.00
	D01 DCU with Printer	1.000		14,500.00	14,500.00
	D02 DCU Without Printer	1.000		12,000.00	12,000.00
	G01 WPU with Agents	1.000		10,000.00	10,000.00
	M01 Rolling Pedestal	1.000		51,000.00	51,000.00
	P01 WPU with IBP	1.000		7,000.00	7,000.00
	T01 WPU with Temperature	1.000		15,000.00	15,000.00
	Agreement Discount			29.000- %	31,755.00-
	Net Value w/out Exp Ship Chg				77,745.00

Expression is specifically designed to withstand demanding environments with strong magnetic fields, Expression delivers the highest quality results, increased patient comfort and safety, and improved productivity with a lifetime of reliability.

WIRELESS TECHNOLOGY IMPROVES EFFICIENCY AND REDUCES DOWNTIME





REPRINT

Invivo Corporation  
 3650 NE 53rd Avenue  
 Gainesville, FL 32609  
 Tel :1-877-INVIVO1  
 Fax :1-352-264-3432

Quote date : 08/23/2012	Page 2 / 7	Quote number : 2300282873
Expiration Date 10/23/2012		
Payment Terms: Net 30 Days		
<b>Formal Quote</b>		

Item	Article - type number/ description	Quantity	Unit	Unit price	Total amount (USD)
------	------------------------------------	----------	------	------------	--------------------

Expression features Invivo's industry-exclusive direct wireless technology makes it easy to move the patient from room to room, expediting patient management and workflow in the MRI suite. Wireless technology helps increase patient comfort and safety too. Shorter cables reduce the risk of cable heating by reducing the potential for creating loops and are less prone to damage reducing replacement costs.

A lot of hard thought went into Expression to make your work easier. That's why you'll find an Electrode Fail Indicator that immediately notifies you if an electrode loses connection with the patient, so you can quickly identify the source of a lead failure during a scan. Wireless SpO2 monitoring that uses a digital signal to ensure precise values for saturation, low and high perfusion, and motion. And trend arrows that instantly provide a visual representation of vital signs trends so physicians can assess the patient's history while also monitoring live readings.

The Expression can be combined with the optional Invivo Essential to provide continuous monitoring through the entire process. Essential helps you create a more satisfying patient experience, Introduces new opportunities in patient monitoring, and makes better use of your human and financial resources.

- " Wireless 2.4 GHz Dual Lead ECG Enabled
- " Wireless 2.4GHz Pulse Oximetry Enabled
- " Non Invasive Blood Pressure Enabled
- " End Tidal CO2 Enabled
- " 3.0 Tesla capable
- " 2.4GHz Wireless Color Display
- " Advanced ECG Filters
- " Active Trend Arrows
- " 360 Degree Alarm Light
- " 8 Hour Smart Battery Technology
- " Express Service Enabled
- " All parameters support Adult, Pediatric and Neonatal patients
- " One (1) year limited warranty and factory service for hardware will be provided by your Invivo/Philips support team.



REPRINT

Invivo Corporation  
 3650 NE 53rd Avenue  
 Gainesville, FL 32609  
 Tel :1-877-INVIVO1  
 Fax :1-352-264-3432

Quote date : 08/23/2012	Page 3 / 7	Quote number : 2300282873
Expiration Date 10/23/2012		
Payment Terms: Net 30 Days		
<b>Formal Quote</b>		

Item	Article - type number/ description	Quantity	Unit	Unit price	Total amount (USD)
0020	866049 Expression MRI Accessories 000000000000866049	1.000	PCE	550.00	550.00
	S14 SpO2 Module and Cable	1.000		3,640.00	3,640.00
	S12 Pediatric SpO2 Accessories	1.000		380.00	380.00
	S11 Adult SpO2 Accessories	1.000		235.00	235.00
	P11 Power Accessories	1.000		1,490.00	1,490.00
	N14 NIBP Hose	1.000		95.00	95.00
	N12 Pediatric NIBP Accessories	1.000		615.00	615.00
	N11 Adult NIBP Accessories	1.000		550.00	550.00
	E14 ECG Module and Gel	1.000		2,000.00	2,000.00
	E12 Pediatric ECG Accessories	1.000		1,410.00	1,410.00
	E11 Adult ECG Accessories	1.000		1,560.00	1,560.00
	D11 CRD Printer Paper	1.000		50.00	50.00
	A14 Agent/EtCO2 H2O Trap&Line	1.000		750.00	750.00
	A12 Pedi Agents/EtCO2 Acces	1.000		470.00	470.00
	A11 Adult Agents/EtCO2 Acces	1.000		550.00	550.00
	Agreement Discount			12.000- %	1,655.40-
	Special Discount			13.000- %	1,793.35-
	Net Value w/out Exp Ship Chg				10,346.25
0030	989803162531 Body Temp Probe (box 10) 000000989803162531	1.000	PCE	490.00	490.00
	Agreement Discount			12.000- %	58.80-
	Special Discount			13.000- %	63.70-
	Net Value w/out Exp Ship Chg				367.50
0040	989803179251 Ferroguard Patient Screener 000000989803179251	1.000	PCE	17,998.94	17,998.94
	Special Discount			25.000- %	4,499.74-
	Net Value w/out Exp Ship Chg				13,499.20
	Ferroguard Patient Screener				
	Ferroguard - Patient Screener (includes 1 x Wall Mounted Ferroguard				



REPRINT

Invivo Corporation  
3650 NE 53rd Avenue  
Gainesville, FL 32609  
Tel :1-877-INVIVO1  
Fax :1-352-264-3432

Quote date :

08/23/2012

Page

4 / 7

Quote number :

2300282873

Expiration Date

10/23/2012

Payment Terms:

Net 30 Days

## Formal Quote

Item	Article - type number/ description	Quantity	Unit	Unit price	Total amount (USD)
------	------------------------------------	----------	------	------------	--------------------

screeener pole; Wall-affixed configuration)

<b>Total Gross Value</b>	141,783.94
<b>Discount Amount</b>	39,825.99-
<b>Net Value w/out Exp Ship Chg</b>	101,957.95
<b>Total</b>	<b>101,957.95</b>



REPRINT

Invivo Corporation  
 3650 NE 53rd Avenue  
 Gainesville, FL 32609  
 Tel :1-877-INVIVO1  
 Fax :1-352-264-3432

Quote Date 08/23/2012	Page 5 / 7	Quote number : 2300282873
Expiration Date 10/23/2012		
Payment Terms: Net 30 Days		
<b>Formal Quote</b>		

Item	Article - type number/ description	Quantity	Unit	Unit price	Total amount (USD)
------	------------------------------------	----------	------	------------	--------------------

**INVIVO CORPORATION TERMS AND CONDITIONS OF SALE**

The products and services listed in the quotation are offered by Invivo Corporation ("Invivo") only under the terms and conditions described below.

1. Taxes. The purchase price stated in the quotation does not include applicable sales, excise, use, or other taxes in effect or later levied. Unless Customer provides Invivo with an appropriate exemption certificate reasonably in advance of the date the product is available for delivery, Invivo shall invoice Customer for those taxes, and Customer shall pay those taxes in accordance with the terms of the invoice.

2. Standard Payment Terms.

2.1. 100% of the Purchase Price shall be due thirty days from Invivo's invoice date.

2.2. Orders are subject to Invivo's on-going credit review and approval.

2.3. Customer shall pay interest on any amount not paid when due at the rate of 1% per month (12.86% per annum) or the highest permissible rate under applicable laws, whichever is less. If Customer fails to pay any amount when due, in addition to any other rights or remedies available to Invivo at law or in equity, Invivo may discontinue the performance of services, discontinue the delivery of the product, or deduct the unpaid amount from any amounts otherwise owed to Customer by Invivo under any agreement with Customer. In any action initiated to enforce the terms of the quotation following a Customer default, Invivo shall be entitled to recover as part of its damages all costs and expenses, including reasonable attorneys' fees, in connection with such action.

2.4. Credit Card. Invivo, at its discretion, will accept a credit card for payment on orders with a net value of \$50,000 or less.

3. The Quote.

3.1. The quotation is subject to change or withdrawal prior to written acceptance by Customer. All purchase orders issued by Customer are subject to acceptance by Invivo. If Buyer postpones delivery beyond the date specified on the face of the quotation, the prices will be subject to renegotiation. If no agreement is reached, the price shall be the price in effect at the time of shipment.

3.2. All sales are final. In the event the Company agrees to accept a return of merchandise, Buyer must first receive a Returned Goods Authorization ("RGA"). If an RGA is issued, Buyer is responsible for all costs associated with the return. Returns will be subject to a 15% restocking fee.

4. Trade - In. If Customer will be trading-in any equipment ("Trade-In"), then:

4.1. Customer represents and warrants that Customer has good and marketable title to such Trade-In;

4.2. Title to the Trade-In shall pass from Customer to Invivo upon Invivo making the new equipment available for first patient use. Removal of the Trade-In from Customer's site shall occur no later than the date Invivo makes the new product available for first patient use, unless otherwise agreed in writing between Invivo and the Customer; and

4.3. Notwithstanding anything to the contrary in any Business Associate Addendum ("BAA"), Customer represents and warrants that Customer has removed or de-identified all Protected Health Information ("PHI") from the Trade-In equipment as of the date the equipment is removed. To the extent Customer has not done so, Customer agrees to reimburse Invivo for any out-of-pocket costs Invivo incurs to remove or de-identify PHI from the Trade-In.

4.4. If (a) the condition of the Trade-In is not substantially the same when Invivo removes the Trade-In (ordinary wear and tear excepted) as it was when Invivo quoted the Trade-In value; or, (b) Customer delays the removal of the Trade-In, then Invivo may reduce the price quoted for such Trade-In or cancel the Trade-In and Customer will pay the adjustment amount within thirty (30) days of receipt of invoice.

4.5. If Invivo does not receive possession of the Trade-In, Invivo will charge Customer, and Customer will pay within thirty (30) days of receipt of invoice, the amount of the Trade-In allowance.

4.6. Evidence that Customer intends to trade in an asset as part of the purchase or lease of any product(s) shall be in the form of: (a) receiving a trade in quote and/or authorization from Invivo on the value of the asset to be traded in; (b) providing Invivo with serial numbers of assets to be traded in; and/or, (c) providing Invivo with a de-installation date to remove an existing asset in order to install Invivo's quoted equipment.

5. Security Interest. Customer hereby grants to Invivo a purchase money security interest in the products until all payments have been made. Customer shall sign any financing statements or other documents necessary to perfect Invivo's security interests in the products. Where permitted by applicable law, Customer's signature on the quotation or on a purchase order issued as a result of the quotation gives Invivo the right to sign on Customer's behalf and file any financing statement or other documents to perfect Invivo's security interest in the product.

6. Delivery.

6.1. Title to any product (excluding software), and the risk of loss or damage to any product shall pass to the Customer F.O.B. Factory - Freight to destination prepaid and added to invoice.

6.2. Claims for merchandise, defective shipping cartons, or missing cartons should be filed within 48 hours by the Customer with Invivo's Customer Service Department. Prior to the shipment of any product, Invivo may change the construction or the design of the product without notice to the Customer as long as the function, footprint, and performance of the product is not substantially altered.

6.3. Invivo will use reasonable efforts to ship the product to the Customer (i) by the mutually agreed upon shipment date, (ii) by the date stated in the quotation, or (iii) as otherwise agreed in writing. Invivo will ship the product according to Invivo's standard commercial practices.

7. Installation.  
 Customer shall (when applicable): 10.1. (i) provide Invivo with a secure location at Customer's premises to store one Invivo remote services network router (or a Customer-owned router acceptable to Invivo at Customer's option) for connection to the Equipment; and (ii) at all times during the warranty period specified in this Agreement provide Invivo with a dedicated broadband Internet access node, including but not limited to public and private interface access, suitable for connection to Customer's network for Invivo use in remote servicing of the product.

8. Product Warranty.

8.1. In addition to the limited warranties stated herein, Invivo may provide limited product-specific warranties that are set forth in separate Invivo warranty documents incorporated herein by reference.

8.2. Subject to the product-specific warranties, and except as otherwise stated therein or except for equipment manufactured in compliance with design or specifications of Customer, Invivo warrants to Customer that the Invivo equipment will perform in substantial compliance with its performance specifications for a period as set forth below from the date of original delivery.

**STANDARD PRODUCT WARRANTY PERIODS**

Patient Monitoring Equipment - One (1) year, part and factory repair labor  
 MRI Coils - Three (3) years, parts and factory repair labor  
 DynaCAD - One (1) year, parts and factory repair labor,  
 Parts and Accessories - Ninety (90) days, replacement Supplies  
 Consumable Items and repaired product - Thirty (30) days, replacement

8.3. Invivo's sole obligations and Customer's exclusive remedy under any product warranty are limited, at Invivo's option, to the repair or the replacement of the product or a portion thereof, or to a credit or refund of a portion of the purchase price paid by Customer. Warranty service outside of normal working hours (i.e., 8:00 A.M. to 5:00 P.M., Monday through Friday, excluding Invivo's observed holidays), will be subject to payment by Customer at Invivo's standard service rates.

8.4. This warranty is subject to the following conditions: the product (a) where applicable, is to be installed by authorized Invivo representatives (or is to be installed in accordance with all Invivo installation instructions by personnel trained by Invivo), (b) is to be operated exclusively by duly qualified personnel in a safe and reasonable manner in accordance with Invivo's written instructions and for the purpose for which the products were intended, (c) is to be maintained and in strict compliance with all recommended and scheduled maintenance instructions provided with the product; and Customer is to notify Invivo immediately if the product at any time fails to meet its printed performance specifications. Invivo's obligations under any product warranty do not apply to any product defects resulting from improper or inadequate maintenance or calibration by the Customer or its agents; Customer or third party supplied interfaces, supplies, or software including without limitation loading of operating system patches to the Licensed Software and/or upgrades to anti-virus software (except DAT file changes) running in connection with the Licensed Software without prior validation approval by Invivo; use or operation of the product other than in accordance with Invivo's applicable product specifications and written instructions; abuse, negligence, accident, loss, or damage in transit; improper site preparation; unauthorized maintenance or modifications to the product; or viruses or similar software interference resulting from connection of the product to a network. Invivo does not provide a warranty for any third party products furnished to Customer by Invivo under the quotation; however, Invivo shall use reasonable efforts to extend to Customer the third party warranty for the product. The obligations of Invivo described herein and in the applicable product-specific warranty document are Invivo's only obligations and Customer's sole and exclusive remedy for a breach of a product warranty.

8.5. THE WARRANTIES SET FORTH HEREIN AND (IF APPLICABLE) IN INVIVO'S WARRANTY DOCUMENT WITH RESPECT TO A PRODUCT (INCLUDING THE SOFTWARE PROVIDED WITH THE PRODUCT) ARE ONLY WARRANTIES MADE BY INVIVO IN CONNECTION WITH THE PRODUCT, THE SOFTWARE, AND THE TRANSACTIONS CONTEMPLATED BY THE QUOTATION, AND ARE EXPRESSLY IN LIEU OF ANY OTHER WARRANTIES, WHETHER WRITTEN, ORAL, STATUTORY, EXPRESS OR IMPLIED, INCLUDING, WITHOUT LIMITATION, ANY WARRANTY OF NON-INFRINGEMENT, MERCHANTABILITY OR FITNESS FOR A PARTICULAR PURPOSE. Invivo may use refurbished parts in the manufacture of the products which are subject to the same quality control procedures and warranties as for new products.

9. Patent Infringement Claims.

9.1. Invivo shall indemnify, defend, and hold harmless Customer against any new claim that a Invivo Product provided in the quotation infringes, misappropriates, or violates any third party intellectual property right, whether patent, copyright, trademark, or trade secret, provided that Customer: (a) provides Invivo prompt written notice of the claim; (b) grants Invivo full and complete information and assistance necessary for Invivo to defend, settle, or avoid the claim; and (c) gives Invivo sole control of the defense or settlement of the claim.

9.2. The provisions of this section shall not apply if the product is sold or transferred.

9.3. If (a) an Invivo Product is found or believed by Invivo to infringe such a claim; or, (b) Customer has been enjoined from using the Invivo Product pursuant to an injunction issued by a court of competent



REPRINT

Invivo Corporation  
 3650 NE 53rd Avenue  
 Gainesville, FL 32609  
 Tel :1-877-INVIVO1  
 Fax :1-352-264-3432

Quote date : 08/23/2012	Page 6 / 7	Quote number : 2300282873
Expiration Date 10/23/2012		
Payment Terms: Net 30 Days		
<b>Formal Quote</b>		

Item	Article - type number/ description	Quantity	Unit	Unit price	Total amount (USD)
------	------------------------------------	----------	------	------------	--------------------

jurisdiction, Invivo may, at its option: (i) procure the right for Customer to use the product; (ii) replace or modify the product to avoid infringement; or (iii) refund to Customer a portion of the product purchase price upon the return of the original product. Invivo shall have no obligation for any claim of infringement arising from: Invivo' compliance with Customer's designs, specifications, or instructions; Invivo' use of technical information or technology supplied by Customer; modifications to the product by Customer or its agents; use of the product other than in accordance with the product specifications or applicable written product instructions; use of the product with any other product; if infringement would have been avoided by the use of a current unaltered release of the products; or use of the Invivo Product after Invivo has advised Customer, in writing, to stop use of the Invivo Product in view of the claimed infringement. Invivo will not be liable for any claim where the damages sought are based directly or indirectly upon the quantity or value of products manufactured by means of the products purchased under this quotation, or based upon the amount of use of the product regardless of whether such claim alleges the product or its use infringes or contributes to the infringement of such claim. The terms in this section state Invivo' entire obligation and liability for claims of infringement, and Customer's sole remedy in the event of a claim of infringement.

10. Limitation of Liability.  
 10.1. The total liability, if any, of Invivo and its affiliates for all damages and based on all claims, whether arising from breach of contract, breach of warranty, negligence, indemnity, strict liability or other tort, or otherwise arising from a product, licensed software, and/or service is limited to the price paid hereunder for the product, licensed software, or service.  
 THIS LIMITATION SHALL NOT APPLY TO:  
 (a) THIRD PARTY CLAIMS FOR BODILY INJURY OR DEATH CAUSED BY INVIVO' NEGLIGENCE OR PROVEN PRODUCT DEFECT;  
 (b) CLAIMS OF TANGIBLE PROPERTY DAMAGE REPRESENTING THE ACTUAL COST TO REPAIR OR REPLACE PHYSICAL PROPERTY DAMAGE;  
 (c) INVIVO OBLIGATIONS UNDER SECTION 11 (INFRINGEMENT CLAIMS);  
 (d) OUT OF POCKET COSTS INCURRED BY CUSTOMER TO PROVIDE PATIENT NOTIFICATIONS, REQUIRED BY LAW, TO THE EXTENT SUCH NOTICES ARE CAUSED BY INVIVO UNAUTHORIZED DISCLOSURE OF PHI,  
 (e) FINES/PENALTIES LEVIED AGAINST CUSTOMER BY GOVERNMENT AGENCIES CITING INVIVO UNAUTHORIZED DISCLOSURE OF PHI AS THE BASIS OF LEVING SUCH FINE/PENALTY AGAINST CUSTOMER. ANY SUCH FINES OR PENALTIES SHALL CONSTITUTE DIRECT DAMAGES

10.2. IN NO EVENT SHALL INVIVO OR ITS AFFILIATES BE LIABLE FOR ANY INDIRECT, PUNITIVE, INCIDENTAL, CONSEQUENTIAL, OR SPECIAL DAMAGES, INCLUDING WITHOUT LIMITATION, LOST REVENUES OR PROFITS, BUSINESS INTERRUPTION, LOSS OF DATA, OR THE COST OF SUBSTITUTE PRODUCTS OR SERVICES WHETHER ARISING FROM BREACH OF THE TERMS IN THE CONTRACT, BREACH OF WARRANTY, NEGLIGENCE, INDEMNITY, STRICT LIABILITY OR OTHER TORT.

11. Confidentiality. Each party shall maintain as confidential any information furnished or disclosed to one party by the other party, whether disclosed in writing or disclosed orally, relating to the business of the disclosing party, its customers and/or its patients, and the quotation and its terms, including the pricing terms under which Customer has agreed to purchase the products. Each party shall use the same degree of care to protect the confidentiality of the disclosed information as that party uses to protect the confidentiality of its own information, but in no event less than a reasonable amount of care. Each party shall disclose such confidential information only to its employees having a need to know such information to perform the transactions contemplated by the quotation. The obligation to maintain the confidentiality of such information shall not extend to information that (a) is or becomes generally available to the public without violation of this Agreement or any other obligation of confidentiality or (b) is lawfully obtained by the receiving Party from a third party without any breach of confidentiality or violation of law.

12. Compliance with Laws.  
 12.1 Each party shall comply with all laws, rules, and regulations applicable to the party in connection with the performance of its obligations in connection with the transactions contemplated by the quotation, including, but not limited to, those relating to affirmative action, fair employment practices, FDA, Medicare fraud and abuse, and the Health Insurance Portability and Accountability Act of 1996 ("HIPAA"). Health care providers are reminded that if the purchase includes a discount or loan, they must fully and accurately report such discount or loan on cost reports or other applicable claims for payment submitted under any federal or state health care program, including but not limited to Medicare and Medicaid, as required by federal law (see 42 CFR 1001.952(H)). 12.2 It is Customer's responsibility to notify Invivo if any portion of the order is funded under the American Reinvestment and Recovery Act ("ARRA"). To ensure compliance with the ARRA regulation, Customer shall include a clause stating that the order is funded under ARRA on its purchase order or other document issued by Customer.

13. Excluded Provider. Invivo represents and warrants that Invivo, its employees and subcontractors, are not debarred, excluded, suspended or otherwise ineligible to participate in a federal health care program, nor have they been convicted of any health care related crime for the products and services provided under this Agreement (an "Excluded Provider"). Invivo shall promptly notify Customer when it becomes aware that Invivo or any of its employees or subcontractors providing services hereunder have become an Excluded Provider, whereupon Customer may terminate this order by express written notice for products and services not yet shipped or rendered.

14. General Terms. The following additional terms shall be applicable to the purchase of a product:  
 14.1. Force Majeure. Each party shall be excused from performing its obligations (except for payment obligations) arising from any delay or default caused by events beyond its reasonable control including, but not limited to, acts of God, acts of third parties, acts of any civil or military authority, fire, floods, war, embargoes, labor disputes, acts of sabotage, riots, accidents, delays of carriers, subcontractors or suppliers, voluntary or mandatory compliance with any government act, regulation or request, shortage of labor, materials or manufacturing facilities.  
 14.2 Bankruptcy. If Customer becomes insolvent, is unable to pay its debts when due, files for bankruptcy, is the subject of involuntary bankruptcy, has a receiver appointed, or has its assets assigned, Invivo may cancel any unfulfilled obligations, or suspend performance; however, Customer's financial obligations to Invivo shall remain in effect.  
 14.3 Assignment. Customer may not assign any rights or obligations in connection with the transactions contemplated by the quotation without the prior written consent of Invivo, which consent shall not be unreasonably withheld, and any attempted assignment without such consent shall be of no force or effect.  
 14.4 Export. Customer shall assume sole responsibility for obtaining any required export authorizations in connection with Customer's export of the products from the country of delivery.  
 14.5 Governing Law. All transactions contemplated by the quotation shall be governed by the laws of the state where the equipment will be installed, without regard to that state's choice of law principles, and expressly excluding application of the Uniform Computer Information Transactions Act ("UCITA"), in any form. EACH PARTY, KNOWINGLY AND AFTER CONSULTATION WITH COUNSEL, FOR ITSELF, IT'S SUCCESSORS' AND ASSIGNS, WAIVES ALL RIGHT TO TRIAL BY JURY OF ANY CLAIM ARISING WITH RESPECT TO THIS AGREEMENT OR ANY MATTER RELATED IN ANY WAY THERETO.  
 14.6 Entire Agreement. These Terms and Conditions of Sale, the terms and conditions set forth in the quotation and the applicable Invivo' product-specific warranty constitute the entire understanding and agreement by and between the parties with respect to the transactions contemplated by the quotation, and supersede any previous understandings or agreements between the parties, whether written or oral, regarding the transactions contemplated by the quotation. The pricing in the quotation is based upon the terms and conditions in the quotation. No additional terms, conditions, consents, waivers, alterations, or modifications shall be binding unless in writing and signed by the parties. Customer's additional or different terms and conditions, whether stated in a purchase order or other document issued by Customer, are specifically rejected and shall not apply to the transactions contemplated by the quotation.  
 14.7 Headings. The headings in the quotation are intended for convenience only and shall not be used to interpret the quotation.  
 14.8 Severability. If any provision of the quotation is deemed to be illegal, unenforceable, or invalid, in whole or in part, the validity and enforceability of the remaining provisions shall not be affected or impaired, and shall continue in full force and effect.  
 14.9 Notices. Notices or other communications shall be in writing, and shall be deemed served if delivered personally, or if sent by facsimile transmission, by overnight mail or courier, or by certified mail, return receipt requested and addressed to the party at the address set forth in the quotation.  
 14.10. Performance. The failure of Customer or of Invivo at any time to require the performance of any obligation will not affect the right to require such performance at any time thereafter. Course of dealing, course of performance, course of conduct, prior dealings, usage of trade, community standards, industry standards, and customary standards and customary practice or interpretation in matters involving the sale, delivery, installation, use, or service of similar or dissimilar products or services shall not serve as references in interpreting the terms and conditions of the quotation.  
 14.11. Obligations. Customer's obligations are independent of any other obligations the Customer may have under any other agreement, contract, or account with Invivo. Customer will not exercise any right of offset in connection with the terms and conditions in the quotation or in connection with any other agreement, contract, or account with Invivo.

15. Licensed Software.  
 15.1. License Grant.  
 15.1.1 Subject to any usage limitations for the Licensed Software set forth on the product description of the quotation, Invivo grants to Customer a nonexclusive and non-transferable right and license to use the computer software package ("Licensed Software") in accordance with the terms of the quotation. The License shall continue for as long as Customer continues to own the product, except that Invivo may terminate the License if Customer is in breach or default. Customer shall return the Licensed Software and any authorized copies thereof to Invivo immediately upon expiration or termination of this License.  
 15.1.2 The License does not include any right to use the Licensed Software for purposes other than the operation of the product. Customer may make one copy of the Licensed Software in machine-readable form solely for backup purposes. Invivo reserves the right to charge for backup copies created by Invivo. Except as otherwise provided under section 1.6, Customer may not copy, reproduce, sell, assign, transfer, or sublicense the Licensed Software for any purpose without the prior written consent of Invivo. Customer shall reproduce Invivo' copyright notice or other identifying legends on such copies or reproductions. Customer will not (and will not allow any third party to) decompile, disassemble, or otherwise reverse engineer or attempt to reconstruct or discover the product or Licensed Software by any means whatsoever.  
 15.1.3 The License shall not affect the exclusive ownership by Invivo of the Licensed Software or of any trademarks, copyrights, patents, trade secrets, or other intellectual property rights of Invivo (or any of Invivo' suppliers) relating to the Licensed Software.



REPRINT

Invivo Corporation  
 3650 NE 53rd Avenue  
 Gainesville, FL 32609  
 Tel :1-877-INVIVO1  
 Fax :1-352-264-3432

Quote date :	Page	Quote number :
08/23/2012	7 / 7	2300282873
Expiration Date		
10/23/2012		
Payment Terms:		
Net 30 Days		
<b>Formal Quote</b>		

Item	Article - type number/ description	Quantity	Unit	Unit price	Total amount (USD)
------	------------------------------------	----------	------	------------	--------------------

15.1.4 Customer agrees that only authorized officers, employees, and agents of Customer will use the Licensed Software or have access to the Licensed Software (or to any part thereof), and that none of Customer's officers, employees, or agents will disclose the Licensed Software, or any portion thereof, or permit the Licensed Software, or any portion thereof, to be used by any person or entity other than those entities identified on the quotation. Customer acknowledges that certain of Invivo's rights may be derived from license agreements with third parties, and Customer agrees to preserve the confidentiality of information provided by Invivo under such third party license agreements.

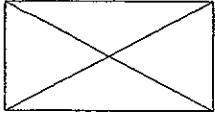
15.1.5 The Licensed Software shall be used only on the product(s) referenced in the quotation.

15.1.6 Customer may transfer the Licensed Software in connection with sale of the product to a healthcare provider who accepts all of the terms and conditions of this License; provided that Customer is not in breach or default of this License, the Terms and Conditions of Sale, or any payment obligation to Invivo.

15.2. Modifications.

15.2.1 If Customer modifies the Licensed Software in any manner, all warranties associated with the Licensed Software and the products shall become null and void. If Customer or any of its officers, employees, or agents should devise any revisions, enhancements, additions, modifications, or improvements in the Licensed Software, Customer shall disclose them to Invivo, and Invivo shall have a non-exclusive royalty-free license to use and to sub-license them.

15.2.2 The Licensed Software is licensed to Customer on the basis that (a) Customer shall maintain the configuration of the products as they were originally designed and manufactured; and, (b) the product includes only those subsystems and components certified by Invivo. The Licensed Software may not perform as intended on systems modified by other than Invivo or its authorized agents, or on systems which include subsystems or components not certified by Invivo. Invivo does not assume any responsibility or liability with respect to unauthorized modification or substitution of subsystems or components.



# Purchase Order

**St. Francis Hosp & Medical Ctr**  
 114 Woodland Street  
 Hartford CT 06105  
 United States

Vendor: 0000001745  
 SIEMENS MEDICAL SOLUTIONS INC.  
 51 VALLEY STREAM PARKWAY  
 MALVERN PA 19355

Dispatch via Phone

Purchase Order	Date	Revision	Page
0100157414	09/28/2011		1
Payment Terms	Freight Terms	Ship Via	
30 DAYS	FOB Destination	BESTWAY	
Buyer	Phone	Fax	
Lisa Condon	860/714-3600	860/714-3468	

Ship To: 114 Woodland Street  
 Hartford CT 06105  
 United States

Bill To: 114 Woodland Street  
 Hartford CT 06105  
 United States

Tax Exempt? Y Tax Exempt ID: EO1451

Line-Sch	Item/Description	Mfg ID/Mfg Item#	Quantity	UOM	PO Price	Extended Amt	Due Date
1- 1	Magnetom Skyra		1.00	EA	2,659,616.00	2,659,616.00	10/05/2011
Schedule Total						2,659,616.00	
Item Total						2,659,616.00	

*lpa*

Order is being placed contingent upon CON approval.  
 Product not to be shipped until approved and released by Supply Chain Management Department.  
 Order can be cancelled at any time without obligation or cost to hospital if CON is not approved.

Total PO Amount 2,659,616.00

Authorized Signature

# SIEMENS

Siemens Medical Solutions USA, Inc.  
51 Valley Stream Parkway, Malvern, PA 19355  
Fax: (866) 309-6992

SIEMENS REPRESENTATIVE  
Tegan Gonzalez - (781) 454-5132

Customer Number: 0000010181

Date: 9/21/2011

ST FRANCIS HOSPITAL  
114 WOODLAND STREET  
HARTFORD, CT 06105

Siemens Medical Solutions USA, Inc. is pleased to submit the following quotation for the products and services described herein at the stated prices and terms, subject to your acceptance of the terms and conditions on the face and back hereof, and on any attachment hereto.

<u>Table of Contents</u>	<u>Page</u>
MAGNETOM Skyra .....	2
General Terms and Conditions .....	8
Warranty Information .....	14
Detailed Technical Specifications .....	15
Cut Sheets .....	following page 39

Proposal valid until 9/30/2011

## SIEMENS / NOVATION GROUP BUY 2011 PROMOTIONAL OFFERING

Confidentially Agreement: This Quotation is strictly confidential and you agree that this information will be held in the strictest of confidence and not shared with any third parties, buying evaluation groups or anyone not directly employed by your facility.

Siemens & Novation Group Buy Promotion:

- Early Access begins June 1, 2011.
- Group Buy ends September 30, 2011.
- Executable orders must be received by Siemens before September 30, 2011.
- Contingent purchase orders (except State CON) are not acceptable.
- Systems must be received by customer no later than September 30, 2013..
- 45 day validity period is not applicable for this proposal.

Accepted and Agreed to by:

Siemens Medical Solutions USA, Inc.

By (sign): \_\_\_\_\_  
Name: Tegan Gonzalez  
Title: Account Executive  
Date: \_\_\_\_\_

ST FRANCIS HOSPITAL

By (sign): Lisa Condon  
Name: Lisa Condon  
Title: Director of Purchasing/Contracting  
Date: 9/29/11

All pages of the signed proposal must be returned to Siemens to process the order - Thank you.



# SIEMENS

Siemens Medical Solutions USA, Inc.  
51 Valley Stream Parkway, Malvern, PA 19355  
Fax: (866) 309-6992

SIEMENS REPRESENTATIVE  
Tegan Gonzalez - (781) 454-5132

---

Quote Nr: 1-2IS5TM Rev. 1

Terms of Payment: 00% Down, 90% Delivery, 10% Installation  
Free On Board: Destination

Purchasing Agreement: Novation GB-2011 - MMMU POS

Novation GB-2011 - MMMU POS terms and conditions apply to Quote Nr 1-2IS5TM

---

## MAGNETOM Skyra

All items listed below are included for this system: *(See Detailed Technical Specifications at end of Proposal.)*

Qty	Part No.	Item Description
1	14418500	<b>MAGNETOM Skyra - System</b> MAGNETOM Skyra - 3T Tim+Dot system - the integration of the next generation Tim "Tim 4G" and Siemens unique Dot Engines (Day optimizing throughput Engines). Short and open appearance (173 cm system length with 70 cm Open Bore Design). Tim 4G with redesigned RF system and all-new coil architecture. DirectRF(tm) technology enabling Tim's new all digital-in/ digital-out design - All-new coil architecture including Dual-Density Signal Transfer Technology - Whole-body superconductive Zero Helium Boil-Off 3T magnet - TrueForm Magnet and Gradient Design - Actively shielded water-cooled Siemens gradient system - TimTX TrueForm for uniform RF distribution in all body regions - Head/Neck 20 DirectConnect, Spine 32 DirectConnect, Body 18, Flex Large/Small 4 Dot offers patient personalization, user guidance and process automation. Brain Dot Engine - personalized, guided and automated workflows - Dot Display and Dot Control Centers for efficient patient preparation. Additional features included: -Tim Application Suite including Neuro, Angio, Cardiac, Body, Onco, Breast, Ortho, Pediatric and Scientific Suite - syngo MR software including 1D/2D PACE, syngo BLADE, iPAT <sup>2</sup> , Phoenix, Inline Technologies. - High performance host computer and measurement and reconstruction system The system (magnet, electronics and control room) can be installed in 31sqm space. For system cooling either the Eco Chiller options or the Separator is required.
1	14418502	<b>Tim [204x48] XQ Gradients #Sk</b> Tim [204x48] XQ-gradients performance level - Tim 4G's newly designed RF system and innovative coil architecture enables high resolution imaging and increased throughput. Up to 204 simultaneously connected coil elements, in combination with the standard 48 independent RF channels, allow for more flexible parallel imaging. Maximum SNR through the new Tim 4G matrix coil technology. XQ - gradients - The XQ - gradients - high performance and linearity to support clinical whole body imaging at 3T. The force compensated gradient system minimizes vibration levels and acoustic noise. The XQ gradients combine 45 mT/m peak amplitude with a slew rate of 200 T/m/s.
1	08464872	<b>PC Keyboard US english #Tim</b> Standard PC keyboard with 101 keys.
1	14416914	<b>Pure White Design #T+D</b> The MAGNETOM Aera / MAGNETOM Skyra design is available in different light and appealing variants which perfectly integrates into the different environments. The color of the main face plate cover of the Pure White Design Variant with the integrated Dot Control Centers and the unique Dot Display is brilliant white surrounded by a brilliant silver trim. The asymmetrical deco area on the left side is colored white matte and also with a brilliant surrounding silver trim The table cover is presented also in the same color and material selection.
1	14418507	<b>Tim Dockable Table #Sk</b> The new Tim Dockable Table is designed for maximum patient comfort and smooth patient preparation. Tim Dockable Table can support up to 250 kg (550 lbs) patients without restricting the vertical or horizontal movement. The one step docking mechanism and the innovative multi-directional navigation wheel ensure easy maneuvering and handling. Critically ill or immobile patients can now be prepared outside the examination room for maximum patient care, flexibility and speed.

# SIEMENS

Siemens Medical Solutions USA, Inc.  
51 Valley Stream Parkway, Malvern, PA 19355  
Fax: (866) 309-6992

SIEMENS REPRESENTATIVE  
Tegan Gonzalez - (781) 454-5132

Qty	Part No.	Item Description
1	14402592	<b>Inline Composing syngo #Tim</b> Automatic anatomical or angiographic composing of multiple adjacent coronal or sagittal images for presentation and further evaluation. Composed images can be automatically loaded into Graphical Slice Positioning for scan planning purposes.
1	14402593	<b>Tim Planning Suite</b> With the Tim Planning Suite, multiple regions in the entire body can be examined in a minimum of time through measurement planning on a single FoV of any desired size.
1	14405224	<b>Composing syngo #Tim</b> This application provides dedicated evaluation software for creation of full-format images from overlapping MR volume data sets and MIPs (starting from syngo MR B13) acquired at multiple stages.
1	14409198	<b>Native syngo #Tim</b> Integrated software package with sequences and protocols for non-contrast enhanced 3D MRA with high spatial resolution. syngo NATIVE particularly enables imaging of abdominal and peripheral vessels and is an alternative to MR angiography techniques with contrast medium, especially for patients with severe renal insufficiency.
1	14416923	<b>Abdomen Dot Engine #T+D</b> The Abdomen Dot Engine: Personalized Exam Strategies - Guidance - Automatic sequence scaling - Auto Navigator - Auto-FoV - Timeline setup and monitoring - Automatic Voice Commands - Auto Bolus Detection - Inline radial range calculation for MRCP - Inline Subtraction - Inline Registration
1	14418746	<b>Cardiac Dot Engine, USA #T+D</b> Cardiac examinations: Dot Cardiac - Customized workflows that are easier to repeat. Using anatomical landmarks, standard views of the heart (such as dedicated long axis and short-axis views), are easily generated and can easily be reproduced using different scanning techniques. Scan parameters are adjusted to the patient's heart rate and automatic voice commands are given.
1	08464740	<b>Flow Quantification #Tim</b> Special sequences for quantitative assessment of flow.
1	14416929	<b>Advanced Cardiac Package #T+D</b> This package contains special sequences and protocols for advanced cardiac imaging including 3D and 4D syngo BEAT functionalities. It supports advanced techniques for ventricular function imaging, dynamic imaging, tissue characterization, coronary imaging, and more.
1	14407334	<b>Argus 4D Ventr.Function syngo #Tim</b> syngo Argus 4D Ventricular Function software processes MR cine images of the heart and generates quantitative results for physicians in the diagnostic process.
1	14416922	<b>Knee Dot Engine #T+D</b> Knee Dot Engine: - Reproducible image quality and streamlined knee examinations. Knee Dot Engine features AutoPositioning and AutoAlign Knee, with automated patient positioning and slice orientation, based on a 3D-localizer. With its new 3D functionality, Dot offers the potential to dramatically speed up scan time and generate 3D datasets for interactive 3D reading, while at the same time providing automatically calculated Inline MPR's for conventional 2D reading.
1	14405341	<b>Mapit syngo #Tim</b> Based on the T1, T2 or T2* properties of the cartilage syngo ParametricMap allows the early detection of osteoarthritic break down of cartilage structures even before morphological changes occur. The method supports therapeutic decisions in individual patients and can be used to control treatments non-invasively, replacing surgeries or biopsies. The assessment of T1, T2 and T2* properties of tissues in other body regions is also possible. syngo ParametricMap provides very fast 2D and 3D high resolution imaging sequences and the Inline calculation of parametric maps for the T1, T2 and T2* properties of the imaged tissue.
1	07365484	<b>Image Fusion syngo</b> This application provides a dedicated evaluation software for spatial alignment (matching) and visualization of image data either from different modalities (CT,MR,NM,PET) or from the same modality but from multiple examinations of the same patient. It supports optimal diagnostic outcome (fusion of morphological and functional information) and therapy planning.
1	14401554	<b>Inline Perfusion #3T</b> Automatic real-time calculation of Global Bolus Plot (GBP), Percentage of Baseline at Peak map (PBP), and Time-to-Peak map (TTP) with Inline technology.

# SIEMENS

Siemens Medical Solutions USA, Inc.  
51 Valley Stream Parkway, Malvern, PA 19355  
Fax: (866) 309-6992

SIEMENS REPRESENTATIVE  
Tegan Gonzalez - (781) 454-5132

Qty	Part No.	Item Description
1	14418563	<b>Neuro Perfusion Evaluation,USA #T+D</b> Neuro Perfusion Evaluation syngo provides a task card for detailed post-processing of brain perfusion data sets. Color display of the relative Mean Transit Time (relMTT), relative Cerebral Blood Volume (relCBV), corrected rel CBV, and relative Cerebral Blood Flow (relCBF) is supported. Flexible selection of the Arterial Input Function (AIF). Furthermore a calculation of maps using the pre-selected local Arterial Input Functions (AIF) is provided. The detailed evaluation of brain perfusion data sets generates parameter maps for TTP and PBP and for the hemodynamic parameters relMTT, relCBV, rel CBVcor and relCBF.
1	14416943	<b>Neuro fMRI Package #T+D</b> The Neuro fMRI Package is a bundle of: - Inline BOLD Imaging - 3D PACE syngo - BOLD 3D Evaluation syngo - fMRI Trigger Converter The bundle comprehends all acquisition and post processing tools for comprehensive BOLD fMRI exams.
1	14416927	<b>MDDW #T+D</b> MDDW (Multi Directional Diffusion Weighted Imaging) provides basic multi-directional diffusion weighting measurements to compute the diffusion tensor. One diffusion-weighted image is generated per slice position, b-value, and direction of diffusion. The package particularly supports clinical applications (e.g. diseases of the white matter).
1	14409110	<b>Arterial Spin Labeling 2D</b> ASL is a non contrast enhanced brain perfusion technique. EPI sequence enhanced for PASL (Pulsed Arterial Spin Labeling) with preparation module (inversion pulse, saturation pulses) and selectable prospective motion correction. Perfusion-weighted color maps and relative cerebral blood flow (relCBF) color maps are calculated with Inline technology.
1	14402527	<b>SWI #Tim</b> Susceptibility Weighted Imaging is a high-resolution 3D imaging technique for the brain with ultra-high sensitivity for microscopic magnetic field inhomogeneities caused by deoxygenated blood, products of blood decomposition and microscopic iron deposits. Among other things, the method allows for the highly sensitive proof of cerebral hemorrhages and the high-resolution display of venous cerebral blood vessels.
1	14416941	<b>Spectroscopy Package #T+D</b> The Spectroscopy Package is a comprehensive software package which bundles Single Voxel Spectroscopy, 2D Chemical Shift Imaging, 3D Chemical Shift Imaging and syngo Spectroscopy Evaluation. Sequences and protocols for proton spectroscopy, 2D and 3D proton chemical shift imaging (2D CSI and 3D CSI) to examine metabolic changes in the brain (e.g. in tumors and degenerative diseases) and in the prostate are included. Furthermore included is the comprehensive syngo Spectroscopy Evaluation Software which enables fast evaluation of spectroscopy data on the syngo Acquisition Workplace.
1	14405328	<b>TWIST syngo #Tim</b> This package contains a Siemens unique sequence and protocols for time-resolved (4D) MR angiographic and dynamic imaging in general with high spatial and temporal resolution. syngo TWIST supports comprehensive dynamic MR angio exams in all body regions. It offers temporal information of vessel filling in addition to conventional static MR angiography, which can be beneficial in detecting or evaluating malformations such as shunts. In case of general dynamic imaging, for example an increase in spatial resolution by a factor of up to 2 at 60 seconds temporal resolution (compared to conventional dynamic imaging) is possible due to intelligent k-space sampling strategies. Alternatively, increased temporal resolution at constant spatial resolution is possible.
1	14416952	<b>Coil Storage Cart #T+D</b> Specially designed non-ferromagnetic cart for easy storage of the most commonly used coils and accessories.
1	14416954	<b>2/4/8-ch Sentinelle BreastCoil #Sk</b> The 2-/4-/8-channel Sentinelle Breast Coil consists of a positioning frame with exchangeable coils with different numbers of channels as described in detail in the E text. The 2-/4-/8-channel Sentinelle Breast Coil can be used as 8-channel imaging coil, 4-channel biopsy coil for lateral biopsy access as well as 2-channel biopsy coil for medial biopsy access. This coil provides a large biopsy access. The preamplifiers are integrated into the coil. The coil is iPAT-compatible. A positioning guidance is provided.

# SIEMENS

Siemens Medical Solutions USA, Inc.  
51 Valley Stream Parkway, Malvern, PA 19355  
Fax: (866) 309-6992

SIEMENS REPRESENTATIVE  
Tegan Gonzalez - (781) 454-5132

Qty	Part No.	Item Description
1	14418512	<b>Peripheral Angio 36 #Sk</b> The new Tim 4G coil technology with Dual Density Signal Transfer and SlideConnect Technology combines key imaging benefits: excellent image quality, high patient comfort, and unmatched flexibility: - 36 channels - Dual Density Signal Transfer - Ultra light-weight - SlideConnect Technology The 36-channel coil includes 36 integrated pre-amplifiers for excellent signal-to-noise ratio. The single SlideConnect Plug allows for fast and easy patient preparation. The Peripheral Angio 36 features: - 36-element design with 36 integrated preamplifiers, distributed over 6 planes with 6 elements each - Operates in an integrated fashion with Body 18 coils and with the Spine 32 . For Whole-Body examinations also with the Head/ Neck 20 - Automatic table feed and active coil switch - Can be utilized head and feet first - Both legs are independently covered with coil elements, maximizing the coil filling factor and the signal-to-noise ratio - No coil tuning - iPAT-compatible - Dual-Density Signal Transfer enables ultra-high density coil designs by integrating key RF components into the local coil - SlideConnect technology for easy coil set up - One cable only for easy handling - Includes special non-ferromagnetic coil cart for safe, user-friendly storage Applications: - High-resolution angiography of both legs incl. Pelvis (by additional use of the Body 18) with highest signal-to-noise ratio - Visualization of the iliac arteries and aorta in combination with Body 18 - Bilateral examinations of long bones of the legs Typically combined with: Head/ Neck 20, Body 18, Spine 32, and all flexible coils such as Flex Large 4 or Flex Small 4
1	14416959	<b>Shoulder 16 Coil Kit #Sk</b> The new Tim 4G coil technology with Dual Density Signal Transfer and SlideConnect Technology combines key imaging benefits: excellent image quality, high patient comfort, and unmatched flexibility. The Shoulder 16 Coil Kit for examinations of the left or right shoulder consists of a base plate and two different sized iPAT compatible 16 channel coils (Shoulder Large 16 and Shoulder Small 16). These will be attached and can be relocated on the base plate. The 16-element coils with 16 integrated pre-amplifiers ensure maximum signal-to-noise ratio. Shoulder Large 16 and Shoulder Small 16 will be connected via a SlideConnect plug for fast and easy coil set-up and patient preparation.
1	14418514	<b>Foot/Ankle 16 #Sk</b> The new Tim 4G coil technology with Dual Density Signal Transfer and DirectConnect Technology combines key imaging benefits: excellent image quality, high patient comfort, and unmatched flexibility. Foot/Ankle 16 for examinations of the left or right foot and ankle region consists of a base plate and an iPAT compatible 16-channel coil and allows high resolution imaging of the foot and ankle within one examination. Foot/Ankle 16 is a cable-less coil and will be connected via DirectConnect for fast and easy patient preparation.
1	14418519	<b>Tim Coil Interface 3T</b> Coil adapter plug for up to 8 receive and 1 transmit channels, in order to connect existing dedicated knee and breast coils ( Tx/ Rx 15-channel Knee Coil, CP Extremity Coil, 4-channel BI Breast Coil, 16-channel AI Breast Coil, 2/4/8-channel Sentinelle BreastCoil) with MAGNETOM Skyra Systems.
1	14418520	<b>Tx/Rx 15-channel Knee Coil 3T</b> New 15-channel transmitter/receiver coil for joint examinations in the area of the lower extremities. Main features : - 15-element design (3x5 coil elements) with 15 integrated preamplifiers, - iPAT-compatible
1	14418511	<b>Body 18 #Sk</b> The new Tim 4G coil technology with Dual Density Signal Transfer and SlideConnect Technology combines key imaging benefits: excellent image quality, high patient comfort, and unmatched flexibility: - 18 channels (inherent) or up to 30 (in combination with the Spine 32) - Dual Density Signal Transfer - Ultra light-weight - SlideConnect Technology The Body 18 is part of the standard configuration. The 18-channel coil with its 18 integrated pre-amplifiers ensures excellent signal-to-noise ratio. The 18 coil elements provide extensive coverage in all directions. The single SlideConnect plug allows for fast and easy patient preparation. The light-weight coil ensures highest patient comfort. The Body 18 Coil features: - 18-element design with 18 integrated preamplifiers (3 clusters of 6 elements each) - Operates in an integrated fashion with the Spine 32 as an 30 channel body coil - Can be combined with further Body 18 coils for larger coverage - Can be positioned in different orientations (0°, 90°, 180°, 270°) for patient specific adaptations - No coil tuning - iPAT compatible in all directions The highly flexible design enables a wide variety of applications including: - Thorax (incl. heart) - Abdomen - Pelvis - Hip Typically combined with: - Head / Neck 20 - Spine 32 - Additional Body 18 coil(s) (optional) - Peripheral Angio 36 (optional) - Flex Large 4 - Flex Small 4 - Loop 3T coils (optional) - Endorectal coil (optional)
1	14407258	<b>MR Workplace Table 1.2m</b> Table suited for syngo Acquisition Workplace and syngo MR Workplace based on syngo Hardware.
1	14407261	<b>MR Workplace Container, 50cm</b> 50 cm wide extra case for the syngo host computer with sliding front door to allow change of storage media (CD/DVD/USB).

# SIEMENS

Siemens Medical Solutions USA, Inc.  
 51 Valley Stream Parkway, Malvern, PA 19355  
 Fax: (866) 309-6992

SIEMENS REPRESENTATIVE

Egan Gonzalez - (781) 454-5132

*Chiller*

*cost? 45-look*

Qty	Part No.	Item Description
1	14416975	<b>Eco Chiller 60kW</b> The KKT ECO 133 -L chiller is a dedicated 20°C cooling system for MAGNETOM Aera and MAGNETOM Skyra which automatically adapts to the different cooling requirements (e.g. system in operation, standby, ...) to reduce the energy consumption for cooling. The cooling system must be used in combination with the IFP (Interface Panel), if there is no on-site chilled water supply at all. The IFP is included in the scope of supply.
1	08857828	<b>UPS Cable #Tim</b> Power cable for connecting the UPS Powerware PW 9130-3000i (14413662) to the ACC of MAGNETOM Tim and MAGNETOM Tim+Dot systems for backing up the computer. Standard cable length: 9 m.
1	14413662	<b>UPS Powerware PW9130G-3000T-XLEU</b> UPS system Eaton PW9130G-3000T-XLEU for MAGNETOM Tim, MAGNETOM Tim+Dot and MAGNETOM Symphony systems for safeguarding computers. Power output: 3.0 kVA / 2.7 kW Bridge time: 5 min full load / 14 min half load Input voltage: 230 VAC
1	14413663	<b>UPS Battery module</b> UPS battery module Eaton PW 9130N-3000T-EBM for all MAGNETOM Tim, MAGNETOM Tim+Dot and MAGNETOM Symphony systems for safeguarding computers. Extension for: PW9130I-3000T Battery type: Closed, maintenance-free Extension of the bridge time to: 24 minutes with a module Dimensions (H x W x D): Battery module: 346 x 214 x 412 mm incl. bracket set Weight: approx. 50 kg
1	MR_STD_RIG_INST	<b>MR Standard Rigging and Installation</b>
1	MR_BTL_INST_ALL	<b>MR Standard Rigging &amp; Install</b>
1	MR_PREINST_DOCK	<b>T+D Preinstall kit for dockable table</b>
1	MR_CRYO	<b>Standard Cryogens</b>
1	MR_PM	<b>MR Project Management</b>
1	MR_INITIAL_32	<b>Initial onsite training 32 hrs</b>
1	MR_FOLLOWUP_P_32	<b>Follow-up training 32 hrs</b>
1	MR_INT_DOT_BCLS	<b>MR Dot Training Class</b>
1	MR_ADD_CLASS_SS	<b>Additional Training Class</b>
1	4MR5142869	<b>Armrest #MR</b>
1	CHILINST_AVT_NOV_GBQ4_M	<b>Chiller Start-up and Warranty for TIM</b>
1	M_MU_POS	<b>Multiple (Two or More) System With POS</b> As part of the FY2011 Novation Group Buy Program, Siemens is providing an additional 2% discount on discountable items for all qualified orders of two or more systems and an additional 1% discount when the purchase includes a POS Service Contract. This quote already reflects the aggregate 3% Multiple System & POS discounts. Siemens will charge for and customer will pay the 2% Multiple System discount if an executed order for the two or more systems is not received by Siemens within two days of the first system order and no later than September 30, 2011. Siemens will charge for and customer will pay the 1% POS Service Contract Discount if an executed POS Service Contract for the applicable system(s) is not received by Siemens within two days of the first system order and no later than September 30, 2011. All systems must be received by customer by September 30, 2012.
1	MR_PR_NGB1_1_TIMPLN	<b>NGB Tim Planning Suite Offset</b>
1	MR_PR_NGB1_1_INLN	<b>NGB Inline Composing syngo Offset</b>
1	MRWSE	<b>MR Wall sign -English</b>

*OPTIMA*

System Total: \$2,592,735

*(40,981)*

*TOT* / 2,659,416.00

# SIEMENS

Siemens Medical Solutions USA, Inc.  
51 Valley Stream Parkway, Malvern, PA 19355  
Fax: (866) 309-6992

SIEMENS REPRESENTATIVE  
Tegan Gonzalez - (781) 454-5132

## OPTIONS:

Qty	Part No.	Item Description	Extended Price	Initial to Accept
1	NNL100200	<b>Nordic fMRI solution- Basic</b> The nordic fMRI Solution is an integrated set of hardware and software components that allows a single clinician to conduct an entire fMRI procedure. The nordic fMRI Solution consists of components: (1) stimulus presentation and software, (2) hardware for auditory and visual stimulus presentation, response collection, and timing synchronization. Key components: Sync and Response Unit - Optical input from Siemens scanner, 2 hand-held grips (2 buttons per grip). Synchronization of stimulus presentation with image acquisition and collection of patient responses. InRoom MRC 18" monitor - 18"LCD display with pedestal for positioning in the MR room. PC and 19" screen - Desktop PC for presentation of paradigms and running of music CD's and DVD's. Includes dual-link graphic output for in-room monitor. nordicAktiva - Stimulus presentation software. Includes a library of 8 standard clinical perceptual and motor paradigms. Software components: The stimulus presentation and workflow software controls the presentation of stimuli during fMRI exams, and has been designed specifically with the clinical user in mind. It offers a collection of standard clinical paradigms, allowing physicians to test perceptual, motor, and cognitive functions in clinical settings. Installation, on-site training and one year warranty provided by Nordic Neuro Lab. This product has been tested and verified for compatibility with the following Siemens' products: MAGNETOM Verio, Trio, Essenza, Espree, Avanto and Symphony. Compatibility with other products cannot be assured and may void service contracts and/or system warranties.	+ \$66,881	<i>X lpc</i>
1	NNL100201	<b>Nordic MR Entertainment System</b> The NNL MRI Entertainment System for Siemens which includes the 18" in-room LCD Monitor is an integrated set of hardware components that allows a movie to be viewed in the MRI room. Key components: InRoom MRC 18" monitor - 18"LCD display with pedestal for positioning in the MR room. PC and 19" screen - Desktop PC for presentation of paradigms and running of music CD's and DVD's. Includes dual-link graphic output for in-room monitor. Installation and one year warranty provided by Nordic Neuro Lab. This product has been tested and verified for compatibility with the following Siemens' products: MAGNETOM Verio, Trio, Essenza, Espree, Avanto and Symphony. Compatibility with other products cannot be assured and may void service contracts and/or system warranties.	+ \$54,217	<i>X</i>

**FINANCING:** The equipment listed above may be financed through Siemens. Ask us about our full range of financial products that can be tailored to meet your business and cash flow requirements. For further information, please contact your local Sales Representative.

**ACCESSORIES:** Don't forget to ask us about our line of OEM imaging accessories to complete your purchase. All accessories can be purchased or financed as part of this order. To purchase accessories directly or to receive our accessories catalog, please call us directly at 1-888-222-9944 ext. 7 or contact your local Sales Representative.

**COMPLIANCE:** Compliance with legal and internal regulations is an integral part of all business processes at Siemens. Possible infringements can be reported to our Helpdesk "Tell us" function at [www.siemens.com/tell-us](http://www.siemens.com/tell-us).

# SIEMENS

Siemens Medical Solutions USA, Inc.  
51 Valley Stream Parkway, Malvern, PA 19355  
Fax: (866) 309-6992

SIEMENS REPRESENTATIVE  
Tegan Gonzalez - (781) 454-5132

## Siemens Medical Solutions USA, Inc. General Terms and Conditions

### 1. GENERAL

**1.1 Contract Terms.** These terms and conditions constitute an integral part of any contract between the Seller identified on the first page hereof to sell products ("Products") and Purchaser and shall govern the sale of the Products. Seller shall not be bound by, and specifically objects to, any terms, conditions or other provisions which are different from or in addition to the provisions of this Agreement (whether or not it would materially alter this Agreement) which is proffered by Purchaser in any purchase order, receipt, acceptance, confirmation, correspondence or otherwise (even if provided to Seller concurrently with this Agreement), unless Seller specifically agrees to any such provision in a writing signed by Seller. Neither Seller's lack of objection to any such terms, nor delivery of the Products or provision of any services hereunder, shall constitute the agreement of Seller to any such terms. Purchaser acknowledges that this is a commercial and not a consumer transaction.

**1.2 Acceptance.** Purchaser shall be deemed to have assented to, and waived any objection to, this Agreement upon the earliest to occur of any of the following: Purchaser's completion or execution of this Agreement; Purchaser's acceptance of all or any part of the Products subject to this Agreement; Purchaser's issuance of a purchase order for any Products identified on Seller's quotation or proposal; or delivery of the Products to the common carrier for shipment pursuant hereto.

**1.3 Refurbished/Used Products.** For Products identified on the Agreement as used or refurbished Products, these Products have been previously owned and used. When delivered to Purchaser, the Products may have received mechanical, electrical and/or cosmetic reconditioning, as needed, and will comply with the manufacturer's specifications. Since pre-owned Products may be offered simultaneously to several customers, the sale of such Products to Purchaser cannot be guaranteed and is subject to continuing availability at the time Purchaser accepts Seller's offer to sell the Products. If the Products are no longer available, Seller will use its best efforts to identify other products in its inventory that may be suitable for purchase by Purchaser, and if substitute products are not acceptable to Purchaser, then Seller will cancel the order and refund to Purchaser any deposits previously paid. The warranty period for any used or refurbished Products will be separately stated on the quotation.

**1.4 Third Party Products.** If this Agreement includes the sale of third party products not manufactured by Seller, then Purchaser agrees and acknowledges that (a) Purchaser has made the selection of these products on its own, (b) the products are being acquired by Seller solely at the request of and for the benefit of Purchaser, in order to eliminate the need for Purchaser to issue a separate purchase order to the manufacturer of the products, (c) no representation, warranty or guarantee has been made by Seller with respect to the products, (d) the obligation of Purchaser to pay Seller for the products is absolute and unconditional, (e) Purchaser will assert no claim whatsoever against the Seller with respect to the products, and will look solely to the manufacturer regarding any such claims, (g) Purchaser will indemnify and hold Seller harmless from and against any and all claims, regardless of the form of action, related to, resulting from or caused by the products or any work or service provided by the manufacturer of the products or any other party, (h) use of the products may be subject to the Purchaser's agreement to comply with any software licensing terms imposed by the manufacturer, as well as any applicable laws, rule and regulations; and (i) the manufacturer, and not Seller, is solely responsible for any required installation, testing, validation, tracking, product recall, warranty service, maintenance, support, and complaint handling, as well as any other applicable FDA regulatory requirements.

### 2. PRICES

**2.1 Quotations.** Unless otherwise agreed to in writing or set forth in the quotation, all prices quoted by Seller are based on U.S. dollars, and include standard and customary packaging. F.O.B. terms are set forth in Section 6.2 hereof. Domestic prices apply only to purchasers located in, and who will use the Products in, the U.S. International prices apply to all purchasers located outside of, or who will use or ship or facilitate shipment of the Products outside of, the U.S. Unless otherwise stated, the quotation shall only be valid for forty-five (45) days from the date of the quotation.

**2.2 Delay in Acceptance of Delivery.** Should the agreed delivery date be postponed by Purchaser, Seller shall have the right to deliver to storage at Purchaser's risk and expense, and payments due upon delivery shall become due when Seller is ready to deliver.

**2.3 Escalation.** Unless otherwise agreed to in writing, except as to goods to be delivered within six (6) months of Seller's acceptance of Purchaser's order, Seller reserves the right to increase its prices to those in effect at the time of shipment.

### 3. TAXES

3.1 Any sales, use or manufacturer's tax which may be imposed upon the sale or use of Products, or any property tax levied after readiness to ship, or any excise tax, license or similar fee required under this transaction, shall be in addition to the quoted prices and shall be paid by Purchaser. Notwithstanding the foregoing, Seller agrees to honor any valid exemption certificate provided by Purchaser.

### 4. TERMS OF PAYMENT

**4.1 Payments; Due Date.** Unless otherwise set forth in the quotation, Seller's payment terms are as follows: an initial deposit of 10% of the purchase price for each Product is due upon submission of the purchase order, an additional 80% of the purchase price is due upon delivery of each Product, and the final 10% of the purchase price is due upon completion of installation or when the Products are available for first patient use, whichever occurs first. Unless otherwise agreed, all payments other than the initial deposit are due net thirty (30) days from the date of invoice. Seller shall have no obligation to complete installation until the payment due upon delivery of the Product is received. All amounts payable pursuant to this Agreement are denominated in United States dollars, and Purchaser shall pay all such amount in lawful money of the United States. Partial shipments shall be billed as made, and payments for such shipments will be made in accordance with the foregoing payment terms. In the event that Purchaser makes any payments hereunder by credit card, Seller has the right to charge the Purchaser any credit card fees imposed on the Seller by the financial institution.

**4.2 Late Payment.** A service charge of 1½% per month, not to exceed the maximum rate allowed by law, shall be made on any portion of Purchaser's outstanding balance which is not paid within thirty (30) days after invoice date, which charge shall be determined and compounded on a daily basis from the due date until the date paid. Payment of such service charge shall not excuse or cure Purchaser's breach or default for late payment. In addition, in the event that Purchaser fails to make any payment to Seller within this thirty (30) day period, including but not limited to any payment under any service contract, promissory note or other agreement with Seller, then Seller shall have no obligation to continue performance under any agreement with Purchaser.

**4.3 Payment of Lesser Amount.** If Purchaser pays, or Seller otherwise receives, a lesser amount than the full amount provided for under this Agreement, such payment or receipt shall not constitute or be construed other than as on account of the earliest amount due Seller. Seller may accept any check or payment in any amount without prejudice to Seller's right to recover the balance of the amount due or to pursue any other right or remedy. No endorsement or statement on any check or payment or in any letter accompanying a check or payment or elsewhere shall constitute or be construed as an accord or satisfaction.

**4.4 Where Payment Due Upon Installation or Completion.** Should any terms of payment provide for either full or partial payment upon installation or completion of installation or thereafter, and the installation or completion is delayed for any reason for which Seller is not responsible, then the Products shall be deemed installed upon delivery and, if no other terms were agreed upon in writing signed by the parties, the balance of payments shall be due no later than thirty (30) days from delivery regardless of the actual installation date.

**4.5 Default; Termination.** Each of the following shall constitute an event of default under this Agreement: (i) a failure by Purchaser to make any payment due Seller within ten (10) days of receipt of notice of non-payment from Seller; (ii) a failure by Purchaser to perform any other obligation under this Agreement within thirty (30) days of receipt of notice from Seller; (iii) a default by Purchaser or any affiliate of Purchaser under any other obligation to or agreement with Seller, Siemens Financial Services, Inc. or Siemens Medical Solutions Health Services Corporation, or any assignee of the foregoing (including, but not limited to, a promissory note, lease, rental agreement, license agreement or purchase contract); or (iv) the commencement of any insolvency, bankruptcy or similar proceedings by or against the Purchaser (including any assignment by Purchaser for the benefit of creditors). Upon the occurrence of any event of default, at Seller's election: (a) the entire amount of any indebtedness and obligation due Seller under this Agreement and interest thereon shall become immediately due and payable without notice, demand, or period of grace; (b) Seller may suspend the performance of any of Seller's obligations hereunder, including, but not limited to, obligations relating to delivery, installation and warranty services; (c) Purchaser shall put Seller in possession of the Products upon demand; (d) Seller may enter any premises where the Products are located and take possession of the Products without notice or demand and without legal proceedings; (e) at the request of Seller, Purchaser shall

# SIEMENS

Siemens Medical Solutions USA, Inc.

51 Valley Stream Parkway, Malvern, PA 19355

Fax: (866) 309-6992

SIEMENS REPRESENTATIVE

Tegan Gonzalez - (781) 454-5132

assemble the Products and make them available to Seller at a place designated by Seller which is reasonable and convenient to all parties; (f) Seller may sell or otherwise dispose of all or any part of the Products and apply the proceeds thereof against any indebtedness or obligation of Purchaser under this Agreement (Purchaser agrees that a period of 10 days from the time notice is sent to Purchaser shall be a reasonable period of notification of sale or other disposition of the Products by or for Seller); (g) if this Agreement or any indebtedness or obligation of Purchaser under this Agreement is referred to an attorney for collection or realization, Purchaser shall pay to Seller all costs of collection and realization (including, without limitation, a reasonable sum for attorneys' fees, expenses of title search, all court costs and other legal expenses) incurred thereby; and (h) Purchaser shall pay any deficiency remaining after collection of or realization by Seller on the Products. In addition, Seller may terminate this Agreement upon written notice to Purchaser in the event that Purchaser is not approved for credit or upon the occurrence of any material adverse change in the financial condition or business operations of Purchaser.

**4.6 Financing.** Notwithstanding any arrangement that Purchaser may make for the financing of the purchase price of the Products, the parties agree that any such financing arrangement shall have no effect on the Purchaser's payment obligations under this Agreement, including but not limited to Sections 4.1 and 4.2 above.

## 5. EXPORT TERMS

**5.1** Unless other arrangements have been made, payment on export orders shall be made by irrevocable confirmed letter of credit, payable in U.S. dollars against Seller's invoice and standard shipping documents. Such letter of credit shall be in an amount equal to the full purchase price of the Products and shall be established in a U.S. bank acceptable to Seller. Purchaser shall procure all necessary permits and licenses for shipment and compliance with any governmental regulations concerning control of final destination of Products.

**5.2** Purchaser shall not, directly or indirectly, violate any U.S. law, regulation or treaty, or any other international treaty or agreement, relating to the export or reexport of any Product or associated technical data, to which the U.S. adheres or with which the U.S. complies. Purchaser shall defend, indemnify and hold Seller harmless from any claim, damage, liability or expense (including but not limited to reasonable attorney's fees) arising out of or in connection with any violation of the preceding sentence. If Purchaser purchases a Product at the domestic price and exports such Product, or transfers such Product to a third party for export, outside of the U.S., Purchaser shall pay to Seller the difference between the domestic price and the international retail price of such Product pursuant to the payment terms set forth herein. Purchaser shall deliver to Seller, upon Seller's request, written assurance regarding compliance with this section in form and content acceptable to Seller.

## 6. DELIVERY, RISK OF LOSS

**6.1 Delivery Date.** Delivery and completion schedules are approximate only and are based on conditions at the time of acceptance of Purchaser's order by Seller. Seller shall make every reasonable effort to meet the delivery date(s) quoted or acknowledged, but shall not be liable for any failure to meet such date(s). Partial shipments may be made.

**6.2 Risk of Loss; Title Transfer.** Unless otherwise agreed to in writing, the following shall apply:

(a) For Products that do not require installation by Seller or its authorized agent or subcontractor, and for options and add-on products purchased subsequent to delivery and installation of Products purchased under this Agreement, delivery shall be complete upon transfer of possession to common carrier, F.O.B. Shipping Point, whereupon title to and all risk of loss, damage to or destruction of the Products shall pass to Purchaser.

(b) For Products that require installation by Seller or its authorized agent or subcontractor, delivery shall be complete upon delivery of the Products to Purchaser's designated site, F.O.B. Destination; title to and all risk of loss, damage to or destruction of such Products shall pass to Purchaser upon completion of the installation by Seller or its authorized agent or subcontractor.

(c) All freight charges and other transportation, packing and insurance costs, license fees, custom duties and other similar charges shall be the sole responsibility of the Purchaser unless included in the purchase price or otherwise agreed to in writing by Seller. In the event of any loss or damage to any of the Products during shipment, Seller and Purchaser shall cooperate in making a claim against the carrier.

## 7. SECURITY INTEREST/FILING

**7.1** From the F.O.B. point, Seller shall have a purchase money security interest in the Products (and all accessories and replacements thereto and all proceeds thereof) until payment in full by Purchaser and satisfaction of all other obligations of Purchaser hereunder. Purchaser hereby (i) authorizes Seller to file (and Purchaser shall promptly execute, if requested by Seller) and (ii)

irrevocably appoints Seller its agent and attorney-in-fact to execute in the name of Purchaser and file, with such authorities and at such locations as Seller may deem appropriate, any Uniform Commercial Code financing statements with respect to the Products and/or this Agreement. Purchaser also agrees that an original or a photocopy of this Agreement (including any addenda, attachments and amendments hereto) may be filed by Seller as a Uniform Commercial Code financing statement. Purchaser further represents and covenants that (a) it will keep the Products in good order and repair until the purchase price has been paid in full, (b) it will promptly pay all taxes and assessments upon the Products or the use thereof, (c) it will not attempt to transfer any interest in the Products until the purchase price has been paid in full, and (d) it is solvent and financially capable of paying the full purchase price for the Products.

## 8. CHANGES, CANCELLATION, AND RETURN

**8.1** Orders accepted by Seller are not subject to change except upon written agreement.

**8.2** Orders accepted by Seller are noncancellable by Purchaser except upon Seller's written consent and payment by Purchaser of a cancellation charge equal to 10% of the price of the affected Products, plus any shipping, insurance, inspection and refurbishment charges; the cost of providing any training, education, site evaluation or other services; and any return, cancellation or restocking fees with respect to any Third Party Products ordered by Seller on behalf of Purchaser. Seller may retain any payments received from Purchaser up to the amount of the cancellation charge. In no event can an order be cancelled by Purchaser or Products be returned to Seller after shipment has been made.

**8.3** Seller shall have the right to change the manufacture and/or design of its Products if, in the judgment of Seller, such change does not alter the general function of the Products.

## 9. FORCE MAJEURE

**9.1** Seller will make every effort to complete shipment, and installation where indicated, but shall not be liable for any loss or damage for delay in delivery, inability to install or any other failure to perform due to causes beyond its reasonable control including, but not limited to, acts of government or compliance with any governmental rules or regulations, acts of God or the public, war, civil commotion, blockades, embargoes, calamities, floods, fires, earthquakes, explosions, storms, strikes, lockouts, labor disputes, or unavailability of labor, raw materials, power or supplies. Should such a delay occur, Seller may reasonably extend delivery or production schedules or, at its option, cancel the order in whole or part without liability other than to return any unearned deposit or prepayment.

## 10. WARRANTY

**10.1** Seller warrants that the Products manufactured by Seller and sold hereunder shall be free from defects in material or workmanship under normal use and service for the warranty period. The final assembled Products shall be new although they may include certain used, reworked or refurbished parts and components (e.g., circuit boards) that comply with performance and reliability specifications and controls. Seller's obligation under this warranty is limited, at Seller's option, to the repair or replacement of the Product or any part thereof. Unless otherwise set forth in the Product Warranty attached hereto and incorporated herein by reference, the warranty period shall commence upon the earlier of the date that the Products have been installed in accordance with 12.6 hereof, which date shall be confirmed in writing by Seller, or first patient use, and shall continue for 12 consecutive months. Seller makes no warranty for any Products made by persons other than Seller or its affiliates, and Purchaser's sole warranty therefor, if any, is the original manufacturer's warranty, which Seller agrees to pass on to Purchaser, as applicable. The warranty provided by Seller under this Section 10 extends only to the original Purchaser, unless the Purchaser obtains the Seller's prior written consent with respect to any sale or other transfer of the Equipment during the term of the warranty.

**10.2** No warranty extended by Seller shall apply to any Products which have been damaged by fire, accident, misuse, abuse, negligence, improper application or alteration or by a force majeure occurrence as described in Section 9 hereof or by the Purchaser's failure to operate the Products in accordance with the manufacturer's instructions or to maintain the recommended operating environment and line conditions; which are defective due to unauthorized attempts to repair, relocate, maintain, service, add to or modify the Products by the Purchaser or any third party or due to the attachment and/or use of non-Seller supplied equipment, parts or software, without Seller's prior written approval; which failed due to causes from within non-Seller supplied equipment, parts or software; which have been damaged from the use of operating supplies or consumable parts not approved by Seller. In addition, no warranty extended by Seller shall apply to any transducer or probe failure due to events such as cracking from high impact drops, cable rupture from rolling equipment over the cable, or delamination from cleaning



# SIEMENS

Siemens Medical Solutions USA, Inc.  
51 Valley Stream Parkway, Malvern, PA 19355  
Fax: (866) 309-6992

SIEMENS REPRESENTATIVE  
Tegan Gonzalez - (781) 454-5132

with inappropriate solutions. Seller's obligation under this warranty is limited to the repair or replacement, at Seller's option, of defective parts. Seller may effectuate such repair at Purchaser's facility, and Purchaser shall furnish Seller safe and sufficient access for such repair. Repair or replacement may be with parts or products that are new, used or refurbished. Repairs or replacements shall not interrupt, extend or prolong the term of the warranty. Purchaser shall, upon Seller's request, return the noncomplying Product or part to Seller with all transportation charges prepaid, but shall not return any Product or part to Seller without Seller's prior written authorization. Purchaser shall pay Seller its normal charges for service and parts for any inspection, repair or replacement that is not, in Seller's sole judgment, required by noncompliance with the warranty set forth in Section 10.1. Seller's warranty does not apply to consumable materials, disposables, supplies, accessories and collateral equipment, except as specifically stated in writing or as otherwise set forth in the Product Warranty attached hereto and incorporated herein by reference, nor to products or parts thereof supplied by Purchaser.

10.3 This warranty is made on condition that immediate written notice of any noncompliance be given to Seller and Seller's inspection reveals that the Purchaser's claim is valid under the terms of the warranty (i.e., that the noncompliance is due to traceable defects in original materials and/or workmanship).

10.4 Purchaser shall provide Seller with full and free access to the Products, network cabling and communication equipment as is reasonably necessary for Seller to provide warranty service. This access includes establishing and maintaining connectivity to the Products via VPN IPsec Tunneling (non-client) Peer-to-Peer connection, modem line, internet connection, broadband internet connection or other secure remote access reasonably required by Seller, in order for Seller to provide warranty service, including remote diagnostics, monitoring and repair services.

10.5 Warranty service will be provided without charge during Seller's regular working hours (8:30-5:00), Monday through Friday, except Seller's recognized holidays. If Purchaser requires that service be performed other than during these times, such service can be made available at an additional charge, at Seller's then current rates. The obligations of Seller described in this section are Seller's only obligations and Purchaser's sole and exclusive remedy for a breach of product warranty.

10.6 SELLER MAKES NO WARRANTY OTHER THAN THE ONE SET FORTH HEREIN AND IN THE ATTACHED PRODUCT WARRANTY COVERING THE APPLICABLE PRODUCT CATEGORY. SUCH WARRANTY IS IN LIEU OF ALL OTHER WARRANTIES, EXPRESS OR IMPLIED, INCLUDING BUT NOT LIMITED TO ANY EXPRESS OR IMPLIED WARRANTY OF MERCHANTABILITY OR FITNESS FOR PARTICULAR PURPOSES, AND SUCH CONSTITUTES THE ONLY WARRANTY MADE WITH RESPECT TO THE PRODUCTS AND ANY DEFECT, DEFICIENCY OR NONCONFORMITY IN ANY PRODUCT, SERVICE OR OTHER ITEM FURNISHED UNDER THIS AGREEMENT.

10.7 In the event of any inconsistencies between the terms of this Section 10 and the terms of the attached Product Warranty, the terms of the attached Product Warranty shall prevail.

## 11. LIMITATION OF LIABILITY

11.1 In no event shall Seller's liability hereunder exceed the actual loss or damage sustained by Purchaser, up to the purchase price of the Products. The foregoing limitation of liability shall not apply to claims for bodily injury or damages to real property or tangible personal property arising as a result of Seller's negligence or a product defect.

11.2 SELLER SHALL NOT BE LIABLE FOR ANY LOSS OF USE, REVENUE OR ANTICIPATED PROFITS, COST OF SUBSTITUTE PRODUCTS OR SERVICES, LOSS OF STORED, TRANSMITTED OR RECORDED DATA, OR FOR ANY INDIRECT, INCIDENTAL, UNFORESEEN, SPECIAL, PUNITIVE OR CONSEQUENTIAL DAMAGES WHETHER BASED ON CONTRACT, TORT (INCLUDING NEGLIGENCE), STRICT LIABILITY OR ANY OTHER THEORY OR FORM OF ACTION, EVEN IF SELLER HAS BEEN ADVISED OF THE POSSIBILITY THEREOF, ARISING OUT OF OR IN CONNECTION WITH THIS AGREEMENT OR THE SALE OR USE OF THE PRODUCTS. THE FOREGOING IS A SEPARATE, ESSENTIAL TERM OF THIS AGREEMENT AND SHALL BE EFFECTIVE UPON THE FAILURE OF ANY REMEDY, EXCLUSIVE OR NOT.

## 12. INSTALLATION - ADDITIONAL CHARGES

12.1 General. Unless otherwise expressly stipulated in writing, the Products covered hereby shall be installed by and at the expense of Seller except that Seller shall not provide rigging or site preparation services unless otherwise agreed to in writing by Seller for an additional charge. Seller will not install accessory items such as cabinets, illuminators, darkroom equipment or processors for X-Ray and CT equipment, unless otherwise agreed to in writing by Seller.

12.2 Installation by Seller. If Seller specifies it will install the Products, the following applies: subject to fulfillment of the obligations set forth in 12.4 below, Seller shall install the Products covered hereby and connect same to the requisite safety switches and power lines to be installed by Purchaser. Except as otherwise specified below, if such installation and connection are performed by Seller's technical personnel, prices shown include the cost thereof, provided that the installation and connection can be performed within the Continental United States or Puerto Rico and during normal business hours. Any overtime charges or other special expenses shall be additional charges to the prices shown.

12.3 Trade Unions. In the event that a trade union, or unions, or other local labor conditions prevent Seller from performing the above work with its own employees or contractors, then Purchaser shall either make all required arrangements with the trade union, or unions, to permit Seller's completion of said work or shall provide the personnel, at Purchaser's sole cost and expense. Moreover, any additional cost incurred by Seller and related to such labor disputes shall be paid by the Purchaser and Seller's obligations under such circumstances will be limited to providing engineering supervision of installation and connection of Seller equipment to existing wiring.

12.4 Purchaser's Obligations. Purchaser shall, at its expense, provide all proper and necessary labor and materials for plumbing service, carpentry work, conduit wiring, and other preparations required for such installation and connection. All such labor and materials shall be completed and available at the time of delivery of the Products by Seller. Additionally, the Purchaser shall provide free access to the premises of installation and, if necessary, safe and secure space thereon for storage of Products and equipment prior to installation by Seller. Purchaser shall be responsible, at its sole cost and expense, for obtaining all permits, licenses and approvals required by any federal, state or local authorities in connection with the installation and operation of the Products, including but not limited to any certificate of need and zoning variances. Purchaser shall provide a suitable environment for the Products and shall ensure, at its sole cost and expense, that its premises are free of asbestos, hazardous conditions and any concealed, unknown or dangerous conditions and that all site requirements are met. Seller shall delay its work until Purchaser has completed the removal of the asbestos or other hazardous materials or has taken any other precautions and completed any other work required by applicable regulations. Purchaser shall reimburse Seller for any increased costs and expenses incurred by Seller that are the result of or are caused by any such delay. In the event that Seller is requested to supervise the installation of the Products, it remains the Purchaser's responsibility to comply with local regulations. Seller is not an architect and all drawings furnished by Seller are not construction drawings.

12.5 Regulatory Reporting. In the event that any regulatory activity is performed by other than Seller authorized personnel, Purchaser shall be responsible for fulfilling any and all reporting requirements.

12.6 Completion of Installation. Installation shall be complete upon the conclusion of final calibration and checkout under Seller's standard procedures to verify that the Products meet applicable written performance specifications. Notwithstanding the foregoing, first use of the Products by Purchaser, its agents or employees for any purpose after delivery shall constitute completion of installation.

## 13. PATENT, TRADEMARK AND OTHER INFRINGEMENT CLAIMS

13.1 Infringement by Seller. Seller warrants that the Products manufactured by Seller and sold hereunder do not infringe any U.S. patent or copyright. If Purchaser receives a claim that any such Product, or parts thereof, infringe upon the rights of others under any U.S. patent or copyright, Purchaser shall notify Seller immediately in writing. As to all infringement claims relating to Products or parts manufactured by Seller or one of its affiliates:

(a) Purchaser shall give Seller information, assistance and exclusive authority to evaluate, defend and settle such claims.

(b) Seller shall then, at its own expense, defend or settle such claims, procure for the Purchaser the right to use the Products, or remove or modify them to avoid infringement. If none of these alternatives is available on terms reasonable to Seller, then Purchaser shall return the Products to Seller and Seller shall refund to Purchaser the purchase price paid by the Purchaser less reasonable depreciation for Purchaser's use of the Products. The foregoing states Seller's entire obligation and liability, and the Purchaser's sole remedy, for claims of infringement.

13.2 Infringement by Purchaser. If some or all of the Products sold hereunder are made by Seller pursuant to drawings or specifications furnished by the Purchaser, or if Purchaser modifies or combines, operates or uses the Products other than as specified by Seller or with any product, data, software, apparatus or program not provided or approved by Seller, then the indemnity obligation of Seller under Section 13.1 shall be null and void and should a claim be made that such Products infringe the rights of any third party under patent, trademark or otherwise, then Purchaser shall indemnify and hold Seller

# SIEMENS

Siemens Medical Solutions USA, Inc.  
51 Valley Stream Parkway, Malvern, PA 19355  
Fax: (866) 309-6992

SIEMENS REPRESENTATIVE  
Tegan Gonzalez - (781) 454-5132

harmless against any liability or expense, including reasonable attorneys' fees, incurred by Seller in connection therewith.

## 14. DESIGNS AND TRADE SECRETS; LICENSE; CONFIDENTIALITY

14.1 Any drawings, data, designs, software programs or other technical information supplied by Seller to Purchaser in connection with the sale of the Products are not included in the sale of the Products to Purchaser, shall remain Seller's property and shall at all times be held in confidence by Purchaser. Such information shall not be reproduced or disclosed to others without Seller's prior written consent.

14.2 For all goods purchased hereunder which utilize software for their operation, such "Applications Software" shall be licensed to Purchaser under the terms of Seller's Software License Schedule as attached hereto.

14.3 Diagnostic/Maintenance Software is not included under 14.2 above, is available only as a special option under a separate Diagnostic Materials License Agreement and may be subject to a separate licensing fee.

14.4 Seller and Purchaser shall maintain the confidentiality of any information provided or disclosed to the other party relating to the business, customers and/or patients of the disclosing party, as well as this Agreement and its terms (including the pricing and other financial terms under which the Purchaser will be purchasing the Products hereunder). Each party shall use reasonable care to protect the confidentiality of the information disclosed, but no less than the degree of care it would use to protect its own confidential information, and shall only disclose the other party's confidential information to its employees and agents having a need to know this information. The obligations of confidentiality set forth herein shall not apply to any information in the public domain at the time of disclosure or that is required to be disclosed by court order or by law.

## 15. ENGINEERING CHANGES

15.1 Seller makes no representation that engineering changes which may be announced in the future will be suitable for use on, or in connection with, the Products.

## 16. ASSIGNMENT

16.1 Neither party may assign any rights or obligations under this Agreement without the written consent of the other and any attempt to do so shall be void, except that Seller may assign this Agreement without consent to any subsidiary or affiliated company, and may delegate to authorized subcontractors or service suppliers any work to be performed under this Agreement so long as Seller remains liable for the performance of its obligations under this Agreement. This Agreement shall inure to and be binding upon the parties and their respective successors, permitted assigns and legal representatives. Seller shall have no obligations under this Agreement to any assignee of Purchaser that is not approved by Seller in advance.

## 17. DAMAGES, COSTS AND FEES

17.1 In the event that any dispute or difference is brought arising from or relating to this Agreement or the breach, termination or validity thereof, the prevailing party shall NOT be entitled to recover from the other party any punitive damages. The prevailing party shall be entitled to recover from the other party all reasonable attorneys' fees incurred, together with such other expenses, costs and disbursements as may be allowed by law.

## 18. MODIFICATION

18.1 This Agreement may not be changed, modified or amended except in writing signed by duly authorized representatives of the parties.

## 19. GOVERNING LAW; WAIVER OF JURY TRIAL

19.1 This Agreement shall be governed by the laws of the Commonwealth of Pennsylvania.

19.2 EACH OF THE PARTIES EXPRESSLY WAIVES ALL RIGHTS TO A JURY TRIAL IN CONNECTION WITH ANY DISPUTE UNDER THIS AGREEMENT.

## 20. COST REPORTING

20.1 Purchaser agrees that it will fully and accurately account for and report in all cost reports and otherwise fully and accurately disclose to federal and state health care program payors and fully and accurately reflect where and as appropriate to the applicable reimbursement methodology, all services and other items, including any and all discounts, received from Seller under this Agreement, in compliance with all applicable laws, rules and regulations, including but not limited to the Social Security Act and implementing regulations relating to Medicare, Medicaid and other federal and state health care reimbursement programs.

## 21. INTEGRATION

21.1 These terms and conditions, including any attachments or other documents incorporated by reference herein, constitute the entire agreement and the complete and exclusive statement of agreement with respect to the subject matter hereof, and supersede any and all prior agreements, understandings and communications between the parties with respect to the Products.

## 22. SEVERABILITY; HEADINGS

22.1 No provision of this Agreement which may be deemed unenforceable will in any way invalidate any other portion or provision of this Agreement. Section headings are for convenience only and will have no substantive effect.

## 23. WAIVER

23.1 No failure and no delay in exercising, on the part of any party, any right under this Agreement will operate as a waiver thereof, nor will any single or partial exercise of any right preclude the further exercise of any other right.

## 24. NOTICES

24.1 Any notice or other communication under this Agreement shall be deemed properly given if given in writing and delivered in person or mailed, properly addressed and stamped with the required postage, to the intended recipient at its address specified on the face hereof. Either party may from time to time change such address by giving the other party notice of such change in accordance with this section.

## 25. RIGHTS CUMULATIVE

25.1 The rights and remedies afforded to Seller under this Agreement are in addition to, and do not in anyway limit, any other rights or remedies afforded to Seller by any other agreement, by law or otherwise.

## 26. END USER CERTIFICATION

26.1 Purchaser represents, warrants and covenants that it is acquiring the Products for its own end use and not for reselling, leasing or transferring to a third party (except for lease-back financings).

# SIEMENS

Siemens Medical Solutions USA, Inc.  
51 Valley Stream Parkway, Malvern, PA 19355  
Fax: (866) 309-6992

SIEMENS REPRESENTATIVE  
Tegan Gonzalez - (781) 454-5132

## Software License Schedule to the Siemens Medical Solutions USA, Inc. General Terms and Conditions

**1. DEFINITIONS:** The following definitions apply to this Schedule:  
"Agreement" shall mean the attached (i) Quotation for Products and/or Services including the Terms and Conditions of Sale and applicable schedules; and/or (ii) Software License Agreement describing the software licensed herein and the specific system for which the license is issued.  
"Licensor" shall mean Siemens Medical Solutions USA, Inc.  
"Licensee" shall mean the end-user to whom Licensor provides Software or Documentation for its internal use under the Agreement.  
"Software" shall mean the software described in the attached Agreement, including the following as contained therein: (i) software programs consisting of a series of statements or instructions to be used directly or indirectly in a programmable controller or computer to bring about a certain result and (ii) databases consisting of systemized collections of data to be used or referenced directly or indirectly by a programmed controller or computer. Notwithstanding the foregoing, "Software" does not include "firmware" as such term is conventionally understood. Diagnostic/Maintenance Software also is not included within the scope of the Software licensed under this Schedule, and is available only as a special option under a separate Diagnostic Materials License Agreement and may be subject to a separate licensing fee.  
"Documentation" shall mean the documents and other supporting materials which are intended to support the use of an associated product, including (but not limited to) instructions, descriptions, flow charts, logic diagrams and listings of the Software, in text or graphic form, on machine readable or printed media.  
"Designated Unit" shall mean a single control unit or computer identified on the first page of the Agreement, on which Software licensed hereunder may be used by Licensee.  
**2. SCOPE:** The following terms and conditions shall apply to all Software and Documentation provided by Licensor to Licensee under the Agreement (whether included with other products listed in the Agreement or listed separately in the Agreement), together with any updates or revisions thereto which Licensor may provide to Licensee, and all copies thereof, except any Software and/or Documentation licensed directly by Licensor's supplier under a separate end-user license agreement accompanying the Software or the Documentation, in which case Licensee agrees to be bound by that license agreement as a condition to using the Software and/or Documentation. Except as expressly provided herein, and provided that in no event shall the warranties or other obligations of Licensor with respect to such Software or Documentation exceed those set forth in this Schedule, this Schedule shall be subject to the liability limitations and exclusions and other terms and conditions set forth in the Agreement. **ANY USE OF THE SOFTWARE, INCLUDING BUT NOT LIMITED TO USE ON THE DESIGNATED UNIT, WILL CONSTITUTE LICENSEE'S AGREEMENT TO THIS SOFTWARE LICENSE SCHEDULE (OR RATIFICATION OF ANY PREVIOUS CONSENT).**  
**3. SOFTWARE AND DOCUMENTATION LICENSE:** Subject to the payment of any applicable annual license fee(s), whether stated separately or included in the purchase price of another product, and to Licensee's acceptance of all of the obligations set forth herein and to the fulfillment of those obligations, Licensor or, if applicable, its licensor or supplier, hereby grants to Licensee a paid-up, nonexclusive and nontransferable (except as expressly provided in this Schedule) limited license to use the Software provided by Licensor under the Agreement solely for Licensee's own use on the Designated Unit and to use the Documentation in support of Licensee's authorized use of the Software, for the purpose of operating the Designated Unit in accordance with the instructions set forth in the user's manual supplied with the Designated Unit and for no other purpose whatsoever. A separate license is required for each Designated Unit on which the Software is to be used. Licensee may obtain from Licensor one copy of the Software licensed hereunder for backup and archival purposes only as is necessary to support Licensee's own authorized use of the Software, provided that Licensee includes on or in all copies (in any form) all copyright, trade secret or other proprietary notices contained on or in the Software as provided by Licensor. Additional copies of the Documentation may be licensed from Licensor at its then applicable charges. Licensee may make the Software and Documentation (including any copies) available only to its employees and other persons on Licensee's premises to whom such disclosure is necessary to enable Licensee to use the Software or Documentation within the scope of the license provided in this Schedule. If the Software is supplied to any unit or agency of the United States Government other than

the Department of Defense, the Software and Documentation are classified as "restricted computer software" and the Government's rights in the Software and Documentation shall be as provided in paragraph (c) (2) of the Commercial Computer Software-Restricted Rights clause in FAR 52.227-19 and any successor laws, rules or regulations thereto. If the Software is supplied to the United States Department of Defense, the Software is classified as "commercial computer software" and the Government is furnished the Software and Documentation with "restricted rights" as defined in paragraph (c) (1) of the Rights in Technical Data and Computer Software clause in DFARS 252.227-7013 and any successor laws, rules or regulations thereto.

**4. PROPRIETARY PROTECTION AND CONFIDENTIALITY:** Ownership of and title to the Software and Documentation and all copies, in any form, licensed under this Schedule are and will remain in Licensor or its suppliers at all times. Licensee shall not (i) remove any copyright, trade secret or other proprietary right notices contained on or in the Software or Documentation as provided by Licensor, (ii) reproduce or modify any Software or Documentation or copy thereof, (iii) reverse assemble, reverse engineer or decompile any Software, or copy thereof, in whole or in part (except and only to the extent that such activity is expressly permitted by applicable law notwithstanding this limitation), (iv) sell, transfer or otherwise make available to others the Software or Documentation, or any copy thereof, except as expressly permitted by this Schedule, or (v) apply any techniques to derive any trade secrets embodied in the Software or Documentation. Licensee shall take all appropriate actions to ensure that: (i) the Software does not leave the Designated Unit's equipment location as set forth above, (ii) the Software is not copied by Licensee or any third parties, and (iii) the Software is not used in any equipment other than the Designated Unit. Licensee shall secure and protect the Software and Documentation and copies thereof from disclosure and shall take such actions with its employees and other persons who are permitted access to the Software or Documentation or copies as may be necessary to satisfy Licensee's obligations hereunder. Prior to disposing of any computer medium, computer memory or data storage apparatus, Licensee shall ensure that all copies of Software and Documentation have been erased therefrom or otherwise destroyed. In the event that Licensee becomes aware that any Software or Documentation or copies are being used in a manner not permitted by the license, Licensee shall immediately notify Licensor in writing of such fact and if the person or persons so using the Software or Documentation are employed or otherwise subject to Licensee's direction and control, Licensee shall use reasonable efforts to terminate such impermissible use. Licensee will fully cooperate with Licensor so as to enable Licensor to enforce its proprietary and property rights in the Software. Licensee agrees that, subject to Licensee's reasonable security procedures, Licensor shall have immediate access to the Software at all times and that Licensor may take immediate possession thereof upon termination or expiration of the associated license or this Schedule. Licensee's obligations under this paragraph shall survive any termination of a license, the Schedule or the Agreement.

**5. UPDATES AND REVISIONS:** During the warranty period or under a separate service contract or software update subscription, revised or updated versions of the Software licensed under this Schedule may be made available, at Licensor's option, to Licensee to use or to test while Licensee continues use of a previous version. Licensee has the right to decide whether to install any such revised or updated versions or to continue use of the previous version after giving due regard to the United States Food and Drug Administration rules and regulations. However, Licensee shall pay Licensor for any services necessitated by any modifications of the Software by Licensee or by Licensee's failure to utilize the current non-investigational version of the Software provided by Licensor. Software updates that provide new features or capabilities or that require hardware changes will be offered to Licensee at purchase prices established by Licensor. Licensor retains the sole right to determine whether an update represents an enhancement of a previously purchased capability or a new capability for which the Licensee will be charged. In addition, some updates may require Applications Training performed by Licensor's personnel that will be offered at Licensor's prevailing rates. Licensor retains the sole right to determine whether an update requires such training.

**6. DELIVERY, RISK OF LOSS AND TITLE:** Notwithstanding the provisions of Section 6 of the attached Terms and Conditions of Sale, if any, the Software and Documentation licensed hereunder shall be delivered on or about the delivery date stated in the Agreement unless a separate delivery

# SIEMENS

Siemens Medical Solutions USA, Inc.  
51 Valley Stream Parkway, Malvern, PA 19355  
Fax: (866) 309-6992

SIEMENS REPRESENTATIVE  
Tegan Gonzalez - (781) 454-5132

date is agreed upon. If Software or Documentation licensed hereunder is lost or damaged during shipment from Licensor, Licensor will replace it at no charge to Licensee. If any Software or Documentation supplied by Licensor and licensed hereunder is lost or damaged while in the possession of Licensee, Licensor will replace it at Licensor's then current applicable charges, if any, for materials, processing and distribution. Notwithstanding the provisions of Section 6 of the attached Terms and Conditions of Sale, if any, the Software and Documentation, in any form, and all copies made by Licensee, including partial copies, and all computer media provided by Licensor are and remain the property of Licensor or its supplier. Licensee has no right, title or interest in the Software, the Documentation, or any computer media provided by Licensor, or copies, except as stated herein, and ownership of any such Software, Documentation and computer media shall at all times remain with Licensor or its suppliers.

**7. LICENSE TRANSFER:** The Software and Documentation, and the license hereunder, may not be assigned, transferred or sublicensed except as hereinafter provided. Upon the sale or lease of the Designated Unit to a third party, Licensee may transfer to such third party, with Licensor's written consent and in accordance with Licensor's then current policies and charges, the license to use the Software and Documentation hereunder, together with the Software, the Documentation, the computer media provided by Licensor, and all copies provided that: (i) Licensee notifies Licensor in writing of the name and address of such third party; (ii) such third party agrees in a written instrument delivered to Licensor to the terms of this Schedule; and (iii) Licensee does not retain any copies of the Software or Documentation in any form.

**8. WARRANTIES:** Licensor warrants that for the warranty period provided by Licensor under the attached Terms and Conditions of Sale, if any, the Software shall conform in all material respects to Licensor's published specifications as contained in the applicable supporting Documentation. This paragraph replaces Paragraphs 10.1 and 10.4 of any such Terms and Conditions of Sale with respect to the Software and Documentation. Such Documentation may be updated by Licensor from time to time and such updates may constitute a change in specification. Licensee acknowledges that the Software is of such complexity that it may have inherent or latent defects. As Licensee's sole remedy under the warranty, Licensor will provide services, during the warranty period, to correct documented Software errors which Licensor's analysis indicates are caused by a defect in the unmodified version of the Software as provided by Licensor. Licensor does not warrant that the Software will meet Licensee's requirements, or will operate in combinations which may be selected for use by Licensee, or that the operation of the Software will be uninterrupted or error free. Licensee is responsible for determining the appropriate use of and establishing the limitations of the Software and its associated Documentation as well as the results obtained by use thereof.

LICENSOR MAKES NO WARRANTY WITH RESPECT TO THE SOFTWARE AND DOCUMENTATION OTHER THAN THOSE SET FORTH IN THIS SECTION. THE WARRANTY HEREIN IS IN LIEU OF ALL OTHER WARRANTIES, EXPRESS OR IMPLIED, INCLUDING BUT NOT LIMITED TO ANY EXPRESS OR IMPLIED WARRANTIES OF MERCHANTABILITY OR FITNESS FOR A PARTICULAR PURPOSE, WHICH ARE HEREBY DISCLAIMED, AND CONSTITUTES THE ONLY WARRANTY MADE WITH RESPECT TO THE SOFTWARE AND DOCUMENTATION.

**9. LICENSE TERM AND TERMINATION:** The license for the Software and Documentation is effective on the shipment date of the Software and Documentation (F.O.B. shipping point or F.A.S., as the case may be) and continues until Licensee's possession of the Software and all copies ceases (except in connection with a transfer of the license as permitted by this Schedule) or until otherwise terminated as provided herein. Licensee may terminate the license for the Software and Documentation at any time after discontinuance of use of the Software and Documentation and all copies, upon written notice to Licensor. If Licensee (i) fails to comply with its obligations herein and does not cure such failure within ten (10) days after receipt of notice from Licensor, or (ii) attempts to assign the Agreement or this Schedule or any rights or obligations hereunder without Licensor's prior written consent, then Licensor may terminate the license hereunder and require the immediate discontinuance of all use of the Software and Documentation and all copies thereof in any form, including modified versions and updated works. Within five (5) days after the termination of the license, Licensee shall, at Licensor's option either: (i) return to Licensor the Software and Documentation, and all copies, in any form, including updated versions, along with any computer media provided by Licensor; or (ii) destroy the affected Software and Documentation, and all copies, in any form, including updated versions, and certify such return or destruction in writing to Licensor.

**10. MISCELLANEOUS:** Since the unauthorized use of the Software and/or Documentation may leave Licensor without an adequate remedy at law, Licensee agrees that injunctive or other equitable relief will be appropriate to

restrain such use, threatened or actual. Licensee further agrees that to the extent applicable, (i) any of Licensor's suppliers of Software and/or Documentation is a direct and intended beneficiary of this Schedule and may enforce it directly against Licensee with respect to the Software and/or Documentation provided by such supplier, and that (ii) **NO SUPPLIER OF LICENSOR SHALL BE LIABLE FOR ANY GENERAL, SPECIAL, DIRECT, INDIRECT, CONSEQUENTIAL, INCIDENTAL OR OTHER DAMAGES ARISING OUT OF ANY SUBLICENSE OF THE SOFTWARE AND/OR DOCUMENTATION. THIS LIMITATION ON LIABILITY SHALL APPLY EVEN IF ANY REMEDY FAILS OF ITS ESSENTIAL PURPOSE.**

**11. ADDITIONAL PROVISIONS RELATING TO THIRD-PARTY SOFTWARE:** If the Software includes software licensed by Licensor from third parties, the following additional provisions shall apply:

(a) If Software is provided by Licensor on separate media and labeled "Recovery Media," Licensee may use the Recovery Media solely to restore or reinstall the Software and/or Documentation originally installed on the Designated Unit.

(b) Licensee is licensed to use the Software to provide only the limited functionality (specific tasks or processes) for which the Designated Unit has been designed and marketed by Licensor. This license specifically prohibits any other use of the software programs or functions, or inclusion of additional software programs or functions that do not directly support the limited functionality, on the Designated Unit. If Licensee uses the Designated Unit to access or utilize the services or functionality of Microsoft Windows Server products (such as Microsoft Windows NT Server 4.0 (all editions) or Microsoft Windows 2000 Server (all editions)), or uses the Designated Unit to permit workstation or computing devices to access or utilize the services or functionality of Microsoft Windows Server products, Licensee may be required to obtain a Client Access License for the Designated Unit and/or each such workstation or computing device. Licensee should refer to the end user license agreement for its Microsoft Windows Server product for additional information.

(c) The Software may contain support for programs written in Java. Java technology is not fault tolerant and is not designed, manufactured, or intended for use or resale as online control equipment in hazardous environments requiring fail-safe performance, such as in the operation of nuclear facilities, aircraft navigation or communication systems, air traffic control, direct life support machines, or weapons systems, in which the failure of Java technology could lead directly to death, personal injury, or severe physical or environmental damage. Sun Microsystems, Inc. has contractually obligated Licensor's supplier to make this disclaimer.

(d) The Software may permit Licensor, its supplier(s), or their respective affiliates to provide or make available to Licensee Software updates, supplements, add-on components, or Internet-based services components of the Software after the date Licensee obtains its initial copy of the Software ("Supplemental Components").

- If Licensor provides or makes available to Licensee Supplemental components and no other end-user software licensing agreement terms are provided along with the Supplemental Components, then the terms of this Software License Schedule shall apply.

- If a supplier of Licensor or affiliates of such a supplier make available Supplemental Components, and no other end-user software licensing agreement terms are provided, then the terms of this Schedule shall apply, except that the supplier or affiliate entity providing the Supplemental Component(s) shall be the licensor of the Supplemental Component(s).

Licensor, its supplier(s), and their respective affiliates reserve the right to discontinue any Internet-based services provided to Licensee or made available to Licensee through the use of the Software.

(e) The Software and Documentation supplied by Licensor's suppliers are provided by such suppliers "AS IS" and with all faults. **SUCH SUPPLIERS DO NOT BEAR ANY OF THE RISK AS TO SATISFACTORY QUALITY, PERFORMANCE, ACCURACY, OR EFFORT (INCLUDING LACK OF NEGLIGENCE) WITH RESPECT TO SUCH SOFTWARE AND DOCUMENTATION. ALSO, THERE IS NO WARRANTY BY SUCH SUPPLIERS AGAINST INTERFERENCE WITH LICENSEE'S ENJOYMENT OF THE SOFTWARE OR AGAINST INFRINGEMENT. IF LICENSEE HAS RECEIVED ANY WARRANTIES REGARDING THE DESIGNATED UNIT OR THE SOFTWARE, THOSE WARRANTIES DO NOT ORIGINATE FROM, AND ARE NOT BINDING ON, LICENSOR'S SUPPLIERS.**

(f) Licensee acknowledges that portions of the Software are of U.S. origin. Licensee agrees to comply with all applicable international and national laws that apply to the Software, including the U.S. Export Administration Regulations, as well as applicable end-user, end-use and destination restrictions issued by U.S. and other governments. For additional information on exporting software supplied by Microsoft, see <http://www.microsoft.com/exporting/>.

Revised 03/15/05

# SIEMENS

Siemens Medical Solutions USA, Inc.  
51 Valley Stream Parkway, Malvern, PA 19355  
Fax: (866) 309-6992

SIEMENS REPRESENTATIVE  
Tegan Gonzalez - (781) 454-5132

## MR Warranty Information

<u>Product</u>	<u>Period of Warranty<sup>1</sup></u>	<u>Coverage</u>
(New Systems and "Proven Excellence" Refurbished Systems Only)		
MR System (not including consumables)	12 month	Full Warranty (parts & labor)
<u>Post Warranty (after expiration of system warranty) – Replacement parts only!</u>		
Magnet	12 month	Parts only
Spare Parts	6 month	Parts only
Consumables	Not Covered	

Note: Optional extended warranty coverage can be obtained by purchase of a service agreement.

<sup>1</sup> Period of warranty commences from the date of first use or completion of installation, whichever occurs first. In the event the completion of installation is delayed for reasons beyond Siemens' control, the stated warranty period shall commence 60 days after delivery of equipment.

# SIEMENS

Siemens Medical Solutions USA, Inc.  
 51 Valley Stream Parkway, Malvern, PA 19355  
 Fax: (866) 309-6992

SIEMENS REPRESENTATIVE  
 Tegan Gonzalez - (781) 454-5132

## Detailed Technical Specifications

### MAGNETOM Skyra

Part No. / Product	Description
14418500 MAGNETOM Skyra - System	<p>MAGNETOM Skyra - the first 3T Tim+Dot system - integrates the next generation Tim - Tim 4G and the Siemens unique Dot Engines (Day optimizing throughput Engines) enabling workflow efficiency combined with excellent diagnostic confidence due to consistent results.</p> <p>The system includes:</p> <p><b>Tim 4G+Dot</b>  <b>Tim 4G</b> provides increased patient comfort and optimized workflow efficiency. Only one patient setup, no repositioning, no changing of coils. Ultra-light-weighted coils with high density of coil elements for maximized patient comfort and increased SNR. Feet-first positioning for almost all examinations possible reduces anxiety and claustrophobia.  <b>Tim 4G</b> is 4G flexibility, accuracy and speed and brings image quality and acquisition speed to a new level.</p> <p><b>Dot</b> helps to take away the complexity in MRI scanning through patient personalization, user guidance and process automation. Exam strategies help customers quickly adapt protocols according to the patient's condition and clinical indication. Integrated decision points allow the user to easily add or remove one or a group of protocols with one click. Complicated exams are facilitated by on-board guidance views. Process automation allows optimal timing for breathing, scanning, and planning. Dot can be easily customized to follow the individual standards of care.</p> <p>Dot is personalized, guided and automated and designed to improve workflow efficiency and image consistency.</p> <p>The MAGNETOM Skyra's 70 cm Open Bore design and 173 cm length gives a patient friendly appearance that can significantly help patients with anxiety or claustrophobia.</p> <p><b>Magnet:</b></p> <ul style="list-style-type: none"> <li>- Ultra-short 163 cm long, whole-body superconductive 3T magnet with active shielding (AS) technology with counter coils</li> <li>- External Interference Shielding (E.I.S.)</li> <li>- Excellent homogeneity enabled TrueForm magnet design which allows for a cylindrically optimized homogeneity volume resulting in high image quality (50 x 50 x 45 cm<sup>3</sup> DEV, typ. 3.6 ppm based on the 24-plane plot method)</li> <li>- The magnet has a helium capacity of approximately 1,200 liters and a typical Helium boil-off rate of 0 l/yr during typical, undisturbed clinical operation depending on the sequences used and examination time, and provided the system is serviced in regular intervals.</li> <li>- It has an integrated magnet cooling system.</li> <li>- The combination of standard active shim with 3 linear channels (1<sup>st</sup> order) and 5 non linear channels (2<sup>nd</sup> order) and passive shim allows for maximized magnetic field homogeneity and consistently high image quality for a wide range of applications</li> </ul> <p><b>Gradient system:</b></p> <ul style="list-style-type: none"> <li>- Actively shielded water-cooled world-class gradient system</li> <li>- All axes force compensated</li> <li>- TrueForm Gradient Design</li> </ul> <p><b>DirectRF - RF Transmit/Receive System:</b></p> <ul style="list-style-type: none"> <li>- Fully integrated Transmit- and Receive path in the magnet housing including extremely compact water-cooled solid state amplifier with 37.5 kW peak power</li> <li>- High dynamic range</li> <li>- Immediate feedback loop for real-time sequence adaptation</li> <li>- Integrated no tune transmit/receive Body Coil</li> <li>- TimTX TrueForm includes innovative techniques in the RF excitation hardware as well as new application and</li> </ul>

# SIEMENS

Siemens Medical Solutions USA, Inc.  
 51 Valley Stream Parkway, Malvern, PA 19355  
 Fax: (866) 309-6992

SIEMENS REPRESENTATIVE  
 Tegan Gonzalez - (781) 454-5132

Part No. / Product	Description
<p>(Continued)  <b>14418500</b>  <b>MAGNETOM Skyra - System</b></p>	<p>processing features to guarantee uniform RF distribution in all body regions. TimTX TrueForm for MAGNETOM Skyra consists of TrueForm excitation, which uses amplitude and phase transmission settings optimized for dedicated body regions. Feeding the 2 ports of the integrated body coil with an optimized weighting yields a homogeneous B1 distribution.</p> <ul style="list-style-type: none"> <li>- The revolutionary Tim 4G technology allows connecting up to 204 coil elements simultaneously enabling higher SNR and iPAT in all directions. No repositioning of patients is needed even for large Field of View examinations.</li> <li>- Dual-Density Signal transfer enables ultra-high density coil design by integrating key RF components into the local coil.</li> </ul> <p><b>Tim 4G Coils:</b>  The new Tim 4G coil technology with Dual-Density Signal Transfer, DirectConnect and SlideConnect technology combines key imaging benefits:  Excellent image quality, high patient comfort, and unmatched flexibility</p> <p>The Tim 4G coils are designed for highest image quality combined with easy handling. The high element density of the coils increases SNR and reduces examination times. DirectConnect and SlideConnect™ technology reduce patient set up time significantly. The coils are designed with the patient in mind. Light weight coils with an open design ensure highest patient comfort resulting in better patient cooperation and image quality. No coil changing with multi-exam studies saves patient setup- and table time.  AutoCoilSelect for dynamic, automatic, or interactive selection of the coil elements within the Field of View fastens the exam preparation at the host.  All coils are time-saving "no-tune" coils.  A comprehensive set of pads for comfortable and stable patient positioning together with safety straps are included.</p> <ul style="list-style-type: none"> <li>- <b>Head/Neck 20</b>  A 20-channel coil with 20 integrated pre-amplifiers ensures excellent signal-to-noise ratio. DirectConnect technology connects all 20 coil elements without cables. Patient-friendly open design for maximum patient comfort. A Look-out mirror is included for claustrophobic patients. iPAT compatible in all directions.</li> </ul> <p>The open and light design of the upper coil part increases patient comfort and is removable for easy patient handling. The lower coil part may remain on the table for most of the examinations can be used without the upper part. The Head/Neck 20 and Spine 32 are smoothly integrated into the patient table, thus enabling high flexibility in imaging and fewer coil changes and easy handling when switching patients. The Head /Neck 20 coil is equipped with two removable cushioned head stabilizers for stable and comfortable patient positioning.</p> <p>The Head/ Neck 20 can be used for applications like head examinations, neck examinations, MR Angiography, combined head/neck examinations or for imaging of the TMJ (temporomandibular joints).</p> <p>Typically combined with the Spine 32 and Body 18 or Peripheral Angio 36 but also other combinations e.g. with flexible coils like the Flex Large 4 are possible.</p> <ul style="list-style-type: none"> <li>- <b>Body 18</b>  The 18-channel coil with 18 integrated pre-amplifiers ensures maximum signal-to-noise ratio. A single SlideConnect Plug connects all 18 coil elements. The light-weight coil ensures highest patient comfort. iPAT compatible in all directions.</li> </ul> <p>Body 18 operates in an integrated fashion with the Spine 32 as an 30 channel body coil</p> <p>Body 18 can be combined with further Body 18 coils for larger coverage and positioned in different orientations (0°, 90°, 180°, 270°) for patient specific adaptations</p> <p>The Body 18 is typically used in combination with the Spine 32 for examinations of the thorax, abdomen, pelvis or hip and operates as a 30 channel body coil (3 rings 10 elements).The Body 18 can also be used for cardiac or vascular applications. Through its combinability with the Spine 32, further Body 18 (optional), the Peripheral Angio 36 (optional), but also the Head/Neck 20 and all flexible coils (e.g. Flex Large 4, Flex Small 4) it contributes for a broad range of indications up to whole-body imaging.</p> <ul style="list-style-type: none"> <li>- <b>Spine 32</b>  The 32-channel coil with 32 integrated pre-amplifiers ensures maximum signal-to-noise ratio. DirectConnect technology connects all 32 coil elements without cables. The patient friendly ergonomic design allows for</li> </ul>

# SIEMENS

Siemens Medical Solutions USA, Inc.  
 51 Valley Stream Parkway, Malvern, PA 19355  
 Fax: (866) 309-6992

SIEMENS REPRESENTATIVE  
 Tegan Gonzalez - (781) 454-5132

Part No. / Product	Description
<p>(Continued)            14418500  <b>MAGNETOM Skyra - System</b></p>	<p>maximum patient comfort. iPAT compatible in all directions.</p> <p>Smoothly integrated into the patient table the Spine 32 may remain on the patient table for nearly all exams.</p> <p>The Spine 32 is typically combined with Body 18, Head/Neck 20, Peripheral Angio 36 or Flex Large 4, Flex Small 4.</p> <ul style="list-style-type: none"> <li>- <b>Flex Large 4/ Flex Small 4</b>            4-element no-tune receiver coils which are made of soft and smooth material. The light weight coils can be wrapped around or used flat. iPAT compatible.</li> </ul> <p>Both coils connected via the Flex Coil interface. One Flex Coil interface is standard.</p> <p>The coils can be used for different examinations ranging from examinations of the extremities to abdominal examinations.</p> <p><b>Tim Table</b></p> <ul style="list-style-type: none"> <li>- The maximum scan range of the Tim Table is 140 cm. A scan range of 205 cm can be achieved with the Tim Whole Body suite (optional)</li> <li>- The maximum patient weight of 250 kg (550 lbs) is valid for horizontal and vertical movements, which ensures maximized patient comfort for obese patients.</li> <li>- The patient table can be lowered to a minimum height of 52 cm from the floor, for easier patient positioning and better accessibility for geriatric, pediatric* or immobile patients. An infusion stand is integrated to ensure fast patient set up also for critical patients.</li> <li>- Multiple Tim4G coils can be connected at once for efficient and patient friendly examinations.</li> <li>- The Tim Table can be moved with two clicks into the isocenter - one click to the upmost position and one click into the isocenter.</li> </ul> <p><b>Dot (Day Optimizing Throughput) Engine</b>            Dot multiplies the power of Tim resulting in excellent image consistency and diagnostic confidence</p> <p><b>Dot Control Centers and Dot Display</b></p> <ul style="list-style-type: none"> <li>- The ergonomically designed Dot Control Centers are integrated left and right into the front covers for controlling table movement and interaction with the Dot Display. The Dot Control Centers are well illuminated for easy visual recognition.</li> <li>- Automated table move up to upmost position, to center position or Home position facilitate smooth patient preparation and will reduce table time</li> <li>- Variable (6 levels) ventilation and lighting inside the magnet bore or volume adjustments are possible for increased patient comfort</li> <li>- The Dot Display provides on board guidance for patient set up where it's needed - directly at the scanner. Information such as Patient name or exam type or required patient position, guidance for ECG set up and immediate visualization of physiological curves will be provided for convenient operation.</li> <li>- Almost all table control functions, including ventilation and illumination of the magnet bore, can be also controlled from the operator console for convenient operation.</li> </ul> <p><b>Dot Technology</b>            Dot makes it easy to get excellent results for virtually any type of patient. Dot gives uniquely tailored, optimized scans configurable to patient condition or clinical question.            Dot provides patient personalization, user guidance and process automation and is of course configurable by the user to adapt to the different clinical needs and standards of care.</p> <p><b>Brain Dot Engine</b>            The Brain Dot Engine simplifies general brain examinations with guided workflows customized to the site specific standards of care. The Brain Dot Engine supports the user in achieving reproducible image quality with increased ease of use and time efficient exams.            The brain workflow can be personalized to the individual patient condition and clinical need. Several predefined strategies are included, which can be easily selected with one click. They can be changed at any time during the brain workflow. Protocols tailored for use of contrast media are integrated.</p> <ul style="list-style-type: none"> <li>- Standard: Standard examination with 2D protocols</li> <li>- Resolution focus: Examination with 3D protocols (with e.g. SPACE) for detailed views</li> </ul>



# SIEMENS

Siemens Medical Solutions USA, Inc.  
 51 Valley Stream Parkway, Malvern, PA 19355  
 Fax: (866) 309-6992

SIEMENS REPRESENTATIVE  
 Tegan Gonzalez - (781) 454-5132

Part No. / Product	Description
<p>(Continued)            14418500            MAGNETOM Skyra - System</p>	<ul style="list-style-type: none"> <li>- Speed focus: Examination with fast 2D protocols (with e.g. HASTE) for further speeding up the exam</li> <li>- Limited patient capabilities: Examination with <i>syngo</i> BLADE protocols</li> <li>- to minimize and correct or the effects of motion automatically</li> </ul> <p>Step-by-step user guidance is seamlessly integrated. Example images and guidance text are displayed for each individual step of the scanning workflow. Both - images and text - are easily configurable by the user.</p> <p>Easy positioning of the patient with AutoPosition. The patient is automatically moved to isocenter without using laser marking.</p> <p>AutoAlign Head automatically proposes slice positioning on the sagittal, coronal, and axial localizer images. AutoAlign provides standardized, reproducible slice positioning independent of patient age, head position, or disease.</p> <p>Automatic real-time calculation of trace-weighted images and ADC maps with Inline Diffusion Technology.</p> <p>Easy rerun or repeat with functionality allows for reduced table time even in case of patients with pain or claustrophobia. An image inside the examination UI can be selected and a rerun of the corresponding series can be triggered with identical sequences or parameters. Alternatively an exam can be repeated with a changed strategy.</p> <p>The Brain Dot Engine as all Dot Engines can be modified by the user to their individual standard of care.</p> <p><b>Tim Application Suite</b>            The Tim Application Suite offers a complete range of clinically optimized sequences, protocols and workflow functionalities for all body regions. Excellent head-to-toe imaging can be accomplished with the sequences and features included in this application suite. To enable this comprehensive application range, nine dedicated application packages have been included.</p> <ul style="list-style-type: none"> <li>- Neuro Suite</li> <li>- Angio Suite</li> <li>- Cardiac Suite</li> <li>- Body Suite</li> <li>- Onco Suite</li> <li>- Breast Suite</li> <li>- Ortho Suite</li> <li>- Pediatric* Suite</li> <li>- Scientific Suite</li> </ul> <p><b>Neuro Suite</b>            Comprehensive head and spine examinations can be performed with dedicated programs. High resolution protocols and fast protocols for uncooperative patients are provided. The Neuro Suite also includes protocols for diffusion imaging, perfusion imaging, and fMRI. It includes for example:</p> <ul style="list-style-type: none"> <li>- EPI sequences and protocols for diffusion, perfusion and fMRI for advanced neurological applications. Diffusion weighted imaging is possible with up to 16 b-values in the orthogonal directions Dynamic Analysis software (included in standard configuration) enables calculation of:               <ul style="list-style-type: none"> <li>- ADC maps</li> <li>- t-test maps from the EPI images for fMRI</li> <li>- Time-to-Peak maps for perfusion analysis.</li> </ul> </li> <li>- Whole spine protocols acquire in multiple steps via software controlled table movement in a single click.</li> <li>- 3D isotropic resolution volume imaging using T1 3D MPRAGE / 3D FLASH, SPACE DarkFluid, T2 SPACE and 3D TSE</li> <li>- T2-weighted high resolution 3D Restore protocols optimized for inner ear examinations</li> <li>- Whole-spine protocols in multiple steps with software controlled table movement</li> <li>- 2D and 3D MEDIC protocols for T2-weighted imaging, particularly for C-spine examinations in axial orientation where reproducibility is difficult due to CSF pulsations and blood flow artifacts</li> <li>- 3D Myelograms with 3D HASTE and 3D True-FISP for anatomical details</li> <li>- Dynamic sacro-iliac joint imaging after contrast administration using a fast T1-weighted FLASH 2D sequence</li> </ul>

# SIEMENS

Siemens Medical Solutions USA, Inc.  
51 Valley Stream Parkway, Malvern, PA 19355  
Fax: (866) 309-6992

**SIEMENS REPRESENTATIVE**  
Tegan Gonzalez - (781) 454-5132

Part No. / Product	Description
<p>(Continued) 14418500 MAGNETOM Skyra - System</p>	<ul style="list-style-type: none"> <li>- Spine diffusion protocols to differentiate osteoporosis versus tumor infiltration and post-radiotherapy changes versus residual tumor with PSIF sequence</li> <li>- Precision filter for high spatial accuracy e.g. for neuro intra-operative imaging and stereotactic planning</li> <li>- 3D CISS (Constructive Interference in Steady State) for excellent visualization of fine structures such as cranial nerves. High resolution imaging of inner ear and spine</li> <li>- AutoAlign Head LS providing a fast, easy, standardized, and reproducible patient scanning supporting reading by delivering a higher and more standardized image quality</li> </ul> <p><b>Angio Suite</b> Excellent MR Angiography can be performed to visualize arteries and veins with or without contrast agent. <i>Contrast-enhanced MRA</i></p> <ul style="list-style-type: none"> <li>- 3D contrast-enhanced MRA protocols for e.g. single step, dynamic, peripheral, whole body MRA with the shortest TR and TE. The strong gradients make it possible to separate the arterial phase from the venous phase.</li> <li>- TestBolus workflow for optimized bolus timing and superb image quality.</li> <li>- CareBolus functionality for accurate determination of the bolus arrival time and the "Stop and Continue" of the 3D ce-MRA protocol after the 2D bolus control scan.</li> <li>- Dynamic ce-MRA for 3D imaging over time.</li> </ul> <p><i>Non-contrast-MRA and venography</i></p> <ul style="list-style-type: none"> <li>- 2D and 3D Time-of-Flight (ToF) protocols for MRA for the Circle of Willis, carotids, neck vessels, and breath-hold protocols for abdominal vessels</li> <li>- Triggered 2D ToF sequences for non-contrast MRA, particularly of the abdomen and the extremities</li> <li>- 2D/3D Phase-Contrast</li> <li>- MR venography with 2D/3D Time-of-Flight (ToF) and Phase-Contrast</li> <li>- TONE (Tilted Optimized Non-saturation Excitation) and MTC (Magnetization Transfer Contrast) techniques for improved Contrast-to-Noise Ratio (CNR)</li> </ul> <p><i>Image processing tools</i></p> <ul style="list-style-type: none"> <li>- MPR, MIP, MinIP, and 3D SSD</li> <li>- Inline MIP for immediate results</li> <li>- Inline subtraction of pre- and post-contrast measurements</li> <li>- Inline standard deviation maps of Phase-Contrast measurements for delineation of arteries and veins</li> </ul> <p><b>Cardiac Suite</b> The cardiac suite covers comprehensive 2D routine cardiac applications, ranging from morphology and ventricular function to tissue characterization. Featuring syngo BEAT 2D in conjunction with iPAT and T-PAT techniques. <i>Cardiac views</i></p> <ul style="list-style-type: none"> <li>- Fast acquisition of the basic cardiac orientations for further examination planning</li> <li>- Cardiac scouting provides users with a step-by-step procedure for the visualization and planning of typical cardiac views, e.g. based on TrueFISP or Dark Blood TurboFLASH: short axis, 4-chamber and 2-chamber views.</li> </ul> <p><i>syngo BEAT</i></p> <ul style="list-style-type: none"> <li>- Unique tool for fast and easy cardiovascular MR imaging</li> <li>- E.g. 1 click change from FLASH to TrueFISP for easy contrast optimization</li> <li>- 1-click to switch arrhythmia rejection on / off</li> <li>- 1-click change from Cartesian to radial sampling to increase effective image resolution and avoid folding artifacts in large patients</li> </ul> <p><i>Visualization of structural cardiovascular pathologies with CMR – syngo BEAT</i></p> <ul style="list-style-type: none"> <li>- Breath-hold and free breathing techniques for strong contrast between the blood and vascular structures. Dark Blood TSE and HASTE imaging are available for the structural evaluation of the cardiothoracic anatomy, including vessels or heart valves. Cine techniques (FLASH &amp; TrueFISP) for high-resolution valve evaluation</li> <li>- Multiple contrasts such as T1- and T2-weighted imaging for use in diseases such as myocarditis (inflammation / hyperaemia), ARVD (fibrous-fatty degeneration) or acute myocardial infarction (edema)</li> <li>- Dark-blood TSE with motion compensation for high-quality vessel wall imaging in small or large vessels</li> </ul> <p><i>Tools for rapid evaluation of left or right ventricular function</i></p>

# SIEMENS

Siemens Medical Solutions USA, Inc.  
 51 Valley Stream Parkway, Malvern, PA 19355  
 Fax: (866) 309-6992

SIEMENS REPRESENTATIVE  
 Tegan Gonzalez - (781) 454-5132

Part No. / Product	Description
<p>(Continued)            14418500  <b>MAGNETOM Skyra - System</b></p>	<ul style="list-style-type: none"> <li>- Acquisition of a stack of short-axis slices (standard segmented FLASH, or advanced segmented TrueFISP)</li> <li>- Automatic adjustment of the acquisition window to the current heart rate</li> <li>- Use of the Inline ECG for graphical ECG triggering setup</li> <li>- Retrospective gating with cine sequences (TrueFISP, FLASH)</li> <li>- Protocols for whole-heart coverage</li> <li>- iPAT integration for highest temporal and spatial resolution</li> <li>- Real-time imaging in case the patient is not able to hold his breath</li> </ul> <p><i>Dynamic imaging and tissue characterization with syngo BEAT</i></p> <ul style="list-style-type: none"> <li>- Protocols for high-contrast and high-resolution tissue characterization</li> <li>- Protocols for stress and rest imaging with TrueFISP or TurboFLASH contrast support the acquisition of multiple slices with high resolution and arbitrarily adjustable slice orientation for each slice</li> <li>- T-PAT with mSENSE and GRAPPA for advanced parallel imaging provides fast high-resolution dynamic imaging</li> <li>- Segmented IR TrueFISP / FLASH with TI scout for optimization of tissue contrast</li> <li>- Advanced tissue characterization with 2D phase-sensitive IR (PSIR) sequences TrueFISP and FLASH contrast. Magnitude and phase-sensitive images with one acquisition</li> <li>- Simple: no adjustment of inversion time (TI) necessary with PSIR technique</li> <li>- Ungated single-shot PSIR imaging for tissue characterization under difficult conditions; free-breathing technique that can be applied even in case of arrhythmia</li> </ul> <p>Physiological Measurement Unit (PMU) - Wireless Physio Control</p> <ul style="list-style-type: none"> <li>- Synchronizes the measurement with the physiological cycles (triggering to minimize motion artifacts caused by cardiac and respiratory movements)</li> <li>- Wireless Sensors</li> <li>- Wireless Vector ECG / respiration and pulse sensors for physiologically synchronized imaging, rechargeable battery-powered - for optimized patient handling</li> <li>- Physiological Signals Display</li> <li>- ECG (3 channels)</li> <li>- Pulse</li> <li>- Respiration</li> <li>- External Trigger Input Display</li> </ul> <p>ECG Triggering:</p> <ul style="list-style-type: none"> <li>- Acquisition of multiple slices, e.g. of the heart, at different phases of the cardiac cycle</li> <li>- Excellent image quality by synchronizing data acquisition with cardiac motion</li> <li>- Peripheral Pulse Triggering:</li> <li>- Reduces flow artifacts caused by pulsatile blood flow</li> <li>- Excellent image quality by synchronizing data acquisition to the pulsatile blood flow</li> <li>- Respiratory Triggering:</li> <li>- Excellent image quality by synchronizing data acquisition with the respiratory motion</li> <li>- External Triggering:</li> <li>- Interface for trigger input from external sources (e.g. Patient Monitoring System) inside the examination room</li> <li>- Interface for trigger input from external sources (e.g. pulse generator, trigger sources for fMRI) outside the examination room</li> <li>- Optical trigger output for fMRI</li> <li>- Retrospective gating for ECG, peripheral pulse, and external trigger input</li> </ul> <p><b>Breast Suite</b>            Extremely high spatial and temporal resolution can be achieved in very short measuring times by using iPAT with GRAPPA.            Excellent soft tissue differentiation, customized protocols (e.g. with fat saturation or water excitation or silicone excitation), as well as flexible multi-planar visualization allow for fast, simple and reproducible evaluation of MR breast examinations.</p>

# SIEMENS

Siemens Medical Solutions USA, Inc.  
51 Valley Stream Parkway, Malvern, PA 19355  
Fax: (866) 309-6992

SIEMENS REPRESENTATIVE  
Tegan Gonzalez - (781) 454-5132

Part No. / Product	Description
<p>(Continued) 14418500 MAGNETOM Skyra - System</p>	<p>This package includes:</p> <ul style="list-style-type: none"> <li>- Quantitative evaluation and fast analysis of the data with colorized Wash-in, Wash-out, Time-To-Peak, Positive-Enhancement-Integral, MIPtime and combination maps with Inline technology or for offline calculation</li> <li>- High-resolution 2D protocols for morphology evaluation</li> <li>- High-resolution 3D protocols covering both breasts simultaneously</li> <li>- Protocols to support interventions (fine needle and vacuum biopsies, wire localization)</li> <li>- Protocols for evaluating breasts with silicone implants</li> <li>- Automatic and manual frequency adjustment, taking into account the silicone signal</li> <li>- Detection of the silicone signal either to suppress the silicone signal, if the surrounding tissue is to be evaluated, or to suppress the tissue signal in order to detect an implant leakage</li> <li>- SPAIR - robust fat sat (robust fat suppression using an adiabatic frequency selective inversion pulse)</li> <li>- DIXON - 2-point Dixon with 3D VIBE, the following contrasts can be obtained: in-phase, opposed phase, fat and water image.</li> <li>- iPAT with GRAPPA for maximum resolution in short time</li> <li>- Inline subtraction and MIP display</li> <li>- Offline subtraction, MPR and MIP display</li> <li>- syngo REVEAL: diffusion imaging for breast exams</li> <li>- IPAT Extension that allows state-of-the-art sagittal breast imaging</li> <li>- iPAT Extension allows bilateral 3D sagittal breast imaging with Fat Sat or Water excitation</li> </ul> <p>The Breast Suite also includes: <b>syngo VIEWS (Volume Imaging with Enhanced Water Signal)</b></p> <ul style="list-style-type: none"> <li>- bilateral - both breasts are examined simultaneously</li> <li>- axial - the milk ducts are directly displayed</li> <li>- fat-saturated or water-excited - fat complicates clinical evaluation and is suppressed</li> <li>- near-isotropic 3D measurement - the same voxel size in all three directions for reconstruction in any slice direction</li> <li>- sub millimeter voxel - highest resolution for precise evaluation</li> </ul> <p><b>Body Suite</b> Body Suite covers your needs for clinical body applications. Ultrafast high resolution 2D and 3D protocols are provided for abdomen, pelvis, MR Colonography, MRCP, dynamic kidney, and MR Urography applications. Siemens unique 2D PACE technique makes body imaging easy allowing for multi-breath hold examinations as well as free breathing during the scans. Motion artifacts are greatly reduced with 2D PACE Inline technology.</p> <p>This package includes:</p> <ul style="list-style-type: none"> <li>- Free breathing 2D PACE applications with 2D/3D HASTE (RESTORE) and 2D/3D TSE (RESTORE)</li> <li>- Optimized fast single shot HASTE protocols and high-resolution 3D RESTORE protocols based on SPACE and TSE for MRCP and MR Urography examinations</li> </ul> <p><b>ABDOMEN:</b></p> <p>2D:</p> <ul style="list-style-type: none"> <li>- T1w (FLASH) breath-hold scans +/- Fat Sat (SPAIR, Q-FatSat, in-/opp-phase)</li> <li>- T2w (HASTE, TSE/BLADE, EPI) breath-hold scans +/- Fat Sat (SPAIR, FatSat, STIR)</li> <li>- T1w (TFL) triggered scans (2D PACE free breathing) in-/opp-phase</li> <li>- T2w (HASTE, TSE/BLADE, EPI) triggered scans (2D PACE free breathing) +/- Fat Sat (SPAIR, FatSat, STIR) as well as HASTE- and TSE-multi-echo</li> <li>- Optimized fast single shot HASTE protocols and high-resolution 3D RESTORE protocols based on SPACE and TSE for MRCP and MR urography examinations</li> </ul> <p>3D:</p> <ul style="list-style-type: none"> <li>- Dixon (VIBE 2pt-Dixon) breath-hold scans, following contrasts can be obtained: in-phase, opposed phase, fat and water image.</li> <li>- Dynamic (VIBE + Q-FatSat) protocols for best visualization of focal lesions with high spatial and temporal resolution</li> <li>- Colonography dark lumen with T1-weighted VIBE</li> </ul> <p><b>PELVIS:</b></p>

# SIEMENS

Siemens Medical Solutions USA, Inc.  
 51 Valley Stream Parkway, Malvern, PA 19355  
 Fax: (866) 309-6992

SIEMENS REPRESENTATIVE  
 Tegan Gonzalez - (781) 454-5132

Part No. / Product	Description
<p>(Continued)            14418500            MAGNETOM Skyra -            System</p>	<ul style="list-style-type: none"> <li>- High-resolution T1w, T2w pelvic imaging (prostate, cervix)</li> <li>- Isotropic T2w SPACE 3D protocols for tumor search in the pelvis</li> <li>- Dynamic volume examinations with 3D VIBE</li> <li>- <i>syngo</i> REVEAL: diffusion imaging for liver and whole body exams</li> </ul> <p><b>Onco Suite</b>            MR imaging has an excellent advantage of soft tissue contrast, multi-planar capabilities and the possibility of selectively suppressing specific tissue e.g. fat or water. This helps visualize pathologies, particularly metastases. The Onco Suite features a collection of sequences as well as protocols and evaluation tools that guide through a detailed screening of clinical indications, such as in hepatic neoplasms.            This package includes:</p> <ul style="list-style-type: none"> <li>- STIR TSE and HASTE, FLASH in-phase and opposed-phase protocols with a high sensitivity to metastases visualization</li> <li>- Dynamic imaging protocols for assessment of the kinetic behavior for lesion visualization and characterization</li> <li>- Quantitative evaluation and fast analysis of the data with colorized Wash-in, Wash-out, Time-To-Peak, Positive-Enhancement-Integral, MIptime and combination maps with Inline technology or for offline calculation</li> <li>- Display and analysis of the temporal behavior in selected regions of interest with the included MeanCurve post processing application. This includes the capability of using additional datasets as a guide for defining regions of interest even faster and easier than before.</li> <li>- <i>syngo</i> REVEAL: diffusion imaging for liver and whole body exams</li> </ul> <p>Dedicated prostate protocols for detection, localization, and staging of tumors and recurrences</p> <ul style="list-style-type: none"> <li>- <i>syngo</i> REVEAL (diffusion-weighted imaging)</li> </ul> <p><b>Ortho Suite</b>            Ortho Suite is a comprehensive collection of protocols for joint and spine imaging. MR imaging is especially suitable for avascular necrosis and internal derangements. The protocols included in this Suite can also be applied for imaging of tumors and infections.            This package includes:</p> <ul style="list-style-type: none"> <li>- 2D TSE protocols for PD, T1 and T2-weighted contrast with high in-plane resolution and thin slices</li> <li>- 3D MEDIC, 3D TrueFISP protocols with water excitation for T2-weighted imaging with high in-plane resolution and thin slices</li> <li>- High resolution 3D VIBE protocol for MR arthrography (knee, shoulder and hip)</li> <li>- 3D MEDIC, 3D TrueFISP, 3D VIBE protocols with water excitation having high isotropic resolution, optimized for 3D post-processing</li> <li>- PD SPACE with fat saturation and T2 SPACE with high isotropic resolution optimized for 3D post-processing</li> <li>- Whole spine single-step or multi-step protocols</li> <li>- Excellent fat suppression in off-center positions, e.g. in the shoulder due to high magnet homogeneity</li> <li>- Dynamic TMJ and ilio-sacral joint protocol</li> <li>- Susceptibility-insensitive protocols for imaging in the presence MR conditional implants per the manufacturer instructions.</li> <li>- Multi-Echo SE sequence with up to 32 echoes for the calculation of T2 time maps (calculation included in the Scientific Suite)</li> <li>- High resolution 3D DESS (Double Echo Steady State): T2 / T1-weighted imaging for excellent fluid-cartilage differentiation</li> </ul> <p><b>Pediatric* Suite</b>            The parameters for pediatric imaging vary significantly in comparison to the parameters for adults. The reasons are developing tissues, body size, faster heart rates and restricted compliance with breath-hold commands. Protocols can be adapted for imaging infants.</p> <p>*MR scanning has not been established as safe for imaging fetuses and infants under two years of age. The responsible physician has to decide about the benefit of the MRI examination in comparison to other imaging procedures.</p> <p><b>Scientific Suite</b>            Scientific Suite supports the scientifically oriented user with an easy access to application-specific data for further</p>

# SIEMENS

Siemens Medical Solutions USA, Inc.  
 51 Valley Stream Parkway, Malvern, PA 19355  
 Fax: (866) 309-6992

SIEMENS REPRESENTATIVE  
 Tegan Gonzalez - (781) 454-5132

Part No. / Product	Description
<p>(Continued)                      14418500                      MAGNETOM Skyra - System</p>	<p>processing and advanced image computation methods.</p> <ul style="list-style-type: none"> <li>- Support of USB memory sticks</li> <li>- Access to the file system by means of a secure and convenient browser</li> <li>- Anonymization of patient data</li> <li>- Easy generation of AVIs and screenshots for integration into presentations and training videos</li> <li>- Export function for tables, statistics and signal-time-courses in a communal format (MeanCurve, Spectroscopy, DTI evaluation)</li> <li>- Advanced image computation methods such as T2 and T1 time calculation, addition, subtraction, multiplication, division, and integration of images</li> </ul> <p>The sequences, features and techniques for acquisition and reconstruction included in the Tim Application Suite are described in detail below.</p> <p><b>Sequences</b>                      Spin Echo family of sequences:</p> <ul style="list-style-type: none"> <li>- Spin Echo (SE) - Single, Double, and Multi Echo (up to 32 echoes); Inversion Recovery (IR)</li> <li>- 2D / 3D Turbo Spin Echo (TSE) - Restore technique for shorter TR times while maintaining excellent T2 contrast; TurboIR: Inversion Recovery for STIR, DarkFluid T1 and T2, TrueIR; Echo Sharing for dual-contrast TSE</li> <li>- 2D / 3D HASTE (Half-Fourier Acquisition with Single Shot Turbo Spin Echo) - Inversion Recovery for STIR and DarkFluid contrast</li> <li>- SPACE for 3D imaging with high isotropic resolution with T1, T2, PD, and DarkFluid Contrast</li> </ul> <p>Gradient Echo family of sequences:</p> <ul style="list-style-type: none"> <li>- 2D / 3D FLASH (spoiled GRE) - dual echo for in- / opposed phase imaging 3D VIBE (Volume Interpolated Breathhold Examination) - quick fat saturation; double echo for in-phase / opposed phase 3D imaging; DynaVIBE: Inline 3D elastic motion correction for multi phase data sets of the abdomen; Inline Breast Evaluation</li> <li>- 2D / 3D MEDIC (Multi Echo Data Image Combination) for high resolution T2 weighted orthopedic imaging and excellent contrast</li> <li>- 2D / 3D TurboFLASH - 3D MPRAGE; single shot T1 weighted imaging e.g. for abdominal imaging during free breathing</li> <li>- 3D GRE for field mapping</li> <li>- 2D / 3D FISP (Fast Imaging with Steady State Precession)</li> <li>- 2D / 3D PSIF - PSIF Diffusion</li> <li>- Echo Planar Imaging (EPI) - diffusion-weighted; single shot SE and FID e.g. for BOLD imaging and Perfusion-weighted imaging; 2D / 3D Segmented EPI (SE and FID)</li> <li>- ce-MRA sequence with Inline subtraction and Inline MIP</li> <li>- 2D / 3D Time-of-Flight (ToF) Angiography - single slab and multi slab; triggered and segmented</li> <li>- 2D / 3D Phase Contrast Angiography</li> <li>- syngo BEAT Tool - TrueFISP segmented; 2D FLASH segmented;</li> <li>- Magnetization-prepared TrueFISP (IR, SR, FS); IR TI scout; Retro gating</li> </ul> <p>Standard Fat/Water Imaging:</p> <ul style="list-style-type: none"> <li>- Fat and Water Saturation. Additional frequency selective RF pulses used to suppress bright signal from fatty tissue. Two selectable modes: weak, strong</li> <li>- Quick FatSat</li> <li>- SPAIR: robust fat suppression for body imaging using a frequency selective inversion pulse</li> <li>- Fat / Water Excitation. Spectral selective RF pulses for exclusive fat / water excitation</li> <li>- Dixon technique for fat and water separation - available both based on VIBE (2 point Dixon)</li> </ul> <p>Standard Techniques:</p> <ul style="list-style-type: none"> <li>- True Inversion Recovery to obtain strong T1-weighted contrast</li> <li>- Dark Blood Inversion recovery technique that nulls fluid blood signal</li> <li>- Saturation Recovery for 2D TurboFLASH, gradient echo, and T1-weighted 3D TurboFLASH with short scan time (e.g. MPRAGE)</li> </ul>

# SIEMENS

Siemens Medical Solutions USA, Inc.  
51 Valley Stream Parkway, Malvern, PA 19355  
Fax: (866) 309-6992

SIEMENS REPRESENTATIVE  
Tegan Gonzalez - (781) 454-5132

Part No. / Product	Description
<p>(Continued) 14418500 MAGNETOM Skyra - System</p>	<ul style="list-style-type: none"> <li>- Freely adjustable receiver bandwidth, permitting studies with increased signal-to-noise ratio</li> <li>- Freely adjustable flip angle. Optimized RF pulses for image contrast enhancement and increased signal-to-noise ratio</li> <li>- MTC (Magnetization Transfer Contrast), Off-resonance RF pulses to suppress signal from certain tissues, thus enhancing the contrast. Used e.g. in MRA</li> <li>- Argus viewer for reviewing cine studies*</li> <li>- Report Viewer for DICOM structured reports including report editing</li> <li>- Dynamic Analysis for addition, subtraction, division, standard deviation, calculations of ADC maps, T1 and T2 values, TTP, t-Test, etc.</li> <li>- Image Filter</li> <li>- 3D post-processing MPR, MIP, MinIP, SSD</li> <li>- Flexible film formats and paper print</li> <li>- Data storage of images and cine AVI files on CD / DVD with DICOM viewer as the viewing tool for hand out to the patients or referrals</li> <li>- Selectable centric elliptical phase reordering via the user interface</li> <li>- Inversion Recovery to nullify the signal of fat, fluid or any other tissue</li> </ul> <p>Standard techniques for Flow Artifact reductions:</p> <ul style="list-style-type: none"> <li>- LOTA (Long-Term Data Averaging) technique to reduce motion and flow artifacts</li> <li>- Pre-saturation techniques using RF saturation pulses to suppress flow and motion artifacts</li> <li>- Tracking SAT bands maintain constant saturation of venous and/or arterial blood flow e.g. for 2D/3D sequential MRA</li> <li>- TONE (Tilted Optimized Non-saturating Excitation - variable excitation flip angle to compensate inflow saturation effects in 3D MRA - selectable on desired flow direction and speed</li> <li>- Gradient Motion rephasing permitting effective reduction of flow artifacts</li> </ul> <p>Standard Motion Correction:</p> <ul style="list-style-type: none"> <li>- <i>syngo</i> BLADE - improves image quality by minimizing and correcting for the effects of motion during an MR sequence acquisition. e.g. head, spine, orthopedic imaging and the abdomen</li> <li>- 1D PACE (Prospective Acquisition CorrEction) allows examination of patients with free breathing</li> <li>- 2D PACE (Precise Motion Correction) detects and corrects respiratory motion e.g. of the heart or liver</li> </ul> <p>MAGNETOM Skyra runs <i>syngo</i> MR software. <i>syngo</i>® is the unique software platform for medical applications. Parallel working and one-click exams are efficiently supported and increase productivity. Parallel scanning and reconstruction are standard.</p> <p>The unique Phoenix technique is the easiest way to exchange protocol data. It supports intelligent extraction of sequence parameters from images acquired on a MAGNETOM Skyra system.</p> <p>Inline technologies, scan@center or AutoVoice Commands speed up the workflow further.</p> <p>The context-sensitive "Online Help" function and <i>syngo</i> Scan Assistant offer support and propose solutions to MR-specific questions and parameter conflicts.</p> <p>Studies can be easily networked and managed using the standard DICOM 3.0 protocol for efficient support of workflow. The following standard functions are supported: Send/Receive, Query/Retrieve, and Basic Print for DICOM-compatible laser cameras (camera is not included in the basic unit), DICOM Worklist, DICOM Storage Commitment (SC) DICOM Modality Perform Procedure Step (MPPS), DICOM Structured Report (SR), DICOM Study Split</p> <p><b>Patient Communication</b></p> <ul style="list-style-type: none"> <li>- The intercom system includes an ergonomically designed patient communication unit for desktop positioning on the <i>syngo</i> Acquisition Workplace and pneumatic headphones for the patient.</li> <li>- Active Noise Cancellation allows for increased user comfort in the control room combined with comprehensive patient supervision.</li> <li>- Control features include an emergency table stop, volume control of speaker and headphones in the examination room, volume control of speaker in the control room, response to the patient's activation of the assistance-call button and provides a connection to an external audio system for music playback (external audio system is not included in the basic unit) .</li> </ul>

# SIEMENS

Siemens Medical Solutions USA, Inc.  
 51 Valley Stream Parkway, Malvern, PA 19355  
 Fax: (866) 309-6992

SIEMENS REPRESENTATIVE  
 Tegan Gonzalez - (781) 454-5132

Part No. / Product	Description
<p>(Continued)            14418500  <b>MAGNETOM Skyra - System</b></p>	<p><b>Computer system</b>            The high performance host computer and the new high performance measurement and reconstruction system are ideally suited for even the most demanding applications. The PC-based computer system uses the intuitive syngo MR user interface. The computer system includes the following components:            High-performance measurement and reconstruction system</p> <ul style="list-style-type: none"> <li>- Two Intel Quadcore Processor <math>\geq</math> E 5540</li> <li>- clock rate of <math>\geq 2 \times 2.53</math> GHz</li> <li>- Main memory (RAM) of 48 GB,</li> <li>- Hard disk for raw data <math>\geq 300</math> GB</li> <li>- Hard disk for system software <math>\geq 100</math> GB</li> <li>- Parallel Scanning and Reconstruction of up to 8 data sets</li> <li>- Reconstruction speed               <ul style="list-style-type: none"> <li>- 12.195 recons per second (256 x 256 FFT, full FoV)</li> <li>- 37.914 recons per second (256 x 256 FFT, 25 % recFoV)</li> </ul> </li> </ul> <p>High-performance host computer</p> <ul style="list-style-type: none"> <li>- Intel Xeon processor <math>\geq</math> W3520 QuadCore</li> <li>- clock rate <math>\geq 2.66</math> GHz</li> <li>- Main Memory (RAM) <math>\geq 4</math> GB</li> <li>- three hard disks               <ul style="list-style-type: none"> <li>- system SW <math>\geq 146</math> GB SAS</li> <li>- data base <math>\geq 146</math> GB SAS</li> <li>- images <math>\geq 146</math> GB SAS</li> </ul> </li> <li>- DVD-R writer for CD-R (approx. 4000 images 256<sup>2</sup> DICOM Standard, ISO 9660 ) and DVD-R (approx. 25 000 images 256<sup>2</sup> DICOM Standard, ISO 9660) storage of DICOM data or other data like AVI files               <ul style="list-style-type: none"> <li>- DVD-ROM drive</li> <li>- Electronic mouse.</li> </ul> </li> </ul> <ul style="list-style-type: none"> <li>- The combination of host computer and the measurement and reconstruction system offers a truly powerful imaging system designed for large image matrix sizes of up to 1024 x 1024. The unrestricted multitasking capability allows time-saving parallel scanning and reconstruction.</li> <li>- High-resolution 19" color LCD flat screen monitor with 1280 x 1024 pixel display, integrated gamma correction for optimum display of radiographic grayscale images and automatic backlight control for long-term brightness stability.</li> </ul> <p><b>Installation:</b></p> <ul style="list-style-type: none"> <li>- The relatively lightweight design of the MAGNETOM Skyra in most cases eliminates the need for structural building reinforcements and thus facilitates installation in upper floors.</li> <li>- The compact integrated design allows for short installation times and reduces the required space to less than 31 sqm (334 sq. ft.) for the entire installation. The necessary room height clearance is only 2.40 m (7' 10").</li> <li>- MAGNETOM Skyra allows siting of the system without a dedicated computer room - no additional cooling or floor requirements.</li> <li>- MAGNETOM Skyra combines state-of-the-art performance with peace of mind. High system availability is ensured by the expert, highly trained Siemens MR service engineers;</li> <li>- Your Siemens service contract (not included in the basic unit) offers a comprehensive range of benefits such as Uptime Remote Diagnostics for improved productivity and maximum uptime.</li> </ul>
<p>14418502  <b>Tim [204x48] XQ Gradients #Sk</b></p>	<p><b>Tim [204x48] performance level</b>            Tim 4G offers DirectRF a completely redesigned RF architecture. This new all digital-in/ digital-out design integrates all RF transmit and receive components at the magnet, eliminating analog cables for true signal purity. This compact and efficient design enables a dynamic feedback control for temporal stability and power linearity. The all-new innovative coil architecture packs more coil elements in a smaller space. Therefore up to 204 coil elements can be simultaneously connected. The newly designed ultra high density array is an essential part supplementing Tim4G. Combined with the 48 independent RF channels advanced iPAT capabilities and SNR are</p>



# SIEMENS

Siemens Medical Solutions USA, Inc.  
51 Valley Stream Parkway, Malvern, PA 19355  
Fax: (866) 309-6992

SIEMENS REPRESENTATIVE  
Tegan Gonzalez - (781) 454-5132

Part No. / Product	Description
<p>(Continued) 14418502 Tim [204x48] XQ Gradients #Sk</p>	<p>enabled. An additional benefit of multiple coil elements and receiver channels is improved performance in multi-directional, i.e. three dimensional, high-speed, high-resolution iPAT in the head-feet, anterior-posterior or left-right directions.</p> <p>This option includes also Advanced High Order Shim.</p> <p><b>XQ gradients</b> Siemens XQ gradients provide actively shielded, water cooled world-class gradients. All axes are force-compensated.</p> <p>The XQ gradients have:</p> <ul style="list-style-type: none"> <li>- Maximum gradient amplitude of 45 mT/m, per axis, i.e. 78 mT/m vector summation gradient performance,</li> <li>- max. slew rate 200 T/m/s per axis, i.e. 346 T/m/s vector summation,</li> <li>- minimal rise time 225 <math>\mu</math>s, from 0 to 45 mT/m amplitude</li> <li>- Max. output voltage for each of the gradient axes 2250 V</li> <li>- Max. output current for each of the gradient axes 900 A</li> <li>- Separate cooling channels that simultaneously cool primary and secondary coils allow the application of extremely gradient intensive techniques in a new class of performance.</li> <li>- 100% duty cycle for fast and demanding techniques such as ultra-short TE MRA in continuous operation, thin slice single breath-hold liver studies and EPI imaging techniques (all optional in appropriate clinical packages).</li> <li>- Variable Field-of-View selection from 0.5 cm to 50 cm (up to 45 cm in z direction) for optimal coverage and highest spatial resolution in diagnostic. The minimum slice thickness in 2D and 3D is 0.1 mm and 0.05 mm, respectively.</li> <li>- Acquisition of sagittal, transverse, coronal, single oblique and double oblique slices with highest resolution.</li> <li>- The extremely compact water-cooled gradient amplifier features a modular expandable design with excellent linearity and pulse reproducibility. It is digitally controlled and has very low switching losses due to ultrafast solid state technology.</li> </ul>
<p>08464872 PC Keyboard US english #Tim</p>	<p>The keys of the numerical key panel are assigned to syngo-specific functions and labeled with the corresponding syngo icons. The keyboard supports the country specific special characters.</p>
<p>14416914 Pure White Design #T+D</p>	<p>The unique color and material selection enhances the visual appeal of the new system design of MAGNETOM Aera / MAGNETOM Skyra, thereby creating an enticing, patient-friendly impression. The Dot Control Centers and the unique Dot Display are neatly integrated into this main face plate. The aesthetically pleasing and ergonomically designed control elements of the Dot Control Centers are well illuminated for easy visual recognition.</p> <p>In particular, the table cover and the asymmetric left deco area cover have also been designed to promote a modern visual appearance. This combination of ingenuity and practical design as presented with "Pure White" design with its brilliant white and the silver trim simply makes MAGNETOM Aera/ MAGNETOM Skyra an overall visually appealing system and creates a patient-friendly environment.</p>
<p>14418507 Tim Dockable Table #Sk</p>	<p>The new MAGNETOM Skyra table with its light appealing design allows for a fast patient preparation and maximized patient comfort.</p> <p>It provides unobstructed foot space for attending staff and direct access to the patient. The patient table can be lowered to a minimum height of 56 cm (18.5") from the floor, for easier moving of immobile patients and better access for geriatric, pediatric patients or immobile patients. The Tim Table can be moved with two clicks into the isocenter - one click to the upmost position and one click into the isocenter. The tabletop travels beyond the rear end of the system, enabling additional patient access.</p> <p>Multiple Tim4G coils can be connected at once for efficient patient set up and patient friendly examinations. The seamless integration of multiple Tim4G coils is possible via 4 SlideConnect and 4 DirectConnect connector slots, which are embedded in the table. This allows for comprehensive examinations without the need of repositioning.</p> <p>The Tim Dockable Table is easily adjustable for height even in the undocked state. A minimum height of 61 cm allows for easy wheelchair access or easy patient movement to the hospital bed.</p> <p>The integrated infusion stand and arm rests allow for fast patient set up anywhere and also for critical patients</p>

# SIEMENS

Siemens Medical Solutions USA, Inc.  
51 Valley Stream Parkway, Malvern, PA 19355  
Fax: (866) 309-6992

SIEMENS REPRESENTATIVE  
Tegan Gonzalez - (781) 454-5132

Part No. / Product	Description
<p><b>14402592</b> Inline Composing syngo #Tim</p>	<p>The Inline Composing option includes the following functions:</p> <ul style="list-style-type: none"> <li>- Inline calculation of full-format images of the spine, the central nervous system or the vessel tree, for example, combined from multiple overlapping steps.</li> <li>- Dedicated composing algorithms, optimized for the generation of anatomical or angiographic full-format images.</li> <li>- Data sets with different FoV, resolution, matrix and slice thickness can be combined.</li> <li>- Generation of full-format images from inline-computed MIPs.</li> <li>- Different inline functions can be combined; e.g. in case of multiple-step angios, Inline subtraction, Inline MIP and Inline Composing can be performed fully automatically.</li> <li>- Full-format acquisitions from Inline Composing are ideal for further measurement planning on large FoV, e.g. with the Tim Planning Suite (optional, urgently recommended).</li> </ul> <p><i>Prerequisite: Software syngo MR B13.</i></p>
<p><b>14402593</b> Tim Planning Suite</p>	<ul style="list-style-type: none"> <li>- Easy planning on a FoV of any desired size (up to 205 cm).</li> <li>- Planning of multiple steps simultaneously, e.g. on a whole-body image, with only one Set-n-Go protocol - which includes several steps.</li> <li>- Tim Planning Suite UI: Dedicated user interface and exclusive tools for effective and smooth working on a large FoV.</li> <li>- Multiple slice groups with their overlap are displayed together and can be easily arranged.</li> <li>- All steps can have independent sets of parameters.</li> <li>- All steps are displayed together with a single mouse click.</li> <li>- Easy positioning of all steps, for example, through Align FoV.</li> <li>- Full support of .</li> <li>- Full support of Phoenix, thus maximum reproducibility, for example, for follow-up studies, multi-centric studies or exchange of experiences across different institutions.</li> <li>- Dedicated protocols are provided for the Tim Planning Suite, for example, for orthopedic, oncological or angiographic indications.</li> <li>- Inline Composing for optimized workflow for the generation of full-format images of anatomic or angiographic data sets is a prerequisite. Efficient measurement planning on these full-format images with Tim Planning Suite.</li> <li>- It is highly recommendable to order application training!</li> </ul> <p><i>Prerequisite: Software syngo MR B13</i></p>
<p><b>14405224</b> Composing syngo #Tim</p>	<p>The option features:</p> <ul style="list-style-type: none"> <li>- Display and storage of full-format images, e.g. of the spine, the central nervous system or the vessel tree (starting from syngo MR B13), combined from multiple overlapping stages.</li> <li>- Dedicated composing algorithms, optimized for the generation of anatomical or angiographic (starting from syngo MR B13) full-format images.</li> <li>- Data sets with different FoV, resolution, matrix and slice thickness can be combined (starting from syngo MR B13).</li> <li>- Generation of full-format images from inline MIPs (starting from syngo MR B13).</li> <li>- Original, detail and reconstructed images can be displayed in different layouts.</li> <li>- Comparison of two reconstructed images for evaluation and diagnosis is thus made possible.</li> <li>- Filming in different layouts is supported.</li> <li>- Measurements of basic functions via reconstructed images is then possible.</li> <li>- Measurements of extended orthopedic functions: scoliotic angle, kyphotic angle, vertical distance measurement and differences in width of the intervertebral spaces.</li> </ul> <p><i>Prerequisite: SW syngo MR B13.</i></p>
<p><b>14409198</b> Native syngo #Tim</p>	<p>syngo NATIVE offers:</p> <ul style="list-style-type: none"> <li>- Non-contrast enhanced MRA</li> <li>- Separate imaging of arteries and veins</li> <li>- Visualization of - e.g. - renal arteries or peripheral vessels</li> </ul> <p>The syngo NATIVE package comprises:</p> <ul style="list-style-type: none"> <li>- syngo NATIVE TrueFISP</li> <li>- syngo NATIVE SPACE</li> </ul>

# SIEMENS

Siemens Medical Solutions USA, Inc.  
 51 Valley Stream Parkway, Malvern, PA 19355  
 Fax: (866) 309-6992

SIEMENS REPRESENTATIVE  
 Tegan Gonzalez - (781) 454-5132

Part No. / Product	Description
14416923 Abdomen Dot Engine #T+D	<p><b>Abdomen Dot Engine</b>  <i>Guidance view</i></p> <ul style="list-style-type: none"> <li>- Step-by-step user guidance is seamlessly integrated.</li> <li>- Example images and guidance text displayed for each step of scanning workflow.</li> <li>- Both images and text are easily configurable by the user</li> </ul> <p><i>Patient View</i></p> <ul style="list-style-type: none"> <li>- Easily tailored to the individual patient.</li> <li>- Several pre-defined, integrated Dot Exam Strategies are included</li> <li>- Single click update of queue and the complete scan set-up.</li> <li>- Integrated contrast media protocols (Vibe Dynamic)</li> </ul> <p><i>Parameter View</i></p> <ul style="list-style-type: none"> <li>- A new view that displays the essential parameters</li> <li>- Can be opened at any time during an examination</li> </ul> <p><b>Automatic sequence scaling</b></p> <ul style="list-style-type: none"> <li>- Auto FoV: optimal FoV is proposed, based on the localizer images.</li> <li>- AutoNavigator: based on automatic breathing pattern detection and scaling of triggered scans.</li> <li>- Breath-hold adaptations</li> </ul> <p><b>Dot Exam Strategies</b>            Personalize to the individual patient condition and clinical need.</p> <ul style="list-style-type: none"> <li>- Predefined strategies:               <ul style="list-style-type: none"> <li>- Standard with breath-hold</li> <li>- Standard with PACE triggering</li> <li>- Limited patient capabilities using syngo BLADE and PACE triggering.</li> </ul> </li> </ul> <p><i>Dot Decisions</i>            Seamlessly integrated into scanning workflow:</p> <ul style="list-style-type: none"> <li>- Select the queue and the appropriate protocol or set of protocols are automatically added.</li> <li>- Abdomen Dot Engine integrates MRCP and Diffusion decision points.</li> </ul> <p><b>Timeline setup and monitoring</b>            Convenient visual overview of multi-phase breath-hold examinations and CM enhancement curve visualization.</p> <p><i>Auto Voice Commands</i></p> <ul style="list-style-type: none"> <li>- Played automatically</li> <li>- Facilitate timing of scanning, breathing and contrast media.</li> <li>- The user controls breath-hold or pauses are actually played</li> <li>- Ability to add pauses between automatic breath-holds.</li> </ul> <p><i>Auto Bolus Detection</i></p> <ul style="list-style-type: none"> <li>- Automatically initiates the dynamic upper abdomen examination based on bolus detection.</li> <li>- The user can override this function.</li> </ul> <p><i>Inline radial range calculation for MRCP</i></p> <ul style="list-style-type: none"> <li>- MRCP is measured</li> <li>- Inline Radial Ranges are automatically generated.</li> </ul> <p><i>Inline Subtraction</i>            Automatically subtracts the native (non-contrast) measurement from the arterial, portal-venous and late phase.</p> <p><i>Inline Registration</i>            The system automatically performs a registration / alignment of the anatomy for the different dynamic phases, of interest when examining nodular enhancing pathologies.</p>

# SIEMENS

Siemens Medical Solutions USA, Inc.  
 51 Valley Stream Parkway, Malvern, PA 19355  
 Fax: (866) 309-6992

SIEMENS REPRESENTATIVE  
 Tegan Gonzalez - (781) 454-5132

Part No. / Product	Description
<p><i>(Continued)</i>            14416923  <b>Abdomen Dot Engine            #T+D</b></p>	<p><b>Customization</b>            Existing Dot Engines can be modified by the user to their individual standard of care.</p> <ul style="list-style-type: none"> <li>- Add / remove protocol steps</li> <li>- Change guidance content (images and text)</li> <li>- Change or add Dot Exam Strategies and Decision Points</li> <li>- Modify the Parameter View</li> </ul>
<p>14418746  <b>Cardiac Dot Engine,            USA #T+D</b></p>	<p><b>Cardiac Dot Engine            Guidance View</b></p> <ul style="list-style-type: none"> <li>- Step-by-step user guidance is seamlessly integrated.</li> <li>- Example images and guidance text are displayed for the individual steps of the scanning workflow.</li> <li>- Both images and text are easily configurable by the user</li> </ul> <p><b>Patient View</b></p> <ul style="list-style-type: none"> <li>- Within the Patient View the user can easily tailor the exam to each individual patient (e.g. patient with arrhythmia, breath hold capability).</li> <li>- Pre-defined Dot Exam Strategies are integrated. The user just selects the appropriate strategy with one click and the queue and the complete scan set-up are automatically updated</li> </ul> <p><b>AutoFoV (automatic Field of View calculation)</b></p> <ul style="list-style-type: none"> <li>- Based on the localizer images the optimal FoV is automatically estimated.</li> <li>- If the patient moves during the examination, this step can be repeated at any time</li> </ul> <p><b>Automated parameter adaptation</b></p> <ul style="list-style-type: none"> <li>- Scan parameters are automatically adapted to the patient's condition (e.g. heart rate)</li> </ul> <p><b>Novel heart localization method</b></p> <ul style="list-style-type: none"> <li>- On-board guidance visually facilitates anatomic landmark settings which are used for calculation</li> <li>- Automated localization</li> <li>- Automated localization of short-axis views</li> </ul> <p><b>Cardiac Views</b></p> <ul style="list-style-type: none"> <li>- Easy selection of cardiac views (e.g. 3 chamber view) during scan planning</li> </ul> <p><b>Inline Ventricular Function Evaluation</b></p> <ul style="list-style-type: none"> <li>- syngo Inline VF performs volumetric evaluation of cardiac cine data fully automatically right after image reconstruction.</li> <li>- If desired, inline calculated segmentation results can be loaded to 4D Ventricular Function Analysis for further review or processing</li> </ul> <p><b>Cardiac specific layout for the Exam task</b></p> <ul style="list-style-type: none"> <li>- layouts show the new physio display and are configured for every step of the exam</li> </ul> <p><b>Automated Naming</b></p> <ul style="list-style-type: none"> <li>- Automated naming of series depending on cardiac views and sequence type</li> </ul> <p><b>Auto Voice Commands</b></p> <ul style="list-style-type: none"> <li>- Seamlessly integrated into scanning workflow.</li> <li>- Played automatically</li> <li>- The user controls breath-hold or pauses are actually played</li> <li>- Ability to add pauses between automatic breath-holds</li> </ul> <p><b>Dot Exam Strategies</b>            The workflow can be personalized to the individual patient condition and clinical need. The following predefined strategies are included. They can be changed at any time during the workflow:</p>

# SIEMENS

Siemens Medical Solutions USA, Inc.  
51 Valley Stream Parkway, Malvern, PA 19355  
Fax: (866) 309-6992

SIEMENS REPRESENTATIVE  
Tegan Gonzalez - (781) 454-5132

Part No. / Product	Description
<p><i>(Continued)</i> 14418746 Cardiac Dot Engine, USA #T+D</p>	<ul style="list-style-type: none"> <li>- <b>Standard:</b> Segmented acquisition techniques</li> <li>- <b>Limited patient capabilities:</b> switch to real-time and single shot imaging if breath-hold is not possible or arrhythmias occur</li> </ul> <p><b>Customization</b> Existing Dot Engines can be modified by the user to their individual standard of care.</p> <ul style="list-style-type: none"> <li>- Add/remove protocol steps</li> <li>- Change guidance content (images and text)</li> <li>- Change or add Dot Exam Strategies and Decision Points</li> <li>- Modify the Parameter View</li> </ul>
<p>08464740 Flow Quantification #Tim</p>	<p>Flow Quantification enables the acquisition of flow encoded images and the evaluation of blood as well as of cerebro-spinal fluid (CSF).</p> <p>Sequences include:</p> <ul style="list-style-type: none"> <li>- ECG triggered 2D phase contrast with iPAT support</li> <li>- Retrospective reconstruction algorithms for full R-R interval coverage</li> <li>- Maxwell Term Compensation</li> </ul>
<p>14416929 Advanced Cardiac Package #T+D</p>	<p>Combining the unique advantages of Tim and <i>syngo</i> BEAT with iPAT and powerful gradients, it allows performing cardiac MR examinations without compromise in image resolution or acquisition speed. <i>syngo</i> BEAT is a unique tool for fast and easy cardiovascular MR imaging. It provides 1-click switch from cine imaging to tagging for wall motion evaluation and 1-click switch from 2D to 3D imaging. <i>syngo</i> BEAT automatically adjusts all parameters associated with the changes.</p> <p><b>Cardiac and Vessel Morphology</b></p> <ul style="list-style-type: none"> <li>- Multi echo technique for e.g. thalassemia assessment</li> <li>- 3D aortopathy imaging with free breathing (SPACE)</li> </ul> <p><b>Global or Regional Wall Motion Analysis with <i>syngo</i> BEAT</b></p> <ul style="list-style-type: none"> <li>- 3D cine acquisition for full CT-like heart coverage</li> <li>- 2D segmented FLASH for visualization of the regional wall motion using various tagging techniques (grid or stripes)</li> </ul> <p><b>Dynamic myocardial imaging with <i>syngo</i> BEAT</b></p> <ul style="list-style-type: none"> <li>- Ultra-fast, high-SNR sequence for dynamic imaging with GRE EPI contrast for stress and rest exams</li> </ul> <p><b>Tissue characterization with <i>syngo</i> BEAT</b></p> <ul style="list-style-type: none"> <li>- Robust myocardial tissue characterization with 3D PSIR (phase-sensitive inversion recovery), e.g. after myocardial infarction or for differentiation of cardiomyopathies</li> <li>- Fast and complete coverage of the myocardium with IR 3D FLASH and TrueFISP</li> </ul> <p><b>Coronary imaging with <i>syngo</i> BEAT</b></p> <ul style="list-style-type: none"> <li>- 3D Whole-Heart non-contrast Coronary MRA</li> <li>- 3D Whole-Heart MRA with advanced free-breathing navigator compensating diaphragm shifts during the acquisition (motion-adaptive respiratory gating)</li> </ul>
<p>14407334 Argus 4D Ventr.Function <i>syngo</i> #Tim</p>	<p>This package includes Argus Function as well as Argus 4D Ventricular Function.</p> <p><b>Argus Function:</b></p> <ul style="list-style-type: none"> <li>- Automatic, semi-automatic, or manual segmentation of the left and semi-automatic or manual segmentation of the right ventricle.</li> <li>- Volumetric analysis and wall thickness analysis.</li> <li>- Output of parametric results, volume-time curves and bull's-eye plots.</li> <li>- DICOM Structured Reporting.</li> </ul>

# SIEMENS

Siemens Medical Solutions USA, Inc.  
 51 Valley Stream Parkway, Malvern, PA 19355  
 Fax: (866) 309-6992

SIEMENS REPRESENTATIVE  
 Tegan Gonzalez - (781) 454-5132

Part No. / Product	Description
<p>(Continued)            14407334            Argus 4D            Ventr.Function syngo            #Tim</p>	<p>Argus 4D Ventricular Function:</p> <ul style="list-style-type: none"> <li>- Calculation of volumetric cardiac data of a given patient very quickly and easily.</li> <li>- Parametric results and volume-time curves are calculated upon automatic creation and adaptation of a 4D model of the left ventricle.</li> <li>- The resulting 4D model of the patient's heart can be visualized superimposed to anatomical images as a reference.</li> </ul>
<p>14416922            Knee Dot Engine            #T+D</p>	<p><b>Knee Dot Engine</b>  <b>Dot Exam Strategies</b>            The workflow can be personalized to the individual patient condition and clinical need. Dot comes with the following predefined strategies, which the user can select or change at any time during the workflow:</p> <ul style="list-style-type: none"> <li>- <b>Standard:</b> Achieve highest image quality in a reasonable scan time with 2D protocols.</li> <li>- <b>Speed focus:</b> Examine e.g. claustrophobic patients or children in the shortest possible time with protocols being accelerated to maximal extend.</li> <li>- <b>Limited patient capabilities:</b> Compensate for the effects of motion, e.g. with syngo BLADE protocols.</li> <li>- <b>High Bandwidth protocol (for reduction of susceptibility artifacts):</b> Is a protocol intended to reduce artifacts when scanning MR conditional implants per the manufacturers instructions. Example images and guidance text are displayed for each individual step of the scanning workflow.</li> </ul> <p><b>Autoposition</b></p> <ul style="list-style-type: none"> <li>- Automatic positioning proposal without laser marker</li> </ul> <p><b>AutoAlign Knee</b></p> <ul style="list-style-type: none"> <li>- Automated proposal of slice group positioning, based on 3D Vibe localizer. Drop down menu for anatomic landmarks, such as Meniscus, Patellar cartilage, ACL, PCL and Femur Cartilage.</li> </ul> <p><b>Guidance View</b></p> <ul style="list-style-type: none"> <li>- Step-by-step user guidance is seamlessly integrated.</li> <li>- Example images and guidance text are displayed for each individual step of the scanning workflow.</li> <li>- Both images and text are easily configurable by the user</li> </ul> <p><b>Customization</b>            Existing Dot Engines can be modified by the user to their individual standard of care.</p> <ul style="list-style-type: none"> <li>- Add/remove protocol steps</li> <li>- Change guidance content (images and text)</li> <li>- Change or add Dot Exam Strategies and Decision Points</li> <li>- Modify the Parameter View</li> </ul>
<p>14405341            Mapit syngo #Tim</p>	<p>Features:</p> <ul style="list-style-type: none"> <li>- 3D VIBE sequence for Inline T1 mapping</li> <li>- Multiecho spin echo sequence for Inline T2 mapping</li> <li>- 3D Multiecho gradient echo sequence for Inline T2* mapping</li> <li>- IPAT compatibility</li> <li>- Protocols for Inline parametric mapping</li> </ul> <p>Using IPAT the 3D sequences provide isotropic imaging extremely high resolution while maintaining clinical measurement times. These data sets allow for the multi planar reconstruction of all planes. 3D is necessary to properly visualize the whole articular cartilage since it typically has a complex shape. In addition the accuracy of isotropic high resolution 3D data sets is superior because partial volume effects between e.g. synovial fluid and cartilage are minimized.</p> <p>For the visualization of the parametric maps in the anatomical context the maps can be displayed as a colored overlay onto anatomical images using the optional package "syngo Image Fusion"</p>
<p>07365484            Image Fusion syngo</p>	<p>CT, MR, NM, or PET Images are accepted as input for image fusion. Studies can be done with the same modality or with different modalities.</p>

# SIEMENS

Siemens Medical Solutions USA, Inc.  
51 Valley Stream Parkway, Malvern, PA 19355  
Fax: (866) 309-6992

**SIEMENS REPRESENTATIVE**  
Tegan Gonzalez - (781) 454-5132

Part No. / Product	Description
	Registration Algorithms:

Part No. / Product	Description
<p>(Continued) 07365484 Image Fusion syngo</p>	<ul style="list-style-type: none"> <li>- Easy-to-use visual alignment with 6 degrees of freedom (3x translation, 3x rotation)</li> <li>- Landmark based registration with convenient landmark editor for point-based registration using anatomical landmarks</li> <li>- Automatic registration</li> <li>- Storage of transformation matrix after registration for later retrieval with datasets</li> </ul> <p><b>Visualization Techniques:</b></p> <ul style="list-style-type: none"> <li>- Side by side visualization of both datasets with correlated pointer and correlated scrolling with dog ears</li> <li>- 2D alpha-blending in monochrome or pseudo-color with adjustable balance between the two superimposed data sets.</li> </ul> <p>Storage of fused results as secondary capture images.</p>
<p>14401554 Inline Perfusion #3T</p>	<p><b>Inline Technology – Processing Instead of Post-processing.</b> Inline Technology helps to streamline the clinical workflow by automating post-processing steps before image viewing. This facilitates getting clinical results immediately. This package integrates Inline technology with perfusion imaging. Automatic real-time calculation of Global Bolus Plot (GBP), Percentage of Baseline at map (PBP) and Time-to-Peak map (TTP) with Inline technology is possible.</p> <p>An optimized EPI sequence for perfusion-diagnostics is included in the standard Tim Application Suite. With this package real-time calculations are done of anatomical images and, in addition, of a global bolus plot and a Time-to-Peak map for visualizing the time dependence of tissue perfusion.</p>
<p>14418563 Neuro Perfusion Evaluation, USA #T+D</p>	<p><b>Post-processing features:</b></p> <ul style="list-style-type: none"> <li>- Flexible selection of the Arterial Input Function (AIF) by the user.</li> <li>- Pixelwise calculation of the hemodynamic parameters relative Mean Transit Time (relMTT), relative Cerebral Blood Volume (relCBV), relative Cerebral Blood Flow (relCBF), corrected relative Cerebral and Blood Flow (relCBF) for compensation of blood brain barrier leakage.</li> <li>- Pixelwise calculation of maximum signal loss due to contrast agent enhancement (Percentage of Baseline at Peak, PBP) and of the time to the maximum signal loss (Time-To-Peak, TTP).</li> <li>- Display of the global signal time course (averaged over all slices) to assess the quality of the exam.</li> <li>- Predefined post-processing protocols available, user definable post-processing protocol are possible.</li> </ul> <p><b>Visualization features:</b></p> <ul style="list-style-type: none"> <li>- Colored display of relMTT-, relCBV-, relCBF-, relCBFcor, PBP- and TTP-maps.</li> <li>- Zoom, pan, annotate.</li> <li>- Colored images can be saved as DICOM images.</li> </ul>
<p>14416943 Neuro fMRI Package #T+D</p>	<p><b>Inline BOLD imaging</b> The BOLD imaging package allows the user to define protocols which, apart from the measurement, configure automatic evaluation of the measured data during the scan. With Inline Technology it is thus possible to generate statistical images (t-value) based on 3D motion corrected and spatially filtered data automatically in real time without any further user interaction. The Inline display of activation cards allows the user to decide during the scan whether enough statistical power has built up for his brain mapping task or if the examination is corrupted by motion. As a result examinations will be shorter with a higher success rate. Functional brain mapping can be easily integrated into the clinical routine e.g. prior to neurosurgical interventions.</p> <p><b>Additional Features:</b></p> <ul style="list-style-type: none"> <li>- Inline retrospective 3D motion detection and correction in 3 rotational and 3 translational directions</li> <li>- Inline t-statistics calculation for variable paradigms and display of t-value images</li> <li>- Statistical evaluation by means of "General Linear Model (GLM)":</li> <li>- Paradigms can be configured</li> </ul>

# SIEMENS

Siemens Medical Solutions USA, Inc.  
 51 Valley Stream Parkway, Malvern, PA 19355  
 Fax: (866) 309-6992

SIEMENS REPRESENTATIVE  
 Tegan Gonzalez - (781) 454-5132

Part No. / Product	Description
	<ul style="list-style-type: none"> <li>- Transitions between passive and active states can be modelled by the hemodynamic response function</li> <li>- Correction of low-frequency trends</li> </ul>

Part No. / Product	Description
(Continued) 14416943 Neuro fMRI Package #T+D	<ul style="list-style-type: none"> <li>- Allows for time delays due to the BOLD-EPI slice order during a measurement</li> <li>- Display of GLM design matrix</li> <li>- Display of a continuously updated t-value card during measurement</li> <li>- Display of colored activation cards continuously updated during measurement, overlaid over the respective BOLD images using Inline technology</li> <li>- MOSAIC image mode for accelerating display, processing and storage of images</li> </ul> <p><b>3D PACE syngo</b>            By tracking the patients head 3D PACE reduces motion resulting in increased data quality beyond what can be achieved with a retrospective motion correction. As a result the sensitivity and specificity of BOLD experiments are increased.            Features:</p> <ul style="list-style-type: none"> <li>- Real time prospective motion correction: Highest accuracy real time motion detection algorithm feeding a real time feed back loop to the acquisition system with updated positioning information</li> <li>- 3D motion correction for 6 degrees of freedom (3 translation and 3 rotation)</li> <li>- Motion related artifacts are avoided in first place instead of correcting for them retrospectively</li> <li>- Significant reduction of motion-related artifacts in statistical evaluations</li> <li>- Increased sensitivity and specificity of BOLD experiments</li> </ul> <p><b>BOLD 3D Evaluation syngo</b>            All tasks from statistical evaluation of the fMRI datasets to reading and exporting results are supported by BOLD 3D Evaluation syngo:</p> <p>Generation of statistical maps:</p> <ul style="list-style-type: none"> <li>- In cases an inline calculated statistical map is not available a statistical map can be generated easily using processing protocols. An intuitive editor UI allows the paradigm definition and offers the selection of head motion correction, image filters and statistical evaluation.</li> <li>- Predefined processing protocols and paradigms are available, which can be edited if required.</li> </ul> <p>Statistical evaluation using General Linear Model (GLM)</p> <ul style="list-style-type: none"> <li>- Transitions between passive and active states modeled by the hemodynamic response function.</li> <li>- Correction of low-frequency trends.</li> <li>- Corrects for time delays due to the BOLD-EPI slice order during a measurement.</li> <li>- Output of a t-value map and the GLM design matrix</li> </ul> <p>Inline monitoring of the fMRI exam</p> <ul style="list-style-type: none"> <li>- During an ongoing BOLD imaging exam results are calculated (by Inline BOLD imaging) and displayed in real time.</li> <li>- The results are displayed and continuously updated as an overlay on online adjustable, free angulated cut planes through the anatomical 3D data set.</li> <li>- The evolving signal time courses in task-related areas of activation can be displayed and monitored.</li> </ul> <p>Visualization of fMRI Results</p> <ul style="list-style-type: none"> <li>- Visualization with 3D volume rendering.</li> <li>- Superimposing on cut planes through the volume.</li> <li>- Interactive Navigation: Zoom, pan and rotate in 3D without noticeable delay. Free double oblique angulation of up to 6 cut planes.</li> <li>- Cine display of the BOLD time series and of EPI volumes in 3 orthogonal cuts for evaluation of non-corrected head motion.</li> </ul> <p>Data Quality Monitoring</p>



# SIEMENS

Siemens Medical Solutions USA, Inc.  
51 Valley Stream Parkway, Malvern, PA 19355  
Fax: (866) 309-6992

SIEMENS REPRESENTATIVE  
Tegan Gonzalez - (781) 454-5132

Part No. / Product	Description
	<p>- Based on the B0 field map, loaded automatically with the fMRI data, areas with less reliable results are indicated.</p> <p><b>fMRI Trigger Converter</b> An optical trigger signal is available to trigger external stimulation devices in fMRI experiments. With the "fMRI Trigger Converter" this signal can be converted to an electrical signal (TTL/BNC and RS 232 interface for PC; modes: toggle or impulse).</p>
<p><b>14416927</b> <b>MDDW #T+D</b></p>	<p>MDDW enables basic acquisition of data sets with multi-directional diffusion weighting to assess anisotropic diffusion properties of brain tissue.</p> <p>It covers:</p> <ul style="list-style-type: none"> <li>- Measurement of up to 12 directions of diffusion weighting with up to 16 different b-values. The maximal b-value is 10.000.</li> <li>- Apparent Diffusion Coefficient (ADC) maps and trace-weighted images.</li> </ul>
<p><b>14409110</b> <b>Arterial Spin Labeling 2D</b></p>	<p>The measurement of relative CBF is done by combination of an ASL preparation module with the 2D multi-slice EPI sequence with full iPAT compatibility. Technically, the ASL module consists of a spatially selective inversion pulse combined with different types of saturation pulses (slice presaturation, label slab saturation) and can be classified under PASL (Pulsed Arterial Spin Labeling). Output quantities are a series of labeled and unlabeled images, a series of inline calculated perfusion weighted color maps and a series of relative cerebral blood flow (relCBF) color maps. Prospective motion correction and spatial filtering can be applied for inline calculation to improve the image quality.</p>
<p><b>14402527</b> <b>SWI #Tim</b></p>	<p>Despite a strong sensitivity for local magnetic field inhomogeneities Susceptibility Weighted Imaging (SWI) as a 3D technology keeps up the signal near large susceptibility leaps due to very thin slices and high resolution in the slice (high image quality e.g. in the area of the forebrain near the frontal sinus). Moreover, the phase information of the MR signal is integrated in the image display. In order to further increase sensitivity for localized microscopic magnetic field inhomogeneities, large-area magnetic field inhomogeneities (e.g. caused by susceptibility leaps near the sinus) are specifically suppressed in the phase images. This allows even smallest amounts of deoxygenated hemoglobin (e.g. in cerebral veins) or from products of hemoglobin decomposition (e.g. from hemorrhages) to be displayed. Interesting measuring times for the ultra-high-resolution 3D protocols are achieved through parallel imaging with iPAT (GRAPPA).</p> <p>The Susceptibility Weighted Imaging package includes:</p> <ul style="list-style-type: none"> <li>- SWI measuring sequence, iPAT compatible</li> <li>- optimized measuring protocols for the head</li> <li>- inline-postprocessing for automatic calculation of relevant images within the scope of image reconstruction:             <ul style="list-style-type: none"> <li>- calculation of susceptibility-weighted images</li> <li>- venous angiography: MIP of a thin slice block</li> </ul> </li> </ul> <p>SWI has been optimized for clinical use to support diagnostics with cerebrovascular diseases (e.g. cerebral insult), venous malformation, brain trauma and tumors.</p> <p><i>Prerequisite: Software syngo MR B13</i></p>
<p><b>14416941</b> <b>Spectroscopy Package #T+D</b></p>	<p>The Single Voxel Spectroscopy option is used to measure proton spectra from single voxels. The spectra may show alterations in brain metabolism e.g. in brain tumors, in degenerative changes of the brain and in metabolic diseases. The possibility of automatic adjustment, measurement and evaluation permits near automatic spectroscopy measurements. The whole procedure, including the evaluation of the spectra using the mandatory spectroscopy evaluation option, takes approx. 6 minutes and can be done by doctors or technologists.</p> <p>The 2D Chemical Shift Imaging option is used to measure 2D proton spectroscopic data to generate metabolite images e.g. in brain tumors, metabolic diseases of the brain and degenerative changes in brain metabolism. The whole procedure, including the generation of metabolite images using the spectroscopy evaluation takes approximately 8 minutes.</p> <p>The 3D Chemical Shift Imaging option is used to measure 3D proton spectroscopic data and allows for the evaluation of the spectra in measured volumes and the generation of metabolite images and spectral maps, e.g. in cases of brain tumors, metabolic diseases of the brain and degenerative changes in brain metabolism. The whole procedure, including the generation of metabolite images using the spectroscopy evaluation takes approximately 10-16 minutes</p>

# SIEMENS

Siemens Medical Solutions USA, Inc.  
51 Valley Stream Parkway, Malvern, PA 19355  
Fax: (866) 309-6992

**SIEMENS REPRESENTATIVE**  
Tegan Gonzalez - (781) 454-5132

Part No. / Product	Description
	<p>Optimized protocols for 3D CSI in the prostate are also included.</p> <p>The evaluation software is fully integrated in <i>syngo</i> MR. Evaluation protocols adapted to the scan protocols carry out a complete and automatic evaluation of the measured data.</p> <p>The following functions are included:</p>

Part No. / Product	Description
<p>(Continued) 14416941 Spectroscopy Package #T+D</p>	<ul style="list-style-type: none"> <li>- Subsequent water suppression with optional phase correction</li> <li>- Apodization</li> <li>- Zero filling</li> <li>- Fourier transformation</li> <li>- Base line correction</li> <li>- Automatic or manual phase correction</li> <li>- Curve fitting and peak labeling</li> <li>- Summaries in tabular form of the essential results specifying the metabolites, their position, integrals and signal ratios in relation to a selectable reference.</li> <li>- Capability of exporting spectroscopy header information and data into a documented external format.</li> <li>- Automated peak normalization to tissue, water or reference.</li> </ul> <p>For CSI the following functions are included:</p> <ul style="list-style-type: none"> <li>- Spectra of selected voxels are automatically calculated, corrected for possible B0 deviations and displayed.</li> <li>- Spectral fit is automatically optimized for each voxel.</li> <li>- CSI data can be represented as spectral maps and colored metabolite images that can be superposed onto anatomical images.</li> </ul>
<p>14405328 TWIST <i>syngo</i> #Tim</p>	<p><i>syngo</i> TWIST provides:</p> <ul style="list-style-type: none"> <li>- Visualization of contrast agent dynamics in the vessel system of interest with maximum flexibility.</li> <li>- Needs only a low amount of contrast agent.</li> <li>- Imaging in all body regions, e.g. carotids, pulmonary and peripheral vessels with brilliant spatial and temporal resolution.</li> <li>- Clear separation of the arterial and venous phase.</li> <li>- High speed acquisition by intelligent k-space strategies and use of iPAT, powered by Tim.</li> <li>- <i>syngo</i> TWIST provides fat suppression using water selective excitation.</li> <li>- Inline technologies, such as subtraction and MIP are provided for optimal workflow.</li> <li>- In case of very high spatial resolution <i>syngo</i> TWIST may even replace conventional static MR angio. Moreover, <i>syngo</i> TWIST does not require any bolus timing - just inject and go.</li> </ul>
<p>14416952 Coil Storage Cart #T+D</p>	<p>The cart may be rolled to convenient locations in the examination room and can be opened up to work like a shelf. The coil storage cart has multiple drawers and trays as well as many other storage spaces for coils, cushions and miscellaneous items.</p> <p>Its dimensions are: Width 140 cm (4' 7") when closed and 280 cm (9' 12") when opened, depth 54 cm (1'9") and height 121 cm (3'12").</p>
<p>14416954 2/4/8-ch Sentinelte BreastCoil #Sk</p>	<p>The 8-channel Sentinelte Breast Coil consists of 2 lateral 3-channel coil elements and a 2-channel coil middle element.</p> <p>The 4-channel Sentinelte Breast Coil consists of 2 lateral 1-channel coil elements and a 2-channel coil middle element.</p> <p>The 2-channel Sentinelte Breast Coil consists of a lateral 1-channel coil element and another lateral 1-channel coil element.</p>

# SIEMENS

Siemens Medical Solutions USA, Inc.  
51 Valley Stream Parkway, Malvern, PA 19355  
Fax: (866) 309-6992

SIEMENS REPRESENTATIVE  
Tegan Gonzalez - (781) 454-5132

Part No. / Product	Description
	<p>The Sentinelle Breast Coil supports the GRID biopsy method.</p> <p>The 2-/4-/8-channel Sentinelle Breast Coil ensures brilliant image quality for high-resolution 2D and 3D MR breast imaging. Techniques for reducing scan times, such as parallel imaging, can be used very well.</p> <p>Together with the Tim Whole Body Suite, the coil can also be operated in "feet first" mode. This function substantially improves the examination flow with claustrophobic patients.</p> <p>For optimal patient positioning, a set of comfortable positioning cushions and aids, such as a height-adjustable</p>

Part No. / Product	Description
<p>(Continued) 14416954 2/4/8-ch Sentinelle BreastCoil #Sk</p>	<p>head rest, is included in the scope of delivery. A set of GRID plates and a Biopsy Training Starter Kit are further included in delivery. (Not for use on humans)</p> <p>The 2-/4-/8-channel Sentinelle Breast Coil measures approx. 1097 x 582 x 279mm (L x W x H) and weights approx. 22kg with base plate and 14kg without base plate.</p>
<p>14418512 Peripheral Angio 36 #Sk</p>	<p>The Peripheral Angio 36 has a 36-element design with 36 integrated preamplifiers distributed over 6 planes with 6 elements each. A uniquely designed non-ferromagnetic coil cart for safe coil storage is included. The PA Matrix Coil is also shipped with a set of positioning cushions for proper handling.</p> <p>No tuning of the fully iPAT-compatible Peripheral Angio 36 is required.</p> <p>With a length of about 1m both legs are covered from the iliac artery level down to the foot arch vessels using multiple, flexible wings. For the visualization of the abdominal aorta and the iliac bifurcation it can be combined with the Body 18 and Spine 32. For larger body coverage eg whole body with up to 205 cm possible coverage, it can be combined with Head/Neck20 or a further Body18 to allow for large Field of View examinations with high patient comfort. Patient set up is done once and no repositioning is necessary For peripheral Angiography the PA Matrix coil will be typically used in feet-first position, but also head-first positioning for whole-body examinations is possible (optional Tim Whole Body Suite required).</p> <p>The dimensions of the Peripheral Angio 36 are: 860 mm x 300 - 640 mm x 280 mm</p>
<p>14416959 Shoulder 16 Coil Kit #Sk</p>	<p>The iPAT compatible Shoulder 16 Large and Shoulder 16 Small are ergonomically designed and adapted to the shape of the shoulder. The different sizes obtain maximum image quality for different body sizes:</p> <ul style="list-style-type: none"> <li>- 165 mm (6.5 in) diameter for small and medium sized shoulders</li> <li>- 200 mm (7.9 in) diameter for large shoulders</li> </ul> <p>The coils can be used either for left or right shoulders. It features sliding attachments to the base plate and can easily be adjusted for comfortable positioning. The coils excels in highest resolution imaging with exceptional signal/noise ratio.</p>
<p>14418514 Foot/Ankle 16 #Sk</p>	<p>The 16-element coil with 16 integrated pre-amplifiers excels in highest resolution imaging with exceptional signal/noise ratio, while taking full advantage of iPAT in all directions.</p> <p>Foot/Ankle 16 is ergonomically designed and features a boot-like coil design. Together with the included stabilization pads the coil allows easy, fast and comfortable patient positioning.</p>
<p>14418519 Tim Coil Interface 3T</p>	<p>This adapter will be required if the following coils will be used on the MAGNETOM Skyra.</p> <ul style="list-style-type: none"> <li>- Tx / Rx 15-channel Knee Coil (two adapters required)</li> <li>- CP Extremity Coil</li> <li>- 4-channel BI Breast Coil</li> <li>- 16-channel AI Breast Coil (two adapters required)</li> <li>- 2/4/8-channel Sentinelle BreastCoil</li> </ul>

# SIEMENS

Siemens Medical Solutions USA, Inc.  
51 Valley Stream Parkway, Malvern, PA 19355  
Fax: (866) 309-6992

**SIEMENS REPRESENTATIVE**  
Tegan Gonzalez - (781) 454-5132

Part No. / Product	Description
	The adapter can be plugged in any the SlideConnect plug of the Skyra system. The Tim Coil Interface has a compact design and measures only approx. 190 mm x 90 mm x 33 mm (W x H x D).
<b>14418520</b> Tx/Rx 15-channel Knee Coil 3T	<p>Thanks to its 15-channel design this coil is perfectly suited for high-resolution images with excellent SNR. With the arrangement of the antennas in three rings of 5 elements each, the coil is specially designed for parallel imaging with high acceleration factors.</p> <p>The coil is positioned on a laterally movable support and therefore allows for comfortable patient positioning of both legs for off-center examinations. Furthermore, the upper part can be removed for easier patient positioning. Additional cushions allow for optimum patient immobilization.</p> <p>The integrated transmission function makes volume-sensitive excitation with greatly reduced RF power possible on the one hand and, on the other, prevents aliasing artifacts (e.g. due to the other knee).</p>
<b>14418511</b> Body 18 #Sk	<p>The Body 18 has a 18-element design with 18 integrated preamplifiers that are arranged in 3 clusters of 6 coil elements each. The Body 18 will be typically used together with the Spine 32 with which it operates in an integrated fashion as a 30-element coil, resulting in 3 rings of 10 elements each for highest SNR and fast imaging. It can be positioned in different orientations and addresses the requirement range for the examinations of obese patient to pediatric patients. The light weight coil improves patient comfort and can be easily connected via SlideConnect technology. No tuning of the fully iPAT-compatible Body 18 is necessary allowing for efficient and patient friendly set-up.</p> <p>For examinations where larger anatomical coverage is required, several Body 18 coils can be used simultaneously. Up to four Body 18 can be used simultaneously, but typically two Body 18 will be used for coverage of the entire abdomen or in the case of large patients.</p> <p>The Body 18 is typically used in combination with the Spine 32 for examinations of the thorax, abdomen, pelvis or hip and is also well suited for cardiac or vascular applications. In addition, the Body 18 can be combined with the Spine 32, further Body 18 (optional), the Peripheral Angio 36 (optional), but also the Head/Neck20 and the 4-channel flex coils (e.g. Flex Large 4, Flex Small 4) it contributes for all large-Field-of-View applications up to whole-body imaging.</p> <p>The dimensions of the Body 18 are 385 mm x 590 mm x 65 mm (L x W x H). Its weight is about 2 kg (4.5 lbs), whereas the patient feels as little weight as 1kg (2,25 lbs).</p>
<b>14407258</b> MR Workplace Table 1.2m	<p>The table design matches the MED-wide uniform design with silver-finished rim, use of friendly colors matching the Siemens color pattern for MAGNETOM and SOMATOM.</p> <ul style="list-style-type: none"> <li>- Width 120 cm</li> <li>- Depth 80 cm</li> <li>- Height 72 cm</li> </ul>
<b>14407261</b> MR Workplace Container, 50cm	<p>The table design matches the MED-wide uniform design with silver-finished rim, use of friendly colors matching the Siemens color pattern for MAGNETOM and SOMATOM.</p> <p>Table height 72 cm, matching the syngo Acquisition Workplace and syngo MR Workplace console table, for installation in the operator room either directly to the left or right of the syngo Acquisition Workplace or syngo MR Workplace console table or separately.</p> <ul style="list-style-type: none"> <li>- Width 50 cm</li> <li>- Depth 80 cm</li> <li>- Height 72 cm</li> </ul> <p>Alternatively this casing is also suited for the Recon image processor (except for the MR systems with the new Tim generation: there the Recon image processor is always placed inside the electronics cabinet).</p>
<b>14416975</b> Eco Chiller 60kW	<p><b>Chiller KKT ECO 133 - L</b></p> <p>Function: Supplies dedicated primary chilled water in cases where no chilled water supply is available on site. Air-cooled version, for outdoor installation up to a maximum distance of 25 m for connection to the IFP, incl. 50 m FOC for control.</p> <p>The cooling capacity of the chiller is 60 kW, the chilled water temperature is 20°C, the water flow is 130 l/min. Ambient temperature: -20 to +48°C Connection rating: 28 kW</p>

# SIEMENS

Siemens Medical Solutions USA, Inc.  
 51 Valley Stream Parkway, Malvern, PA 19355  
 Fax: (866) 309-6992

SIEMENS REPRESENTATIVE  
 Tegan Gonzalez - (781) 454-5132

Part No. / Product	Description
	Voltage: 3/PE 400 V to 480 V / 50/60 Hz Fuse rate: 80 A Power consumption: 66 A Dimensions: 2000 mm x 1100 mm x 2100 mm (height x width x depth). Weight: 760 kg  Noise level at a distance of 10 m at outside temperatures of: 21°C 47 dB(A) 32°C 52 dB(A) 48°C 58 dB(A)  IFP (Interface Panel) Main functions of the IFP:

Part No. / Product	Description
(Continued) 14416975 Eco Chiller 60kW	<ul style="list-style-type: none"> <li>- Interface function between the KKT chiller and the MR cabinet.</li> <li>- Water supply for MREF, MBB, CBB and TX box.</li> </ul> Additional devices such as integrated differential pressure control, a pressure gage, and a filter are used in order to guarantee the precise functioning of the cooling circuit, especially for the cold head compressor (MREF). The connection must be made locally with 2" lines up to a maximum distance of 25 m.  Dimensions: 800 mm x 1150 mm x 210 mm (height x width x depth). Weight: 67 kg
08857828 UPS Cable #Tim	Power cable to connect the 3 KVA Powerware 9125 small UPS system (pn PWR9125H3000) to the ACC cabinet of the MAGNETOM Avanto/ Espree/ Tim Trio for backing up the host computer and imager.  Configuration includes connection box.  The standard cable length is 9 m.
14413662 UPS Powerware PW9130G-3000T-XLEU	Voltage range: 180 - 276 V Input frequency: 50 / 60 Hz Output voltage: 230 VAC Dimensions (H x W x D): UPS 346 x 214 x 412 mm incl. UPS bracket set Weight: approx. 36 kg
MR_STD_RIG_INST MR Standard Rigging and Installation	MR Standard Rigging and Installation  This quotation includes standard rigging and installation of your new MAGNETOM system  Standard rigging into a room on ground floor level of the building during standard working hours (Mon. - Fri. / 8 a.m. to 5 p.m.) It remains the responsibility of the Customer to prepare the room in accordance with the SIEMENS planning documents Any rigging requiring a crane over 80 tons and/or special site requirements (e.g. removal of existing systems, etc.) is an incremental cost and the responsibility of the Customer. All other "out of scope" charges (not covered by the standard rigging and installation) will be identified during the site assessment and remain the responsibility of the Customer.
MR_PM MR Project Management	A Siemens Project Manager (PM) will be the single point of contact for the implementation of your Siemens equipment. The assigned PM will work with the customer's facilities management, architect or building contractor to assist you in ensuring that your site is ready for installation. Your PM will provide initial and final drawings and will coordinate the scheduling of the equipment, installation, and rigging, as well as the initiation of on-site clinical education.
MR_INITIAL_32	MR_INITIAL_32 Up to (32) hours of on-site clinical education training, scheduled consecutively (Monday - Friday)

# SIEMENS

Siemens Medical Solutions USA, Inc.  
51 Valley Stream Parkway, Malvern, PA 19355  
Fax: (866) 309-6992

SIEMENS REPRESENTATIVE  
Tegan Gonzalez - (781) 454-5132

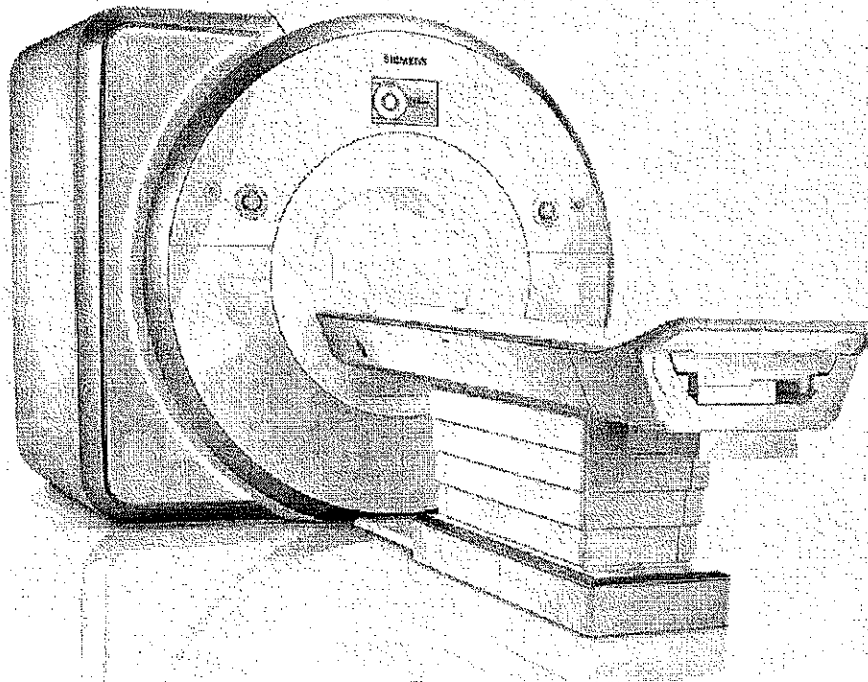
Part No. / Product	Description
Initial onsite training 32 hrs	during standard business hours for a maximum of (4) imaging professionals. Training will cover agenda items on the ASRT approved checklist. Uptime Clinical Education phone support is provided during the warranty period for specified posted hours. <b>This educational offering must be completed (12) months from install end date. If training is not completed within the applicable time period, Siemens obligation to provide the training will expire without refund.</b>
MR_FOLLOWUP_32 Follow-up training 32 hrs	Up to (32) hours of follow-up on-site clinical education training, scheduled consecutively (Monday – Friday) during standard business hours for a maximum of (4) imaging professionals. Uptime Clinical Education phone support is provided during the warranty period for specified posted hours. <b>This educational offering must be completed (12) months from install end date. If training is not completed within the applicable time period, Siemens obligation to provide the training will expire without refund.</b>
MR_INT_DOT_BCLS MR Dot Training Class	Tuition for (1) imaging professional to attend Classroom Course at Siemens Training Center. The objectives of this class are to introduce the user interface of the common syngo platform, including Dot, and instructions on building protocols, demonstration of software functions, and hands-on sessions. This class includes lunch, economy

Part No. / Product	Description
(Continued) MR_INT_DOT_BCLS MR Dot Training Class	airfare, and lodging for (1) imaging professional. All arrangements must be arranged through Siemens designated travel agency. This educational offering must be completed (12) months from install end date. If training is not completed within the applicable time period, Siemens obligation to provide the training will expire without refund.
MR_ADD_CLASS Additional Training Class	Tuition for (1) attendee for a customer classroom course of choice at one of the Siemens training centers. Includes economy airfare and lodging for (1) attendee. All arrangements must be arranged through Siemens designated travel agency. <b>This educational offering must be completed (12) months from install end date. If training is not completed within the applicable time period, Siemens obligation to provide the training will expire without refund.</b>
4MR5142869 Armrest #MR	An MR-compatible arm rest that supports the patient's arm on the magnet patient table when starting intravenous lines. The board is removed after the IV is inserted.  This product has been tested and verified for compatibility with the following Siemens' products: MAGNETOM Trio, Verio, Espree, Essenza, Avanto and Symphony. Compatibility with other products cannot be assured and may void service contracts and/or system warranties.
CHILINST_AVT Chiller Start-up and Warranty for TIM	Start up and initial set up service performed by the chiller manufacturer or designated service representative. This service does not include the piping and other prerequisite siting, of the waterchiller, which are the responsibility of the customer. 12 months warranty and performed by the chiller manufacturer.
MRWSE MR Wall sign - English	Highly durable 1mm PVC wall signs with high-tack, double-back tape. Sticks to most any surface. English. 12" x 18".

# SIEMENS

## MAGNETOM SKYRA TYPICAL ROOM PLAN

MR



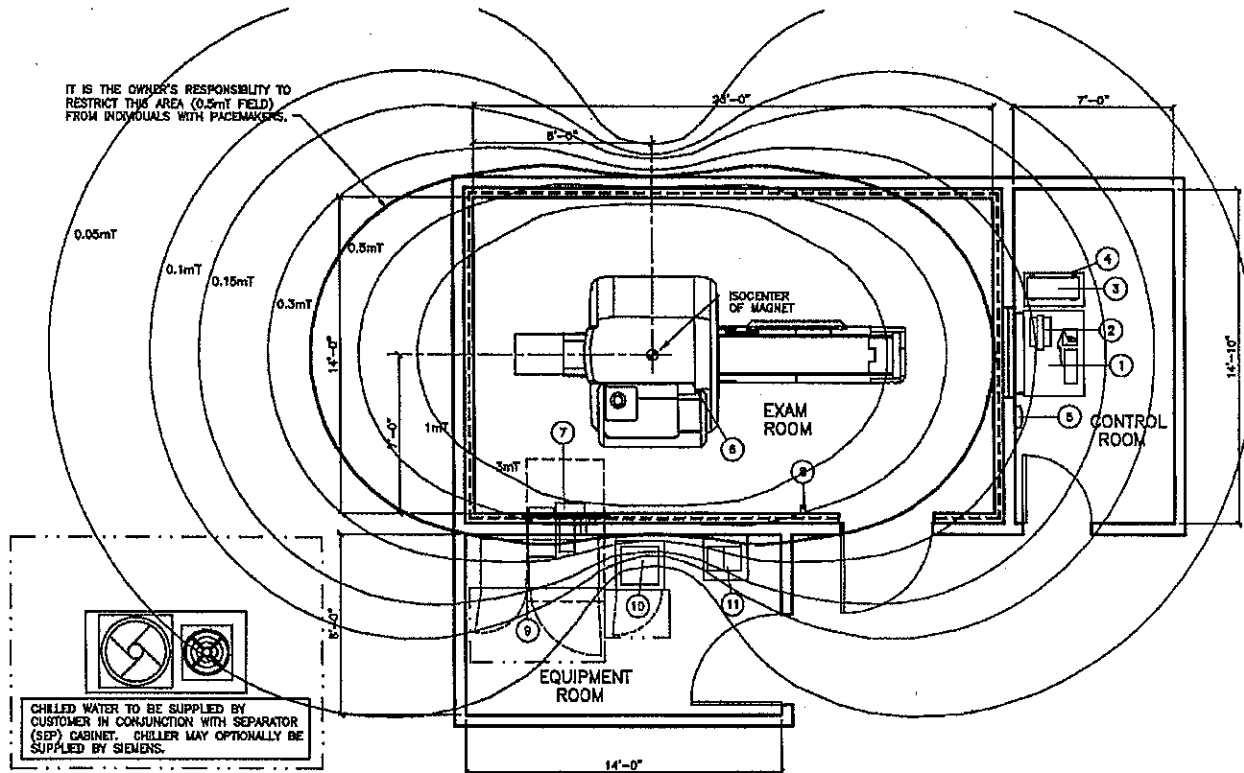
The intended use for this Cut Sheet is to communicate the spatial requirements as well as the basic architectural, electrical, structural, and mechanical requirements for this piece of imaging equipment. The information provided in this document is for reference only, during the pre-planning stage, and therefore does not contain any site specific detailed requirements. This information is subject to change without notice. Federal, state and/or local requirements may impact the final placement of the components. It is the customer's responsibility to ensure that the final layout and placement of the equipment complies with all applicable requirements.

# SIEMENS

FOR REFERENCE ONLY,  
NOT FOR CONSTRUCTION.

## MAGNETOM SKYRA TYPICAL ROOM PLAN

# MR



**TYPICAL PLAN**

SCALE: 1/8" = 1'-0"

### EQUIPMENT LEGEND

NO	DESCRIPTION	SMS SYM	WEIGHT (LBS)	BTU/HR TO AIR	DIMENSIONS (INCHES)			REMARKS
					W	D	H	
①	MRC OPERATING CONSOLE AND KEYBOARD	⊗	132	---	45 11/16	35 1/4	28 3/8	
②	COLOR MONITOR FOR MRC	⊖	22	239	18 5/16	16 15/16	4 3/4	ON CONSOLE/COUNTER
③	HOST PC MRC	⊕	49	2,388	11	27	18 1/8	
④	CONTAINER FOR HOST 500	⊖	238	---	19 5/8	31 1/2	28 3/8	
⑤	ALARM BOX	⊕	2	---	9	4	9	
⑥	3T MAGNET WITH COVERS AND PATIENT TABLE	⊕	15,802	9,383	90 1/2	181 3/4	87 3/8	
⑦	RF-FILTER PLATE	⊕	285	853	46 1/2	21 3/4	21 1/2	
⑧	MAGNET STOP	⊕	1	---	3	5	3	
⑨	ELECTRONICS CABINET (GPA/EPC CABINET)	⊕	2,756	13,649	61 1/2	26	77 1/2	
⑩	SEP CABINET	⊕	750	3,415	25 5/8	25 5/8	73 5/8	
⑪	POWERWARE 9130 UPS WITH EBM (OPTION)	⊕	186	1,257*	16 7/8	12 7/8	16 1/4	*1,755 ON BATTERIES



# SIEMENS

FOR REFERENCE ONLY,  
NOT FOR CONSTRUCTION.

## MAGNETOM SKYRA SPECIFICATIONS

# MR

POWER REQUIREMENTS	
VOLTAGE RANGE: 480 VAC $\pm 10\%$ FOR ALL LINE AND LOAD CONDITIONS. VOLTAGE BALANCE: 2% MAXIMUM DIFFERENCE BETWEEN PHASES	
FREQUENCY:	60 Hz $\pm 1.0$ Hz
LINE IMPEDENCE:	95 mOHMS
STAND BY POWER:	7.2 kVA
HIGHEST AVERAGE POWER	58 kVA
CONNECTION VALUE (LESS THAN 5 MINUTES)	110 kVA
MOMENTARY POWER	140 kVA
RECOMMENDED TRANSFORMER	150 kVA
MR SYSTEM OVERCURRENT PROTECTION	175 A
RECOMMENDED UPS	TBD
UPS SYSTEM OVERCURRENT PROTECTION	TBD
MAX. ALLOWABLE VOLTAGE DROP AT MAX. POWER	6.0%

NOISE LEVELS	
SYSTEM ROOM	NOISE LEVEL / dB(A)
CONTROL ROOM	<55
EXAMINATION ROOM	88.3 dB(A) AVERAGE VALUE OVER 8 HOURS INSIDE EXAM ROOM.
EQUIPMENT ROOM	<65

IT IS THE CUSTOMER'S RESPONSIBILITY TO ENSURE THAT ALL LOCAL/  
STATE/OSHA NOISE REGULATIONS ARE ADHERED TO. ADDITIONAL NOISE  
DATA MAY BE PROVIDED BY SIEMENS PROJECT MANAGER UPON REQUEST.

POWER REQUIREMENTS
DEMAND AND CAPACITY REQUIREMENTS NOTES
1) IF EQUIPMENT UPGRADE IS ANTICIPATED, INSTALLING ELECTRICAL POWER TO MEET THE REQUIREMENTS OF THE HIGHER POWER GRADIENT PACKAGE AT THE TIME OF INITIAL INSTALLATION WILL REDUCE THE COST TO UPGRADE THE ELECTRICAL SYSTEM LATER.
2) RECOMMENDED TRANSFORMER SIZE (SYSTEM WITHOUT UPS) IS BASED ON INDUSTRY STANDARD ISOLATION TRANSFORMER KVA RATINGS. SOURCE IMPEDANCE FEEDING THE MAGNETOM SYSTEM, INCLUDING ANY ISOLATION TRANSFORMERS, MUST MEET EQUIPMENT REQUIREMENTS AS LISTED HERE. SIEMENS RECOMMENDS A TRANSFORMER WITH COPPER WINDINGS, AN ELECTRO-STATIC SHIELD, AND A LOW IMPEDANCE (<3%) TO ENSURE THAT SOURCE IMPEDANCE REQUIREMENTS ARE MET.
3) OVERCURRENT PROTECTION IS SPECIFIED FOR SYSTEMS WITHOUT AN UNINTERRUPTIBLE POWER SUPPLY (UPS). ADDITION OF A UPS REQUIRES A HIGHER CAPACITY MAINS CONNECTION (DEPENDENT UPON UPS MODEL AND SIZE). MAXIMUM FAULT CURRENT IS DEPENDENT UPON THE IMPEDANCE OF THE FACILITY ELECTRICAL SYSTEM. CUSTOMER'S ARCHITECT OR ELECTRICAL CONTRACTOR TO SPECIFY AIC RATING OF OVERCURRENT PROTECTION BASED ON FACILITY IMPEDANCE CHARACTERISTICS.
4) MOMENTARY POWER IS BASED ON A MAXIMUM RMS VALUE FOR A PERIOD NOT TO EXCEED FIVE (5) SECONDS, AS DEFINED IN NEC 517.2. STAND-BY AND AVERAGE CURRENT ARE SUBSTANTIALLY LOWER.
5) THE CONDUCTOR SIZE SHOULD BE SELECTED TO MEET THE VOLTAGE DROP REQUIREMENTS, TAKING INTO CONSIDERATION THE MAINS CAPACITY, RUN LENGTH, AND ANY ADDITIONAL TRANSFORMERS USED TO OBTAIN THE PROPER EQUIPMENT VOLTAGE LEVEL. NEMA STANDARD XR-9-1989 (R1994,R2000) PROVIDES GENERAL GUIDELINES FOR SIZING CONDUCTORS, TRANSFORMERS, AND ELECTRICAL SYSTEMS FOR MEDICAL IMAGING SYSTEMS.
6) LONG-TIME POWER IS BASED ON THE HIGHEST AVERAGE RMS VALUES FOR A PERIOD EXCEEDING 5 MINUTES DURING CLINICAL SYSTEM OPERATION, AS DEFINED IN NEC 517.2.
7) A CIRCUIT BREAKER WITH A HIGH INRUSH RATING (>8x RATED CURRENT) IS REQUIRED TO PERMIT SWITCH-ON OF THE UPS SYSTEM WITHOUT SPURIOUS TRIPPING. CIRCUIT BREAKERS WITH AN ADJUSTABLE MAGNETIC TRIP (SIEMENS FDB SERIES OR SIMILAR) ARE HIGHLY RECOMMENDED.

CEILING HEIGHTS
EXAM ROOM 7'-11" MINIMUM CONTROL ROOM 6'-11" MINIMUM EQUIPMENT ROOM 7'-3" MINIMUM

REMOTE SYSTEM DIAGNOSTICS
SIEMENS REMOTE SERVICES (SRS) REQUIRES A CONNECTION BETWEEN THE SRS REMOTE SERVER AND SIEMENS SYSTEMS VIA REMOTE LOCAL AREA NETWORK ACCESS, TO ENSURE THE UPTIME OF YOUR SYSTEM.
THIS SERVICE REQUIRES ONE OF THE FOLLOWING CONNECTION METHODS:
1. (PREFERRED) VPN - WHERE THE CUSTOMER HAS AVAILABLE A VPN CAPABLE FIREWALL OR OTHER VPN APPLIANCE.
2. (OPTIONAL) *SRS ROUTER* - CONNECTED TO ANALOG PHONE LINE VIA *ANALOG MODEM*, ETHERNET CONNECTION TO CUSTOMER'S LAN, AND A POWER OUTLET.
NOTE: - *SUPPLIED BY SIEMENS*

FOR MORE INFORMATION
FOR MORE DETAILED PLANNING REQUIREMENTS FOR THIS SYSTEM, SEE THE TYPICAL FINAL DRAWING SET NUMBER: 10024

# SIEMENS

FOR REFERENCE ONLY,  
NOT FOR CONSTRUCTION.

## MAGNETOM SKYRA SPECIFICATIONS

# MR

### CHILLED WATER SUPPLY

A CHILLED WATER SUPPLY IS REQUIRED TO THE MRI SYSTEM 24 HOURS A DAY, YEAR ROUND FOR THE COLD HEAD AND GRADIENT SYSTEMS. THIS CAN BE PROVIDED BY A CENTRAL CHILLED WATER SUPPLY OR A SEPARATE STAND ALONE CHILLER THAT MEETS THE STATED REQUIREMENTS. THE CHILLED WATER CAN ALSO BE SUPPLIED BY A DEDICATED KRAUS ECO CHILLER AND INTERFACE PANEL.

WITHOUT THE USE OF A DEDICATED KRAUS CHILLER, A SEP (SYSTEM SEPARATOR CABINET), MUST BE INCLUDED WITH THE SIEMENS ORDER. THE PIPE SIZE BETWEEN THE KRAUS CHILLER AND INTERFACE PANEL, OR BETWEEN THE WATER SUPPLY AND SEP MUST BE 2 INCH UP TO 82 FEET, 2-1/2 INCH UP TO 148 FEET, CONSULT FOR LONGER PIPE. PERMISSIBLE MATERIALS THAT CAN BE USED FOR THE PIPING ARE: STAINLESS STEEL (V2A, V4A), NON-FERROUS METAL (COPPER, BRASS), SYNTHETIC MATERIAL, PLASTICS, BRAZING SOLDER, HARD SOLDER, OR FITTING SOLDER TYPE 3 AND 4. THERE ARE MATERIALS THAT MAY CAUSE DAMAGE TO THE COOLING SYSTEM AND CANNOT BE USED, THESE MATERIALS ARE ALUMINUM, IRON, CARBON STEEL, ZINC, ZINC PLATED STEEL, OR STANDARD STEEL PIPES.

THESE REQUIREMENTS ARE REQUIRED FOR NEW INSTALLATIONS, IF EXISTING WATER PIPES COMPLY WITH SIEMENS WATER SPECIFICATIONS, THEY DO NOT NEED TO BE REPLACED.

NORMAL TAP WATER MUST BE AVAILABLE FOR FILLING THE SECONDARY WATER CIRCUIT. THERE SHALL BE A HOSE BIB LOCATED WITHIN 65' OF THE SEP, IFP, ACC OR THE KRAUS CHILLER.

THE SUPPLY AND RETURN CHILLED WATER PIPES MUST BE LABELED. THE LOCATION OF THE LABELS MUST BE AT ALL CONNECTION AND REFILLING POINTS AND MUST CONTAIN FLOW DIRECTION AND CONTENTS.

### ENVIRONMENTAL REQUIREMENTS

1) AIR CONDITIONING IS TO PROVIDE A TEMPERATURE OF 70°F ±5°F IN THE CONTROL & EQUIPMENT ROOMS 65°F-71°F IN EXAM ROOM. RELATIVE HUMIDITY OF 40-60% (NON-CONDENSING) IS REQUIRED EXAMINATION ROOM AND 40-80% (NON-CONDENSING) IN ALL OTHER AREAS WHERE SIEMENS EQUIPMENT IS INSTALLED. THESE CONDITIONS ARE TO BE MET AT ALL TIMES; 24 HOURS A DAY, 7 DAYS A WEEK.

2) A DEDICATED AIR CONDITIONING AND HUMIDIFICATION SYSTEM IS RECOMMENDED FOR THE EXAM ROOM. A MINIMUM FRESH AIR EXCHANGE RATE OF 6 TIMES PER HOUR FOR THE EXAM ROOM IS REQUIRED. AIR SUPPLY AND RETURN ABOVE THE FINISHED CEILING IN THE EXAM ROOM IS RECOMMENDED. EACH ROOM SHOULD HAVE A DEDICATED CONTROL AND SENSOR TO MONITOR AND ADJUST THE AIR.

3) THE HEAT INTO THE EXAM ROOM IS LESS THAN 10,236 BTU/HR. THE HEAT INTO THE EQUIPMENT ROOM IS TYPICALLY 32,415 BTU/HR, MAXIMUM 40,946 BTU/HR. THIS HEAT DISSIPATION IS FROM THE SIEMENS EQUIPMENT ONLY. AUXILIARY SUPPORT EQUIPMENT (ie UPS) AND LIGHTING MUST BE CONSIDERED FOR TOTAL HEAT LOADS.

4) IT IS IMPORTANT FOR FRESH AIR INTAKE SYSTEMS TO EXHAUST AIR DIRECTLY OUT OF THE BUILDING. THE EXHAUST AIR MUST NOT BE DEFLECTED INTO ANOTHER ROOM. THE MAGNET ROOM EXHAUST AIR SHOULD BE INSTALLED AT LEAST 6'-6" ABOVE FINISHED FLOOR.

5) THE AIR INTAKE OF THE AIR CONDITIONING SYSTEM MUST NOT BE LOCATED IN THE VICINITY OF THE QUENCH VENT EXHAUST.

6) IF THE INPUT DRAWS UPON AIR FROM OUTSIDE THE BUILDING, IT IS RECOMMENDED TO INSTALL AN ON-SITE FILTER TO REMOVE DUST PARTICLES GREATER THAN 10 MICRONS.

### CHILLED WATER REQUIREMENTS

WATER REQUIREMENTS TO BE MEASURED AT THE SEP CABINET.

FLOW RATE:	26.42 GPM ±2.64 GPM
WATER TEMPERATURE:	43°F - 53°F
BTU DISCHARGE TO THE WATER	204,728 BTU/HR
WATER PRESSURE	MAXIMUM 87 PSI
LOSS OF PRESSURE FOR SEP CABINET	14.5 PSI MAXIMUM
CHILLED WATER ACIDITY RANGE	6 pH TO 8 pH
CHILLED WATER HARDNESS	<260 ppm CALCIUM CARBONATE
CHLORINE GAS CONCENTRATION	<200 ppm
FILTRATION	500 µm

FOR INSTALLATION OF A KRAUS ECO CHILLER, IT IS THE RESPONSIBILITY OF THE CUSTOMER/MECHANICAL CONTRACTOR TO PROVIDE A MIXTURE OF WATER WITH 35%-38% ETHYLENE GLYCOL PRIOR TO CHILLER START UP. DO NOT USE PROPYLENE GLYCOL OR AUTOMOTIVE ANTI-FREEZE.

THE AMOUNT OF THE MIXTURE MUST FILL THE CHILLER, MR SYSTEM AND PIPING (SUPPLY AND RETURN), SEE EXAMPLES BELOW.

(1) GALLON OF UNDILUTED GLYCOL, OR (2) GALLONS OF WATER/GLYCOL MIXTURE MUST REMAIN ON SITE FOR USE AFTER START UP.

MIXTURE VOLUME INCLUDING SUPPLY & RETURN+15 GAL. CHILLER & MR

PIPE DIAMETER	TOTAL LENGTH	MIXTURE VOLUME	GLYCOL NEEDED
2"	100'	31.3 GALLONS	11.9 GALLONS
2"	200'	47.6 GALLONS	18.1 GALLONS
2.5"	100'	40.5 GALLONS	15.4 GALLONS
2.5"	200'	66.0 GALLONS	25.1 GALLONS

MIXTURE VOLUME =  $3.14 \times (\text{PIPE RADIUS})^2 \times \text{PIPE LENGTH} + 15 \text{ GALLONS}$ .  
GLYCOL AMOUNT = 35-38% OF MIXTURE VOLUME.

### QUENCH VENT NOTES

LIQUID AND GASEOUS HELIUM ARE USED IN THE OPERATION OF A SUPERCONDUCTING MRI SYSTEM. THE MECHANICAL CONTRACTOR SHALL PROVIDE A VENT, ACCORDING TO SIEMENS SPECIFICATIONS, TO EXHAUST GASEOUS HELIUM FROM THE MAGNET TO OUTSIDE THE BUILDING. PLEASE SEE THE SIEMENS TYPICAL DRAWINGS FOR DETAILS.

# SIEMENS

FOR REFERENCE ONLY,  
NOT FOR CONSTRUCTION.

## MAGNETOM SKYRA SPECIFICATIONS

# MR

### PROTECTING THE ENVIRONMENT

PROTECTING THE IMMEDIATE ENVIRONMENT FROM THE EFFECT OF THE MAGNETIC FIELD REQUIRES CONSIDERATION. INFORMATION STORED ON MAGNETIC DATA CARRIERS SUCH AS DISKS, TAPES, AND CREDIT CARDS MAY BE ERASED IF IN CLOSE PROXIMITY. CAUTION WITH REGARD TO HEART PACEMAKERS MUST BE EXERCISED. MOST PACEMAKER UNITS EMPLOY A REED RELAY WHICH MAY CHANGE OPERATING MODE WHEN EXPOSED TO AN EXTERNAL MAGNETIC FIELD. THEREFORE, PACEMAKER USERS MUST BE KEPT AT A SPECIFIED DISTANCE FROM THE MAGNET WHICH IS DETERMINED BY THE MAGNETIC FIELD STRENGTH.

### PROTECTING THE MAGNETIC FIELD

THE SIEMENS MAGNETOM UTILIZES A SUPERCONDUCTIVE MAGNET WITH AN EXTREMELY HOMOGENEOUS FIELD WITHIN THE MAGNET TO PROVIDE DISTORTION-FREE IMAGING. THE PRESENCE OF FERROMAGNETIC MATERIAL WITHIN THE VICINITY OF THE MAGNET CAN ADVERSELY AFFECT THE UNIFORMITY OF THE USEFUL MAGNETIC FIELD. THIS APPLIES TO STATIONARY FERROUS MATERIAL (STRUCTURAL STEEL) WHICH IS TO BE MINIMIZED. STATIONARY STEEL COMPENSATION MAY BE ACHIEVED BY MAGNET POSITIONING AND SELECTIVE USE OF SHIMS. FIELD DISTORTION ENCOUNTERED BY MOVING FERROMAGNETIC OBJECTS IS MORE DIFFICULT TO COMPENSATE AND MAY REQUIRE THE USE OF MAGNETIC SHIELDING.

### MAGNETIC FRINGE FIELDS

MAGNETIC FIELDS MAY AFFECT THE FUNCTION OF DEVICES IN THE VICINITY OF THE MAGNET. THESE DEVICES MUST BE OUTSIDE CERTAIN MAGNETIC FIELDS. THE DISTANCES LISTED ARE FROM THE MAGNET ISOCENTER AND DO NOT CONSIDER ANY MAGNETIC ROOM SHIELDING.

X/Y AND Z AXIS	DEVICES
6'-11" / 10'-6" 3.0mT	SMALL MOTORS, WATCHES, CAMERAS, CREDIT CARDS, MAGNETIC DATA CARRIERS (SHORT-TERM EXPOSURE)
7'-7" / 13'-2" 1.0mT	COMPUTERS, MAGNETIC DISK DRIVES, OSCILLOSCOPES, PROCESSORS
8'-7" / 15'-2" 0.5mT	CARDIAC PACEMAKERS, X-RAY TUBES, INSULIN PUMPS, B/W MONITORS, MAGNETIC DATA CARRIERS (LONG-TERM STORAGE)
11'-2" / 20'-1" 0.15mT	COLOR MONITORS, SIEMENS CT SCANNERS
12'-6" / 22'-4" 0.1mT	SIEMENS LINEAR ACCELERATORS
16'-1" / 26'-11" 0.05mT	X-RAY IMAGE INTENSIFIERS, GAMMA CAMERAS, PET/CYCLOTRON, ELECTRON MICROSCOPES, LINEAR ACCELERATORS

THE OWNER/USER IS TO VERIFY THE LOCATION OF THE 0.5mT FIELD AND ENSURE THAT IT IS MAINTAINED AS A RESTRICTED AREA.

### MAGNET SITING REQUIREMENTS

IT MUST BE ENSURED THAT THE MAGNET IS LOCATED SO THAT THE STABILITY AND HOMOGENEITY OF THE MAGNETIC FIELD ARE NOT ADVERSELY AFFECTED BY EXTRANEIOUS FIELDS AND STATIC OR DYNAMIC FERROMAGNETIC OBJECTS.

X/Y AND Z AXIS	SOURCE OF INTERFERENCE
4'-0"	FLOOR STEEL REINFORCEMENT < 20 LBS./ FT <sup>2</sup> IRON BEAMS < 66 LBS./FT.
18'-0" / 21'-3"	STRETCHERS UP TO 110 LBS.
13'-1"	A/C CHILLERS
19'-8" / 22'-11"	TRANSPORT DEVICES UP TO 440 LBS.
21'-3" / 26'-2"	VEHICLES UP TO 2,000 LBS.
22'-11" / 31'-2"	ELEVATORS, TRUCKS UP TO 10,000 LBS.
39'-4" / 26'-2"	AC TRANSFORMERS LESS THAN 100 KVA
41'-0" / 32'-8"	AC TRANSFORMERS LESS THAN 250 KVA
42'-7" / 39'-4"	AC TRANSFORMERS LESS THAN 650 KVA
45'-11" / 49'-2"	AC TRANSFORMERS LESS THAN 1600 KVA
9'-10" / 6'-6"	AC CABLES, MOTORS LESS THAN 100 AMPS
22'-11" / 9'-10"	AC CABLES, MOTORS LESS THAN 250 AMPS
131'-2"	ELECTRIC RAILWAY SYSTEMS

FOR IRON OBJECTS LOCATED UP TO 45' FROM THE Z AXIS, THE DISTANCES FOR THE Z AXIS MUST BE USED. REDUCTION IS POSSIBLE WITH STEEL SHIELDING.

### MAXIMUM CABLE LENGTH

THERE ARE 3 DIFFERENT LENGTHS OF CABLE THAT ARE AVAILABLE FOR THE MRI SYSTEM DIFFERENTIATED BY MAXIMUM LENGTHS FROM THE MAGNET TO THE FILTER PANEL (INSIDE) AND FROM THE FILTER PANEL TO THE ELECTRONICS (OUTSIDE).

INSIDE	OUTSIDE
20'	4'
20'	32'
20'	39'

THE VERTICAL DISTANCE FOR CABLE TRAVEL FROM THE FILTER PANEL TO THE CABLE TRAY, AND FROM THE CABLE TRAY TO THE MAGNET MUST BE CONSIDERED.

THE MAXIMUM DISTANCE FROM THE ACC CABINET TO THE CONTROL CONSOLE IS 75 FEET.

# SIEMENS

FOR REFERENCE ONLY,  
NOT FOR CONSTRUCTION.

## MAGNETOM SKYRA SPECIFICATIONS

### MR

#### RF SHIELDING

THE EXAMINATION AREA MUST BE SHIELDED TO PROVIDE A REDUCTION OF RADIO FREQUENCY WAVES EMANATING FROM EXTERNAL TRANSMITTERS. THE REQUIRED ATTENUATION IS 90dB IN THE FREQUENCY RANGE OF 15-128 MHZ. IF CO-SITING TWO SYSTEMS EACH ROOM SHOULD BE 100 dB. THE RF SHIELD MUST BE TESTED BEFORE AND AFTER MAGNET PLACEMENT IN THE RF ROOM AND AFTER THE SIEMENS RF FILTER PANEL IS INSTALLED.

THE RF-SHIELDING MUST BE INSULATED FROM ALL GROUNDS SUCH THAT THE ONLY GROUND IS THE SINGLE POINT GROUND ON THE OUTSIDE OF THE RF-ROOM WALL. RESISTANCE  $\geq$  100 OHMS.

ALL ELECTRICAL LINES INTO THE RF ROOM MUST BE ROUTED THROUGH RF FILTERS (PROVIDED BY RF SHIELDING SUPPLIER). ALL ELECTRICALLY NON-CONDUCTIVE SUPPLY LINES (E.G. FIBER OPTIC CABLES, OR HOSES) INTO THE RF ROOM MUST BE ROUTED THROUGH RF SEALED WAVEGUIDES (PROVIDED BY RF SHIELDING SUPPLIER).

FOR PRESSURE EQUALIZATION PURPOSES THE RF DOOR SHOULD OPEN TO THE OUTSIDE OF THE RF ROOM. AS AN ALTERNATIVE A 24"x24" OPENING IN THE RF ROOM FOR PRESSURE EQUALIZATION IS REQUIRED.

#### BUILDING VIBRATIONS

VIBRATION OF THE SITE HAS THE ABILITY TO AFFECT THE STABILITY AND HOMOGENEITY OF THE MAGNETIC FIELD. THEREFORE EXTERNAL VIBRATIONS OR SHOCKS AFFECTING THE MAGNET MAY DEGRADE IMAGE QUALITY. IN THE THREE SPATIAL ORIENTATIONS THE BUILDING MUST NOT EXCEED ACCELERATION OF 0.001m/s or -80dB(g)  $g=9.81$  m/s

THE REQUIREMENT FOR  $a_{max}$  IS MEASURED AS MAXIMUM RMS VALUE PER FREQUENCY COMPONENT <0.5Hz IN THE FOURIER TRANSFORMATION OF THE RECORDED SIGNAL (SPECTRUM).

THE VIBRATION LEVEL OF CONTINUOUS VIBRATIONS (CAUSED BY AIR CONDITIONER, COMPRESSOR, ETC.) AT THE LOCATION OF THE MAGNET MUST NOT EXCEED THE SPECIFIED VALUES.

FOR ALL NON-CONTINUOUS TRANSIENT VIBRATIONS THE FIGURES SHOULD BE MULTIPLIED BY 4 (OR 12dB).

CONTACT SIEMENS PROJECT MANAGER FOR MORE DETAILS.

#### TRANSPORTING REQUIREMENTS

LARGEST ITEM - MAGNET - 18,298 LBS.

MAGNET DIMENSIONS: 7'-6" HIGH x 7'-7" WIDE x 10'-5" LONG FOR STANDARD DELIVERY. BY REMOVING THE TABLE, THE LENGTH CAN BE REDUCED TO 6'-5". THE ROOF HATCH OPENING SHOULD BE 4" LARGER THAN THE MAGNET DIMENSIONS.

TO TRANSPORT THE GPA/ACC CABINET (2,756 POUNDS) A MINIMUM ROOM HEIGHT OF 6'-9" WITH TRANSPORT ROLLERS, OR 6'-5" WITHOUT TRANSPORT ROLLERS IS REQUIRED.

# **ATTACHMENT 9**

**Table 4: Patient Population Mix**

**SAINT FRANCIS HOSPITAL AND MEDICAL CENTER**

<b>Description:</b>	<b>Current FY 2012</b>	<b>Year 1 FY 2013</b>	<b>Year 2 FY 2014</b>	<b>Year 3 FY 2015</b>	<b>Year 4 FY 2016</b>
1. Medicare *	38.6%	39.1%	39.0%	39.0%	39.0%
2. Medicaid*	23.6%	23.5%	23.5%	23.5%	23.5%
3. CHAMPUS & TriCare	0.3%	0.3%	0.3%	0.3%	0.3%
<b>Total Government</b>	62.6%	62.9%	62.8%	62.8%	62.8%
1. Commercial Insurers*	34.8%	34.5%	34.6%	34.6%	34.6%
2. Uninsured	2.0%	1.9%	1.9%	1.9%	1.9%
3. Workers Compensation	0.7%	0.7%	0.7%	0.7%	0.7%
<b>Total Non-Government Payers</b>	37.4%	37.1%	37.2%	37.2%	37.2%
<b>Total Payer Mix</b>	100.0%	100.0%	100.0%	100.0%	100.0%

\* includes managed care activity.

**12. C. (i) Please provide one year of actual results and three years of Saint Francis Hospital and Medical Center projections of revenue, expense and volume statistics without, incremental to and with the CON proposal in the following reporting format:**

**Saint Francis Hospital and Medical Center**

Description	FY 2011	FY 2012		FY 2013		FY 2014		FY 2014	FY 2014	FY 2014
	Actual Results	Projected W/out CON	Projected With CON	Projected W/out CON	Projected With CON	Projected W/out CON	Projected With CON	Incremental	Projected	Projected With CON
<b>NET PATIENT REVENUE</b>										
Non-Government	269,851,357	287,099,320	287,099,320	311,396,218	311,396,218	329,473,382	329,473,382	253,489	329,473,382	329,726,871
Medicare	258,456,390	257,704,366	257,704,366	268,472,263	268,472,263	272,096,639	272,096,639	42,444	272,096,639	272,139,083
Medicaid and Other Medical Assistance	82,731,828	91,174,192	91,174,192	92,904,666	92,904,666	94,145,461	94,145,461	8,944	94,145,461	94,154,405
Other Government	1,701,806	585,859	585,859	993,948	993,948	1,017,440	1,017,440	2,274	1,017,440	1,019,714
Total Net Patient Revenue	612,741,382	636,563,737	636,563,737	673,767,095	673,767,095	696,732,922	696,732,922	307,151	696,732,922	697,040,073
Other Operating Revenue	30,869,665	34,822,996	34,822,996	30,651,803	30,651,803	31,264,839	31,264,839	-	31,264,839	31,264,839
Revenue from Operations	643,611,046	671,386,733	671,386,733	704,418,898	704,418,898	727,997,761	727,997,761	307,151	727,997,761	728,304,912
<b>OPERATING EXPENSES</b>										
Salaries and Fringe Benefits	300,958,979	310,753,976	310,753,976	330,549,802	330,549,802	341,252,023	341,252,023	-	341,252,023	341,252,023
Professional / Contracted Services	93,536,847	90,165,508	90,165,508	89,000,334	89,000,334	92,587,074	92,587,074	(245,700)	92,587,074	92,341,374
Supplies and Drugs	114,547,580	114,518,398	114,518,398	110,312,805	110,312,805	114,758,444	114,758,444	5,513	114,758,444	114,763,957
Bad Debts	15,406,823	18,947,560	18,947,560	20,337,630	20,337,630	21,030,852	21,030,852	9,448	21,030,852	21,040,300
Other Operating Expense	78,774,642	83,922,171	83,922,171	87,879,011	87,879,011	91,302,266	91,302,266	-	91,302,266	91,302,266
Subtotal	603,224,870	618,307,614	618,307,614	638,079,582	638,079,582	660,930,660	660,930,660	(230,739)	660,930,660	660,699,921
Depreciation/Amortization	28,954,676	34,284,451	34,284,451	34,169,101	34,169,101	35,180,758	35,180,758	307,655	35,180,758	35,488,413
Interest Expense	9,560,860	12,191,556	12,191,556	12,461,558	12,461,558	11,722,588	11,722,588	-	11,722,588	11,722,588
Lease Expense	5,037,394	5,276,600	5,276,600	5,263,228	5,263,228	5,263,228	5,263,228	-	5,263,228	5,263,228
Total Operating Expenses	646,777,801	670,060,221	670,060,221	689,973,469	689,973,469	713,097,234	713,097,234	76,916	713,097,234	713,174,150
Gain/(Loss) from Operations	(3,166,754)	1,326,511	1,326,511	14,445,428	14,445,428	14,900,527	14,900,527	230,235	14,900,527	15,130,762
Non-Operating Income/(Loss)	(12,703,120)	(10,417,045)	(10,417,045)	(1,050,000)	(1,050,000)	-	-	-	-	-
Revenue Over/(Under) Expense	(15,869,874)	(9,090,534)	(9,090,534)	13,395,428	13,395,428	14,900,527	14,900,527	230,235	14,900,527	15,130,762
FTEs	3,554.4	3,534.2	3,534.2	3,695.8	3,695.8	3,732.8	3,732.8	-	3,732.8	3,732.8
*Volume Statistics:										
Patient Days	157,959	157,301	157,301	163,731	163,731	165,312	165,312	-	165,312	165,312
Discharges	31,842	32,274	32,274	34,099	34,099	34,440	34,440	-	34,440	34,440
Average Length of Stay	4.96	4.87	4.87	4.80	4.80	4.80	4.80	-	4.80	4.80
MRI exams:	11,580	12,337	12,337	12,583	12,583	12,583	12,583	250	12,583	12,833

Provide projected inpatient and/or outpatient statistics for any new services and provide actual and projected inpatient and/or outpatient statistics for any existing services which will change due to the proposal.

**12. C. (i) Please provide one year and volume statistics with**

**Saint Francis Hospital and Medical**

Description	FY 2015		FY 2015		FY 2016		FY 2016	
	Projected W/out CON	Projected Incremental	Projected With CON	Projected Incremental	Projected W/out CON	Projected Incremental	Projected With CON	Projected With CON
<b>NET PATIENT REVENUE</b>								
Non-Government	345,445,721	542,516	345,988,237	838,521	362,210,391	838,521	363,048,912	363,048,912
Medicare	275,769,943	86,911	275,856,854	131,379	279,492,838	131,379	279,624,217	279,624,217
Medicaid and Other Medical Assistance	95,403,007	17,452	95,420,459	26,612	96,677,529	26,612	96,704,141	96,704,141
Other Government	1,041,487	6,891	1,048,378	9,280	1,066,103	9,280	1,075,383	1,075,383
<b>Total Net Patient Revenue</b>	<b>717,660,158</b>	<b>653,770</b>	<b>718,313,928</b>	<b>1,005,792</b>	<b>739,446,861</b>	<b>1,005,792</b>	<b>740,452,653</b>	<b>740,452,653</b>
Other Operating Revenue	31,890,136	-	31,890,136	-	32,527,939	-	32,527,939	32,527,939
Revenue from Operations	749,550,294	653,770	750,204,064	1,005,792	771,974,800	1,005,792	772,980,592	772,980,592
<b>OPERATING EXPENSES</b>								
Salaries and Fringe Benefits	352,302,298	-	352,302,298	-	363,722,155	-	363,722,155	363,722,155
Professional / Contracted Services	96,317,226	(245,700)	96,071,526	(245,700)	98,282,932	(245,700)	98,037,232	98,037,232
Supplies and Drugs	119,381,836	11,491	119,393,327	17,917	124,193,490	17,917	124,211,407	124,211,407
Bad Debts	21,662,540	19,869	21,682,409	30,761	22,350,726	30,761	22,381,487	22,381,487
Other Operating Expense	94,980,655	149,099	95,129,754	149,099	98,808,826	149,099	98,957,925	98,957,925
Subtotal	684,644,556	(65,241)	684,579,315	(47,923)	707,358,127	(47,923)	707,310,204	707,310,204
Depreciation/Amortization	36,580,104	615,308	37,195,412	615,308	38,038,185	615,308	38,653,493	38,653,493
Interest Expense	11,400,217	-	11,400,217	-	11,624,809	-	11,624,809	11,624,809
Lease Expense	5,263,228	-	5,263,228	-	5,421,125	-	5,421,125	5,421,125
<b>Total Operating Expenses</b>	<b>737,888,105</b>	<b>550,067</b>	<b>738,438,172</b>	<b>567,385</b>	<b>762,442,246</b>	<b>567,385</b>	<b>763,009,631</b>	<b>763,009,631</b>
Gain/(Loss) from Operations	11,662,189	103,703	11,765,892	438,407	9,532,554	438,407	9,970,961	9,970,961
Non-Operating Income/(Loss)	-	-	-	-	-	-	-	-
Revenue Over/(Under) Expense	11,662,189	103,703	11,765,892	438,407	9,532,554	438,407	9,970,961	9,970,961
FTEs	3,770.1	-	3,770.1	-	3,807.8	-	3,807.8	3,807.8
*Volume Statistics:								
Patient Days	166,963	-	166,963	-	168,634	-	168,634	168,634
Discharges	34,784	-	34,784	-	35,132	-	35,132	35,132
Average Length of Stay	4.80	-	4.80	-	4.80	-	4.80	4.80
MRI exams:	12,583	506	13,089	766	12,583	766	13,349	13,349

Provide projected inpatient and/or outpatient statistics



12.C(ii). Please provide three years of projections of incremental revenue, expense and volume statistics attributable to the proposal in the following reporting format:

SAINT FRANCIS HOSPITAL AND MEDICAL CENTER											
Fiscal Year 2014											
Type of Service Description	MRI -3T	(1)	(2)	(3)	(4)	(5)	(6)	(7)	(8)	(9)	(10)
Type of Unit Description:	Exams	Rate	Gross Revenue	Allowances/ Deductions	Charity Care	Bad Debt	Net Revenue	Operating Expenses	Gain/(Loss) from Operations		
# of Months in Operation	11	Col. 2 * Col. 3	Col. 4 - Col.5 -Col.6 - Col.7	Col. 4 / Col. 4 Total	Col. 8 - Col. 9						
Year 1											
FY Projected Incremental											
Total Incremental Expenses:	\$67,468										
Total Facility by											
Payer Category:											
Medicare		\$ 6,339.62	\$399,396	\$356,952			\$42,444	\$17,002	\$25,442		
Medicaid		\$6,339.62	\$253,585	\$244,641			\$8,944	\$10,795	(\$1,851)		
CHAMPUS/TriCare		\$6,339.62	\$6,340	\$4,066			\$2,274	\$270	\$2,004		
<b>Total Governmental</b>			\$659,320	\$605,658	\$0	\$0	\$53,662	\$28,067	\$25,595		
Commercial Insurers		\$6,339.62	\$906,565	\$655,295	\$7,775	\$5,450	\$238,045	\$38,592	\$199,453		
Uninsured		\$6,339.62	\$19,019	\$9,025	\$3,998	\$3,998	\$5,996	\$810	\$5,186		
<b>Total NonGovernment</b>			\$925,584	\$655,295	\$16,800	\$9,448	\$244,041	\$39,401	\$204,640		
<b>Total All Payers</b>			\$1,584,904	\$1,260,953	\$16,800	\$9,448	\$297,703	\$67,468	\$230,235		

SAINT FRANCIS HOSPITAL AND MEDICAL CENTER										
Fiscal Year 2015										
Type of Service Description	(1)	(2)	(3)	(4)	(5)	(6)	(7)	(8)	(9)	(10)
Type of Unit Description:	Exams	Rate	Units	Gross Revenue	Allowances/ Deductions	Charity Care	Bad Debt	Net Revenue	Operating Expenses	Gain/(Loss) from Operations
# of Months in Operation	12			Col. 2 * Col. 3				Col. 4 - Col.5 -Col.6 - Col.7	Col. 1 Total * Col. 4 / Col. 4 Total	Col. 8 - Col. 9
<b>Year 2</b>										
<b>FY Projected Incremental</b>										
Total Incremental Expenses:	\$530,198									
<b>Total Facility by Payer Category:</b>										
Medicare		\$ 6,973.57	129	\$899,591	\$812,680			\$86,911	\$135,169	(\$48,258)
Medicaid		\$6,973.57	78	\$543,939	\$526,487			\$17,452	\$81,730	(\$64,278)
CHAMPUS/TriCare		\$6,973.57	3	\$20,921	\$14,030			\$6,891	\$3,143	\$3,748
<b>Total Governmental</b>			210	\$1,464,450	\$1,353,196	\$0	\$0	\$111,254	\$220,043	(\$108,789)
Commercial Insurers		\$6,973.57	288	\$2,008,389	\$1,484,259	\$8,532	\$9,102	\$506,496	\$301,773	\$204,723
Uninsured		\$6,973.57	8	\$55,789	\$28,871	\$10,767	\$10,767	\$16,151	\$8,383	\$7,768
<b>Total NonGovernment</b>			296	\$2,064,178	\$1,484,259	\$37,403	\$19,869	\$522,647	\$310,155	\$212,491
<b>Total All Payers</b>			506	\$3,528,628	\$2,837,455	\$37,403	\$19,869	\$633,901	\$530,198	\$103,703

12.C(ii). Please provide three years of projections of incremental revenue, expense and volume statistics attributable to the proposal in the following reporting format:

SAINT FRANCIS HOSPITAL AND MEDICAL CENTER										
Fiscal Year 2016										
Type of Service Description	MRI - 3T	(2)	(3)	(4)	(5)	(6)	(7)	(8)	(9)	(10)
Type of Unit Description:	Exams	Rate	Units	Gross Revenue	Allowances/ Deductions	Charity Care	Bad Debt	Net Revenue	Operating Expenses	Gain/(Loss) from Operations
# of Months in Operation	12			Col. 2 * Col. 3				Col. 4 - Col. 5 -Col. 6 - Col. 7	Col. 1 Total * Col. 4 / Col. 4 Total	Col. 8 - Col. 9
<b>Year 3</b>	<b>(1)</b>									
<b>FY Projected Incremental</b>										
Total Incremental Expenses:	\$536,624									
<b>Total Facility by Payer Category:</b>										
Medicare		\$ 7,670.93	195	\$1,495,831	\$1,364,452			\$131,379	\$136,608	(\$5,229)
Medicaid		\$7,670.93	119	\$912,841	\$886,229			\$26,612	\$83,366	(\$56,754)
CHAMPUS/TriCare		\$7,670.93	4	\$30,684	\$21,404			\$9,280	\$2,802	\$6,478
<b>Total Governmental</b>			318	\$2,439,356	\$2,272,085	\$0	\$0	\$167,271	\$222,776	(\$55,505)
Commercial Insurers		\$7,670.93	438	\$3,359,867	\$2,535,770	\$19,560	\$17,167	\$787,370	\$306,842	\$480,528
Uninsured		\$7,670.93	10	\$76,709	\$42,725	\$13,594		\$20,390	\$7,006	\$13,384
<b>Total NonGovernment</b>			448	\$3,436,576	\$2,535,770	\$62,285	\$30,761	\$807,760	\$313,848	\$493,912
<b>Total All Payers</b>			766	\$5,875,932	\$4,807,855	\$62,285	\$30,761	\$975,031	\$536,624	\$438,407

12.C(ii). Please provide three years of projections of incremental revenue, expense and volume statistics attributable to the proposal in the following reporting format:

# SAINT FRANCIS HOSPITAL AND MEDICAL CENTER

## Acquisition of 3T MRI Certificate of Need Application

### WITHOUT THE PROJECT

#### ASSUMPTIONS

#### General

- 1) The projection for FY 2012 equals eleven (10) months actual and one (1) month projected.
- 2) The projection for FY 2013 equals the hospital's budget.

#### Volume

- 3) Inpatient volume for patient days and discharges.
  - a) FY 2012 equals eleven (11) months actual and one (1) month projected.
  - b) FY 2013 patient days and discharges equal the budget.
  - c) FY 2014 – FY 2016 patient days and discharges were increased by 1.0% over the previous year.
- 4) Outpatient visits for FY 2014 – FY 2016 were increased by 2.0% over the previous year.
- 5) MRI Exams:
  - a) FY 2012 equals ten (10) months actual and two (2) months projected.
  - b) FY 2013 equals the budget.
  - c) FY 2014, FY 2015 and FY 2016 are assumed not to increase without the project.

#### Revenue

- 6) Price increases are as follows:

FY 2014:	10.00%
FY 2015:	10.00%
FY 2016:	10.00%
- 7) Free Care is projected at 1.06% of gross revenues consistent with historical experience.

# SAINT FRANCIS HOSPITAL AND MEDICAL CENTER

## Acquisition of 3T MRI Certificate of Need Application

### WITHOUT THE PROJECT

#### ASSUMPTIONS

##### Continued

- 8) Listed below are the projected payer rate increases to project FY 2014 through FY 2016.

	<u>FY 2014</u>	<u>FY 2015</u>	<u>FY 2016</u>
Blue Cross	4.0%	3.0%	3.0%
Commercial /Managed Care	5.0%	4.0%	4.0%
Other Non-Gov	1.0%	1.0%	1.0%
Medicare / Medicare Managed Care	0.0%	0.0%	0.0%
Medicaid	0.0%	0.0%	0.0%
Tri-Care Champus	1.0%	1.0%	1.0%

- 9) State Disproportionate Share Pool and Hospital User Tax is included in Medicaid and Other Medical Assistance Net Revenue. For FY 2014 through FY 2016 these funds were held constant at FY 2012 amounts.

#### Expenses

- 10) Listed below are the inflation rates used to project FY 2014 through FY 2016. Expenses were increased annually by the inflation factors.

	<u>2014-2016</u>
Salaries and Wages	2.0%
Employee Benefits	3.0%
Professional Fees	3.0%
Supplies and Drugs	3.0%
Purchased Services	3.0%
Other	3.0%

- 11) Salaries and Benefits, Professional and Contracted Services, Supplies and Drugs and Other operating expenses were also increased by the percentage increase in hospital discharges.
- 12) Bad Debt expense is projected at 3.0% of net patient revenues consistent with historical experience.
- 13) Depreciation expense for FY 2014 through FY 2016 was increased by 3.0%.

**SAINT FRANCIS HOSPITAL AND MEDICAL CENTER**

**Acquisition of 3T MRI  
Certificate of Need Application**

**WITHOUT THE PROJECT**

**ASSUMPTIONS**

**Continued**

- 14) Interest equals hospital's outstanding bonds and letter of credit fee arrangements.
- 15) Lease expense for FY 2014 through FY 2016 equals FY 2013 budget.

# SAINT FRANCIS HOSPITAL AND MEDICAL CENTER

## Acquisition of 3T MRI Certificate of Need Application

### INCREMENTALLY DUE TO THE PROJECT

#### ASSUMPTIONS

##### General

- 1) Expected date of operation for the new 3T MRI is November 2013.

##### Volume

- 2) Incremental volume for the proposed acquisition of the 3T MRI:

FY 2014	250
FY 2015	506
FY 2016	766

##### Revenue

- 3) FY 2014 - FY 2016 Net Revenue was calculated by multiplying the incremental increase in the number of MRI exams for each payer by the net revenue per MRI exam for each payer increased by the estimated payer percentage rate increase

##### Expenses

- 4) Professional / Contracted services were reduced for the fees paid to Alliance Imaging for the Mobile MRI exams.
- 5) Supplies & Drugs for the project equal \$ 22.05 per MRI exam for FY 2014. FY 2015 and FY 2016 the medical supply cost per MRI exam was inflated by 3.0% over the previous year.
- 6) Bad Debt expense was projected at 3.0% of net revenues.
- 7) Other expense for the project is the Maintenance Contract on the 3T MRI. For FY 2015 and FY 2016 the maintenance contract equals \$149,099.

Note: Due to a one year warranty on the new 3T MRI, there is no projected expense for FY 2014.

- 8) Depreciation expense was increased by the Project for FY 2014, FY 2015 and FY 2016.  
{See Depreciation Schedule}

**SAINT FRANCIS HOSPITAL AND MEDICAL CENTER**  
**Acquisition of 3T MRI**

**CALCULATION OF DEPRECIATION EXPENSE**  
**FOR THE PROJECT**

<u>DESCRIPTION</u>	<u>COST</u>	<u>ESTIMATED USEFUL LIFE</u>	<u>FY 2014 DEPRECIATION</u>	<u>ANNUAL DEPRECIATION</u>
<b>BUILDING:</b>				
Construction - renovation	\$ 763,000			
Other including fees and Arch.& Eng.	<u>150,000</u>			
<b>Total Building</b>	913,000	25 years	18,260	36,520
<b>MRI - Siemens 3T</b>	2,659,616	5 years	265,962	531,923
<b>MEDICAL EQUIPMENT:</b>	223,266	5 years	22,327	44,653
<b>NON MEDICAL EQUIPMENT:</b>	22,118	10 years	1,106	2,212
<b>TOTAL PROJECT COSTS</b>	<u>\$ 3,818,000</u>		<u>\$ 307,655</u>	<u>\$ 615,308</u>



# SAINT FRANCIS HOSPITAL AND MEDICAL CENTER

## Acquisition of 3T MRI Certificate of Need Application

### WITH THE PROJECT

### ASSUMPTIONS

#### General

- 1) The projection for FY 2012 equals eleven (10) months actual and one (1) month projected.
- 2) The projection for FY 2013 equals the hospital's budget.

#### Volume

- 3) Inpatient volume for patient days and discharges.
  - a) FY 2012 equals eleven (11) months actual and one (1) month projected.
  - b) FY 2013 patient days and discharges equal the budget.
  - c) FY 2014 – FY 2016 patient days and discharges were increased by 1.0% over the previous year.
- 4) Outpatient visits for FY 2014 – FY 2016 were increased by 2.0% over the previous year.
- 5) MRI Exams:

FY 2012	12,337
FY 2013	12,583
FY 2014	12,833
FY 2015	13,089
FY 2016	13,349

#### Revenue

- 6) Price increases are as follows:

FY 2014:	10.00%
FY 2015:	10.00%
FY 2016:	10.00%
- 7) Free Care is projected at 1.06% of gross revenues consistent with historical experience.

**SAINT FRANCIS HOSPITAL AND MEDICAL CENTER**

**Acquisition of 3T MRI  
Certificate of Need Application**

**WITH THE PROJECT**

**ASSUMPTIONS**

**Continued**

- 8) Listed below are the projected payer rate increases to project FY 2014 through FY 2016.

	<u>FY 2014</u>	<u>FY 2015</u>	<u>FY 2016</u>
Blue Cross	4.0%	3.0%	3.0%
Commercial /Managed Care	5.0%	4.0%	4.0%
Other Non-Gov	1.0%	1.0%	1.0%
Medicare / Medicare Managed Care	0.0%	0.0%	0.0%
Medicaid	0.0%	0.0%	0.0%
Tri-Care Champus	1.0%	1.0%	1.0%

- 9) State Disproportionate Share Pool and Hospital User Tax is included in Medicaid and Other Medical Assistance Net Revenue. For FY 2014 through FY 2016 these funds were held constant at FY 2012 amounts.

**Expenses**

- 10) Listed below are the inflation rates used to project FY 2014 through FY 2016. Expenses were increased annually by the inflation factors.

	<u>2014-2016</u>
Salaries and Wages	2.0%
Employee Benefits	3.0%
Professional Fees	3.0%
Supplies and Drugs	3.0%
Purchased Services	3.0%
Other	3.0%

- 11) Salaries and Benefits, Professional and Contracted Services, Supplies and Drugs and Other operating expenses were also increased by the percentage increase in hospital discharges.
- 12) Professional / Contracted services were reduced for the fees paid to Alliance Imaging for the Mobile MRI exams.

**SAINT FRANCIS HOSPITAL AND MEDICAL CENTER**

**Acquisition of 3T MRI  
Certificate of Need Application**

**WITH THE PROJECT**

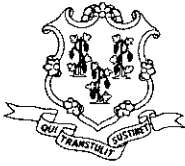
**ASSUMPTIONS**

**Continued**

- 13) Supplies & Drugs for the project equal \$ 22.05 per MRI exam for FY 2014. FY 2015 and FY 2016 the medical supply cost per MRI exam was inflated by 3.0% over the previous year.
- 14) Bad Debt expense is projected at 3.0% of net patient revenues consistent with historical experience.
- 15) Other expense for the project is the Maintenance Contract on the 3T MRI. For FY 2015 and FY 2016 the maintenance contract equals \$149,099.

Note: Due to a one year warranty on the new 3T MRI, there is no projected expense for FY 2014.

- 16) Depreciation expense for FY 2014 through FY 2016 was increased by 3.0%. Additionally, depreciation for these years was increased by the project {see project depreciation schedule}
- 17) Interest equals hospital's outstanding bonds and letter of credit fee arrangements.
- 18) Lease expense for FY 2014 through FY 2016 equals FY 2013 budget.



STATE OF CONNECTICUT  
DEPARTMENT OF PUBLIC HEALTH  
*Office of Health Care Access*

October 19, 2012

VIA FAX ONLY

Christopher Hartley  
Senior Vice President Planning  
Business Development and Government Relations  
St. Francis Hospital and Medical Center  
114 Woodland Street  
Hartford, CT 06105

RE: Certificate of Need Application, Docket Number 12-31785-CON  
Proposal for the Acquisition of a Magnetic Resonance Imaging Scanner

Dear Mr. Hartley:

On September 21, 2012, the Office of Health Care Access ("OHCA") received your Certificate of Need application filed on behalf of St. Francis Hospital and Medical Center ("Hospital") for the acquisition of a Magnetic Resonance Imaging ("MRI") Scanner. OHCA has reviewed the CON application and requests the following additional information pursuant to General Statutes §19a-639a(c):

1. On page 9 of the CON application, the Hospital states that it will continue to provide mobile MRI services at its outpatient location in Avon. Please provide the historical (3 years) and projected (3 year) utilization of the Avon location.
2. Explain in detail the role of the mobile MRI being continued at the Avon location and the Hospital's role at that location.
3. On page 12 of the CON application, the Hospital provides the existing Hospital based MRI scanner in the Hospital's service area. Please update the table to include **all** providers of MRI services in the Hospital's service area.

In responding to the questions contained in this letter, please repeat each question before providing your response. Paginate and date your response, i.e., each page in its entirety. Information filed after the initial CON application submission (i.e. completeness letter, late file submissions, and the like) must be numbered sequentially from the Applicant document preceding it. As the current submission for the application concludes with page 339, please begin with the completeness response with page 340. Reference Docket Number: 12-31785-CON and submit one (1) original and six (6) hard copies of your response in its entirety, including any

*An Equal Opportunity Employer*  
410 Capitol Ave., MS#13HCA, P.O.Box 340308, Hartford, CT 06134-0308  
Telephone: (860) 418-7001 Toll-Free: 1-800-797-9688  
Fax: (860) 418-7053

supporting documentation. Submit a scanned copy of your response in Adobe format, an electronic copy in MS Word format and any worksheets in MS Excel, including all attachments, on CD.

Sincerely,

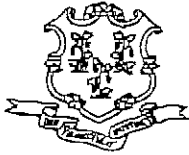
A handwritten signature in black ink, appearing to read 'Steve Lazarus', with a stylized, sweeping flourish at the end.

Steve Lazarus  
Associate Health Care Analyst

\*\*\*\*\*  
\*\*\* TX REPORT \*\*\*  
\*\*\*\*\*

TRANSMISSION OK

TX/RX NO 3092  
RECIPIENT ADDRESS 918607148093  
DESTINATION ID  
ST. TIME 10/19 15:59  
TIME USE 00'28  
PAGES SENT 3  
RESULT OK



STATE OF CONNECTICUT  
DEPARTMENT OF PUBLIC HEALTH  
OFFICE OF HEALTH CARE ACCESS

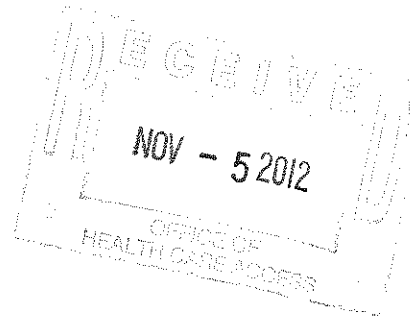
FAX SHEET

TO: Chris Hartley  
FAX: (860) 714-8093  
AGENCY: \_\_\_\_\_  
FROM: Steven Lazani  
DATE: 10/19/12 TIME: 3:50 pm  
NUMBER OF PAGES: 3  
*(including transmittal sheet)*

Comments: 12-31785-corr  
Con completion Letter Enclred.

November 5, 2012

Steve Lazarus  
Associate Health Care Analyst  
State of Connecticut  
Department of Public Health  
Office of Health Care Access  
410 Capitol Ave, MS#13HCA  
PO Box 340308  
Hartford, CT 06134



**RE: Completeness Letter - Certificate of Need Docket Number 12-31785-CON  
for Proposal for the Acquisition of a Magnetic Resonance Imaging Scanner**

1. On page 9 of the CON application, the Hospital states that it will continue to provide mobile MRI services at its outpatient location in Avon. Please provide the historical (3 years) and projected (3 year) utilization of the Avon location.

**The following are the Avon Center's actual volumes:**

**FY 2010 - 1,192  
FY 2011 - 1,215  
FY 2012 - 1,189**

**Projected Volume**

**FY 2013 - 1,207  
FY 2014 - 1,225  
FY 2015 - 1,243  
FY 2016 - 1,262**

The volumes are based on 1.5% increase in each year.

2. Explain in detail the role of the mobile MRI being continued at the Avon location and the Hospital's role at that location.

**The Avon mobile MRI service is located at the St FrancisCare Access Center, 35 Nod Hill Road and shares immediate adjacency to Radiology Associates of Hartford outpatient imaging office. Saint Francis Hospital and Medical Center has a contractual agreement with Alliance Imaging, Inc., to provide four days of mobile MRI service at this location, inclusive of the mobile MRI unit and the MRI technical staff. Saint Francis Hospital and Medical Center holds the CON for this approved mobile service and pays Alliance Imaging, Inc., according to the existing contracted technical fee schedule. Additionally, Saint Francis Hospital and Medical Center has an exclusive contract with Radiology Associates of Hartford to provide professional interpretation services for imaging studies performed at Saint Francis Hospital and Medical Center Department of Radiology Imaging Services, on the main hospital campus and outpatient off-site Saint Francis Hospital and Medical Center Radiology service locations.**

**The mobile MRI unit at the Avon location services only outpatients from the immediate surrounding area. We believe continuing the mobile MRI service is necessary to maintain the availability of MRI services to the patient population in Avon and surrounding areas. MRI services provided at the Avon location are independent of the services provided at 114 Woodland Street, Hartford, the main hospital campus. Please note the volumes for the Avon location were not included in the utilization numbers and projections included as justification for this MRI application. In addition, the actual days of mobile MRI services being purchased by Saint Francis Hospital and Medical Center from Alliance Imaging is being reduced through the elimination of the 95 Woodland site (ie: 3 days/week).**



3. On page 12 of the CON application, the Hospital provides the existing Hospital based MRI scanner in the Hospital's service area. Please update the table to include all providers of MRI.

Please see below updated table:

Hospital	Number of MRI Machines	FY 2010 Total Volume	FY 2011 Total Volume	Increase/Decrease And Percent difference ft'11 over 'FY'10
Bristol	1	3,465	3,232	(233) (7%)
CCMC	1	3,634	4,094	460 13%
Charlotte Hungerford	1	6,434	6,480	46 1%
Hospital of Central CT	1	6,965	7,703	738 11%
Hartford Hospital	2	8,322	7,742	(580) (7%)
John Dempsey	1	7,185	6,876	(309) (4%)
Johnson Memorial	1	1,378	1,511	133 10%
Manchester Memorial	1	3,840	3,731	(109) (3%)
Middlesex Hospital	1	10,803	10,579	(224) (2%)
Midstate Medical Center	1	6,942	7,534	592 9%
Rockville General	1	1,896	1,833	(63) (3%)
Saint Francis Hospital and Medical Center	3	13,849*	14,221*	372 3%
Jefferson Radiology	10- (Bloomfield, Avon, Glastonbury, Windsor, Wethersfield, Farmington, Hartford, West Hartford, Granby, Enfield)	N/A	N/A	N/A
CT Valley Radiology	2 (Bloomfield and Hartford)	N/A	N/A	N/A
Radiology Associates of Hartford	3 (Enfield, Glastonbury and Avon)	N/A	N/A	N/A
Advanced Medical Imaging of Northwest CT	1- (Torrington)	N/A	N/A	N/A
Evergreen Imaging Center	1-(South Windsor)	N/A	N/A	N/A
Tolland Imaging Center	1- (Tolland)	N/A	N/A	N/A
Mandell and Blau	7- (South	N/A	N/A	N/A

	Windsor, Glastonbury, Enfield, New Britain, West Hartford, Southington and Middletown)			
Grove Hill Medical Center	1- (New Britain)	N/A	N/A	N/A
Farmington Imaging Center	1- (Farmington)	N/A	N/A	N/A
West Hartford Open MRI	1- (West Hartford)	N/A	N/A	N/A
Open MRI of Southington	1- (Southington)	N/A	N/A	N/A
Radiology and Imaging	1 - (Enfield)	N/A	N/A	N/A
Radiologic Associates	2- ( 2 in Bristol)	N/A	N/A	N/A
<b>Total</b>	<b>47</b>	<b>74,713</b>	<b>75,536</b>	<b>823 1.1%</b>

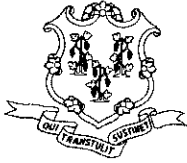
The above table is as complete as Saint Francis Hospital and Medical Center is aware. The sources used to update the table are OHCA Financial Form 450 for the Acute Care hospitals, and the internet websites for Jefferson Radiology, CT Valley Radiology, Radiology Associates of Hartford, Advanced Medical Imaging of Northwest CT, Evergreen Imaging Center, Mandell and Blau, Grove Hill Medical Center, Farmington Imaging Center, West Hartford Open MRI, Open MRI of Southington, Radiology and Imaging, and Radiologic Associates.

Please let us know if there is additional information you may need. I can be reached at 714-5573.

Sincerely,



Christopher Hartley  
Senior Vice President  
Planning & Business Development  
Government Relations



**STATE OF CONNECTICUT**  
DEPARTMENT OF PUBLIC HEALTH  
*Office of Health Care Access*

December 11, 2012

Via Fax Only

Christopher R. Hartley  
Senior Vice President Planning,  
Business Development & Government Relations  
Saint Francis Hospital and Medical Center  
114 Woodland Street  
Hartford, CT 06105

RE: Certificate of Need Application; Docket Number: 12-31785-CON  
Saint Francis Hospital and Medical Center  
Acquisition of a MRI Scanner

Dear Mr. Hartley:

This letter is to inform you that, pursuant to Section 19a-639a(d) of the Connecticut General Statutes, the Office of Health Care Access has determined that the above-referenced application has been deemed complete as of December 5, 2012.

If you have any questions regarding this matter, please feel free to contact me at (860) 418-7012.

Sincerely,

A handwritten signature in black ink, appearing to read "Steven W. Lazarus".

Steven W. Lazarus  
Associate Health Care Analyst

\*\*\*\*\*  
\*\*\* TX REPORT \*\*\*  
\*\*\*\*\*

TRANSMISSION OK

TX/RX NO 3201  
RECIPIENT ADDRESS 918607148093  
DESTINATION ID  
ST. TIME 12/11 14:28  
TIME USE 00'23  
PAGES SENT 2  
RESULT OK



STATE OF CONNECTICUT  
DEPARTMENT OF PUBLIC HEALTH  
OFFICE OF HEALTH CARE ACCESS

FAX SHEET

TO: MR. HARTLEY  
FAX: \_\_\_\_\_  
AGENCY: 860 . 714 . 8093  
FROM: Steven Lazarus  
DATE: 12/11/12 TIME: 1:15  
NUMBER OF PAGES: \_\_\_\_\_  
*(including transmittal sheet)*

Comments: Deemed Complete Enclosed